Technical Report

TR-11-01

# Long-term safety for the final repository for spent nuclear fuel at Forsmark

## Main report of the SR-Site project

## Volume III

Svensk Kärnbränslehantering AB

March 2011

**Svensk Kärnbränslehantering AB**
Swedish Nuclear Fuel
and Waste Management Co

Box 250, SE-101 24 Stockholm
Phone +46 8 459 84 00

ISSN 1404-0344
SKB TR-11-01
ID 1271592
Updated 2015-05

# Long-term safety for the final repository for spent nuclear fuel at Forsmark

## Main report of the SR-Site project

## Volume III

Svensk Kärnbränslehantering AB

March 2011

*Keywords:* Safety assessment, Long-term safety, Final repository, Spent nuclear fuel, Forsmark.

A pdf version of this document can be downloaded from www.skb.se

## Update notice

The original report, dated March 2011, was found to contain both factual and editorial errors which have been corrected in this updated version. The corrected factual errors are presented below.

### Updated 2015-05

| Location | Original text | Corrected text |
|---|---|---|
| Page 723, paragraph 1, last two sentences | …the release of C-14 would be about 10 GBq. A release of Rn-222 would be about 25 GBq if… | …the release of C-14 would be about 25 GBq. A release of Rn-222 would be about 45 GBq if… |
| Page 723, Table 13-11, heading | …a single canister /SKB 2006g, a/. | …a single canister /SKB 2006g/, updated with inventory data used in SR-Site. |
| Page 723, Table 13-11, Table head, column 2 | (10 GBq release) | (25 GBq release) |
| Page 723, Table 13-11, Table head, column 3 | (25 GBq release) | (45 GBq release) |
| Page 723, Table 13-11, row 1, column C-14 | 0.036 | 0.033 |
| Page 723, Table 13-11, row 2, column C-14 | $4.4 \cdot 10^{-5}$ | $5.5 \cdot 10^{-5}$ |
| Page 723, Table 13-11, row 2, column Rn-222 | 0.22 | 0.20 |
| Page 723, Table 13-11, row 3,column C-14 | 0.0028 | 0.0035 |
| Page 723, Table 13-11, row 3, column Rn-222 | 7.2 | 8.3 |

### Updated 2012-12

| Location | Original text | Corrected text |
|---|---|---|
| Page 664, paragraph 4 | | Text in paragraph 4 updated |
| Page 665, all text and figure 13-20 | | All text and figure 13-20 updated, last paragraph is new |
| Page 666, paragraph 1 | | New paragraph |
| Page 723, paragraph 2, line 1 | /SKB 2006g, h/ | /SKB 2006g, a/ |
| Page 723, Table 13-1, heading | /SKB 2006g, h/. | /SKB 2006g, a/. |
| Page 730, paragraph 2, line 2 | /Bond et al. 2007/ | /Bond et al. 1997/ |
| Page 846 | | *New reference*: Bradbury and Baeyens, 2005 |
| Page 847 | | *New reference*: Bäckblom et al. 2004 |

### Updated 2011-10

| Location | Original text | Corrected text |
|---|---|---|
| Page 594, paragraph 6, heading | Quantitative consequence analysis/discussion – containment and retardation | Quantitative consequence analysis/discussion |
| Page 596, paragraph 5, line 6 | ...criterion of 1 MPa, which is most unlikely. | ...criterion of 1 MPa, where advection conditions need to be considered, which is most unlikely. |
| Page 638, paragraph 2, last line | ...in the central corrosion case (see Section 13.5.4). | ...in e.g. the corrosion scenario (see Section 13.5.4). |
| Page 640, paragraph 1, line 1 | In the central corrosion case,... | In e.g. the central corrosion case,... |
| Page 654, paragraph 2, line 1 | The handling assumes... | The handling of pulse releases assumes... |
| Page 743, second last paragraph, line 2 and 3 | ...as SSI in the general guidelines to their regulations /SSI 2008b/ | ...as SSM in the general guidelines to their regulations /SSM 2008b/ |
| Page 744, last paragraph, line 1 | /SKI 2002/. | /SSM 2008a/. |
| Page 746, paragraph 6, line 1 | Can1, Ensure containment | Can1, Provide corrosion barrier; ensure containment |
| Page 748, paragraph 1, line 4 | ...is calculated to be 500 mSv/hour... | ...is calculated to be 130 mSv/hour... |
| Page 748, last paragraph, last line | ...would be about 15 mSv/hour. | ...would be about 4 mSv/hour. |
| Page 751, second last paragraph, line 3 | After a couple of hours of exposure | After about eight hours of exposure |
| Page 755, paragraph 4, line 2 | /SKI 2002/. | /SSM 2008a/. |
| Page 755, paragraph 5, line 2 | Can1, Ensure containment | Can1, Provide corrosion barrier; ensure containment |
| Page 755, paragraph 5, line 5 | Bf1 | BF1 |
| Page 760, Figure 14-5 | Positive powers of y-axis | Figure 14-5 updated Negative powers of y-axis |
| Page 770, paragraph 1, line 1 | The travel paths of solutes... | The length of the travel paths of solutes... |
| Page 810, paragraph 4, line 2 | ...travel paths of solutes in the groundwater will increase with... | ...length of the travel paths of solutes in the groundwater will increase with... |
| Page 873, under heading A1.2, paragraph 1, line 3 | (SSMFS 2002:1) | (SSMFS 2008:21) |

# Contents

## Volume I

## Volume II

## Volume III

# 11 Selection of scenarios

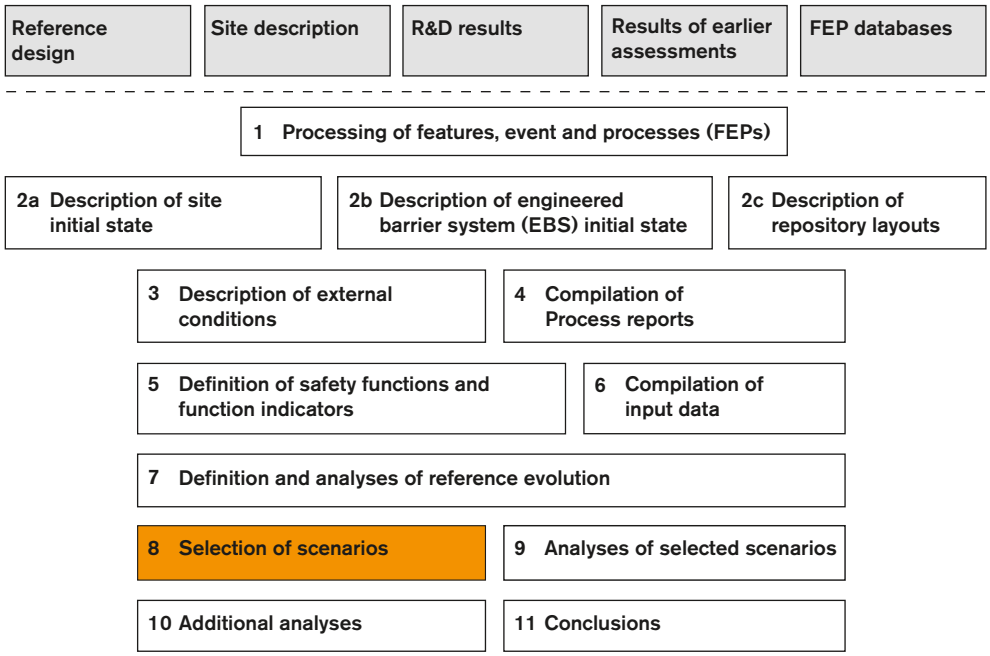


***Figure 11-1.*** *The SR-Site methodology in eleven steps (Section 2.5), with the present step highlighted.*

## 11.1 Introduction

As mentioned in Section 2.5.8, a key feature in managing uncertainties in the future evolution of the repository system is the reduction of the number of possible evolutions to analyse by selecting a set of representative scenarios.

The selection focuses on addressing the safety relevant aspects of the evolution expressed at a high level by the safety functions containment and retardation which are further characterised by reference to safety function indicators, as discussed in Chapter 8.

In Section 2.5.8 the regulatory requirements in the selection of scenarios were discussed and a general methodology for the selection of scenarios was presented. The methodology explains i) how a main scenario, closely related to the reference evolution, is defined and ii) the principles for selecting a number of additional scenarios, based on safety functions.

In the following, the selection of additional scenarios based on safety functions is carried out in Section 11.2.1, a structure for the further analyses of these scenarios is presented in Section 11.2.2, leading to a template for the account of the analyses given in Section 11.2.3. All selected scenarios are summarised in Section 11.3. A discussion on uncertainties in relation to scenario selection was given in Section 2.8.

## 11.2 Scenarios derived from safety functions; selection and structuring for analysis

### 11.2.1 Selection of additional scenarios

#### *Uncertainties not covered by the reference evolution*

As discussed above, the main scenario is based on the reference evolution that covers the evolution of the repository system for a **realistic** initial state of the repository and for an example of a **credible** evolution of external conditions over the assessment period.

However, as implied by the terms 'realistic' and 'credible', significantly different conditions and hence different repository evolutions cannot be ruled out. There are uncertainties regarding the initial state, the processes governing the evolution and the external conditions. Not all these uncertainties are covered in the reference evolution on which the main scenario is based and they need to be explored in a set of additional scenarios. The evaluation of uncertainties explores whether more extreme initial state and external conditions need to be included in the analyses, and if uncertainties related to the handling of processes warrant further analyses.

#### *Approach to selection of additional scenarios*

A structured selection approach is required in order to obtain a set of additional scenarios that can be argued to be comprehensive. The purpose of the scenarios is to aid in a critical evaluation of repository safety and it is, therefore, natural to use the safety functions and the safety function indicators discussed in Chapter 8 when seeking a structure for scenario selection.

The approach taken in SR-Site is to use the safety functions with their indicators and indicator criteria as expressed in Figure 10-2 to define a set of scenarios that are distinguished by their different status of the safety functions. The scenarios thus consider cases where the possibility and consequences of partially or completely losing one or several of the safety functions are evaluated. Examples are scenarios where canisters fail due to corrosion, to isostatic overpressure or to shear movements in fractures intersecting the deposition hole. The scenarios are defined without consideration of their likelihood.

In the analyses of the selected scenarios, all conceivable routes to the loss of the safety function that defines the scenario are critically examined, in order to evaluate the likelihood of the scenario, its consequences and its potential contribution to the risk summation for the repository. From the understanding of the functioning of the repository system, this examination is focussed on the factors contributing to the particular safety function, thus focussing the evaluation of each scenario on a limited set of uncertain factors. The FEP chart, Figure 8-4, is an aid when identifying such factors. The basis for the evaluation is the analysis of the reference evolution, where all the factors covered in the FEP chart are analysed for reference conditions.

The approach taken when selecting scenarios is thus to ask the question: What characterises a failed repository? The answer to that question is a list of states where one or several safety functions are not upheld, e.g. a situation where advection is the dominant transport mechanism in the buffer. The analyses of the so selected scenarios then focus on identifying and quantifying all conceivable routes to these failed states. The goal, for each scenario, is to either dismiss it, since no credible such route can be identified, or to assess its likelihood and consequences so that it can be included in the risk summation for the repository. For the latter scenarios, it may, as feedback to future design development, be appropriate to consider whether modifications to the design could eliminate or reduce the potential for occurrence of the scenario.

#### *Elaboration of list of safety functions for the scenario selection*

The primary safety function of a KBS-3 repository is containment. Therefore, an obvious step when selecting scenarios based on safety functions is to select three **canister scenarios** based on the three safety functions directly related to canister containment, i.e. scenarios characterised by (Figure 10-2)

A. Canister failure due to corrosion, safety function Can1.

B. Canister failure due to isostatic load, safety function Can2.

C. Canister failure due shear load, safety function Can3.

For the further selection of scenarios, the list of safety functions requires some elaboration, since many of the safety functions are overlapping or inter-connected. The buffer safety function 'limit advective transport' is e.g. connected to the canister safety function 'provide corrosion barrier' in that corrosion is strongly enhanced if advective conditions prevail in the buffer. A comprehensive evaluation of the canister corrosion scenario must thus encompass also an evaluation of advection in the buffer. In general, each of the above three scenarios related to canister failure needs to be combined with relevant states of the buffer in order to obtain a comprehensive evaluation.

#### *Derivation of critical buffer states*

From the safety functions, six buffer states related to safety can be derived:

1. A basic state is the **intact buffer**, where all buffer safety functions are upheld.
2. Another state directly derivable from the safety functions is the **buffer with advective conditions**, relating to loss of the safety functions Buff1a or Buff1b. A special case of advective conditions occurs when the buffer is not able to keep the canister in its intended vertical position so that, in the most extreme case, the canister has sunk to the bottom of the deposition hole. The buffer diffusion barrier is then lost and the mass transfer between the groundwater and the canister is controlled by advection in the surrounding rock and possibly also in the buffer. This relates to the buffer function Buff5 (prevent canister sinking).
3. Another state needing consideration is the **transformed buffer**. This is related to the buffer function Buff4 that concerns the maximum temperature of the buffer. There are, however, a number of additional potential causes for, or routes to, buffer transformation that also need to be considered in order to fully evaluate this buffer state.
4. A **frozen buffer** must be considered, relating to the buffer function Buff6b.
5. A **dense buffer** considers a situation where the density of the buffer is higher than that given in the design premises. This state relates to the buffer function Buff3 (damp rock shear) and Buff6a (limit swelling pressure on the canister).
6. Finally, a **buffer housing active microbes** implies a situation where microbial reduction of sulphate needs to be considered in the buffer itself. This state relates to the function Buff2.

These are six buffer states, five of which that may be characterised as 'failed', that emerge from the list of safety functions, and also from the general understanding of the role of the buffer and its evolution over time in a KBS-3 repository. Of these, the first four are treated as distinct buffer scenarios (one intact and three failed). The last two, the dense buffer and the buffer housing active microbes are included in the analyses of the relevant canister scenarios as indicated in Figure 11-2. Both these are related to the buffer density and swelling pressure, and are readily analysed within the appropriate canister scenarios, hereby reducing the number of scenarios and the complexity of the account of the scenarios.

### 11.2.2 Structure for analysis of the additional scenarios

#### *Approach*

The analysis of the additional scenarios uses the reference evolution as a point of departure. The analysis of each of the scenarios then focuses on an evaluation of possible uncertainties of relevance to the particular scenario, including uncertainties that are not addressed in the analysis of the reference evolution. These uncertainties may be related to the initial state of the repository, to processes governing repository evolution or to external influences.

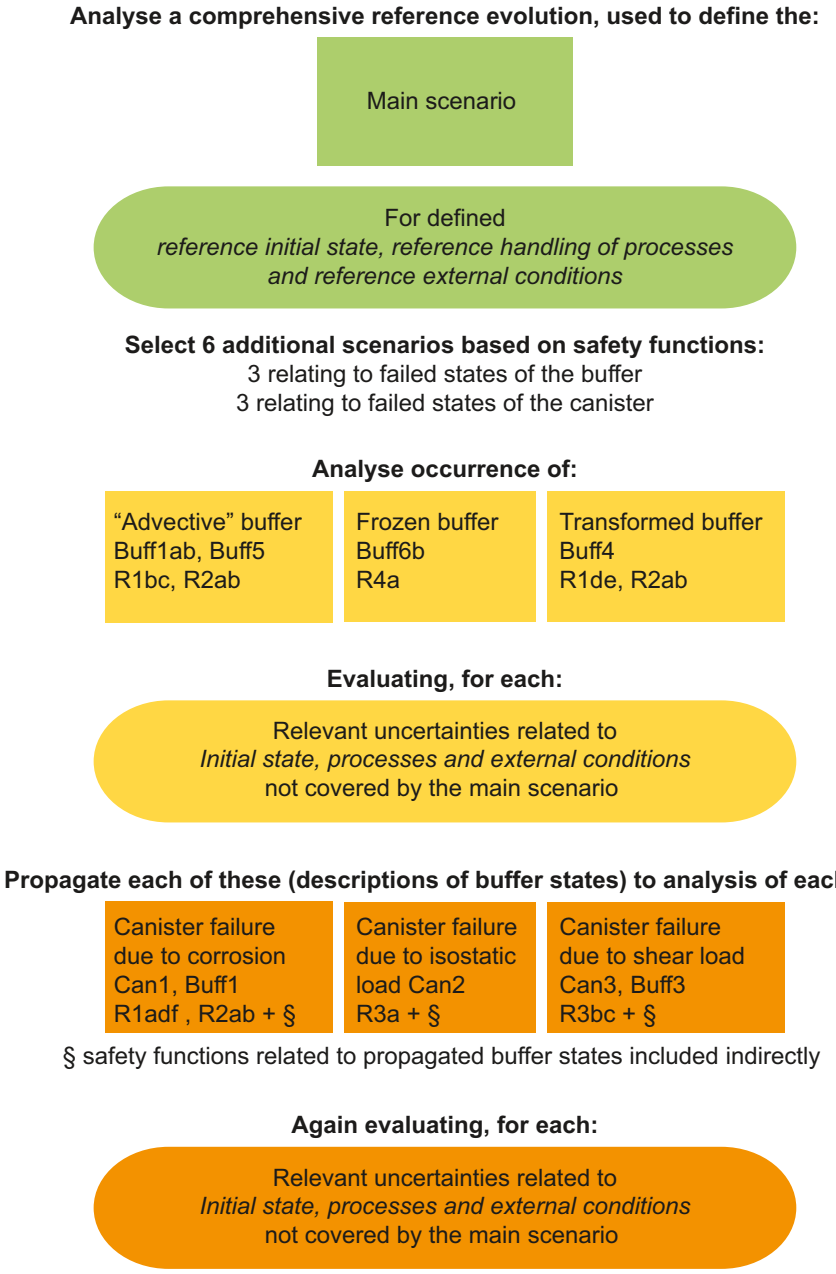


***Figure 11-2.*** *The main components of the scenario selection and analysis procedure where safety functions of the canister and the buffer are used to derive the additional scenarios (yellow and orange squares). The safety function indicators of relevance in each scenario are given with the same nomenclature as in Figure 8-2.*

For example, in the analysis of the buffer advection scenario, the following issues are among those addressed.

- Could the initial density of the buffer – density being a critical factor for the occurrence of buffer advection – for any reason be lower than the reference initial density assumed in the reference evolution?
- Are there remaining conceptual uncertainties related to the buffer colloid release/erosion process (leading to loss of density) that are not addressed by the models used to quantify this process in the reference evolution? This includes effects of piping and erosion during the saturation of the repository.
- Could the groundwater composition and flow be less favourable to safety due to the induction of buffer advection than the composition and flow that follow from the reference external conditions, a repetition of the Weichselian glacial cycle, in the reference evolution?

### *Combination of scenarios related to buffer functions and canister functions*

Each of the three failed buffer states is evaluated as a separate scenario, critically examining all identified routes to them, as described under the previous sub-heading. Their consequences in terms of canister failures and release of radionuclides are, however, not evaluated until they are combined with the three canister scenarios defined above. By this procedure, much of the issue of combining scenarios is handled. Figure 11-2 shows schematically how the scenario analysis based on safety functions is carried out. Note that, if the analysis of a particular buffer scenario comes to the conclusion that it is to be considered as residual, then it is not propagated to the canister scenarios defined above.

The safety functions related to the rock are evaluated **within** each of these combinations through the consideration also of uncertainties related to geosphere and external conditions when evaluating both the buffer states and the canister failure modes (see buffer advection example above). This is necessary since e.g. the potential occurrence of advective conditions in the buffer is directly related to the groundwater composition through the safety function R1c (groundwater minimum ionic strength) and the occurrence of canister failures due to rock shear is directly related to rock movements through the safety functions R3b and c, see further Figure 11-2.

### *Approach to retardation*

The approach presented so far concerns direct failure modes of the canister, and how the buffer safety functions relate to these failure modes, i.e. it is related to the primary safety function of the repository. The approach taken to evaluate also the secondary safety function, retardation, is to determine, for each of the canister failure modes, uncertainties related to retardation. This approach is strongly motivated by the fact that each canister failure mode has distinct consequences for retardation, thus requiring a specific evaluation of uncertainties related to this characteristic.

Within each scenario, uncertainties related to the relevant aspects, for that particular scenario, of retardation properties of the fuel, the canister, the buffer, the deposition tunnel backfill and the geosphere are evaluated. Many of the uncertainty issues overlap with those relevant for containment. For example, advective conditions in the buffer are relevant for both containment, through the inward transport of canister corroding agents, and for retardation, in relation to the outward transport of radionuclides. This evaluation is made in Chapter 13, following a similar but simpler approach to that used in the evaluation of scenarios related to containment, see Section 11.2.3.

### *Classification as 'less probable' or 'residual'*

A key point in the evaluation of the scenarios is to arrive at an assessment of whether there is any possibility of the scenario occurring. If this is the case, the scenario is classified as 'less probable' and included in the risk summation, otherwise it is defined as 'residual'.

There is no numerical limit to the probability below which a scenario is considered as residual in SR-Site. The approach taken is that if it can be argued that a scenario is not physically reasonable, given cautious evaluations of current knowledge of e.g. barrier properties, processes and effects of future climate changes, then the scenario is considered as residual.

A more precise definition, covering all possible situations, is not seen as possible or meaningful to formulate; the reader is referred to the implementation in Chapter 12 for detailed applications of the approach.

### *Common causes affecting several scenarios, combination of scenarios*

As mentioned above, through the combination of buffer- and canister-related scenarios, much of the issue of combining scenarios is handled. There are, however, some additional considerations regarding scenario combinations.

Combinations of the canister failure scenarios need to be considered. Are the identified failure modes independent, so that their risk contributions can be added, i.e. are their causes independent? Furthermore, is the response to a particular failure cause independent of whether another cause is acting simultaneously? The combination of isostatic load and loads caused by a rock shear movement on a canister

illustrates both these issues: Is the likelihood of an earthquake independent of whether a major ice sheet, potentially generating high groundwater pressures, exists above the repository? If these two load situations can exist simultaneously, is the canister response to an earthquake-induced shear movement independent of the existence of an isostatic overpressure?

Also combinations of the buffer states need to be considered in a similar way. The freezing temperature of the buffer is e.g. dependent on the buffer density which is lowered when advective conditions prevail in the buffer.

When the analyses described in Figure 11-2 are completed, the issue of combinations is revisited through a structured approach aiming at a comprehensive treatment of scenario combinations, see further Section 12.9.

#### *Risk summation*

The risk contributions from each of the scenarios form the basis for a risk summation, when the scenario analyses are completed.

Risk contributions from scenarios that are independent are added, if combinations do not lead to higher consequences than the individual scenarios. If combinations may lead to higher consequences, the likelihood and consequences of each such combination are also assessed.

In the summation, it is also observed whether some sub-sets of the scenarios are mutually exclusive, in which case the total consequence of the sub-set cannot exceed that of the scenario with the highest consequence in the sub-set. This is a way of bounding the risk from a set of mutually exclusive scenarios (or cases within a scenario) if the basis for apportioning probabilities among the members of the set is limited.

#### *Relation to reference evolution*

For several safety function indicators, criteria exist such that if the criterion is fulfilled, a certain phenomenon, negatively impacting safety, is excluded. Freezing of the buffer is e.g. excluded if the buffer temperature is above −4°C. If the criterion was assessed to be fulfilled in the reference evolution, then the evaluation focuses on conceivable routes, beyond those covered by the reference evolution, to a violation of the criterion. Guided by the FEP chart, see Section 8.5, uncertainties related to initial state and external conditions as well as conceptual uncertainties associated with processes are explored.

If the indicator is not associated with a criterion, or if the criterion was assessed to be violated in the reference evolution, then it is evaluated if the value of the safety function indicator could be less favourable for safety than is the case in the reference evolution. Again, uncertainties related to initial state, external conditions and processes are explored.

### 11.2.3 Template for assessment of scenarios based on safety functions

A common template is followed in the analysis of all scenarios derived from safety function indicators. The template is given below, and, for each heading, a brief description of the information that can be expected under it is given. Minor modifications of the structure for a specific scenario are made as appropriate, but the contents given below are always covered.

Note that the template covers only the analysis of containment potential in Chapter 12. Consequence calculations for the canister failure modes assessed in the scenarios are carried out in Chapter 13, according to procedures described in that chapter.

#### *Safety function indicator(s) considered*

The safety function under consideration is stated. If the scenario concerns a safety function for which a criterion of adequate safety function has been determined, it is stated that this criterion is assumed to be violated. The degree to which it is violated is specified as the analysis continues.

In some cases, several safety functions are evaluated within the same scenario, since they all relate to circumstances that are relevant to a common safety issue. If this is the case, all involved functions and their dependencies are explained. The function indicator "buffer hydraulic conductivity" related to the safety function Buff1 is e.g. related to the indicators "buffer swelling pressure", "minimum ionic strength of groundwater", "limited salinity" and "backfill density".

#### *Treatment of this issue in the reference evolution*

The treatment in the reference evolution is described briefly.

#### *Qualitative description of routes to this situation*

The table of uncertainties derived from the analysis of the reference evolution is revisited, in order to identify uncertainties requiring further treatment in the scenario under consideration. Based on this table and the FEP chart, the factors contributing to the possible occurrence of the scenario are presented. The presentation results in a listing of i) initial state factors, ii) processes and iii) external conditions to be considered.

#### *Quantitative assessment of routes to this situation*

A critical evaluation of the analysis of the reference evolution is carried out, in order to exhaustively evaluate all conceivable routes to the situation characterising the scenario. Uncertainties possibly remaining after the treatment in the reference evolution are addressed. For example, initial state conditions not covered by the reference initial state are addressed as are external conditions not covered by the reference external evolution. Conceptual uncertainties related to the processes involved are discussed.

An analysis of the importance of the sequence in which different processes or events occur is made.

Unless overridden by assumptions related to this particular scenario, the scenario is analysed for the reference glacial cycle, the global warming variant and other relevant climate cases, to satisfy SSM's requirement that each scenario is to be analysed for several alternative climate evolutions.

#### *Categorisation as "less probable" or "residual" scenario*

Based on an assessment of plausibility of the routes to the situation, the scenario is characterised as either a "less probable" scenario if its occurrence cannot be ruled out or otherwise as a "residual" scenario. In the former case, the consequences of the scenario are included in the risk summation for the repository, which means that an assessment of the likelihood of the scenario's occurrence is made. In some cases it is relevant to consider both the probability that a single deposition hole is affected and the probability of all (or many) holes being affected. In the "residual scenario" case, the consequences of the scenario are not included in the risk summation for the repository.

#### *Conclusions*

Conclusions, based on the results under the previous headings, are drawn.

## 11.3 Summary of scenario selection

Table 11-1 summarises the result of the scenario selection carried out as described in this chapter.

The reference evolution described in Chapter 10, is defined as the main scenario and forms the basis for selection of additional scenarios.

The safety functions are used as a basis for the selection of additional scenarios. These comprise three buffer scenarios, representing 'failed' states of the buffer and three canister scenarios, representing distinct canister failure modes. The buffer scenarios are analysed first and each buffer state is then considered in the analyses of the canister failure modes. Should, however, the analyses of any of the

buffer states lead to the conclusion that it can be ruled out, that state is not propagated. The outcome of the analyses in Chapter 12 determines whether a combination is 'less probable' and hence included in the risk summation, or 'residual'.

Scenarios related to future human actions and other scenarios analysed e.g. in order to understand barrier functions are included as necessary if not covered by the results of the already analysed scenarios. These latter points are discussed in Section 2.5.8.

The completeness of the set of selected scenarios is discussed in Chapter 15.

In summary, the scenario methodology is an investigation of all routes to the three identified canister failure modes aiming at ruling them out or at quantifying them, considering all conceivable evolutions of the system. The safety functions of the repository components and the understanding of the development of the repository system emerging from the analysis of the reference evolution form the basis for exhaustive evaluations of such routes.

**Table 11-1 Result of scenario selection. Green cells denote conditions for the base case of the main scenario, red cells denote deviations from those conditions.**

| **Main scenario/Reference evolution** | | | | |
|---|---|---|---|---|
| **Name** | **Initial state EBS** | **Initial state Site** | **Process handling** | **Handling of external conditions** |
| Base case. | Reference ± tolerances. | Site descriptive model (with variants/ uncertainties). | According to **Process reports**. | Reference climate (repetitions of Weichselian glacial cycle) No future human actions (FHA). |
| Global warming variant. | Reference ± tolerances. | Site descriptive model (with variants/ uncertainties). | According to **Process reports**. | Extended warm period No future human actions (FHA). |
| **Additional scenarios based on potential loss of safety functions ("less probable" or "residual" based on outcome of analysis)** | | | | |
| **Name** | **Initial state EBS** | **Initial state Site** | **Process handling** | **Handling of external conditions** |
| Buffer advection. | Scrutinise uncertainties of relevant initial state factors, internal processes and external conditions possibly leading to violation of safety function indicator under consideration. Analysis of reference evolution used as starting point. | | | |
| Buffer freezing. | See above. | | | |
| Buffer transformation. | See above. | | | |
| | Consider each of above three buffer states + intact buffer when analysing the three canister scenarios below. | | | |
| Canister failure due to isostatic load. | Scrutinise uncertainties of relevant initial state factors, internal processes and external conditions possibly leading to violation of safety function indicator under consideration. Analysis of reference evolution used as starting point. | | | |
| Canister failure due to shear load. | See above. | | | |
| Canister failure due to corrosion. | See above. | | | |
| **Hypothetical, residual scenarios to illustrate barrier functions** | | | | |
| **Name** | **Initial state EBS** | **Initial state Site** | **Process handling** | **Handling of external conditions** |
| Several cases, covering together the KBS-3 barriers. | As base case of main scenario, except factors related to the hypothetical loss of barriers. | | | |
| **Scenarios related to future human actions** | | | | |
| **Name** | **Initial state EBS** | **Initial state Site** | **Process handling** | **Handling of external conditions** |
| Boring intrusion. | As base case of main scenario. | As base case of main scenario. | As base case of main scenario, except processes affected by boring. | Reference climate + boring. |
| Additional intrusion cases, e.g. nearby rock facility. | As base case of main scenario. | As base case of main scenario. | As base case of main scenario, except processes affected by intrusion. | Reference climate + intrusion activity. |
| Unsealed repository. | As base case of main scenario, but insufficient sealing. | As base case of main scenario. | As base case of main scenario, modified according to initial state. | Reference climate. |

# 12 Analyses of containment potential for the selected scenarios

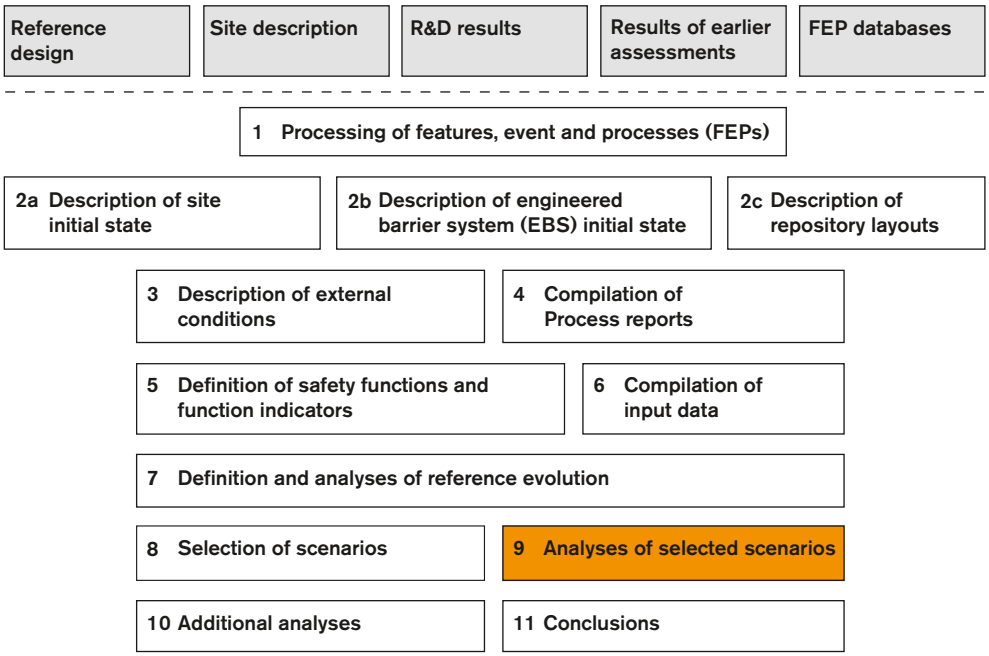


***Figure 12-1.*** *The SR-Site methodology in eleven steps (Section 2.5), with the present step highlighted. This chapter deals with the analysis of containment potential in step 9. The retardation potential is analysed in Chapter 13.*

## 12.1 Introduction

### 12.1.1 General

This chapter deals with analyses of the containment potential for most of the scenarios selected in Chapter 11.

Scenarios derived from safety function indicators are analysed in Section 12.2 through 12.8. The three buffer scenarios are treated in Sections 12.2 to 12.4 and then propagated to the three canister scenarios analysed in Sections 12.6 to 12.8.

The chapter also provides, in Section 12.9, an analysis of possible combinations of the above scenarios.

Analyses of the retardation potential for the scenarios analysed in this chapter are carried out in Chapter 13.

The containment potential of the main scenario is not analysed in detail in this chapter since it is closely related to the containment potential for the reference evolution that was analysed in Chapter 10, see further Section 12.1.2.

Hypothetical, residual scenarios to illustrate barrier functions are also not analysed in this chapter, since the affected barrier properties are postulated and not the outcome of an analysis. Assumptions regarding such barrier states and analyses of consequences are presented in Chapter 13, Section 13.7.

Both containment and retardation potential for FHA scenarios are analysed in Section 14.2, where also an account of the methodology for the FHA scenarios is given.

### 12.1.2 Definition of the main scenario

The main scenario corresponds closely to the reference evolution described in Chapter 10. The definition of the main scenario thus includes the detailed prerequisites given for the general evolution in Section 10.1.1. The aim of that description is to present a reasonable evolution of the repository system, and that is also the aim with the main scenario. Therefore, most of the developments and results described in Chapter 10 apply to the main scenario. As for the reference evolution, there are two variants of the main scenario; the Weichselian base case and the global warming variant.

There are also a number of uncertainties associated with the reference evolution. Those uncertainties requiring further consideration regarding containment are compiled in Table 10-27. All these are revisited in the analyses of the additional scenarios in the subsequent sections, where uncertainties are addressed as appropriate for the scenario in question. Therefore, it is not meaningful to assess these uncertainties here to arrive at a more precise judgement on the evolution of the main scenario. Rather, a brief assessment of the containment potential of the main scenario is given in Section 12.9.2, after the analyses of the additional scenarios, when such an assessment can be based on the outcome of the more detailed evaluation of uncertainties in the additional scenarios.

### 12.1.3 Climate development for the scenario analyses

As mentioned in Section 6.2.4, in addition to the external evolution for the reference scenario, complementary climate cases, with potentially larger impacts on repository safety than the reference glacial cycle, have been analysed as documented in the **Climate report**. These results are utilised as appropriate in the analyses of the containment potential of the additional scenarios. The climate cases are shown in Figure 12-2.

The reference glacial cycle constitutes the external conditions for the reference evolution, analysed in Chapter 10, with the *global warming* climate case as a variant also analysed in Chapter 10.

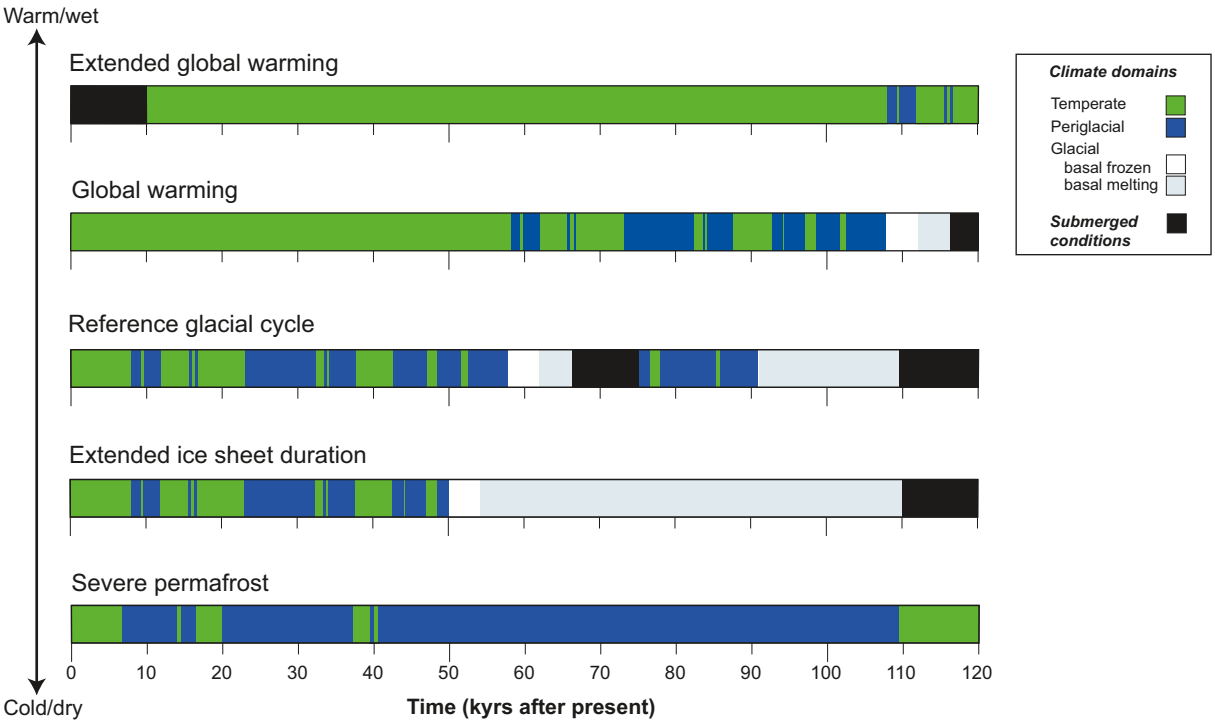


***Figure 12-2.*** *Summary of future climate cases analysed in the SR-Site safety assessment. The maximum ice sheet configuration climate case, with maximum ice thicknesses, is not shown. However, it is contained within the temporal development of the extended ice sheet duration case. For a description of the climate domains, see the* ***Climate report****, Section 1.2.3.*

The longest period of temperate climate conditions for the coming 120,000 years, resulting in the longest period of groundwater formation from precipitation, is found in the *extended global warming* climate case. This case is relevant for the assessment of the extent of buffer erosion potentially leading to advective conditions in the buffer, see Section 12.2.

The most extended period of periglacial climate conditions, with longest periods of permafrost and deepest frozen ground at Forsmark, is found in the *severe permafrost case*. This case is relevant for the analysis of buffer freezing in Section 12.3. The largest uncertainty for the development of permafrost and frozen ground is however connected to the reference glacial cycle, meaning that the widest uncertainty interval for freezing occurs in this climate case.

The longest period of glacial conditions, and associated period of groundwater formation from glacial melt water, is found in the *extended ice sheet duration* case. Also this case is relevant for the assessment of buffer advection in Section 12.2.

The maximum future ice sheet thickness, and resulting largest increase in hydrostatic pressure at repository depth, is found in the *maximum ice sheet configuration* case. This case is not depicted in Figure 12-2. However it is contained within the temporal development of the extended ice sheet duration case. It is relevant for the analysis of canister failure due to isostatic load in Section 12.7.

The six climate cases together cover the expected maximum range within which climate and climate related conditions of importance for long-term repository safety may vary within the time scales analysed in SR-Site, i.e. over multiple glacial cycles. The *actual* development of climate and climate related processes of importance for a KBS-3 repository at the Forsmark site are expected to lie within the range covered by the six climate cases in Figure 12-2.

## 12.2 Buffer advection

### 12.2.1 Introduction

#### *Safety function indicator(s) considered*

A central safety function of the buffer is to prevent advective transport of species between the groundwater and the canister, (safety function indicators Buff1a and b) ensuring that diffusion is the dominant mechanism of transport. In order to maintain this safety function, the buffer must have a sufficiently low hydraulic conductivity. A prerequisite for an appropriate and homogeneous hydraulic conductivity is also a certain minimum buffer swelling pressure, which ensures tightness and self-sealing of the material.

In this scenario, conceivable routes to a violation of the buffer hydraulic conductivity criterion are examined. Basically, there are two routes to a situation where advection could be an important mechanism for transport in the buffer.

- A drop in dry density caused by loss of buffer material which would give a hydraulic conductivity sufficiently high for advection to dominate over diffusion, or too low a swelling pressure to maintain the self-sealing ability.
- Transformation of the montmorillonite in the buffer to another mineral with different hydraulic properties.

The results of these routes could lead to either:

- *High conductivity case:* A case where so much buffer material is lost that water can flow through the buffer,
- *Fracture case:* A case where the buffer has lost its sealing properties and a conductive fracture is formed in it.

For an intact canister, advection concerns the transport of corroding agents to the canister. For a defective canister, transport of radionuclides to the groundwater is affected.

A number of factors influence, directly or indirectly, the buffer hydraulic conductivity. The hydraulic conductivity is directly influenced by the buffer density, and the type of cations in the buffer. These factors also influence the buffer swelling pressure. The swelling pressure is further influenced by the ionic strength of the surrounding groundwater.

There are a number of safety function indicators that can be seen as "sub-indicators" to the "master" indicator buffer hydraulic conductivity. These are all used to evaluate this scenario:

- Buffer swelling pressure > 1 MPa.
- Minimum cation charge concentration in the groundwater $\Sigma q[M^{q+}] > 4$ mM.
- Limited groundwater salinity.

A maximum temperature of 100°C or a pH of < 11 can also be seen as sub-indicators for this scenario. The consequences of these are evaluated in Section 12.4.

A special case of this scenario is the effect of a sinking canister. This is dealt with in Section 12.2.4.

### *Treatment of this issue in the reference evolution*

In the reference evolution, advection as a transport mechanism in the buffer is assumed to the extent suggested by the results of calculations of the base case for the reference evolution in Section 10.3.11, where 23 out of approximately 6,000 deposition positions are calculated to experience advective conditions within one million years for the base case realisation of the semi-correlated hydrogeological DFN model.

### *Bounding cases*

For the reference evolution, the mean number of canisters calculated probabilistically to fail during the one million year assessment period due to buffer colloid release/erosion leading to buffer advection and hence enhanced corrosion is 0.12 for the semi-correlated hydrogeological DFN model, see Section 10.4.9. There, it is also demonstrated that the consequences in terms of canister failures are similar (on average 0.17) if **advection is assumed initially in all deposition positions**. (In both these cases rejection according to EFPC is assumed.)

This result is important for the treatment of the buffer advection scenario. Irrespective of the outcome of the complex interplay of a number of uncertain factors influencing the occurrence of buffer advection, the consequences in terms of canister failures are always bounded by the case where advection is assumed for all canisters throughout the assessment period, and these failure rates are similar to those for the reference evolution where only a small fraction of the deposition holes are affected by advective conditions in the buffer. The reason for this simplifying circumstance is that the time taken to erode the buffer to the extent that advection occurs is shorter than that required to cause corrosion failure once the advective conditions are established. For both processes, the groundwater flow rate at the deposition position in question is an important determining factor, and dependence on other factors influencing erosion and corrosion, respectively, is such that the time required to reach advective conditions is, in general, shorter than that required to cause corrosion failure once advective conditions are established. It is also noted again that it is only in the small number of holes that have high advective flow rates in the intersecting fractures that erosion and subsequent enhanced corrosion could lead to canister failures in one million years.

As also discussed in the reference evolution Section 10.3.11, a situation where erosion does not occur is also conceivable given the incomplete understanding of this process as such and uncertainties regarding future groundwater compositions.

Three important cases can therefore be envisaged before this scenario is analysed:

1. a case where advective conditions occur to the extent given by the reference evolution treated in Chapter 10,
2. a case where advective conditions occur in every deposition hole throughout the assessment period,
3. a case where diffusive conditions are preserved in every deposition hole throughout the assessment period.

These three cases, two of which are bounding, are used as a background for the discussion below.

As mentioned in the reference evolution, the buffer colloid release/erosion process is poorly understood and leads already in the reference evolution to loss of buffer mass to the extent that advection cannot be ruled out for a few deposition holes during the first glacial cycle. In a one million year perspective, case 2 is therefore not vastly different from the reference evolution case 1, in particular since advective conditions in the buffer are tolerated by the canister throughout the assessment period for the majority of deposition holes and for around 100,000 years for all holes, according to the calculations in Chapter 10. The three cases can, therefore, be said to reasonably reflect the current uncertain knowledge of the extent of buffer colloid release/erosion. They are however encompassing in the sense that it is difficult to conceive of a worse situation than case 2 or a more favourable situation than case 3.

#### *Qualitative description of routes to buffer advection (including initial state aspects and external conditions)*

As mentioned, the buffer density plays a key role for the buffer's ability to prevent advection. The density may decrease due to erosion induced by piping as the buffer saturates, through buffer expansion into the deposition tunnel as a saturated buffer swells or through erosion caused by dilute groundwater for glacial conditions. Buffer expansion into the deposition tunnel will be counteracted by the tunnel backfill material, meaning that factors affecting the density and compressibility of the backfill material could also indirectly influence buffer hydraulic conductivity.

Of these factors, colloid release/erosion caused by dilute groundwater has by far the highest impact on density in the reference evolution and it is the only factor that causes any considerable alteration of buffer density over the one million year assessment period in that evolution.

The overall conclusion from the analysis of the reference evolution is, therefore, that the buffer is expected to function as intended until intruded by dilute groundwater, and, if dilute conditions prevail for tens of thousands of years, there is currently little confidence that advection is prevented in the deposition positions intersected by the fractures with the highest flow rates. At the end of the one million year assessment period, 23 deposition positions are calculated to experience advective conditions for the base case realisation of the semi-correlated hydrogeological DFN model.

The following factors of importance for buffer advection are identified, based on the discussion above, on Table 10-27 describing uncertainties identified in the reference evolution and on the FEP chart, Figure 8-4.

**Initial state factors involved**

- Buffer density (amount of dry mass deposited).
- Backfill density (amount of dry mass deposited above the deposition hole).
- Type of buffer material used (This is not an uncertain factor, but the evolution will, in some respects, be different for e.g. the two materials considered in SR-Site).

**Processes involved**

A number of different processes could lead to a drop in buffer density:

- piping/erosion during the early stage,
- swelling/expansion into the backfill,
- buffer erosion/colloid release.

For a given density, the hydraulic conductivity and swelling pressure will be determined by the following processes:

- ion exchange,
- osmosis.

The hydraulic conductivity and swelling pressure of the buffer will also be determined by the process of montmorillonite transformation.

**External conditions involved**

- Geosphere conditions yielding very high or very low ionic strengths of groundwater.
- Geosphere conditions leading to increased flow.

There are thus a large number of factors that need to be considered in the buffer advection scenario.

### 12.2.2 Quantitative assessment of routes to buffer advection

In the reference evolution, the reference buffer and backfill densities are addressed, as are reasonably high and low ionic strengths and durations of such conditions for a glacial cycle. The possibility for the transformation of the montmorillonite in the buffer is also evaluated.

#### *Initially deposited dry buffer mass*

The effect of a variation in the composition of the buffer material is not discussed in the reference evolution. It is expected that the defined delivery and quality control systems will ensure that all material will meet the specified requirements. These material requirements have not yet been fully defined. However, considering the very small difference in the important properties between the two reference materials in SR-Site at the target density (see Section 5.5), it can be concluded that variation in the material composition will have a rather limited effect on buffer performance. As seen in the assessment of the geochemical evolution of the buffer in Section 10.3.8 and in /Sena et al. 2010/ the composition of buffer material, especially exchangeable cations, tends to equilibrate to similar values for both materials as a result of the interaction with the Forsmark groundwater. The allowed variability of composition for the selected buffer material will be defined at time of purchase of the buffer. Under all circumstances this variability is expected to be small.

The overall conclusion regarding initially deposited buffer dry mass is that the initial buffer mass and composition is expected to be well within the design specifications.

#### *Initially deposited dry backfill mass*

The expected uncertainties in the amount of initially deposited backfill are discussed in Section 5.6. If less backfill is deposited this could potentially lead to buffer swelling into the deposition tunnel and a loss of buffer mass. However, according to the production and control procedures described in Section 5.6, there is no reason to believe that failures in the backfilling process will lead to significant contributions to the generation of advective conditions in the buffer.

#### *Swelling*

If the initial density of the tunnel backfill is lower than the design target or if the buffer saturates ahead of the backfill and expands into a pile of dry backfill blocks, the buffer can expand into the backfill which in turn gives a lower average buffer density. These cases have been evaluated in the reference evolution (Section 10.3.9). The case with a dry backfill and pellets in the slot at the roof has been identified as the one that has the strongest impact on the final buffer density. Table 10-3 shows the final density of the buffer around the canister for different assumptions about the pellet filling. According to calculations in the reference evolution, there is sufficient margin in backfill density to ensure acceptable performance for all reasonable combinations. Therefore, this issue is not further considered here.

#### *Erosion caused by piping*

Erosion caused by piping is discussed in the reference evolution in Section 10.2.4. If the pressure of the water flowing into a deposition hole is higher than the swelling pressure, the buffer will not be able to seal and a channel (pipe) may form. The channel will most likely end in the deposition tunnel. As long as the tunnel is not sealed and the hydrostatic pressure has not been restored, there will be a flow in the pipe. The flow may erode the buffer and some material may be lost. The potential loss can be calculated from the accumulated flow of water.

For the maximum allowed inflow to the deposition hole (150 $m^3$) an erosion of up to 41 kg was calculated (Section 10.2.4). At the dry density of the buffer $\rho_d$ =1,570 kg/$m^3$, this would correspond to a volume of 0.026 $m^3$.

Overall, the uncertainties in the parameters related to piping are in these circumstances rather limited and it is unlikely that the erosion from piping should be substantially higher than in the reference evolution. This issue is, therefore, not further considered here.

#### *Erosion of backfill*

Erosion of backfill material during the operational phase could lead to a local loss of backfill density at the top of a deposition hole. This could, in turn, lead to expansion of buffer material into the backfill and a loss of buffer density. However, as seen in Section 10.2.4, the maximum loss (redistribution) of backfill during this phase is estimated at 1,640 kg which is insignificant compared to the backfill losses that would lead to advective condition in the buffer according to Section 10.3.11 (220 tonnes). This issue is, therefore, not further considered here.

#### *Buffer erosion/Colloid release*

Buffer colloid formation and release during a glacial cycle is discussed in the reference evolution, Section 10.3.11. Several uncertain aspects of the colloid release process are mentioned in connection with the analysis of the reference evolution. These include the conceptual uncertainty in the erosion model /Neretnieks et al. 2009/, behaviour of the selected buffer material, the duration of periods of low ionic strength groundwater and the groundwater flow rates during these periods. These uncertainties are the main reason for selecting the bounding cases for the buffer erosion scenario described in Section 12.2.1.

A quantitative treatment of the impact on the extent of erosion of uncertainty in factors affecting the erosion process is given in a subsection below.

#### *Ion-exchange and osmosis*

Figure 5-14 shows the swelling pressure for the two reference buffer materials as a function of dry density for different water salinities. Comparing the two materials gives a good indication on the effect of ion-exchange as well. MX-80 is Na-bentonite that was exposed to NaCl solutions, whereas Ibeco RWC is Ca-bentonite that was exposed to $CaCl_2$ solutions. Neither the exchangeable cation nor the salinity has any major effect on the buffer properties at the reference density. However, the effect of both processes becomes much stronger at lower densities. The effect of high salinity becomes important for the swelling pressure at a dry density of ~1,400 kg/$m^3$. For the salinities expected in Forsmark (Table 10-8), the effect can be neglected for dry densities > 1,000 kg/$m^3$. The ion-exchange characteristics are not important until the density drops to about 1,000 kg/$m^3$, but below that value the effect is very strong.

The groundwater composition, Ca/Na-ratio and total salinity, will determine how much buffer mass can be lost before advection starts to be important.

The effect of groundwater salinity will only be important if large amounts of buffer are lost, i.e. in combination with colloid release. The processes are mutually exclusive since colloid formation only occurs at low calcium concentrations but they could occur in sequence if the ground water composition is changing.

In conclusion, the uncertainties regarding the effects of increased salinities are unimportant compared to the uncertainties in the colloid formation process.

#### *Montmorillonite transformation*

Transformation of the montmorillonite in the buffer to other minerals as an effect of elevated temperature is evaluated in the reference evolution and in the buffer transformation scenario (Section 12.4).

### *Geosphere conditions*

The development of the buffer is dependent on conditions imposed by the geosphere on the buffer. Key parameters are the following.

1. Flows and gradients during the construction phase. These will determine the magnitude of mass loss from piping/erosion.
2. Ionic strength of the groundwater for all time scales. A low charge concentration of cations in the groundwater will make it possible for the buffer to form a colloidal phase that can be transported away with the groundwater. A high ionic strength will affect the buffer hydromechanical properties, which may result in a higher hydraulic conductivity and a lower swelling pressure, in the case where some mass loss has occurred. The Ca/Na ratio will affect the ion-exchange capacity which can affect the buffer properties at very low densities.
3. The groundwater flow will determine how much buffer mass can be transported away in the colloid formation case.

Flows and gradients during the construction phase are treated above under 'Erosion caused by piping'. The latter two factors are treated in the sensitivity analysis immediately below.

### *Quantitative sensitivity analysis of buffer erosion/colloid release*

The following is a quantitative treatment of the impact on the extent of erosion of uncertainty in factors affecting the erosion process.

The extent of buffer erosion is calculated with the model described in Section 10.3.11. The calculated extent of erosion will depend on the groundwater composition required for erosion to occur, the fraction of time during the one million year assessment period during which the groundwater has the composition favouring erosion and the quantitative extent of the corrosion process for these conditions. An additional factor of importance is the amount of buffer that is required to be eroded away before advective conditions occur in a deposition hole. The following have been assumed or concluded regarding these factors in SR-Site.

- The *criterion* determining whether the process occurs states that the groundwater cation charge concentration, $\Sigma q[M^{q+}]$, should exceed 4 mM to avoid erosion see Section 10.3.11.
- The *fraction of time* of the one million year assessment period during which erosion occurs was assumed to be 25 percent of the time in the two percent of the deposition holes exposed to the highest flow rates, based on analyses summarised in Sections 10.3.7 and 10.4.7.
- The *amount of buffer* that needs to be eroded in order for advective conditions to arise in the deposition hole is assumed to be 1,200 kg based on the discussion in Section 10.3.9.
- The *quantitative model* for quantifying the extent of erosion gives the erosion rate, $R_{\text{Erosion}}$, as $A \cdot \delta \cdot v^{0.41}$

  where $v$ is the groundwater velocity in a fracture intersecting the buffer, $\delta$ is the aperture of the intersecting fracture, and $A$ is a constant, see Section 10.3.11 and further /Neretnieks et al. 2009/.
- The *groundwater velocity* and the *fracture aperture* are obtained from the groundwater flow calculations. The natural variability of these entities is covered by determining the flow conditions in each of the ensemble of 6,000 deposition position in the repository. The hydrogeological DFN model with semi-correlated relation between fracture length and transmissivity (Section 10.3.6) is used in the calculation.
- The calculation result also depends on the *criteria for deposition hole rejection* applied in the layout and simulated in the hydrogeological modelling. This is not an uncertainty in the same sense as the above factors, but a design choice. In SR-Site it is assumed that deposition holes are rejected according to the EFP criterion and to the transmissivity related criterion described in Section 5.2.2.

With the above assumptions, it is calculated that on average 0.6 deposition holes out of the repository's 6,000 experience advective conditions after 100,000 years. At the end of the one million year assessment period, the corresponding number is almost 20, see 'Semi-correlated base case' in Figure 12-3. These results were obtained through averaging over ten realisations of the semi-correlated hydro-

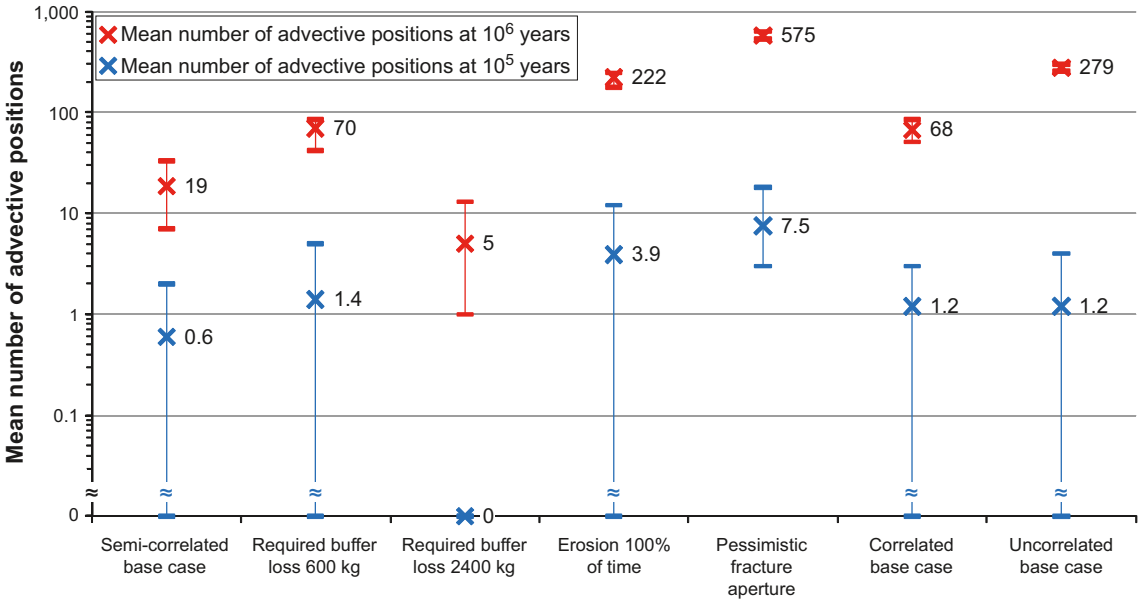


***Figure 12-3.*** *Calculated extent of erosion at 100,000 years and at one million years for a number of cases. The crosses denote mean values and the bars denote the variability over the several realisations of the hydrogeological DFN models.*

geological DFN model. (The earlier cited value of 23 was obtained with the base case realisation of this DFN model.) Each realisation covers the 6,000 deposition positions and thus covers spatial variability within that realisation. The variability between realisations is shown by the ranges in Figure 12-3.

The following sensitivity calculations were carried out, essentially by varying one of the above mentioned factors at a time. Results are shown in Figure 12-3.

- The *amount of buffer* assumed to be required to be eroded away in order for advective conditions to arise in the deposition hole was changed from 1,200 kg by a factor of two up and down, respectively i.e. to i) 600 kg and ii) 2,400 kg. This yielded changes in the calculated number of deposition holes by factors larger than two.
- Uncertainties relating to the nature of the *criterion* determining whether erosion occurs and also to the *fraction of time* during which the criterion is fulfilled is addressed by assuming erosion throughout the one million year assessment period. As seen in Figure 12-3, this causes the number of deposition positions experiencing advective condition to increase by a factor of more than ten in the one million year perspective, yielding approximately 220 deposition holes with advective conditions after one million years. The corresponding number for 100,000 years is approximately 4 out of the 6,000 deposition holes. There are uncertainties in both the factors covered by this variation and neither less nor more extensive erosion than in the base case can be excluded. The sensitivity case calculated here puts an upper bound on the possible variation.
- In the hydrogeological model, fracture apertures ($\delta$) are obtained from the fracture transmissivity ($T$) according to $\delta = 0.5\ T^{0.5}$, see further Section 10.3.6. An alternative, for buffer erosion more pessimistic, relation was also evaluated: $\delta = 0.28 \cdot T^{0.3}$ /Joyce et al. 2010, Selroos and Follin 2010/. This yields an almost 30-fold increase in the calculated number of deposition positions experiencing advective conditions at one million years. However, in the **Data report** the second of the two relationships is shown to be overly pessimistic since the relationship yields fracture apertures larger than those measured at the site using electrical resistivity measurements. Hence, for the quantification of buffer erosion the first relationship is justified for use in SR-Site.
- An important aspect of conceptual uncertainties relating to the *groundwater velocity* in fractures intersecting the deposition holes is illustrated by calculations with the hydrogeological DFN models based on the uncorrelated and fully correlated relations between fracture size and transmissivity (see Section 10.3.6 for details). As seen in Figure 12-3, these both yield a larger extent

of buffer erosion. Both the uncorrelated and the fully correlated models represent extremes of the correlation structure. In particular, the uncorrelated model lacks support in observations. The semi-correlated model used as the base case is seen as the most realistic representation, but it is not possible to quantify the degree of correlation in a rigorous manner. Therefore, the span represented by the three models is considered as a reasonable illustration of the conceptual uncertainties associated with the hydrogeological DFN models.

Regarding varying groundwater flow conditions over a glacial cycle, it is demonstrated in Section 10.4.6 that the time averaged value over the reference glacial cycle of $q^{0.41}$, relevant for buffer erosion is around 80 percent of that for temperate conditions, see ML2 data in Figure 10-147. Using the temperate values is thus pessimistic and gives some margin for alternative evolutions to the reference glacial cycle. The issue of temporal variability is, therefore, not treated further here.

In conclusion, with base case assumptions (Semi-correlated base case), around one of six thousand deposition positions is calculated to be advective at $10^5$ years and less than one percent at $10^6$ years.

The sensitivity cases analysed here show that a considerable variation around the base case calculation result in the extent of erosion is possible. However, less than ten percent of the deposition positions reach advective conditions after one million years even for the most unfavourable cases. Also, the sensitivity cases give far less variation of the extent than the two bounding cases identified at the beginning of this section, i.e. no erosion and advective conditions initially in all deposition holes.

The conceptual model for quantifying the extent of erosion is associated with uncertainties that are difficult to quantify:

- there are potentially mitigating effects like clogging of the water conductive fracture with detritus material from the eroded bentonite /Neretnieks et al. 2009/,
- there are also potentially aggravating effects, e.g. gravitational effects but these are argued to be small or negligible /Neretnieks et al. 2009/,
- there are additional factors that could lead to a decrease in the clay dispersion rate, see further the concluding discussion of uncertainties in Section 10.3.11.

The influences of the sensitivity cases on the extent of corrosion are evaluated in the corrosion scenario, Section 12.6.2. Full documentation of all calculations of buffer erosion/colloid release and canister corrosion is given in /SKB 2010d/.

#### *Global warming variant and other climate cases*

The occurrence of buffer advection is strongly linked to the presence of low ionic strength groundwaters at repository depth. As demonstrated in the reference evolution Section 10.3.6, an extended initial period of temperate conditions could give rise to longer periods of exposure to dilute groundwaters indicating that the global warming variant could lead to more colloid release than the base case evolution. However, in the global warming variant, it is only the initial temperate period that is prolonged. Also, the relatively limited effect of a global warming variant is encompassed in the assumption that two percent of the deposition holes will experience dilute groundwater during 25 percent of a glacial cycle, since the fraction of deposition holes would be only 0.02 in 60,000 years of temperate conditions, see Section 10.3.6. Also, this limited difference relative to the base case applies only for the first glacial cycle, whereas the effects of global warming are assumed to not affect subsequent cycles in the global warming variant. The issue is therefore not further treated in SR-Site for the global warming variant.

Regarding other climate cases, the *extended global warming* case and the *extended ice sheet duration* case (see Section 12.1.3) could imply more extensive intrusion of dilute water than in the reference evolution. Such developments are covered by the bounding case where advection is assumed initially in all deposition holes.

### 12.2.3 Conclusions

As evidenced by the above account, there are a number of uncertainties regarding the evolution of the buffer density. All conceivable initial states and subsequent developments are however, from the point of view of advection, which is the issue in this scenario, covered by the three cases outlined at the beginning of the analysis of the scenario, Section 12.2.1. This analysis applies to the high conductivity case, see Section 12.2.1.

For the fracture case, see Section 12.2.1, no route leading to this situation has been identified and it is thus considered as a residual scenario. Canister corrosion for a fractured buffer can be illustrated with expressions given in /Neretnieks et al. 2010/. The life time of the canister is considerably longer for a fractured buffer than for an eroded buffer, for otherwise identical circumstances, see examples in /Neretnieks 2006b/. No additional such calculation cases have been performed in SR-Site.

Regarding event sequences, the evolution can certainly be affected by the order in which swelling, mass losses, intrusion of various types of groundwater, etc. occur. Again, however, these situations are bounded by the three cases considered.

Should transport in the buffer not be controlled by diffusion, corrosion of the canister could ultimately be controlled by advection of corroding agents in the groundwater. This is illustrated in the reference evolution. The extent of corrosion is further treated in the corrosion scenario, Section 12.6, to which the three cases of buffer advection are propagated, i.e. advection as calculated with base case assumptions and the two bounding cases of initial advection in all deposition holes and no advection throughout the assessment period. As concluded above, all three hydrogeological model variants are also propagated to further analyses. This yields the nine cases in Figure 12-4 to consider.

The occurrence of buffer advection cannot be ruled out and the buffer advection scenario is thus considered as a less probable scenario, to be further addressed in combination with the canister scenarios. The probability that the scenario will occur cannot be quantified in an exact way. It is represented by the nine cases in Figure 12-4, in three of which no advective positions occur.

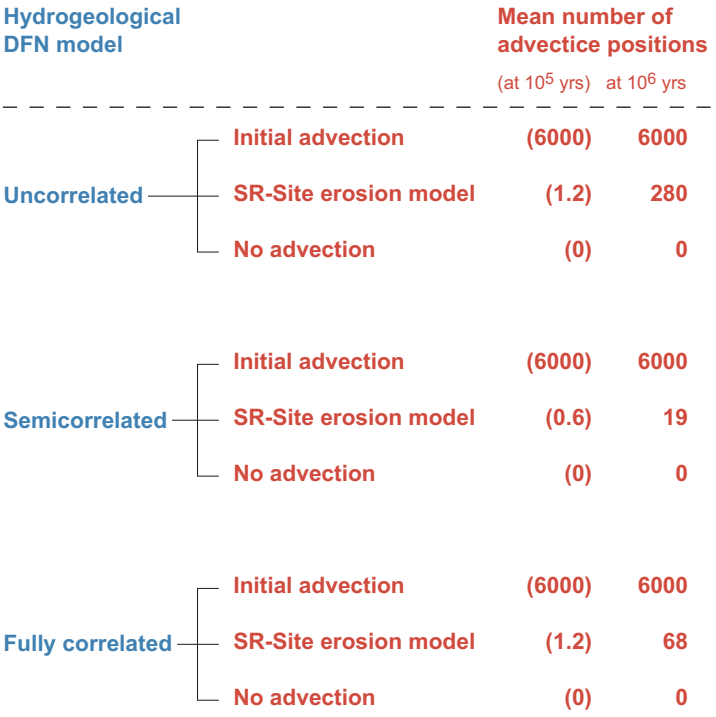


***Figure 12-4.*** *Erosion cases propagated to further analysis of canister corrosion.*

### 12.2.4 Special case of advective conditions: Canister sinking

#### *Function indicator(s) considered*

A central safety function of the buffer is to prevent advective transport of species between the groundwater and the canister. To ensure this, a certain buffer thickness is required. If the canister sinks or tilts in the deposition hole, this minimum thickness cannot be guaranteed. A swelling pressure of 200 kPa is needed to keep the canister in position in the deposition hole (Buff5). This function indicator assumes that the buffer consists of bentonite.

#### *Treatment of this issue in the reference evolution*

Since the loss of buffer mass needed for the advective conditions as described in Sections 10.3.9 and 10.3.11 is less than the loss needed to get to a situation where the canister would sink, advective conditions due to canister sinking *per se* can never occur in the reference evolution. Advective condition will already prevail when the canister sinks.

#### *Qualitative description of routes to canister sinking*

The swelling pressure could be reduced by:

1. Loss of buffer material,
2. A transformation of the montmorillonite to a non-expandable mineral.

If sufficient buffer mass was lost to bring the average swelling pressure around the canister down to 200 kPa, advection would likely already be the dominant transport mechanism, hence item 1 above is covered in the reference evolution and in the general buffer advection scenario above. Transformation of the montmorillonite in the buffer is discussed in the transformation scenario, Section 12.4.

#### *Quantitative assessment of routes to canister sinking*

The routes to loss of swelling pressure are discussed in the scenarios mentioned above.

#### *Categorisation as "less probable" or "residual" scenario*

The consequences of the loss of large amounts of buffer material are discussed in the reference evolution and further in the general buffer advection scenario above. Since considerably higher mass losses are required to cause canister sinking than are required for advective conditions, and since advective conditions is the safety related concern also in the case of canister sinking, the occurrence of canister sinking would not lead to consequences beyond those already quantified in Section 12.2.3.

#### *Conclusion*

The only way the canister could sink to the bottom of the deposition hole is in the case of a large loss of buffer material. If this happens the diffusive barrier of the buffer is lost long before the canister starts to sink. Therefore, loss of the diffusive barrier caused by canister sinking does not have to be treated as a scenario on its own.

## 12.3 Buffer freezing

### 12.3.1 Introduction

#### *Indicator criterion violated*

This scenario concerns the criterion of minimum buffer temperature, namely that the temperature in the buffer should not fall below −4°C to avoid formation of ice in the buffer.

If the buffer minimum temperature criterion is violated, this could potentially affect both containment and retardation. It has previously been shown that the bentonite will retain its properties after a freezing cycle, but containment could be jeopardised through mechanical impact on the canister by a freezing buffer and the retardation potential may be impaired in the case of severe ice lens formation.

### *Treatment of buffer freezing in the reference evolution*

The possibility of buffer freezing was excluded from the reference evolution which is based on a plausible glacial cycle in which permafrost (that is the 0°C isotherm) develops to a maximum depth of 259 m at Forsmark (Section 10.4.3). When including all known surface and subsurface uncertainties (e.g. uncertainties in air temperature, climate humidity, surface wetness, vegetation, snow cover, bedrock thermal conductivity and diffusivity, and geothermal heat flux) and setting them all in the condition most favourable for permafrost growth, the uncertainty interval for the permafrost reaches a maximum depth of 463 m in the reference evolution. Correspondingly, the uncertainty interval for the perennially frozen ground reaches a maximum depth of 422 m. The freezing of buffer material requires temperatures of −4°C or lower, see Section 8.3.2. In the reference evolution, the −4°C isotherm reaches a maximum depth of 148 m. Including the most pessimistic combination of all uncertainties relevant for the reference glacial cycle, the uncertainty interval for the −4°C isotherm reaches a maximum depth of 316 m (Section 10.4.3). This shows that even in this most pessimistic case, buffer freezing temperatures do not reach repository depth in the reference evolution.

### *Qualitative description of routes to buffer freezing*

The route to this scenario is development of permafrost under periglacial climate conditions.

The following factors of importance for the occurrence of buffer freezing are identified, based on the discussion above, on Table 10-27 describing uncertainties identified in the reference evolution and on the FEP chart Figure 8-4.

**Initial state factors**

- Thermal conductivity of bedrock.
- Heat capacity of bedrock.
- Geothermal heat flow.
- Hydraulic conductivity of bedrock.
- Groundwater salinity.
- Porosity of bedrock.
- Heat output of the spent fuel, including its diminishing over time.

**Processes**

- Heat conduction in bedrock.
- Heat conduction in buffer.
- Freezing of buffer.

**External conditions**

- Periglacial climate conditions leading to lowered temperature at ground surface.
- Soil coverage at ground surface.
- Vegetation coverage at ground surface.
- Snow coverage at ground surface.
- Glacial conditions leading to changes in temperature at ground surface.
- Submerged conditions leading to changes in temperature at ground surface.

For more details on the processes involved in the development of permafrost and perennially frozen ground, see the **Climate report**, Section 3.4.4 and /Hartikainen et al. 2010/.

### 12.3.2 Quantitative assessment of routes to buffer freezing

Three types of sensitivity studies were made to investigate if and under what conditions permafrost, perennially frozen ground and sub-zero temperature ground may reach repository depth:

- Lowering of constant ground surface temperatures.
- Lowering of the air temperature curve reconstructed for the last glacial cycle.
- Assumptions of extremely dry conditions during periods of cold climate; e.g. that no ice sheet, sea, vegetation or winter snow exist at the site during a full glacial cycle.

#### *Sensitivity study on lowering of constant ground surface temperatures*

Sensitivity tests on the evolution of permafrost for different constant temperatures were first made. Site-specific data on physical-, thermal-, and hydrological bedrock properties were used, see the **Climate report**. These calculations were made for two cases, with and without the heat contribution from a repository using the 1D permafrost model, see the **Climate report**, Section 3.4.4. The results show that, with heat from the spent fuel included (i.e. conditions corresponding to the first future glacial cycle), the ground surface temperature must be *lower* than −8°C for permafrost (0°C isotherm) to reach repository depth (450 m) (Figure 12-5). If no heat from spent fuel is taken into account (subsequent glacial cycles), the 0°C isotherm reaches repository depth in ~120,000 years if the ground temperature is −8°C. (Figure 12-5). At present, the annual mean air temperature at Forsmark is c. +5°C, see the **Climate report**, Section 2.4.2. The air temperature is often a few degrees lower than the ground surface temperature /Hartikainen et al. 2010/. The results thus indicate that an air temperature lowering of more than 13°C is required to make permafrost develop to repository depth when considering constant temperatures.

#### *Sensitivity study on lowering of the air- and ground surface temperature curves reconstructed for the last glacial cycle*

Permafrost simulations were made to investigate how much air- and ground surface temperatures need to be lowered in a more realistic *variable* climate for permafrost, perennially frozen ground, and sub-zero temperatures to develop to repository depth. Specifically, it was investigated how much the local temperature curve used for the assessment of permafrost in the reference evolution, Section 10.4.3, was required to be lowered to get the 0, –2 and –4°C isotherms to reach the 450 m repository depth. The temperature of 0°C corresponds to the freezing point of fresh water at normal

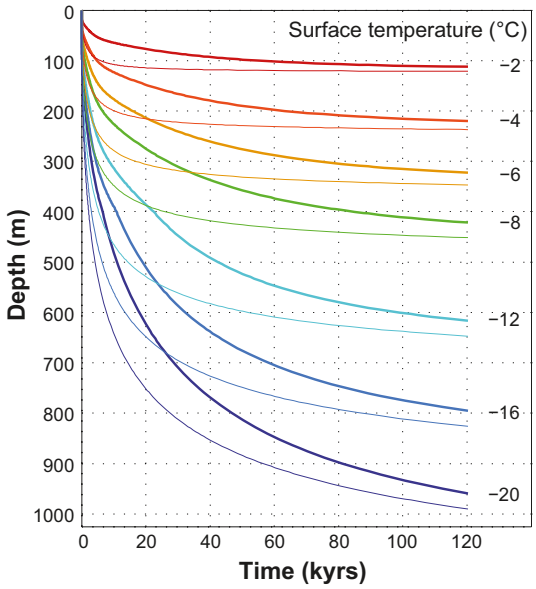


***Figure 12-5.*** *Calculated evolution of permafrost depth (defined by the 0°C isotherm) at the repository location in Forsmark for different constant ground surface temperatures. Bold lines: with repository heat contribution. Thin lines: without repository heat contribution.*

pressure, as well as the definition of permafrost. The temperatures of –2 and –4°C are the freezing temperature for the backfill material in the deposition tunnels and for freezing of the buffer clay, respectively, see Sections 8.3.2 and 8.4.4. Based on results from SR-Can /SKB 2006c/, temperature lowerings of 4, 6, 8, 10, 12, 14 and 16°C were studied. These sensitivity experiments were made with the 2D permafrost model, see the **Climate report**, Section 3.4.4 and /Hartikainen et al. 2010/.

In the 2D permafrost simulations performed for SR-Site, the significant uncertainties associated with descriptions of the surface conditions motivated an analysis of two variants, one with humid surface conditions and one with dry conditions, see the **Climate report**, Section 3.4.4 and /Hartikainen et al. 2010/. As a pessimistic case, the dry variant of the reconstruction of last glacial cycle conditions was used for this sensitivity experiment since it results in deeper permafrost than the humid variant. Mean thermal properties of the subsurface were used. Note that these simulations only cover the initial 50,000 years of the glacial cycle, which however includes the period with deepest permafrost during the glacial cycle, see the **Climate report**, Section 3.4.4.

The resulting temporal evolution of maximum 0, –2 and –4°C isotherm depths over the repository are shown in Figures 12-6 to 12-8. Figure 12-6 also includes the depth of the perennially frozen ground, which is somewhat shallower than the permafrost depth due to the prevailing pressure- and salinity conditions at depth. The results show that the temperature curve reconstructed for the last glacial cycle needs to be lowered by 8°C to make permafrost reach the repository depth (Figure 12-6). Furthermore, the results show that a lowering of the reconstructed temperature curve of more than 10°C and around 14°C are needed to get the –2°C and –4°C isotherms to reach the repository depth (Figures 12-7 and 12-8). These lowerings are large, especially for the –2°C and –4°C isotherms, for instance considerably larger than the estimated maximum uncertainty in the air temperature curve (±6°C) used as input to the simulations, see Section 10.4.3 and the **Climate report**, Appendix 1 and Section 3.4.4.

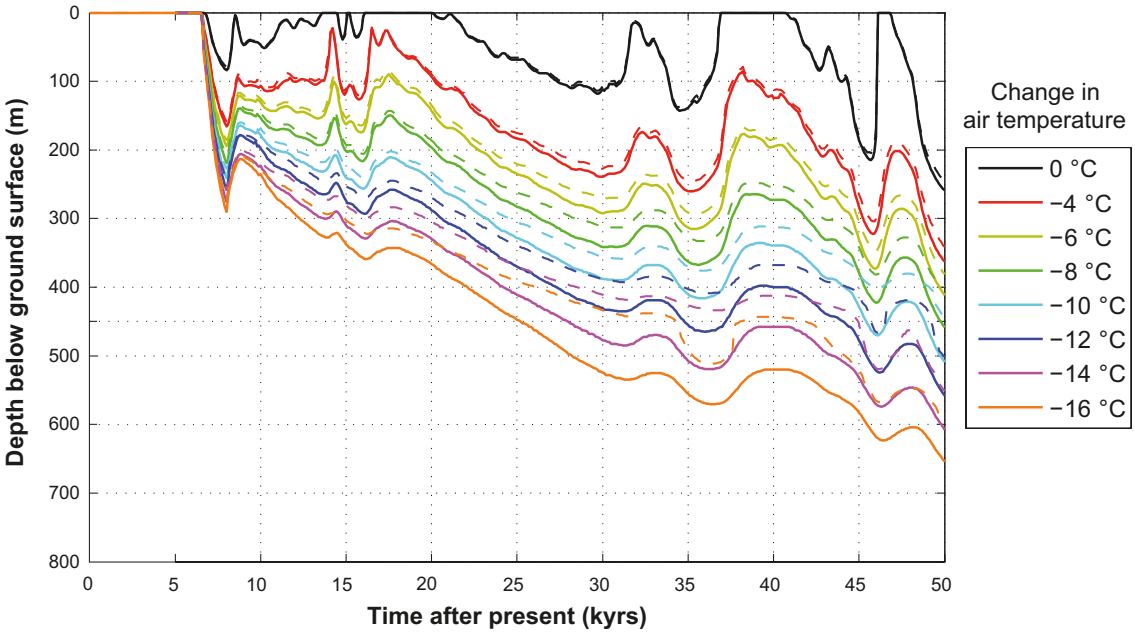


***Figure 12-6.*** *Evolution of 0°C isotherm (permafrost) depth (solid lines) and depth of perennially frozen ground (dashed lines) at the repository location for the reference glacial cycle (dry climate variant, see the* ***Climate report****, Section 3.4.4). The figure also shows corresponding results for simulations where the temperature curve reconstructed for the last glacial cycle has been lowered by –4, –6, –8, –10, –12, –14 and –16°C. The results are extracted from the 2D permafrost modelling conducted for the Forsmark site, see the* ***Climate report****, Sections 3.4.4 and 5.5 and /Hartikainen et al. 2010/.*

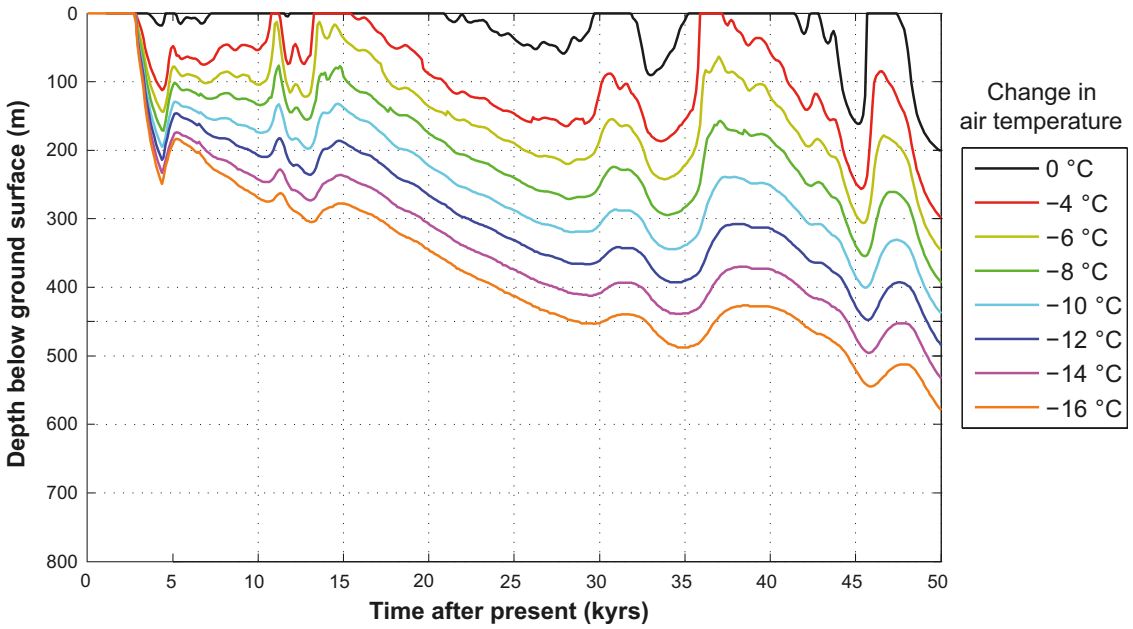


***Figure 12-7.*** *Evolution of maximum –2°C isotherm depth at the repository location for the reference glacial cycle (dry climate variant). The figure also shows corresponding results for simulations where the temperature curve reconstructed for the last glacial cycle has been lowered by –4, –6, –8, –10, –12, –14 and –16°C. The results are extracted from the 2D permafrost modelling conducted over the Forsmark site, see the* ***Climate report****, Sections 3.4.4 and 5.5 and /Hartikainen et al. 2010/.*

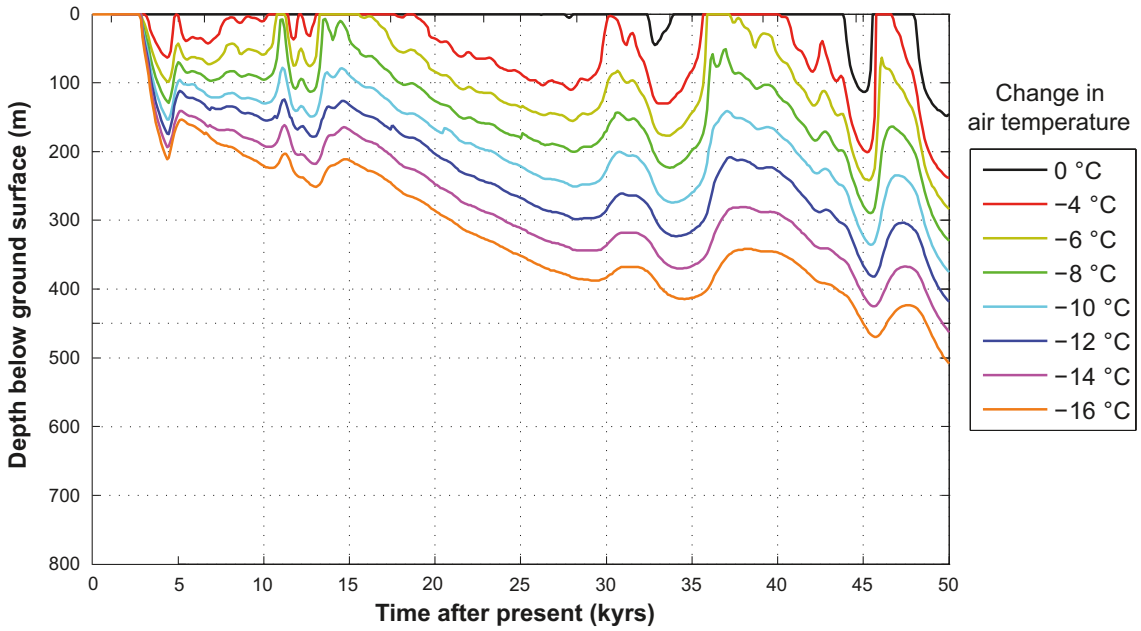


***Figure 12-8.*** *Evolution of maximum –4°C isotherm depth at the repository location for the reference glacial cycle (dry climate variant). The figure also shows corresponding results for simulations where the temperature curve reconstructed for the last glacial cycle has been lowered by –4, –6, –8, –10, –12, –14 and –16°C. The results are extracted from the 2D permafrost modelling conducted over the Forsmark site, see the* ***Climate report****, Sections 3.4.4 and 5.5 and /Hartikainen et al. 2010/.*

### *Sensitivity study on assumptions of no ice sheet, sea, vegetation or winter snow during a full glacial cycle (Severe permafrost case)*

The main uncertainty in all permafrost simulations conducted for SR-Site is the uncertainty in the input air temperature curve, see the **Climate report**, Section 3.4.4. This uncertainty was, together with all other known climate-, surface- and subsurface uncertainties relevant for the reference glacial cycle, treated in Section 10.4.3. In this present sensitivity study, the remaining uncertainties, on e.g. ice sheet and sea coverage are treated based on the results of the severe permafrost case, see the **Climate report**, Section 5.5.

The main assumption in the severe permafrost case is that a very dry periglacial climate dominates, a climate not supporting ice sheet growth over the Forsmark site at any time during the full glacial cycle. To favour permafrost growth further, the effects of protective snow cover and vegetation were excluded, in line with the assumption of a very dry climate. In addition, the repository location was assumed to always remain above sea level, in line with the assumption of no ice sheet. Heat generated by the repository is however included in the simulation, since it is relevant for the first future glacial cycle. The 2D permafrost model was used for the simulations. For further information on the permafrost models and the setup of these simulations, see Sections 10.4.1 and 10.4.3, **Climate report**, Section 4.5.5 and /Hartikainen et al. 2010/.

In the severe permafrost case, all known uncertainties compatible with the main assumption of having no ice sheet over Forsmark are included. It should to be noted that the main assumption for the severe permafrost case, of having no ice sheet over the site, is incompatible with the temperature curve reconstructed for the last glacial cycle, and its uncertainty range towards lower temperatures handled in the reference evolution, Sections 10.4.1 and 10.4.3, since these temperatures result in an ice sheet over Forsmark, see the **Climate report**, Section 3.1.4. Nevertheless, in order to make a pessimistic choice of temperature curve for the severe permafrost case air temperatures were assumed to fall according to the reconstructed temperature curve for the reference glacial cycle (Figure 12-9). For further discussion and motivation for this approach, see the **Climate report**, Section 5.5.

The air temperature curve reconstructed for the last glacial cycle was used to calculate ground surface temperatures for the severe permafrost case, see Figure 12-9, using an empirical relationship between air and ground temperatures. For details of this calculation, see /Hartikainen et al. 2010/.

Evolution of the depth of permafrost, perennially frozen ground and the –2 and –4°C isotherms over the repository for the severe permafrost case is shown in Figure 12-10. As one variant of the severe permafrost case, a simulation was made to study the effects of uncertainties in bedrock thermal properties together with uncertainties in surface conditions (except air temperature, see above). In order to obtain the largest uncertainty range, the dry climate variant was combined with the bedrock thermal properties enhancing permafrost development, and the humid climate variant with thermal properties diminishing permafrost development (Figure 12-11).

The results show that the maximum depth of permafrost over the repository in the severe permafrost case is 393 m (Figure 12-10), with the uncertainty interval reaching down to 456 m (Figure 12-11). This occurs after more than 90,000 years into the future. The maximum depth of perennially frozen ground, occurring at the same time, is 359 m with an uncertainty interval down to 408 m. The –2 and –4°C isotherms reach depths of 311 and 234 m respectively, with the uncertainty intervals reaching down to 359 and 268 m. Table 12-1 summarises all results from the severe permafrost case, together with the results from the reference evolution.

The values in Table 12-1 are valid for the first future glacial cycle of the 1 Myr long safety assessment period. For the second and following glacial cycles, the heat from the repository is negligible, resulting in up to 37 m deeper permafrost and frozen ground, see the **Climate report**, Section 4.5.3.

Further results from the 2D permafrost simulations made for the severe permafrost case, regarding e.g. salinity concentrations, ground water flow and vertical temperature profiles for various surface cover types, are found in the **Climate report**, Section 3.4.4 and /Hartikainen et al. 2010/.

The conclusion that can be drawn from the results of the severe permafrost case is that the uncertainties remaining from the analysis of the reference evolution, Section 10.4.3, i.e. mainly the uncertainty in ice sheet and sea coverage, yielded larger depths for the permafrost, perennially frozen ground, −2 and −4°C isotherms, but with a smaller uncertainty range (Table 12-1). For most parameters, the uncertainty

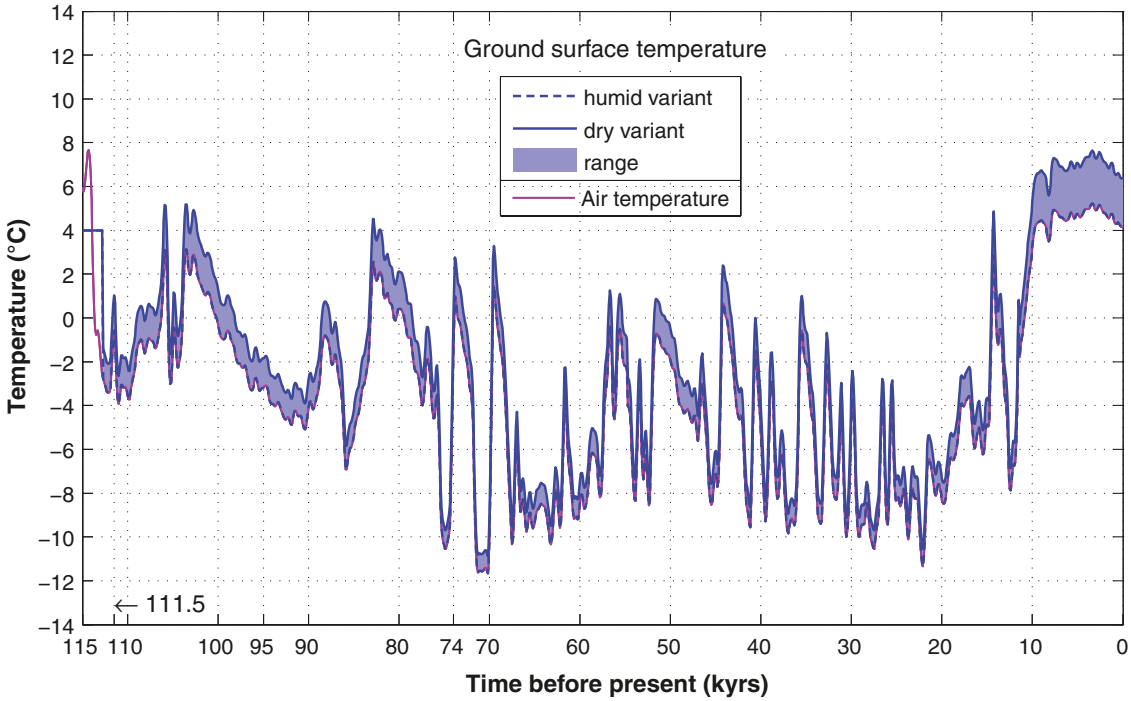


***Figure 12-9.*** *Example of evolution of air temperature and modelled ground surface temperatures used for the severe permafrost case. In this plot, the temperature has not been projected into the future. For a description of the modelling of ground surface temperature, see /Hartikainen et al. 2010/.*

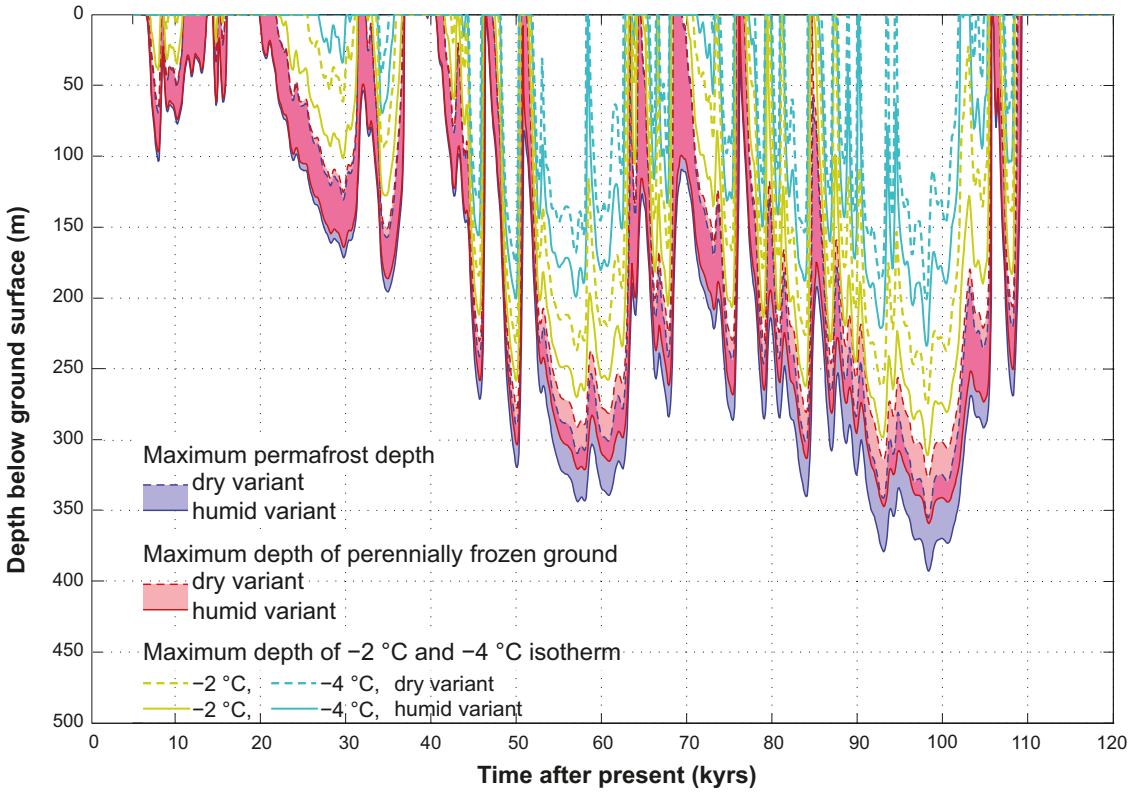


***Figure 12-10.*** *Evolution of maximum permafrost depth, maximum depth of perennially frozen ground and maximum depth of –2 and –4°C isotherms over the repository for the severe permafrost case. The upper permafrost surface, for periods of degradation from above, is not shown. The shaded area in blue and red represents the range when considering the dry and humid climate variants of the severe permafrost case. The lilac colour indicates that the results for permafrost and perennially frozen ground overlap.*

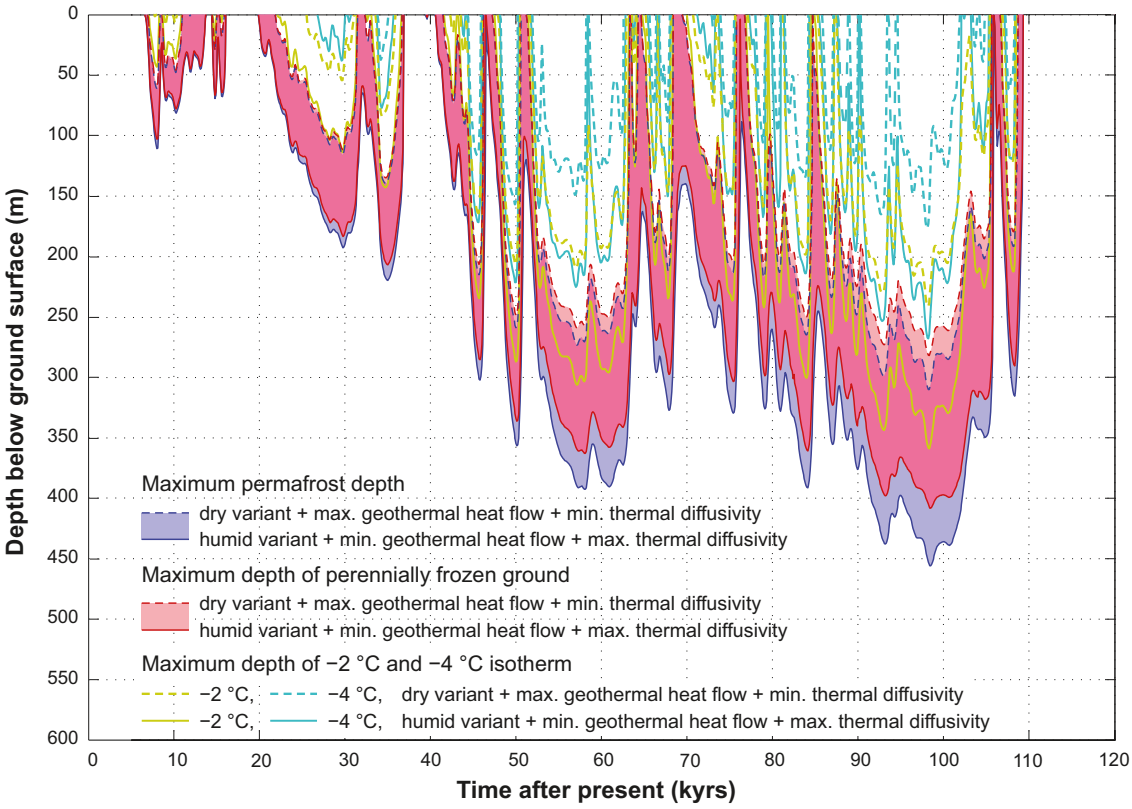


***Figure 12-11.*** *Evolution of maximum permafrost depth, maximum depth of perennially frozen ground and maximum depth of –2 and –4°C isotherms over the repository for the severe permafrost case considering combined uncertainties in surface conditions and thermal properties favourable for permafrost growth. The shaded area in blue and red represents the range when considering the dry and humid climate variants. The lilac colour indicates that the results for permafrost and perennially frozen ground overlap.*

**Table 12-1 Maximum depths of permafrost (0°C isotherm), perennially frozen ground, −2°C isotherm and −4°C isotherm for the severe permafrost case and the reference evolution. The uncertainty interval for the reference glacial cycle includes the unlikely combination of having all uncertainties, including air temperature, set to the most pessimistic values favouring permafrost growth. The uncertainty interval for the severe permafrost case includes all relevant uncertainties for this case (set to their most pessimistic settings), which excludes air temperature since lower air temperatures than the reconstructed last glacial cycle air temperature curve are not compatible with the main assumption of having no ice sheet development over the site.**

| | Maximum permafrost depth (0°C isotherm) [uncertainty interval] | Maximum depth perennially frozen ground [uncertainty interval] | Maximum depth −2°C isotherm (i.e. freezing temperature of backfill) [uncertainty interval] | Maximum depth −4°C isotherm (i.e. freezing temperature of buffer clay) [uncertainty interval] |
|---|---|---|---|---|
| Reference evolution | 259 m [down to 463 m] | 246 m [down to 422 m] | 200 m [down to 388 m] | 148 m [down to 316 m] |
| Severe permafrost case | 393 [down to 456] | 359 [down to 408] | 311 [down to 359] | 234 [down to 268] |

ranges reach maximum depths that are a few tens of metres shallower in the severe permafrost case than in the reference evolution (Table 12-1). The largest depth of perennially frozen ground is achieved not in the severe permafrost case but from making the unrealistic combination of setting all uncertainties relevant for the reference evolution to their values most favourable for permafrost growth, see Table 12-1 and Section 10.4.3. In the analysis of maximum possible freezing depths, the situation is bounded by the consideration of both the reference glacial cycle and severe permafrost case, including their respective uncertanty ranges.

### *Can climate get cold enough to cause buffer freezing?*

Reconstructed late glacial climatic conditions for southern Sweden indicate that continental arctic conditions prevailed prior to ~15,000 years before present. At that time, mean July temperatures were around 10–12°C /Lemdahl 1988, Coope et al. 1998, Hohl 2005/, i.e. about 5–7 degrees colder than at present. The difference between the present warm interglacial temperatures and the *coldest* temperatures during the last glacial cycle as recorded in the GRIP ice core is in the order of 12°C (Figure 12-12). Using an alternative way of interpreting $^{18}O$ values from the ice core in terms of air temperature, /Lang et al. 1999/ suggested that this cold event reflects a temperature change of 16°C, which is several degrees more than in /Dansgaard et al. 1993/. However, according to all interpretations, this was a very short-lived climate event, /Lang et al. 1999/. This exemplifies a typical feature of temperature climate archives namely that they show that climate is highly variable on both long and short time scales, see the **Climate report**, Section 4.3.4 and /IPCC 2007/, variability for example seen in the GRIP proxy temperature data, Figure 12-12. When severe very cold conditions occur, these conditions do not persist for long periods of time. Such climate variability is observed also in frequency analyses of climate records, e.g. /Moberg et al. 2005, Witt and Schumann 2005/.

How low could temperatures have been at Forsmark during the last glacial cycle? Recent global- and regional climate modelling suggest that the proglacial regions, south, southeast and southwest of the Last Glacial Maximum (LGM) ice margin in northern Europe, experienced annual mean air temperatures around 0 to −6°C (some 9 to 12 degrees colder than at present) /Kjellström et al. 2009, Figure 3-27, Brandefelt and Otto-Bliesner 2009/. The LGM model results for the Forsmark area are not relevant to this discussion, since at that time Forsmark was covered by the ice sheet. However, /Kjellström et al. 2009/ also made a climate simulation for a stadial period during Marine Isotope Stage 3 during the Weichselian, at 44,000 years BP, with postulated ice-free conditions at Forsmark. The resulting cold and dry periglacial climate had an annual mean air temperature in the Forsmark region of c. −7.5°C (around 13 degrees lower than at present) /Kjellström et al. 2009, Figure 4-4 and Tables 4-2 and 5-1/. The annual mean air temperature of −7.5°C is well in line with the temperature in the reconstructed temperature curve for this specific period (Figure 12-9) which is around −8°C. The results show a consistency between the independent temperature obtained from the climate model

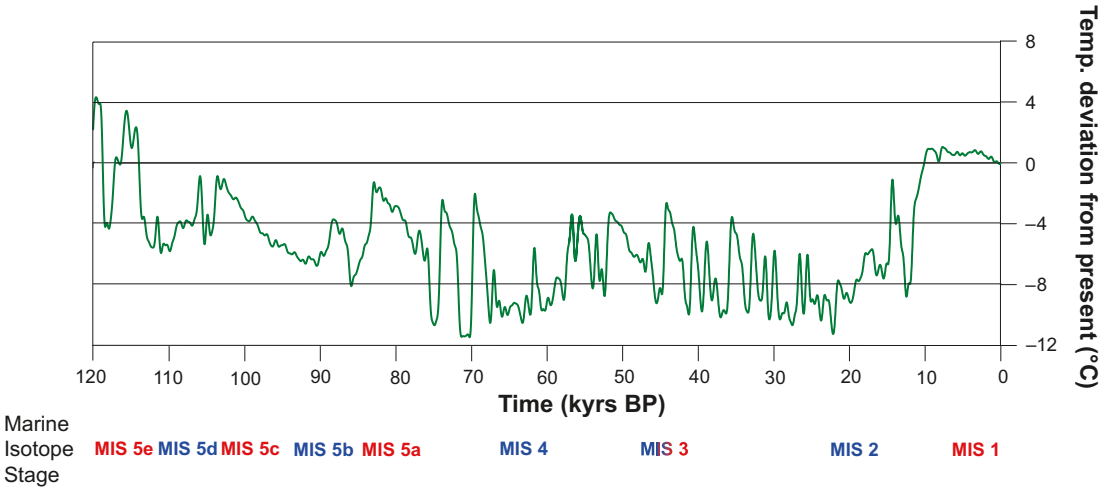


***Figure 12-12.*** *GRIP proxy temperature curve. During the last glacial cycle, temperature was highly variable on both long and short time scales. Modified from /Dansgaard et al. 1993/.*

and the temperature curve reconstructed for the last glacial cycle, both showing that during cold last glacial cycle stadials, with restricted duration, temperatures in the Forsmark area often may have dropped to be more than 10°C colder than at present.

Furthermore, the air temperature curve reconstructed for the last glacial cycle for the Forsmark region (Figure 12-9) suggests that mean annual air temperatures during the *coldest* stadials of the glacial cycle may have been around −11 to −12°C (16 to 18 degrees colder than at present). However, considering the uncertainties in e.g. the transfer functions between $^{18}O$ and air temperature and the adaptation of the curve for Fennoscandian conditions, temperatures could have been even lower, see the **Climate report**, Appendix 1. In this context, it should also be noted that the mean annual ground surface temperature, relevant for permafrost growth, typically is a few degrees *higher* than the air temperature, see Figure 12-9, the **Climate report**, Section 3.4.4 and /Kjellström et al. 2009, Figure 3-57/.

During the last glacial cycle, really low air temperatures only prevailed during stadials with relatively short duration, typically some thousands of years long (Figure 12-12). This prevented permafrost from developing to great depths (Figure 10-102), and would do so also under even more extreme glacial cycle conditions (Figures 12-10 and 12-11). For more information on the last glacial cycle climate, see the **Climate report**, Section 4.3.

If climate were to shift towards colder glacial cycles, it is unlikely that the variability within the climate system would drastically change. Very cold periods have been short lived in the past and nothing suggests that this would not be the case also during future glacial cycles. Variability is a characteristic feature of Earth's climate system. However, for a discussion on a less variable climate, see further below.

Assuming a similar climate variability to that during the last glacial cycle, it requires a lowering of the entire last glacial cycle temperature curve by as much as 14°C in order to make the −4°C isotherm reach repository depth at Forsmark (Figure 12-8). Also when considering the significant estimated maximum uncertainty in the reconstructed air temperature curve (±6°C), this corresponds to an unrealistically large change in glacial climate conditions.

Furthermore, during the coldest phases of glacial cycles, Fennoscandia is covered by an ice sheet, and the glacial domain prevails at Forsmark. Calculations using the ice-sheet model indicate that, if the temperature falls by 9 degrees, an ice sheet will develop that covers the Forsmark region, see the **Climate report**, Section 5.4.2. When this happens, permafrost either develops at a much lower rate or decreases, see the **Climate report**, Sections 3.4.4 and 4.5. In association with major ice sheet advances over the site, the area is also submerged for a considerable time after deglaciation, which further prevents permafrost development. If future glacial cycles were to be colder than in the past, this would most likely produce larger ice sheets and longer periods of ice sheet coverage at the sites, reducing the depth of the permafrost and −4°C isotherm.

The effect of an unlikely future climate with considerably less glacial climate variability than during the past 2 million years can be determined by reference to the sensitivity test results presented in Figure 12-5. If the ground temperature is −8°C at Forsmark, it would take about 120,000 years for permafrost (0°C isotherm) to develop to repository depth (if heat from spent fuel is present). At present, the annual mean air temperature at Forsmark is around +5°C, see the **Climate report**, Section 2.4.2. Since the air temperature often is a few degrees lower than the ground surface temperature, Figure 12-9 and /Hartikainen et al. 2010, Kjellström et al. 2009, Figure 3-57/, the results indicate that an air temperature lowering of more than 13°C is required to make permafrost develop to repository depth when considering constant temperatures. Such low temperatures could occur occasionally during a glacial cycle (Figures 12-9 and 12-12), but such cold periods prevail for considerably shorter times than 120,000 years, see Section 4.3 and Appendix 1, both in the **Climate report**. In the **Climate report** a theoretical estimate is performed of the maximum pressure, taking into account the equilibrium state between bentonite and ice.

### *Conclusion on freezing of backfill*

During permafrost periods in the reference evolution, freezing of the backfill (−2°C isotherm) in the ramp and shafts occurs down to a maximum depth of 200 m, with an uncertainty interval down to 388 m (Table 12-1). In the severe permafrost case, freezing of the backfill occurs down to a maximum depth of 311 m (Figure 12-10), with an uncertainty interval down to 359 m (Figure 12-11, Table 12-1). Possible consequences of this are discussed in Section 10.4.8.

### 12.3.3 Conclusions

Based on the model studies described above, including sensitivity studies of all known uncertainties, perennially frozen ground and the −2 and −4°C isotherms do not reach repository depth in the reference evolution, nor in the severe permafrost case. If adapting the most pessimistic combination of all uncertainties related to permafrost development in the reference evolution, the 0°C isotherm may reach repository depth. However, this case, which is considered quite unrealistic, does not result in freezing at repository depth during the first future glacial cycle since the repository heat and the prevailing pressure and salinity conditions at depth counterbalance the freezing process. After repository heat has declined, i.e. for the second future glacial cycle, and for all following glacial cycles in the 1 Myr assessment period, the most pessimistic combination of uncertainties results in that water at repository depth freezes. However, it should again be emphasised that this combination of uncertainties is considered quite unrealistic, and consequently, that freezing at repository depth also for these glacial cycles are considered unrealistic. In addition, it should be noted that there is a large margin for freezing of the buffer clay and repository tunnel back fill for all assessment period glacial cycles, even when adopting this most pessimistic combination of uncertainties.

Ice formation in the buffer material requires temperatures of –4°C or lower. The results in Figures 12-10 and 12-11 show that in the pessimistic cold and dry severe permafrost case, there is ample margin before the −4°C isotherm would reach repository depth. The results in Figure 12-8 show that the temperature curve reconstructed for the last glacial cycle needs to be lowered by ~14°C in order for the −4°C isotherm reach a depth of 450 m. Even when including the significant uncertainty in the reconstructed air temperature curve, see the **Climate report**, Appendix 1 and /Hartikainen et al. 2010/, such low temperatures are considered unrealistic based on what is known about past climate conditions and climate variability. The possibility that the buffer clay would freeze, under any feasible future climate development, is therefore considered as ruled out.

#### *Categorisation as “less probable” or “residual” scenario*

Since the conclusion of the analysis of this scenario is that the buffer will not freeze, this is considered as a residual scenario.

#### *Quantitative consequence analysis/discussion – containment and retardation*

If the consequences in terms containment of a postulated freezing were to be analysed, a bounding case would be one where all canisters are damaged due to freezing. This is similar to the situation where all canisters fail due to isostatic over-pressure, analysed as a postulated “what-if” case in Section 13.7.1.

#### *Global warming variant and other climate cases*

The occurrence of permafrost is delayed in the Global warming variant, see Section 10.6.1. The delay would also delay the onset of possible buffer freezing and thus any consequences would also be delayed and reduced. Buffer freezing is, therefore, not further treated for the Global warming variant.

Since the severe permafrost climate case (see Section 12.1.3) has been used in the above analysis and since that case was defined to maximise the potential for buffer freezing, no additional climate cases need to be considered.

#### *Combination of buffer erosion and freezing*

The results from the permafrost simulations show that, in the reference evolution and in the severe permafrost case, freezing of ground water does not occur at repository depth during the first glacial cycle, although the 0°C isotherm may reach repository depth under very pessimistic assumptions. Therefore, groundwater in erosion cavities does not freeze during the first glacial cycle when a buffer erosion case is combined with a freezing case based on the reference evolution or severe permafrost case. Such a combined case is therefore not further treated in this report.

For the second future glacial cycle, and all following glacial cycles in the 1 Ma assessment period, the heat from the spent fuel has declined, resulting in the situation that under the most pessimistic

and quite unrealistic combination of uncertainties, water may freeze at repository depth during these glacial cycles. Therefore, an analysis of freezing of water in buffer erosion cavities is presented in the **Climate report**, Appendix 3. The results show that, if freezing were to occur at repository depth, the maximum freezing induced pressure in buffer erosion cavities would be 26–27 MPa, which is considerably lower than the critical pressure for canister collapse described in the scenario treating canister collapse due to isostatic load (Section 12.7.2).

## 12.4 Buffer transformation

### *Indicator criterion violated*

This scenario concerns all conceivable routes to an alteration of the montmorillonite in the buffer material. This refers to a transformation of the montmorillonite in the buffer to non-expandable minerals (e.g. illite), but also accumulation of impurities that could change the properties of the buffer. This mainly concerns the function indicators on maximum buffer temperature and limited pH:

1. The temperature in the buffer should not exceed 100°C.
2. The pH of the groundwater should not exceed 11.

There may also be other processes that affect the stability of the montmorillonite. A *temperature gradient over the buffer* may cause transport of silica from the hot to the cold part. Presence of *metallic iron in contact with bentonite* could also alter the montmorillonite.

If the buffer material is transformed, this could possibly affect both containment and retardation by affecting other function indicators. Containment could be jeopardized indirectly through a lack of swelling pressure, which could lead to enhanced sulphide corrosion and create conditions suitable for microbially induced corrosion on the canister surface. Retardation could be affected by an increased hydraulic conductivity in the buffer, or by a loss of swelling pressure, which in turn could lead to the formation of pathways.

### *Treatment of routes to transformation in the reference evolution*

According to Section 10.3.4 there are substantial margins to the 100°C function indicator even with account taken of uncertainties in the thermal conductivity in the rock. Based on this, temperatures above 100°C were not considered in the reference evolution.

According to Section 10.3.12, there may be a short period with pH > 11 in the contact between the bottom plate and the buffer. However, the duration of the conditions with elevated pH will be very short. Based on this, alteration from high pH was not considered in the reference evolution.

The movement of silica in the thermal gradient is discussed in Section 10.3.10, see Figure 10-64. The expected thermal gradients gave a very small redistribution of silica.

Contact between metallic iron and the buffer is only possible if there is a defect in the copper shell. This is not addressed in the reference evolution.

### *Qualitative description of routes to buffer transformation*

The following factors of importance for the occurrence of buffer transformation are identified, based on the discussion above, on Table 10-27 describing uncertainties identified in the reference evolution and on the FEP chart, Figure 8-4.

#### High temperature

This route to the transformation scenario can be due to:

1. a residual power in the canister, which is higher than the design value,
2. a misinterpretation of the thermal properties of the rock at the site,
3. a lower initial water content in the buffer than the design value,
4. a drying of the buffer, leading to a decreased thermal conductivity.

The only identified cause for route 4 is ventilation of the deposition hole for an extended period of time. The consequences of drying of the rock and its effect on the thermal properties of the buffer are discussed in Section 10.3.8. There is no foreseen evolution of the near field that could lead to those conditions and drying of the buffer is not considered further.

**High pH**

High pH groundwaters in contact with the buffer could occur if the quality control system for repository construction fails or malfunctions. The possible routes could either be a misjudgement of the pH arising from the cement used, or the use of a wrong cement mixture.

**Thermal gradient**

The thermal gradient is dependent on the thermal power from the canister and the thermal properties of the rock. However, the sensitivity to the parameters is small and the conclusions from the reference evolution are expected to be valid for all possible conditions.

**Interaction with metallic iron**

This process will occur if the canister insert gets in contact with the buffer material. Recent laboratory experiments under repository conditions have shown that reactions between montmorillonite and metallic iron in an oxygen-free environment may be relatively fast and in some cases also lead to a general breakdown of the montmorillonite structure /Lantenois et al. 2005/.

Another possibility would be if stray equipment or material containing iron or steel was left in a deposition hole during buffer emplacement. However, in SR-Site it is assumed that the QC system will ensure that the deposition holes are cleaned before the buffer is deposited.

### *Quantitative consequence analysis/discussion*

The effect of the thermal period on the buffer is described in Section 10.3.10. The conclusion is that the expected temperature increase will have no significant effect on the buffer properties.

A buffer temperature exceeding the function indicator could lead to the following consequences.

1. A transformation of the montmorillonite in the buffer to non-expandable minerals (illite). This would give a higher hydraulic conductivity and a decrease in swelling pressure.
2. An accumulation of impurities in the buffer on the hot (or cold) side. This would be caused by temperature-dependent solubilities. This accumulation could potentially lead to clogging of the pore space and a change in the rheological or/and the hydraulic properties.

The transformation of montmorillonite to illite is discussed in Section 10.3.10. It is evident that the transformation is very slow even if repository timescales are considered. /Karnland and Birgersson 2006/ undertook a review of different kinetic models for smectite to illite conversion. Figure 12-13 shows the results from different models. The models of Cuadros /Cuadros and Linares 1996/ (Cuadros 1) estimate a much faster alteration rate than the one that was used in the SR-Can assessment (Huang). However, the Cuadros experimental work did not include specific determinations of all rate-determining constants and parameters, as was done by /Huang et al. 1993/. Cuadros, therefore, used natural analogues to adjust their model (Cuadros 5) in order to represent the conditions in nature, where bentonite persists over geological time scales.

There are two kinds of data uncertainties for this process.

- Uncertainties in the temperature calculation. This is described in the section above.
- Uncertainties in the data used in the alteration calculation /Karnland and Birgersson 2006/ and in the reactive transport calculation.

The potentially most critical data uncertainties are in the frequency factor for a first order reaction (Arrhenius equation) and the activation energy in the kinetic expression for the alteration rate.

Using the Huang model, a temperature of 125°C for 10,000 years would not have any significant effect on the swelling pressure and hydraulic conductivity function indicators /Karnland and Birgersson 2006/. However, the experimentally achieved model parameters have to be determined at temperatures

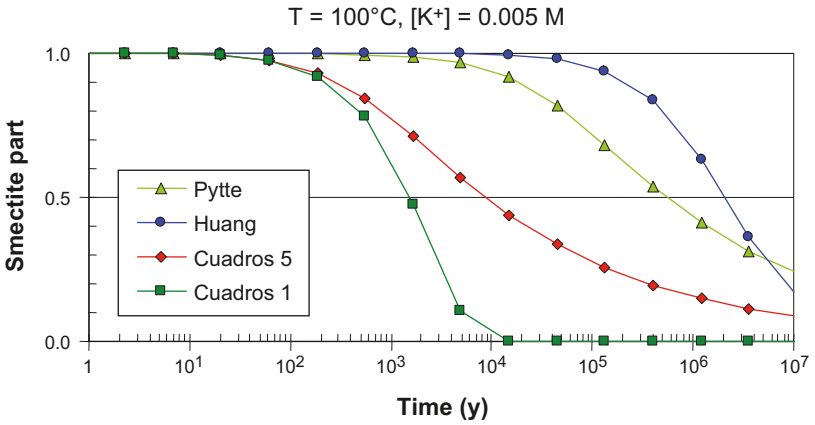


***Figure 12-13.*** *Comparison of kinetic models for the smectite to illite transformation. Lines show the calculated remaining proportion of smectite versus time for a constant temperature of 100°C and a constant potassium concentration of 0.005 M.*

significantly higher than the maximum repository temperature. The uncertainty in the model predictions is thereby increasing with decreasing temperature. The kinetic model is thereby only used for the justification of the temperature criterion, but not for a detailed long term prediction of the transformation with attention to the decreasing temperature. As seen in Figure 10-16, the temperature in the warmest part of the buffer decreases below 60°C already after 200 years. This means that the uncertainties in the kinetic models will only impact a very limited period of the repository evolution.

Figure 12-14 /Karnland and Birgersson 2006/ shows the swelling pressure of the MX-80 buffer material as a function of the dry density. The arrows in the figure indicate the swelling pressure for the reference density, a material with 30% transformation and a material with 50% conversion to illite. A conversion of 30% of the montmorillonite to illite would still give a swelling pressure above the 1 MPa function indicator. Figure 12-13 shows that with the Huang model a temperature of 100°C for a period of over 1,000,000 years is needed to get a degree of conversion of 30%. It is evident that the period with elevated temperature under any reasonably postulated set of conditions will never be close to that value. The problem with the kinetic model is not the long timescale but rather a more exact effect of the decreasing temperature. The scoping calculation by use of the temperature is though considered useful since it does not lead significant alteration despite the over-pessimistic temperature assumptions.

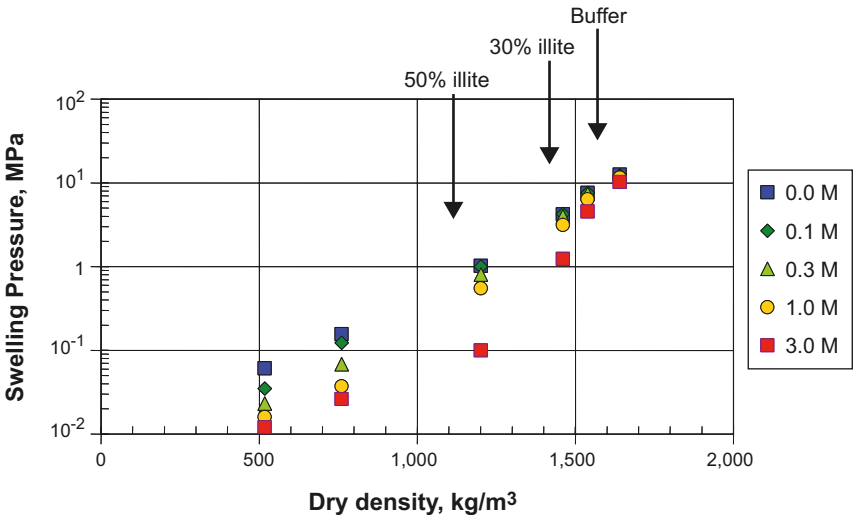


***Figure 12-14.*** *Swelling pressure of MX-80 material in contact with pure water and NaCl solutions. Dots show measured values. Buffer indicates the swelling pressure of unaltered buffer material at KBS-3 target density, 30% illite indicates the pressure at the maximum acceptable transformation, and 50% illite illustrates the pressure at 50% illitization.*

An effect of steam on the properties of bentonite has been identified by /Couture 1985/ and is discussed by /Pusch 2000a/ and /Karnland and Birgersson 2006/. There is an observed effect of vapour that could influence the maximum free swelling of the bentonite. However, no obvious mineral alteration was identified by Couture although the experiments were performed at temperatures significantly higher than the maximum temperature in a repository. The consequence of steam on the long-term performance of the buffer is thereby expected to be limited.

**High pH**

If high pH (pH > 11) groundwaters were to contact the buffer, some alteration or dissolution would be expected. The extent of the transformation is dependent on the actual pH of the water, the local hydrologic situation and the amount of cement producing the high pH (mass balance). However, in SR-Site it is assumed that the quality control systems will be sufficient to avoid the introduction of cements that could give rise to high pH waters in the repository.

**Thermal gradient**

The effect of the temperature gradient on the redistribution of impurities has been calculated by /Sena et al. 2010/ and /Karnland and Birgersson 2006/. This process has been shown to have a very limited effect. The temperature gradient is only affected by the absolute temperature to a limited degree, and the dependence of this process on the temperature is, therefore, limited.

**Interaction with metallic iron**

Currently, a mechanistic understanding is lacking and a quantitative model does not exist. However, no interaction between buffer bentonite and metallic iron is expected to occur as long as the copper canister is intact.

**Summary**

Since there still are some uncertainties on the effect of high temperatures on the long-term performance of the buffer, a case with an altered buffer zone next to the canister cannot be entirely excluded. The consequences of such a case would be a loss of swelling pressure next to the canister, and a correlated consolidation of this part due to the swelling pressure in the remaining buffer. However, a major part of the buffer has to be transformed in order for the buffer swelling pressure to fall below the pressure criterion of 1 MPa, where advection conditions need to be considered, which is most unlikely. If such a low pressure occurred, this would mean that it could be possible for sulphate-reducing bacteria to survive and sulphide corrosion to be enhanced.

The interaction between iron and buffer material is still under investigation. It is likely that only the region closest to the insert would be affected, assuming that there was any contact between the insert and the buffer, and the overall transport properties of the buffer would be maintained. However, today it cannot be excluded that the entire diffusion barrier could be lost. This, however, would have consequences only for retardation.

**Global warming variant and other climate cases**

There is nothing connected to the global warming variant (essentially 60,000 years before first permafrost) that would make buffer transformation worse. The climate on the surface has no bearing on any of the processes discussed in this section. The issue is therefore not further treated for the global warming variant. Nor do any of the other climate cases described in Section 12.1.3 have any relevance for the buffer transformation scenario.

### *Categorisation as "less probable" or "residual" scenario*

High temperature, high pH and high temperature gradients are not expected to have any significant effect on buffer stability under any plausible conditions. Transformations of buffer material to such an extent that the beneficial containment and retardation properties are affected are, therefore, considered as a residual scenario.

If the buffer gets in contact with metallic iron some alteration will occur. The extent of this is currently unknown. The process can only occur after copper canister failure. It is not relevant for failures when buffer is missing.

#### *Conclusions*

Processes that may alter or transform the montmorillonite, as described above, are not expected to have any significant effect on the important buffer properties. However, since there are uncertainties over the combined effect of elevated temperatures and high pH, a case where the buffer next to the canister is altered and the swelling pressure is lost to a level where bacteria can survive is appropriate to study. This case is treated as a residual scenario.

## 12.5 Conclusion from analyses of buffer scenarios

From the results of the analyses of the three buffer scenarios above, the following conclusions are drawn regarding propagation of buffer conditions to the analyses of canister scenarios.

- The buffer advection scenario is propagated as three cases to the canister scenarios: i) advective conditions in every deposition hole throughout the assessment period, ii) advective conditions as calculated with base case assumptions in Section 12.2.2, iii) no advective conditions in any deposition hole at any part of the assessment period.
- The buffer freezing scenario is regarded as residual. It is, therefore, not propagated to the canister scenarios in SR-Site.
- The buffer transformation scenario is regarded as residual. It is, therefore, not propagated to the canister scenarios in SR-Site.

In addition to the buffer scenarios treating altered buffer states, also the case of an intact buffer needs to be considered, and this is covered by case iii) in the first bullet point.

## 12.6 Canister failure due to corrosion

### 12.6.1 Introduction

Canister corrosion was evaluated for a number of situations in the reference evolution. As demonstrated in Chapter 10, canister corrosion leads to failure only for advective conditions in the buffer, and for such conditions only in the most highly flowing deposition holes, in general after several hundreds of thousands of years.

The buffer conditions are thus crucial for the evaluation of the canister failure due to corrosion scenario. Based on the findings in the analyses of the buffer scenarios, the cases of intact buffer and of advective conditions in the buffer need to be propagated to this corrosion scenario. As described in the analysis of the buffer advection scenario, Section 12.2, three cases for buffer advective conditions are propagated for further analyses.

#### *Safety function indicator(s) considered*

This scenario concerns the safety function Can1, ‘Provide corrosion barrier’, that is directly related to the containment potential of the canister.

This is one of the top-level safety functions, meaning that a number of sub-functions must be evaluated in order to fully assess the canister corrosion scenario. Several results from other scenarios, in particular regarding the buffer are, therefore, propagated to this scenario.

#### *Treatment of canister corrosion in the reference evolution*

Canister failures due to corrosion occur in the reference evolution, for the case of advective conditions in the buffer. For an intact buffer, the margins protecting against corrosion failures were demonstrated to be considerable.

The two tasks for this corrosion scenario are thus to i) evaluate whether all uncertainties for the corrosion case with advective conditions in the buffer are appropriately addressed in the reference evolution and ii) whether for an intact buffer there are any remaining uncertainties that could challenge the conclusion that corrosion failures will not occur.

#### *Qualitative description of routes to corrosion*

The following factors of importance for the occurrence of canister failures due to corrosion are identified, based on the discussion above, on Table 10-27 describing uncertainties identified in the reference evolution and on the FEP chart, Figure 8-4.

**Initial state factors involved**

- Initial minimum copper coverage.
- Deposition hole rejection criteria.
- Corroding agents in buffer and backfill.

**Processes and rock conditions involved**

- Copper corrosion.
- Diffusive transport of corroding species through the buffer (for intact buffer).
- Advective transport in a deposition hole with an eroded buffer.
- Groundwater flow.
- Groundwater concentrations of sulphide.
- The possibility of oxygen penetration.

**External conditions involved**

- Glacial conditions leading to enhanced groundwater flow.
- Glacial conditions leading to changed groundwater composition (oxygen, and sulphide).

### 12.6.2 Quantitative assessment of corrosion

Remaining uncertainties regarding each of the factors mentioned above are addressed below followed by corrosion calculations based on the additional uncertainties identified for a buffer in advective conditions.

#### *Initial copper coverage*

The initial copper coverage was evaluated extensively in the **Canister production report**, leading to the initial state values cited in Section 5.4.3, Table 5-9. The derivation of the initial state is based on the reference design, production and control methods described in the **Canister production report** and summarised in Section 5.4.2. This issue is, therefore, not further treated here.

As seen in Table 5-9 the minimum copper thickness is 47.5 mm for more than 99 percent of the canisters, and somewhat lower values may exist for the remaining small fraction. For the corrosion analyses presented in this section, only a limited part of the canister surface is exposed to the corroding agent. For an eroded buffer where advection is the dominant transport process, a height of the canister corresponding to the thickness of the buffer around the canister, 35 cm, is assumed to be corroded (see Section 10.4.9). For an intact buffer, where diffusion is the dominant transport process, the concentration profile in the buffer from species entering through a fracture in the deposition hole will have its maximum over an even smaller area. The probability that the area with (pessimistically) assumed reduced copper thicknesses around the seals will actually be exposed to corrosion is thus small. Therefore, the thickness is assumed to be 47 mm in the corrosion analyses (see the **Data report**, Section 4.1). More sophisticated analyses are not seen as warranted in light of the considerable uncertainties associated with many other factors in the corrosion calculations, in comparison to the rather limited range of values of initial copper coverage discussed here.

Furthermore, a reduction in copper coverage by a small cavity on the outside, say at the mm scale, would not decrease the time required for penetration due to corrosion in proportion to the reduced coverage, as the copper outer surface would be evened out as corrosion proceeds. It is only cavities on the inner surfaces that would result in a proportionate decrease in penetration time.

As mentioned in Section 10.2.5, subsection 'Canister corrosion', initial corrosion by atmospheric oxygen before emplacement and from initially entrapped oxygen is expected to cause corrosion depths less than 500 μm at most, and will thus have a negligible impact on the minimum copper coverage of the canisters.

Alternative design copper thicknesses are evaluated as part of the BAT analyses in Section 14.3.

#### *Deposition hole rejection criteria*

Deposition holes are rejected according to the EFPC criterion in the reference evolution. This is a design decision and it is seen fully feasible to implement the EFPC, see Section 5.2.3. Therefore, rejection according to EFPC is assumed also in the corrosion scenario. Alternative rejection criteria are evaluated as part of the BAT analyses in Section 14.3.

#### *Buffer and backfill impurities*

The analysis of the reference evolution demonstrates that constituents initially present in the buffer and the backfill, i.e. entrapped oxygen and impurities (pyrite, organic matter) as well as other sources of organic matter (rock biofilms) and hydrogen from corroding rock bolts and other iron components contribute negligibly to copper corrosion, see Section 10.3.13. Mass balance considerations lead to the conclusion that corrosion depths from these constituents would be less than a few mm and furthermore that time intervals comparable to the one million year assessment period are required for all constituents to reach the canister. Considering that the initial content of these constituents puts a fundamental limit on the extent of corrosion caused by these, and that this extent is negligible, this issue is not further considered in this scenario.

#### *Copper corrosion*

In the analysis of the reference evolution corrosion is evaluated as caused by oxygen (atmospheric, and initially entrapped), sulphide (transported via groundwater, or produced by sulphate reducing bacteria, as mentioned above) as well as corroding agents formed by radiolysis of water or irradiation of nitrogen in air. Section 10.3.13 gives the extent of this corrosion as limited to a few mm in the $10^6$ year assessment perspective, and with these margins and most of the processes bounded by mass balance (otherwise by mass transport), these corrosion mechanisms are not further treated in this scenario. However, there is a need to revisit the discussion on corrosion of copper with water under hydrogen gas production, for low pH conditions, and for the mechanism suggested by /Szakálos et al. 2007/.

In Section 8.3.4 it is stated that chloride-assisted corrosion of copper is ruled out if simultaneously $pH > 4$ and $[Cl^-] < 2$ M, and there is a thus a need to analyse additional evolutions to rule out unfavourable pH conditions and high ionic strength conditions. During temperate conditions the acidity of groundwaters is highest in the upper parts of the rock where recharge of meteoric waters dominates because rain water is saturated with atmospheric $CO_2$, which is an acid, and several biological processes produce $CO_2$ in the soil layers. When these waters penetrate further down in the rock, the acidity is neutralised through several water-rock reactions. Typical pH values for waters at Forsmark are illustrated in Figure 10-45. In addition to the enhanced infiltration of fresh meteoric waters, another process that may result in low-pH groundwaters is the upconing of deep saline groundwaters which results in mixtures with fresh groundwaters. If the mixtures become oversaturated with calcite, the acidity of the mixture increases when calcite precipitates: $Ca^{2+} + HCO_3^- \rightarrow CaCO_3 + H^+$. This effect is larger when waters of meteoric origin, rich in $HCO_3^-$, rather than glacial melt waters are mixed with deep Ca-rich groundwaters. The present-day groundwater data at Forsmark together with sensitivity analysis results of mixing calculations show that the lowest pH that may be attained is around 6.3, and this agrees with the analysis presented in Section 10.3.7. In Section 10.6.3 a transitory rise in atmospheric $CO_2$ concentrations is discussed. As long as the increased $CO_2$ levels are limited to a period of hundreds to thousands of years, it would not affect the acidity of groundwaters at repository level. The controls on atmospheric $CO_2$ concentrations subsequent to a reduction in fossil fuel emissions indicates that although enhanced $CO_2$ concentration values would persist over such timescales, concentrations would be lower than the peak value, see the **Climate report**, Sections 5.1 and 5.2.

The groundwater data at Forsmark indicate that in volumes of rock outside fracture zones the salinity has been stable during the Weichselian, and large oscillations in groundwater salinities are therefore not expected in the future. The analyses of different possible climatic episodes presented in Sections 10.3.7 and 10.4.7 show that salinity can increase due to upconing during the short glacial transit above the repository area. The analyses reported in Sections 10.4.6 and 10.4.7 show that the upconing effect is moderate and the resulting ionic strengths in the repository volume are below 0.5 M. Because the most pronounced upconing takes place during an ice advance, where the ice profile is steepest, the analysis of the reference evolution includes the highest salinities that can be expected at Forsmark. It is therefore concluded that there is no need to analyse consequences of chloride-assisted copper corrosion.

In the **Fuel and canister process report** (Section 3.5.4, subsection 'Corrosion in the absence of oxygen'), the reaction of copper with water to give a not clearly identified corrosion product and hydrogen gas is discussed. The scientific basis for the suggested reaction is debated, but the consequences for the canister in the repository can be estimated from the published data on hydrogen equilibrium pressure /Szakálos et al. 2007/ and mass transport considerations, see further /SKB 2010d/. These "what-if"-calculations show that the copper shell is very far from being penetrated, even for an assessment time of $10^6$ years. It is only in the case of an eroded buffer and then only for the deposition holes with the highest flow rate that the corrosion depth is in the mm scale after $10^6$ years.

### *Diffusion in intact buffer*

As demonstrated in /SKB 2010d/ the flow rate controlled transport resistance in the buffer/rock interface determines the rate of transport of species from the groundwater to the canister. The transport resistance due to the buffer diffusivity is negligible in comparison. Therefore, there is no reason to handle buffer diffusion any further in this corrosion scenario for the intact buffer. In the case of advective conditions in the buffer, diffusion of dissolved species in the buffer porewater is, by definition, irrelevant.

### *Corrosion geometry*

For the diffusive case with the buffer present, the corrosion geometry is given by the dimensions of the near-field repository components. There are no significant uncertainties to evaluate in this case.

As discussed in the context of the reference evolution at Section 10.4.9, the corrosion geometry for the case with advective conditions in the deposition hole is uncertain, varying in time and difficult to quantify. In Section 10.4.9 a cautious geometry was used in the calculation examples. An extreme, bounding geometry is evaluated below as a sensitivity case.

The canister is first exposed along a line around half its circumference and this situation does not change with time, see Figure 12-15. Corrosion would then proceed radially in the copper material, corresponding to a corroded area with an equivalent height, $h_{corr}$, of $\pi \cdot d_{can}/2$, where $d_{can}$ is the thickness of the copper shell. This yields an exposed area of

$$A_{corr} = ½ \cdot \pi^2 \cdot r_{can} \cdot d_{can}$$

This extreme value is about a factor of five smaller than the cautious value in the reference evolution. (A smaller area yields a higher corrosion rate since all incoming sulphide is assumed to react with the exposed canister surface.)

In the corrosion scenario, the cautious geometry is used since it is seen as unrealistic and overly pessimistic to base the calculations in the corrosion scenario on the above extreme geometry. For this extreme geometry to arise and persist would require the erosion to first go on for a long time (hundreds of thousands of years) and then abruptly stop due to changed groundwater conditions at just this eroded position, and then remain in this state for another long time (again hundreds of thousands of years). However, the sensitivity of the corrosion result to the pessimistic corrosion geometry is analysed below.

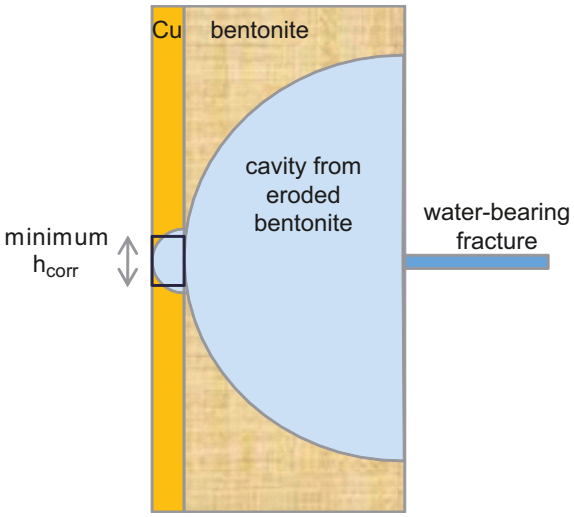


***Figure 12-15.*** *Illustration of erosion and corrosion geometry in the erosion/corrosion model. The corroded copper volume is modelled with a constant height, with an extreme, minimum value derived from a growing semi-circular cross section into the copper.*

### *Groundwater flow and glacial conditions leading to enhanced groundwater flow*

The groundwater flow is one of the factors determining the equivalent flow rates around the deposition holes. In the reference evolution, conceptual uncertainties regarding groundwater flow for temperate conditions were evaluated for the advection case, Section 10.4.9, by considering the three fracture size/transmissivity correlation functions treated in the Forsmark hydrogeological DFN model in **Site description Forsmark** and further handled in the uncertainty analysis described in Section 10.3.6. These three variants of the hydro DFN model are used in the further quantitative evaluations of the extent of corrosion below.

Regarding varying groundwater flow conditions over a glacial cycle, it is demonstrated in Section 10.4.6 that the time averaged values over the reference glacial cycle of q (Darcy flux), $q^{½}$ and $q^{0.41}$, relevant for copper corrosion under advective conditions, copper corrosion under diffusive conditions and buffer erosion, respectively, are all around 80 percent of the corresponding entities for temperate conditions, see ML2 data in Figure 10-147. Using the temperate values is thus pessimistic and gives some margin for alternative evolutions to the reference glacial cycle.

To address this further, it is noted that increased flow in comparison with temperate conditions occurs when the margin of an advancing ice sheet reaches the repository footprint or the margin of a retreating ice sheet leaves the footprint, see Section 10.4.6. More severe cases of increased flow could thus occur if a margin of an ice sheet came to a halt on top of the repository. This is addressed as follows.

During the deglaciation of the Weichselian ice sheet, the general ice sheet retreat temporarily halted several times. This is seen from dated ice marginal moraines, including the deposits from the Younger Dryas stadial in e.g. southern Sweden, see the **Climate report**, Section 4.2.2. During such halts in the deglaciation, the ice margin either oscillated back and forth or moved slowly within a zone that could be many km wide, in the case of the Younger Dryas several tens of km. During the formation of individual moraine ridges, the ice margin is estimated to have been at stable positions for up to a few hundred years, see the **Climate report**, Section 4.2.2. It has to be assumed that similar types of stillstands may occur also during phases of ice sheet advance.

Although not the case during the last deglaciation and in the SR-Site reference glacial cycle, future periods of frontal stillstands could occur at the Forsmark site during ice advance, maximum or retreat phases, given suitable climate conditions. An extreme case in terms of hydraulic gradients and associated increased groundwater flow would occur if the ice front came to a temporary halt with the frontal part of the ice sheet situated above the repository. According to /Vidstrand et al. 2010/ there is an approximately two km wide influence zone with significantly increased groundwater flux associated with an ice sheet margin over Forsmark. This situation is valid if there is no permafrost

at the Forsmark site. If permafrost is present, which is the case in the reference evolution, and also very likely during a future glaciation of the Forsmark site, a zone of increased groundwater flow is significantly less pronounced /Vidstrand et al. 2010/. Using a two km wide near-frontal zone with significantly increased groundwater flux is therefore a pessimistic choice for the analysis of the probability for a future situation with an ice sheet margin stillstand over the repository.

Assuming that future periods of ice margin stillstands would have the same characteristics as the stillstands associated with the most recent deglaciation, briefly described above and in more detail in the **Climate report**, Section 4.2.2, one could make an estimate of the probability of having such a situation occurring at the Forsmark site. By generalising the development of the last deglaciation, one could postulate ten temporary halts of shorter duration and one major halt of longer duration, corresponding to the Younger Dryas event, for a deglaciation of a full-sized ice sheet equivalent to the one of the LGM. Furthermore, for the halts of shorter duration, completely stable ice margin conditions are set to persist for 200 years, while during the major stillstand, a completely stable position of the ice margin is pessimistically set to a full 1,000 years. This is somewhat longer than the time period that the ice margin was located somewhere within the 20–25 km wide Younger Dryas zone in Sweden, which lasted around 900 years. In reality, it is likely that, during such long phases, the ice margin would move slowly and/or oscillate within an ice marginal zone, see the **Climate report**, Section 4.2.2. Nevertheless, in order to cover uncertainties in future ice sheet behaviour, a completely stable margin position for 1,000 years is assumed for the major stillstand. In this way, the major stillstand constitutes a pessimistically chosen case in terms of the duration of a high hydraulic gradient and associated high groundwater fluxes.

The deglaciation of the Weichselian ice sheet, from its LGM position in Poland and Germany to the Scandinavian mountain range, occurred along a distance of ~2,500 km /Fredén 2002/. For each of the postulated stillstands, there is a ~2 km wide frontal zone with significantly increased groundwater fluxes /Vidstrand et al. 2010/. For each advance or deglaciation phase, the probability of having a 200 year long stillstand at Forsmark is therefore 0.008 (10·2 km/2,500 km), while the probability of having the postulated 1,000 year long stillstand at Forsmark is 0.0008 (2 km/2,500 km). For a complete glacial cycle with two phases of ice advance and two phases of deglaciation over Forsmark, i.e. a glacial cycle similar to the SR-Site reference glacial cycle, the probabilities for the 200 year and 1,000 year ice margin stillstands at Forsmark are 0.03 (0.008·4) and 0.003 (0.0008·4), respectively. For the full assessment period of 1 million years, comprising eight repeated identical glacial cycles, the probabilities grow correspondingly larger. There is thus a relatively low probability that the ice margin zone with high groundwater flux would come to a temporary halt above the repository, especially when considering the rarer stillstands of long duration. In this context, it should again be pointed out that the assumption of a completely stable ice margin over the repository for 1,000 years is a highly pessimistic case compared to what is known from the last deglaciation, see further the **Climate report**, Section 4.2.2.

For the question of increased flow during a stillstand, also the presence or absence of permafrost should be considered. In the reference glacial cycle, the simulated ice sheet is cold-based, and advances over permafrost, during the phases of ice sheet advance whereas it is warm-based during the deglaciations, see Section 10.4.1. Only the latter situation gives rise to increased flow. In estimating the probability of having an ice margin stillstand over Forsmark, it is reasonable to include also this development. In line with this, it is assumed that half of the stillstands are cold-based and half are warm-based. The resulting probability of having a warm based, 200 year stillstand over the repository during one glacial cycle is thus estimated at 0.015 (0.03/2), while the probability of a warm based 1,000 year stillstand is estimated at 0.0015 (0.003/2). For the one million year assessment period, these figures should be multiplied by eight, yielding probabilities of 0.12 and 0.012 for 200 year and 1,000 year stillstands, respectively.

**Intact buffer**

For an intact buffer, $q^{1/2}$ is the relevant entity to consider. Assuming according to Figure 10-132 that $q$ is increased by a factor of 100 during the stillstand, $q^{1/2}$ increases by a factor of ten. A one thousand year stillstand then gives an impact on corrosion corresponding to 10,000 years of temperate flow, which is only one percent of the one million year assessment period. Considering that the probability of this to occur once during one million years is 0.012 leads to the conclusion that this impact is negligible. The same conclusion is reached for the 200 year stillstands.

**Advection in buffer**

For a buffer with advective conditions, the Darcy flux, $q$, is normally the relevant entity to consider, but for the high flow rates of concern in this case, the dependence on Darcy flux is as $q^{1/2}$ /Neretnieks et al. 2010/ and the effect is thus negligible according to the above. Even with a linear dependence on $q$, the effect would be negligible considering the low probabilities involved.

In conclusion, the Darcy flux distributions at 2000 AD for the three hydrogeological DFN models do not have to be modified to account for varying flow conditions over a glacial cycle.

### *Groundwater concentrations of sulphide*

For corrosion calculations in the reference evolution, it was assumed that the distribution of groundwater concentrations of sulphide over a glacial cycle is equal to that for temperate conditions reported in Section 10.3.7. This is regarded as a pessimistic assumption, see Section 10.4.7. These concentrations also include effects of microbial sulphate reduction. Also, it was pessimistically assumed in the corrosion calculations reported for the reference evolution that sulphide concentrations at a given position in the repository do not vary in time, but a randomly sampled value from the distribution of sulphide concentrations is assumed to prevail throughout the one million years assessment period. As also shown for the reference evolution, assignment of the mean value of the distribution to all deposition holes results in lower consequences in terms of failed canisters at one million years.

No reason to pursue this pessimistic approach any further has been identified. However, some simple studies of the sensitivity of the corrosion result to the properties of the sulphide distribution are presented below. The distribution consists of 46 data points ranging from $1.2 \cdot 10^{-7}$ M representing a detection limit, to a maximum value of $1.2 \cdot 10^{-4}$ M. It is noted that the second highest value is $1.2 \cdot 10^{-5}$ M, i.e. an order of magnitude lower than the highest. Since it is only the combination of high sulphide concentrations and high flow rates that yield corrosion failures, it is of interest to study the sensitivity of the corrosion results to details of the high-end tail of the sulphide distribution. (The corresponding dependence on the high-end tail of the flow distribution is covered by the multiple realisations of the flow models.)

The following sensitivity cases are analysed:

- The highest point in the distribution i.e. $[HS^-] = 1.2 \cdot 10^{-4}$ M is deleted from the distribution.
- A point with twice the highest, i.e. $[HS^-] = 2.4 \cdot 10^{-4}$ M is added to the distribution.
- The mean value of $[HS^-]$ is used for all deposition positions. This is equivalent to saying that $[HS^-]$ at a given position will vary over time with an average value equal to the mean value of the $[HS^-]$ distribution = $5 \cdot 10^{-6}$ M.

### *Oxygen penetration*

Penetration of oxygenated groundwater to the deposition holes was ruled out in the reference evolution, see Section 10.4.7. This issue needs, however, to be analysed also for situations with increased flow caused by an ice sheet margin stationary over a repository for longer periods than expected in the reference evolution.

The understanding of oxygen penetration is discussed in Section 10.4.7. There, it is demonstrated that the degree of oxygen penetration for steady state flow conditions is controlled by:

- the duration of the steady state episode,
- the concentration of oxygen at the inlet of the flow paths,
- the extent to which microbial processes contribute to oxygen consumption,
- the surface area of the reducing minerals in the rock and the kinetics of their reactions with oxygen,
- the $F$ factors of the recharge flow paths connecting the surface to the deposition holes.

In the following, each of these factors is discussed and quantified in order to arrive at a quantitative assessment of the extent of oxygen penetration and potential consequences in terms of corrosion.

**Duration**

According to the section on glacial conditions leading to enhanced groundwater flow above, situations with 200 year and 1,000 year stillstands can be considered, with probabilities of occurrence in combination with warm-based glaciers, of 0.12 and 0.012, respectively.

**Oxygen concentration**

According to Section 10.4.7, see also /Sidborn et al. 2010/, there is a theoretical upper limit on the oxygen concentration of intruding glacial melt water of 1.5 mM. This concentration is pessimistically assumed in the following.

**Microbial activity at the surface**

As mentioned in Section 10.4.7, during a period of glaciation, the amount of degradable organic substances is uncertain, although microbial activity is observed at the surface of most glaciers, and in glacial melt water /Hallbeck 2009/. Microbial activity is pessimistically disregarded here.

**Mineral surface area and reaction kinetics**

The same data as used in Section 10.4.7 is used here. A cautious value for the specific reactive surface is used based on the size and geometric shape of biotite grains in the rock mass at Forsmark.

The pH of the water is assumed to be equal to 8. Higher pH values would result in increased mineral dissolution rates and homogeneous oxidation rates, and therefore, in an increased oxygen consumption rate, and in a decreased penetration of oxygen both into the rock matrix and along the fracture. The results are however not very dependent on the pH in the range 7 to 8, but this effect begins to be important at pH 8.5. It is indicated in /Salas et al. 2010/ that groundwaters with a large glacial meltwater component are characterised by pH values around 9, and therefore the pH value assumed here is considered cautious.

No account is taken here for the reducing capacity of fracture filling minerals. Along the fracture path, the oxygen-rich waters will encounter Fe(II) minerals which in Forsmark correspond to a concentration of Fe(II) increased by a factor of 3 in a 0.2 mm thick layer of rock adjacent to the fracture surface. This increased reducing capacity close to the fracture surface is pessimistically not included in the calculations. The effect is however discussed in the calculations reported in /Sidborn et al. 2010/.

**Diffusivity and porosity**

The penetration of oxygen is evaluated for a rock matrix having the characteristics of intact rock. Close to the fracture surface the porosity is higher, and therefore the diffusion of oxygen and other dissolved substances is faster. Because of this, the diffusion of oxygen into the rock matrix is deeper than in the present calculations, and the penetration along the fracture is shorter. Due to the difficulty of assigning cautious values for the effective diffusivity and porosity in the altered zone close to fractures, values for the bulk rock matrix are used for the base-case calculations in /Sidborn et al. 2010/, but an example of increased $D_e$ and porosity is included in that report as a parameter sensitivity analysis. The increased rock porosity close to fracture surfaces is pessimistically disregarded here.

***F* factors**

Flow-related transport resistance values for steady state recharge flow conditions with the ice margin right above the repository were reported in Section 10.4.6 and used there for assessments of penetration of dilute water. In these calculations, the flowing fractures in the part of the flow domain that hosts the repository are described with an explicit hydrogeological discrete fracture network model (DFN). This part is surrounded by two successive volumes. Next to the DFN volume, the advective flow system is modelled using an Equivalent Continuous Porous Medium (ECPM) approach based on up-scaling of a DFN representation. Outside of the ECPM, a Continuous Porous Medium (CPM) approach is used with assumed homogeneous properties. In the calculation of penetration of dilute water, only the explicit DFN part was accounted for. There is, however, no reason to disregard the part of the flow path going through the two continuum representations of the flow domain. The initial part of the recharge flow paths, i.e. close to ground surface, will predominantly be in the CPM part of the domain, and it is desirable to capture the oxygen depletion along the full flow path.

To obtain an ECPM representation of the fractures in the full domain, a variant representation of the groundwater flow model described in Section 10.3.6 was produced, namely the *Extended spatial variability case*. In this variant, an ECPM representation, based on up-scaling of an explicit discrete fracture network representation, is used throughout the regional model domain. However, the repository region is still represented by an explicit DFN, see Section 10.3.6 and /Joyce et al. 2010/ for details. Recharge particle tracking is done in this model with boundary conditions from the glacial case model presented in Section 10.4.6. Ice front locations II and III, i.e. when the ice front is in close proximity to the repository, are considered. Along the recharge flow paths, advective travel time and flow-related transport resistance are calculated for use in the calculations of oxygen penetration.

It should be noted that the model of /Joyce et al. 2010/ underestimates the length of the recharge flow paths due to the finite extent of the domain used. In the super-regional scale model of /Vidstrand et al. 2010/, recharge paths are obtained, for the corresponding ice front locations, that extend well beyond the upstream boundary of the model domain used in /Joyce et al. 2010/. Hence, the flow-related transport resistance ($F$) values used in the present assessment are likely under-predicted.

**Extent of oxygen penetration**

Using the $F$-values obtained according to the approach described above, that is, using the *Extended spatial variability case*, for ice front location III and applying the EFPC rejection criterion, 31 deposition positions out of the 6,000 experience oxygen concentrations above $10^{-7}$ M, and of these, the oxygen concentration is higher than ~1 mM for 6 positions. For ice front location II the deposition location most affected (in a different volume of the repository not affected by ice front location III), has an $O_2$ concentration slightly below 0.15 mM.

**Corrosion for diffusive conditions**

A 1,000 year exposure to 1.5 mM of $O_2$ in a fracture intersecting a deposition hole with an intact buffer yields a corrosion of about 0.3 mm in the most exposed deposition hole in the repository, for the flow conditions discussed above and assuming spalling in all deposition holes. Note that i) all deposition holes are included in this calculation, not only those for which the corresponding $F$ factors imply oxygen penetration and ii) the theoretically maximal oxygen concentration is assumed.

It is concluded that corrosion due to oxygen penetration with diffusive conditions in the deposition hole can be neglected.

**Corrosion for advective conditions**

The same corrosion model as used for sulphide corrosion for assumed advective conditions in the deposition hole was applied for the deposition positions to which oxygen was calculated to penetrate as mentioned above. The enhanced flow rates calculated for these positions were used in the corrosion calculation.

The calculations result in a corrosion rate slightly below 6 μm/yr for the deposition location mostly affected by the high $O_2$ concentration for ice front location III. The following three most affected positions have corrosion rates of 3.6, 1.7 and 0.9 μm/yr respectively. This yields corrosion depths after 1,000 years of at most 6 millimetres. A 200 year stillstand would result in a corrosion depth of about 1.2 mm for the position most affected. These corrosion depths do not include surface roughening due to localised corrosion, see below.

The following is noted.

- The particular position for which the high oxygen concentration occurs is not among those predicted to experience advective conditions in the erosion calculations carried out with the same hydrogeological DFN model (the same DFN realisation of the semi-correlated base case). This is because the hydrogeological boundary conditions for the two situations are different.
- Only ice front location III results in substantial oxygen penetration. The distance between ice front location II and III is 1.7 km. It is assumed here that for the 1,000 year duration of the ice front standstill, the ice margin does not move forth and back distances in the scale of several hundreds of metres. If the ice front should oscillate around its margin position, then the hydrogeological conditions would change in such a way that no single deposition location would be affected by oxygen penetration during any significant period of time.

- Any localised corrosion in connection with oxygen corrosion under glacial conditions would be in the form of uneven general corrosion (rather than true pitting), and as documented in the **Fuel and canister process report**, Section 3.5.4, the extent of this roughening could be estimated to be some hundred μm, for corrosion depths in the mm scale.

**Conclusion**

With the pessimistic assumptions i) that a theoretical upper limit on oxygen concentration is used, ii) that the reducing potential of fracture filling minerals and microbial processes are neglected, and iii) that no credit is taken for the fact that different canister positions are the most exposed to erosion and corrosion, respectively, and iv) that small oscillations of the ice front during the 1,000 years stillstand are not considered, then the calculated corrosion depths are in the millimetre scale. Furthermore, the probabilities of the 1,000 year and 200 year stillstands occurring during the one million year assessment period are estimated at 0.012 and 0.12, respectively. Therefore, it is concluded that effects of oxygen penetration can be excluded from the corrosion scenario.

### *Event sequences*

The sequences of events that are considered in this scenario concern the succession of climate domains with their associated variations in groundwater flow and geochemical conditions. As averages over glacial cycles are used for these entities, justified by the fact that corrosion failures generally take several glacial cycles to develop, the detailed event sequences are of secondary importance for estimation of the number and timing of the resulting corrosion failures. Hence one important aspect of the regulatory requirement on treatment of alternative climate evolutions has been addressed.

### *Quantitative sensitivity analysis of canister corrosion*

**Intact buffer**

For an intact buffer, the analysis of additional uncertainties did not result in any situations that challenge the conclusion from the reference evolution that there are considerable margins to canister failures. Therefore, no additional corrosion calculations are carried out for the case of an intact buffer.

**Advection in buffer**

In the buffer advection scenario, Section 12.2, three cases to be propagated to the corrosion scenario were identified.

- A case where advective conditions occur to the extent given by the reference evolution treated in Chapter 10.
- A bounding case where advective conditions occur in every deposition hole throughout the assessment period.
- A case where diffusive conditions are preserved in every deposition hole throughout the assessment period.

The third case corresponds to an intact buffer and has been treated above. That case does not represent a situation with advective conditions in the buffer, but is included to represent the conceptual uncertainty regarding buffer colloid release/erosion. Further understanding of that process could lead to the exclusion of colloid release from future assessments. In addition to these three cases, also the sensitivity cases based on *erosion related factors* identified in the buffer erosion scenario are studied from the point of view of corrosion below.

The uncertainty analyses of factors contributing to corrosion above have led to the following conclusions regarding base case assumptions and sensitivity cases for *corrosion related factors*.

- The initial copper coverage is assumed to be 47 mm, as in the reference evolution.
- EFPC rejection of deposition positions is applied.
- Corrosion due to impurities in buffer and backfill is neglected.
- Buffer diffusion is irrelevant for the advection case. However, before advective conditions arise, diffusion controlled sulphide corrosion in a partially eroded buffer will occur. The extent of this corrosion is difficult to quantify. Here, the case with initial advection in all deposition holes puts

a bound also on the extent of corrosion with a partially eroded buffer followed by corrosion under advective conditions.

- The cautious corrosion geometry from the reference evolution is used, with the bounding pessimistic geometry as a sensitivity case.
- Regarding flow conditions, the three cases of uncorrelated, semi-correlated and fully correlated relations between fracture length and transmissivity are propagated to corrosion calculations. Temperate flow conditions are pessimistically assumed and glacier stillstands are disregarded for sulphide corrosion since they give negligible additional contributions.
- As in the reference evolution, present day sulphide concentrations are pessimistically assumed and, also pessimistically, a deposition position is assumed to experience the same, randomly sampled sulphide concentration throughout the assessment period. Three sensitivity cases are defined to study the sensitivity to the properties of the sulphide distribution.
- Corrosion contributions from oxygen penetration are disregarded, since they are unlikely and, also with a number of pessimistic assumptions, limited in extent.

A base case using all ten realisations of the semi-correlated hydrogeological DFN model, the site specific sulphide distribution and base case assumptions regarding buffer erosion yields on average 0.12 failed canisters in one million years as already reported in the reference evolution, Section 10.4.9.

The sensitivity to uncertainties in *erosion related factors* is studied by calculating the number of failed canisters for the sensitivity cases for buffer erosion studied in the buffer advection scenario, Section 12.2.2. The results are shown in Figure 12-16, which thus corresponds to the erosion cases in Figure 12-3 of Section 12.2.2, but where the cases F, H and J with initial advection have been added.

As seen in the Figure, the sensitivity to all assumptions regarding buffer erosion is limited. The highest impact is obtained for the different hydrogeological DFN models. It is noteworthy that even assuming advective conditions initially in all deposition holes has a limited impact on the extent of corrosion for a given hydrogeological model variant. This finding justifies the simplification of only propagating the base case and the two bounding cases from the analysis of buffer erosion.

Figure 12-17 shows results of the sensitivity cases based on uncertainties in *corrosion related factors* identified above, i.e. sensitivities related to the distribution of sulphide concentrations and to the corrosion geometry. (The impact of the different hydrogeological DFN models is shown in Figure 12-16). The cases show the following.

- Assuming the mean value of $[HS^-]$ for all deposition positions, which is equivalent to assuming that $[HS^-]$ at a given position will vary over time with an average equal to the mean value of the entire $[HS^-]$-distribution, i.e. $5 \cdot 10^{-6}$ M, yields no corrosion failures for the semi-correlated hydrogeological DFN model. The same result is obtained with the uncorrelated and the fully correlated hydro DFN models (not shown in the Figure). This is a significant result. Although it cannot be justified to assume a temporal variability that is represented by the given sulphide distribution, it is not unreasonable to assume that the sulphide concentrations would vary over time and thus serve to reduce the expected number of canister failures considerably. The result is a reflection of the fact that canister failures occur only when the highest flow rates are combined with the highest sulphide concentrations, and when both these entities are pessimistically assumed to be constant in time over the entire one million year assessment period for a given deposition position.
- Omitting or adding another data point with the highest sulphide concentration, i.e. 0.12 mM, has a significant impact on the result. As mentioned above this point is about one order of magnitude higher than the next highest point in the distribution.
- Assuming the unrealistic, pessimistic corrosion geometry leads to an increase in the mean number of failed canisters by about a factor of five meaning that the dependence is roughly inversely proportional to the exposed canister surface in this case.

Full documentation of all calculations of buffer erosion/colloid release and canister corrosion is given in /SKB 2010d/.

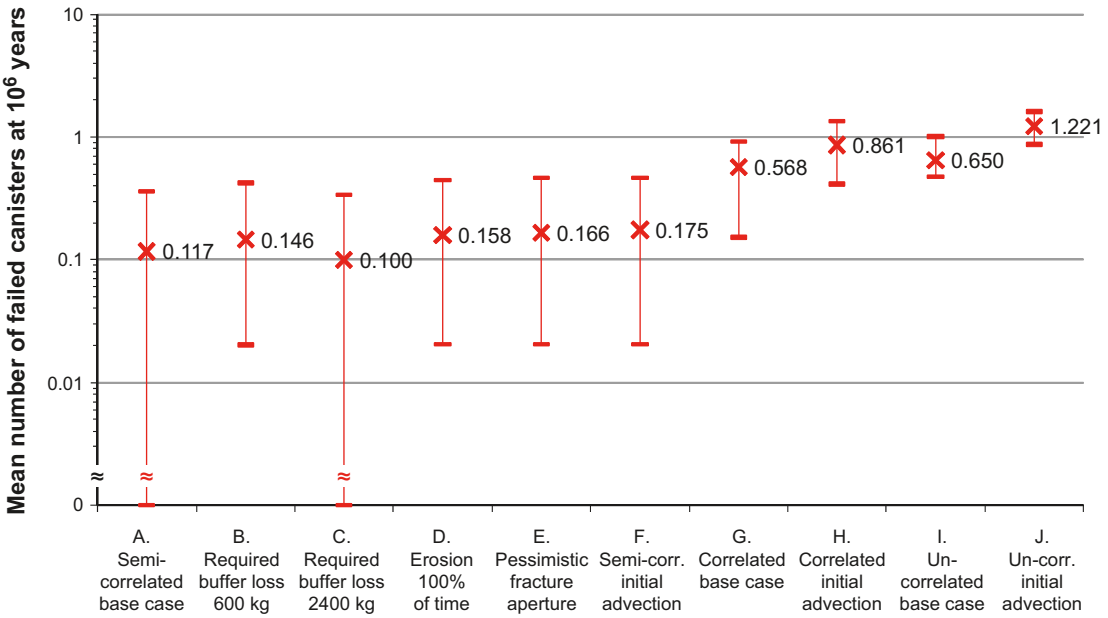


***Figure 12-16.*** *Calculated mean number of failed canisters at one million years for the sensitivity cases identified in the buffer advection scenario, Figure 12-3 in Section 12.2.2, and with base case assumption for corrosion. The crosses denote mean values and the bars denote the variability over the several realisations of the hydrogeological DFN models.*

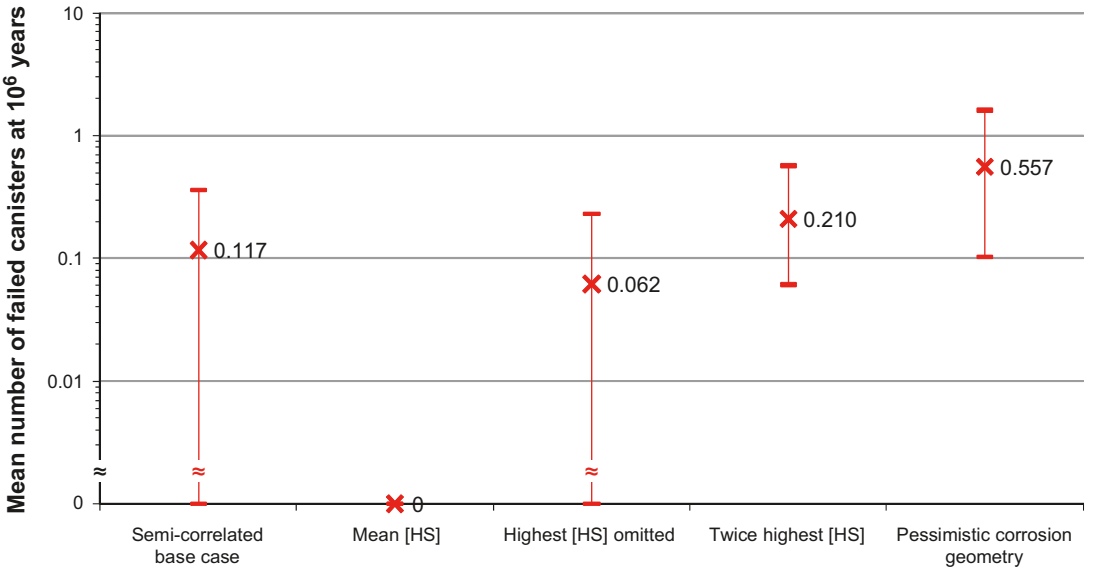


***Figure 12-17.*** *Calculated mean number of failed canisters at one million years for the sensitivity cases identified in the corrosion scenario and with base case assumptions for erosion. The crosses denote mean values and the bars denote the variability over the several realisations of the hydrogeological DFN models.*

### 12.6.3 Conclusions

The canister failure due to corrosion scenario is a less probable scenario, since this type of canister failure cannot be ruled out in the one million year assessment period.

For the assessment of consequences in terms of dose and risk, the three buffer cases (no advection, erosion according to the SR-Site model, initial advection) need to be combined with the three hydrogeological DFN models, with the base case assumptions used above for other erosion and corrosion related parameters. Evidently, the bounding case where advective conditions occur in every deposition hole throughout the assessment period is unrealistic, but this case is still kept within the scenario, to illustrate the impact of the uncertainties covered by this case.

Figure 12-18 shows the cases that have been formulated for the corrosion scenario. The three hydrogeological DFN model variants of the Forsmark site are included to cover uncertainties in the correlation structure (blue objects). The next branching represents the three cases of buffer advection (red) propagated from the buffer advection scenario. Finally, the mean number of failed canisters calculated for each of the situations is given in orange.

The case with the semi-correlated hydrogeological DFN variant combined with the SR-Site model for buffer erosion is seen as a *central corrosion variant*, based on which assessments of radionuclide transport and dose should primarily be made. This position is adopted because of the following considerations.

- The semi-correlated DFN model is more compatible with site data than the other two variants since its description of the relation between fracture size and transmissivity is most consistent with observations.
- The SR-Site model for buffer erosion is the best available representation of current knowledge of this process, although there are conceptual uncertainties associated with the model.

The remaining combinations of hydro DFN models and erosion cases are seen as illustrative cases providing bounds on uncertainties in the aspects of corrosion they represent.

The cases discussed above are propagated to analyses of the retardation potential for the corrosion scenario, Section 13.5.

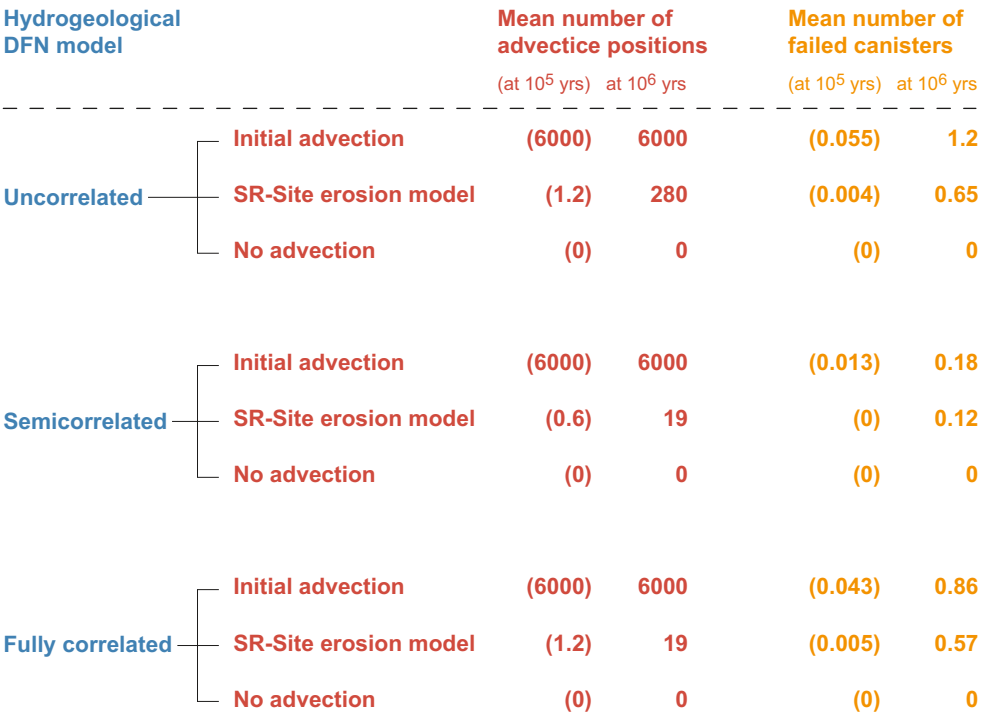


***Figure 12-18.*** *Mean number of advective deposition positions and mean number of failed canisters for the calculation cases identified as relevant for the corrosion scenario.*

#### *Global warming variant and other climate cases*

The above conclusions are valid also in relation to the global warming variant of the reference evolution. Such a variant could possibly impact negatively on the extent of erosion during the initial temperate period. In the one million year assessment period, this impact is very limited and it is covered by the case with initial advection in all deposition holes. Nor do any of the other climate cases described in Section 12.1.3 have any relevance for the corrosion scenario.

## 12.7 Canister failure due to isostatic load

### 12.7.1 Introduction

#### *Safety function indicator(s) considered*

This scenario concerns the safety function relating to the canister's ability to withstand isostatic loads, safety function Can2.

This safety function is directly related to containment, as the containment is assumed to be breached if the safety function is not maintained.

#### *Treatment of this issue in the reference evolution*

Canister failure due to isostatic load was not included in the reference evolution, since peak loads in the reference evolution (43.5 MPa) are below the design load of the canister (45 MPa).

#### *Propagated buffer conditions*

According to Section 12.5, three different buffer conditions are propagated to the canister scenarios. Two of these concern advective conditions in the buffer and the third is the intact buffer. Since advective conditions are related to an eroded buffer which has a lower swelling pressure than an intact buffer, such conditions are less likely to induce isostatic collapse.

Furthermore, in Section 12.3, it was concluded that neither an intact buffer nor groundwater in potential buffer erosion cavities will freeze, not even for pessimistic assumptions of future climate conditions at the Forsmark site.

Based on these considerations, only the intact buffer is further treated in the analysis of potential canister failures due to isostatic load.

#### *Qualitative description of routes to canister failure due to isostatic load (including initial state aspects and external conditions)*

The evolution in this scenario is assumed to be identical to that of the reference glacial cycle variant of the reference evolution, except for factors related to isostatic collapse of a canister.

According to the FEP chart, this safety function would be jeopardised if the isostatic load on the canister, determined by the groundwater pressure, equal to the buffer porewater pressure, and the buffer swelling pressure, exceeds the design load of 45 MPa.

The groundwater pressure is determined by repository depth for non-glacial conditions. For the Forsmark site, this means pressures of around 4.5 MPa. For glacial conditions the alteration of the hydrostatic pressure due to the presence of the ice sheet is added. This pressure is, in the reference evolution, assumed to correspond to the maximum ice thickness at the site, as it cannot be significantly greater than this. At Forsmark, the additional hydrostatic pressure is 26 MPa, see Section 10.4.1.

The buffer swelling pressure is determined by the buffer density and chemical composition, including the species of adsorbed cation. In the reference evolution, the maximum buffer swelling pressure, corresponding to an unaltered buffer of 2,050 kg/m$^3$ (the upper limit of the reference density interval), was determined to 13 MPa.

The following factors of importance for the occurrence of canister failure due to isostatic load are identified, based on the discussion above, on Table 10-27 describing uncertainties identified in the reference evolution and on the FEP chart, Figure 8-4.

**Initial state factors involved**

- Canister strength.
- Buffer density.
- Repository depth (determining groundwater pressure if no glacial load).

**Processes involved**

- Buffer swelling.
- Buffer chemical alterations and density losses.
- Convergence of deposition hole.

**External conditions involved**

- Ice sheet thickness and hydrology.

These factors are discussed quantitatively in the following under the three headings glacial load, buffer swelling pressure and canister strength.

### 12.7.2 Glacial load

#### *Introduction*

As mentioned in Section 10.4.1, for glacial conditions an additional hydrostatic pressure related to the ice sheet thickness is added to the hydrostatic pressure for ice free conditions. The extremes regarding hydrostatic pressure in the glacial climate domain depend on the ice sheet configuration and on its hydraulic systems. Under the Antarctic ice sheet, sub-glacial lakes have been observed. The hydrostatic pressure in these lakes is typically assumed to correspond to the ice overburden pressure. A hydro-thermo-mechanical balance is assumed, where supply of basal melt water, re-freezing and ice deformation result in a hydrostatic equilibrium where the ice sheet rests, or floats, on the water surface, e.g. /Pattyn et al. 2004/. As further justified below, it is reasonable to assume that also for the Fennoscandian ice sheet, the maximum ice sheet thickness sets a limit to the maximum hydrostatic pressure that may occur at the ice sheet bed-substrate interface.

#### *Sensitivity to climate forcing*

To investigate the maximum ice sheet thickness that may occur in Fennoscandia, the ice sheet model described in Section 10.4.1 was run using a set of temperature evolutions where local annual air temperatures were decreased linearly by 1°C per 2,000 years, from present-day temperatures down to various constant levels. In these sensitivity tests, temperatures were lowered between 4 and 16°C, see Figure 12-19 and in the **Climate report**, Section 5.4. In these calculations, ice sheets only develop for temperature lowerings of 7°C and more (Figure 12-19). In all cases, the ice sheet model simulated a total time period of 100,000 years, after which approximate steady-state conditions were obtained with little further change in ice volume and area. The resulting maximum ice sheet thicknesses are shown in Figure 12-20.

As expected, the maximum ice sheet thickness increases with colder climates (Figure 12-20, black line). However, the degree of increase in thickness with temperature lowering declines as colder cases are considered. For a temperature lowering of more than approximately 13°C, colder climates do not generate thicker ice sheets. The model result that there is such a limit on the maximum ice thickness, is in line with what is known of Antarctic ice-sheet variations, see below.

These simulated temperature cases are extreme as regards their prolonged duration. Variations in temperature of this magnitude have occurred in the past, e.g. /Dansgaard et al. 1993/, but never of this long duration without interruptions, see the **Climate report**, Section 4.3.4. The extreme nature of these sensitivity cases is reflected also in the resulting ice sheet configurations for the colder cases.

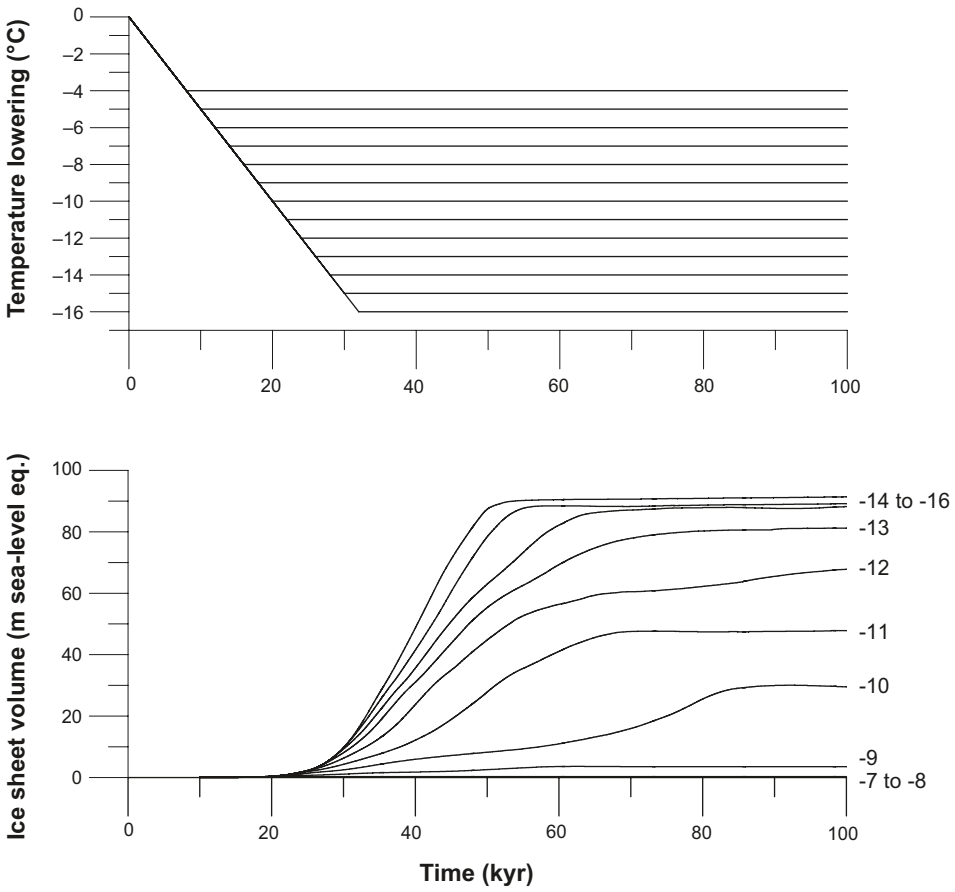


***Figure 12-19.*** *Temperature lowering schemes (upper graph) and resulting development of Fennoscandian/ Eurasian ice-sheet volume (lower graph).*

Here, the ice sheet covers all of northern and central Europe, and extends southward all the way to the Alps. Geological observations of traces from Fennoscandian ice sheets show that such large ice configurations have never occurred during the Quaternary period, and can thus be considered unrealistic.

The maximum ice thickness for Forsmark in the reference glacial cycle was 2,920 metres (Figure 12-20). In the sensitivity tests, the maximum ice sheet thicknesses developed at Forsmark were 3,670 metres. The uniform and high values reflect that the site has an interior location within these unrealistically large ice sheets. For more information on these simulations and motivation for considering these extreme ice sheets unrealistic, see the **Climate report**, Section 5.4.

### *Estimate of maximum ice thickness at Forsmark during the past 2 million years*

From geological information, it is known that the maximum ice extent of Pleistocene Fennoscandian ice sheets (i.e. those occurring during the past ~2 million years) were larger than that of the Weichselian ice sheet, and occurred during the Saalian glaciation, e.g. /Svendsen et al. 1999, 2004, Lambeck et al. 2006, Colleoni et al. 2009/. At the peak of the Saalian glaciation, around 140,000 years BP, the ice sheet reached up to c. 200 km further south and more than 1,000 km further east than the Weichselian ice sheet. Modelling of the maximum Saalian ice sheet configuration indicated that the maximum ice thickness of this ice sheet was c. 3,200 m over the Forsmark region, see the **Climate report**, Section 5.4. According to /Lambeck et al. 2006/ the maximum Saalian ice thickness over the Forsmark region at 140,000 years BP was around 3,400 m. Similar values may be inferred from /Colleoni et al. 2009/. Based on this information, the maximum expected ice sheet thickness for Forsmark is set to 3,400 m. From the results of the extreme cases in the sensitivity test (Figure 12-20), it is unlikely that the ice thickness at Forsmark could, under any circumstances, exceed 3,700 metres. The results of the sensitivity tests can be considered as high values since it is unlikely that a Fennoscandian ice sheet would, in reality, ever reach its maximum equilibrium size, i.e. the sizes simulated in these experiments. For a description of uncertainties in the model simulations, see the **Climate report**, Sections 3.1.4, 3.1.7 and 5.4.2.

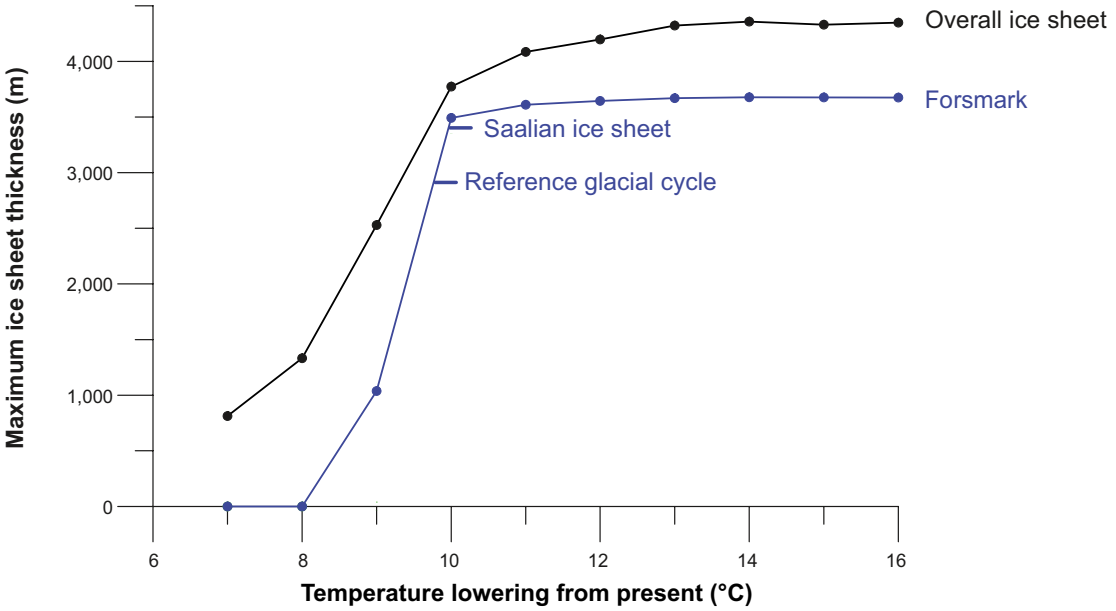


***Figure 12-20.*** *Maximum modelled ice sheet thicknesses for the schematic climate evolutions in Figure 12-19. The curves represent maximum ice thicknesses for the Forsmark region (blue) and the overall largest ice-sheet thickness (black). The short lines marked Reference glacial cycle show the maximum ice thickness obtained for that case. Short lines marked Saalian ice sheet show the estimated maximum ice thickness for the largest ice sheet configuration during the past 2 million years supported by geological observations, see the* ***Climate report****, Section 5.4.*

### *Estimate of maximum overall ice sheet thicknesses during the past 2 million years*

In the climate cooling sensitivity tests, the maximum simulated *overall* thickness of the ice sheets is 4,360 metres. This is 1,000 m more than the maximum overall ice thickness of the reference glacial cycle which is 3,300 metres. Estimating the maximum thickness of the largest geologically feasible Pleistocene ice sheet yields a maximum *overall* Saalian ice thickness of 3,600 metres. Other simulations of the Saalian ice sheet result in a maximum ice thickness of 4,500 m, over the Kara Sea in the Arctic /Lambeck et al. 2006/.

For comparison, the maximum ice sheet thickness occurring on Earth today is ~4,500 m for parts of the East Antarctic ice sheet /Lythe et al. 2001/. The Greenland ice sheet has a maximum thickness of ~3,400 m /Bamber et al. 2001/. In a colder glacial climate, the maximum ice thickness of the Antarctic ice sheet will probably not change significantly. In a colder climate, the marginal parts of the Antarctic ice sheet grow significantly, whereas, at the same time, more interior parts keep the same thickness or even gets thinner due to moisture starvation /Huybrechts 1990, Näslund et al. 2000/. Therefore, it is likely that the maximum thickness of the Antarctic ice sheet seen also over an entire glacial cycle is around 4,500 m. This value is close to the largest overall ice thickness obtained in the sensitivity test, 4,360 metres (Figure 12-20). These results are also in line with a largest inferred thickness of the Laurentide ice sheet of 4,300 metres /Tarasov and Peltier 2004/. These observations and results suggest that Pleistocene ice sheets up to date have not grown thicker than approximately 4,500 m, which gives an upper limit for ice sheet thickness.

### *Hydrostatic pressures exceeding ice overburden pressure*

Hydrostatic pressures exceeding ice overburden can occur in some situations, for example in relation to jökulhlaups, i.e. large sudden outburst floods of glacial melt water from subglacial or supraglacial ice-dammed water reservoirs /Roberts et al. 2000/. In a few cases, higher pressures of non-jökulhlaup origin have been registered also in the ablation area of smaller glaciers. These high pressures are of artesian character, with the amount of pressure being ultimately determined by upglacier ice thickness and the presence of meltwater. This may also occur in near-frontal parts of ice sheets /Roberts 2005/. However, during times of maximum ice sheet thickness over Forsmark, e.g. during the Last Glacial

Maximum, these site is located within the ice sheet interior, far from the ablation area and the margin. For this ice sheet configuration, surface melting is thus absent or negligible above and upstream of the Forsmark site, due to the high ice surface elevation and associated low air temperatures. In addition, climate is at its coldest at this time during the glacial cycle, also precluding surface melt in these high-polar regions of the ice sheet. Therefore, it is reasonable to assume that maximum hydrostatic pressures at Forsmark are dependent only on the local ice thickness during periods of maximum ice thickness, and not on ice thickness and surface melting upstream of the site.

#### *Conclusions*

For the reference glacial cycle, the additional hydrostatic pressure related to ice thickness over Forsmark is 26 MPa (Table 12-2). The *maximum* expected additional hydrostatic pressure, pessimistically derived from the largest ice sheet configuration during the past 2 million years, as supported by geological observations, is 30 MPa. Adding the hydrostatic pressure for ice free conditions, 4.5 MPa, yields a total maximum hydrostatic pressure at Forsmark of 34.5 MPa. Maximum ice thicknesses of the more extreme and unrealistic ice sheet configurations discussed above, with associated additional hydrostatic pressures, are also presented in Table 12-2.

**Table 12-2. Maximum ice sheet thickness and associated additional hydrostatic pressure at Forsmark for various Fennoscandian ice sheet configurations.**

| | Maximum ice thickness (m) | Hydrostatic pressure contribution (MPa) |
|---|---|---|
| **Reference glacial cycle** | 2,920 | 26 |
| **Largest Fennoscandian ice sheet during past 2 Myrs (Saalian ice sheet)** | 3,400 | 30 |
| **Extreme ice sheets from climate sensitivity test** | 3,670 | 32 |

### 12.7.3 Buffer swelling pressure

#### *Buffer initial density*

The saturated density of the buffer according to the reference design is 1,950–2,050 kg/m$^3$. The initial diameter of the deposition hole cannot reasonably be smaller than the reference value of 1.75 m since this is determined by the diameter of the boring machine. Furthermore, the diameter of the hole will be inspected before being accepted for deposition, as further described in the **Underground openings construction report**.

The upper reference density limit of 2,050 kg/m$^3$ results in around 13 MPa swelling pressure for MX-80 and Ibeco RWC according to Figure 5-14. For the maximum allowed montmorillonite content this would yield a swelling pressure of around 15 MPa /Karnland 2010/. It is, furthermore, noted that a saturated clay density of 2,100 kg/m$^3$ yields both a calculated and experimentally observed swelling pressure of around 21 MPa.

According to Section 5.5.3, the maximum saturated density around the canister will be 2,022 kg/m$^3$ if no spalling occurs (spalling will lead to a lower density). The upper density limit of 2,050 kg/m$^3$ is therefore seen as pessimistic.

It is also noted that the total stress on the canister is not the sum of the bentonite swelling pressure and the hydrostatic pressure. According to /Harrington and Birchall 2007/ the total stress σ can be expressed as:

$$\sigma = \Pi + \alpha\, p_w$$

where Π is the original swelling pressure, $p_w$ is the porewater pressure and α a constant of proportionality. Experimentally, α has been found to be in the range of 0.86–0.92. In the experiments by /Harrington and Birchall 2007/ with MX-80 with an original swelling pressure of ~8 MPa the bentonite retains a proportion of its original swelling ranging between 48 and 67% at porewater pressures of 46 MPa. There are indications of a reduction in the rate of decline in swelling pressure

as backpressure increases, indicative of a rise in α values at high water pressures. Linear regression suggests α = 1 at a porewater pressure of around 64 MPa.

Based on the findings by /Harrington and Birchall 2007/, for a hydrostatic pressure of 34.5 MPa and a swelling pressure of 15 MPa, the total pressure is estimated at around 46.7 MPa (15 MPa + 0.92·34.5 MPa).

#### *Buffer compaction*

The buffer will have a higher swelling pressure than the backfill in a saturated state. No compaction of the buffer from the swelling of the backfill is therefore expected. However, there is a possibility that the backfill will saturate and develop its swelling pressure ahead of the buffer. This situation has not been directly evaluated in SR-Site, but it is briefly discussed in /Börgesson and Hernelind 2009/, where it is stated that the case is not of primary interest since there will be very little compression of the buffer blocks and rings and the uniaxial compression strength of the blocks is in the same range as the fully developed swelling pressure from the backfill.

#### *Buffer chemical alterations and density losses*

The buffer swelling pressure is determined by the buffer density and chemical composition, including the species of adsorbed cation. All identified chemical changes (ion exchange, osmosis and mineral transformation, see Section 10.3.10) of the buffer result in unaltered or decreased swelling pressure (possibly with the exception of a marginal effect for high density Ca bentonite). It is, therefore, pessimistically assumed that no such changes take place.

According to the FEP chart, the mechanisms through which buffer mass may be lost are piping, erosion or swelling into the deposition tunnel. It is pessimistically assumed that no buffer mass is lost over time due to these processes.

#### *Conceptual uncertainties*

No process has been identified that could increase the swelling of the buffer to a higher value than the original starting value. The pressure is expected to be as specified above or lower for all possible conditions.

#### *Convergence of deposition holes*

A possible issue is the convergence of deposition holes. No residual uncertainty has been identified that would challenge the conclusion from the reference evolution, namely that convergence effects are negligible, see Section 10.3.5.

### 12.7.4 Canister strength

As mentioned in Section 5.4.3, extensive analyses of the canister's ability to withstand isostatic load have been undertaken as part of the canister design analysis /Raiko et al. 2010/. These analyses are focussed on demonstrating that the canister can withstand the design load of 45 MPa. It is demonstrated that this is achieved with considerable margin, both as regards avoidance of local plastic collapse of the insert due to variation in material properties and allowed defect sizes in relation to expected and detectable defects. It is likely that with these local properties of the insert, the canister can be demonstrated to withstand considerably higher loads, but the limit has not been quantified. It has also been demonstrated that the insert can be manufactured with a fully sufficient accuracy regarding its critical dimensions relating to isostatic loads.

Also, the global collapse load for the cylindrical part of a canister (without defects) has been calculated to 99 MPa and 128 MPa for BWR and PWR inserts, respectively /Raiko et al. 2010/. Results from pressure tests of real canisters show that the collapse load for the canister is approximately 100 MPa or higher /Raiko et al. 2010/.

Hence, the following conclusions are drawn.

- *Total collapse*, i.e. the criterion for canister failure, of the insert is not expected to occur below at least 90 MPa according to both model calculations and laboratory tests.
- *Local collapse* is excluded for loads up to 45 MPa with a considerable margin.

### 12.7.5 Combined assessment

According to Section 12.7.3, a maximum swelling pressure of 15 MPa could occur in the buffer.

The groundwater pressure is around 4.5 MPa at Forsmark for ice-free conditions. According to Section 12.7.2, an additional ground water pressure of at most 30 MPa could occur as a result of a maximum glacial load supported by geological evidence.

This would give a maximum feasible isostatic load on the canister of 49.5 MPa at Forsmark if the hydrostatic and swelling pressures are added. However, applying an α-value of 0.92 in the addition as suggested in Section 12.7.3 results in a total pressure of around 46.5 MPa.

According to Section 12.7.4, local collapse is avoided with substantial margin for 45 MPa, suggesting that local collapse would be avoided also at 49.5 MPa. The margin to total collapse (90 MPa), i.e. the criterion for canister failure, is considerable.

Overall, the following conclusions can be drawn.

- Total collapse is the relevant failure criterion since only this type of failure will lead to the release of radionuclides from the canister.
- There is ample margin to prevent canister failure due to isostatic load, even for the most extreme load situations.

#### *Different event sequences*

There are no different event sequences to consider in the discussion of this scenario, since pessimistic assumptions are made and maximum effects are sought for all involved factors. During the one million year assessment time, the canister will be subjected to some eight glaciations leading to repeated load cycles. The number of events is, however, far too low to have any fatigue effect on the mechanical stability of the cast iron insert.

#### *Combination of isostatic load and shear movement*

See the shear load scenario, Section 12.8.2, where it is concluded that the combined case can be excluded from consideration.

#### *Global warming variant and other climate cases*

The occurrence of high groundwater pressures is directly related to glacial conditions. The delay of glacial conditions expected for the global warming variant would thus be beneficial for repository safety in this respect. The issue is therefore not further treated for the global warming variant.

Since the *maximum ice sheet configuration* climate case (see Section 12.1.3) has been used in the above analysis and since that case was defined to maximise the isostatic load on the canister, no additional climate cases need to be considered.

#### *Categorisation as "less probable" or "residual" scenario*

Based on the above assessment, this scenario, i.e. a canister failure due to isostatic load, is considered as "residual", meaning that its consequences are excluded from the risk summation.

The consequences in terms of radionuclide transport and annual effective dose of a postulated isostatic collapse are addressed in Section 13.7.1.

## 12.8 Canister failure due to shear load

### 12.8.1 Introduction

#### *Safety function indicator(s) considered*

This scenario primarily concerns the safety function relating to shear loads on the canister. If the shear load on the canister is too large, the canister is assumed to lose its containment capacity (safety function Can3).

Safety function indicators and criteria relevant to the evaluation of this failure mode are i) the requirement that shearing across the deposition hole should be less than 0.05 m (R3b) and ii) that the saturated buffer density must not exceed 2,050 kg/m$^3$ for the R3b criterion to be applicable (Buff 3).

This safety function is directly related to containment, as the containment is assumed to be breached if the safety function indicator criterion R3b is violated. Should this occur, also the retarding capacity of the system is affected, since the rock shear event is assumed to affect the retarding properties of the buffer and the rock negatively.

#### *Treatment of failure due to shear load in the reference evolution*

The possibility of canister failure due to shear load is of low probability and is, therefore, excluded from the reference evolution, see Section 12.1.2. This is motivated by the results of the analysis of the reference evolution reported in Section 10.4.5.

The analysis below evaluates whether all uncertainties were appropriately considered in the reference evolution and also provides an upper bound on the likelihood for canister failures due to shear load.

This upper bound is related to the result of the pessimistically derived frequency of canister failures due to shear loads in Section 10.4.5 and illustrated in Figure 10-124.

#### *Qualitative description of routes to failure due to shear load*

The evolution in this scenario is assumed to be identical to that of the base case of the reference evolution, except for factors related to collapse of the canister due to shear load.

As indicated in the FEP chart, the ability of the cast iron insert to withstand shear loads is determined by the canister design and by the quality of the production and NDT (non-destructive testing). The shear stress on the canister is determined by the nature of the slip along the fracture intersecting the deposition hole and the way in which this shear load is propagated through the buffer. The buffer density affects this propagation, meaning that the initial buffer density must be evaluated. The shear load is determined by the likelihood that the deposition hole is intersected by a fracture of a particular size, which, in turn, depends on the properties of the fracture network within the host rock and the likelihood with which unsuitable fractures can be detected and avoided in deposition holes.

Also the likelihood that earthquakes of a sufficient magnitude will occur during the assessment period needs to be evaluated.

The following factors of importance for possible occurrence of a canister failure due to shear load are identified, based on the discussion above, on Table 10-27 describing uncertainties identified in the reference evolution and on the FEP chart, Figure 8-4.

**Initial state factors involved**

- Insert strength and the occurrence of defects (casting quality).
- Copper shell mechanical properties.
- Buffer density.
- Buffer material properties.
- Fracture network properties.
- Efficiency in the implementation of deposition hole rejection.

**Processes involved**

- Canister: Deformation of copper canister; creep.
- Canister: Deformation of cast iron insert.
- Buffer: Swelling/mass redistribution.
- Buffer transformation.
- Geosphere: Reactivation of fractures as a consequence of earthquakes.

**External conditions involved**

- Earthquakes.

#### *Propagated buffer conditions*

According to Section 12.5, three different buffer conditions are propagated to the canister scenarios. Two of these concern advective conditions in the buffer and the third is the intact buffer. Since advective conditions are related to an eroded buffer which has a lowered swelling pressure than an intact buffer, such conditions are of less concern when canister failures due to shearing are evaluated. Therefore, only the intact buffer is further treated in the analysis of canister failures due to shear loads and it is evaluated if the intact buffer may under any circumstances have a higher density than that specified in the initial state. (In addition, the transformed buffer is discussed as a residual case below.)

### 12.8.2 Quantitative assessment of routes to canister failure by shear load

The response of the canister-buffer system to shear loads has been extensively studied within the canister design analysis /Raiko et al. 2010/, forming an important basis for the **Canister production report**. The aim of those studies has been to establish that the canister fulfils the design premise stating that the copper corrosion barrier should remain intact after a 5 cm rock shear movement at 1 m/s for buffer material properties of a 2,050 kg/m$^3$ Ca-bentonite. This applies for all locations and angles of the shearing fracture in the deposition hole, and for temperatures down to 0°C. The insert should maintain its pressure-bearing properties to isostatic loads after such shear movements.

In the design analysis a number of the factors listed above are by necessity taken into account and evaluated. This regards the following factors related to the initial state: the strength of the insert, the copper shell mechanical properties, the buffer density and the buffer material properties. The design analysis also considers deformation of the copper canister and the cast iron insert, including creep in the copper.

The overall conclusion of the design analysis is that the canister fulfils the design premise relating to shear load, as further discussed in Section 5.4.3. In the design analysis report, this conclusion is reached after discussing all relevant uncertainties of the phenomena included in the analysis, i.e. uncertainties in the above mentioned initial state factors and processes have been considered. These are, therefore, not discussed here.

The design analysis considers material properties down to 0°C in accordance with the design premise. As demonstrated in the buffer freezing scenario, Section 12.3, temperatures below 0°C are ruled out for the Forsmark site, meaning that the results of the design analysis are valid for all relevant temperatures in the repository.

Consequences of alterations of the buffer are discussed in Section 10.4.5, and argued to be of no concern, in a stylised calculation case where a substantial part of the buffer is assumed to be cemented. This, in combination with the fact that buffer alteration is considered to be a residual scenario in Section 12.4, yields the conclusion that buffer alterations are not a concern for the shear load scenario.

In the reference evolution, Section 10.4.5, it is argued that there is a margin in the results obtained in the design analysis such that, in many of the shearing cases analysed, e.g. for different angles of intersection and points of impact, there is evidence that the canister would in fact sustain also the load from a 10 cm shearing. This is further strengthened by the fact that the initial state of the buffer resulting from an analysis of the reference procedures for buffer production and installation yields

an upper limit on buffer density of 2,022 kg/m$^3$, which is lower than the design premise upper limit of 2,050 kg/m$^3$. Also, the failure criterion for the canister is the acceptable defect size for surface defects in the insert. The copper shell is assumed to be penetrated at the same moment as this criterion is exceeded. The strains in the copper shell are low (with the exception of model singularities) compared to copper material ductility requirements. However, uncertainties due to a copper thickness of slightly less than 50 mm are not evaluated.

In the following, uncertainties relating to factors associated with the geosphere are discussed.

#### *Fracture network*

The discrete fracture network (DFN) uncertainties are treated by the use of alternative DFN models that together span a wide range of uncertainties (see the **Data report** for details). In the reference evolution (Section 10.4.5), all three DFN models suggested for the Forsmark site were propagated through all calculations, which resulted in a range (min-max) of the number of potentially damaged canisters. In deriving the frequency of canister failures as a function of time in Section 10.4.5, the maximum value of this range was chosen.

Further, for the analyses summarised in Section 10.4.5, all earthquakes were pessimistically assumed to occur on the deformation zone (A2) that affects the largest number of canisters. Also, as argued in /Munier 2010/, the use of FPI criteria considerably lessens the impact of DFN uncertainties on the number of canisters intersected by potentially critical fractures.

#### *Efficiency in the implementation of deposition hole rejection*

The number of canisters that may fail due to shear load during the assessment period depends on the success of detecting and avoiding large fractures in deposition holes. The EFPC deposition hole rejection criterion has been shown to be effective in finding critical structures and enables the detection of > 97% of the critical canister positions irrespective of DFN model /Munier 2010/. The remaining positions are propagated to the assessment of seismic impact (Section 10.4.5). However, the EFPC simulations are based on idealisations of fractures as being perfectly planar, infinitely thin discs for computational convenience. Most real fractures are not so anonymous and, rather, display many properties that can be used as proxies for size /Cosgrove et al. 2006/. It is therefore, likely, as argued in /Munier 2010/, that critical fractures that escaped detection in the simulations used as input for this assessment will indeed be detected by a carefully designed investigation programme /SKB 2010b/. Hence, it is likely that the number of potentially damaged canisters will be lower than predicted in this assessment.

#### *Earthquakes, in particular those of post-glacial origin*

The largest uncertainty concerns the estimated frequency of earthquakes during different time frames. In the reference evolution (Section 10.4.5) all relevant estimates of long-term earthquake frequencies were considered, thereby enabling the definition of a frequency range. This frequency range was then combined with the range of the number of critically positioned canisters to yield, eventually, a range of numbers of potentially damaged canisters.

In deriving the frequency of canister failures as a function of time in Section 10.4.5, the maximum value of this range was chosen.

#### *Reactivation of fractures as a consequence of earthquakes*

Uncertainties regarding the reactivation of fractures as a consequence of earthquakes are discussed in the reference evolution, Section 10.4.5. Several pessimistic approaches are used when quantifying the reactivation of fractures and these are not repeated here.

#### *Combination with isostatic load*

As discussed in Section 10.4.5, the stability of fractures in the rock is increased during periods of high isostatic load. This is a consequence of how stresses in the upper crust are expected to develop as a

result of a typical future glacial cycle according to analyses of large scale ice-crust-mantle interactions /Lund et al. 2009/. Accordingly, the combined effects of high isotatic pressures and shear load across canisters do not have to be further considered.

#### *Cumulative effects of several earthquakes*

The induced slip on large fractures, as a response to an earthquake, might be less than the canister failure criterion due to the fracture's position, orientation, local stress field and other properties. However, it is possible that slips along a particular fracture might accumulate to exceed the failure criterion as a response to repeated large earthquakes.

It is questionable if large earthquakes can be treated as independent events, which is implied by the above use of a time-independent, frequency based approach. In fact, large earthquakes within a glacial cycle are most probably *dependent* events such that the release of elastic energy relaxes the fault so that another large earthquake along the same fault is less likely. Similarly, but on another scale, slip relaxes the target fracture such that a repeated slip is less likely, and in particular slip of the same amount and orientation.

By taking strain rate into consideration, the time necessary for a fault to accumulate sufficient stress for a repeated earthquake was estimated in Section 10.4.5. With the assumptions made in Section 10.4.5, it was estimated that a maximum of 2 large seismic events can occur on the same fault within the assessment period of $10^6$ years. The slip vectors on the fractures crossing the canisters were then pessimitically assumed to be perfectly parallel which implicitly assumes that the same zone reactivates and that the earthquake mechanism (slip velocity, stress drop, shear mode, etc.) is identical. The positive effect of buffer restoration between the seismic events was disregarded and, further, a constant slip velocity (1 m/s) regardless of displacement on target fractures was assumed. Altogether, therefore, the cumulative effect of repeated earthquakes as treated in Section 10.4.5 is judged to yield an upper, pessimistic, estimate of the number of failed canisters.

#### *Global warming variant and other climate cases*

The external conditions of relevance to the occurrence of large earthquakes have already been considered in the above analysis.

### 12.8.3 Conclusions

#### *Categorisation as "less probable" or "residual" scenario*

Based on the above assessment, this scenario is considered as "less probable", meaning that its consequences are to be included in the risk summation.

The above analysis demonstrates that the handling of uncertainties for this scenario was exhaustive in the reference evolution. Therefore, probabilities of canister failures estimated in Section 10.4.5, Figure 10-124, are used for the consequence calculations in Section 13.6 and considered as bounding for the risk contribution from the shear load scenario.

## 12.9 Summary and combinations of analysed scenarios

### 12.9.1 Summary of results of the analyses

In summary, the following conclusions were reached when the selected scenarios were analysed, as described above.

- Buffer advection: This situation may occur in the reference evolution. The additional analyses in Section 12.2, considering conceptual uncertainties and additional interpretations of the hydraulic properties of the site, suggest a range in the possible extent of buffer advection. *These consequences were propagated to the canister corrosion scenario.*

  (Regarding canister sinking to the bottom of the deposition holes, in terms of consequences, this is a special case of buffer advection. The additional analyses in Section 12.2.4 led to the conclu-

sion that canister sinking, if it occurs, is preceded by advective conditions in the buffer due to buffer erosion. The consequences of a possible canister sinking are, therefore, covered by the general treatment of buffer advection.)

- Buffer freezing: Buffer freezing was ruled out in the reference evolution, also for an eroded buffer. The additional analyses in Section 12.3 also led to the conclusion that freezing of an intact buffer is ruled out and hence should be considered as a residual scenario. This applies also to the freezing of water in cavities of a partially eroded buffer. *The possibility of buffer freezing was, therefore, not propagated to the canister scenarios.*
- Buffer transformation: The analyses of a high buffer temperature, or other circumstances leading to the transformation of the buffer material in Section 12.4 led to the conclusion that this should be considered as a residual scenario. *The possibility of buffer transformation was, therefore, not propagated to the canister scenarios.*
- Canister failure due to corrosion: This failure mode is included in the reference evolution, where it occurs for the case of advective transport through an eroded buffer. The additional analyses in Section 12.6, with input from the buffer advection scenario, Section 12.2, led to the conclusion that buffer advection is indeed the main potential cause of corrosion failures. Evaluating all the advective situations and other uncertainties related to corrosion led to a range of potential extents of corrosion failure. *These are propagated to the analysis of consequences for the corrosion scenario in Section 13.5.*
- Canister failure due to isostatic load: This failure mode was ruled out in the reference evolution and the analysis in Section 12.7 led to the conclusion that it should be considered as a residual scenario. Consequences for a hypothetical case of canister failure due to isostatic load are analysed in Section 13.7.1.
- Canister failure due to shear load: This failure mode was analysed in the reference evolution, where it had a low probability of occurrence even with a number of pessimistic assumptions, Section 10.4.5. This conclusion remains after the additional analyses in Section 12.8. *The pessimistically estimated frequency of canister failures due to shear load is propagated to the analyses of consequences for the shear load scenario in Section 13.6.*

### 12.9.2 Assessment of containment potential for the main scenario

As mentioned in Section 12.1.2, an assessment of the containment potential of the main scenario is postponed until after the analysis of the additional scenarios, so that the assessment can be based on also the evaluation of uncertainties carried out in the analysis of additional scenarios. Since only two of the additional scenarios lead to the conclusion that canister failures cannot be ruled out, and since the uncertainty span for the additional scenarios is broader than that of the main scenario, only these two failure modes need to be considered in the evaluation of the containment potential of the main scenario.

Based on the analyses of the corrosion scenario in Section 12.6.2, the central corrosion variant is seen as representative for the main scenario, since it has an appreciable likelihood of occurrence given the cautious assumptions underpinning it and since it is compatible with the reference evolution of the repository.

Regarding canister failure due to shear load in the main scenario, the probability of shear failure in the reference evolution is low; on average 0.078 canisters in one million years even with a number of pessimistic assumptions regarding earthquake probability, location of earthquakes to fracture zones, extent of secondary movements for a give fracture size, the selection of geological DFN model, assumptions on the implications of the location and angle of shearing fractures on the impact on the buffer/canister system, handling of multiple earthquakes, etc. Therefore, it is seen as justified to exclude this failure mode from the main scenario. Note, however, that this does not reduce the calculated risk since the shear load scenario is based on all the pessimistic assumptions mentioned and no reduction in probability of the shear load scenario is made for these pessimisms when it is propagated to the consequence calculations.

In conclusion, the containment potential for the main scenario is assessed as equal to that of the central corrosion variant in Section 12.6.2.

### 12.9.3 Combinations of analysed scenarios and phenomena

Combinations of the analysed scenarios need to be considered. However, it is important to note that several such combinations have already been addressed, since, in the methodology for scenario analysis adopted, the buffer scenarios were analysed first. Results of those buffer scenarios that were not found to be residual were then propagated to the analyses of the canister scenarios. Also gradually developing phenomena need to be considered.

According to the summary above, the scenario analyses in this chapter demonstrate that the only appreciable safety related degradations of the engineered barrier system that cannot be ruled out are loss of buffer due to erosion, corrosion of the copper canister when buffer erosion has proceeded to the stage when advective conditions have arisen and canister failure due to shear movements on fractures intersecting the deposition hole. In addition, the canister may be subject to considerable isostatic loads, although not to the extent that canister failures occur. Buffer freezing and buffer transformation were ruled out.

In the following discussion of combinations, the emphasis is on combinations of physical phenomena rather than on combinations of the formal scenarios. To direct the discussion towards an account of combinations of potentially detrimental phenomena, the thermal, hydraulic, mechanical and chemical impacts on the buffer and on the canister are considered, in light of the results of the analyses of the reference evolution and the scenarios.

- The thermal impact on the canister and the buffer occurs initially in terms of elevated temperatures and during permafrost conditions in terms of the lowest temperatures. As reported in Section 10.3.4, the safety related thermal requirements on the repository are met and no challenge to this conclusion has been identified in the scenario analyses, in particular as regards buffer transformation (Section 12.4). As also mentioned above, buffer freezing is ruled out in the analysis of the buffer freezing scenario. Thermal aspects are, therefore, not further considered in the following.
- Two mechanical phenomena of relevance for long-term safety have been identified: canister failure due to shear movements in fractures intersecting the deposition hole and canister failure due to isostatic pressure. Furthermore, thermally induce spalling is included in the transport analyses that it affects. A number of additional mechanical phenomena, mainly related to the host rock are ruled out either in the reference evolution or in the screening in the **Geosphere process report**.
- The hydraulic impact on the buffer and the canister is indirect as part of the buffer erosion and canister corrosion processes, that are considered in the following. Groundwater transport of solvents could also contribute to the deterioration of the buffer, but this process was considered negligible in the analysis of the buffer transformation scenario.
- Also the chemical impact on the buffer and the canister is included as part of the buffer erosion and canister corrosion processes, that are considered in the following.

Phenomena that have been excluded in the **Process reports**, the reference evolution or the scenario analyses are hence not further considered here, but their exclusion is further justified in Section 14.4 where it is verified that FEPs omitted in earlier parts of the assessment are of negligible significance in the light of the completed scenario and risk analysis.

The analyses of the reference evolution and the scenarios hence leave the following processes or phenomena of which combinations need to be considered:

- loss of buffer due to erosion,
- corrosion of the copper canister when buffer erosion has proceeded to the stage that advective conditions have arisen,
- canister failure due to shear movements in fractures intersecting the deposition hole,
- isostatic loads on the canister.

Loss of buffer due to erosion and canister corrosion during advective conditions are already combined in the corrosion scenario and are therefore treated together in the following, leaving three phenomena for which to consider combinations and gradual developments.

### *Buffer erosion and canister corrosion in combination with shear movement*

*Impact of erosion on effects of shear movements*: If the buffer is eroded, then the likelihood of failures due to shear movements is significantly reduced due to the reduced buffer stiffness, in particular near a potentially shearing fracture. This combination is thus favourable for safety and it is pessimistic to neglect it.

*Impact of erosion on radiological consequences of a shear movement failure*: Failure due to a shear movement in a deposition hole with an intact buffer that is subsequently eroded is addressed in the consequence analyses of the shear scenario, see Section 13.6. The likelihoods of these two phenomena are not independent since both are positively correlated to fracture size.

*Impact of corrosion on canister response to shear movement*: It needs to be considered whether a partly corroded canister is more sensitive to shear movements. It is first noted that it is the canister insert that is the load bearing component and that the insert is unaffected by copper corrosion. Furthermore, an intact copper shell sustains a 5 cm shear movement with a large margin. Corrosion has been demonstrated to reduce the copper shell by at most a few mm for an intact buffer, and, considering the large margins for an intact 50 mm canister, it is unreasonable that such a corrosion depth should jeopardise that integrity of the copper shell in case of a shear movement. Appreciable corrosion could occur if the buffer is eroded. However, erosion of the buffer is favourable as regards the mechanical impact of shear movements on the canister, see above. Therefore, the possible increased sensitivity of a corroded canister to shear movements is counteracted by the fact that the stresses are reduced, particularly in the corroded area where the buffer is lost. It is noted that the shear analyses are performed for 50 mm copper since the resulting copper thickness after production had not been finally assessed when this analysis was carried out, whereas the corrosion analyses for advective conditions uses a copper coverage of 47 mm; this is considered to be a negligible difference.

*Impact of corrosion on radiological consequences of a shear movement failure*: Since a canister having experienced a shear movement failure is not assigned any transport resistance for radionuclides, corrosion will, in the analysis, not have a negative impact on the consequences of a shear movement failure.

*Impact of shear movements on buffer erosion*: Shear movements that do not lead to failure are less than 5 cm in extent, since the canister is designed to resist 5 cm movements. Such minor movements give a limited impact on buffer thickness and thus also on the time required to reach advective conditions according to the sensitivity analyses in Section 12.2.2. A shear movement may also lead to an enhanced flow in the shearing fracture. However, the mean number of deposition holes that are calculated to experience 5 cm shear movements or larger during the one million year assessment period is around 0.08, whereas at least several tens of holes are calculated to experience severe erosion during one million years with the assumptions in SR-Site, see Figure 12-3. Therefore, even if much smaller shear movements were considered to lead to enhanced flow, the overall impact on the extent of buffer erosion in the repository would be small.

*Impact of shear movements on corrosion*: Shear movements will induce stresses in the copper shell, even if the movement does not cause canister failure. For stresses to have an impact on corrosion (by stress corrosion cracking), high concentrations of detrimental anions are needed (as well as oxidising conditions). Such conditions are not expected in the repository environment (Section 10.2.5) and there is no reason that a shear movement would induce such an environment.

### *Buffer erosion and canister corrosion in combination with isostatic load*

*Impact of erosion on isostatic load*: Erosion of the buffer leads to a lowered isostatic load on the canister. This combination is thus favourable for safety and it is pessimistic to neglect it.

*Impact of corrosion on resilience to isostatic load*: A partially corroded canister surface does not influence the canister's resilience to isostatic loads negatively since it is the insert that bears the load.

*Impact of isostatic load on erosion and corrosion*: There is no reason to assume that an increased isostatic load has a negative impact on the buffer erosion and the canister corrosion processes, other than it is in some situations associated with an increased groundwater flow. This latter phenomenon is included in the analyses of buffer erosion and canister corrosion scenarios.

### *Shear movement in combination with isostatic load*

*Impact of isostatic load on shear movement*: As concluded in Section 10.4.5, subsection 'Combined isostatic and shear loads', an isostatic load during a shear displacement does not yield a more severe impact on the canister than the corresponding case without isostatic load. It was also concluded that, since large earthquakes will not occur in connection with high isostatic loads, this case is unrealistic.

*Impact of shear movement on resilience to isostatic load:* Also as concluded in Section 10.4.5, subsection 'Combined isostatic and shear loads' the canister is expected to maintain its resilience to isostatic loads after experiencing a 5 cm shear movement, in accordance with the design premises for the canister.

### *Gradually developing phenomena*

Erosion and corrosion are by their nature gradually developing phenomena and have been analysed as such. However, corrosion is considered in detail for an intact buffer or for a missing buffer. Therefore, also corrosion for an eroding buffer needs to be considered, see below. Shear movements occur as discrete events. However, the accumulated effect of several minor shear movements can be seen as a gradually developing load on the canister. This is already addressed in the analyses of shear movements, see Section 10.4.5, subsection 'Cases of shear load to consider'. Isostatic loads develop gradually as the buffer swells and, in particular, as ice sheets develop resulting in increased groundwater pressures. These developments are, however, slow and it is the peak loads that need to be considered, as is done in the analyses already reported. There is, therefore, no need to further address gradual developments of isostatic load.

*Corrosion for an eroding buffer*: Corrosion for an eroding buffer is pessimistically bounded by the case where the buffer is assumed to be lost initially. The consequences in terms of corrosion are not vastly different from the case where the buffer erodes according to the adopted erosion model. Both cases are propagated to the consequence analysis for the corrosion scenario in Section 13.5.

### *Completeness of the scenarios*

Combinations of scenarios and phenomena are an important aspect of the discussion of scenario completeness. This discussion is provided as part of the conclusions of the safety assessment, see Section 15.3.6.

### *Conclusion*

The above account demonstrates that relevant combinations and gradual developments of phenomena either have been addressed in earlier parts of the assessment and in some cases propagated to consequence calculations, or can, with relatively simple complementary arguments, be shown to not give rise to additional cases for further consideration. The only exception concerns a case where a shear failure is followed by buffer erosion. This case was also propagated to consequence calculations.

# 13 Analysis of retardation potential for the selected scenarios

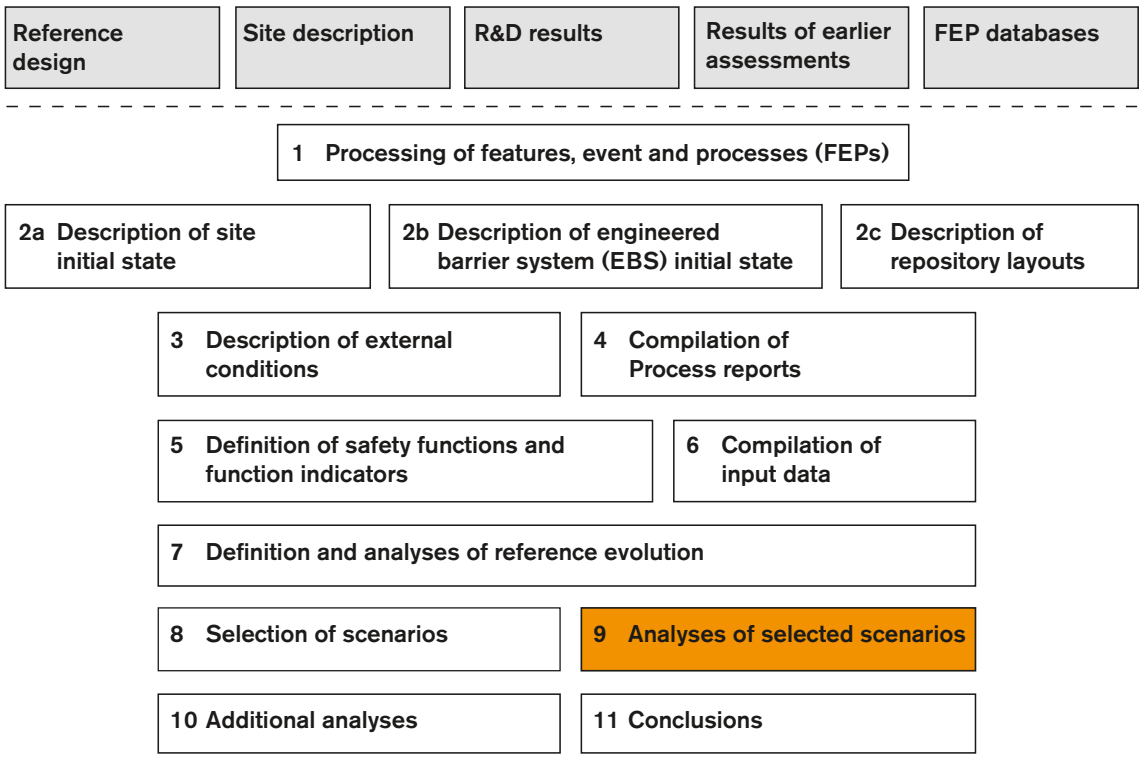


***Figure 13-1.*** *The SR-Site methodology in eleven steps (Section 2.5), with the present step highlighted. This chapter deals with the analysis of the retardation potential of the repository.*

## 13.1 Introduction

This chapter describes analyses of radionuclide release, transport and dose impacts for the scenarios selected in Chapter 11 and for which the containment potential was analysed in Chapter 12. In terms of safety functions, this chapter contains analyses of the repository's retardation potential.

Two issues related to radionuclide transport and dose calculations that can to a large degree be treated independent of the scenario or the nature of the failure mode of the canister are addressed first in this chapter:

- The modelling of radionuclide transport and dose estimation in the biosphere is described in some detail in Section 13.2.
- The issue of potential criticality for a failed canister is treated in Section 13.3.

The models used for radionuclide transport in the water phase for the near field and the geosphere are then described in Section 13.4.

The analyses of the two scenarios based on safety functions for which canister failures could not be excluded, i.e. the scenarios 'canister failure due to corrosion' and 'canister failure due to shear load' are described in Sections 13.5 and 13.6, respectively. In the following, these two scenarios are often referred to as the corrosion scenario and the shear load scenario, respectively, for simplicity.

Canister failures in the main scenario occur according to the central corrosion variant of the corrosion scenario and are thus covered by the analysis of this particular variant in Section 13.5.

Analyses of hypothetical, residual scenarios to illustrate barrier functions are presented in Section 13.7. This section also includes the scenario 'canister failure due to isostatic load'. Radionuclide transport in the gas phase is analysed in Section 13.8, common to all scenarios where it can occur.

Finally, a risk summation is provided in Section 13.9.

All modelling and modelling results for the near field and the far field are discussed in more detail in the SR-Site **Radionuclide transport report**. Details of the biosphere modelling are found in references given in Section 13.2.

## 13.2 Biosphere assessments and derivation of landscape dose conversion factors for a glacial cycle

The Swedish regulations state that human health and the environment must be protected from harmful effects of ionising radiation both during operation of the repository and in the future (see Section 1.4). More specifically, harm to humans should be assessed as the mean annual risk over a lifetime to a representative individual of the most exposed group (see Section 2.6.2 for details). For this assessment, the annual effective doses to future inhabitants of the Forsmark area per unit constant release rate or per unit released in a single pulse to potential release areas (biosphere objects) are calculated for each radionuclide. These doses are referred to as *Landscape dose conversion factors* (LDFs). Multiplying the maximum LDFs over all biosphere objects and time points with modelled radionuclide release rates from the geosphere under different release scenarios, results in estimates of the annual doses used to assess compliance with the regulatory risk criterion. The results from such calculations are reported for a number of release scenarios later in this chapter (Sections 13.5–13.8). For the assessment of the effects on the environment, the whole-body absorbed dose rates to individual organisms are calculated and compared to a no-effect dose rate. If harmful effects at the level of the individual organisms can be excluded, then this also ensures the sustainability of populations and of ecosystem functions.

Over the time scales of relevance for the safety assessment, the biosphere will undergo considerable changes, in particular due to the long-term climatic variation involving glacial cycles and the associated displacements of the shoreline (see Chapter 10). As the site emerges from the sea, the potential activity concentrations in surface water are expected to increase and radionuclides which may have accumulated in the regolith can enter into the terrestrial food web in existing or wetlands converted to agriculture. Thus, the potentially highest exposure of humans and other organisms to radionuclides from the repository is expected when at least parts of the site have emerged from the sea. However, at what stage in the ecosystem succession, and in what part of the landscape a specific radionuclide will cause maximum exposure will vary due to the properties of the specific radionuclide and of the potential release location.

In the following sections, the approach, methods and main results from the biosphere assessment are presented. A comprehensive account of the biosphere assessment can be found in the **Biosphere synthesis report**, and the details of this work are presented in a number of technical reports referenced therein (see Figure 13-3). In Section 13.2.1, the approaches and central concepts for the biosphere assessment are presented. The methods to identify and delimit biosphere objects are described in Section 13.2.2. This section also gives an account of how the biosphere objects are connected to each other and how the *Landscape development model* is used to describe the development of the biosphere objects during a reference glacial cycle, with emphasis on the first interglacial period. Details of the work concerning biosphere objects and the Landscape Development Model are presented in /Lindborg 2010/. Section 13.2.3 gives an overview of the *Radionuclide model for the biosphere*, presented in detail in /Andersson 2010/, and presents the methods for calculation of *Landscape dose conversion factors* (LDF values). In Section 13.2.4, the resulting LDF values for a full glacial cycle are presented. Section 13.2.5 gives an overview of methods for estimation of doses to non-human biota /Torudd et al. 2010/ and in Section 13.2.6 the uncertainties in the risk estimates are discussed.

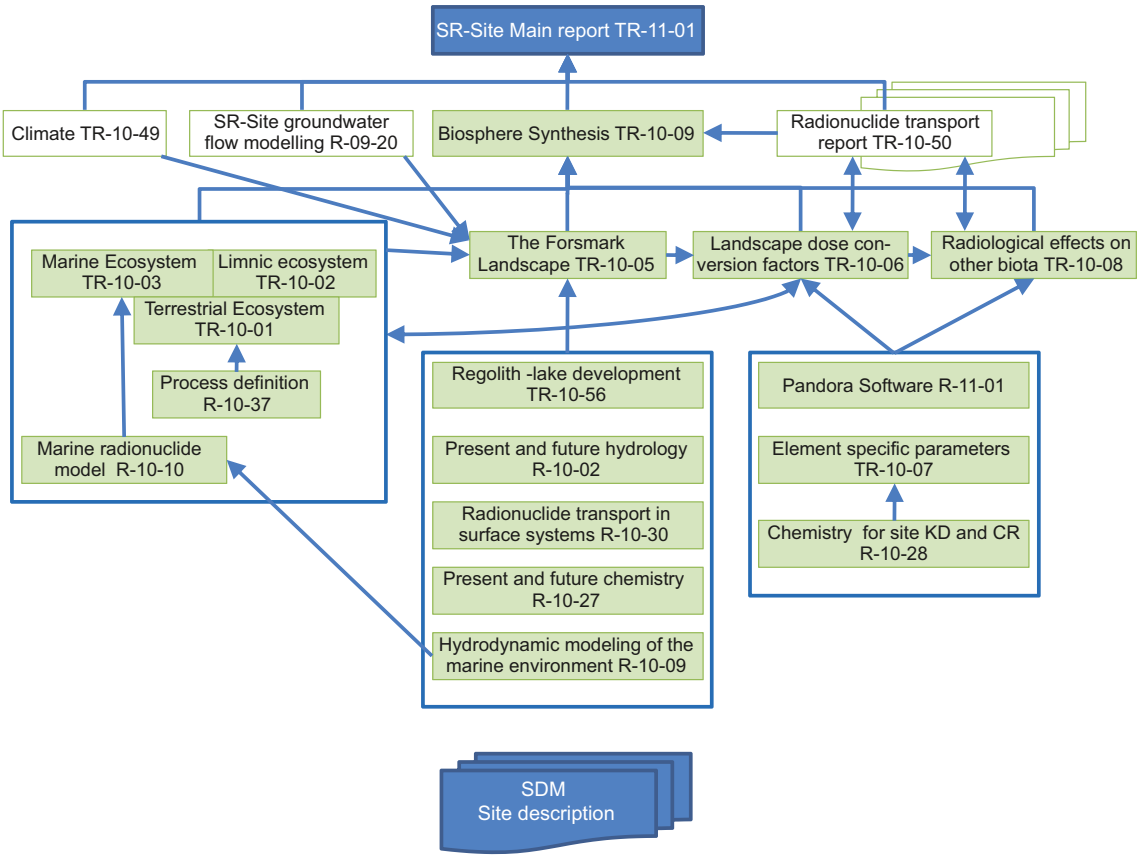


***Figure 13-2.*** *The hierarchy of biosphere reports (grey) and their dependencies of information from other reports within SR-Site project. Arrows indicate major interactions during project workflow, but most reports rely to some extent on information from all other reports, and the production of the information has been an iterative process. See the* ***Biosphere synthesis report*** *for a short description of the contents of each report.*

### 13.2.1 Approaches and central concepts in the biosphere assessments

The main objectives of the biosphere assessments in the SR-Site project are to produce values of the landscape dose conversion factors that allow translation of a potential release from a geological repository to the exposure of humans inhabiting the Forsmark site in the future, and to assess the exposure of other organisms in the area. The landscape dose conversion factors are used in the safety assessment for obtaining estimates of doses to humans, which, in turn, are used in demonstrating compliance with the regulatory criteria.

To accomplish this, areas with potential discharge of deep groundwater from the repository, here called *biosphere objects*, have been identified at the site, and the long-term development of these areas has been modelled. A biosphere object is defined as an area of the landscape that potentially may receive radionuclides released from a future repository, either through discharge of deep groundwater or by contaminated surface water, at any time during a glacial cycle. In SR-Site, the biosphere at Forsmark is represented by a set of interconnected biosphere objects (see the **Biosphere synthesis report** for an overview and /Lindborg 2010/ for details).

The transport and accumulation of radionuclides in the biosphere objects throughout a full glacial cycle has then been described with the radionuclide model for the biosphere. The biological uptakes by various organisms, some of which are potential food sources for humans, have been calculated from activity concentrations in the environment (air, soil, water and food). Finally, assumptions on land use and human habits have been used in combination with activity concentrations in the environment, to calculate landscape dose conversion factors for future human inhabitants. The activity concentrations have also been used to assess the potential future exposure of other organisms at the site.

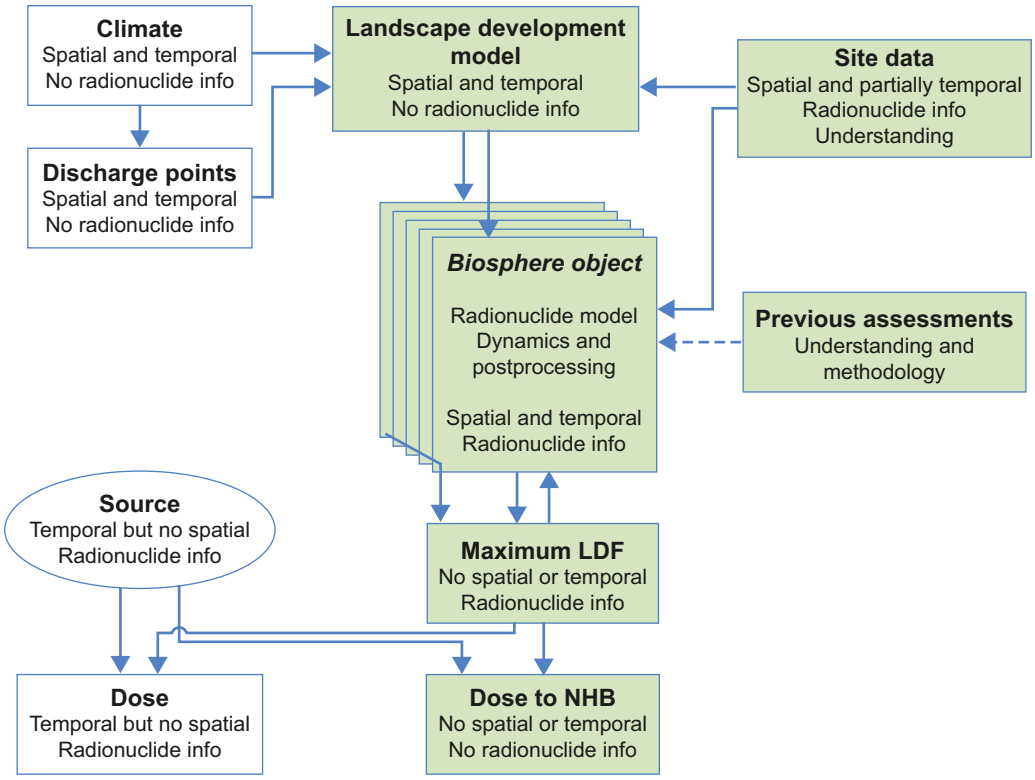


***Figure 13-3.*** *Major dependencies and spatial/temporal dimensions of models used in the biosphere assessment (grey). Climate scenarios and discharge points provide information, in temporal and spatial terms (but no radionuclide-specific information), that is used in the Landscape development model. The Radionuclide model provides temporally and spatially resolved radionuclide information. The maximum unit release dose (LDF) over all objects and time steps is a factor with no temporal or spatial dimension, used in the SR-Site calculation chain (see Section 13.4) to calculate doses to humans by multiplication with the source term (which has a temporal, but no spatial dimension). For doses to non-human biota (NHB), the source is directly used in the calculations of effects.*

### *Assessment philosophy*

The assessment philosophy has been to make estimations of the radiological risk for humans and the environment as realistic as possible, based on the knowledge of present-day conditions and of the past and expected future development of the Forsmark site. This has been relatively straightforward for the current situation when knowledge of the site is good and uncertainty is relatively low, for instance in the representation of well-investigated biosphere processes and properties that can be observed at the site today (see Section 4.10). However, it is much more difficult to determine the level of realism in assumptions related to future scenarios, human habits and biosphere properties. In these cases, the uncertainties are larger and therefore it is inevitable that some cautious assumptions have to be introduced in the assessments.

The landscape dose conversion factors obtained from the biosphere assessment are best estimates for the most exposed group from deterministic simulations. These deterministic simulations are the combined results of process understanding, the most precise description of the site available, and relevant assumptions on the habits of future human inhabitants. In addition, the effects of parameter uncertainties, assumptions and conceptual uncertainties on the estimated LDFs have been addressed through probabilistic simulations, alternative models and informed assumptions. This approach is consistent with recommendations from the ICRP /ICRP 2007/ and with the guidelines from the Swedish authority /SSM 2008b/.

To be able to provide the calculation chain (presented in Section 13.4) with an *a priori* dose conversion factor, the LDF was calculated for a release rate of 1 Bq/y, i.e. it represents a unit release dose. Because there is no temporal or spatial resolution when this factor is applied, the LDF used in the assessment was cautiously chosen as the maximum value over all times and biosphere objects. This maximum LDF is then used to calculate the dose (see Figure 13-3). Thus, this LDF contains no

spatial or temporal resolution and is certainly an overestimate. For detailed analysis or interpretations, including e.g. analysis of time varying releases due to transient hydrogeological conditions, the temporal and spatial dimensions of the surface systems should be considered (see further discussion in the **Biosphere synthesis report**).

### 13.2.2 Location and temporal development of biosphere objects

The identification of biosphere objects in the Forsmark area is based on the modelling of flow paths from the repository to the ground surface (Figure 13-4, see further Section 4.2 in /Joyce et al. 2010/). To locate potential discharge areas, the end position of flow paths from the particle tracking simulations were related to present and future features of the Forsmark landscape, such as lakes and shallow parts of the sea floor. According to /Joyce et al. 2010/, the discharge pattern is determined mainly by the local topography and deterministic deformation zones, and the pattern does not vary significantly among model realisations. With few exceptions, the discharge points cluster together in space and time into a limited number of areas. For the identification of discharge areas, it was assumed that the location of these clusters indicates areas likely to be affected by discharge of deep groundwater from the repository.

The locations of discharge points in the Forsmark landscape show that: 1) deep groundwater from the repository is primarily attracted to low points in the landscape, e.g. shallow parts of the sea, along the shoreline, and in lakes, streams and wetlands, 2) discharge areas covered by the sea tend to be relatively large, whereas discharge areas above sea level are narrower and primarily located

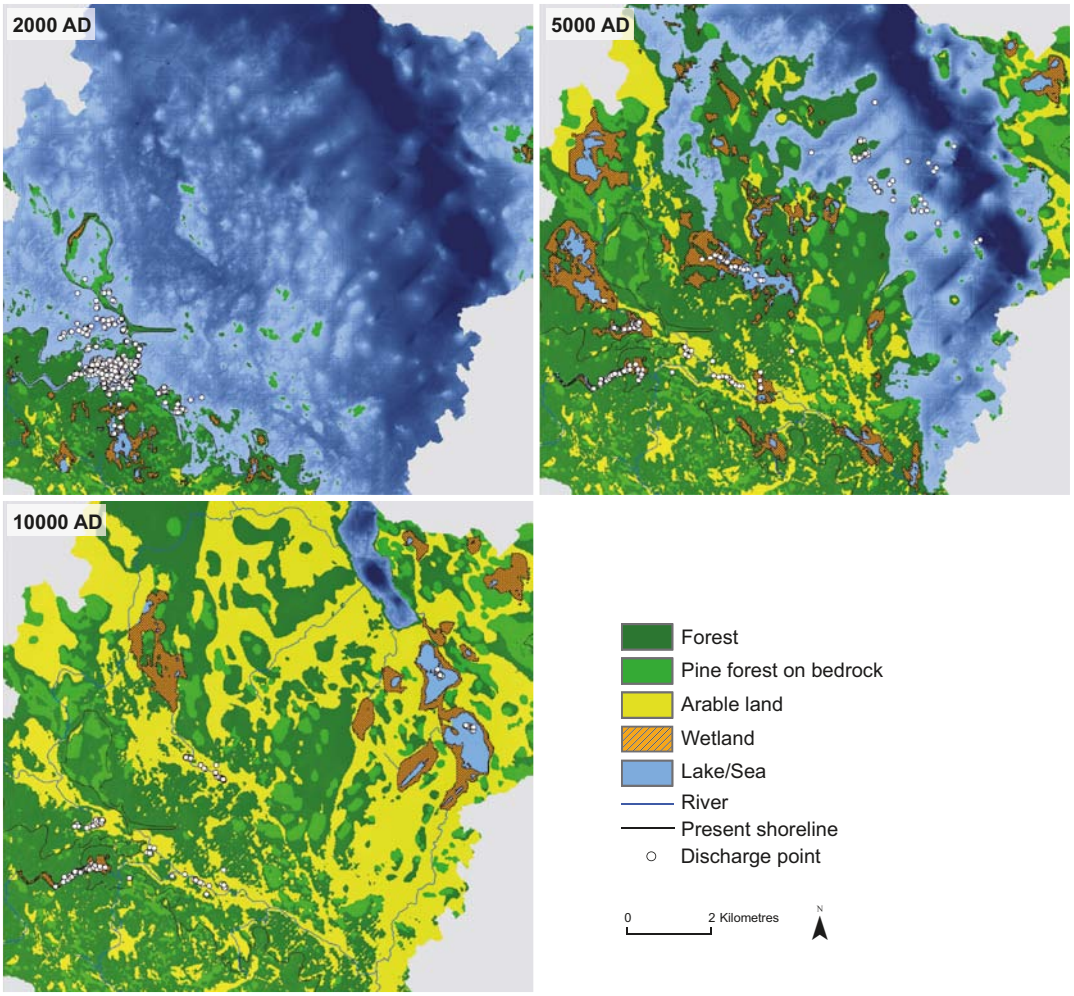


***Figure 13-4.*** *Discharge points from the particle tracking simulations (see Section 4.2 in /Joyce et al. 2010/) at three different times. The discharge points are displayed on maps of the Forsmark landscape at corresponding times, predicted from the Landscape Development Model, see /Lindborg 2010/.*

in lake basins (which may be open or infilled), 3) discharge areas are located in a limited number of basins in the Forsmark landscape (Figure 13-5, see further the **Biosphere synthesis report** and Chapter 5 in /Lindborg 2010/).

The long-term development of the site is determined mainly by climate variations, both directly and indirectly through the resulting shoreline displacement (Section 10.3.3, see also the **Biosphere synthesis report**). The shoreline displacement affects the size and position of potential discharge areas in two important ways. First, the size of a discharge area that receives groundwater from the repository over extended periods of time (e.g. areas situated above the repository) decreases substantially when the area emerges from the sea. Secondly, changes in the hydrological forces due to the moving shoreline directly affect the discharge of deep groundwater; the discharge in terrestrial areas will cease with time, whereas new discharge areas will appear in the emerging landscape and in shallow parts of the sea along the new coastline (Figure 13-4, for more details see Chapter 5 in /Lindborg 2010/).

Thus, clusters of discharge points were used to identify the location of biosphere objects in the Forsmark area. During the submerged phase, the outer boundary of each biosphere object was determined from the future sub-catchments (called basins), whereas the shoreline of the lake at time for isolation from the sea delineates the biosphere object during the lake and terrestrial phases. Key geometrical characteristics of the objects were determined from the local (i.e. sea or lake basin) topography, whereas the regional geometry defined landscape characteristics, like hydrological links between biosphere objects and sizes of catchment areas. In total, 17 biosphere objects were identified (Figure 13-5). Most of these objects contained a discharge area during some period of the Holocene interglacial, but some additional biosphere objects located downstream of the discharge areas were also identified (see discussion in the **Biosphere synthesis report**, for details see /Lindborg 2010/).

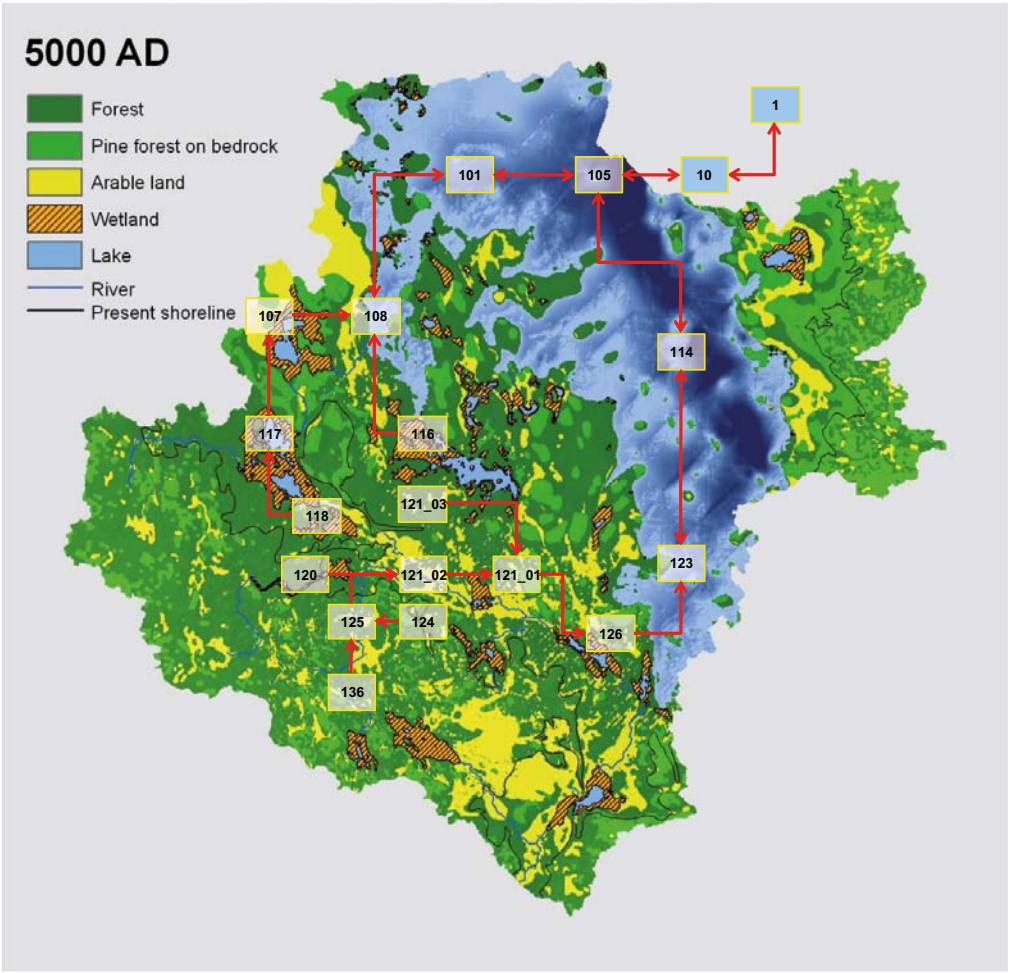


***Figure 13-5.*** *The location and hydrological connections of biosphere objects in the SR-Site assessment, displayed on a map of the Forsmark landscape at 5000 AD.*

The main features of the landscape relief in the Forsmark area, like the locations of higher and lower altitude areas, are determined mainly by the bedrock topography. The small-scale undulations of the bedrock surface are smoothed by glacial and post-glacial deposits, which, to a limited extent, are redistributed by wave erosion when the shoreline moves over the area (see Section 10.3.3). Since the bedrock topography is expected to be marginally affected by weathering, and since the shoreline displacement is expected to be repeated during future glacial cycles, it is argued that the landscape development during the present ice-free period will give an acceptable representation also of the landscape development during future ice-free periods of repeated glacial cycles /Lindborg 2010/.

Since each biosphere object is associated with the local topography of a sea/lake basin, the physical boundaries of the object reflect the geometry of the bedrock and the overlying till and glacial sediments, which changes marginally during the modelled non-glacial period. In contrast, the properties of the biosphere objects change continuously, e.g. due to shoreline displacement, wave erosion and sedimentation, lake infilling and ecosystem succession (see Section 10.3.3).

As a combined effect of the ongoing shoreline displacement, redistribution of marine sediments, infilling of lakes, and climate variations, the landscape properties and features will change continuously in at least partly predictable ways. By combining information from the contemporary *Digital elevation model* /Strömgren and Brydsten 2008/ with the envisaged shoreline displacement according to the **Climate report**, output from the *Coupled regolith-lake development model* /Brydsten and Strömgren 2010/ (see also Section 10.3.3) and biotic information from the ecosystem modelling /Andersson 2010, Aquilonius 2010, Löfgren 2010/, a *Landscape development model* that describes the long-term development of the site at the landscape level has been developed. The Landscape development model produces a description over time in spatial detail (20·20 m) of landscape properties and features, including topography, location of the shoreline, regolith depth, areas and depths of present and future lakes and sea basins, stream network, and vegetation and potential land use. This description is used to extract time-dependent properties of the biosphere objects that are input parameters to the radionuclide model for the biosphere (see next section).

For the quantitative modelling of transport and accumulation of radionuclides in the biosphere (Section 13.2.3), it is assumed that the landscape development during repeated glacial cycles will be similar to that of the present cycle /Lindborg 2010/. Future sea and lake ecosystems are assumed to have similar characteristics to the aquatic ecosystems existing at the site today. The wetlands that will develop around future lakes are assumed to be similar to the rich fens presently found in the area. If drained, these wetlands will provide an organic soil rich in nutrients that may be suitable for cultivation, at least for a limited period.

### 13.2.3 The Radionuclide model for the biosphere

The radionuclide model for the biosphere can handle different types of sources and properties of radionuclides. However, the model has been designed for a constant release rate of radionuclides, under which steady-state conditions are likely to be approached within the time frames of the assessment, and parameter values have been assigned accordingly. This simplifying approach is possible since the releases from the fuel matrix and corroded metals in the repository are in most cases approximately constant on the time scale of the biosphere assessment (i.e. 20,000–70,000 years), as demonstrated in later sections of this chapter. To assess the potential doses to humans for release scenarios with approximately constant release rates, the radionuclide model was used to calculate LDFs (see below). In addition, a modified version of the LDF, which can be applied to releases reaching the biosphere in a single pulse, was calculated.

The radionuclide model was also used to illustrate the consequences of a number of hypothetical release scenarios where losses of barrier functions of the repository are assumed already at deposition (see Section 13.7.3). For these simulations, which are described in more detail in /Avila et al. 2010/, two approaches were taken.

1. Releases were multiplied by the LDFs obtained with a constant release rate distributed to the biosphere objects in accordance with the time dependent distribution of release points over an interglacial. This is more appropriate than the use of the basic LDFs for these release scenarios, since they concern situations where all deposition positions are affected by a hypothetical barrier loss and hence cause releases.

2. Since these situations lead to transient releases that vary significantly over an interglacial, time-dependent dose modelling in the biosphere was also carried out. Here, the time dependent far-field release was used as input data to the radionuclide model to calculate annual effective dose to a representative member of the most exposed group. Also here, the release was distributed over all biosphere objects in accordance with the density of discharge points in the landscape.

In addition, dose consequences of releases from rare, early canister failures due to earthquakes, i.e. early failures in the shear load scenario, Section 13.6.2, are handled with time-dependent modelling as in case 2 above. However, here the entire release was input to each landscape object in order to capture the landscape object in which the highest consequences would arise due to release from a single canister.

Radionuclides released from the repository are in the radionuclide model assumed to be transported with groundwater to the deeper parts of the regolith in a biosphere object. Additionally, it is assumed that the released radionuclides also reach a hypothetical well drilled into the bedrock, as soon as a biosphere object has emerged from the sea. The activity concentration in well water (Bq/m$^3$) was calculated by dividing the release rate (Bq/y) by the well capacity (m$^3$/y). The capacity of the well was selected to represent drilled wells in the central part of the site investigation area, where they would have the possibility to receive released radionuclides from the repository /Avila et al. 2010/.

### *Modelling radionuclide transport and accumulation in biosphere objects*

The radionuclide model for the biosphere is a compartment model, where system components that are considered internally homogeneous in their properties are represented by distinct compartments. A graphical representation of the conceptual model is shown in Figure 13-6, where each box corresponds to a model compartment. Definitions of the model compartments are presented in Table 13-1.

The arrows in Figure 13-6 represent radionuclide fluxes between compartments and fluxes into and out of the system. Radionuclide fluxes are linked to the movement of matter in the biosphere, i.e. water flow, particle transport and gas emanation and transport. Radionuclide transfer mediated by biota, like uptake and release by primary producers, has also been represented. The arrow reaching the lower regolith compartment represents radionuclide releases from the geosphere into the biosphere objects. These releases are directed to the deeper parts of the regolith, which at the site normally consists of glacial till deposited on the bedrock (see Section 4.10.2 and the **Biosphere synthesis report**).

Radionuclides released to the lower regolith compartment are distributed to the upper layers of the ecosystems by advection and diffusion. The representation of the waterborne transport of radionuclides between compartments is based on detailed hydrological modelling with MIKE-SHE /Bosson et al. 2010/. The effect of radionuclide sorption on the advective and diffusive transport is taken into account by assuming equilibrium between the porewater and the solid phase of the different compartments. The model also considers the transport of radionuclides absorbed to suspended particles, driven by surface water fluxes, sedimentation and resuspension processes (see the **Biosphere synthesis report** and /Avila et al. 2010/).

The radionuclide transport mediated by biota is, for both terrestrial and aquatic ecosystems, described in the model through fluxes driven by net primary production. It is assumed that equilibrium is established between the activity concentrations of radionuclides in the newly produced biomass and in the corresponding environmental media (upper regolith for terrestrial and water for aquatic ecosystems). Losses from the upper regolith and surface waters via degassing processes are pessimistically neglected for all radionuclides, except for C-14 for which this process has been explicitly considered since uptake from air through photosynthesis is the dominant pathway for incorporation into terrestrial primary producers (see the **Biosphere synthesis report** and /Andersson 2010/).

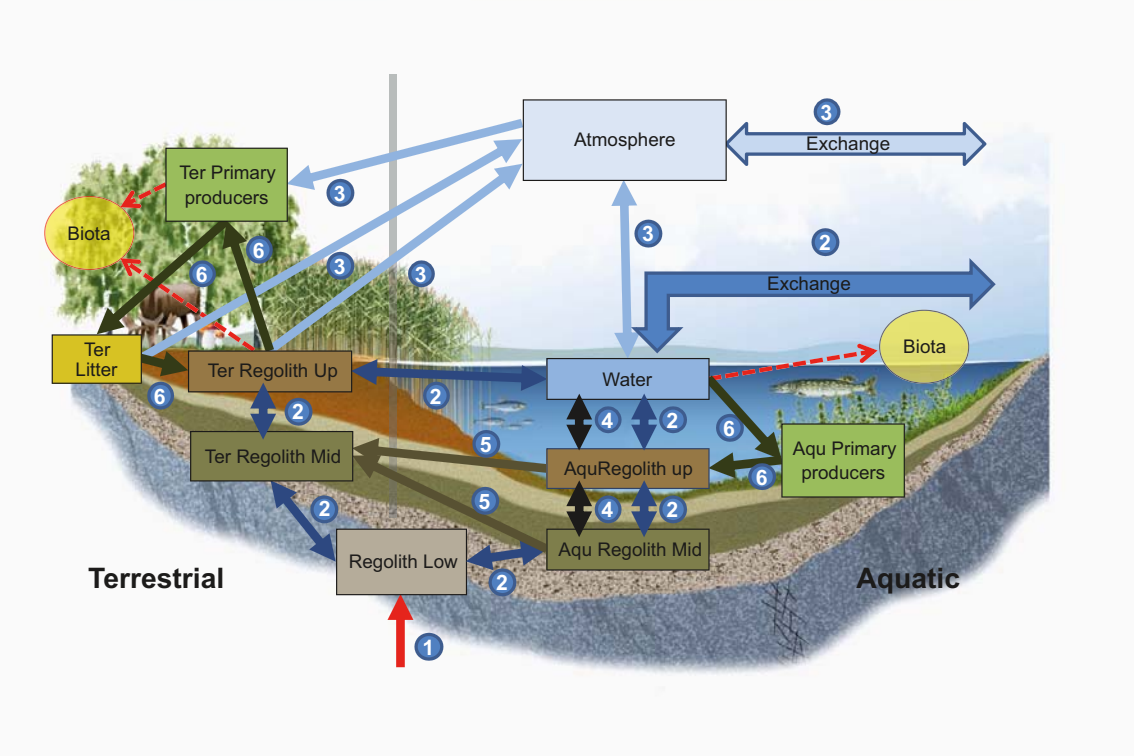


***Figure 13-6.*** *Conceptual illustration of the Radionuclide model for the biosphere. Boxes represent compartments, thick arrows fluxes, and dotted arrows concentration computations for non-human biota (these are not included in the mass balance). The model represents one object which contains an aquatic (right) and a terrestrial part (left) with a common lower regolith and atmosphere. The source flux (1 Bq/y) is represented by a red arrow (1). The radionuclide transport is mediated by different major processes, indicated with dark blue arrows for water (2), light blue for gas (3), black for sedimentation/resuspension (4), dark brown for terrestrialisation (5), and green for biological uptake/decomposition (6). Import from and export to surrounding objects in the landscape is represented by arrows marked "exchange". A detailed explanation can be found in /Andersson 2010/ and descriptions of the compartments are given in Table 13-1.*

**Table 13-1. Compartments in the radionuclide model for the biosphere used in the conceptual approach adopted Figure 13-6 (for further description see /Andersson 2010/).**

| Model name | Description |
|---|---|
| Regolith Low | The lower part of the regolith overlying the bedrock, primarily composed of till. It is common to the terrestrial and aquatic parts and its origin is from the glaciation. |
| Aqu Regolith Mid | The middle part of the regolith in the aquatic part of biosphere objects, usually consisting of glacial and postglacial clays, gyttja and finer sediments which originate mainly from the period after the retreat of the glacial ice sheet, or from later resuspended matter mixed with organic sediments. |
| Aqu Regolith Up | The part of the aquatic regolith with highest biological activity, comprising c. 5–10 cm of the upper aquatic sediments where resuspension and bioturbation can maintain an oxidising environment. |
| Ter Regolith Mid | The middle part of the terrestrial regolith, containing glacial and postglacial fine material, i.e. former sediments from the seabed / lake bottoms. |
| Ter Regolith Up | The upper part of the terrestrial regolith which has the highest biological activity, like the peat in a mire, or the plowing layer in agricultural land. |
| Litter | Dead plant material overlying the regolith. |
| Water | The surface water (stream, lake, or sea water). |
| Aqu Primary Producers | The biotic community in aquatic habitats, comprising both primary producers and consumers. |
| Ter Primary Producers | Terrestrial primary producers. |
| Atmosphere | The lower part of the atmosphere where released radionuclides are fully mixed. |

Biosphere objects may, beside a release to the lower regolith, also receive radionuclides with surface water from contaminated biosphere objects located upstream or in adjacent marine bays (exchange arrows in Figure 13-6). In initial simulations, the radionuclide model was implemented for each identified biosphere object in a network according to the flux of surface water in the landscape (see Figure 13-5). These simulations showed that the maximum unit release dose was always found in a biosphere object that received a direct release from the geosphere, and that the dose resulting from the indirect release to the same object via an adjacent object was typically an order of magnitude lower /Avila et al. 2010/. As the aim of the biosphere assessment is to identify the most exposed group across all biosphere objects, indirect contamination was not considered in the assessment, in order to simplify the analysis with separate simulations for each object, see the **Biosphere synthesis report**.

### *Temporal development of biosphere objects in the radionuclide model*

The radionuclide model has two parts when it is applied to a biosphere objects, one aquatic (right side in Figure 13-6) and one terrestrial (left side). The temporal development of an object is handled by varying the sizes and properties of these two parts in accordance with the simulated natural development of the specific biosphere object (see /Lindborg 2010/ for details). Thus, most biosphere objects are expected to experience four main stages:

- Sea stage – the biosphere object is a sea bay which, as the landscape emerges from the sea, is continuously reduced in size. During this period the object is totally dominated by the aquatic part, and the fluxes from the deep regolith layers are consequently directed only to the aquatic sediments (mid and upper regolith).
- Transitional stage – the sea bay is isolated and transforms into a lake or a stream (aquatic part), surrounded by wetland (terrestrial part). The isolation of a lake in the Forsmark area takes typically around 500 years /Lindborg 2010/ and during this period, saltwater flooding will occur periodically. Fluxes from the deep regolith layers are apportioned to the aquatic and the terrestrial parts according to their relative sizes. During the transitional stage, parameter values for the aquatic part are changed linearly from sea to lake values.
- Lake stage – the surrounding wetland expands into the lake, and the aquatic sediments are gradually covered by a layer of peat. This process is represented by a flux of radionuclides bound to the regolith from the aquatic to the terrestrial regolith layers. The lake stage ends when the lake has been fully transformed into a wetland, intersected by a small stream.
- Terrestrial stage – the biosphere object has reached a mature state and no further natural succession occurs. The end stage is a wetland with a small stream. If the wetland has a suitable size and regolith composition for agriculture /see Lindborg 2010/, it may potentially be cultivated at any time in the future and this agricultural use is represented in the model.

### *Definition of most exposed group*

The most exposed group is defined as the group of individuals that receives the highest exposure across all potential release areas (i.e. biosphere objects) in the landscape. A representative individual of the most exposed group is assumed to spend all his/her time in the contaminated area, and to get his/her full supply of food and water from this area.

### *Assumptions on human behaviour and land use*

When the wetland in a biosphere object has emerged to sufficiently high elevation above the sea level to avoid periodic seawater flooding, it can be drained and used for agricultural purposes. It is assumed in the assessment that human inhabitants will drain and subsequently use wetlands situated 2 metres or more above sea level for crop (cereals, root crop, and vegetables) and livestock production (see the **Biosphere synthesis report** and /Avila et al. 2010/). The organic layers (peat and gyttja) on drained and cultivated wetlands will rapidly become oxidised and compacted, resulting in an agricultural soil that is a mixture of potentially contaminated organic matter and deeper mineral layers (glacial and postglacial deposits) where radionuclides may have accumulated since the early sea stage (cf. Chapter 4 in /Lindborg 2010/).

The production capacity of human food in a biosphere object is directly determined by the size of the contaminated object and the sustainable yield of natural food and agricultural products. The number of individuals that can be sustained in a biosphere object is thus proportional to the area of the object. It is assumed that all available food sources from both aquatic and terrestrial parts of a biosphere object are utilised by human inhabitants. Additionally, it is assumed that wetlands will at least partly be converted to agricultural land when this is possible. No assumptions are made regarding food preferences of future individuals. Instead, the human diet is directly determined by the potential production of different types of food in the object. Biosphere objects that can be drained and cultivated can typically feed a population in the range of 100–1,000 persons, whereas biosphere objects that cannot be cultivated can support approximately 10 individuals during the sea stage and only one or a few individuals during the lake and terrestrial stages, see the **Biosphere synthesis report** and /Avila et al. 2010/.

Once a wetland is drained, further contamination of the soil through groundwater is assumed to not be of quantitative importance, and any additional contamination will reach the soil only through irrigation with surface water. The highest activity concentrations of radionuclides in agricultural soil are therefore expected in the period directly after drainage. Thus, the 50 years following immediately after drainage are cautiously used to assess the average annual dose from the use of contaminated agricultural soil during a human lifetime. The wetland is assumed to be converted to agricultural land at the point in time when it results in the largest annual dose (see further explanation in the **Biosphere synthesis report**).

Future humans are assumed to acquire their drinking water by equal contributions from a well drilled into the bedrock, and from the surface water in the lake or stream passing through the object. Livestock are assumed to consume water from the same sources. Exposure from contaminated drinking water is considered from the point in time when a biosphere object has emerged from the sea. Exposure originating from irrigation with contaminated surface water is considered in the production of vegetables. Surface water for irrigation of agricultural soils will be readily available in all considered biosphere objects, and irrigation with water from a drilled well has consequently been deemed unlikely (see the **Biosphere synthesis report** and /Avila et al. 2010/).

#### *Mathematical implementation*

The radionuclide model consists of a system of ordinary differential equations, representing the rate of change of the radionuclide content (Bq) in a model compartment (Figure 13-6 and Table 13-1), as a function of the radionuclide fluxes (Bq/y) into and out from the compartment, of radioactive decay and of ingrowth /Andersson 2010/. The model has the same mathematical formulation for all biosphere objects. The differences between biosphere objects are captured by using object-specific parameter values describing the geometry of the biosphere objects, the depth of regolith layers, and the rate and timing of transitions between sea, lake and terrestrial stages.

The radionuclide fluxes are modelled in the same way for all radionuclides. Element-specific values describe e.g. retention (partitioning coefficients, $K_d$) and biological uptake (concentration ratios, CR). Additionally, for C-14 the uptake by biota is modelled using a specific activity approach /Avila and Pröhl 2008/, and gas exchange between the upper regolith/surface water compartments and the atmosphere has also been considered for this radionuclide.

The radionuclide model was implemented in the software package Pandora /Åstrand et al. 2005/ and /Ekström 2011/. Pandora is an extension of the codes Matlab and Simulink. A brief description of the development, functionality and features of the Pandora tool is presented in the **Biosphere synthesis report**, and the tool is described in detail in /Ekström 2011/.

#### *Estimating activity concentrations*

The radionuclide model was used to dynamically model the inventories in the ten compartments of the biosphere object (see Figure 13-6). The activity concentrations in upper regolith, atmosphere and surface water were used to assess exposure to humans (see below) and to non-human biota (Section 13.5.7). Activity concentrations in human food (Bq/kg C) were calculated from concentrations in environmental media (upper regolith and surface water), assuming equilibrium between the concentrations in food and in the corresponding environmental media (see the **Biosphere synthesis report** and /Avila et al. 2010/).

### *Assessment of human exposure*

The average exposure over the entire life of individuals was assessed by averaging predicted unit release annual doses over a period of 50 years. Adults have been shown to provide a sufficiently good approximation of the average lifetime exposure (see discussion in /Avila et al. 2010/). The contributions to human exposure from all relevant pathways were summed as outlined in /Avila and Bergström 2006/. A brief description of the assumptions and calculations of human exposure from inhalation, external exposure, and consumption of contaminated food and water can be found in the **Biosphere synthesis report** and details are presented in /Avila et al. 2010/ and /Nordén et al. 2010/.

### *Landscape dose conversion factors*

Potential doses to humans were assessed by multiplying release rates of different radionuclides to the biosphere by a radionuclide-specific *Landscape dose conversion factor (LDF)*. For each radionuclide, LDFs were calculated over time for each biosphere object, and the highest value over time among all objects was pessimistically chosen to represent the most exposed group. The basic LDFs are applicable to continuous long-term releases. Beside the basic LDF, a modified LDF was calculated for pulse releases with an extension of years to hundreds of years.

The LDF for each potentially released radionuclide is defined as the mean annual dose to a representative individual of the most exposed group, resulting from a constant release rate of 1 Bq/y of this radionuclide. The modified LDF for a pulse release of each potentially released radionuclide is defined as the mean annual dose to a representative individual of the most exposed group, resulting from a unit pulse release. For both factors, the exposure is averaged over the lifetime of an individual, and the unit is Sv/y per Bq/y for the basic LDF and Sv/y per Bq for the modified LDF. For a further discussion of the LDF concept, see the **Biosphere synthesis report** and details in /Avila et al. 2010/.

#### LDF values for different climatic conditions

LDF values were calculated for three different periods of the reference glacial cycle; a period of submerged conditions following the deglaciation, the whole interglacial period, and a prolonged period of periglacial conditions. Additionally, LDFs were calculated for the global warming climate case. The modified LDF values for a pulse release were calculated for the interglacial period only.

The calculation period starts at the time for the deglaciation around 9000 BC, when the landscape is covered by the sea (i.e. *submerged conditions*). The length of the submerged period differs between biosphere objects since it takes almost 10,000 years from the emergence of the first biosphere object from the sea, until the shoreline has passed over the whole model area.

The *interglacial period*, i.e. the period from deglaciation to the onset of periglacial conditions, see the **Climate report**, is represented by climate conditions similar to those of today. It is, in accordance with the reference glacial cycle, assumed to prevail for 18,400 years (i.e. from –9000 to 9400 AD) and includes both submerged and temperate conditions. As land has emerged sufficiently from the sea, wetlands are assumed to be converted to arable land. Drinking water for humans and livestock during the terrestrial stage of this period is supplied by equal parts from surface water and from a contaminated well drilled into the bedrock (see Chapter 8 in the **Biosphere synthesis report**).

The initial period of temperate climate conditions is followed by a period of *periglacial conditions* in the reference glacial cycle. During this period, the climate is colder than today, with episodes of deep permafrost. For the LDF calculation, periglacial conditions are assumed to prevail until the onset of the next glaciation around 59,600 AD. During this period, it is assumed that agriculture is not possible, and drinking water from a contaminated deep drilled well is not accessible (see Chapter 8 in the **Biosphere synthesis report**).

Exposures of humans under *glacial conditions*, when the site is covered by an ice sheet, are unlikely. Nevertheless, if releases occur, humans may be exposed to radionuclides through ingestion of sea food when the ice margin is situated above or close to the repository. As a cautious estimate of the exposure from releases during glacial conditions, the LDFs from the open sea stage during a temperate climate (i.e. submerged conditions) are used in the assessment.

In the SR-Site *global warming* climate case, it is assumed that the temperate climate domain is extended by approximately 50,000 years compared with the reference glacial cycle (i.e. the temperate climate domain prevails until 59,600 AD, see Section 5.1 in the **Climate report**). Assumptions concerning human usage of the landscape during this period are the same as for the interglacial, i.e. wetlands are converted to arable land when possible and drinking water for humans and livestock is supplied in equal parts from surface water and water from a contaminated well drilled in the rock.

#### *Uncertainty analyses*

Sensitivity and uncertainty analyses of LDF values were performed for the most dose-contributing radionuclides. Both the effects of parameter uncertainties and conceptual uncertainties were quantified. The results from a selection of these analyses are summarised in Section 13.2.6. The results are further discussed in the **Biosphere synthesis report** and details are presented in /Avila et al. 2010/.

For each input parameter, a combination of site-specific data, generic data, and expert judgement were used to determine a best estimate, and to characterise the uncertainty in the parameter estimate with a probability density function. The parameter uncertainty included natural interannual variation (expected at the site during the interglacial period) and measurement uncertainties. For each selected radionuclide, probabilistic simulations were then performed by applying Monte Carlo simulations for the landscape object that showed the highest LDF value in the deterministic simulations.

Some parameters that occur in the model as time series do not vary independently (e.g. the development of the different regolith layers or different parameters describing aquatic production) and were therefore excluded from the probabilistic simulations. Instead, these parameters were varied systematically as a group, preserving their correlation structure.

A number of conceptual uncertainties were addressed with alternative models. These analyses included e.g. evaluation of the pattern of groundwater discharge using particle tracking in hydrogeological models /Bosson et al. 2010/. Other analyses included evaluation of the effects on the LDFs of a finer discretisation of the lower regolith compartment, evaluation of the effects of periglacial conditions using an alternative parameter set, evaluation of the effects of irrigation, and evaluation of how assumptions on land use and human diet affect LDFs /Avila et al. 2010/.

#### *Input data*

The radionuclide model for the biosphere relies on nearly 140 input parameters, of which a third represent radionuclide- or element-specific properties. The input data include physical constants and parameters that describe the development of the individual biosphere objects. Other parameters describe the characteristics of the ecosystems where radionuclides are likely to accumulate, the surface hydrology which drives transport within and between biosphere objects, element distribution between the solid and aqueous phases, and equilibrium concentration ratios for organisms (see the **Biosphere synthesis report** for more details).

A majority of the parameter values have been estimated from field measurements at the site as part of the site investigations, or have been modelled from the predicted development of the site. These parameter values, which are chosen as typical for the site, are associated with uncertainties due to natural variation and also to the methods used to measure and model them. There are also parameters describing the exposed individuals and the dose coefficients for external exposure, inhalation, and ingestion of food and drinking water. Fixed, slightly cautious values have been chosen for these parameters, in line with international recommendations /ICRP 2007/.

### 13.2.4 Resulting LDF values

Maximum LDFs for a constant release rate of radionuclides (1 Bq/year) were calculated for interglacial and periglacial conditions, and for the global warming climate case. Maximum LDFs for periods when the biosphere objects are submerged were used as a cautious estimate of unit release rate annual doses during the glacial climate domain. Results for the 19 radionuclides that contributed the most to human exposure are presented in Figure 13-7. LDFs for the 40 assessed radionuclides are presented in /Avila et al. 2010/ and in the **Data report**.

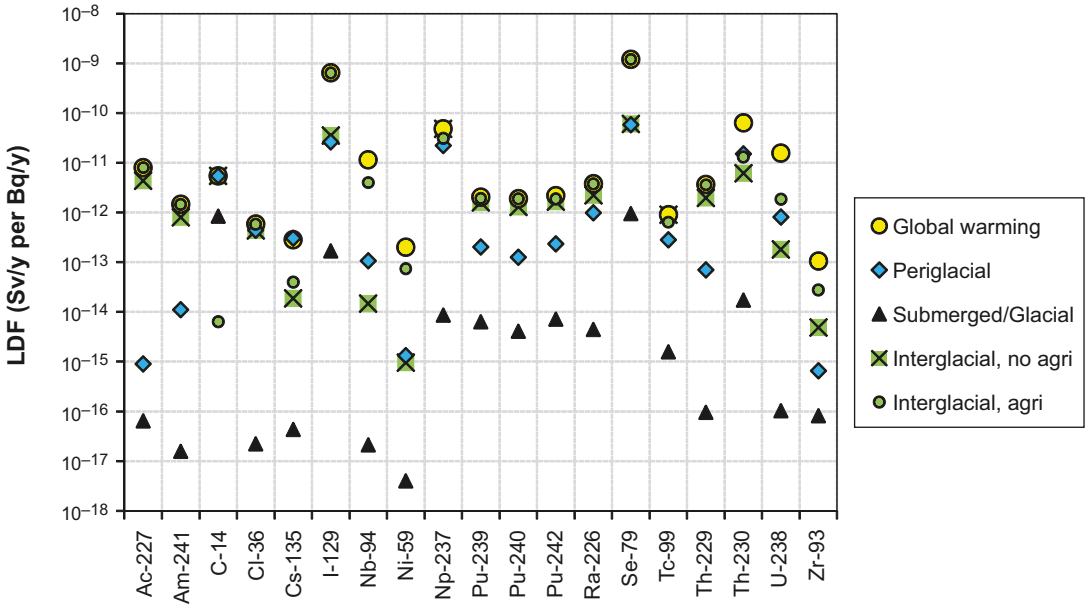


***Figure 13-7.*** *Resulting LDFs (i.e. the highest LDF over time among all biosphere objects) for different climate conditions /Avila et al. 2010/. LDFs for the initial submerged period were used to represent glacial conditions in the assessment. The effect on the LDFs of using agricultural products as food is visualised by including and excluding food from arable land during the interglacial period.*

The LDFs are consistently higher for the interglacial period than for any of the other climate domains in the reference glacial cycle (Figure 13-7). For instance, LDF values for glacial conditions are less than the values for interglacial conditions by two orders of magnitude or more, and also LDFs for periglacial conditions are lower than the corresponding values for the interglacial period, although they are higher than the LDFs for glacial conditions. For most radionuclides, the LDFs for the interglacial period differ marginally between the situations with and without agriculture (Figure 13-7). However, for a few radionuclides (i.e. C-14, I-129, Nb-54, Ni-59, U-238), the LDFs differ by more than an order of magnitude between these two situations (see further the **Biosphere synthesis report** and /Avila et al. 2010/).

Thus, the highest doses from a constant release rate from the repository are expected under interglacial conditions when humans are exposed to radionuclides that have accumulated in a wetland that has been converted to arable land, and when contaminated well water is utilised by human inhabitants and livestock. The only exception is C-14, for which the LDF also is highest in the interglacial period, but the maximum LDF occurs when agriculture is not possible. Accordingly, the LDFs for the interglacial period are the maximum values applicable during the reference glacial cycle and have been used for the dose assessments in e.g. the corrosion scenario (see Section 13.5).

The global warming climate case is represented by a 50,000 year extension of temperate conditions. Consequently, radionuclides that do not reach steady state activity concentrations within the initial temperate period (–9000 to 9400 AD) will continue to accumulate during the extended temperate period. However, most radionuclides have approached steady state at 9400 AD, and additional accumulation and the associated increase in LDF is marginal for dose-dominating radionuclides (exemplified for biosphere object 121-3 in Figure 13-8). Therefore, the LDFs for most radionuclides calculated for the global warming case do not differ significantly from those for reference glacial cycle. However, two radionuclides, Cs-135 and U-238 (the latter not included in the figure), have maximum LDFs approximately an order of magnitude larger in the global warming climate case than under the reference glacial cycle, which can be explained by several factors as discussed in /Avila et al. 2010/. However, due to the small contributions of Cs-135 and U-238 to the total risk estimate resulting from a long term release (see Section 13.5.4), this tenfold increase in the LDFs of these nuclides would not affect the final risk estimates significantly. It is therefore concluded that, from the perspective of the biosphere, the global warming case is not significantly different than the reference glacial cycle.

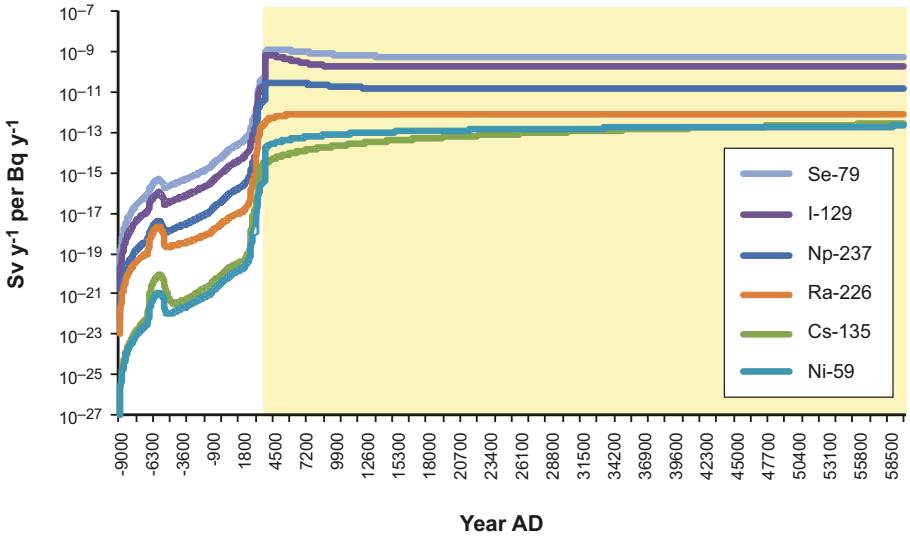


***Figure 13-8.*** *Development of the LDF for a number of radionuclides in biosphere object 121-3 in the global warming climate case. Yellow colour indicates when agriculture is possible /Avila et al. 2010/.*

The LDFs clearly vary among biosphere objects, and the degree of variation depends on the properties of different radionuclides (Figure 13-9). For radionuclides for which food ingestion is the dominant exposure pathway (i.e. C-14, Cl-36, I-129, Nb-94, Np-237, Se-79, Sn-126, and Tc-99), the LDFs typically vary by two to three orders of magnitude among objects (excluding object 105). However, for radionuclides for which drinking water is an important exposure pathway (e.g. Am-241, Pa-231, Pu-239, Pu-240, Pu-242, Ra-226 and Th-229), the variation in LDFs among objects is typically less than a factor of three. For most radionuclides, the rank order of objects with respect to LDF is similar. Biosphere object 121-3 (Figure 13-8) yields the highest LDF for a majority of the examined radionuclides, whereas biosphere object 105, which is in the sea stage during the entire interglacial, consistently has three orders of magnitude or more lower LDFs for all radionuclides /Avila et al. 2010/.

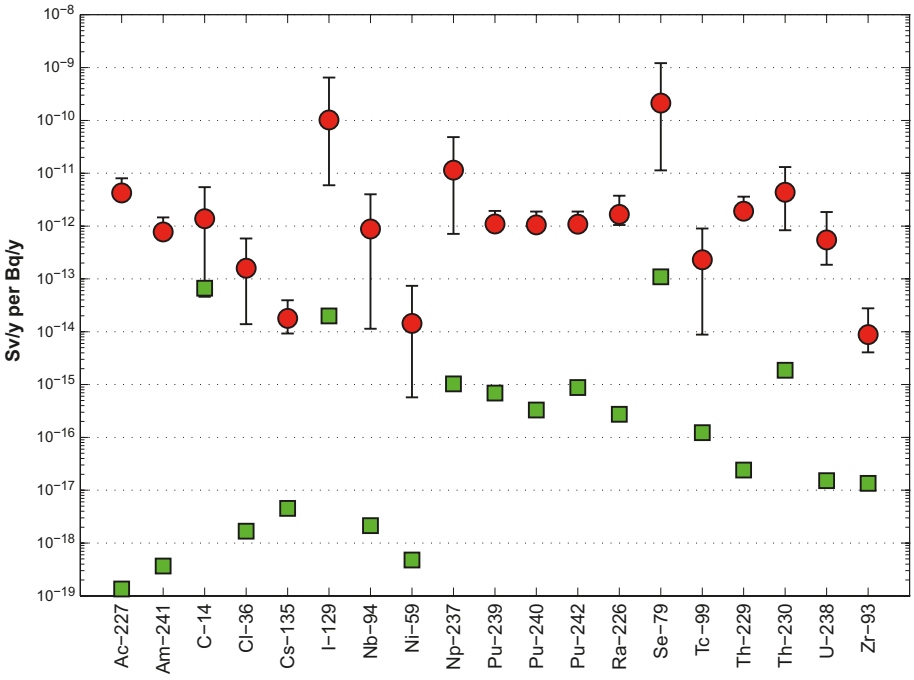


***Figure 13-9.*** *Mean (red circles), minimum and maximum LDF for a selection of radionuclides across biosphere objects (excluding object 105). The LDF values for object 105, which is submerged during the whole interglacial, are shown separately (green squares) /Avila et al. 2010/.*

In e.g. the central corrosion case, a fraction of the inventory in a canister is assumed to be instantaneously released from the fuel upon water contact, propagated through the geosphere, and released to the biosphere as a pulse with a duration of years to hundreds of years (see Section 13.5.2). The modified LDF values for radionuclides that may be present in pulse releases are presented in Table 13-2. The values correspond to the maximum annual doses obtained in a simulation with a pulse unit release of 1 year duration, occurring at any time point within a period with temperate conditions.

#### *Comparison of the SR-Site LDFs with results from earlier studies*

The method used for calculating landscape dose factors in SR-Site has been updated in several important ways since the last two biosphere assessments of a deep repository (i.e. SR-Can /SKB 2006a/ and SR 97 /SKB 1999a/), and data from the site have been used to modify parameters from values used in the past, with improved justification for the values used in the present assessment. The changes in methodology and parameter values, and their consequences for exposure, are discussed in detail in /Avila et al. 2010/.

The maximum values of the ecosystem specific dose conversion factors (EDF) used in SR 97 /Bergström et al. 1999/ were systematically higher than the LDFs calculated in the present assessment, with the exception of a few radionuclides (e.g. C-14) (Figure 13-10). These differences are attributable to important methodological differences between the two assessments, including the delineation of the sub-catchment, assumptions on where a release will reach discharge areas and enter the ecosystems, as well as differences in the approach to evaluate the well /Avila et al. 2010/. Moreover, in the SR 97 assessment, generic parameter values were used in most cases, whereas site-specific data obtained during the site investigation programme have been broadly applied in the SR-Site assessment.

### 13.2.5 Approach and methods for assessment of radiological effects on the environment

To ensure the protection of the environment, adverse effects on non-human biota from a potential radionuclide release in the Forsmark area were assessed (see details in /Torudd 2010/). The assessment was carried out using the approach developed within the European projects FASSET /FASSET 2004/, ERICA /Beresford et al. 2007/ and PROTECT /Howard et al. 2010/, and recommended by ICRP /ICRP 2007/. Thus, the potential effects were evaluated of a radionuclide releases on individual specimens of a variety of types of organism occurring at the site. This approach is based on the rationale that if there are no detrimental effects at the level of individuals, then negative consequences at the population or ecosystem levels can also be excluded see /Torudd 2010/.

**Table 13-2. Modified landscape dose conversion factors derived for pulse releases (from /Avila et al. 2010/). Asterisk denotes the radionuclides contributing most to dose in the pulse release cases (see Section 13.5.4).**

| Radionuclide | LDF pulse Sv/y per Bq |
|---|---|
| Se-79* | $9.7 \cdot 10^{-14}$ |
| I-129* | $5\,6 \cdot 10^{-14}$ |
| Cl-36 | $4.3 \cdot 10^{-15}$ |
| Tc-99 | $2.8 \cdot 10^{-15}$ |
| Sn-126 | $2.3 \cdot 10^{-15}$ |
| Ag-108m | $5.1 \cdot 10^{-16}$ |
| Nb-94 | $3.2 \cdot 10^{-16}$ |
| Cs-135 | $1.8 \cdot 10^{-16}$ |
| Ni-59 | $9.7 \cdot 10^{-18}$ |

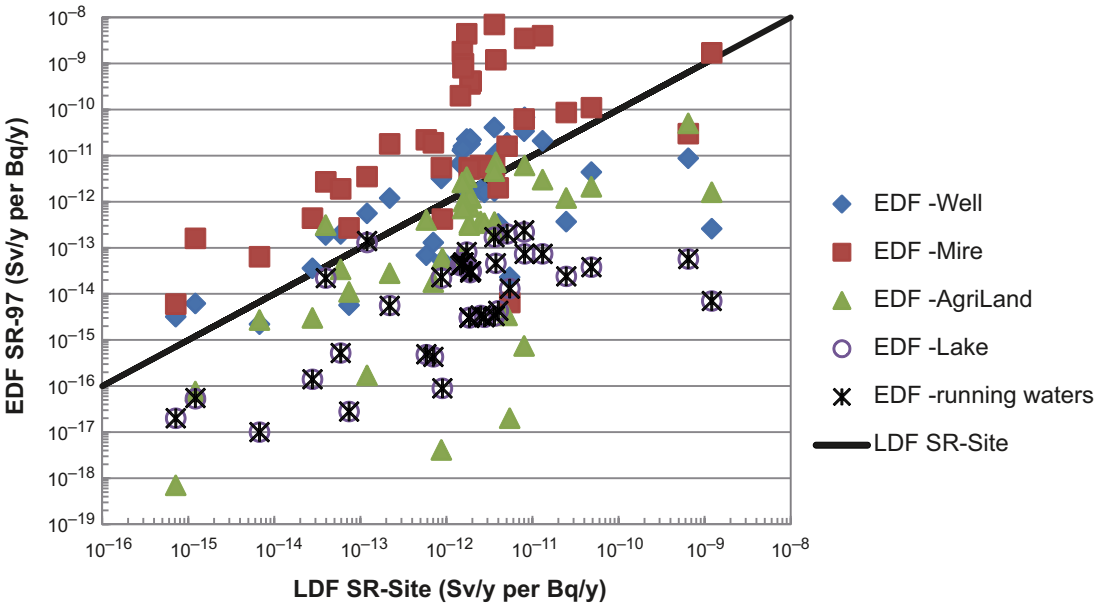


***Figure 13-10.*** *Comparison of the SR-Site LDFs with corresponding dose conversion factors (EDF) reported in SR 97 /SKB 1999a/. The solid line represents a 1:1 relationship between SR-Site and the SR 97 dose factors, and each point represents a specific radionuclide /Avila et al. 2010/.*

The primary focus was put on species that are presently found in the Forsmark area and that occupy habitats where they can be exposed to discharges from the repository. In addition, a number of reference organisms defined in the ERICA tool see /Brown et al. 2008/, were included in the assessment. Instead of using a unit release rate as for the assessment of doses to humans, it was desired to conduct an analysis to understand the likely importance of effects on the environment. Consequently, calculated radionuclide releases to the surface from the probabilistic calculation of the central corrosion case (Section 13.5.4) were used as input to the calculations. By selecting these release rates, the maximum potential impact on the environment in any time period is assessed.

The activity concentrations in water and upper regolith of the aquatic and terrestrial ecosystems, calculated with the radionuclide model for the biosphere, were used as input in the ERICA tool to obtain activity concentrations in different types of organism. The ERICA tool then estimated the total absorbed dose rates, both internal and external. The sum of the absorbed dose rates was evaluated against a screening no-effect dose rate of 10 $\mu Gyh^{-1}$ /Andersson et al. 2009/. The results from the assessment are summarised in Section 13.5.7. A more detailed presentation of the methods and results is given in the **Biosphere synthesis report** and a full description of the assessment can be found in /Torudd 2010/.

### 13.2.6 Uncertainties and cautiousness in the risk estimates

There are two major types of uncertainties associated with the final LDFs. The first type is related to uncertainties in the parameter values. The effect of these uncertainties on the LDFs can be evaluated through systematic and/or random variations of parameter values (see /Avila et al. 2010/ and /Ekström 2011/). The second type, conceptual uncertainties, is related to model assumptions or to conceptual descriptions, which in turn are based on our understanding of the system and on model simplifications. Conceptual uncertainties have to be evaluated by the use of alternative approaches and models, or by discussing the potential outcome of erroneous assumptions.

The effect of these two types of uncertainty differs among radionuclides. To illustrate the approaches used to evaluate uncertainty, the following discussion is presented, based on the modelling of a continuous release in the central corrosion case. It focuses on the most relevant parameters, based on a sensitivity analysis /Avila et al. 2010/, and on the radionuclides contributing most to dose, especially Ra-226 (see Section 13.5.4). A more detailed discussion of uncertainties in the LDF modelling is found in the **Biosphere synthesis report**.

### *Influence of parameter uncertainties on the final LDF estimates*

The deterministic LDFs were calculated by selecting input parameters using expert judgement, with an intention that the LDF should reflect a reasonable value, given the uncertainties. This approach should therefore produce results that represent the central tendency of a full analysis of parameter uncertainty. To substantiate this approach, probabilistic simulations were used to propagate parameter uncertainties through the model to establish how they affect the LDF estimates. The LDF distributions calculated in this way were approximately log-normal, with a 90% confidence interval of LDFs typically spanning two orders of magnitude (Figure 13-11).

The central tendency of distributions that span several orders of magnitude can be thought to be represented by either the median or the mean of the distribution. Due to the log-normal distribution of LDFs, the arithmetic mean was systematically higher than the median value. Because of the nature of information used to establish the input distributions for the probabilistic approach, there is uncertainty whether the distribution represents actual site behaviour. Often, parameter distributions reflect generic information; as a result the calculated LDF distributions may have excessively broad ranges, and the mean value may be skewed to excessively high values. Nevertheless, for most radionuclides, including all major dose-contributing nuclides, the deterministic LDFs and the arithmetic mean were within a factor three.

The deterministic LDFs were generally close to the median and slightly lower than the mean of the probabilistic simulations, with a few exceptions. For a few radionuclides, use of the mean calculated probabilistically would have resulted in LDFs that were an order of magnitude larger than the LDFs used in the safety assessment (e.g. Tc-99, Th-230 and U-238). However, the potential release of these nuclides to the biosphere is expected to be insignificant (see Section 13.5.4). Thus, it can be concluded that there is reasonable agreement between the deterministic approach to calculating LDFs for use in the safety assessment, and a probabilistic approach that propagates parameter uncertainties relevant for evaluating the safety of the repository. This is discussed in more detail in the **Biosphere synthesis report** and in /Avila et al. 2010/.

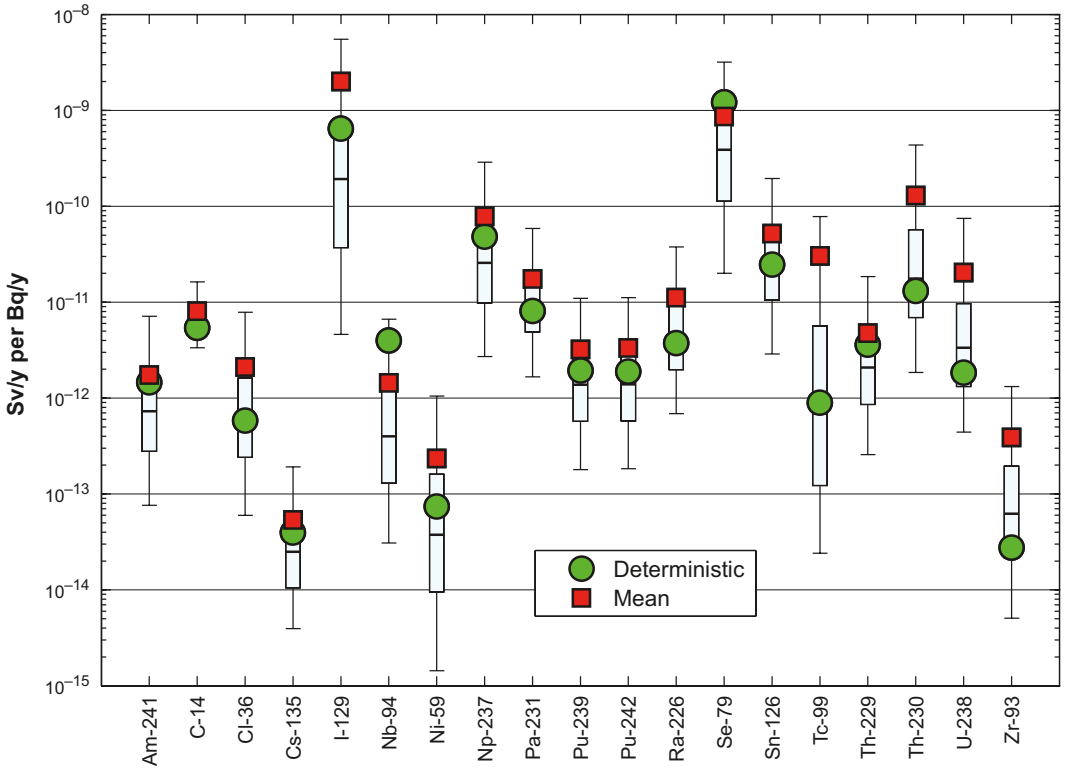


***Figure 13-11.*** *Variation in interglacial LDFs obtained from probabilistic simulations for a subset of the analysed radionuclides. The LDF distributions are taken at the time when the median of the probabilistic output reached its peak. The mean, median, 5 percentile and 95 percentile from the probabilistic simulations are shown. The deterministic LDFs are also shown for comparison (from /Avila et al. 2010/).*

### *Discharge of radionuclides into the biosphere*

The identification of the potential discharge areas for deep groundwater determines the characteristics of areas that are likely to be affected by radionuclides from the repository. The hydrogeological models /Joyce et al. 2010, Bosson et al. 2010/ predict that discharge areas will primarily be located in low points of the landscape such as lakes, wetlands and shallow parts of the sea floor. According to /Joyce et al. 2010/, the discharge pattern is determined mainly by the local topography and the deterministic deformation zones, and the pattern does not vary significantly among model realisations. Detailed surface hydrological modelling confirmed the overall pattern of the location of discharge areas in Forsmark /Bosson et al. 2010/.

Several characteristics of the biosphere objects (including area of sub-catchment, timing of emergence from the sea and depth of regolith layers) affect the transport and accumulation of radionuclides. These features are not independent properties, but they vary together in response to the topography and geometry of the landscape. There are uncertainties in the location and configuration of the biosphere objects that are submerged today, associated mainly with uncertainties in the sea floor bathymetry and regolith characteristics. However, the identified biosphere objects span a wide range in different characteristics, such as topographical location, geometric features and thickness of different regolith layers, and they are therefore assumed to be representative both for the present and the future landscape.

Although there are many characteristics that affect the predicted development of activity concentrations in a discharge area, the steady state activity concentrations in soil and water are primarily determined by the sizes of the watershed and the local drainage area (sub-catchment). The biosphere objects that yield the highest environmental activity concentrations are objects with a small sub-catchment and no inflow of surface water from an upstream watershed. These objects can typically support 80 individuals, and the most extreme object has a local drainage area which is only three times larger than the lake/wetland area (24 ha). In theory, smaller biosphere objects with smaller sub-catchments could sustainably support a group of say 10–20 individuals. However, a thorough analysis of the Forsmark landscape fails to identify any discharge area with a smaller sub-catchment than 24 ha and a reasonable likelihood of persistent release from the repository /Lindborg 2010/.

The use of maximum LDF values in the calculation chain (see Figure 13-3) disregards the fact that discharges may affect several objects, and that different nuclides will give maximum LDF values during different successional stages of the biosphere. Thus, the maximum LDF used in the assessment overestimates the potential risk.

In the LDF calculations, a unit release rate of 1 Bq/y is used (see Section 13.2.3). This concept overestimates the LDF during low flow conditions, e.g. when a biosphere object is submerged, compared with periods with high water flows, because the source term to the biosphere is not a constant but varies with the flow conditions. The flow conditions affect the fluxes from the repository by an order of magnitude, as shown in Figure 13-33. The maximum LDF value is unaffected by this variation in flow conditions, but in the interpretation of the development of LDF over time (Figure 13-8), this has to be considered.

It is concluded that the biosphere objects used to represent the future Forsmark landscape give a reasonable representation of the range of discharge areas that may receive contaminated groundwater from the repository, and consequently uncertainties with respect to the properties of future discharge areas have been incorporated in the LDF values used in the safety assessment. It is also concluded that the concept of unit release rate and the application of maximum LDF values in the risk assessment means that the risk is overestimated (see further /Avila et al. 2010/).

### *Accumulation of radionuclides in the regolith*

Uncertainties in parameters describing radionuclide retention in regolith layers have an impact on the overall uncertainty of LDF results. For the dose-dominating Ra-226, the partitioning coefficient between the solid and liquid phases (i.e. the $K_d$ value) for the lower regolith layer explained approximately 60% of the overall uncertainty, and additionally 7% was explained by $K_d$ for the upper and mid-regolith layers, see the **Biosphere synthesis report**. The main reason for the large variation in $K_d$ value for Ra-226 was that the available site data were insufficient to give a reliable estimate of the natural variation. Instead, the $K_d$ value for Ra-226 was estimated from literature data /IAEA 2010/, spanning a wide range of geographical conditions and soils types.

However, the available site data are in the same order of magnitude as the best estimate from the literature, suggesting that an appropriate site-specific estimate would not be likely to deviate by orders of magnitude from the value used in the assessment, see the **Biosphere synthesis report**. To validate the LDF for Ra-226 used in SR-Site, and to estimate the effect of a reasonable span in the uncertainty of the estimate, LDFs for Ra-226 were recalculated using recently (autumn 2010) collected site data (see /Avila et al. 2010/ and references therein).

The analysis showed that the LDF for Ra-226 used in SR-Site deviates less than a factor of two from the LDF calculated with $K_d$ values based on site data. This was not surprising as the $K_d$ value for organic sediments based on site data closely matched the literature value of 2.5 $m^3$ $kg^{-1}$, and the $K_d$ value for inorganic sediments was within an order of magnitude of the literature value. However, literature data clearly exaggerate the uncertainty of Ra-226 retention at the site, and consequently the uncertainty in $K_d$ estimated from the site data was used in the probabilistic simulations that addressed the effect of parameter uncertainty. Thus, we conclude that the $K_d$ values for Ra-226 used in SR-Site are representative for the site, and that the LDF value for Ra-226 is reasonable with respect to the uncertainty in $K_d$ value for Ra-226 at the site.

**Discretisation of the regolith compartments**

In the radionuclide model**,** the lower regolith is represented by a single compartment. A single-compartment model will tend to produce earlier breakthrough and more dispersion of radionuclides that are accumulating in the regolith, than a model with a finer discretisation. To examine the effect of discretisation on dilution and dispersion, the lower regolith compartment was split into a varying number of compartments, stacked on top of each other /Avila et al. 2010/. The analysis showed that a finer discretisation of the lower regolith compartment increases the retention in deeper soil layers, but that this has a limited effect on the calculated LDFs for most radionuclides (including the dose-dominating nuclides). Moreover, for radionuclides that are affected by the discretisation, the single-compartment representation used in SR-Site leads to pessimistic LDF estimates as compared to estimates based on finer discretisation of the lower regolith (see the **Biosphere synthesis report** and /Avila et al. 2010/.

### *Human behaviour and utilisation of the landscape*

A potential release of radionuclides from the repository will reach the biosphere in spatially restricted discharge areas, i.e. biosphere objects. It is concluded that the highest activity concentrations in the landscape over time will be found in biosphere objects that receive direct releases of radionuclides from the geosphere /Avila et al. 2010/.

In the assessment it is assumed that the most exposed group spend all of their time in the contaminated area, and get their full supply of food and water from the biosphere object. It is further assumed that a contaminated wetland will be drained and used for agricultural purposes at the point in time which would result in the maximum annual dose for unit release rate. These assumptions are unlikely in a cultural or landscape utilisation perspective. For example, a sustainable agricultural use of the drained organic soils that are typical for the biosphere objects is possible only for a period of 50–100 years /Lindborg 2010/. In contrast, the thick and partly continuous layers of clay and sand in the central parts of Öregrundsgrepen can be sustainably cultivated for thousands of years.

Thus, a more realistic scenario for a future self-supporting society in the area is that the mainly lightly contaminated central parts of Öregrundsgrepen will be intensively cultivated and contribute the major part of the food consumed, even by the most exposed group. Some of the small biosphere objects may occasionally be cultivated and may then complement the food produced in the more suitable agricultural areas in Öregrundsgrepen, but probably the biosphere objects will primarily be utilised for extensive collection of naturally produced foods. Thus, the assumption that a representative individual of the most exposed group will spend all his or her time in the contaminated area and get his/her full supply of food and water from this biosphere object is strongly pessimistic. The effect of uncertainties in the composition of the human diet was investigated in a separate probabilistic simulation. According to the results, uncertainties in dietary composition affect the LDFs less than a factor 2 (see further /Avila et al. 2010/).

For the LDF calculations it was assumed that vegetables are irrigated with contaminated surface water. The effects of irrigation with well water and long-term irrigation were explored in separate simulations. Irrigation with well water increased activity concentrations in vegetables somewhat for most examined nuclides, but the effects on the most dose-contributing radionuclides was typically below a factor of two. Long-term irrigation of uncontaminated minerogenic soil with contaminated surface water did not result in higher concentrations in vegetables than those resulting from draining and cultivating a wetland in an adjacent contaminated discharge area /Avila et al. 2010/. From these simulations it was concluded that assumptions on the origin of contaminated irrigation water did not significantly affect the calculated LDFs, and that long-term irrigation with contaminated surface water would not lead to significantly higher doses than those arising from the initial cultivation of the contaminated organic soil /Avila et al. 2010/.

### *Summary and conclusions*

The biosphere assessment is built on knowledge and results from extensive investigations of the site. The site investigations have underpinned the conceptual description of the site and contributed to a systematic mapping of processes that may be important for transport and accumulation of radionuclides in the biosphere, in order to ensure that all relevant processes have been included in the assessment. The investigations have also enabled the use of parameter estimates that correspond to conditions at the site today and in the future, in the different modelling steps.

A number of different biosphere objects have been identified as potential release areas for radionuclides from the repository. The objects are situated in a dynamic landscape, ranging from fully submerged to entirely terrestrial, and they include considerable variation in size, timing of succession and object-specific properties. Even if the exact future landscape development is difficult to predict, the modelled landscape development can be seen as a systematic evaluation of possible futures, based on the understanding of how present-day geometries have developed and an expected shoreline displacement regime.

An ecosystem-based approach has been used to dynamically model the transport and accumulation of radionuclides in the biosphere objects over a 70,000 years long ice-free period of the reference glacial cycle. Effects of different climate conditions have also been evaluated in the modelling approach. Human utilisation of natural resources was, in the assessment, based on the productivity of natural and cultivated food in the object. The annual dose to future inhabitants of the Forsmark area was calculated per unit constant release rate to each biosphere object and for each radionuclide. The calculated LDFs have been selected from the biosphere object and point in time which gives the highest unit release dose, and consequently LDFs from different nuclides do not necessarily match the same group of exposed individuals with respect to point in time or location in the landscape.

Additional simulations and alternative models have been used to explore how uncertainties and assumptions may affect the final LDF estimates. From these analyses it is concluded that neither object discretisation, nor parameter uncertainties, nor assumptions on human utilisation of natural resources will have significant effects on the calculated LDFs. However, the analyses highlighted that a large proportion of LDF uncertainty can be attributed to parameters describing the partitioning of radionuclides between the solid and liquid phases (i.e. $K_d$ values) and biological uptake (i.e. CR values). Consequently, the uncertainties can be reduced by better estimates of these parameters from the site, or by alternative modelling approaches for sorption and uptake of radionuclides that are less sensitive to parameter uncertainties (see further discussion in the **Biosphere synthesis report**).

Even though the intent of the biosphere modelling effort has been to make the assessment as realistic as possible, a systematic evaluation of the effects of assumptions and other sources of uncertainties on the SR-Site LDFs shows that the handling of system and model uncertainties tends to be cautious, see the **Biosphere synthesis report**. Site representative values were used for model parameters, and their uncertainties were not handled pessimistically, whereas the definition of the most exposed group was clearly cautious. However, the effect of quantified uncertainties was limited and is therefore not expected to have a significant effect on the assessment endpoint. Taken together there is confidence that the maximum LDFs used in SR-Site are robust estimates for the most exposed group, reflecting process understanding and the most precise description of the site available.

## 13.3 Criticality

If a canister failure occurs, the issue of nuclear criticality has to be considered, since, if this occurred, it could have a strong influence on the further development of the failed canister and of repository areas in its vicinity.

The possibility of nuclear criticality in the canister interior, process F3 Induced fission (criticality) in the process table for the fuel in Section 7.4.1, has been dismissed in a number of studies, see e.g. the SR-Can report /SKB 2006a/. The issue has most recently been analysed by Agrenius /SKBdoc 1193244/.

In the repository, the normal spent fuel criteria for safety against criticality must apply. This means that the effective neutron multiplication factor $k_{eff}$, including uncertainties, must not exceed 0.95. Agrenius /SKBdoc 1193244/ has calculated the effective neutron multiplication factor $k_{eff}$ after disposal. Uncertainties in the determining parameters such as the position of the assemblies in the canister, the manufacturing tolerances and the size of fuel compartments in the insert, and temperature, variation with enrichment, were taken into account. The calculations were performed for fresh fuel with an initial enrichment of 5% U-235. For a loaded and sealed canister filled with argon the $k_{eff}$ value is less than 0.4 and the system is strongly subcritical.

If it is assumed that the canister is leaking and that the canister storage positions and the fuel assemblies are water filled, the reactivity will increase. With all fuel element locations occupied in a canister deposited in the repository, surrounded by 35 cm bentonite and filled with water, the following results are found:

BWR: $k_{eff} = 0.9959 \pm 0.0002$

PWR: $k_{eff} = 1.0888 \pm 0.0002$

It can therefore be concluded that the reactivity criteria could not be met for a failed canister with the pessimistic assumption that the fuel is fresh. A more realistic assumption would be to take credit for the burnup of the fuel, which will decrease the reactivity. Agrenius /SKBdoc 1193244/ also calculated the neutron multiplication factor for irradiated fuel with various initial enrichments including the isotopic concentrations for two sets of isotopes. These calculations showed, using state-of-the-art methods and a reasonable assessment of the uncertainties, that taking credit for the burn-up of the fuel, the criterion $k_{eff} \leq 0.95$ could be met for both BWR and PWR fuel of a given burnup. The results are further discussed in the **Fuel and canister process report**, Section 2.1.3. Acceptance criteria for encapsulation of fuel assemblies are defined to ensure that the fuel assemblies shall not, under any circumstances, be encapsulated if the criticality criteria cannot be met, see further Section 5.3.4.

The risk of criticality as a result of redistribution of material has been analysed by /Behrenz and Hannerz 1978/ and by /Oversby 1996, 1998/. The conclusions were that criticality outside the canister has a vanishingly small probability, requiring several highly improbable events. After the report of a possibility of criticality outside a canister by /Bowman and Venneri 1994/ that was dismissed in a review by /Van Konynenburg 1995/, several other studies have concluded that criticality in a geologic repository as a result of redistribution of fissile material is a highly unlikely event.

The possibility of nuclear criticality in the vicinity of the proposed Yucca Mountain repository was explored recently by /Nicot 2008/. It was concluded that external nuclear criticality is not a concern at the proposed Yucca Mountain repository for any of the deposited waste. Some of the waste intended for Yucca Mountain contains higher levels of fissile material than what is intended for disposal in a Swedish repository.

In conclusion, credit for burnup has to be taken to demonstrate that the canister remains subcritical in the repository for all reasonably conceivable scenarios (Table 2-3 in the **Fuel and canister process report**). The probability of criticality inside or outside the canister is considered to be negligibly small, based on the results reported in /SKBdoc 1193244/ and in /Van Konynenburg 1995, Oversby 1996, 1998, Nicot 2008/.

## 13.4 Models for radionuclide transport and dose calculations

Figure 13-12 shows the models and data used in the radionuclide transport and dose calculations. In the following, a brief description is given of the near-field model COMP23 in Section 13.4.1 and of the far-field model FARF31 in Section 13.4.2, which also describes a separate model, MARFA, for modelling of varying flow and colloid-facilitated transport in the geosphere.

Radionuclide transport and dose consequences for some cases have been calculated with simplified, analytical models that yield similar results to the numerical models. The analytical models are briefly explained in Section 13.4.4.

### 13.4.1 The near-field model COMP23

The near-field radionuclide transport model used in SR-Site to handle radionuclide transport in the water phase is COMP 23 /Cliffe and Kelly 2006, Kelly and Cliffe 2006/. This is an updated version of the compartment model used in the SR 97 assessment and it was originally developed from the NUCTRAN code /Romero 1995, Romero et al. 1999/. In SR-Site, a Matlab/Simulink implementation /Vahlund and Hermansson 2006/ is used to solve the COMP23 model instead of the original Fortran implementation.

COMP23 models processes related to radionuclide release and transport in the canister interior, the buffer and the deposition tunnel backfill, i.e. the summary processes F17, Bu25 and BfT21, respectively in the process tables in Section 7.4. These incorporate the processes radioactive decay (F1), metal corrosion (modelled as a constant metal corrosion rate, F11), fuel dissolution (F12), dissolution of gap inventory (modelled as an instantaneous release, F13), speciation of radionuclides (i.e. dissolution/precipitation of nuclides with shared elemental solubilities, F14), diffusion (Bu11) and sorption (Bu12) in the buffer and advection (BfT9), diffusion (BfT10) and sorption (BfT11) in the deposition tunnel backfill. It also handles the release of radionuclides to exit paths from the near field, see below.

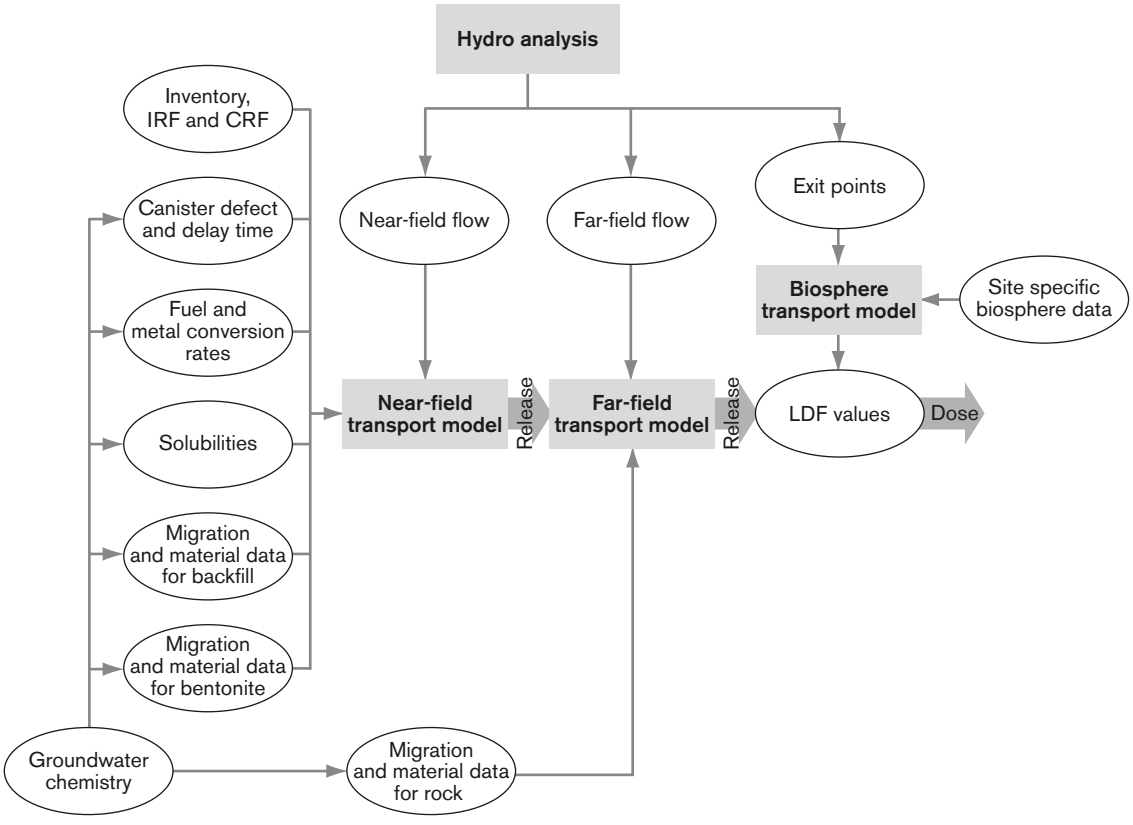


***Figure 13-12.*** *Models and data for the consequence calculations.*

COMP23 is a multiple-path model that calculates transient nuclide transport in the near field of a repository by use of a network of coupled resistances and capacitances in analogy with an electrical circuit network. Analytical solutions, instead of fine discretisation, at sensitive zones, for example at the exit point of a small canister hole and at the entrance to fractures, are embedded to enhance calculation speed.

Figure 13-13 shows the canister, deposition hole and the deposition tunnel backfill and how these are modelled by COMP23 in SR-Site. Three exits from the near field are included: a fracture intersecting the deposition hole at the vertical position of the canister lid, denoted Q1, an excavation damaged zone, EDZ, in the floor of the deposition tunnel (if such a zone is assumed to exist), Q2, and a fracture intersecting the deposition tunnel, Q3. In the hydrogeological modelling, the number of fractures intersecting a deposition hole and the properties of these fractures are determined statistically based on the DFN description of the rock, see further the **Data report**, Section 6.6. If more than one fracture intersects a deposition hole, the transport capacity of the several fractures are added and pessimistically assigned to the single fracture modelled by COMP23. The equivalent flow rate through Q2 is also calculated as an integral part of the hydrogeological modelling. Data on transport properties for the EDZ used in these calculations are given in the **Data report**, Section 6.5. The flow rate in the deposition tunnel and the distance to the nearest Q3 fracture through which radionuclides

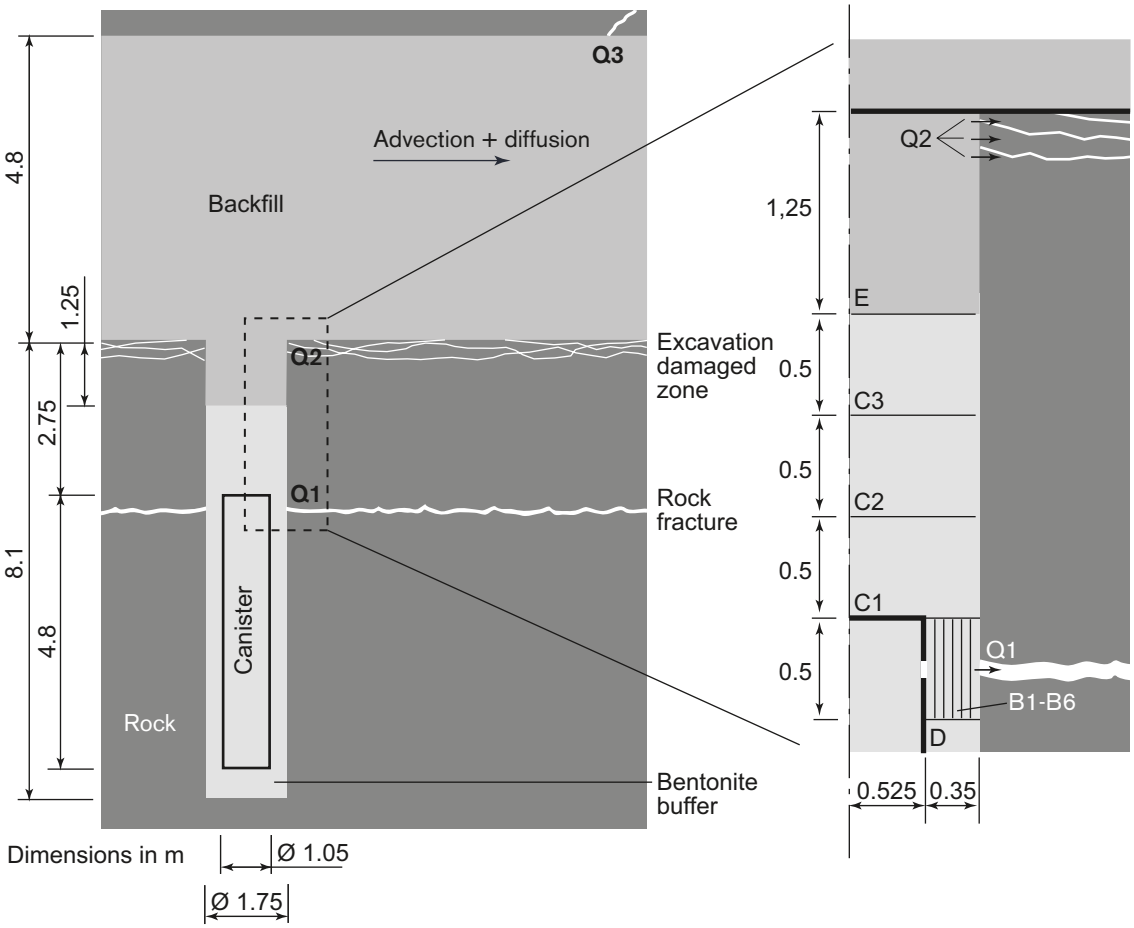


***Figure 13-13.*** *The near field and detail of its model representation as compartments B1–B6, C1–C3, D and E in the model COMP23. The transport paths Q1, Q2 and Q3 to a fracture intersecting the deposition hole, to the excavation damaged zone, and to a fracture intersecting the deposition tunnel, respectively, are also shown. (Potentially a minor EDZ around the deposition hole could exist, but as shown in the* ***Underground construction report*** *such a zone would have very low – if any – connected hydraulic conductivity and is thus not included in the model.) The differentiation of compartments shown in this figure is relevant for a pinhole failure in the canister. All other analysed failure modes require less differentiated representations of the near field.*

are released to the geosphere from the tunnel are given by the hydrogeological modelling. Transport by advection/diffusion in the tunnel is included in the near-field simulations and the computational domain is extended in the downstream direction to include the Q3 fracture.

Effects of spalling in deposition holes are treated by a modification of the input equivalent flow rates for the transport path Q1, as described in Section 10.3.6 and further in the **Data report**, Section 6.6. The handling of spalling does not require any modification of the numerical model.

Advective conditions in the buffer are simply treated by equating the outflux from the canister interior compartment with the release to Q1. The release paths Q2 and Q3 are not modelled when advective conditions are assumed in the buffer since releases to Q1 completely dominate over those to Q2 and Q3 for such cases.

### 13.4.2 The far-field models FARF31 and MARFA

The far-field radionuclide transport models used in SR-Site to handle radionuclide transport in the water phase are FARF31 /Norman and Kjellbert 1990, Elert et al. 2004/ and MARFA /Painter and Mancillas 2009/.

FARF31 has been employed already in earlier assessments, e.g. SR 97 /SKB 1999a/ and SR-Can /SKB 2006a/, whereas MARFA has been developed for use within SR-Site. Development of MARFA is still on-going as detailed below. Within SR-Site, MARFA is primarily used for calculations employing code functionality not available in FARF31. The two codes are partially used also in parallel within SR-Site to show that they produce consistent results.

The two codes solve migration along one-dimensional paths and handle, using the nomenclature in the process tables in Section 7.4, the process Ge24 ‘Transport of radionuclides in the water phase’, consisting of the sub-processes advection (an aspect of process Ge11), dispersion, matrix diffusion with equilibrium sorption (Ge12 and Ge13), and radioactive decay (F1, including decay chains). MARFA can in addition also handle equilibrium sorption within the flowing phase, i.e. not only within the stagnant water of the matrix.

In FARF31, the equations are solved analytically in Laplace space and subsequently numerically inverted to obtain the breakthrough curves. It is noted that the equations are expressed in terms of accumulated travel time rather than distance along the flow path. This feature makes it easy to calculate travel times in a stand-alone groundwater flow model, see Section 10.3.6, and subsequently radionuclide transport in a decoupled fashion.

FARF31 was originally developed to be used with a groundwater flow model adopting a continuum representation of the rock. In SR-Site, groundwater flow is primarily modelled through a discrete fracture network (DFN) where individual fractures are represented explicitly. Here, the conceptualisation of a migration path is slightly different than in a continuum-based groundwater flow model. Rather than macroscopic stream tubes encompassing both rock and flow paths, the equation now describes flow paths through the actual open pore space, i.e. through the connected fracture network /RETROCK 2005/. However, the governing equations are identical for the two conceptualisations. The entities calculated in the DFN-based groundwater flow models are the advective travel time ($t_w$) and flow-related transport resistance ($F$) along flow paths. FARF31 has been modified to use these inputs directly.

MARFA (Migration Analysis of Radionuclides in the Far Field) uses a particle-based Monte Carlo method to simulate the transport of radionuclides in a sparsely fractured geological medium. MARFA uses a time-domain random walk algorithm /Painter et al. 2008/, wherein noninteracting particles representing packets of radionuclide mass are moved through the system according to rules that mimic the underlying physical transport and retention processes. MARFA is specifically designed to work with output from discrete fracture network (DFN), continuous porous medium (CPM), or nested DFN/CPM flow models.

The main advantage of MARFA relative to FARF31 is that different retention models can be specified for different sub-units of the system, e.g. different models for hydraulic rock, hydraulic conductor (deformation zone), and hydraulic soil domains. Furthermore, also the engineered part of the system, i.e. tunnels, can be assigned retention. Finally, the flow magnitude, but not direction, can be changed along the pathlines. This provides an opportunity to address, in at least an approximate sense, e.g. glacial conditions where flow may be almost stagnant during ice cover, but very high when the ice front passes above the repository.

Immobilisation processes, known to occur in the field, are not readily quantified and not included in the codes. However, in the **Radionuclide transport report**, these processes are evaluated through screening calculations, and their implications on the safety assessment discussed in detail. The exclusion of these processes in the radionuclide transport codes is judged cautious in terms of resulting doses for most relevant situations, with the possible exception of the case in which there is precipitation with subsequent dissolution due to e.g. changed chemical conditions /RETROCK 2005/. Radionuclides that exhibit sensitivity to redox conditions are most strongly influenced by such processes on account of the fact that they can transition from being essentially immobile to being in a highly mobile state over very short distances in proximity to a redox front. Situations where this might compromise the safety function of the repository, however, are considered to be unlikely on account of the uncharacteristic configuration of redox boundary conditions that such an accumulation and remobilisation process would require.

A limitation with the flow path concept used in FARF31 is that only steady-state velocity fields can be addressed (adopting the snapshots in time approach for transport modelling), whereas the flow field is expected to evolve in time due to shoreline displacement. In MARFA, changes in flow magnitude can be handled.

Colloid-facilitated transport is not included in FARF31. For rapid reversible sorption/desorption onto colloids, an expression is derived which modifies the MARFA input parameters which quantify radionuclide retention in the host rock matrix. In principle, the same modification could be done in FARF31, but colloid-facilitated transport is chosen to be handled in MARFA since this case is combined with changes in flow conditions.

### 13.4.3 Biosphere representation

The biosphere is mainly represented by multiplying the radionuclide releases from the near field or from the geosphere by an appropriate dose conversion factor, i.e. the LDF, derived as explained in Section 13.2.3.

The so obtained doses, or, in the case of the near field, dose equivalent releases, are the main calculation end-points in the consequence calculations presented in this chapter. The conversion to dose is done to obtain a convenient measure of the impact of the releases, where also a total measure is obtained as the summed dose.

In some release situations, a pulse is rapidly released to the biosphere, and the LDF that is derived for a steady state release, is not a suitable conversion factor. In such cases the pulse LDFs described in Section 13.2.4 are applied.

In a few cases of relatively early releases, the LDFs would represent an overestimation of the dose consequences, again since a steady state release situation is far from established. In some of these cases, time dependent releases are transferred to the same biosphere model as used for the derivation of LDFs and a time dependent dose, taking into account both the temporal variation of the release and the development of the landscape, is obtained, see Section 13.2.3.

There are also a few cases, calculated for illustrative purposes, where a large number of canisters are assumed to fail. In such cases, LDF values calculated for a release spread over the landscape objects according to the distribution of release locations over time during the modelled interglacial period are applied, rather than the basic LDFs where the landscape object yielding the highest dose is pessimistically used to represent the biosphere, see Section 13.2.3.

### 13.4.4 Simplified analytical models

Analytical simplified versions of the near- and far-field transport models have been developed /Hedin 2002b/. These models use the same input data as the corresponding numerical models and doses are calculated using the same LDF values as in the numerical approach. The models may be executed probabilistically and yield results in good agreement with the deterministic and probabilistic calculation cases in the SR 97 assessment /Hedin 2002b, SKB 2004b/. In the SR-Can assessment they were shown to be in good agreement for the corrosion scenario, for the shear load scenario and for releases from a pinhole failure of the canister /SKB 2006a/. A single realisation with the analytical models executes in around 0.1 second on a 2 GHz Personal Computer, making them well suited for probabilistic calculations. The corresponding calculation time for the numerical models is of the order of 10 seconds.

The analytical models have been benchmarked against the numerical models for several calculation cases in this chapter. The roles of the analytical models are to i) quickly and preliminarily evaluate calculation cases to be used in the planning of the transport calculations, ii) serve as one of several quality assurance measures of the numerical calculations by identifying potential differences in results obtained with the analytical and numerical models and seeking explanations for these (are they due to modelling errors or to differences in the nature of the models?), and iii) demonstrating an understanding of the nature of the models facilitated by the simple nature of the analytic models.

The analytical models have not been quality assured according to the procedures used for the numerical models for radionuclide transport, since they are not a formally approved tool for transport calculations in SR-Site.

These models are applied in parallel to the numerical models to key variants of the corrosion scenario, Section 13.5.10, and the shear load scenario, Section 13.6.5.

### 13.4.5 Selection of radionuclides

The selection of radionuclides is based on radiotoxicity, inventory, half-life and shared solubility. The selection is further described in the **Radionuclide transport report**. Some of the selected, short-lived nuclides were omitted in cases where they would have decayed to insignificance at the time of the start of the calculation, see the **Radionuclide transport report**.

The following fission and activation products were selected: Ag-108m, C-14, Cd-113m, Cl-36, Cs-135, Cs-137, Eu-152, H-3, Ho-166m, I-129, Mo-93, Nb-93m, Nb-94, Ni-59, Ni-63, Pd-107, Se-79, Sm-151, Sn-121m, Sn-126, Sr-90, Tc-99 and Zr-93.

The following decay chain nuclides (ordered by chain) were selected: Pu-240, U-236, Th-232, Cm-245, Am-241, Np-237, U-233, Th-229, Cm-246, Am-242m, Pu-242, Pu-238, U-238, U-234, Th-230, Ra-226, Pb-210, Am-243, Pu-239, U-235, Pa-231 and Ac-227. Some nuclides with short half-lives in comparison to their progeny were only included by adding their initial inventory to that of their progeny. This applies to e.g. Cm-244, Pu-241, Cm-243 and Pa-233.

## 13.5 Canister failure due to corrosion

### 13.5.1 Introduction

As reported in Section 12.6, in the ‘canister failure due to corrosion’ scenario (called briefly the corrosion scenario below) canisters fail as a result of enhanced corrosion due to advective conditions in the deposition hole following the loss of buffer through erosion.

For this failure mode, both the canister and the buffer are bypassed, and the rock retention is small since substantial copper corrosion after buffer erosion only occurs in deposition holes with high flow rates, which are in general associated with flow paths to the surface of low geosphere retention.

Six variants yielding varying extents of corrosion failures were identified in the corrosion scenario, see Figure 12-18 in Section 12.6.3, for which radionuclide transport and dose calculations are reported in the following. A *central corrosion variant* was identified as the one on which assessments of radionuclide transport and dose should primarily be made.

In the following, the conceptualisation of the transport conditions including the handling of pulse releases for the instantaneously released fraction of the inventory is accounted for in Section 13.5.2 and input data for these *base case transport assumptions* are given in Section 13.5.3. Data from the central corrosion variant from the corrosion analysis are used with the base case transport data yielding a *central corrosion case* that is analysed in Section 13.5.4.

In Section 13.5.5, reasons to consider alternative transport data are examined. This analysis corresponds to the analysis of containment conditions in Section 12.6.2. Section 13.5.6 presents calculations of alternative cases, both as concerns transport assumptions and data, including findings in Section 13.5.5, and alternative corrosion variants identified in Section 12.6.2. Some cases in Section 13.5.6 are analysed with the MARFA code.

Results of calculations of doses to non-human biota for the central corrosion case are given in Section 13.5.7. Alternative safety indicators for the central corrosion case are given in Section 13.5.8. Section 13.5.9 gives a summary of the results for the corrosion scenario.

## 13.5.2 Conceptualisation of transport conditions

### *Evolution of the canister after canister failure*

According to the analysis of copper corrosion for advective conditions, Section 10.4.9, a band, 0.35 m high and covering half the circumference of the canister, is assumed to be evenly corroded. This means that when penetration occurs, a large amount of damage must be assumed in the copper shell.

The time required to penetrate the cast iron insert is pessimistically neglected since it is difficult to estimate a reasonable development for this process for this failure mode. Also, because penetration of the copper shell in general occurs after several hundred thousand years for the few canisters exposed to the highest corrosion rates, the additional time to penetrate the cast iron insert is of less importance.

Once the copper canister and the cast iron insert have failed, the void in the insert is assumed to be rapidly filled with water due to the high flow rate and the lack of transport resistances in the absence of the buffer and with a large amount of damage also to the cast iron insert.

### *Radionuclide release*

Advective conditions in the buffer must be assumed also for the consequence calculations for the corrosion scenario. There is no buffer hindering the outward transport of radionuclides meaning that this is controlled by the flow through the deposition hole, q. The following three contributions to the outward transport can be distinguished.

- The instantaneously accessible fraction of radionuclides, IRF, that is assumed to be rapidly dissolved in the water void volume and subsequently flushed out of the canister. This gives rise to a pulse of uncertain duration, the uncertainty stemming from e.g. uncertainties in the detailed development of the canister failure through which the IRF is made accessible.
- A contribution from the corrosion of metal parts in the fuel assemblies and the congruent release of radionuclides embedded in the metal parts. These inventories are collectively called the corrosion release fraction, abbreviated CRF.
- A contribution from fuel dissolution and the congruent release of radionuclides embedded in the fuel matrix.

In a case where the buffer is severely eroded, a colloid filter (buffer function indicator Buff7) cannot be guaranteed. This means that the use of elemental solubilities as a limit for radionuclide release could be questioned, since it cannot be excluded that the solid particles formed by various radionuclides reaching saturation would leave the canister and migrate further. In this case, however,

this is of minor concern, since the flow through the deposition hole is often too high for solid phases to precipitate (with the exception of uranium). This is demonstrated in Section 13.5.6 by analysing a case where solubility limits are included.

The release into the fracture is thus controlled by the corrosion rate and the fuel dissolution rate, with two exceptions:

1. For uranium, a concentration limit is still an effective constraint on release, due to the large amount of U-238 present in the fuel. This limits the near-field releases of uranium isotopes, but also leads to increased near-field releases of Th-230, Th-229 and Pa-231 generated by the re-precipitated U-234, U-233 and U-235, respectively.
2. It cannot be excluded that co-precipitation processes and sorption/immobilisation in the remaining bentonite in the deposition hole could confine Th-230 to the near field. If this is the case, its daughter nuclide, the considerably more mobile Ra-226, would be released. The so generated Ra-226 is assumed to be released to the flowing groundwater in the fracture intersecting the deposition hole. This causes higher releases of Ra-226, since there is a contribution not only directly from the fuel dissolution, but also from the confined Th-230. Since Ra-226 is often the main contributor to dose, this also causes higher total doses. Sorption of Th in the near field is thus assumed. The effect of disregarding Th sorption is analysed as a separate calculation case.

Furthermore, as the flow rate in the intersecting fracture is high, the retention of the rock is in general limited for these deposition holes.

#### *Release of activation products*

The inventory of activation products in the metal parts of the fuel assemblies has often been assigned to the instantaneously accessible fraction, since it has been considered unnecessary to develop a model for the metal parts as nuclides in these are dispersed by the buffer. However, in the corrosion scenario this assumption would lead to unrealistically high releases of e.g. Ni-59 and Nb-94. Therefore, corrosion of metal parts of the fuel assemblies is included in the near-field model, with corrosion rates given in the **Data report**. The geosphere transport and the release-to-dose conversion in the biosphere is done as for the bulk of the nuclides, i.e. with the far-field model FARF31 and using LDF values. The fraction of the inventory for which corrosion of metal parts determines the release rate is called the corrosion release fraction, CRF. The CRF is given in the **Data report**, in the same manner as other fractions of the inventory.

#### *Release of instantaneous release fraction*

The fraction of the inventory assumed to be instantaneously released from the fuel upon water contact is expected to be released to the geosphere in a matter of years in the corrosion scenario, since the flow rates at the deposition positions with the eroded buffer and failed canister are high, see further Table 13-4. Since these nuclides are in general non-sorbing and since the flow related retardation properties in the geosphere are poor for the flow paths associated with the deposition positions in question, they are generally released as pulses of durations of tens of years from the geosphere to the biosphere. In this case, the LDF values would yield overly pessimistic estimates of doses, as discussed in Section 13.2.3. Therefore, the LDF pulse values given in Table 13-2 are applied to the total IRF inventory in a canister at the time of canister failure for Cl-36, Ni-59, Se-79, Nb-94, Tc-99, Sn-126, I-129 and Cs-135. A number of nuclides with an IRF, and with half-lives up to 10,000 years (e.g. Sr-90, Cs-137, C-14), were excluded from the analysis since they would decay to insignificance before a failure would occur in the corrosion scenario.

Note that it is also pessimistic to apply the pulse LDF approach even though some of the species in some realisations of a probabilistic transport calculation in the geosphere would result in releases to the biosphere of longer duration. This is because the maximum dose for a given mass released to the biosphere is obtained when the entire mass is released at once, noting that the LDF pulse values are by definition taken for the point in time in the landscape development where the consequences are maximal.

Note also that it is pessimistically assumed that the development of the canister failure is such that all the fuel rods become accessible simultaneously, i.e. a sudden breaching of the cladding for all fuel rods is assumed.

The handling of pulse releases assumes that if several canisters fail, no two canisters will affect the same biosphere object simultaneously. This is justified by the fact that on average less than one canister fails due to advection/corrosion and further since calculated failure times are spread over hundreds of thousands of years.

### 13.5.3 Input data to transport models

Input data to the transport models for the corrosion scenario are summarised in Table 13-3. All data in the table are qualified in the **Data report**, except the failure times that are obtained as output from the erosion/corrosion calculations reported in Section 12.6.2 and in detail in /SKB 2010d/. However, the input to those latter calculations is qualified in the **Data report**.

**Table 13-3. Input data for the corrosion cases.**

| Entity | Nuclide/ Element specific | Data | Section in Data report |
|---|---|---|---|
| Number of failed canisters | – | As calculated with corrosion model, see Section 12.6.2. | – |
| Failure times | – | As calculated with corrosion model, see Section 12.6.2. | – |
| Radionuclide inventory | N | Mean inventory taken over all fuel types. | 3.1 |
| Instantaneous release fraction of inventory | N | Distributions according to the **Data report**. | 3.2 |
| Corrosion release fraction of inventory | N | Distributions according to the **Data report**. | 3.2 |
| Corrosion release rate | – | Log-triangular ($10^{-4}$/yr, $10^{-3}$/yr, $10^{-2}$/yr) | 3.2 |
| Fuel dissolution rate | – | Log-triangular ($10^{-8}$/yr, $10^{-7}$/yr, $10^{-6}$/yr) | 3.3 |
| Concentration limits | E | Calculated distribution based on distribution of several groundwater compositions* | 3.4 |
| Rock porosity | – | Constant = 0.0018 | 6.8 |
| Rock diffusivities | – | Log-normal distributions; mean values:<br>Cations: $6.6 \cdot 10^{-7}$ m$^2$/yr<br>Anions: $2.1 \cdot 10^{-7}$ m$^2$/yr | 6.8 |
| Rock partitioning coefficients | E | Truncated log-normal distributions | 6.8 |
| **Hydrogeological data related to flow and transport**<br>Darcy flux at deposition hole ($U_0$)<br>Rock transport resistance, $F$, for paths beginning at release point Q1<br>Rock advective travel time, $t_w$, for paths beginning at release point Q1 | – | Correlated distributions from several DFN model calculations propagated from hydrogeological analyses:<br>**Uncorrelated model**<br>Base case and 5 additional realisations<br>**Semi-correlated model**<br>Base case and 10 additional realisations<br>**Fully correlated model**<br>Base case and 5 additional realisations<br>Only deposition holes where failures occur are included. | 6.7 |
| Rock Peclet number | – | Constant = 10 | 6.7 |
| Max. penetration depth in rock matrix | – | Constant = 12.5 m | 6.7 |
| Biosphere LDF factors | N | Calculated LDF values, see Section 13.2. | 7.2 |

* As noted above, concentration limits are not applied in the central corrosion case, with the exception of U. Concentration limits for U, and for other elements to be used in other calculation cases, are calculated probabilistically by using distributions of groundwater compositions for either temperate, permafrost, glacial or submerged conditions and combining the calculated distributions into the one distribution used in the transport calculation. See further the **Radionuclide transport report**, where also sensitivities to different groundwater types, thermodynamic data etc. are analysed.

#### *Hydrogeological data related to flow and transport*

Hydrogeological data, obtained from the modelling described in Section 10.3.6 are used. As described in Section 10.3.6, three fracture size/transmissivity correlation functions are considered yielding three variants of the hydrogeological DFN model. Several realisations of each of these three variants are propagated to the corrosion scenario, see Table 13-3. In a probabilistic central corrosion case, data from all the ten additional realisations of the semi-correlated DFN model are used. In all calculations for this scenario, deposition positions are rejected according to the EFPC criterion (Section 5.2.2) in the output from the hydrogeological modelling.

It is only data for the few deposition holes for which canister failures due to corrosion occur that are used for this corrosion case. This means that all deposition holes of relevance experience a high flow rate and in general also a low geosphere transport resistance, since these properties are strongly correlated.

Data for the four deposition holes of relevance for the base case realisation of the semi-correlated DFN model are given as an example in Table 13-4. The advective flow through the deposition hole, q, is obtained from the hydrogeological calculations and multiplied by a factor of two to account for the locally increased flow due to the void from the eroded buffer.

It is noted that the calculated hydraulic and transport properties of these deposition holes are from the extreme tails of distributions derived from a complex hydrogeological model with stochastic components (the generated fracture network). All ten realisations of the semi-correlated model variant are used in order to obtain more reliable representations of these tails. (For the uncorrelated and fully correlated DFN model variants, for which consequences are analysed in Section 13.5.6, all five available realisations are used.)

Figure 13-14 is a graphical representation of failure time vs *F*-value for the deposition positions where failures occur in three of the cases propagated from the analysis of containment potential for the corrosion scenario. The figure shows results obtained with the base case realisations of the semi-correlated, uncorrelated and fully correlated hydrogeological DFN models, respectively.

### 13.5.4 Calculation of the central corrosion case

#### *Deterministic calculations*

Figure 13-15 shows near-field releases converted to dose equivalent releases through multiplying the release rate by the LDF-value for each nuclide in a stylised, deterministic case where a canister is assumed to fail at 114,000 years after deposition (the earliest failure time of the analysed realisations). As mentioned in Section 13.4.3, the conversion to dose is done to obtain a convenient measure of the impact of the releases, where also a total measure is obtained as the summed dose. Advection occurs in the buffer void and the dose equivalent releases are primarily determined by the fuel dissolution rate set to $10^{-7}$/yr. The contributions from the instantaneously released fraction of nuclides, IRF, are not included in the figure, since it is more convenient to show these separately.

**Table 13-4. Data for the four deposition holes where canisters fail due to advection/corrosion for the base case realisation of the semi-correlated DFN model. The ten additional realisations are used in the calculations below.**

| Time of failure (yr) | Rock transport resistance, F (yr/m) | Advective travel time, $t_w$ (yr) | Advective flow through deposition hole q ($m^3$/yr) |
|---|---|---|---|
| 200,786 | 471,800 | 122.6 | 0.144 |
| 218,215 | 149,800 | 27.54 | 0.166 |
| 299,149 | 11,970 | 23.14 | 0.084 |
| 886,073 | 35,890,000 | 1,968 | 0.026 |

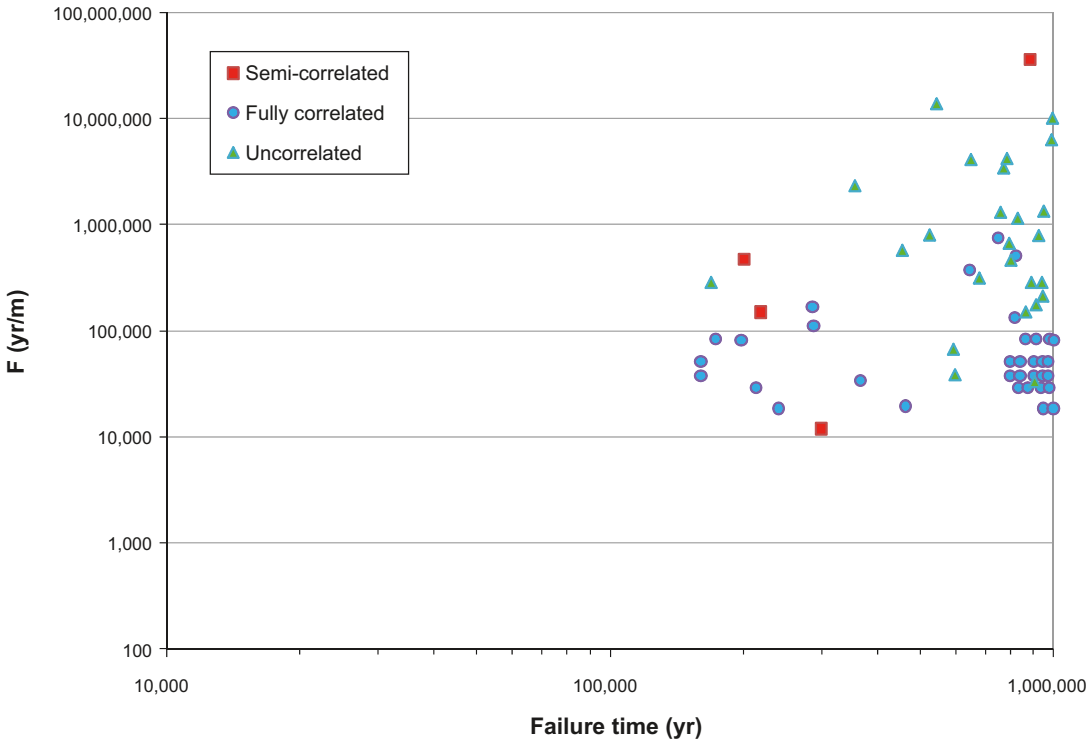


***Figure 13-14.*** *Graphical representation of pairs of failure times and F values for base case realisations of the semi-correlated, uncorrelated and fully correlated hydrogeological DFN models propagated from the analysis of containment potential for the corrosion scenario.*

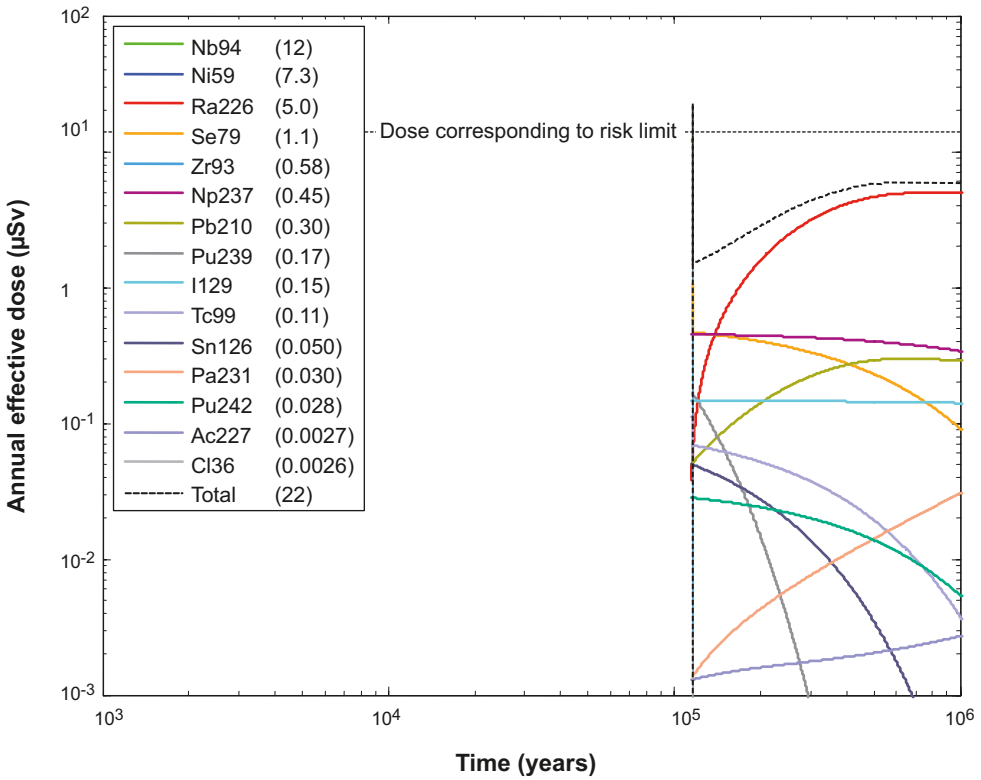


***Figure 13-15.*** *Near-field annual effective dose equivalent release for a deterministic calculation of the central corrosion case. The legends are sorted according to descending peak annual effective dose over one million years (given in brackets in μSv). The curves for Nb-94 and Ni-59 are hidden under the curve showing the total dose.*

The dose equivalent releases caused by releases from the near field are dominated by Nb-94, Ni-59 and Ra-226. Most uranium released from the fuel is precipitated in the canister interior, since the concentration limit of uranium always applies because of the large amount of U-238 present, see Section 13.5.2. The precipitated uranium isotopes U-234, U-233 and U-235 generate the daughter nuclides Th-230, Th-229 and Pa-231, respectively.

The dose equivalent releases from the geosphere for the same calculation case are shown in Figure 13-16. The doses caused by releases from the far field are dominated by Ra-226, Ni-59, Se-79, Np-237 and I-129. It is noted that the peak dose appears at the end of the assessment period in Figure 13-16, indicating that the time of the peak dose is not strongly related to the time of the canister failure. This also indicates that a distribution of failure times will not cause risk dilution, an issue that is addressed further in Section 13.9.4.

The numerical calculation results have been compared to results obtained with analytical models and the agreement is good. This was expected since the situation to model is simple and the release rates straightforward to express analytically. See further Section 13.5.10.

Table 13-5 shows peak annual doses from the pulse releases from the instantaneously released fraction, IRF, for the deterministic calculation. The IRF inventory at 100,000 years has been multiplied by the pulse LDF values given in Table 13-2.

It is noted that these doses are, for some nuclides, higher than the peak doses from the continuous releases in Figure 13-16.

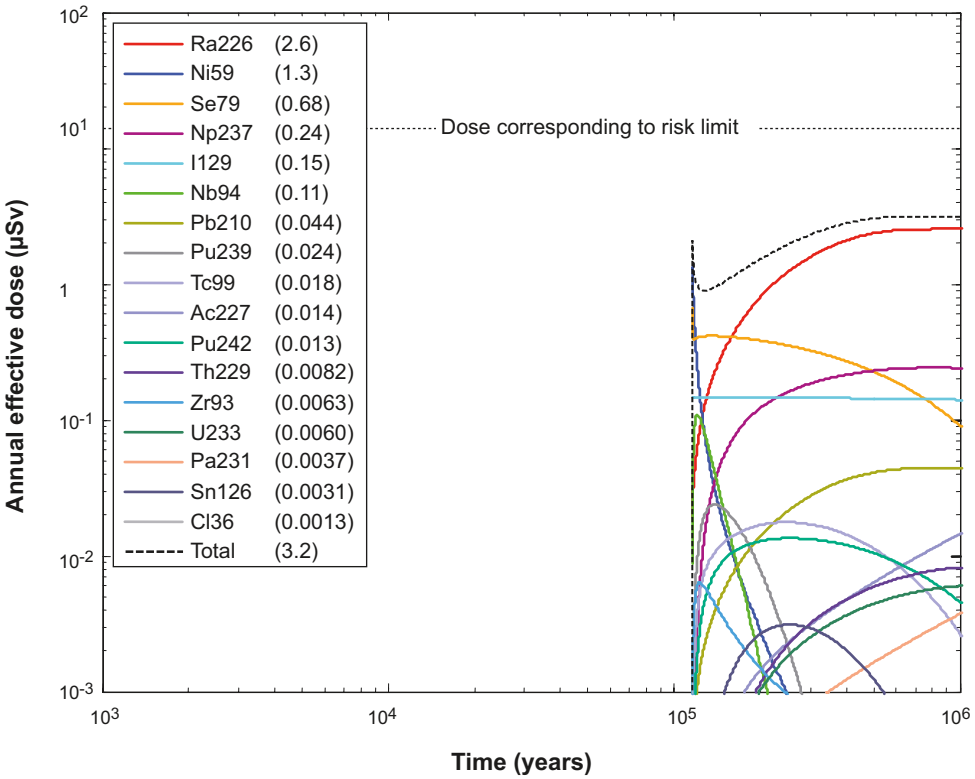


***Figure 13-16.*** *Far-field annual effective dose for a deterministic calculation of the central corrosion case. The legends are sorted according to descending peak annual effective dose over one million years (given in brackets in µSv).*

**Table 13-5. Peak annual dose from the pulse releases from the instantaneously released fraction, IRF.**

| Nuclide | Peak annual dose (μSv) | Nuclide | Peak annual dose (μSv) |
|---|---|---|---|
| Cl-36 | 0.12 | Tc-99[a] | 6.8 |
| Ni-59 | 0.012 | Sn-126 | 0.019 |
| Se-79 | 1.72 | I-129 | 3.82 |
| Nb-94 | 0.026 | Cs-135 | 0.21 |

[a]This value applies to the near-field dose equivalent release only. The far-field pulse release is modelled with the far-field transport model since sorption in the geosphere is considerable for Tc-99. The pulse release of Tc-99 is thus included in the results shown in Figure 13-16.

### *Probabilistic calculation*

Figure 13-17 shows near field dose equivalent releases for a probabilistic calculation encompassing 2,800 realisations with input data distributions according to Table 13-3. Input distributions of failure times and geosphere transport data were obtained from the ten realisations of the semi-correlated DFN model, each yielding data for the ensemble of 6,000 canisters. Figure 13-18 shows the corresponding far-field releases. The first releases occur after around 114,000 years when the first canister fails. The average number of failed canisters in the probabilistic calculation of failure times is 0.12, see Section 12.6.2. This is reflected in the calculation results here.

The dose equivalent releases from the near field and the dose after transport through the geosphere are both dominated by Ra-226. Much of the Ra-226 released from the near field is transmitted through the geosphere since the failed canisters are located in deposition holes intersected by large, highly transmissive fractures with low retention. The release of Ra-226 from the geosphere is almost exclusively due to Ra released from the near field and not to in-growth in the geosphere. This, in turn, is related to the fact that the parent nuclide Th-230 is assumed to be confined to the near field.

The failure times are reflected as distinct features in the release curves, in particular for the near field. The pulse like features are due to release controlled by corrosion of the metal parts of the fuel assemblies (e.g. Ni-59 and Nb-94). The corrosion times (ranging between 100 and 10,000 years, see Table 13-3) are such that the releases appear as pulses on the time scale of the dose curves.

Some statistics for the far-field release are shown in Figure 13-19. Note that these are derived only for the realisations of the failure times where failures actually occur in the corrosion calculations. Since the mean number of failed canisters is about 0.12, the most likely outcome of the corrosion calculations is zero failures. This is not reflected in the percentiles in Figure 13-19, other than for the mean value. Taking this into account would bring the 99th and 95th percentiles closer to the mean.

### Contribution from the IRF pulse

The contribution from the IRF pulse in the probabilistically calculated mean dose is treated as follows. The probability of canister failure, $p_{Fail}$, is determined for each 100,000 year interval from the calculated distribution of canister failure times for the central corrosion case. The width of the dose curves in the biosphere is typically 1,000 years. The likelihood that an exposure due to a pulse release, $p_{Expo}$, is present at a given point in time during the 100,000 year interval is thus $10^{-2} \cdot p_{Fail}$. (The likelihood of overlaps between pulses is very small due to the low probabilities.) The total dose associated with a pulse release $D_{TotPulse}$ is determined at the start of each 100,000 year interval. The probabilistically calculated mean dose is then obtained as $D_{TotPulse} \cdot p_{Expo}$. The result of this procedure for the central corrosion case is shown in Table 13-6. As seen in the table, the highest mean dose is around $1.0 \cdot 10^{-3}$ μSv, i.e. more than four orders of magnitude below the dose corresponding to the risk limit. The pulse releases thus give negligible contributions to the probabilistically calculated mean dose. They do, however, need to be considered in the account of risk dilution. This is done in Section 13.9. It is also noted that this treatment assumes that temperate conditions are prevailing. Including probabilities of periglacial and glacial climate conditions would reduce the mean dose further.

For other calculation cases of the corrosion scenario, the pulse contribution to the mean dose is not calculated. All cases are, however, considered in the treatment of risk dilution, see Section 13.9.4.

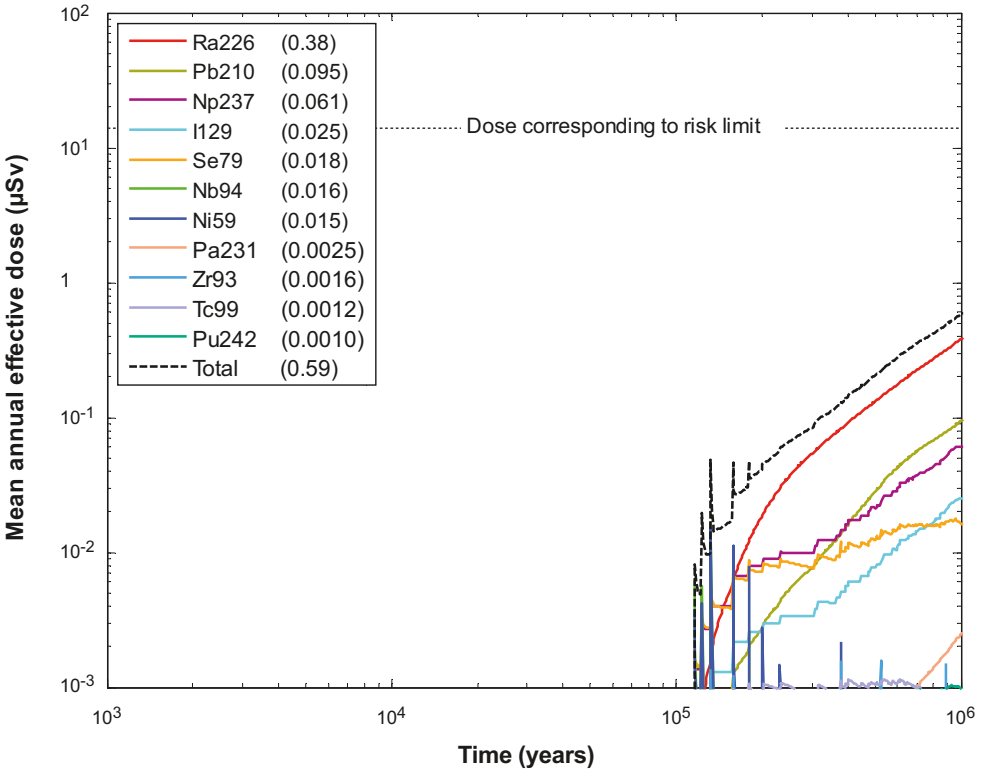


***Figure 13-17.*** *Near-field mean annual effective dose equivalent release for a probabilistic calculation of the central corrosion case. The average number of failed canisters is 0.12. The legends are sorted according to descending peak mean annual effective dose over one million years (given in brackets in µSv).*

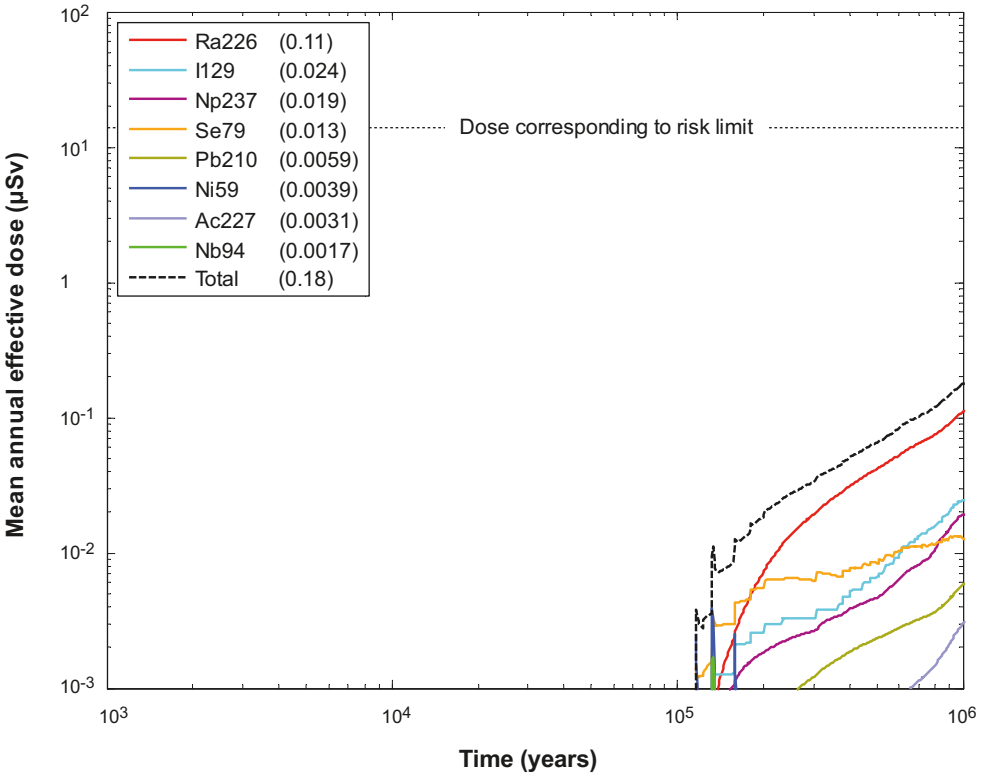


***Figure 13-18.*** *Far-field mean annual effective dose for the same case as in Figure 13-17. The legends are sorted according to descending peak mean annual effective dose over one million years (given in brackets in µSv).*

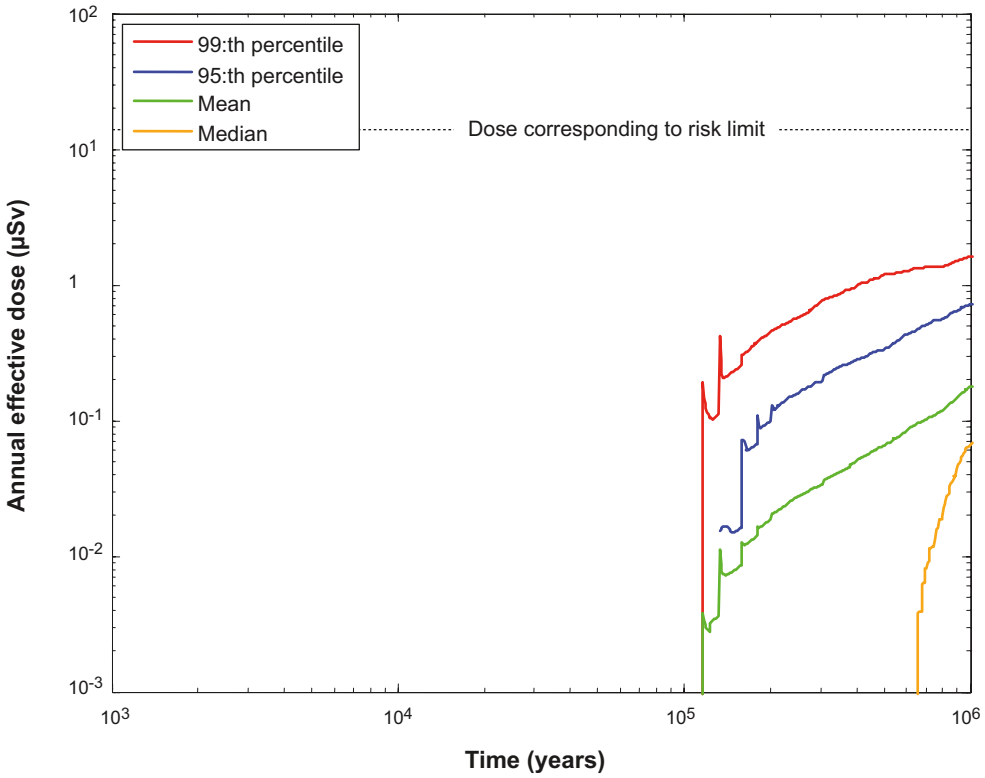


*Figure 13-19. Far-field annual effective dose (mean, median, 95th and 99th percentiles) for the probabilistic calculation of the central corrosion case.*

**Table 13-6. Contribution from the pulse release for the probabilistically calculated mean dose for the central corrosion case.**

| Time interval [yr] | $p_{Fail}$ | $p_{Expo}$ | $D_{TotPulse}$ [μSv] | Mean dose [μSv] |
|---|---|---|---|---|
| 0–100,000 | 0 | 0 | 0 | 0 |
| 100,000–200,000 | $1.25 \cdot 10^{-2}$ | $1.25 \cdot 10^{-4}$ | 5.92 | $7.4 \cdot 10^{-4}$ |
| 200,000–300,000 | $4.17 \cdot 10^{-3}$ | $4.17 \cdot 10^{-5}$ | 5.54 | $2.3 \cdot 10^{-4}$ |
| 300,000–400,000 | $1.04 \cdot 10^{-2}$ | $1.04 \cdot 10^{-4}$ | 5.25 | $5.5 \cdot 10^{-4}$ |
| 400,000–500,000 | $8.33 \cdot 10^{-3}$ | $8.33 \cdot 10^{-5}$ | 5.01 | $4.2 \cdot 10^{-4}$ |
| 500,000–600,000 | $1.46 \cdot 10^{-2}$ | $1.46 \cdot 10^{-4}$ | 4.81 | $7.0 \cdot 10^{-4}$ |
| 600,000–700,000 | $1.46 \cdot 10^{-2}$ | $1.46 \cdot 10^{-4}$ | 4.64 | $6.8 \cdot 10^{-4}$ |
| 700,000–800,000 | $1.25 \cdot 10^{-2}$ | $1.25 \cdot 10^{-4}$ | 4.49 | $5.6 \cdot 10^{-4}$ |
| 800,000–900,000 | $2.29 \cdot 10^{-2}$ | $2.29 \cdot 10^{-4}$ | 4.37 | $1.0 \cdot 10^{-3}$ |
| 900,000–1,000,000 | $1.67 \cdot 10^{-2}$ | $1.67 \cdot 10^{-4}$ | 4.26 | $7.1 \cdot 10^{-4}$ |

### 13.5.5 Analysis of potential alternative transport conditions/data

The transport data used in the calculation of the probabilistic central corrosion case are those provided in the **Data report** and presented in Table 13-3. The data have been selected for certain conditions and, in the following, it is analysed i) whether the evolution in the corrosion scenario is compatible with these conditions and ii) whether any alternative evolutions of the system, that could imply less favourable transport conditions, need to be considered.

This analysis corresponds to the analysis of the possible routes to alternative containment conditions in Section 12.6, but is simplified based on the analyses already made in the derivation of data in the **Data report**.

### *Number of failed canisters and failure times*

The number of failed canisters is an outcome of the analysis of the containment potential for the corrosion scenario, and has thus been exhaustively analysed in Section 12.6.2. This led to several corrosion variants for which consequences are analysed in Section 13.5.6.

### *Radionuclide inventory, IRF and CRF*

It is not relevant to include these entities here since they are not affected by external factors, but by conditions determining the initial state. Uncertainties related to the initial state are fully explored in the **Data report**.

### *Fuel dissolution rate*

#### Introduction

At the time when water enters a failed canister, fuel dissolution is expected to begin. Based on a review of the experimental data available at the time /Werme et al. 2004/ suggested a constant fractional dissolution rate with a triangular probability density function in the $\log_{10}$-space with lower limit, best estimate, and upper limit of $10^{-8}$, $10^{-7}$, and $10^{-6}$ per year, respectively. The review of more recent experimental data discussed in the **Fuel and canister process report** and the **Data report**, Section 3.3, support these data and the mentioned distribution is qualified for use in SR-Site although support can be found for even lower values. The arguments for the suggested distribution presented in the **Fuel and canister process report** and the **Data report** are shortly summarised here, as an introduction to the subsequent discussion of its robustness under conditions that lead to the analysed failure scenarios.

Fuel dissolution has been implemented in the near-field transport model as two components. One component represents fuel being mobilised at a rate described by the fuel corrosion rate (i.e. the oxidative dissolution rate of the fuel). In the model the fuel corrosion rate, given by the forementioned distribution, is constant and independent of the concentration of uranium species in the intruding water. The other component represents fuel dissolution due to the upholding of the U(IV) concentration at the solubility limit, which is pessimistically assumed high. In general, the former, oxidative component dominates over the latter non-oxidative component for the data on corrosion rate, groundwater flow and uranium solubility used in SR-Site.

The suggested distribution corresponds to fuel dissolution rates calculated from laboratory studies spanning up to four years. Since the expected repository environment is reducing, the fuel dissolution rate adopted in the analysis must be the one expected in an oxygen-free environment and in the presence of iron and its anoxic corrosion products. However, oxidants are also produced radiolytically. Therefore, the experimental data upon which the analysis is based have been obtained both with relatively fresh spent fuel, and α-doped $UO_2$ ($UO_2$(s) doped with the alpha-emitters U-233 or Pu-238).

Fresh spent fuel represents the real properties of the fuel matrix, but has an unrealistically high radiation field with large contribution of β- and γ-radiations. For this reason it is tested under relatively high hydrogen concentrations (> 1 mM). On the other hand, α-doped $UO_2$ represents better the radiation field of the fuel expected to contact groundwater, but does not represent other properties of the fuel matrix. In this case the data have been obtained with low concentrations of reductants, or no reductants present.

For all fuel dissolution studies carried out in the presence of hydrogen or actively corroding iron, the levels of molecular oxidants in the solution or gas phase are below the detection limit and the same holds for oxidised states of all redox sensitive radionuclides. The release rates of non-redox sensitive fission products such as Cs and Sr decrease by more than two orders of magnitude during one year. The absence of oxidised species in the test solutions in spite of the relatively high radiation field of fresh spent fuel shows that radiolytic oxidants have been consumed either by oxidising the fuel surface or by recombining with hydrogen to give water. Post leaching spectroscopic analysis of fuel surfaces shows no signs of surface oxidation.

Experimental studies with $UO_2$, doped with the alpha-emitters U-233 or Pu-238, have been carried out in the presence of low concentrations of dissolved hydrogen, sulphide ions or actively corroding iron. These experiments with alpha-doped $UO_2$(s) indicate clearly that the presence of a small amount of sulphide and strict anoxic conditions are sufficient to cancel any oxidising effect due to α-radiolysis from a few thousand year old fuel. In most tests with U-233-doped $UO_2$ (0, 5 and 10%) under inert ($N_2$) and reducing (Fe(s)) conditions, very low total uranium concentrations were measured, especially in the presence of an iron strip. Estimation of the matrix dissolution rate confirms previously measured low values.

An $UO_2$ pellet with a high doping level (385 MBq/g corresponding to 50 years old fuel) was tested more recently /Muzeau et al. 2009/, and a very clear effect of α-radiolysis was observed under Ar atmosphere, with U concentrations increasing quickly with time in carbonate solutions. The same system, tested under 1 bar $H_2$ atmosphere, showed a slight decrease in U concentration. This suppressing effect of hydrogen, indicates that oxidative dissolution (corrosion) of fuel occurs at extremely low rates if at all in an environment similar to that expected in the failed canister.

As discussed in the **Fuel and canister process report**, similar or lower rates are estimated by an electrochemical model, from experimental data in an EU project and by a steady-state fuel dissolution model which uses experimentally determined kinetic parameters and accounts for the effects of the presence of both Fe(II) and hydrogen.

The driving force for the oxidative dissolution (or corrosion) of spent fuel is its radiation field, which decreases with time due to radioactive decay. This decrease is taken into account in fuel dissolution models used in other studies of geologic disposal, leading to a lower production of radiolytic oxidants with time and decreasing dissolution rates. Even though there is hardly any uncertainty in the fact that the radiolytic dissolution rate of spent fuel will decrease with time, the SR-Site model pessimistically neglects this decrease and assumes a constant dissolution rate, which varies within broad ranges to cover conceptual and other uncertainties.

The following is a summary of conditions for which the range of fuel dissolution rates given in the **Data report** is valid. For each condition, a brief discussion of whether it can be considered as fulfilled for the possible evolutions discussed in SR-Site is provided.

**Redox conditions**

*Range in which the fuel dissolution rate is valid according to the **Data report***: In the corrosion scenario, canister failures occur after typically hundreds of thousands of years. In such time frames, the alpha radiation field of the spent fuel is expected to have decreased to such low levels that there will be no measurable effect of alpha radiolysis on fuel dissolution, see the **Fuel and canister process report**. After a canister failure, the hydrogen producing iron corrosion of the insert will continue for tens of thousands of years. As long as there is corroding iron, both hydrogen and Fe(II) concentrations will be sufficient to assure reducing conditions. If the groundwaters penetrating the failed canister contain sulphate, microbial sulphate reduction might result in the precipitation of Fe(II)-sulphide. In the longer perspective, the Fe(II) concentrations and the redox potential of groundwaters inside the canister will be determined by equilibrium with magnetite or possibly iron sulphides, while hydrogen concentrations may decrease to those produced by water radiolysis when all metallic iron has corroded.

If the reducing conditions in the flowing groundwaters are disturbed by penetration to repository depth of oxidising glacial melt waters, the fuel may dissolve at higher rates. However, the reducing capacity of the canister components needs to be considered since a continuous supply of oxidants is needed to support a higher dissolution rate. About $4 \cdot 10^{-3}$ moles of oxygen/year are needed to support a fuel corrosion rate of $10^{-6}$/year (neglecting any consumption of oxygen by interaction with magnetite, sulphides or copper). This means that both the redox potential of the groundwater and the mass-balance of oxygen need to be considered. Under oxidising conditions with $P_{O2}$ up to 0.2 bar, that is, air saturation, the long term rates measured at the pH interval 7 to 9 /Forsyth and Werme 1992, Forsyth 1997/ may be used, and the spent fuel dissolution rate is then in the interval $10^{-4}$ to $10^{-5}$/year. All other environmental parameters (temperature, pH etc.) affect in various degrees the dissolution rate under oxic conditions, but they are discussed below only for reducing conditions because limiting rates have been defined for oxidising conditions, as set out above.

*Ranges in evolution cases studied:* The possibility of oxidising conditions has been extensively studied, since it also would affect canister corrosion negatively, see in particular Section 12.6.2. The conclusion was that oxidising conditions can be ruled out.

*Need for assessments of additional evolutions:* The analysis of a glacial episode in Section 12.6.2 shows that the penetration of oxygen rich glacial melt waters is a low probability event that is deemed to be possible only if a set of extreme assumptions are made. However, even if these extreme assumptions were to be assumed, and oxygen postulated to reach a breached canister, the large reducing capacity of the remains of the failed copper canister and of the iron insert, would imply that anoxic conditions would prevail inside the canister. Even if the mass transfer of oxygen to the canister were to be higher than $4 \cdot 10^{-3}$ moles/year, it is unreasonable that all the oxygen would react with the fuel. The remaining copper and the iron/iron corrosion products would act as a sink and consequently no additional evolutions need to be assessed.

**pH**

*Range in which the fuel dissolution rate is valid according to the **Data report**:* $4 < pH < 11$.

*Ranges in evolution cases studied:* The possibility of high pH conditions has been extensively studied in the buffer alteration scenario, since it also would affect the buffer negatively, see Section 12.4. There, it is concluded that pH values above 11 can be excluded. The possibility of low pH conditions has been studied in the corrosion scenario, since it also could affect canister corrosion negatively in combination with high chloride concentrations, see Section 12.6. There, it is concluded that pH values below 6.3 can be excluded.

*Need for studies of additional evolutions to rule out unfavourable pH conditions:* None, since exhaustive such studies have already been performed.

**Temperature**

*Range in which the fuel dissolution rate is valid according to the **Data report**:* < 70°C.

*Ranges in evolution cases studied:* Elevated temperatures only occur early in the repository evolution, see Section 10.3.4, whereas canister failures in the corrosion scenario occur after typically hundreds of thousands of years. In such time frames, the fuel temperature is close to the background temperature of the host rock, i.e. well below 70°C.

*Need for studies of additional evolutions to rule out unfavourable temperature conditions:* None according to the above.

**Ionic strength**

*Range in which the fuel dissolution rate is valid according to the **Data report**:* Up to 1 M ionic strength and there is no indication for increased fuel dissolution rates even at higher ionic strengths.

*Ranges in evolution cases studied:* The ionic strengths of groundwaters expected during the whole period of repository evolution are lower than 0.5 M.

*Need for analyses of additional evolutions to rule out unfavourable ionic strengths:* The groundwater data at Forsmark indicate that the salinity has been stable during the Weichselian, and large oscillations in groundwater salinities are therefore not expected in the future. The analysis of different possible climatic episodes presented in Sections 10.3.7 and 10.4.7 shows that salinity can increase due to upconing during the short glacial transit above the repository area. The analyses reported in Sections 10.4.6 and 10.4.7 show that the upconing effect is moderate and the resulting ionic strengths in the repository volume are below 0.5 M. Because the most pronounced upconing takes place during an ice advance, where the ice profile is steepest, the analysis of the reference evolution includes the highest salinities that can be expected at Forsmark, and no additional analyses are required.

**Chemical influence of major and minor groundwater components**

*Range in which the fuel dissolution rate is valid according to the **Data report**:* $HCO_3^-$ < 0.01 M. The beneficial effect of molecular hydrogen in homogeneous radiolysis is based on its reaction with the OH-radical, which converts the very oxidising radical (OH·) to water and a very reducing radical (H·). Bromide ions are strong reductants and react ~250 times faster with the OH-radical than the $H_2$ molecule. It is said that bromide scavenges the OH-radical, thus decreasing the beneficial effect of hydrogen on homogeneous water radiolysis. The radical-rich beta and gamma radiations are expected to have decayed to negligible levels at the time of canister failure in the corrosion scenario. This together with the absence of very saline waters during repository evolution and the very low alpha activity makes any influence of bromide on fuel dissolution very improbable.

*Ranges in evolution cases studied:* The carbonate concentrations during the whole repository evolution are expected to be below 0.01 M.

*Need for analyses of additional evolutions to rule out unfavourable conditions:* The total concentration of inorganic carbon, which at pH values close to neutral is close to the concentration of $HCO_3^-$, is highest in the upper parts of the rock where recharge of meteoric waters dominates, because several biological processes produce $CO_2$ in the soil. In deep saline waters, rich in $Ca^{2+}$, the concentration of carbonate is kept low because of equilibrium with calcite. Typical carbonate concentrations for waters at Forsmark are illustrated in Figure 10-45. Thus, the only process that can increase bicarbonate concentrations in groundwaters is the enhanced infiltration of fresh meteoric waters. The data at Forsmark shows that the waters having a large influence of meteoric recharge all have carbonate concentrations around or below 0.01 M, and it is therefore concluded that there is no need to analyse the fuel dissolution rate for higher total carbonate concentrations.

**Additional factor identified: Transport of uranium with clay colloids in the groundwater**

When the buffer is partially or completely eroded, a cavity filled with a slurry (gel/sol) of water containing colloidal clay particles may exist in the deposition hole. Should the canister be breached under such circumstances, the clay particles themselves are not expected to affect the oxidative fuel dissolution rate. Dissolved U(IV) would, however, be expected to sorb strongly to the clay particles. This sorption increases the amount of U(IV) released into solution from the re-precipitated $UO_2$(s) or the fuel matrix. In this case, the amount of U(IV) sorbed on clay particles may be calculated as the $K_d$ value for U(IV) on clay particles multiplied by the U(IV) concentration in solution, determined by $UO_2$(s) solubility. No limit to the U(IV) release rate from $UO_2$(s) to satisfy U(IV) solubility limits in the canister void is then posed. In the case when all re-precipitated $UO_2$(s) is dissolved due to sorption to clay particles, the remaining U(IV) needed to saturate clay particles is released from the fuel matrix, resulting in an increase of the fuel dissolution rate. To calculate this enhanced U release, the values for $UO_2$(s) solubility and $K_d$ for U(IV) on clay particles are taken from the **Data report**. The rate at which the clay particles with sorbed uranium are carried away are set by the concentration of clay particles and water flow rate. These depend on the scenario analysed.

*Need for studies of additional evolutions to rule out unfavourable conditions:* Fuel dissolution in the presence of a clay slurry needs to be considered. This is done as described below.

The eroded void volume of the deposition hole is assumed to be filled with clay particles that enhance the dissolution rate of the $UO_2$ fuel matrix. The outward transport rate of U, $R_U$ (mole/yr), is then obtained as

$$R_U = C_{Sol}U \cdot q \cdot (1 + C_{Clay} \cdot K_d)$$

where

$C_{Sol}U$ is the solubility of U(IV) (mole/m$^3$),

q is the advective flow at the deposition hole (m$^3$/yr),

$C_{Clay}$ is the concentration of clay in the flowing fluid (kg/m$^3$),

$K_d$ is the partitioning coefficient between solid phase and solution for U in a clay slurry (m$^3$/kg).

In /Birgersson et al. 2009/ the void ratio when the transport of bentonite is by colloid dispersion is determined to be 73, which corresponds to a dry density of 37.6 kg/m$^3$. This concentration will not be maintained in a large void in the deposition hole, since there will be a concentration gradient from the source of the colloids to the fuel. The location of the source could be remaining bentonite in the deposition hole, the backfill in the tunnel or through a fracture from another deposition hole/tunnel in the repository. Since it is impossible to determine the location of the source, and it may change with time, the value for $C_{Clay}$ cannot be calculated. Instead a fixed value of 10 kg/m$^3$ is selected and judged to be a reasonable estimate of an upper bound of the mean value taken over the entire void volume.

Using $C_{Clay}$ = 10 kg/m$^3$ and distributions of $K_d$, $C_{Sol}U$ and q for the central corrosion case, the contribution from U transport on clay particles to the fuel dissolution rate is calculated probabilistically and compared to the probabilistically sampled ordinary fuel dissolution rate for the central corrosion case.

The following also applies in the modelling.

- This process is only active during the relatively limited periods when the deposition position is exposed to dilute groundwater such that clay colloids can form. This is not taken into account in the calculation.
- Inflowing groundwater may have U concentrations exceeding $10^{-9}$ mol/L, but the influence of the occupation of sorption sites of clay particles by natural uranium present in the groundwater is pessimistically neglected.
- Should sorption to clay colloids be modelled as irreversible and assuming that all sorption sites were to be occupied by U, then a transport rate of the order of $2.5 \cdot 10^{-3}$ moles/yr is calculated for a sorption site density of $2.0 \cdot 10^{-6}$ moles/g /Bradbury and Baeyens, 2005/, cited in /Ochs and Talerico 2004/, q = 100 L/yr, and $C_{Clay}$ = 10 g/L. This, in turn, corresponds to a fuel dissolution rate of approximately $3 \cdot 10^{-7}$/yr, i.e. slightly lower than the maximum value of the "ordinary" distribution. An upper limit on the transport rate determined by the product of the sorption site density, q, and $C_{Clay}$ is imposed in the calculation of the distribution in Figure 13-20, curve B. (Irreversible sorption, as well as U occupancy of all available sites is, however, ruled out for the conditions in the deposition hole, based on the description of the sorption process in the **Buffer, backfill and closure process report**.)
- Although advective conditions are assumed to prevail in the deposition hole, there will be parts of the path between the inner parts of the, assumed damaged, fuel elements and the canister exterior where the transport is diffusion controlled. A certain continuous outward, clay assisted transport of $UO_2$ then requires a corresponding flux of $UO_2$ over the diffusion controlled path. The geometry for this transport is difficult to assess, but un upper bound can be estimated as follows: Assume a pessimistically high cross sectional area of 0.1 m$^2$ and a pessimistically low diffusion path length of 1 mm. Taking then the highest U solubility in the distribution used in SR-Site, i.e. $4.2 \cdot 10^{-4}$ mol/m$^3$, and assuming a U diffusivity in water (at 11°C) of 0.01 m$^2$/yr, one obtains a maximum U flux of $4.2 \cdot 10^{-4}$ mol/yr, assuming a zero concentration 1 mm away from the fuel. With 8,400 mol U/canister this corresponds to a fractional dissolution rate of approximately $5 \cdot 10^{-8}$/yr. This pessimistic bound suggests that the effect of U transport with clay particles is negligible in the radionuclide transport calculations. A bound using these diffusion data in combination with the distribution of U solubility is imposed in curve A in Figure 13-20.

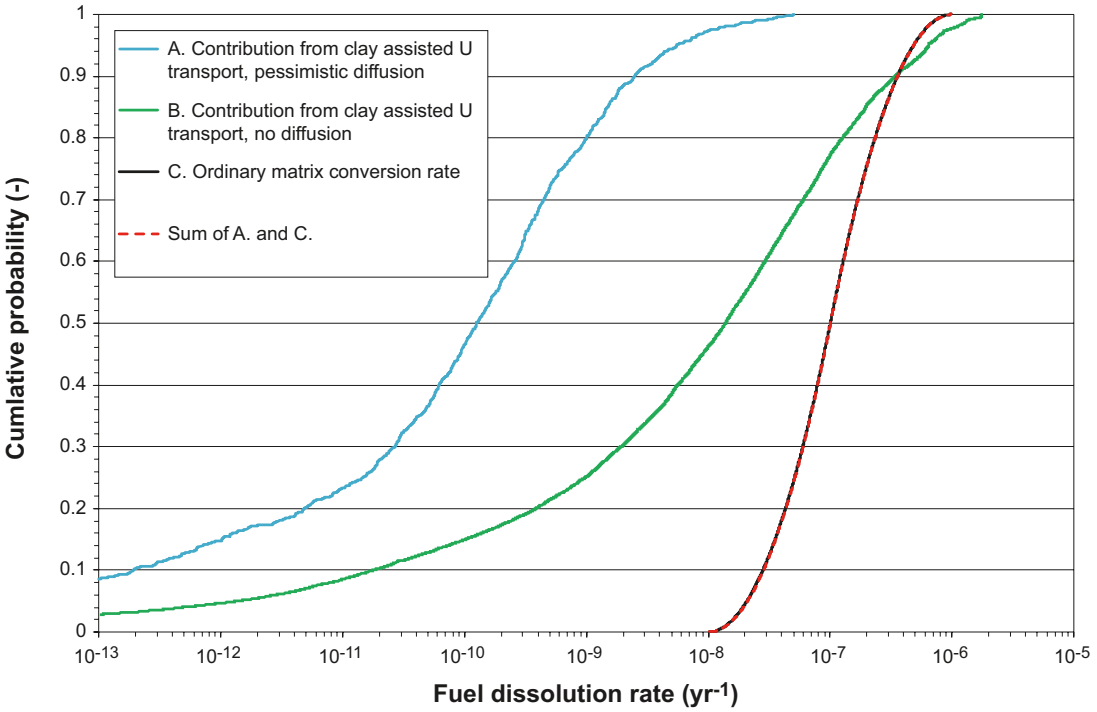


***Figure 13-20.*** *Cumulative distributions of fuel dissolution rate. The contribution from clay assisted U transport has a negligible impact on the distribution for the ordinary matrix conversion rate. See text for further explanations.*

As seen in Figure 13-20, the clay assisted fuel dissolution rate (curve B) is considerably lower than the "ordinary" dissolution rate (curve C) up to the 90$^{th}$ percentile of the distribution, whereas it is comparable or slightly higher above the 90$^{th}$ percentile. If also the pessimistic diffusion limitation is imposed (curve A), the clay assisted dissolution rate is well below the "ordinary" dissolution rate over the entire range. Therefore, it is concluded that the contribution to fuel dissolution from U transport is negligible.

**Intrinsic conditions**

The following intrinsic conditions/processes have been considered in the **Fuel and canister process report** which provided the bases for the derivation of fuel dissolution data in the **Data report**: Alpha self irradiation, enhanced diffusion (ASIED), helium build-up and the influence of high burn-up.

**Conclusion**

Based on the above account, it is concluded that the distribution of fuel dissolution rates given in the **Data report** is valid for all evolutions that need to be considered in SR-Site, even for groundwater conditions in which a clay slurry may contribute to the outward transport of uranium.

### *Metal corrosion rate*

*Range in which metal corrosion release rates are valid:* The release rates of the activation products from the metallic parts given in the **Data report** are based on a range of corrosion rates for stainless steel under anoxic conditions. These corrosion rates were estimated from a number of relevant studies carried out at temperatures up to 140°C and salinities up to anoxic sea water. The important parameters are thus salinity (especially chloride concentration) and redox conditions.

*Ranges in evolution cases studied:* In the corrosion scenario, canister failure occur after typically hundreds of thousands of years. In such time frames, the fuel temperature is close to the background temperature of the host rock, i.e. no increase of corrosion rates due to high temperatures is expected. The highest chloride concentrations expected during the whole repository evolution time are of the order 0.35 mol/L, i.e. much lower than in anoxic sea water. Hence the corrosion rates used in the **Data report** are valid (with a large margin) for the corrosion scenario.

*Need for analyses of additional evolutions:* The important parameters for the metal corrosion rate are the chloride concentrations and the redox conditions. As stated in the previous section about fuel dissolution, the analysis of the reference evolution includes the highest salinities that can be expected at Forsmark. The analysis of the redox conditions for the reference evolution shows a variability of redox potentials, always with anoxic conditions. Only the penetration of oxygen rich glacial melt waters can possibly lead to a deviation, and as described in Section 10.4.7 this is a very low probability event that is deemed to be possible only if in addition a set of extreme assumptions are made. Even if extreme assumptions were to be made, and oxygen postulated to reach a breached canister, the large reducing capacity of the remains of the failed copper canister and of the iron insert, would imply that anoxic conditions would prevail inside the canister. It is therefore concluded that there are no additional evolutions that need to be assessed.

### *Rock porosity, rock diffusivities and rock sorption coefficients*

**Rock porosity and effective diffusivity**

The rock porosity and effective diffusivity provided in the **Data report** (Section 6.8) are valid for all conditions in the host rock during repository evolution. The host rock conditions discussed in the **Data report** are groundwater composition, in-situ temperature, and in-situ stress. However, it is argued that the effective diffusivity and, especially, the porosity are relatively insensitive to host rock conditions.

Concerning the groundwater composition, which affects the porewater composition, the salinity may affect the degree of anion exclusion in the porous system. This is judged to have an insignificant effect on the porosity but a minor effect on the effective diffusivity. In the **Data report**, this is treated as data uncertainty, and the data provided should encompass not only reasonable groundwater

compositions during repository evolution, but also a larger range of groundwaters seen in crystalline rock. Also, anions are transported through the geosphere virtually without retention in the corrosion scenario, i.e. it is not warranted to explore even less favourable cases of anion exclusion.

The in-situ temperature affects the diffusivity in free solution, as described by well known relations, and thus also the effective diffusivity. The data provided are valid for temperatures ranging from somewhat elevated temperatures, compared to present day conditions, to temperatures just above freezing. Within this temperature range, the variation in the effective diffusivity is small. To exemplify, the diffusivity at room temperature is about a factor of two larger than that at temperatures just above freezing. This is treated as data uncertainty in the **Data report**. Since temperatures below freezing are irrelevant and since temperatures above present day values are favourable, there is no reason to explore more extreme cases than those covered by the **Data report**.

The porosity provided in the **Data report** is based on laboratory measurements at atmospheric pressure. However, corrections are made so that the data given should represent in-situ stress conditions. The provided effective diffusivity is based on measurements at, and should represent, in-situ stress conditions. The in-situ stress will change during the glacial cycle, primarily due to the extra load from an ice sheet during glaciation. However, this additional stress is judged to have a very minor effect on the porosity and minor effect on effective diffusivity, and is treated as data uncertainty in the **Data report**. Also, in the 'Canister failure due to isostatic load' scenario, Section 12.7, maximum ice thicknesses were found to be within the range covered by the input to the determination of porosity data in the **Data report**.

Finally, it is seen as unlikely that potential erosion products from the buffer would act as diffusion resistance at the fracture/rock interface, preventing radionuclides from entering the microporous system.

In summary, there is no need for additional studies, as the subject has been exhaustively studied and the data are provided in the **Data report**.

### Pore connectivity

An entity closely related to the effective diffusivity is the pore connectivity. In the **Data report** the in-situ pore connectivity is suggested to be unlimited on all scales relevant for safety assessment calculations (that is on the scale of at least several tens of metres). During glaciation, the microporous system could be affected by the additional in-situ stress originating from the ice cap. However, this effect is included in the data uncertainty assessment of the effective diffusivity, and even at glaciation unlimited pore connectivity is expected.

Also, for the transport conditions in the corrosion scenario, the pore connectivity would have to be reduced to the centimetre scale before affecting the geosphere retention in any significant way.

### Sorption partitioning coefficient

The sorption partitioning coefficient, $K_d$, is for many radionuclides sensitive to conditions in the host rock. In the **Data report** the groundwater composition is singled out as the most important condition, while in-situ temperature and stress are subordinate conditions with a minor or even very minor impact. For radionuclides sorbing by surface complexation, pH, the carbonate concentration and the concentrations of various other ligands that can directly compete to bind radionuclides at the expense of sorption, are of importance. For radionuclides sorbing by cation exchange, the concentrations of competing cations are of importance.

For many nuclides, the $K_d$ value is sensitive to redox conditions, which are determined by the presence of redox controlling pairs such as $Fe^{2+}/Fe(OH)_3$ or $SO_4^{2-}/FeS_{(am)}$, and is also related to pH and dissolved carbonate concentration. The redox conditions of the host rock are discussed in Section 6.1 of the **Data report**.

In the case of nuclides sorbing by cation exchange, $K_d$ values have been corrected to encompass the range of groundwater compositions projected during repository evolution. Input data for this correction have been modelled groundwater compositions at a great number of locations at the repository,

delivered in Section 6.1 of the **Data report**. This has resulted in distributions of $K_d$ values in which the lower tail of the distributions corresponds to unfavourable groundwater conditions. However, for nuclides sorbing by surface complexation, the complexity of the sorption mechanism has prevented making such detailed corrections. Here, based on expert judgment, compiled data have been sorted to be (fairly) representative for the Forsmark host rock, or not. Unrepresentative data have to the extent possible been discarded.

In summary, there are great uncertainties associated with $K_d$ values, which are also reflected in the wide $K_d$ ranges given in the **Data report**. As the lower tails of the distributions imply no geosphere retention for, in particular, the dose determining Ra-226 in the corrosion scenario, and as a wide range of conditions are covered by the data in the **Data report**, it is not deemed warranted to explore additional ranges of $K_d$ values. In addition to the transport conditions for the central corrosion case, where the full range of $K_d$ values for reducing conditions is used, also a case where rock $K_d$ values for oxidising conditions are used when an ice sheet passes above the repository with flow rates also varying in accordance with the changing external conditions, is explored, see Section 13.5.6.

#### *Hydrogeological data related to flow and transport*

The hydrogeologic flow-related migration data are presented in the **Data report** in Section 6.7. The different data sets that are of relevance for the corrosion scenario are:

- Equivalent flow rate ($Q_{eq}$) and Darcy flux ($U_0$) for the Q1 release path.
- Flow-related transport resistance ($F$).
- Advective travel time ($t_w$).
- Peclet number ($Pe$).
- Maximum penetration depth in rock matrix ($x_0$).

Canister failures in the corrosion scenario occur when the buffer is lost in the deposition hole. Backfill material from tunnels will also be lost, but it is judged that this loss will be small relative to the total amount of backfilled material (Section 10.3.11) and hence not modify the flow conditions in the tunnels. However, flow in fractures intersecting deposition holes may be changed locally because of the modified properties of the fractures. Specifically, eroded buffer from the deposition holes may fill up the fracture void space and hence change the flow characteristics.

#### Equivalent flow rate and Darcy flux

If the eroded buffer remains within the fracture close to the deposition hole, it is likely that groundwater flow (and associated equivalent flow rate and Darcy flux) will be decreased. Also, the radionuclide release rate from the near field is virtually independent of the flow rate for the transport conditions in the corrosion scenario. The flow rate is sufficiently high to carry away all radionuclides released from the spent fuel, and there is thus no need to consider higher flow rates from this point of view. Any reduction in flow rate due to remaining buffer in the fractures is pessimistically disregarded.

#### Flow-related transport resistance and advective travel time

The flow paths through the geosphere are not believed to be affected by the modified properties implied by the eroded buffer. Darcy flux at deposition hole locations is inversely correlated to flow-related transport resistance and advective travel time. Thus, if the eroded material implies a decrease in flow at deposition hole locations, the flow-related transport resistance and advective travel time will increase. Repository evolutions leading to increased flow rates were explored in the analysis of containment for the corrosion scenario, Section 12.6, leading to the conclusion that no additional cases need to be analysed with respect to corrosion, in which case essentially temperate flow rates were used. However, for the analysis of radionuclide transport, it is warranted to explore the effects of flow varying in accordance with the changing conditions during a glacial cycle. This is done as a variant case, see Section 13.5.6.

**Peclet number and maximum penetration depth in rock matrix**

The penetration depth of the rock matrix is not assessed to be affected by the presence of buffer material in the fractures, see also discussion on pore connectivity above. Also, the Peclet number is not assessed to be affected by the presence of some buffer material in the fracture network.

No other issues of concern related to the corrosion scenario have been identified. The data presented in the **Data report** are thus judged relevant for the corrosion scenario. Furthermore, no other repository evolutions compatible with the corrosion scenario have been identified that would imply less favourable flow and transport conditions.

#### *Biosphere LDF factors*

All climate conditions emerging from the analyses of the evolution of the system are covered by the different sets of LDFs available. LDFs for the interglacial period are used in the central corrosion case.

As concluded in Section 13.2.4, the highest doses from a constant release rate from the repository are expected under temperate conditions when humans are exposed to radionuclides that have accumulated in a wetland that has been converted to arable land, and when contaminated well water is utilised by human inhabitants and livestock. Hence, the LDFs for the interglacial period used in the calculations are maximum values during the reference glacial cycle. For the global warming climate case, LDFs were significantly (about an order of magnitude) larger than under the reference glacial cycle only for Cs-135 and U-238, see Figure 13-7. Since neither of these nuclides contributes significantly to the total annual dose in the corrosion scenario, there is no need to apply any LDFs other than those used in the central corrosion case to cover biosphere uncertainties.

#### *Overall conclusion regarding additional cases to analyse*

The analyses in this section demonstrate that i) the evolution in the corrosion scenario is compatible with conditions for which data in the **Data report** have been determined and ii) no alternative evolutions of the system that could imply less favourable transport conditions, need to be considered. However, a case with host rock conditions varying in accordance with the changing conditions during a glacial cycle needs to be explored.

### 13.5.6 Calculation of alternative cases

#### *Overview of cases*

Figure 13-21 gives an overview of calculation cases for the corrosion scenario. The three hydrogeological DFN models (blue) are combined with three erosion cases (red) yielding nine corrosion variants to consider in the derivation of calculation cases for radionuclide transport and dose. Of these, the three ‘no advection’ variants are not further treated as they do not lead to canister failures.

The central corrosion case consists of the semi-correlated hydrogeological DFN model, the SR-Site erosion model and base case transport assumptions and data as presented above. Five cases of alternative transport conditions are analysed for the central corrosion variant:

- A case with solubilities included.
- A case in which Thorium is assumed to be mobile in the near field.
- A case with varying climate conditions.
- A cases with colloid facilitated transport in the geosphere.
- A case with varying climate conditions and colloids in the geosphere.

(The case mentioned in the fourth bullet point is shown only in the **Radionuclide transport report**.) The other four relevant corrosion variants are analysed for the base case transport conditions. Additional corrosion variants are reported in the **Radionuclide transport report**.

### *Mobile Thorium in the near field*

Figures 13-22 and 13-23 show near-field dose equivalent releases and far-field doses, respectively, for the central corrosion case when disregarding sorption of Thorium in the near field. Both doses caused by release of Ra-226 and the total dose are lower than in the central case, showing that the assumption of Thorium sorption in the near field made in the central corrosion case is pessimistic. Note also that considerably less Ra-226 is released from the near field compared to the central corrosion case (radiological impact 0.0024 vs 0.38 μSv), but that the far-field releases are more similar (0.063 vs 0.11 μSv). This is due to the fact that, in the case where Thorium sorption in the near field is disregarded, Th-230 is released from the near field and thus generates Ra-226 in the geosphere rather than in the near field.

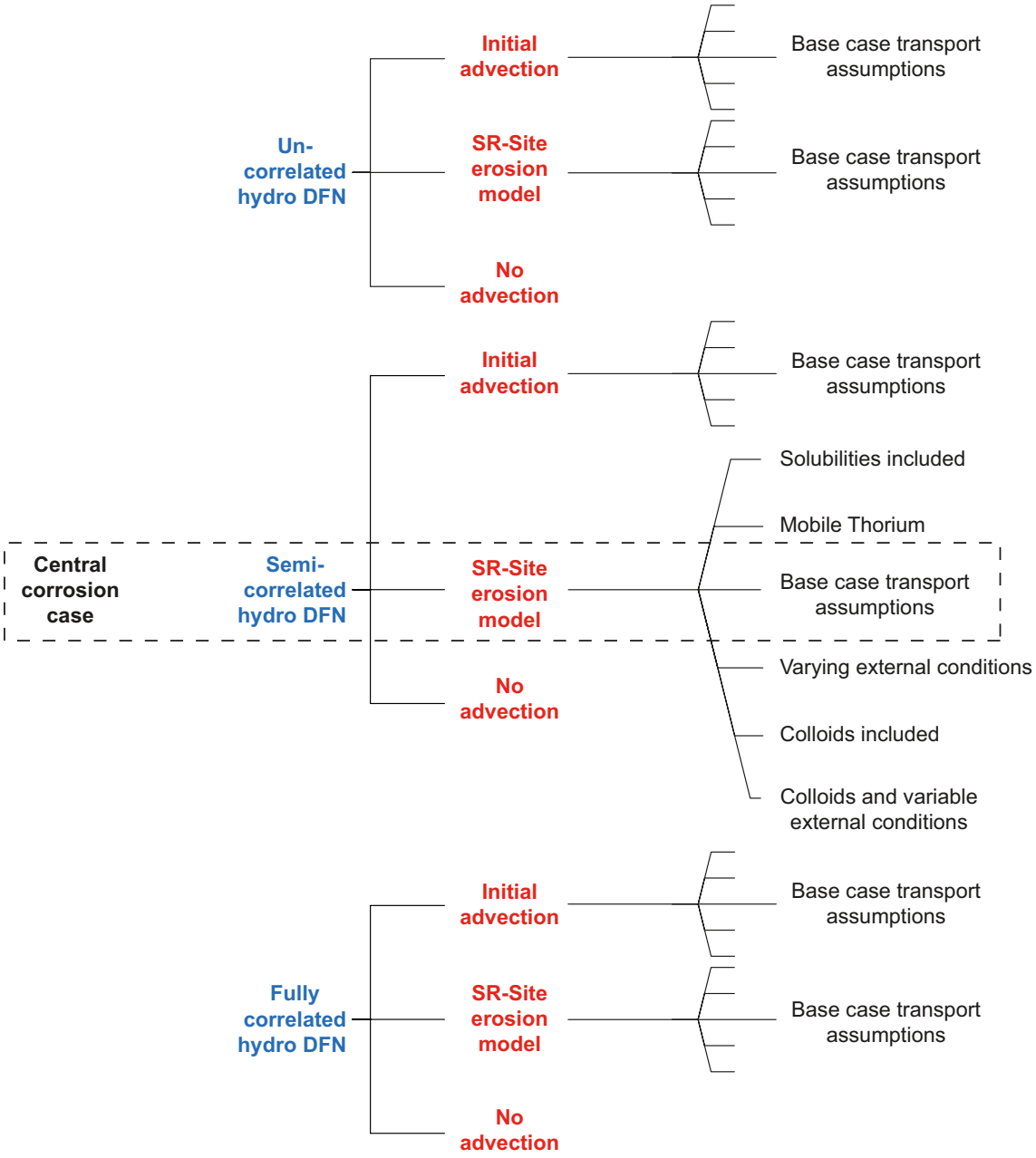


***Figure 13-21.*** *Overview of calculation cases for the corrosion scenario.*

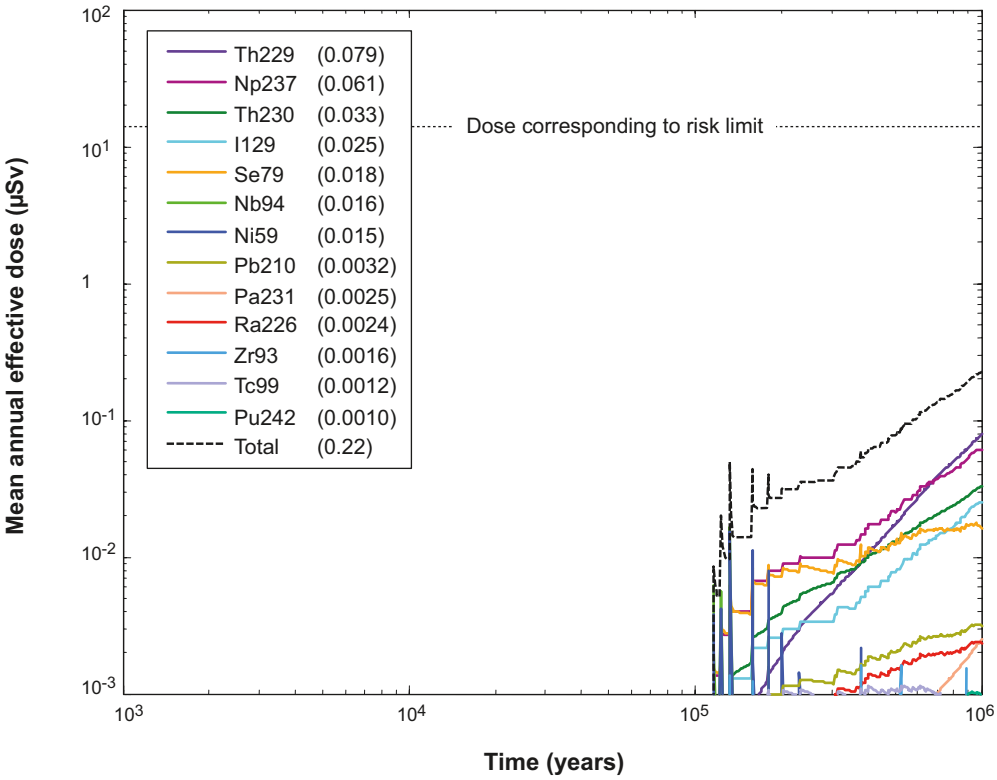


***Figure 13-22.*** *Near-field mean annual effective dose equivalent release for the probabilistic central corrosion case, disregarding Th sorption in the near field. The legends are sorted according to descending peak mean annual effective dose over one million years (given in brackets in µSv).*

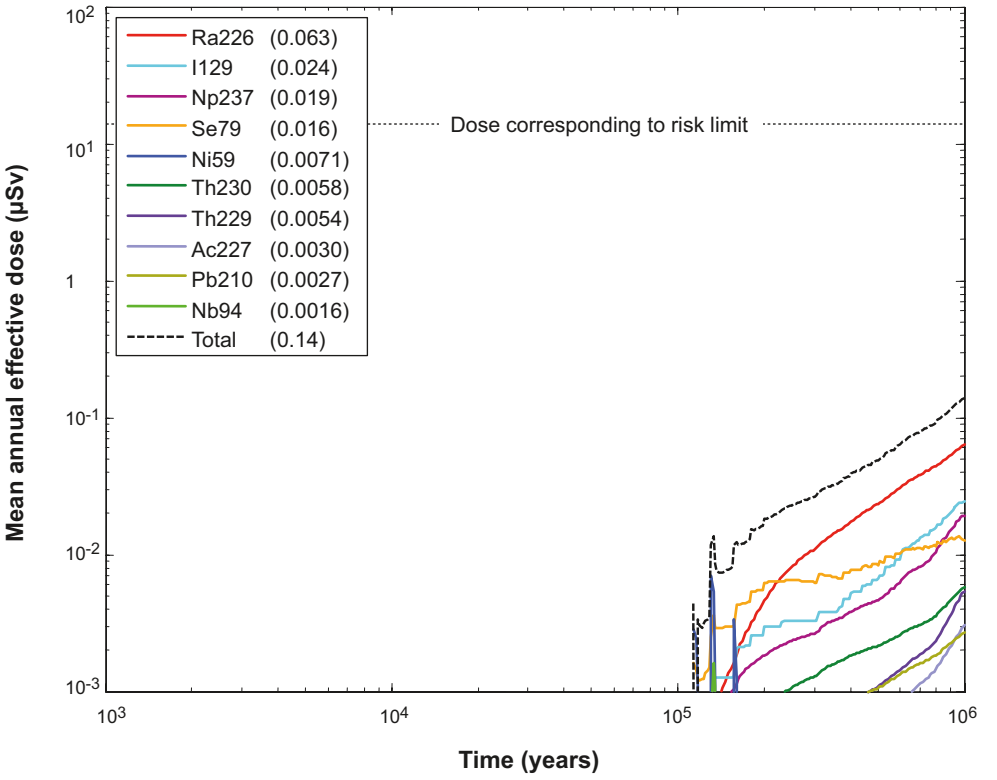


***Figure 13-23.*** *Far-field mean annual effective dose for the probabilistic central corrosion case, disregarding Th sorption in the near field. The legends are sorted according to descending peak mean annual effective dose over one million years (given in brackets in µSv).*

### *Solubilities included in the near field*

Figures 13-24 and 13-25 show near-field dose equivalent release and far-field annual doses, respectively, for the central corrosion case when including solubilities in the near field. The near-field dose caused by release of Pb-210 is considerably higher than for the central corrosion case since Ra-226 is confined to the canister interior where it generates Pb-210. The far-field doses are, however, similar to those of the central corrosion case. Pb-210 decays considerably in the geosphere, due to in particular its short half-life.

### *Uncorrelated and fully correlated hydrogeological DFN model*

Far-field annual doses for the central corrosion case but with hydrogeological data for the uncorrelated relation between DFN fracture size and transmissivity used in the calculation of canister failure times and radionuclide transport are shown in Figure 13-26. The corresponding far-field annual doses for the fully correlated DFN model are shown in Figure 13-27. The mean numbers of failed canisters are 0.65 and 0.57, respectively, and the first releases occur after around 100,000 years.

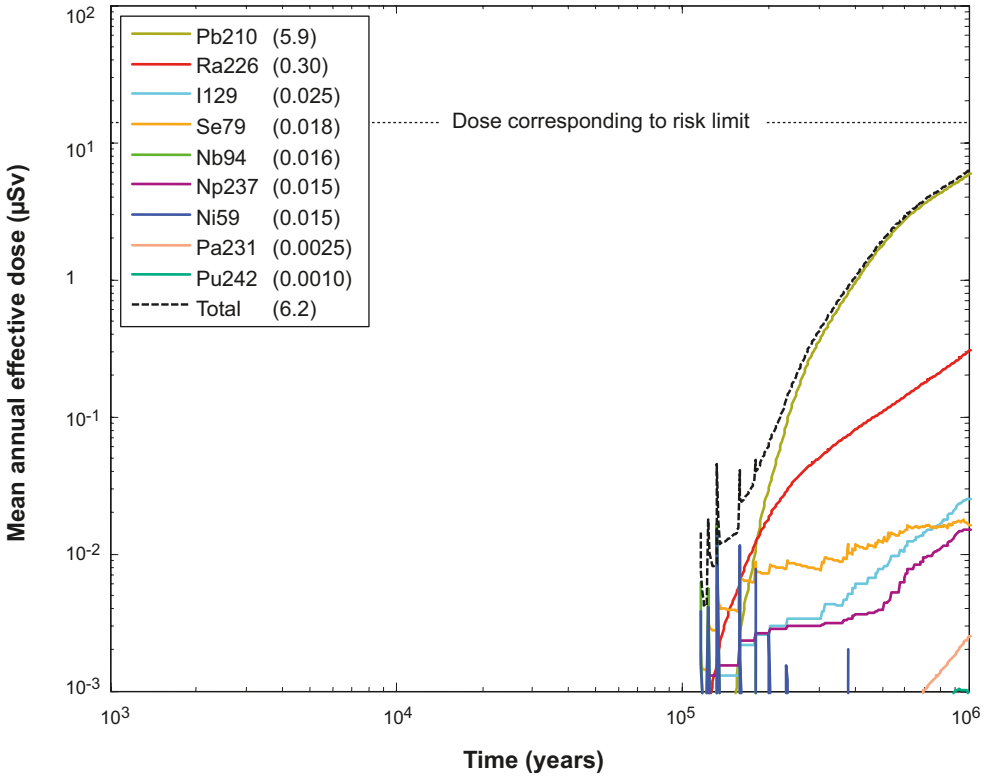


***Figure 13-24.*** *Near-field mean annual effective dose equivalent release for the probabilistic central corrosion case, including solubility limits in the near field. The legends are sorted according to descending peak mean annual effective dose over one million years (given in brackets in µSv).*

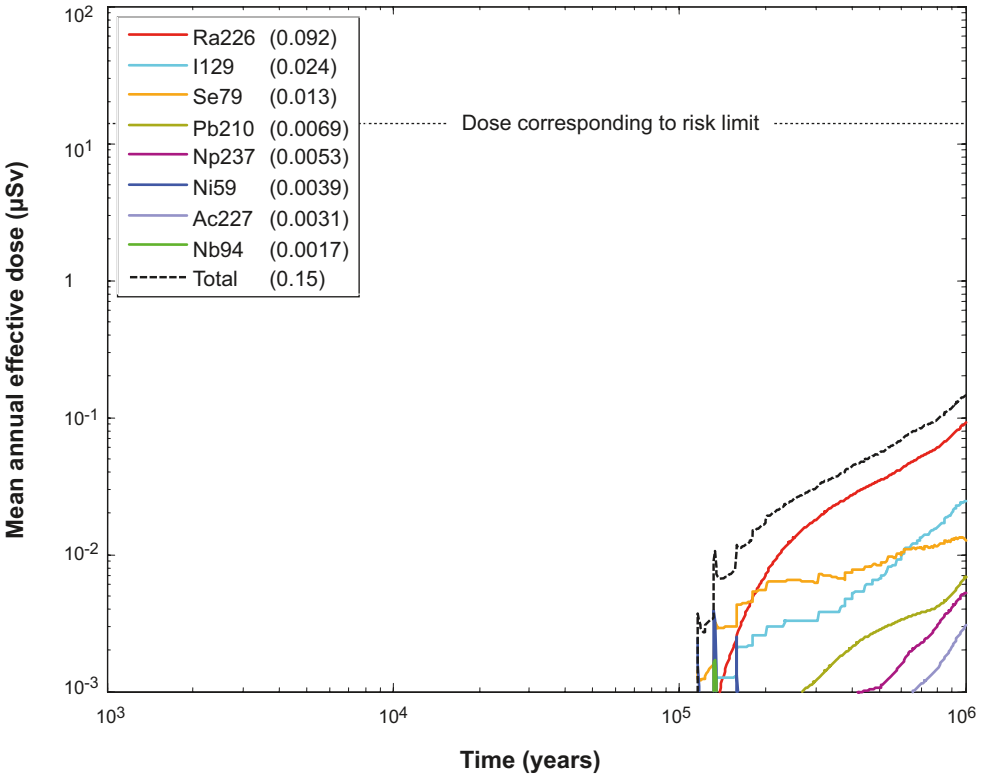


***Figure 13-25.*** *Far-field mean annual effective dose for the probabilistic central corrosion case, including solubility limits in the near field. The legends are sorted according to descending peak mean annual effective dose over one million years (given in brackets in µSv).*

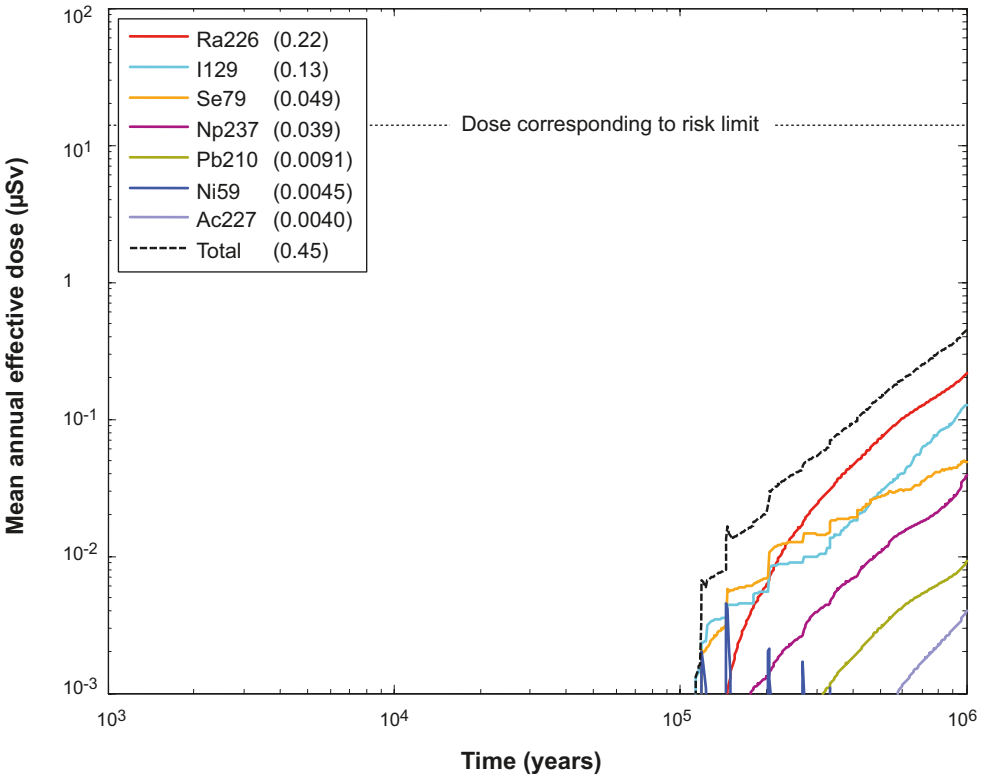


***Figure 13-26.*** *Far-field mean annual effective dose for a probabilistic calculation for the corrosion failure with the uncorrelated hydrogeological DFN model. The legends are sorted according to descending peak mean annual effective dose over one million years (given in brackets in µSv).*

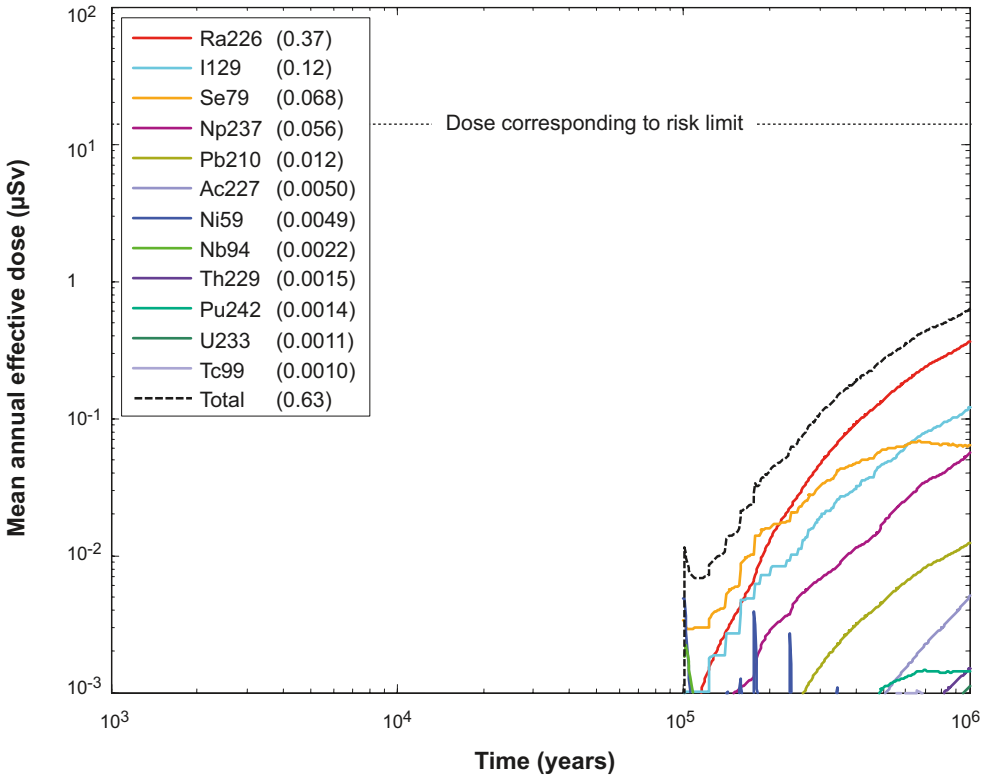


***Figure 13-27.*** *Far-field mean annual effective dose for a probabilistic calculation for the corrosion failure with the fully correlated hydrogeological DFN model. The legends are sorted according to descending peak mean annual effective dose over one million years (given in brackets in μSv).*

### *Cases with initial advection in all deposition holes*

Consequences for the extreme case assuming initial advection in all deposition holes are shown for the near field and the far field in Figures 13-28 and 13-29, respectively. The mean number of failed canisters is 0.17.

The first releases occur slightly before 50,000 years. The dose equivalent releases from the near field are dominated by pulse release from metal corrosion of Nb-94 and the more continuous release of Ra-226. The doses caused by releases from the far field are dominated by the pulse release from Nb-94 and the more continuous release of Se-79 and Ra-226.

The relatively small difference between this case and the central corrosion case is due to the fact that most canisters will not fail even if the buffer is missing since the time required to corrode through the canister exceeds the one million year assessment period for the majority of canisters.

The corresponding cases for the uncorrelated and fully correlated hydrogeological DFN models yield similar results, see the **Radionuclide transport report**. Total doses for these cases are also included in the summary of cases given in Figures 13-39 and 13-40 in Section 13.5.9.

### *Varying external conditions*

Flow related transport data for temperate climate conditions are used in the above cases. The effect of varying flow conditions and other climate related geosphere data are analysed with the MARFA model.

Future climate evolution at the Forsmark site is described in detail in the **Climate report** and summarised in Section 10.4.1. Future glacial cycles will have a significant effect on groundwater flow and chemistry. A pessimistic abstraction of the groundwater flow field evolution is developed to assess the impacts of future glacial cycles on radionuclide transport in the corrosion scenario.

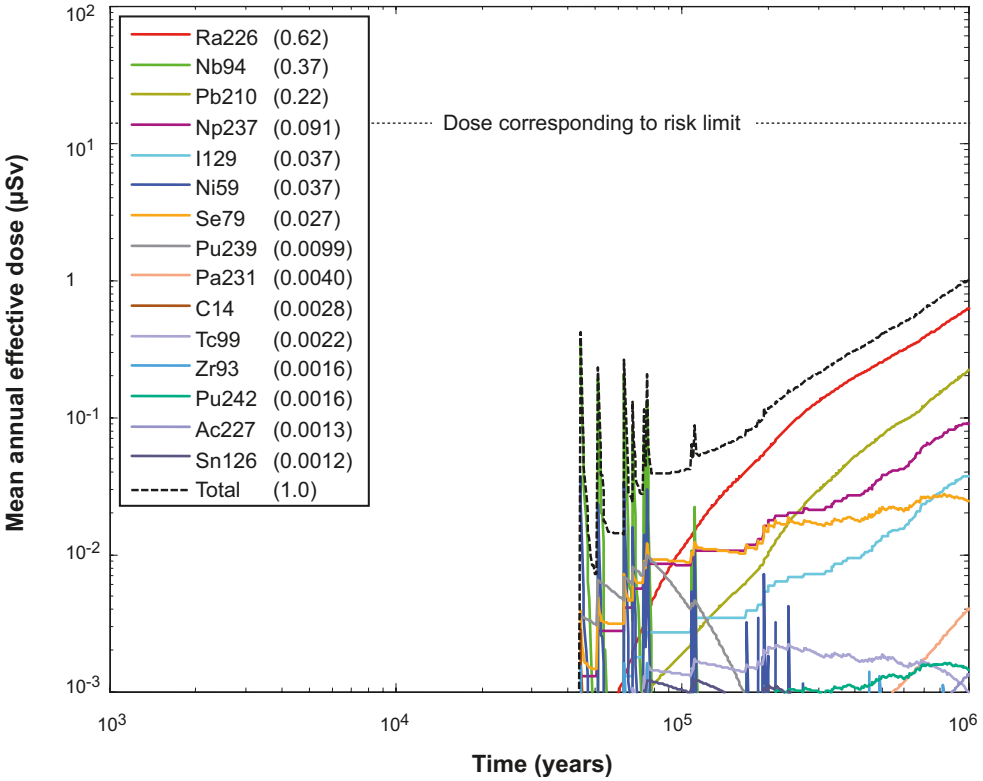


***Figure 13-28.*** *Near-field mean annual effective dose equivalent release for a probabilistic calculation for the corrosion failure with initial advection in the buffer and otherwise as the central corrosion case. The legends are sorted according to descending peak mean annual effective dose over one million years (given in brackets in µSv).*

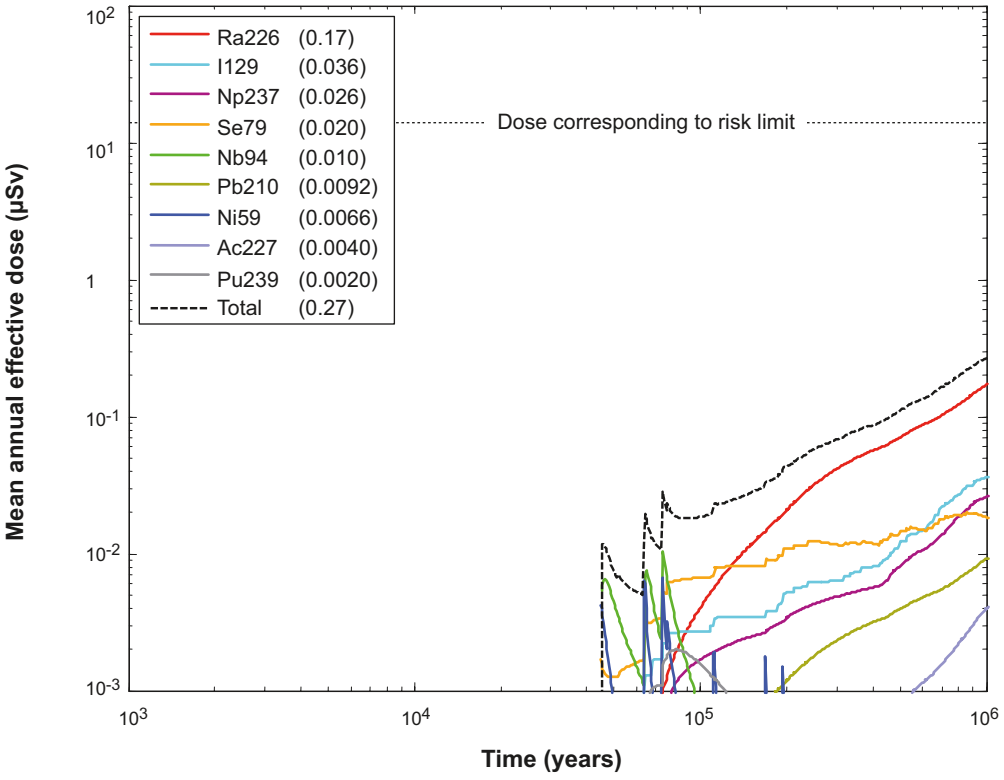


***Figure 13-29.*** *Far-field mean annual effective dose for a probabilistic calculation for the corrosion failure with initial advection in the buffer and otherwise as the central corrosion case. The legends are sorted according to descending peak mean annual effective dose over one million years (given in brackets in µSv).*

A simplification of the glacial cycle is developed in the **Climate report**, Section 4.5.4 to support the abstraction, see Figure 13-30. The simplified cycle has two temperate periods, three periglacial periods, two glacial periods, and two submerged periods in the 120,000 year cycle. It is noted that the summed percentages of each climate period coincide with the corresponding percentages for the original, non-simplified cycle. In the abstraction, the cycle repeats 8 times in the 1 million year assessment period of interest. Table 13-7 provides times for each flow change in the first 120,000 year cycle.

Detailed simulations of transient flow during a glacial cycle have been undertaken /Vidstrand et al. 2010/ and are summarised in Section 10.4.6. These simulations show that both the direction and magnitude of groundwater flow are affected by the glacial cycle. As an alternative to representing the full details of transient groundwater flow fields in the transport simulations, a pessimistic bounding abstraction is developed.

The abstraction includes changes in flow magnitude, but uses pathlines from the temperate period /Joyce et al. 2010/ and ignores changes in flow direction. This abstraction is pessimistic because it greatly overestimates the vertical component of the flow velocity compared with detailed simulations /Vidstrand et al. 2010/, and also ignores lengthening of the flow paths that may occur during some of the climate periods.

**Table 13-7. Duration of each climate period in the simplified 120,000 year cycle. The percentage of each accumulated period is also indicated.**

| Period | Calendar time (kyrs) | Duration (kyrs) | Accumulated duration (kyrs) |
|---|---|---|---|
| Temperate | 0–8 | 8 | 8 |
| Periglacial | 8–12 | 4 | 4 |
| Temperate | 12–35 | 23 | 8+23 = 31 (26%) |
| Periglacial | 35–58 | 23 | 4+23 = 27 |
| Glacial | 58–65 | 7 | 7 |
| Submerged | 65–75 | 10 | 10 |
| Periglacial | 75–89 | 14 | 27+14 = 41 (34%) |
| Glacial | 89–111 | 22 | 7+22 = 29 (24%) |
| Submerged | 111–120 | 9 | 10+9 = 19 (16%) |

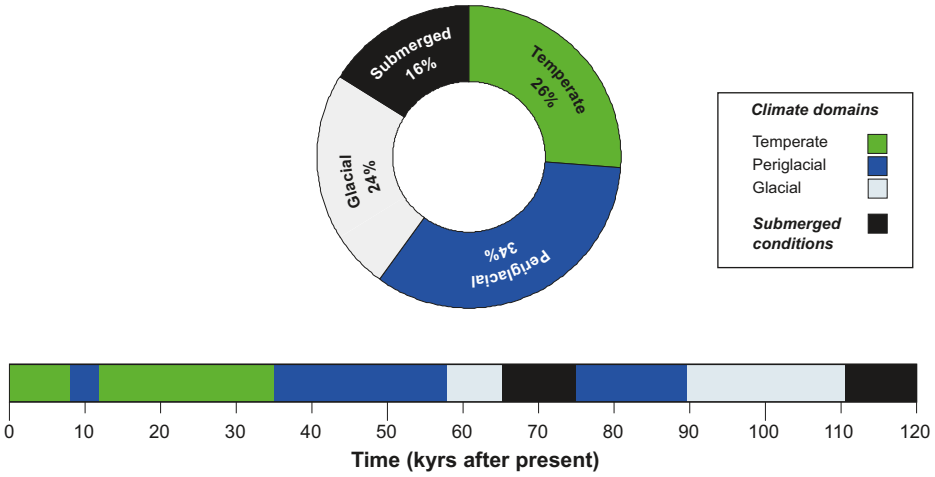


***Figure 13-30.*** *Simplified glacial cycle for use in the geosphere transport assessment, see the* ***Climate report****, Section 4.5.4.*

The glacial periods summarised in Figure 13-30 and Table 13-7 need to be further subdivided into advancing, glacial maximum and retreating phases, because the groundwater velocity will be very different in these three phases. For the advancing ice sheet, it takes 366 years for the ice sheet to move between ice front locations I and IV, see Section 10.4.6 and /Vidstrand et al. 2010/ for details. For the retreating ice sheet it takes 61 years to move between ice front locations IV and I. As an approximation, it is judged that when the ice front is beyond these ice front locations, the influence of the ice front on the repository will be small, i.e. conditions close to periglacial or submerged will prevail. However, even beyond these times, there is some influence, even if not comparable to the peak, see Figure 13-31 which shows the Darcy flux at repository depth within the repository footprint (measurement locality 2 in /Vidstrand et al. 2010/). Specifically, during the ice advance, the increase in Darcy flux relative to temperate conditions prevails approximately for 2,000 years. It is decided to represent the glacial advancing period as having duration of 1,800 years, which is much longer than the time to move between ice front locations I and IV, but slightly shorter than the time 2,000 years. The more rapid retreating phase is modelled as having duration of 300 years; i.e. the ratio in duration between advance and retreat phases is maintained. It is also noted that the increase in Darcy flux during the advancing phase is smaller than during the retreating phase. This is due to the fact that the advancing phase is characterised by permafrost in front of the ice sheet, whereas the retreating ice sheet is warm based such that no permafrost is present, see Section 10.4.6 and /Vidstrand et al. 2010/ for details.

Flow scaling factors for each climate domain are obtained from the calculated Darcy flux distributions at deposition hole locations in the super-regional groundwater flow model of /Vidstrand et al. 2010/ summarised in Section 10.4.6. In Figure 10-146 the Darcy flux distributions are shown in terms of maximum, median, and minimum values. The median values from Figure 10-146 and the duration of each flow period in Table 13-7 are used to obtain time-dependent flow factors (Figure 13-32). In developing the flow factors, the glacial state with a 2-km tongue of permafrost was assumed for the glacial retreating phase. The latter assumption is regarded as slightly pessimistic because the fluxes in the glacial case without permafrost of /Vidstrand et al. 2010/ were developed for an advancing ice sheet but applied here for a retreating ice sheet. In the far-field calculations performed with MARFA, the advective travel time and flow-related transport resistance for the temperate period are inversely scaled by the values in Figure 13-32 to obtain corresponding values for other stages in the glacial cycle.

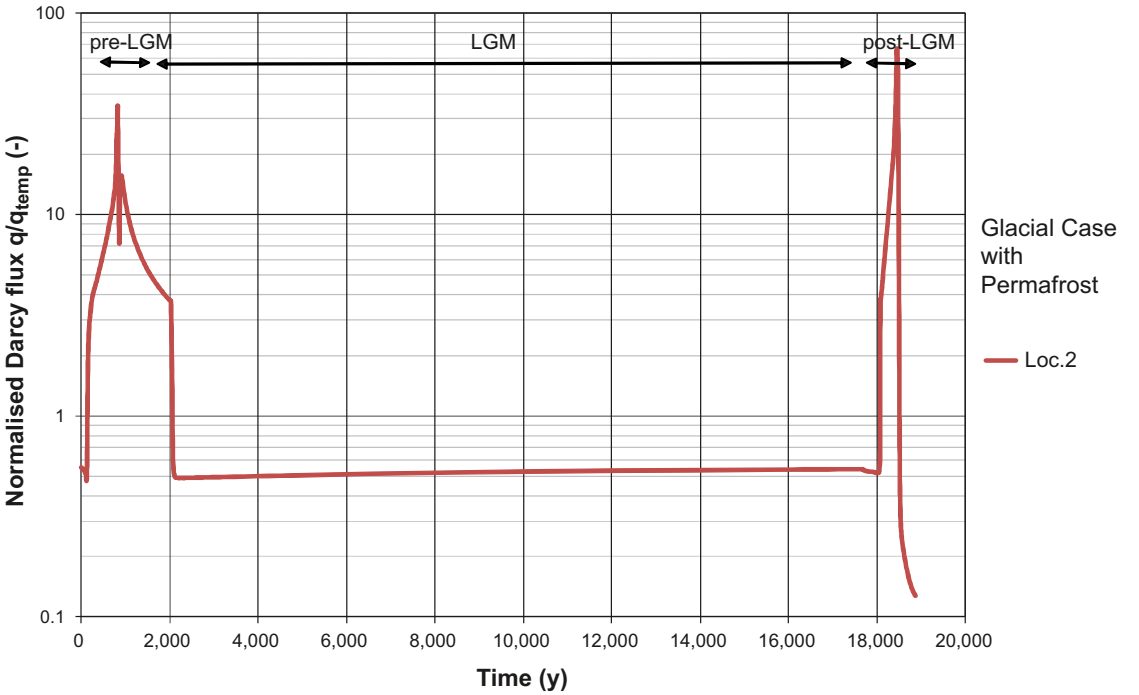


***Figure 13-31.*** *Change in Darcy flux relative to the temperate period as the ice sheet advances and retreats over the repository location. Figure is modified after Figure G-12 of /Vidstrand et al. 2010/.*

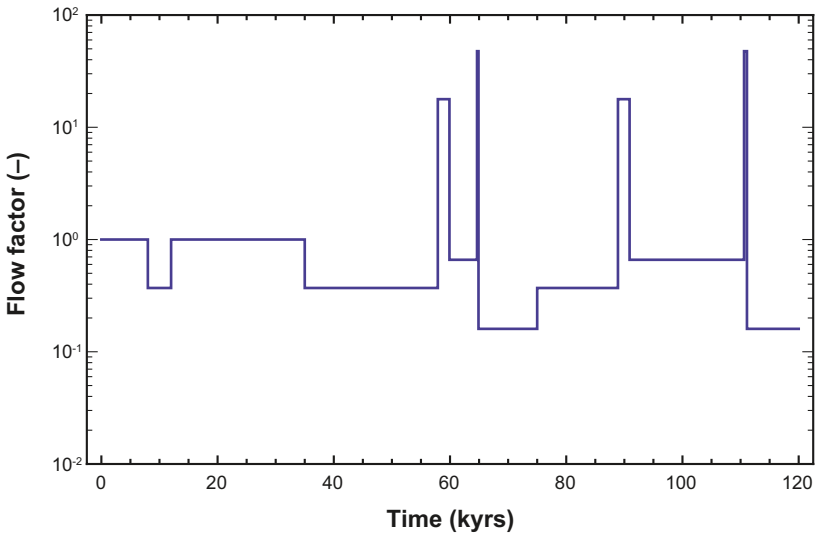


***Figure 13-32.*** *Flow scaling factors for one glacial cycle (of eight) for use in far-field radionuclide transport simulations. The spikes at the end of each glacial period have 300 year duration, but are not resolved on the scale of this figure. The scaling factor is defined relative to the Darcy flux in the temperate period.*

The transport simulations are identical to the temperate period base case described in Section 13.5.4 except for the flow changes shown in Figure 13-32 and the use of sorption $K_d$-values for oxidising conditions for the redox sensitive elements during ice front passages (i.e. during the time periods when flow scaling factors are 20 and 50, respectively). In addition, different landscape dose factors (LDFs) are applied for different periods in the glacial cycle. The near-field release calculations used as input to the MARFA simulations do not take into consideration the changes in flow. This simplification is based on the fact that releases of radioelements that are not solubility limited will be limited by the rate of fuel dissolution, which is independent of flow rate. It should also be noted that instantaneous release fractions are not included in this simulation.

Expected annual dose versus time for this case is shown in Figure 13-33. Also the case without flow changes, i.e. with temperate flow throughout the assessment period, is shown. The results are based on 2,800 realisations of the central corrosion case where both near-field and far-field parameters follow distributions given in the **Data report**.

The results in Figure 13-33 indicate that the flow, $K_d$ and LDF changes collectively cause no significant increase in peak dose. The main effect is the sharp downward spikes in dose during the time of glacial approach and retreat. Although the radionuclide mass discharge to the biosphere is increased sharply during these periods due to changes in flow and, more importantly, changes in $K_d$ for redox-sensitive radionuclides, this increase is more than compensated by the greatly reduced LDF values during these periods.

The results without flow changes can also be compared to the corresponding case calculated using FARF31, see Figure 13-18 of Section 13.5.4, showing very similar total dose results.

### *Colloid facilitated transport*

The presence of bentonite material in the deposition tunnel backfill and in the buffer in the deposition hole is expected to result in bentonite colloids in the groundwater near deposition holes and along the geosphere transport pathways. Radionuclides that have a strong affinity for bentonite will sorb onto bentonite colloids and may be transported through the geosphere with reduced interaction with the rock matrix, i.e. with a reduced retention. Colloid facilitated transport involves a complicated combination of processes, many of which can mitigate the transport. Mitigating processes include colloid retardation in fractures, physical filtration (straining) of colloids in fractures, colloid flocculation and sedimentation, radionuclide desorption from colloids, saturation of sorption sites on colloids, and competition for sites on colloids. These processes are uncertain or involve uncertain parameters that are difficult to quantify in short duration experiments. Rather than attempting to

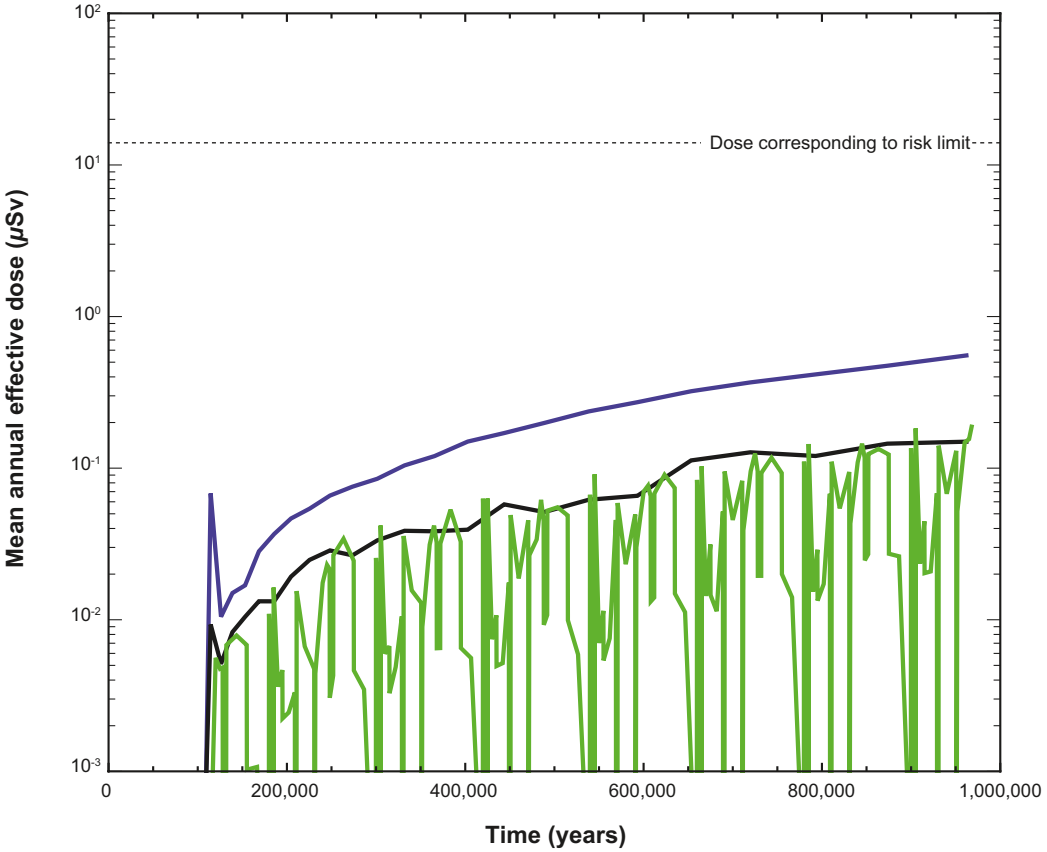


***Figure 13-33.*** *Expected doses with and without flow changes. The solid blue curve is the near-field release expressed as an annual effective dose. The black and green curves are far-field annual effective dose without and with flow changes, respectively.*

develop detailed process models for colloid facilitated transport, potential mitigating processes are ignored so as to place an upper bound on the possible effect. Ignoring these potential mitigating processes and taking into consideration that sorption of radionuclides onto bentonite is understood to be a reversible process on the time scale of geosphere transport, see the **Buffer, backfill and closure process report**, the effect of colloids in facilitating transport may be modelled through the introduction of effective transport parameters, as described in Appendix I of the **Radionuclide transport report**.

Colloid concentrations that can be stably supported are highly sensitive to groundwater chemistry. It has been determined from a review of laboratory and field data /Wold 2010/ that 10 mg/L is a reasonably pessimistic value for colloid concentrations for typical groundwater chemistries. However, this value may be much higher during brief periods when highly dilute glacial melt water enters the geosphere. The maximum concentration of clay colloids in very dilute waters has been determined to be ~40 g/L at the buffer/groundwater boundary /Birgersson et al. 2009/ and the **Geosphere process report**. However, it is unreasonable to assume that this concentration can be maintained throughout the geosphere. For the radionuclide transport calculations a value of 10 g/l has been selected to be a pessimistic value for colloid concentrations in very dilute waters. The pessimistic value for dilute waters (i.e. 10 g/L) is used during periods of glacial retreat/advance and during the second halves of the glacial maximum and temperate periods, to illustrate consequences of periods of potential dilute water intrusion according to the analyses in Chapter 10. The lower value of 10 mg/L is used for other periods.

The partitioning coefficient for sorption onto bentonite colloids $K_c$ may be related to the same parameter for sorption onto bentonite buffer material $K_d$ as $K_c = \gamma K_d$ where $\gamma$ is a ratio of specific surface areas for colloidal and bulk bentonite. Given that bentonite is a fine-grained material and that equilibrium partitioning coefficients for bentonite are typically measured using colloidal suspensions with particle sizes less than 1 μm, $\gamma \approx 1$ is a reasonable assumption. Thus, $K_d$ distributions from Section 5.3 of the **Data report** were used for $K_c$.

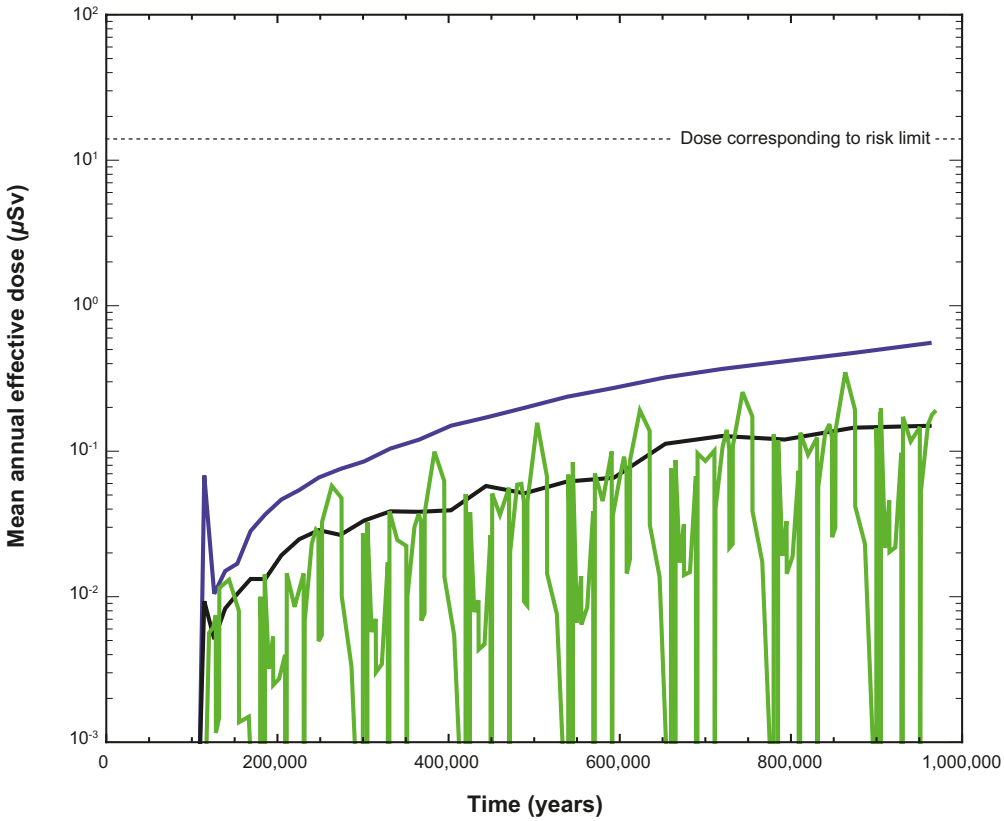


***Figure 13-34.*** *Expected dose with unsteady flow and colloid-facilitated transport. The solid blue curve is the near-field release expressed as an annual effective dose. The green curve is far-field annual dose with flow changes and colloid-facilitated transport. The case with no flow changes and no colloid-facilitated transport is shown for comparison purposes (black curve).*

Results using 2,800 realisations of the central corrosion case are shown in Figure 13-34. By comparison with Figure 13-33, it can be seen that colloids enhance the mean annual dose by a modest factor (< 3) and only during the last halves of the temperate periods. In all cases the mean annual dose is less than the dose-equivalent near-field release. That the mean annual dose would be bounded by the dose-equivalent near-field release is not obvious *a priori* because of the potential for colloid-induced pulse remobilization (i.e. build up of radionuclide mass in the geosphere during periods of low mobility that is subsequently released during periods of high mobility). The results in Figure 13-34 clearly show that colloid-induced pulse remobilization is not an issue and that the dose-equivalent near-field release can be used as an upper bound on the mean annual dose.

### 13.5.7 Doses to non-human biota for the corrosion scenario

Doses to non-human biota for the probabilistic central corrosion case have been calculated according to the methodology described in Section 13.2.5. The total dose rates to organisms in terrestrial, freshwater and marine ecosystems in Forsmark are presented in Table 13-8, and the results are presented in more detail in the **Biosphere synthesis report** and in /Torudd 2010/. All the total dose rates are well below the screening dose rate (10 μGy $h^{-1}$) recommended in the ERICA Integrated Approach /Beresford et al. 2007/. It is, therefore, concluded that radionuclide releases predicted for this case will not lead to detrimental biological effects on individuals of species found at the site. As discussed in Section 13.2.5, the lack of biological detriment to individuals is regarded as clear evidence that the populations comprising those individuals are similarly protected.

The results are readily applicable to other corrosion cases, by scaling the releases of the nuclides in question, which are at most about one order of magnitude higher than those for the central corrosion case. This means that the conclusion for the central corrosion case holds also for all other corrosion cases considered in SR-Site.

**Table 13-8. Whole-body dose rates for terrestrial, freshwater and marine biota in Forsmark, given the mean release according to the probabilistic central corrosion case. Estimates from deterministic calculations are given together with the 95th percentile from probabilistic simulations (from /Torudd 2010/).**

| | Dose rate (μGy $h^{-1}$) | |
|---|---|---|
| **Reference organism** | **Deterministic estimate** | **95th percentile** |
| **Terrestrial** | | |
| Amphibia | $2.9 \cdot 10^{-5}$ | $5.9 \cdot 10^{-5}$ |
| Bird | $2.7 \cdot 10^{-5}$ | $5.9 \cdot 10^{-5}$ |
| Detritivorous invertebrate | $6.4 \cdot 10^{-5}$ | $1.4 \cdot 10^{-4}$ |
| Flying insect | $6.1 \cdot 10^{-5}$ | $1.4 \cdot 10^{-4}$ |
| Gastropod | $5.9 \cdot 10^{-5}$ | $1.4 \cdot 10^{-4}$ |
| Grasses and herbs | $3.7 \cdot 10^{-5}$ | $8.5 \cdot 10^{-5}$ |
| Mammal, large | $2.2 \cdot 10^{-5}$ | $4.9 \cdot 10^{-5}$ |
| Mammal, small | $2.5 \cdot 10^{-5}$ | $5.2 \cdot 10^{-5}$ |
| Lichen and bryophytes | $6.7 \cdot 10^{-4}$ | $1.2 \cdot 10^{-3}$ |
| Reptile | $2.9 \cdot 10^{-5}$ | $5.8 \cdot 10^{-5}$ |
| Shrub | $7.6 \cdot 10^{-5}$ | $2.0 \cdot 10^{-4}$ |
| Soil invertebrate | $6.3 \cdot 10^{-5}$ | $1.4 \cdot 10^{-4}$ |
| Tree | $6.1 \cdot 10^{-5}$ | $1.6 \cdot 10^{-4}$ |
| **Freshwater** | | |
| Bird | $1.6 \cdot 10^{-5}$ | $4.4 \cdot 10^{-5}$ |
| Bivalve mollusc | $3.7 \cdot 10^{-4}$ | $7.7 \cdot 10^{-4}$ |
| Crustacean | $2.7 \cdot 10^{-4}$ | $4.8 \cdot 10^{-4}$ |
| Gastropod | $2.7 \cdot 10^{-4}$ | $5.3 \cdot 10^{-4}$ |
| Insect larvae | $1.9 \cdot 10^{-3}$ | $5.1 \cdot 10^{-3}$ |
| Mammal | $1.8 \cdot 10^{-5}$ | $4.3 \cdot 10^{-5}$ |
| Pelagic fish | $1.7 \cdot 10^{-5}$ | $4.0 \cdot 10^{-5}$ |
| Phytoplankton | $3.4 \cdot 10^{-3}$ | $9.7 \cdot 10^{-3}$ |
| Vascular plant | $5.2 \cdot 10^{-4}$ | $1.2 \cdot 10^{-3}$ |
| Zooplankton | $2.2 \cdot 10^{-4}$ | $4.9 \cdot 10^{-4}$ |
| **Marine** | | |
| Benthic fish | $1.1 \cdot 10^{-6}$ | $1.8 \cdot 10^{-6}$ |
| Benthic mollusc | $1.9 \cdot 10^{-6}$ | $3.1 \cdot 10^{-6}$ |
| Bird | $3.2 \cdot 10^{-7}$ | $9.0 \cdot 10^{-7}$ |
| Crustacean | $6.3 \cdot 10^{-7}$ | $1.2 \cdot 10^{-6}$ |
| Macroalgae | $1.4 \cdot 10^{-6}$ | $1.8 \cdot 10^{-6}$ |
| Mammal | $8.5 \cdot 10^{-8}$ | $2.2 \cdot 10^{-7}$ |
| Pelagic fish | $3.4 \cdot 10^{-7}$ | $1.0 \cdot 10^{-6}$ |
| Phytoplankton | $2.9 \cdot 10^{-6}$ | $6.2 \cdot 10^{-6}$ |
| Polychaete worm | $3.0 \cdot 10^{-6}$ | $4.6 \cdot 10^{-6}$ |
| Vascular plant | $1.3 \cdot 10^{-6}$ | $1.9 \cdot 10^{-6}$ |
| Zooplankton | $3.4 \cdot 10^{-7}$ | $6.9 \cdot 10^{-7}$ |

### 13.5.8 Alternative safety indicators for the corrosion scenario

As mentioned in Section 2.6.3, four alternative indicators to risk are used in SR-Site; release of activity from the geosphere, radiotoxicity flux from the geosphere, concentrations of radionuclides in ecosystems and natural geosphere fluxes of radionuclides. The following reference values are used when evaluating these indicators.

- The Finnish activity constraints. These constraints are strictly applicable only in the Finnish regulatory context, but are nevertheless deemed useful as reference values for SR-Site.
- The reference value for radiotoxicity flux from the geosphere suggested by the EU SPIN project.
- Measured concentrations of naturally occurring radionuclides in ecosystems at the Forsmark site or other, comparable sites.
- Naturally occurring fluxes of radionuclides at the site, in particular of U-238 and Ra-226.

### *Release of activity from the geosphere*

The constraints on activity release from the geosphere issued by the Finnish regulator STUK yield an index calculated as described in Section 2.6.3. Figure 13-35 shows the result of applying this activity constraint to mean releases calculated for the probabilistic central corrosion case, see the **Radionuclide transport report** for details. The releases from the geosphere are around three orders of magnitude lower than the STUK constraint.

### *Radiotoxicity flux from the geosphere*

As mentioned in Section 2.6.3, the radiotoxicity flux from the geosphere may be used as an alternative indicator for late time frames. An EU project /Becker et al. 2002/ suggests a reference value of 60 Sv/yr for a typical area of 200 km$^2$ that could tentatively be used for comparisons to calculated fluxes of radionuclides from the repository.

For the probabilistic central corrosion case, the mean activity release for each nuclide was converted to radiotoxicity flux by using ingestion dose coefficients, see further the **Radionuclide transport report**. This yielded the result shown in Figure 13-36. The peak release from the geosphere is around $10^{-2}$ Sv/yr, i.e. more than three orders of magnitude below the suggested reference value. The IRF pulses are not included in this calculation.

The relevance of the reference value can be argued. It is seen as more significant that for a totally hypothetical situation where an individual alone would ingest all repository-derived radionuclides released from the geosphere in the central corrosion case, the maximum received dose over one million years would only be around one order of magnitude above that caused by typical background radiation in Sweden. It is noted that the result is based on the probabilistic calculation of the central corrosion case, whereas a deterministic calculation not taking into account the probability of 0.12 of this case would yield about one order of magnitude higher dose.

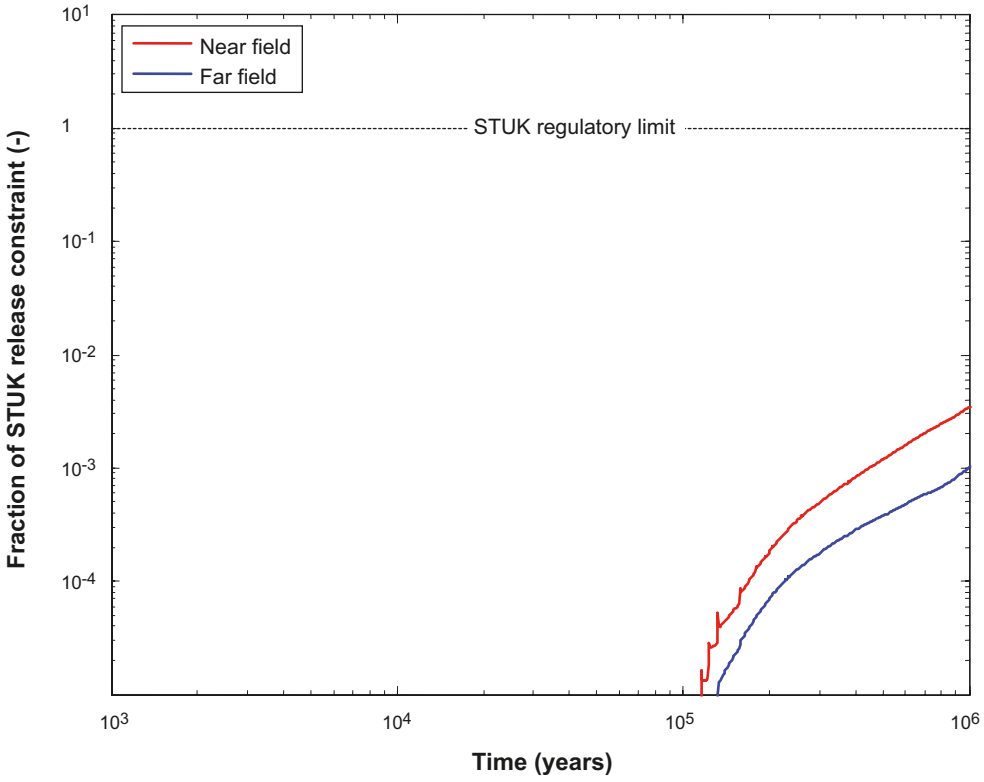


***Figure 13-35.*** *Releases as a fraction of the activity release constraint index adopted by the Finnish regulator.*

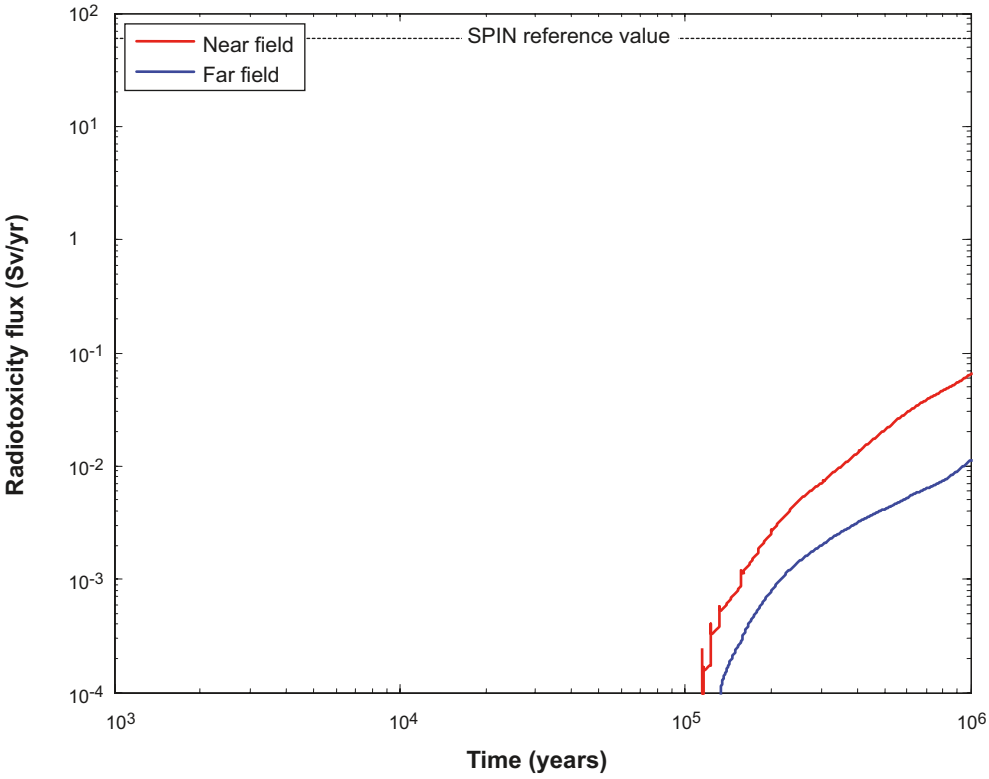


***Figure 13-36.*** *Radiotoxicity fluxes from near field and geosphere for the central corrosion case.*

### *Concentrations in ecosystems*

Another alternative indicator is the calculated concentration of radionuclides in the biosphere, which can be compared to the natural content of radionuclides in soil, sediment, groundwater and surface water. This comparison is here made for the most dose-contributing radionuclide Ra-226. In addition, the comparison has been done for all isotopes with measured activity concentrations and is further described and discussed in the **Biosphere synthesis report**.

In the biosphere assessment, maximum activity concentrations of radionuclides are calculated for different environmental media with the radionuclide transport model for the biosphere, given a constant unit release per year of each radionuclide (see Section 13.2.4). These concentration factors (i.e. concentration per Bq/yr) were here multiplied by the maximum activity release rate (Bq/yr) from the geosphere according to the mean release of the probabilistic central corrosion case, to get maximum activity concentrations in different environmental media. The maximum concentration factor and the maximum activity release rate were not coupled in time, giving a pessimistic approach.

Biosphere object 136 (Figure 13-5) was chosen as a representative object for the Forsmark site for the comparison, since the calculated activity concentrations for this object can be compared to the natural content of Ra-226 in different media (soil, sediment, groundwater, lake water and sea water) measured in the basin and in its vicinity as part of the site investigations. The calculated activity concentrations of Ra-226 in different media in this object were of similar magnitude as the highest calculated concentrations among all biosphere objects. The difference was at most 1.6 times lower in object 136 (noted for sediments). As shown in Table 13-9, the calculated activity concentrations for Ra-226 from a release are at least three orders of magnitude lower than the measured background activity concentrations for all the compared environmental media.

**Table 13-9. Calculated activity concentration for Ra-226 in different environmental media in Biosphere object 136 (Bolundsfjärden), resulting from the mean release of radionuclides given the probabilistic central corrosion case, compared with measured activity concentrations (median values) from Forsmark. For reference, measured concentrations from Laxemar and from reference sites available in the literature are presented. N represents the number of samples.**

| | Calculated activity concentration | Measured activity concentration Forsmark (N) | Measured activity concentration Laxemar (N) | Reference sites |
|---|---|---|---|---|
| **Lake water (Bq/l)** | $4.5 \cdot 10^{-7}$ | $6.0 \cdot 10^{-3}$ (4) | | $4.6 \cdot 10^{-4}$ [1)] |
| **Sea water (Bq/l)** | $3.1 \cdot 10^{-9}$ | $3.1 \cdot 10^{-3}$ (1) | | $1.1 \cdot 10^{-3}$ [1)] |
| **Near surface groundwater (Bq/l)** | $4.2 \cdot 10^{-5}$ | $7.2 \cdot 10^{-2}$ (11) | $5.9 \cdot 10^{-2}$ (10) | $4.2 \cdot 10^{-3}$ [2)] |
| **Limnic sediment (Bq/kg dw)** | $2.9 \cdot 10^{-3}$ | 36 (2) | 70 (1) | |
| **Marine sediment (Bq/kg dw)** | $3.5 \cdot 10^{-4}$ | 8.5 (1) | 8.5 (1) | |
| **Top soil (Bq/kg dw)** | $2.2 \cdot 10^{-3}$ | 39 (4) | 16 (1) | 2–1,000 [3)] |

[1)] /Aastrup 1981/
[2)] /Porcelli et al. 2001/
[3)] /UNSCEAR 2008/

### *Geosphere fluxes of radionuclides*

The naturally occurring fluxes of U-238, U-234 and Ra-226, are estimated based on i) measured activities in the groundwater during the site investigations, ii) an estimate of the surface area to which hypothetical releases from the ensemble of deposition positions in the repository would occur for present day conditions, and iii) an estimate of the fraction of the average groundwater discharge originating from repository depth. See Section 2.3 in the **Radionuclide transport report** for details. The resulting natural fluxes are $4.7 \cdot 10^5$ Bq/yr U-238, $1.2 \cdot 10^6$ Bq/yr U-234 and $7.6 \cdot 10^6$ Bq/yr Ra-226.

Figure 13-37 shows the far-field release rates of U-238, U-234 and Ra-226 for the probabilistic central corrosion case compared to the estimated naturally occurring fluxes at Forsmark. The repository derived flux of Ra-226 for the central corrosion case is about two orders of magnitude below the naturally occurring flux of Ra-226. For the U isotopes, the fluxes from the repository are about six orders of magnitude below the natural fluxes, irrespective of whether rock $K_d$-distributions for U(IV) or U(VI) are used.

It is noted that the releases from the repository could be concentrated to one or a few of the landscape objects in the release area. There are about ten objects in the area used in the derivation of the naturally occurring fluxes, suggesting that the natural fluxes would exceed those from the repository even if all the release from the repository were to occur to a single landscape object.

The naturally occurring fluxes of U-238, U-234 and Ra-226 have been converted to effective dose by using the basic LDF values. The result is shown together with the far-field annual effective dose in the central corrosion case in Figure 13-38. The result is similar to that in Figure 13-37 since the dose is dominated by Ra-226 in the central corrosion case.

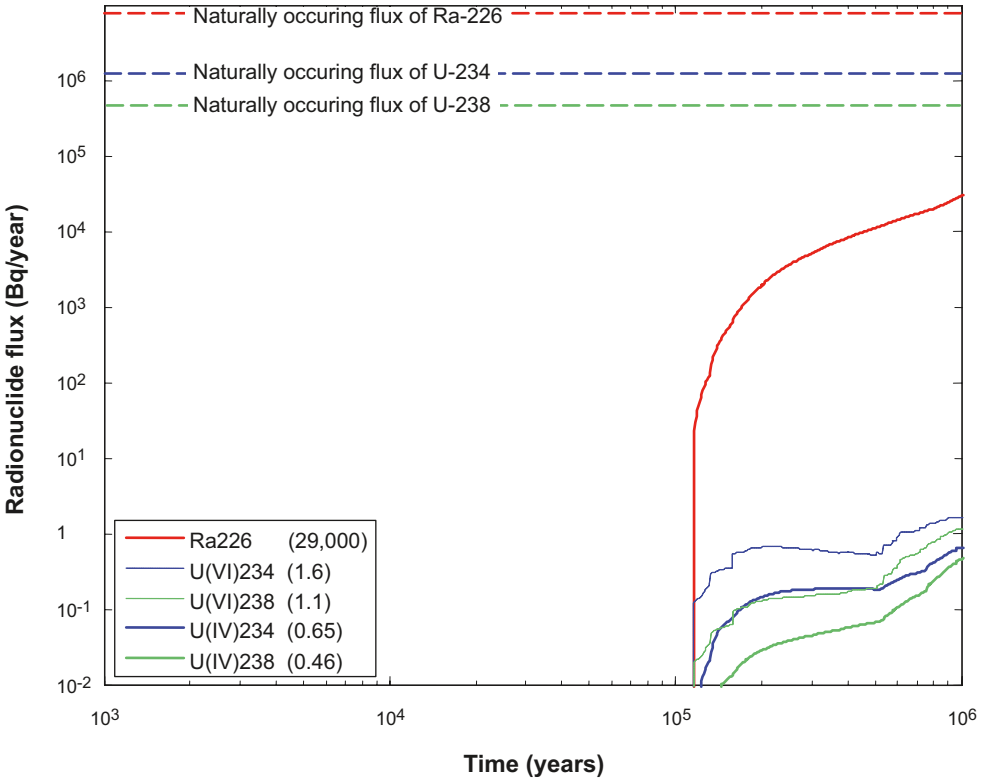


***Figure 13-37.*** *Far-field release rates (Bq/year) of U-238, U-234 and Ra-226 in the central corrosion case compared to the naturally occurring fluxes at Forsmark.*

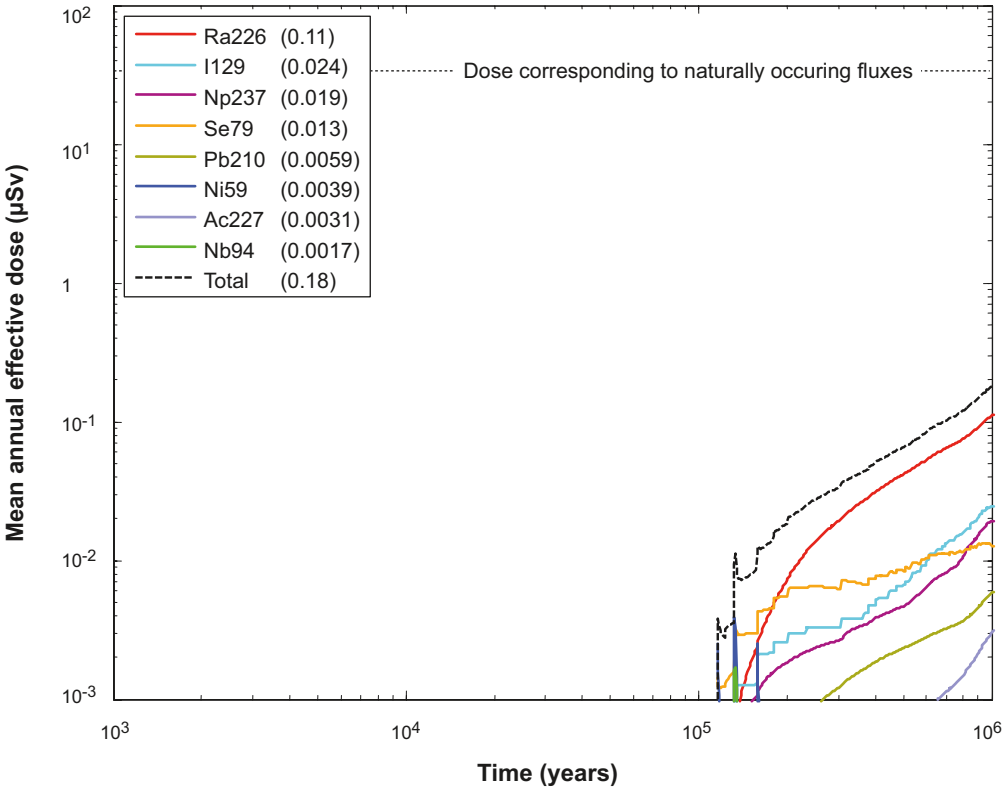


***Figure 13-38.*** *Far-field mean annual effective dose in the central corrosion case compared to the annual effective dose coming from naturally occurring fluxes of U-238, U-234 and Ra-226 at Forsmark converted to annual effective dose using the basic LDF values.*

### *Conclusions*

Four alternative indicators to risk are used in SR-Site, yielding the following results for the central corrosion case:

- Peak releases of activity from the geosphere are about three orders magnitude below the activity constraints issued by the Finnish regulator STUK.
- The peak radiotoxicity flux from the geosphere is more than three orders of magnitude lower than the reference value for the radiotoxicity flux from the geosphere suggested by the EU SPIN project.
- Calculated radionuclide peak concentrations in ecosystems at Forsmark from repository releases of Ra-226 are about three orders of magnitude below measured concentrations of naturally occurring Ra-226 at Forsmark.
- Peak geosphere fluxes caused by Ra-226 releases from the repository are about two orders of magnitude below naturally occurring fluxes of Ra-226 at the site, as estimated from site data; the difference is larger for U-234 and U-238. The total release of all repository derived nuclides converted to dose is also around two orders of magnitude lower than the summed dose from releases of the three mentioned naturally occurring nuclides.

The results are readily applicable to other corrosion cases, for most indicators by simply scaling with the release of Ra-226, which is at most one order of magnitude higher than that for the central corrosion case.

## 13.5.9 Summary of results of calculation cases for the corrosion scenario

Figures 13-39 (near field) and 13-40 (far field) summarise the probabilistic calculations done for the corrosion scenario with COMP23/FARF31. Peak mean annual doses vary roughly within an order of magnitude between the cases.

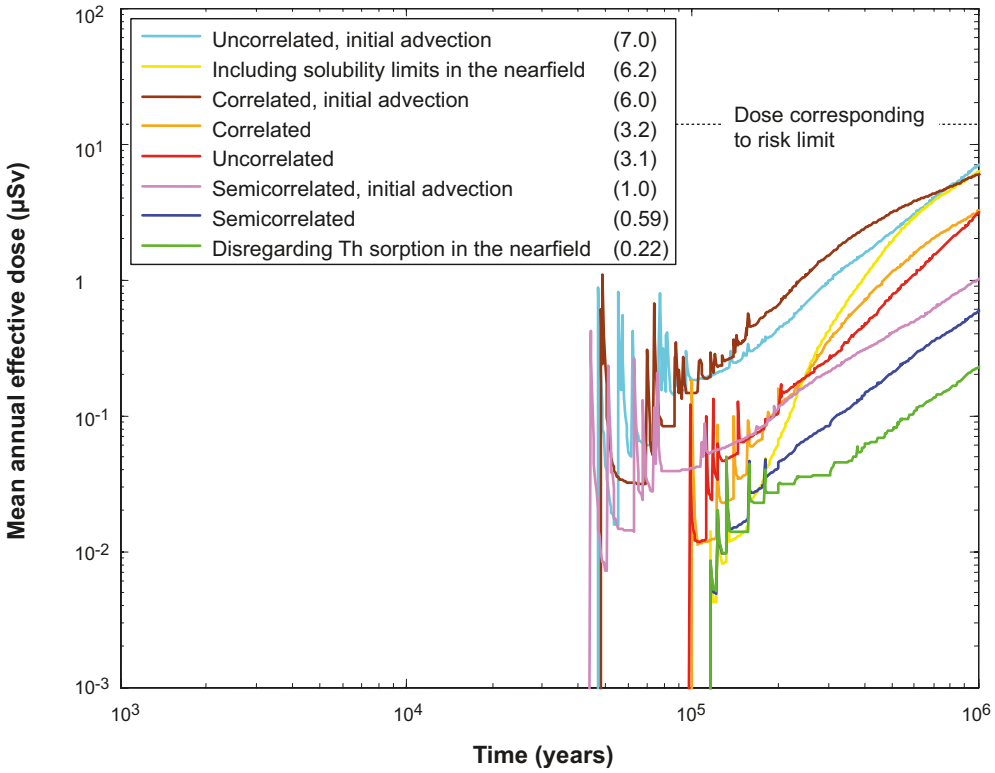


***Figure 13-39.*** *Summary of near-field mean annual effective dose equivalent release for all probabilistic calculations performed with COMP23 for the corrosion scenario.*

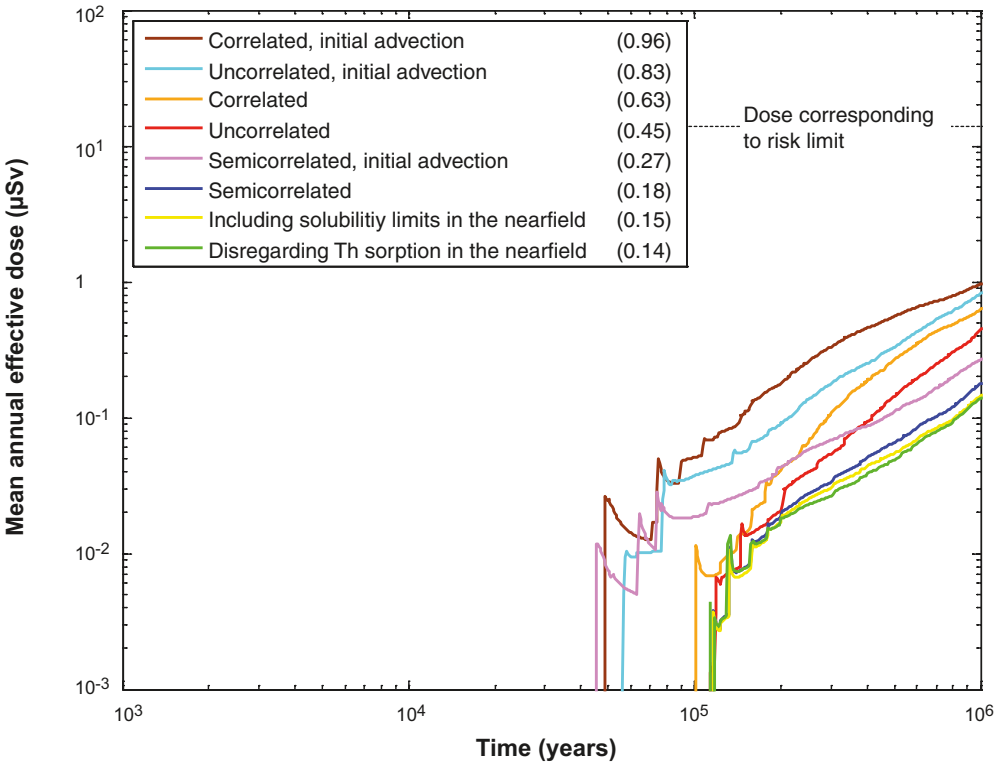


***Figure 13-40.*** *Summary of far-field mean annual effective dose for all probabilistic calculations performed with COMP23/FARF31 for the corrosion scenario. The peak doses are given in parentheses in μSv.*

### 13.5.10 Calculations with the analytical models

As mentioned in Section 13.4.4, simplified, analytical models are available for the modelling of radionuclide transport in the near field and the far field.

The analytical models have been applied to the six corrosion variants of the corrosion scenario.

Regarding the application of the models to the corrosion scenario, the following, further simplifying, conditions are noted. The near-field release is determined by the rate of radionuclide release to water in the void space because the flow rate in the Q1 fracture is not a limitation (canister failures due to corrosion only occur in the deposition holes with the highest flow rates). Therefore, the release rate from the near field is simply modelled as the dissolution rate of the fuel, alternatively the corrosion rate of the metal parts, in both cases multiplied by the inventory. As in the numerical models, the IRF is not included but handled separately.

The release rate from the far field is in most cases calculated as the release rate from the near field times a geosphere transmission factor /Hedin 2002b/. This yields a good approximation in cases of a continuous release over long times.

However, in some cases of relatively short duration, releases caused by corrosion of the metal parts of the fuel, the treatment is overly pessimistic. In such cases the release of the entire inventory in the metal parts, $M_0$, as a pulse to the geosphere is also considered. This yields a peak release rate from the geosphere of $M_0/\tau$ where $\tau$ is obtained from /SKB 2006a, Appendix B/. Hydrodynamic and molecular dispersion in the flowing fracture are pessimistically neglected when this expression is used. Also, radioactive decay is neglected in the expression since no appreciable decay will take place during the short transients of concern here.

Since both the above approaches overestimate the release rate from the far field, the smaller of the two is chosen in each realisation.

It is also noted that chain decay in the geosphere is not accounted for when applying the transmission factors for geosphere retention. The theory for a full, analytical treatment of chain decay in transmission factors has been developed, but is not yet implemented in the analytical model. Using the numerical models, it has been demonstrated that chain decay of parent nuclides of Ra-226 in the far field has a negligible impact on the releases of Ra-226 in the corrosion scenario.

The result of the analytical modelling of the probabilistic central corrosion case is shown in Figure 13-41. As seen by comparing the results in Figure 13-41 with those of the corresponding numerical case in Figure 13-18, the agreement of the peak doses is very good for nuclides emerging from the fuel matrix, whereas doses from nuclides embedded in metal parts (Ni-59 and Nb-94) are somewhat overestimated with the analytical model. This is due to the pessimistic modelling of nuclide release from corrosion of metal parts discussed above.

The modelling results of the six corrosion variants are shown in Figure 13-42. Each case was modelled with 20,000 realisations using Latin Hypercube Sampling. As seen by comparing the results in Figure 13-42 with those in Figure 13-40, which shows far-field annual effective dose for all corrosion cases calculated with FARF31, the agreement between results obtained with the two sets of models is good. All peak doses over one million years are the same to within less than ten percent.

The fact that the numerical calculations are in good agreement with the analytical calculations enhances confidence in the dose equivalent releases provided here and in the **Radionuclide transport report** for two reasons. First, the comparison provides a quality assurance check on the numerical modelling of dose equivalent releases. This check applies not only to the numerical calculations but also to the data/parameter transfers, as the data for the analytical calculations were taken directly from the **Data report** independently of the numerical calculations. Second, it demonstrates that dose equivalent releases for the corrosion cases are controlled by relatively simple processes that are straightforward to understand and model.

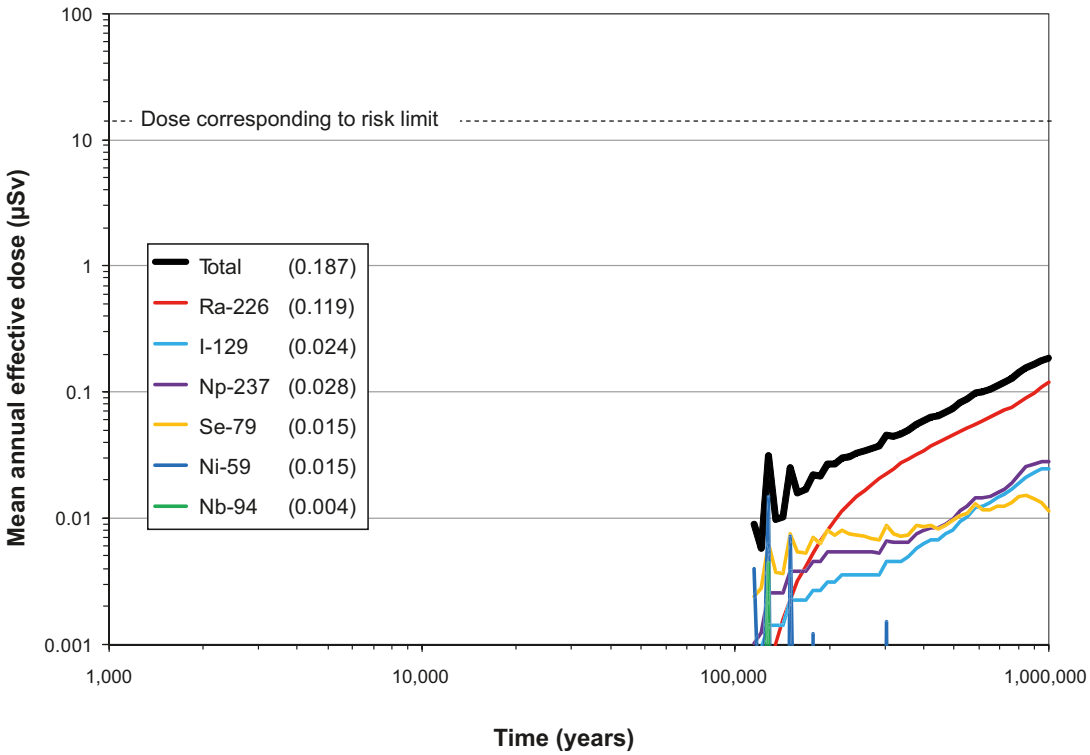


***Figure 13-41.*** *Far-field mean annual effective dose for the central corrosion case, obtained with analytical models. The legends are sorted according to descending peak mean annual effective dose over one million years (given in brackets in µSv).*

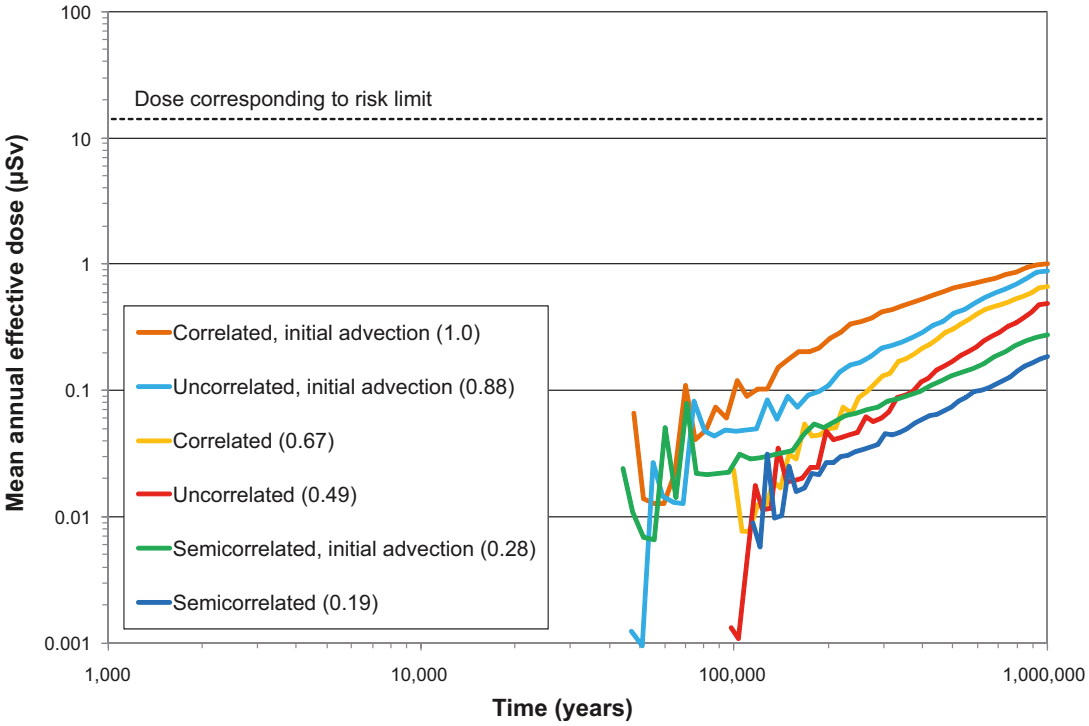


***Figure 13-42.*** *Summary of far-field mean annual effective dose for analytical, probabilistic calculations of the six corrosion variants of the corrosion scenario. The peak doses are given in parentheses in μSv. These results can be compared to the corresponding results obtained with numerical models in Figure 13-40.*

## 13.5.11 Sensitivity analyses

### *Introduction*

This section presents results of sensitivity analyses of the results of the dose calculations, i.e. the sensitivity of the uncertainty in calculated dose to uncertainties in the input parameters is analysed. All analyses concern the probabilistic calculation of the central corrosion case, Section 13.5.4.

It is of interest to determine i) the variables that correlate with the dose over the entire dose range and ii) the parameter values that are related to high and low doses. Ra-226 dominates the dose in most of the realisations in the central corrosion case and it is thus of particular interest to clarify sensitivities of the Ra-226 dose to input parameters.

### *Global sensitivity analysis*

The first purpose is thus to perform a so called global sensitivity analysis, i.e. to identify the input parameters that have the greatest influence on the spread of the results. The contribution to output spread depends on both the spread of the input parameter and the model's sensitivity to variations in that particular input parameter. A range of methods for this type of sensitivity analysis exists /Saltelli et al. 2000/. Several studies and reviews have demonstrated that standardised rank regression is a suitable method for sensitivity analysis of non-linear systems where the calculation end point is a monotonic function of the input variables /Saltelli et al. 1993, Helton 1993, Hamby 1994, Iman and Conover 1979/. This applies to the present non-linear and monotonic system /Hedin 2003/, and the standardised rank regression coefficient (SRRC) is, therefore, used for identifying the most important variables contributing to dose uncertainty.

A standardised rank regression analysis of the total dose at $10^6$ years on the input variables yields, in descending order, the fuel dissolution rate $D_{Fuel}$, the transport resistance along the geosphere flow path, $F$, and the failure time $t_{Failure}$ as the input parameters most affecting dose results, see Figure 13-43. Regressing on Ra-226 dose at $10^6$ years yields a similar result due to the dominance of Ra-226. The ranking of the two most important variables is switched in this case and this is consistent with the fact that the fuel dissolution rate, $D_{Fuel}$, affects all nuclides whereas the $F$ parameter only affects sorbing nuclides and is hence relatively more important for the Ra-226 dose, than for the total dose which is in some of the realisations dominated by the non-sorbing I-129. It is also noted that the three variables $F$, $t_w$ and $t_{Failure}$ are correlated, meaning that their significance is not necessarily as high as indicated by the SRRC method. This was further investigated with a tailored regression model, as described below. Standardised rank regression analysis on maximum total dose over time yields an almost identical result as regressing on total dose at one million years (not shown in the figure). However, regressing on e.g. peak Ni-59 equivalent dose from the near field (not shown in the figure) identifies also the corrosion release rate, $CRR$, as a sensitive input variable. This is consistent with the fact that in some realisations of the central corrosion case, the peak dose of Ni-59 occurs shortly after canister failure and is then caused by the releases congruent with the corrosion of the metal parts of the fuel assemblies.

### *Main risk contributors*

The standardised rank regression analysis identifies the variables that co-vary with the dependent variable, the total dose, over the entire dose range. To determine the variables that are related to the highest doses, a conditional mean value analysis /Hedin 2002a/ was carried out. Here, the subsets of input parameter values related to the top percentile of the dose are selected. For each such subset, the mean value of the logarithmically transformed data was determined for each parameter and compared to the corresponding mean value of the entire input distribution. A dimensionless, normalised measure, α99, is obtained by dividing the difference between the two mean values by the standard deviation of the entire distribution.

The so determined conditional mean value identifies variables that take on significantly different values in the top percentile realisations than in the entire dose distribution. In descending order, the $t_{Failure}$, $D_{Fuel}$, $F$ and $t_w$ parameters were identified as most significant, see Figure 13-44. Similarly, α1-values, relating to the lowest percentile of the dose distribution were determined. Also α99 − α1 values were determined to distinguish extreme outcomes from others. The highest ranking variables were here, in descending order, $D_{Fuel}$, $F$, $t_w$, which is strongly correlated to $F$, and $t_{Failure}$.

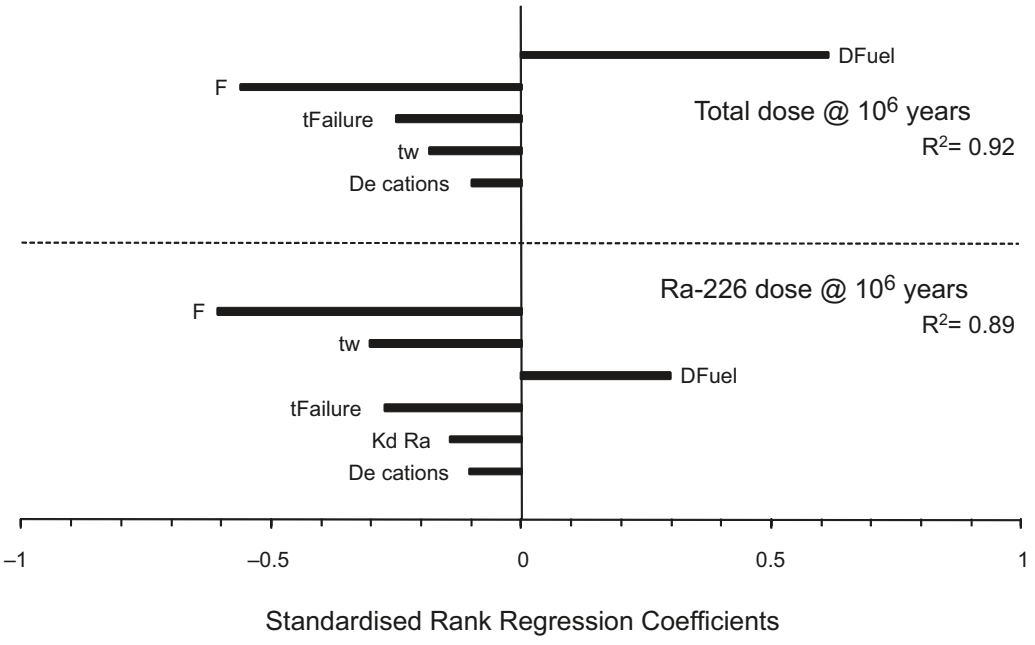


***Figure 13-43.*** *Results of standardised rank regression. Regressing on total dose at $10^6$ years and on Ra-226 dose at $10^6$ years yields similar results due to the dominance of Ra-226.*

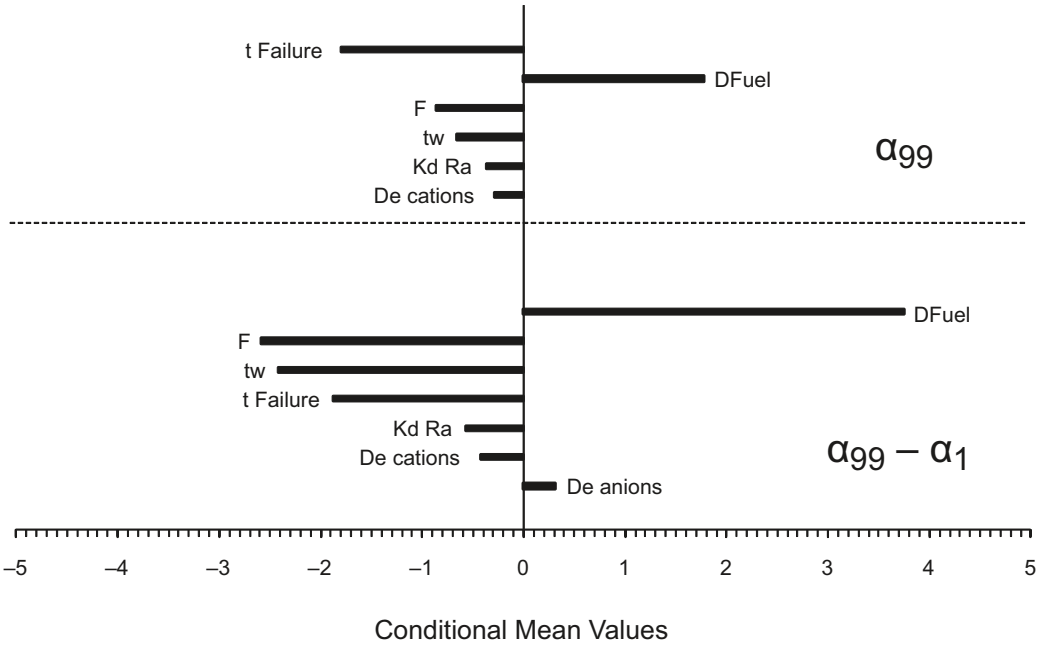


***Figure 13-44.*** *Conditional mean values.*

### *Tailored regression model*

The understanding and mathematical formulation of the transport models used in the dose calculations can be utilised to further explain the results. The release rate of Ra-226 is determined by the amount of its parent nuclide, Th-230, liberated from the fuel matrix and subsequently assumed to sorb in the near field. This amount is proportional to the product of the fuel dissolution rate, $D_{Fuel}$, and the time, $t$, elapsed between the canister failure and the point in time for which the dose is calculated, i.e. it is proportional to $D_{Fuel} \cdot t$. In the studied case $t = 10^6 - t_{Failure}$. It can further be shown that the released Ra-226 is transported through the geosphere with a certain transmission efficiency, $\theta$, that in its full expression depends in a complex way on all the uncertain parameters relating to geosphere transport, see e.g. /Hedin 2002b/. However, it can also be demonstrated that most of the variability of $\theta$ is captured by the simpler expression /Hedin 2003/:

$$\theta \propto \exp\left(-cF^{0.5}\,(K_d D_e)^{0.25}\right)$$

where $c$ is a positive constant determined by well known properties like the density of the rock and the half-life of Ra-226. This suggests that the Ra-226 dose varies according to

$$\log(DoseRa226) = Constant + \log(D_{Fuel}t) - cF^{0.5}\,(K_d D_e)^{0.25}$$

and that a tailored regression model according to the above expression could be successful in explaining the calculated results. Figure 13-45 shows how such a regression model is able to predict the calculated results when successively more terms are included in the model. As seen in the figure, the agreement when all terms are included is good, with an $R^2$-value of 0.99.

These expressions also reveal combinations of input variables of importance. Obviously, combinations of high $D_{Fuel}$ and $t$ values and combinations of low values of the three factors occurring in the exponent of the first expression favour high doses. This result also illustrates that the variable $t_w$, identified as important for the Ra-226 dose by the SRRC method above is not needed to explain the Ra-226 dose. It is concluded that $t_w$ is identified in the SRRC method only since it is correlated to the $F$ parameter. (This can be further analysed through use of partial rank correlations in the SRRC method.)

A partition plot, Figure 13-46, showing how high and low dose results relate to the variable groups $D{\cdot}t$ and $F^{0.5}(K_d{\cdot}D_e)^{0.25}$ confirms the explanatory power of these variable groups.

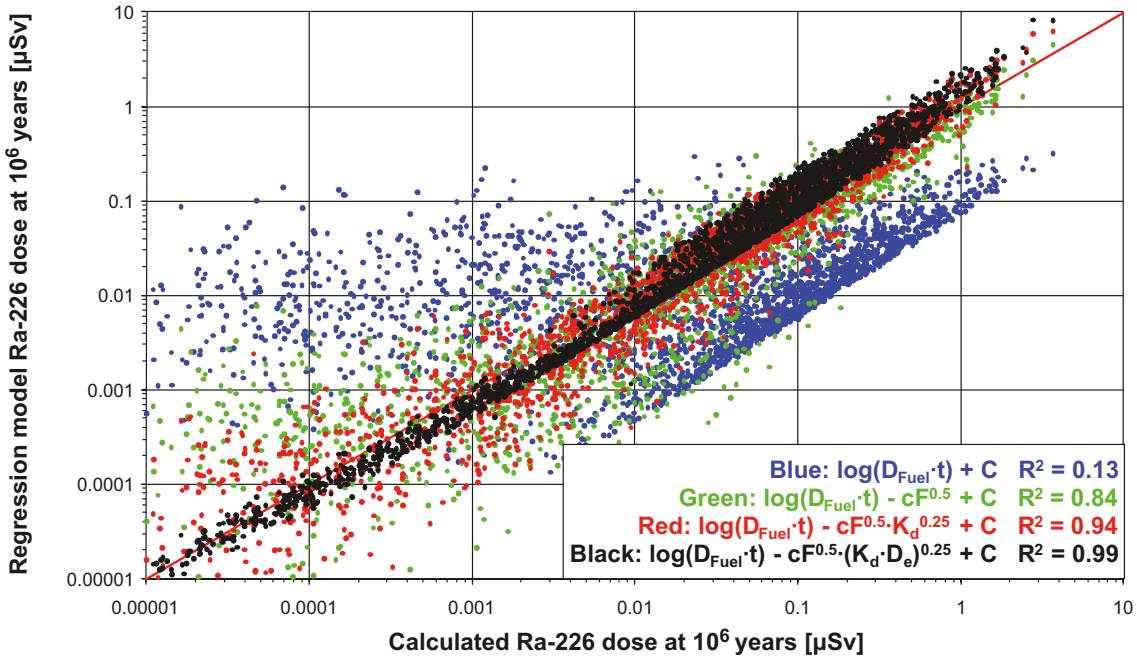


***Figure 13-45.*** *Four tailored regression models, including successively more variables, for the Ra-226 dose at one million years.*

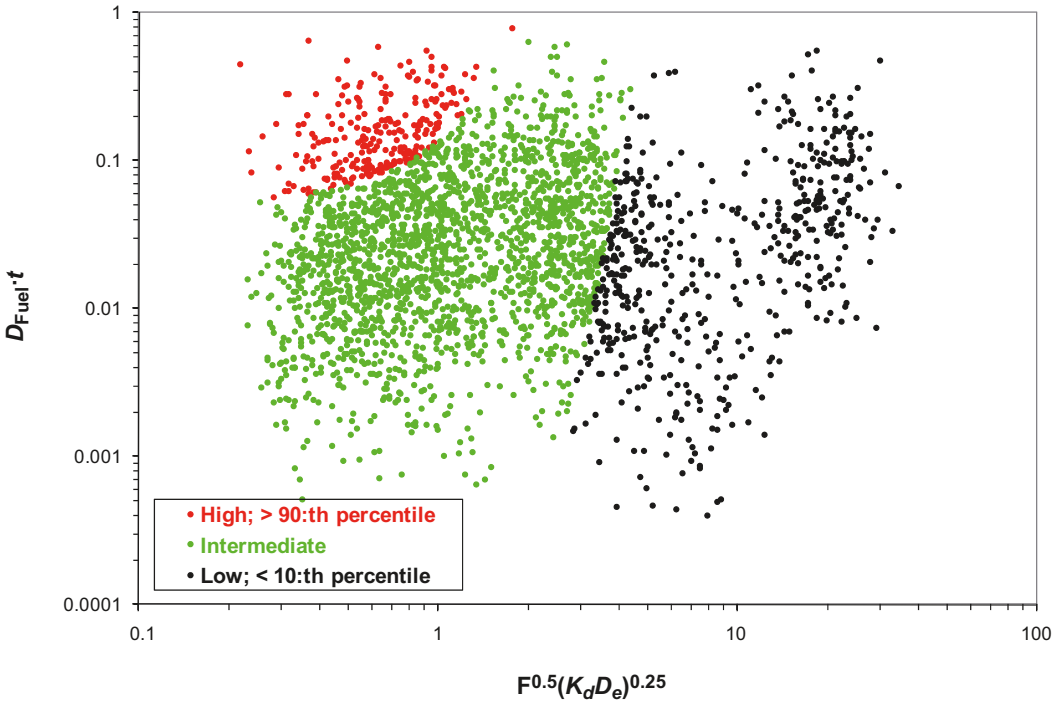


***Figure 13-46.*** *Partition plot demonstrating how the two groups of variables on the axes relate to high and low dose results for Ra-226.*

### *Conclusions*

The above analyses show that it is possible to identify the uncertain input parameters to which the probabilistic result is most sensitive with relatively simple methods. This is in part due to the nature of the conceptualisation of the calculation cases in the corrosion scenario, where the buffer is omitted and the near-field release is essentially controlled only by the fuel dissolution rate.

The fuel dissolution rate, $D_{Fuel}$, and the geosphere transport resistance factor, $F$, emerge generally as the uncertain input parameters to which the result is most sensitive. The uncertainty in corrosion release rate, $CRR$, has a significant impact on the result of near-field releases immediately after failure for nuclides that are released congruently with metal corrosion.

It is also noted that a number of different assumptions regarding transport conditions were analysed in Section 13.5.6, where it was found that the sensitivity to these assumptions is low, see Figures 13-39 and 13-40. Similar results are expected for all corrosion variants since they differ from the central corrosion case only through somewhat altered input distributions for the failure times and the hydrogeological transport parameters.

Finally, it is noted that, in the corrosion scenario, the canister failure times and positions are determined by the distribution of advective flow at the deposition holes and of the distribution of sulphide concentrations. As concluded in Section 12.6.2, it is only combinations of the highest flows with the highest concentrations that have the potential of yielding canister failures.

## 13.6 Canister failure due to shear load

### 13.6.1 Conceptualisation of transport conditions

Canister failure due to rock shear was demonstrated to have a low probability in the reference evolution. The only identified cause for this failure mode is the event of large earthquakes in the vicinity of the repository, see further Section 10.4.5.

Pessimistic estimates of the extent of this failure mode in Section 10.4.5 indicate that the probability that one out of the 6,000 canisters has failed at the end of the one million year assessment period is 0.079. A failure frequency as a function of time is also provided in Section 10.4.5, Figure 10-124, and this is used in the probabilistic assessment of the canister failure due to shear load scenario, briefly called the shear load scenario in the following.

A calculation case is formulated, based partially on the analyses carried out in Section 10.4.5. The following data and assumptions are used.

- In the affected deposition holes the faulting is supposed to be so large that it causes massive failure of the canister. A delay time of 100 years between failure and the onset of radionuclide transport is assumed, based on a pessimistic estimate of the time required to fill the canister with water, see further the **Data report**. Thereafter, no credit is taken from limited transport resistance in the canister.
- The shear movement will not affect the buffer to the extent that its protection against advective flow will be impaired, but the effective amount of buffer between the canister and the shearing fracture is assumed to be reduced from 35 to 25 cm. In Section 10.4.5, canister failures are pessimistically assumed to occur for shear movements exceeding 5 cm in fractures intersecting deposition holes. The reduction in buffer thickness by 10 cm is selected in relation to this criterion.
- The canister failure location is assumed to fully coincide with the location of the shearing fracture. Furthermore, the shear is assumed to increase the fracture transmissivity significantly. The $Q_{eq}$ value for the intersecting fracture is, therefore, assumed to be sufficiently high (1 $m^3$/yr) that it does not contribute to the transport resistance in the near field. Nor are any transport resistances related to the geometric constraint of the fracture intersection with the buffer assumed, meaning that the flux through the buffer is that obtained with a zero concentration of radionuclides on the buffer exterior.
- The shearing fracture is likely to be among the larger in the modelled fracture network and its properties after shearing are difficult to assess. Therefore, no credit for radionuclide retention in the geosphere is taken.
- Solubility limits are imposed since, contrary to case in the corrosion scenario, the buffer is in place in the shear load scenario.

All other data and assumptions are handled probabilistically, with data from the **Data report**. This concerns the radionuclide inventory, the fuel dissolution rate, the metal corrosion rate and buffer sorption and diffusion data.

### 13.6.2 Consequence calculations

#### *Postulated failure at 100,000 years*

Figure 13-47 shows the result of a calculation where the failure of one canister at 100,000 years is postulated. As for the corrosion scenario, the contributions from the instantaneously released fraction of nuclides, IRF, are not included here. Note that the near-field dose equivalent release and the far-field dose are the same since no retention in the far field is assumed. The total dose is dominated by Ra-226, which is efficiently transferred through the buffer. The solubility of Ra-226 has a very limited impact on the result. The slight decrease of Ra-226 dose at the end of the calculation period is due to the decrease in inventory of U-234 in the fuel matrix.

#### *Distribution of failures between 1,000 and 1,000,000 years*

Figure 13-48 shows a probabilistic evaluation of rock shear failures for the period between 1,000 and one million years and using the frequency of canister failures due to shear load from the reference evolution cited above. The doses are dominated by releases of Ra-226 after about 100,000 years. Before that, releases of Nb-94 and C-14 dominate. It is seen that the peak dose of 0.15 µSv, occurring at one million years is about two orders of magnitude below the dose corresponding to the regulatory risk limit, 14 µSv.

Due to the assumed high equivalent flow rate in the Q1 buffer/rock interface, the outward transport capacity from the near field is in general sufficiently high to carry away all radionuclides released from the fuel, thus rendering solubility limits in the near field ineffective. As an illustration, a probabilistic case where no credit was taken for co-precipitation of Ra/Ba was calculated, i.e. where the solubility of Ra was increased by a factor of 1,000. This led to an increase of the release rate of Ra by only a factor of about 1.5, see further the **Radionuclide transport report**.

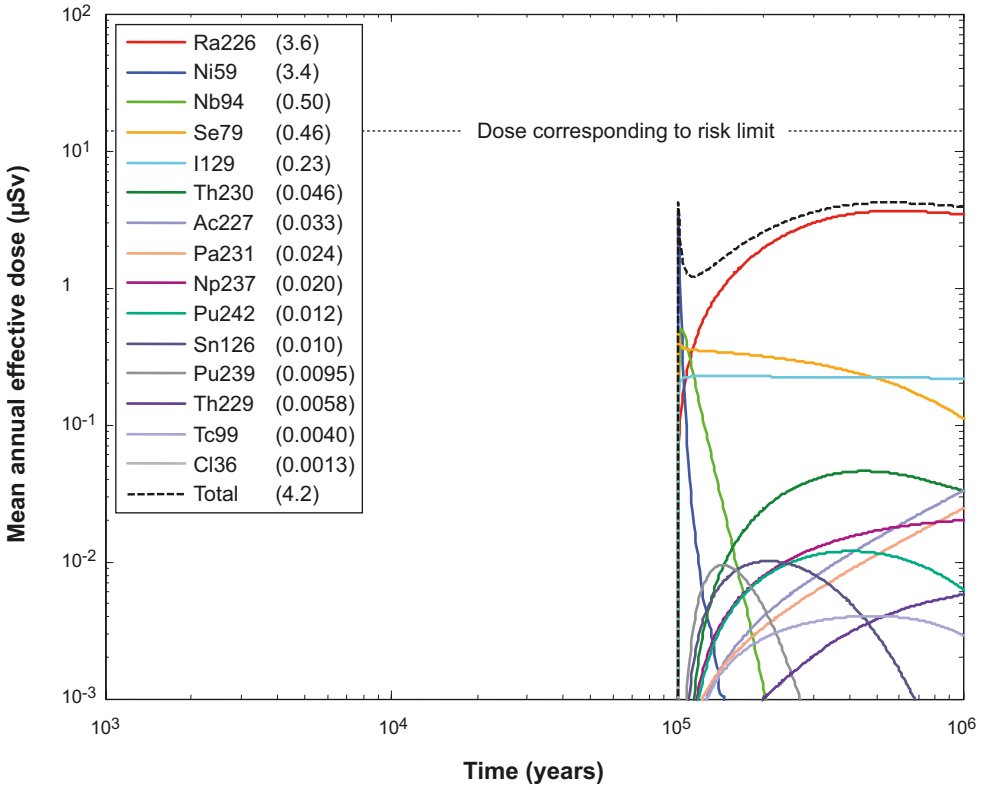


*Figure 13-47. Far-field annual effective dose for a probabilistic calculation postulating failure of one canister due to rock shear at 100,000 years.*

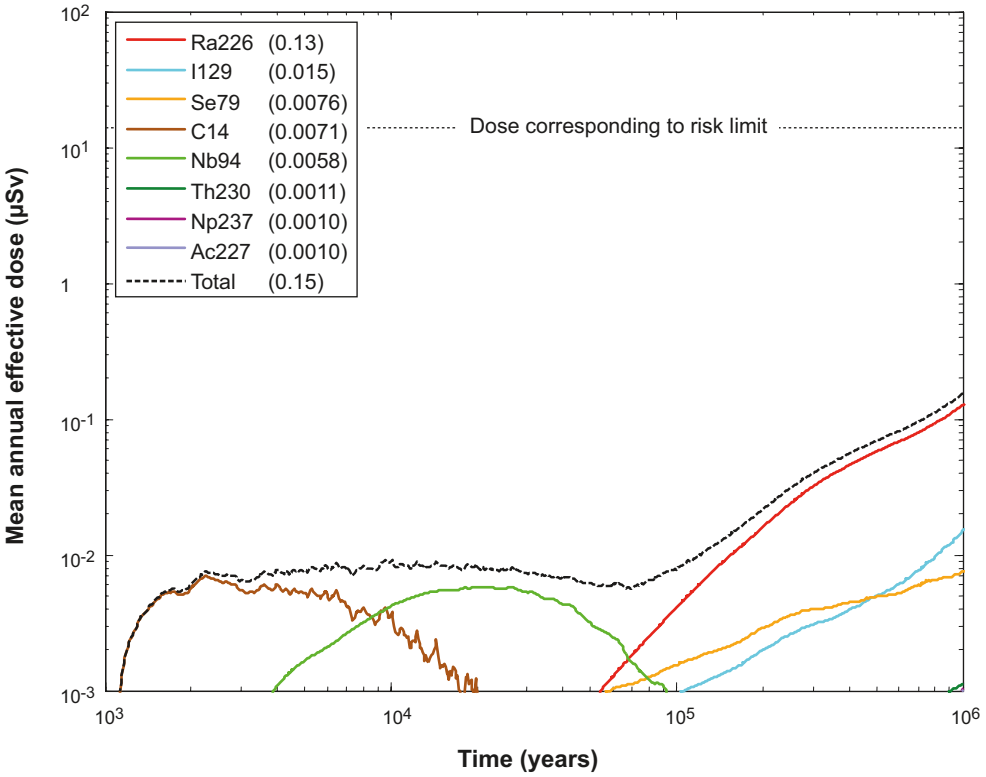


***Figure 13-48.*** *Probabilistically calculated consequences of shear failure, for the period between 1,000 years and one million years. The legends are sorted according to descending peak mean annual effective dose over one million years (given in brackets in µSv).*

### *Distribution of failures up to 1,000 years*

For times up to 1,000 years after closure, the frequency of earthquakes is assessed to be lower, with a probability that one out of the 6,000 canisters has failed at the end of the initial 1,000 year period being $2.4 \cdot 10^{-5}$, see further Section 10.4.5. Also, the use of LDF values overestimates the doses in this time perspective since i) the LDF is a pessimistic upper bound for releases occurring continuously over an entire interglacial period taking into account accumulation, whereas a large part of the interglacial period has elapsed without any releases when the repository is sealed and ii) it is not meaningful to use the LDF concept for a radionuclide that decays to insignificance over an interglacial period, since the concept is based on a continuous uniform release over the period.

A more detailed calculation of the shear load failure case for the initial 1,000 years was therefore done. In this calculation, releases from the near field were determined as for all other cases, and also the IRFs were included. Since no credit is taken for geosphere retention in the shear scenario, the near-field releases were used as direct input to the biosphere modelling. Since it is not possible to determine a location of the releases among the identified potential landscape objects, the mean release over all realisations as a function of time was fed to each object and the time dependent development of radionuclide transport and dose in the landscape was calculated for each object. The object giving the highest dose was then determined for each point in time and for each radionuclide. This entity is pessimistically defined as the calculated dose consequence for the case of a shear failure during the initial 1,000 years. A well was included in each landscape object in the same way as for the LDF calculations. The modelling of failures and of consequences in terms of releases and doses was continued to 10,000 years to facilitate comparisons with the LDF results for the one million year time frame presented above.

The peak dose is almost four orders of magnitude lower than that corresponding to the regulatory risk limit, see Figure 13-49. Releases of Sr-90, Cs-137 and C-14 dominate the initial 1,000 years. (Note the extended dose scale, required as the most of the dose curves lie below the scale used for other figures). The curve shape of C-14 is due to the release dynamics and to the temporal development of the landscape, in particular the transitions from sea to lake occurring at different times for different biosphere objects. The modelling of the dose consequences in the two time frames are compared in Figure 13-50.

As for the corrosion scenario, the calculated consequences of the shear load scenario represent a contribution to the calculated risks associated with releases from the repository. This is further addressed in Section 13.9.

### *Risk dilution*

Risk dilution for the shear load scenario needs to be considered, since canisters fail at probabilistically determined times.

An illustration is obtained by comparing the results in Figure 13-47 (postulated, deterministic failure time) with those in Figure 13-48 (distribution of failure times). If the result in Figure 13-47 is multiplied by the overall probability of the event occurring during the assessment period, i.e. 0.079, then the dose at one million years (0.28 μSv) is close to that obtained at one million years in Figure 13-48 (0.15 μSv).

This is because the consequences are determined i) by in-growth of Ra-226 and ii) by the build-up of Th-230 released from the fuel and precipitated in the canister interior or sorbed in the buffer, and thus in general occur long after the failure time. The in-growth of Ra-226 is essentially controlled by the build-up of its parent nuclide Th-230, that occurs over a time scale comparable to the half-life of Th-230 which is approximately 75,000 years. The build-up of Th-230 occurs over times determined by the fuel dissolution rate which are of the order of one million years.

Risk dilution, including a treatment of the pulse releases, is further discussed in Section 13.9.4.

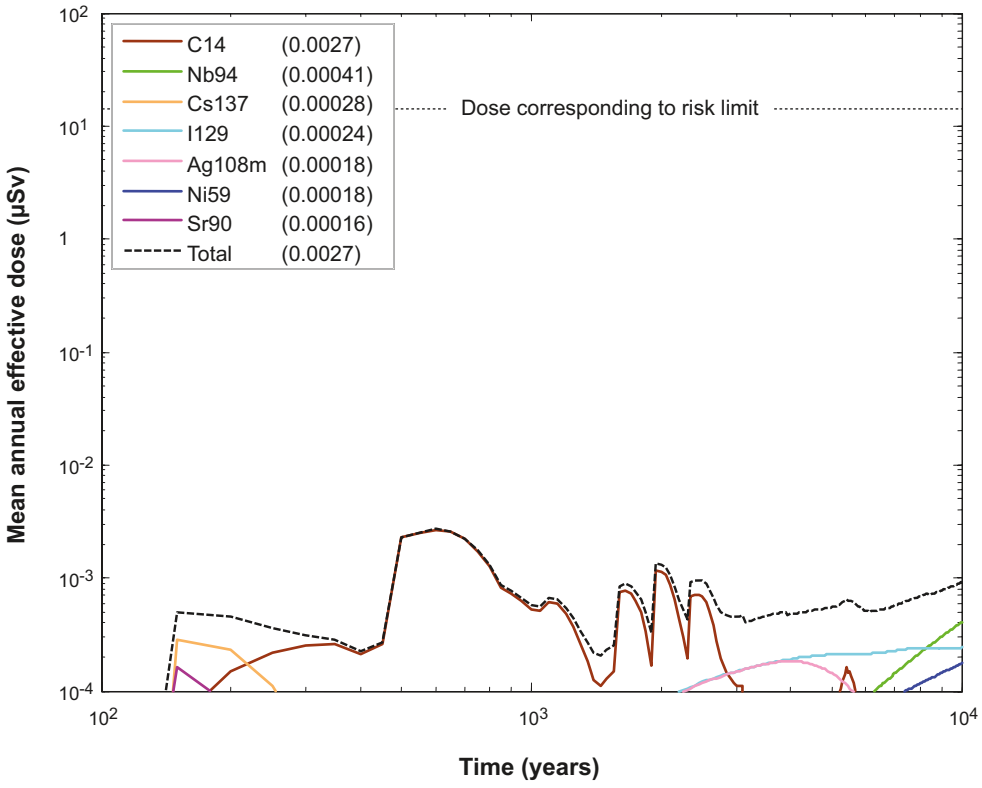


***Figure 13-49.*** *Probabilistically calculated consequences of shear failure, occurring for the period up to 10,000 years.*

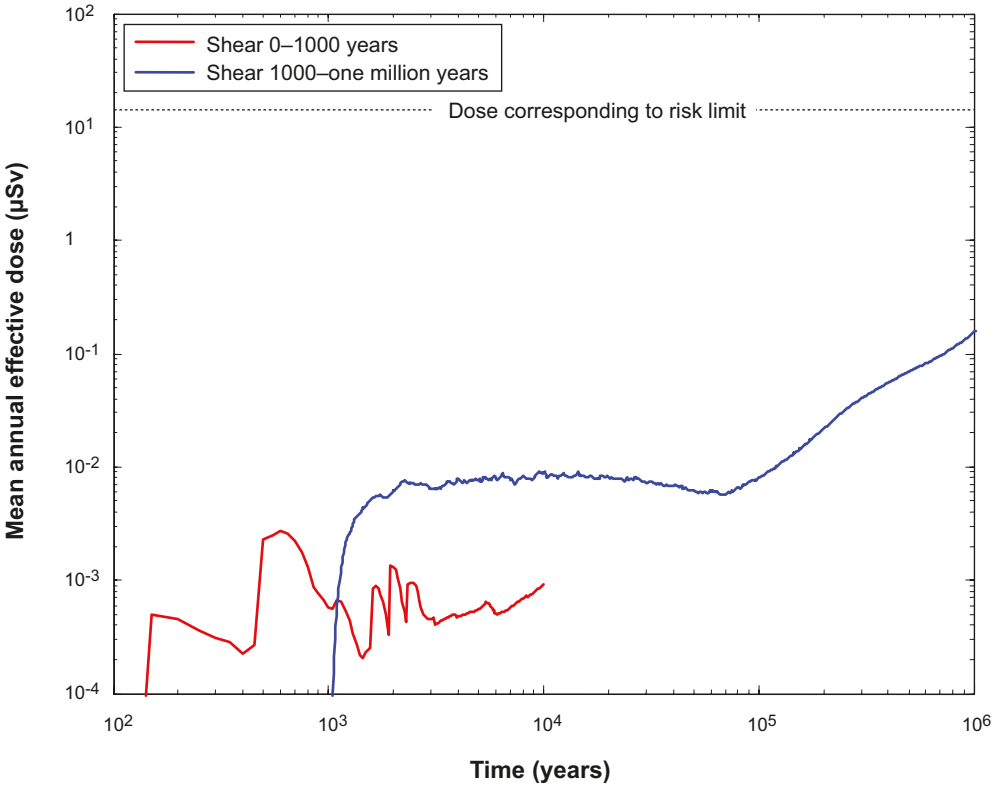


***Figure 13-50.*** *A comparison of mean annual effective doses for early shear load failures modelled transiently in the biosphere and failures in the $10^3$–$10^6$ year time frame modelled using LDF values.*

### *Global sensitivity analysis*

A global sensitivity analysis on the results of the probabilistic shear load case using the SRRC method as for the central corrosion case yields results according to Figure 13-51.

Regressing the total dose at $10^6$ years on the input variables yields, in descending order, the fuel dissolution rate $D_{Fuel}$, the solubilities of Radium and Thorium, and the failure time $t_{Failure}$ as the input parameters most affecting dose results. Regressing on Ra-226 dose at $10^6$ years yields a similar result due to the dominance of Ra-226. The significance of the solubility of Thorium is due to decay of Th-230 to Ra-226 in the buffer, where the release of Th-230 to the buffer is controlled by the solubility of Th. A further scrutiny of individual realisations reveals that the significance of the limited solubility overall is due to a relatively limited number of realisations with low solubilities, whereas the total dose is dominated by the larger number of realisations where the solubilities are sufficiently high not to limit the release. Solubilities of neither Th nor Ra, where co-precipitation with Ba is taken into account do therefore significantly limit the mean release rate of Ra-226. This conclusion is corroborated by the fact that the case with the omitted buffer, where neither sorption in the buffer nor solubility limits are included, see Section 13.6.3 yields increases in Ra-226 mean dose by only a factor of 2.

Regressing instead on the maximum of total dose over time yields the failure time and the corrosion release rate, *CRR*, as significant variables. This is consistent with the fact that, for early failures, the highest doses occur due to release of e.g. Ni-59 and Nb-94 congruently with the corrosion of structural parts of the fuel elements.

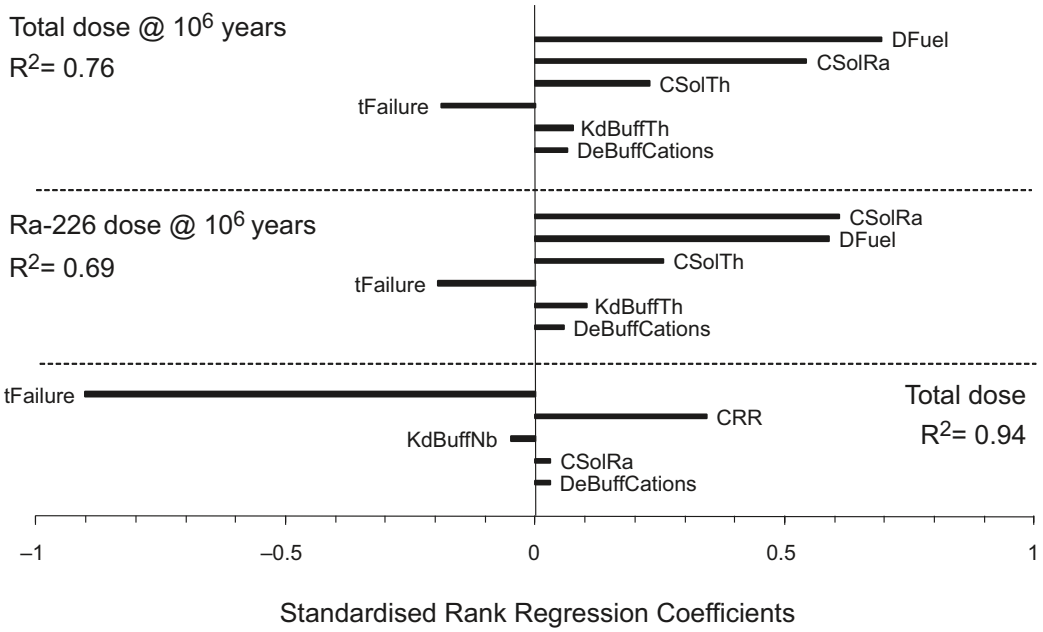


***Figure 13-51.*** *Results of standardised rank regression. Regressing on total dose at $10^6$ years and on Ra-226 dose at $10^6$ years yields similar results due to the dominance of Ra-226. Regression on the maximum of total dose over time identifies CRR as an additional sensitive input parameter.*

### 13.6.3 Combination of the shear load and the buffer advection scenarios

As noted in the discussion of buffer erosion in combination with shear movement in Section 12.9.3, the consequences of a shear failure followed by buffer erosion need to be considered, since it is reasonable to assume that the groundwater flow in a fracture that has undergone a major secondary shear movement could be high. Buffer erosion could then ultimately lead to loss of the buffer and its retardation function in the deposition hole with the canister failed due to shearing. A similar situation could arise if the buffer material is transformed through interaction with iron ions from the failed canister, as discussed in the buffer transformation scenario in Section 12.4.

The case with shear failures distributed between 1,000 and one million years was therefore calculated also for near-field conditions with a missing buffer. The conceptualisation of the near field is thus the same as in the corrosion scenario, but near-field flow data are stylised and geosphere retention is disregarded as in other consequence calculations for the shear load scenario. The results are shown in Figure 13-52.

The result is similar to that where the buffer is present in Figure 13-48, in particular beyond 100,000 years. The peak annual effective dose from Ra-226 increases by about a factor of 2 from 0.13 μSv to 0.25 μSv. The retardation in the buffer and the limited solubility of the dose driving Ra-226, both of which contribute to retardation only when the buffer is present, are thus of minor importance in the shear load scenario. This result is also consistent with the limited effect of imposing solubility limits as a variant case in the corrosion scenario, where solubility limits are otherwise not imposed due to the absence of the buffer.

The main difference for the radionuclides contributing most to dose is for Nb-94, as this is significantly retained in the buffer when it is present. However, Nb-94 contributes to dose mainly before 100,000 years. The above case is only relevant after the buffer has been eroded. Since the near-field hydrogeological conditions are stylised with respect to radionuclide transport in the above case, they are not necessarily relevant for estimating the time taken for buffer erosion to cause advective conditions in the deposition hole. The first advective positions occur after several tens of thousands of years in the buffer advection scenario. However, considering the unknown nature of the hydraulic conditions in the deposition hole after a shear failure, the results in Figure 13-52 are seen as cautiously representative of a combined scenario for times beyond 10,000 years.

This combined case is further considered in the risk summation in Section 13.9.

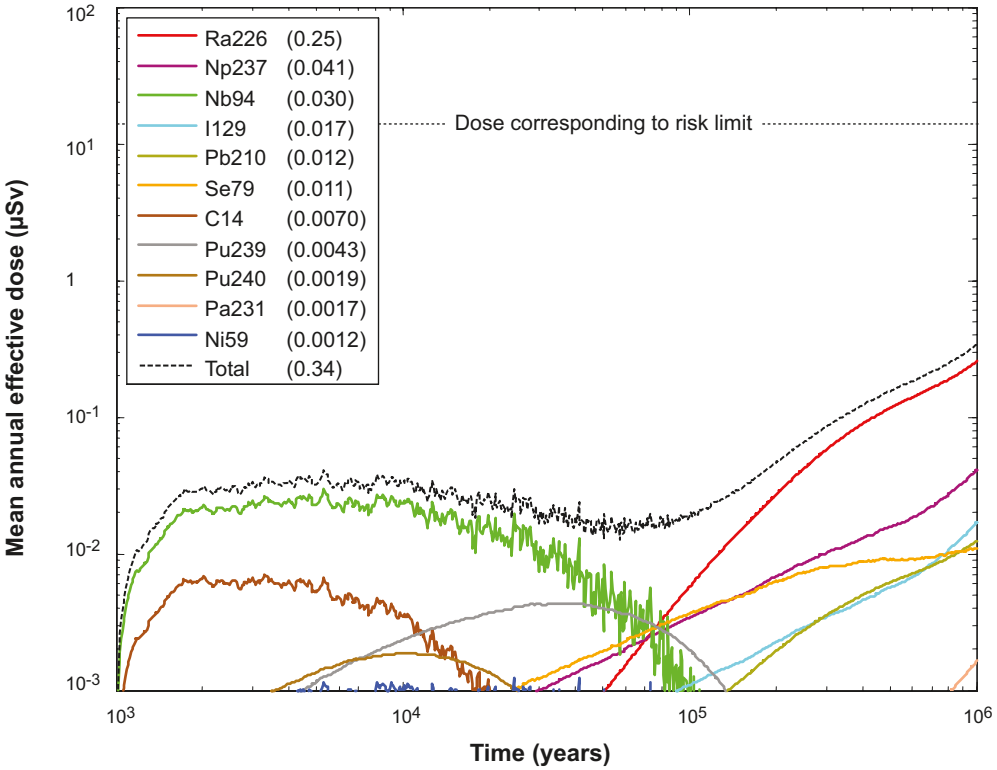


***Figure 13-52.*** *Probabilistically calculated consequences of shear failure with advective conditions in the deposition hole, for the period between 1,000 years and one million years. The legends are sorted according to descending peak mean annual effective dose over one million years (given in brackets in µSv).*

### 13.6.4 Analysis of potential alternative transport conditions/data

The transport data used in the calculation of the probabilistic base case calculation are those provided in the **Data report**. The data have been selected for certain conditions and in the following, it is analysed i) whether the evolution in the shear scenario is compatible with these conditions and ii) whether any alternative evolutions of the system, that could imply less favourable transport conditions, need to be considered.

This analysis corresponds to the analysis of the possible routes to alternative containment conditions in Section 12.8.2, but is simplified based on the analyses already done in the derivation of data in the **Data report**.

#### *Number of failed canisters and failure times*

This is the outcome of the analysis of the containment potential for the shear load scenario, and has thus been exhaustively analysed in Section 10.4.5.

#### *Radionuclide inventory, IRF and CRF*

It is not relevant to include these entities here since they are not affected by external factors, but by conditions determining the initial state. Uncertainties related to the initial state are fully explored in the **Data report**.

#### *Metal corrosion rate*

Even for a very early shear failure the temperature is not expected to be above 70°C for a water filled canister. Therefore, as for the corrosion scenario, see Section 13.5.4, the corrosion rates used in the **Data report** are valid (with a large margin) also for the shear load scenario.

### *Fuel dissolution rate*

In this case the buffer is in place and the expected hydrogen concentrations are relatively high, as discussed later in Section 13.7.2. On the other hand the radioactivity of the fuel may be higher at the time of water contact. However, the iron corrosion will continue for tens of thousands years and during this time fuel activity will decrease to levels below the alpha activity threshold /Muzeau et al. 2009/. Even for a very early shear failure the temperature is not expected to be above 70°C for a water filled canister.

### *Solubilities*

#### Redox conditions

The solubility of several of the important radionuclides is strongly dependent on the prevailing redox conditions in the near field of the repository. For example, the solubility of technetium increases by many orders of magnitude for a pe > 0. However, since the redox chemistry inside the canister will be dominated by the iron corrosion products (magnetite), the redox potential is expected to stay low under all circumstances.

*Need for studies of additional evolutions to rule out unfavourable redox conditions:* None; the vast amounts of iron and its anoxic corrosion products will buffer the redox conditions inside a defective canister.

#### pH

Natural groundwaters will have a pH in the range of about 6–9. The dissolution of low pH cement used for grouting and plugs could locally give a pH of ~11.

*Need for studies of additional evolutions to rule out unfavourable pH conditions*: As stated in Section 13.5.5, a pH above 11 or below 6.3 can be excluded. This range is already covered in the assessment of solubilities.

#### Temperature

The most relevant uncertainty associated with the thermodynamic data is the effect of temperature on the stability of aqueous species and solid compounds. In the database used a selection of reaction enthalpy is included, although in some cases no enthalpy data are available. The approach to correct the equilibrium constants for temperature effects follows the Van't Hoff equation, which relates the change in temperature to the change in the equilibrium constant, given that the standard molar enthalpy of reaction ($\Delta_f H_0$) is considered constant at all temperatures /Allard et al. 1997, p 434/. The calculations in SR-Site are based on fixed temperature of 25°C, since it is judged that the small temperature variations that can be expected in the repository when solubility limits are important will have marginal effect on the calculated values.

*Need for studies of additional evolutions to rule out unfavourable temperature conditions*: Solubility limits are generally only important for the long-term assessment. This means that temperatures above 25°C are of limited or no concern. Even in the case of an early failure the period with temperatures > 25°C will be short compared to the assessment timescale. Temperatures between ~0–25°C may on the other hand be important for solubility. Since there is a scarcity of enthalpy data, no temperature effects have been included in the solubility calculations in SR-Site. Instead a sensitivity study has been made in the documentation of the solubility assessment /Grivé et al. 2010/. The conclusion is that the effect of temperature < 25°C on the elemental solubilities is limited.

#### Groundwater ionic strength

The treatment of *activity corrections* also represents an uncertainty to the current solubility assessment. The range of ionic strength (I) in the groundwaters used /Duro et al. 2006/ is from $10^{-3}$ to 2 mole/dm$^3$. The most appropriated procedure to conduct activity corrections in this range would be the Specific Interaction Theory (SIT) /Allard et al. 1997, p 331/. However, this approach is still not

implemented in the geochemical codes used and, therefore, the extended Debye-Hückel approach /Allard et al. 1997, pp 328–329/ has been used for activity corrections. The results obtained by using the extended Debye-Hückel approach are comparable with the ones obtained by the SIT for those cases where the comparison is possible. Higher ionic strength than 1 mole/dm$^3$ would lead to an increased uncertainty in the obtained results.

*Need for studies of additional evolutions to rule out unfavourable ionic strength conditions*: As discussed for the fuel dissolution in Section 13.5.5, the reference evolution includes the highest salinities that can be expected at Forsmark, and no additional analyses are required.

**Minor components in groundwaters**

The lack of data on phosphate species and solid phases is an important drawback in the prediction of the solubility of some elements, mainly for rare earth elements and trivalent actinides. The consideration of phosphate in the groundwater composition may cause a change in the selected solubility controlling phases as well as in the solubility limits recommended for some of the radionuclides. Inclusion of phosphate phases and species could potentially lead to either higher or lower solubilities for radio-elements.

*Need for studies of additional evolutions to rule out unfavourable conditions*: There will be a competition for phosphate between the iron together with its corrosion products and the components in the spent fuel. The total concentrations of phosphate in the Forsmark groundwaters are generally low and are therefore not expected to have any significant impact on the solubilities. Therefore, it is concluded that no additional studies of the effect of phosphate on the solubilities are required.

**Conclusions**

The suggested handling of, and data for, solubilities in the **Data report** are sufficient to cover the shear failure scenario.

### *Buffer porosities*

This case involves no loss of buffer mass. The suggested handling of, and data for, porosities in the **Data report** are, therefore, sufficient to cover the shear failure scenario. Furthermore, as shown in Section 13.6.3, a loss of buffer following shear failure has a limited impact on the consequences.

### *Buffer diffusivities and buffer partitioning coefficients*

Cases leading to decreased retardation of radionuclide transport may be expressed through alterations of the parameters that affect radionuclide interactions with bentonite. These are separated into the following:

Intrinsic or structural parameters:
- Bentonite composition.
- (Assumed) tightness with regard to $CO_2$ exchange with the host formation.

External or environmental parameters such as:
- Changes in assumed groundwater composition, or $pCO_2$ imposed by the host formation leading to changes in porewater composition (very high or very low pH, high ionic strength, high concentration of competing cations/complexing ligands).
- Temperature.

The effects of different factors will be different for each radionuclide (or group of radionuclides). The validity range of sorption and diffusion coefficients is dependent on the uncertainties considered to be associated with each parameter in data derivation in the **Data report**. Different assumptions regarding these uncertainties would have led to a different validity range.

Lower buffer density will correspond to higher diffusion coefficients. Sorption will only be affected by the density if the porewater chemistry is significantly changed due to the higher water/solid ratio, but the effect of this ratio is of little importance in comparison to bentonite and groundwater composition. Smectite (montmorillonite) is the principal source of sorption sites; its content determines the magnitude of sorption. $K_d$ values are selected for a CEC of 85 meq/100 g in the **Data report**. Changing this internal factor to a lower value will lead to a lower $K_d$, but the effect is small considering the range of the $K_d$ values. A lower CEC is easily compensated by e.g. a slight variation of pH within the given uncertainty range. The content of accessory minerals of the bentonite influences porewater composition. Calcite in bentonite is needed to establish carbonate buffering. Absence of calcite would increase the dependency on groundwater composition; the corresponding effects on porewater composition were not quantified in /Ochs and Talerico 2004/. Absence of salts gives porewater results that lie within the parameter space already considered. Higher salt content is only relevant if it leads to a porewater salt concentration higher than that covered by the parameter space considered (ionic strength up to ~0.76 M /Ochs and Talerico 2004/). Tightness with regard to $CO_2$ is relevant because $CO_2$ exchange influences porewater pH. Completely open/closed systems were considered in the data derivation and thus already included in the selected range of sorption parameters.

Salinities of groundwater up to seawater was considered in /Ochs and Talerico 2004/. Higher salinity may lead to lower $K_d$ values, in particular for Cs/Sr/Ra. Increased chloride concentrations will lead to lower sorption of most radionuclides due to complexation, but this effect will, in most cases, be within the range already considered. Double layer effects will be decreased; therefore anion exclusion effects will be less important at high salinity. $D_e$ could increase for anions at high salinity. The lowest porewater pH considered for sorption was 6.6 /Ochs and Talerico 2004/. A lower porewater pH may lead to a different distribution of $K_d$ values.

*Need for studies of additional evolutions to rule out unfavourable conditions:* A loss of buffer density or a change in montmorillonite content is not directly foreseen in the shear load scenario, but this issue is discussed further in the subsection immediately below. The evolution of pH and ionic strength of the groundwater is discussed in Section 13.5.5. The range of possible ionic strength is already considered in the data for diffusivities and $K_d$ values in the **Data report**. However, as seen in the sensitivity study presented in Table 10-8, a combination of high groundwater flow, the MX-80 bentonite and a low groundwater pH could lead to a porewater with a pH that is slightly lower than the pH 6.6 that was used as the lower limit for the derivation of $K_d$ values in the **Data report**. This means that there could be cases where the $K_d$ values selected are inappropriate. This case requires a high flow, which is the case in the shear load scenario, but a high flow also means that the sorption in the buffer will contribute very little to the retardation of radionuclides. Also the limited additional consequences of this case are bounded by those of the combination of shear load and buffer advection, see below.

#### *Buffer hydraulic conductivity and swelling pressure*

To ensure that diffusion is the dominant transport mechanism in the buffer the safety function indicator criteria for hydraulic conductivity and swelling pressure should be upheld (see Section 8.3.2). The fulfilment of these criteria is basically dependent on the density and montmorillonite content in the buffer. Neither of these is expected to be directly affected by a shear failure of the canister. However, there may be indirect effects:

1. As described in Section 12.4 it cannot be excluded that metallic iron will have an effect on the montmorillonite. Currently, there is no reliable method to quantify this effect.
2. A combination of canister failure due to the shear load scenario and the buffer advection scenario would lead to a case with advective conditions in the deposition hole.

A severe transformation of the buffer caused by the metallic iron from the canister insert according to 1 above would lead to a similar situation as 2.

*Need for studies of additional evolutions to rule out unfavourable conditions*: A failed canister due to shear load in combination with advective conditions in the deposition hole needs to be considered. This can represent both cases described above. The consequences of such a case are presented in Section 13.6.3.

#### *Rock data*

Rock data are either stylised and pessimistic (applies to $Q_{eq}$) or irrelevant since geosphere retention is pessimistically neglected (applies to all other rock data).

#### *Biosphere LDF factors*

As for the corrosion scenario, all climate conditions emerging from the analyses of the evolution of the system are covered by the different LDF values available.

#### *Overall conclusion regarding additional cases to analyse*

The transport data provided in the **Data report** and used in the probabilistic base case calculation of the shear load scenario give a sufficient coverage of transport conditions for the shear load scenario.

### 13.6.5 Doses to biota, alternative safety indicators, analytical calculations and collective dose

#### *Doses to biota*

Releases for the shear load scenario have not been analysed with respect to doses to biota in SR-Site. However, since the releases are generally lower for this scenario than for the corrosion scenario, and since the margin to the reference value is, according to Section 13.5.7, several orders of magnitude in the latter, it is concluded that the effects on the environment for the shear load scenario are of no concern.

#### *Alternative safety indicators*

The same alternative safety indicators as for the corrosion scenario (Section 13.5.8) have been applied to the calculated releases for the shear load scenario, see further the **Radionuclide transport report**. Since the releases are generally lower for this scenario than for the corrosion scenario, the margins to the reference values are several orders of magnitude also for the shear load scenario.

#### *Analytical calculations*

The probabilistic case with shear failure with advective conditions in the deposition hole, for the period between 1,000 years and one million years (Figure 13-52), has been calculated also with the analytical models, see the **Radionuclide transport report**. The agreement is good and the peak dose, occurring at one million years is 0.36 μSv, compared to 0.34 μSv in Figure 13-52 for the numerical model.

#### *Collective dose*

SSMFS 2008:37 states the following: "The collective dose as a result of the expected outflow of radioactive substances during a period of 1,000 years after closure of a repository for spent nuclear fuel or nuclear waste shall be calculated as the sum, over 10,000 years, of the annual collective dose."

In the shear load scenario, releases occur before 1,000 years and hence the collective dose is calculated for this scenario. The release during the first 1,000 years is dominated by C-14 and it is also the most important contributor to the collective dose. The complete, i.e. integrated over 50,000 years, collective dose commitment from C-14 releases during the first thousand years is estimated by multiplying the integrated release of C-14 during the initial 1,000 year period by a conversion factor of 109,000 manSv per PBq. This conversion factor has been recommended by the UNSCEAR /UNSCEAR 2000, Annex A/ for estimating the complete collective dose commitment to the global population from releases of C-14 to the atmosphere. It has been calculated under the assumption that the future world population stabilises at $10^{10}$ people, and that the global inventory of stable carbon does not increase from its present value. Estimations of collective dose commitments from C-14 releases made with several different models have given very similar results /UNSCEAR 2000/. This consistency

between model predictions has been attributed to the long half-life of C-14, relative to its rate of environmental transport, which makes the estimated dose commitments insensitive to the detailed structure of the models or to the values of the parameters used in them. It is also concluded that doses following a release to soils or surface oceans are about the same as those for an atmospheric release /UNSCEAR 2000/.

According to /UNSCEAR 2000/, 75% of the complete dose commitment from a single release is delivered within 10,000 years. To estimate the incomplete collective dose commitment, i.e. the collective dose integrated over 10,000 years, the complete collective dose commitment is multiplied by 0.75.

The integrated release of C-14 during the initial 1,000 years is about 0.5 MBq. This yields a collective dose summed over 10,000 years for the shear load scenario of about $4 \cdot 10^{-5}$ manSv.

## 13.7 Hypothetical, residual scenarios to illustrate barrier functions

In this section, hypothetical, residual scenarios to illustrate barrier functions are analysed. They encompass i) the scenario ‘canister failure due to isostatic load’, considered as residual according to the analysis in Section 12.7, ii) a failure mode where a hypothetical initial defect in the form of a penetrating pinhole in the copper shell grows into a larger defect and iii) a number of hypothetical cases where different barriers are assumed to be completely lost. The canister failure due to isostatic load scenario is analysed in Section 13.7.1. The pinhole case is analysed in Section 13.7.2, using the COMP23 model for the near field and both the FARF31 and MARFA codes for far-field transport. Hypothetical cases illustrating consequences of assumed barrier losses in addition to the pinhole case are analysed in Section 13.7.3.

### 13.7.1 Canister failure due to isostatic load

This section analyses the consequences of the scenario treating canister failure due to isostatic load, analysed in Section 12.7. This scenario was classified as residual in Section 12.7.5, since no routes to this failure mode were found. The following treatment is thus for a hypothetical, postulated failure mode.

For this failure mode, the canister (both the cast iron insert and the copper shell) is bypassed, whereas the buffer and the geosphere are assumed to have intact retention properties. Failure of the canister due to isostatic load would probably mean that the insert buckles slightly inwards, the copper shell follows and opens up near the lid. The dimensional changes are, however, expected to be small.

Three exits from the near field are modelled: a fracture intersecting the deposition hole at the vertical position of the canister lid, denoted Q1, an excavation damaged zone, EDZ, in the floor of the deposition tunnel, Q2, and a fracture intersecting the deposition tunnel, Q3, see Figure 13-13 in Section 13.4.1. Geosphere transport data are from the base case of the semi-correlated hydrogeological DFN model. Thermally induced spalling is assumed to have occurred in the wall of the deposition hole meaning that the transport resistance at the interface Q1 is decreased.

The consequences of postulated failures of one canister due to isostatic collapse 10,000 years and 100,000 years after repository closure are shown in Figure 13-53. Since both hypothetical global causes (glacial load) and local causes (deficient material properties, higher than intended buffer density) for this failure mode can be envisaged, simultaneous failure of more than one canister needs to be considered and would yield consequences in proportion to the number of failed canisters, provided that all releases occur to the same biosphere object. If a large number of canisters fail, it is more appropriate to use the LDF values for a distributed release (Section 13.2.3) when converting release to dose, since the release can be expected to be distributed over several landscape objects. Illustrations of consequences of extreme cases where all canisters fail at 10,000 and 100,000 years are also shown in Figure 13-53. It is noted that the cases where one canister fails yield lower dose consequences at one million years compared to single canister failures due both to corrosion (where the buffer is eroded away, Figure 13-16), and to shearing (where geosphere retention is neglected, Figure 13-47). Additional cases are shown in the **Radionuclide transport report**.

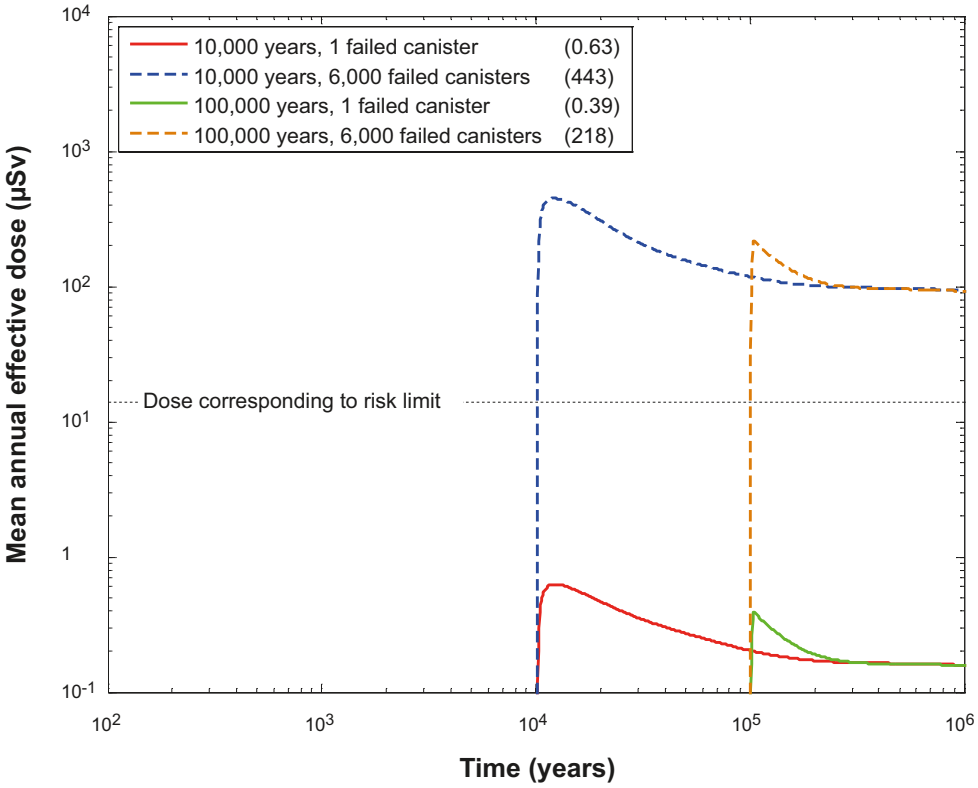


***Figure 13-53.*** *Postulated failures of one and of all 6,000 canisters at 10,000 years and at 100,000 years. The failed canisters are assumed to have no resistance to radionuclide transport. The single canister failures are calculated with the basic LDF values whereas for the global failures, LDF values for a distributed release are applied.*

### 13.7.2 The growing pinhole failure

As mentioned in the introduction, this failure mode is hypothetical since the initial state of the canisters implies that there will be no penetrating pinhole defects in the copper shell.

An analysis of this failure mode is, however, relevant in addressing important aspects of the internal evolution of the canister. For the pinhole failure mode, the pinhole in the canister wall initially offers a considerable transport resistance that is subsequently lost as the defect expands with time, whereas the buffer and the geosphere have intact retention properties. It is, therefore, also a convenient case for demonstrating the retarding capacity of the buffer and the geosphere and for exploring uncertainties relating to these components of the repository. Furthermore, the initially small defect is eventually expected to evolve into a large defect, which resembles the case of a failure caused by general corrosion of the canister, when the buffer is still intact. Although the likelihood of this latter failure mode was found negligible in the analysis of the corrosion scenario, Section 12.6, it is of interest to understand its consequences.

The evolution of the near field (canister and buffer) after canister failure for the pinhole case and input data for the transport models, valid for the pinhole case, are described in the **Radionuclide transport report**, where also a number of calculation cases not shown here are found.

One canister is postulated to have an initial, penetrating defect. Water penetrates through the defect into the canister and the time to establish a continuous water pathway between the fuel and the canister exterior is pessimistically assumed to be 1,000 years. After an additional pessimistically estimated 9,000 years, the pinhole suddenly grows so large that all transport resistance is lost. Three exits from the near field are modelled: a fracture intersecting the deposition hole at the vertical position of the assumed pinhole defect (near the canister lid), denoted Q1, an excavation damaged zone, EDZ, in the floor of the deposition tunnel, Q2, and a fracture intersecting the deposition tunnel, Q3, see Figure 13-13 in Section 13.4.1. Geosphere transport data are from the base case of the semi-correlated hydrogeological DFN model.

### *Calculations with COMP23 and FARF31*

Figures 13-54 to 13-57 show results for the near-field dose equivalent release and the far-field dose, as summed dose and decomposed into the three exit paths for a probabilistic base case calculation.

The near-field dose equivalent release is dominated by the non-sorbing nuclides I-129 and C-14, Figure 13-54. The peak values, occurring at 10,000 years when the canister is assumed to lose all its transport resistance, are due to the IRF and/or CRF of these nuclides. The release path Q1 dominates the initial releases and those immediately after 10,000 years, whereas the three release paths give more equal contributions longer after the failures, Figure 13-55.

The far-field peak total dose, Figure 13-56, is reduced by about a factor of 5 compared with that for the near field. Non-sorbing nuclides dominate also the far-field dose. The reduction in dose between near field and far field is larger for sorbing species. The initial dominance of Q1 is less pronounced for the far field, Figure 13-57, and here, the release paths Q2 and Q3 dominate in the long term.

Several additional cases have been calculated to examine sensitivities to various transport conditions. The results are summarised in the text below and in Figure 13-58, and details are provided in the **Radionuclide transport report**.

Thermally induced spalling may occur in the walls of the deposition holes and decrease the transport resistance in the interface between the buffer and the rock, see Section 10.3.5. For the base case calculation it is pessimistically assumed that all deposition holes experience spalling. An additional probabilistic case without spalling is, therefore, analysed. This yields a reduction of about a factor of 40 in total dose equivalent near-field release from Q1, whereas the effects on Q2 and Q3 are very limited. The total dose from the near field and the far field are reduced by factors of about 4 and 1.5, respectively. It is also noted that the occurrence of spalling does not affect the transport conditions in the corrosion and shear load scenarios.

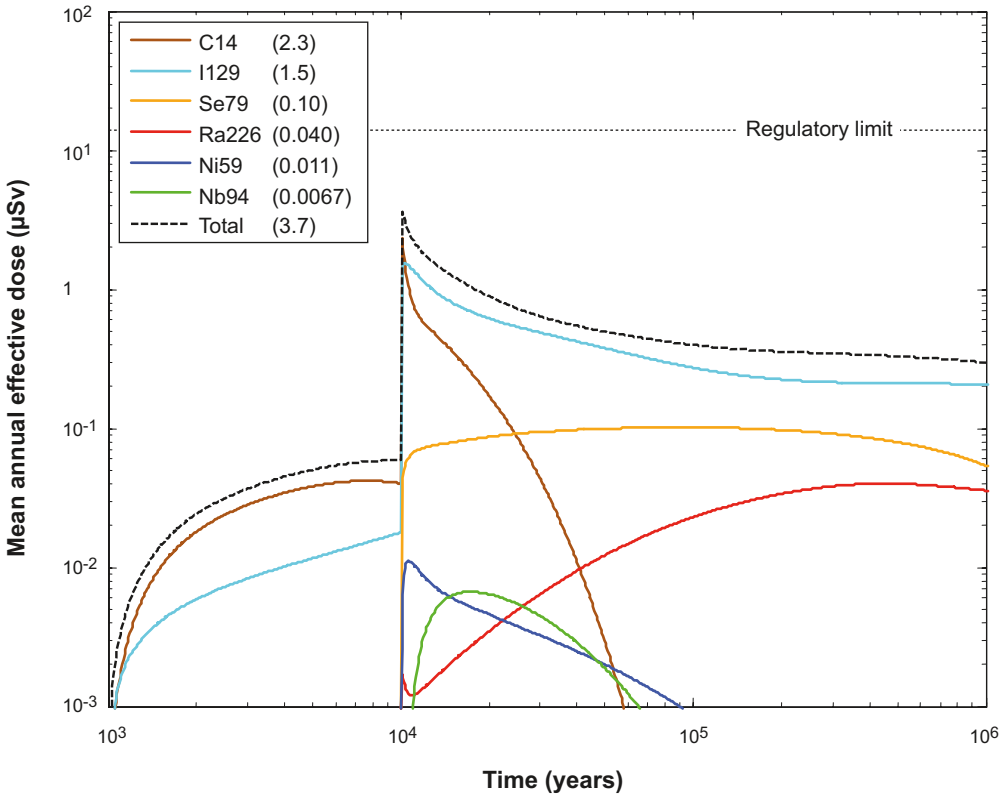


***Figure 13-54.*** *Near-field mean annual effective dose equivalent release for a probabilistic calculation for the base case for the pinhole failure mode. Summed doses for all release paths (Q1+Q2+Q3). The legends are sorted according to descending peak mean annual effective dose over one million years (given in brackets in µSv).*

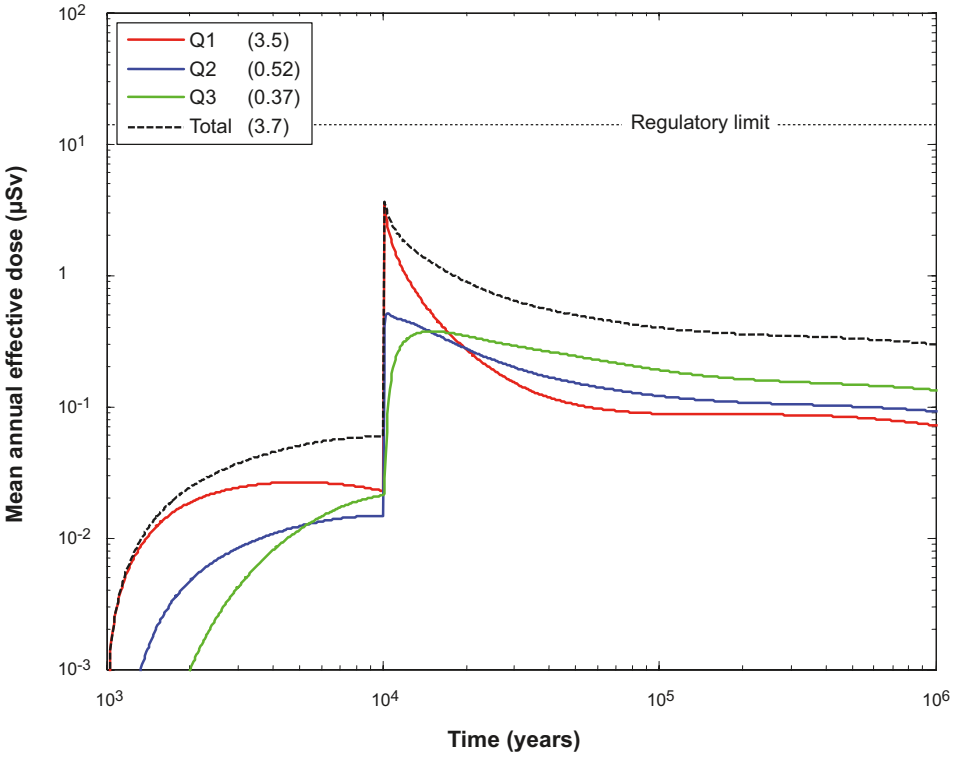


***Figure 13-55.*** *Near-field mean annual effective dose equivalent release for a probabilistic calculation for the base case for the pinhole failure mode. Doses decomposed into Q1, Q2 and Q3. The legends are sorted according to descending peak mean annual effective dose over one million years (given in brackets in μSv).*

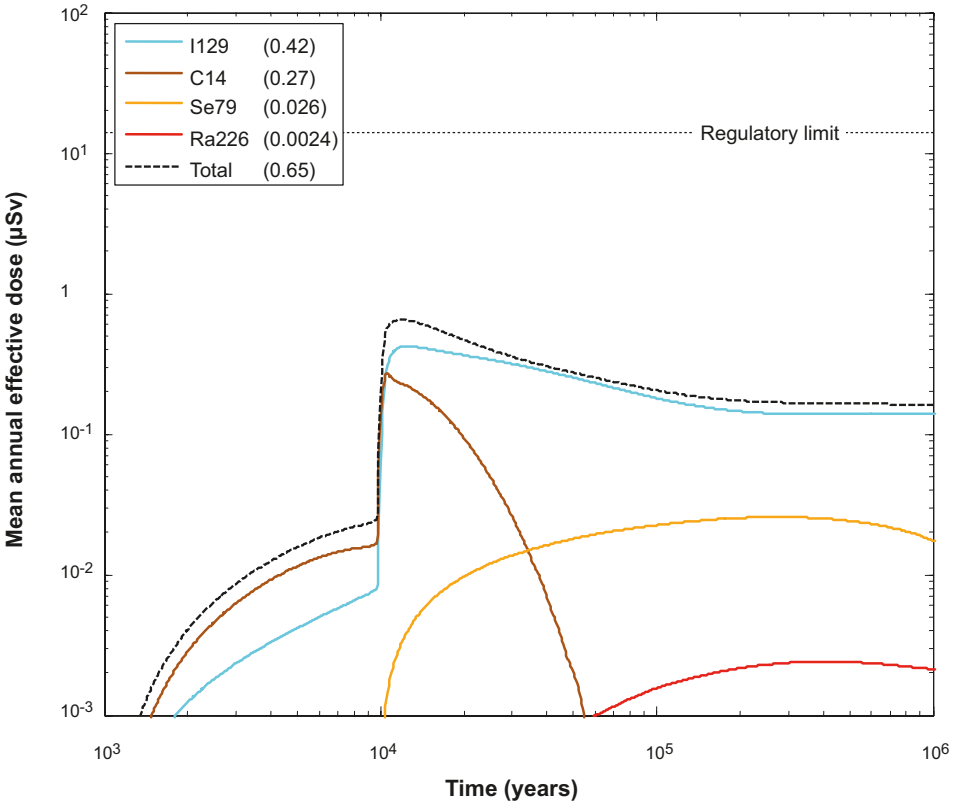


***Figure 13-56.*** *Far-field mean annual effective dose for a probabilistic calculation for the base case for the pinhole failure mode. Summed doses for all release paths (Q1+Q1+Q3). The legends are sorted according to descending peak mean annual effective dose over one million years (given in brackets in μSv).*

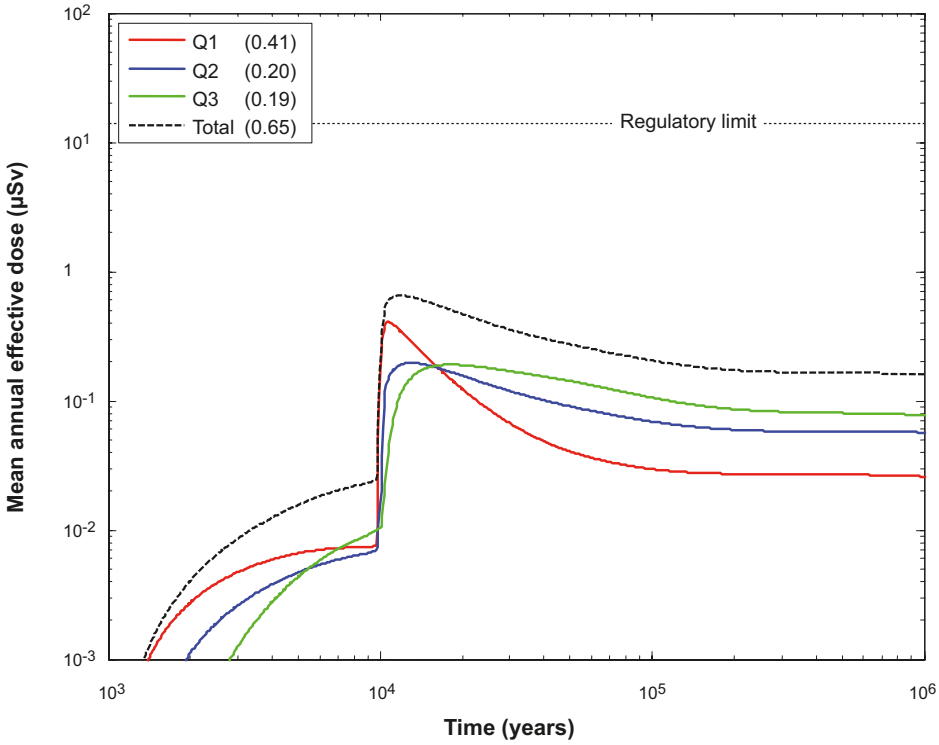


***Figure 13-57.*** *Far-field mean annual effective dose for a probabilistic calculation for the base case for the pinhole failure mode. Doses decomposed into Q1, Q2 and Q3. The legends are sorted according to descending peak mean annual effective dose over one million years (given in brackets in μSv).*

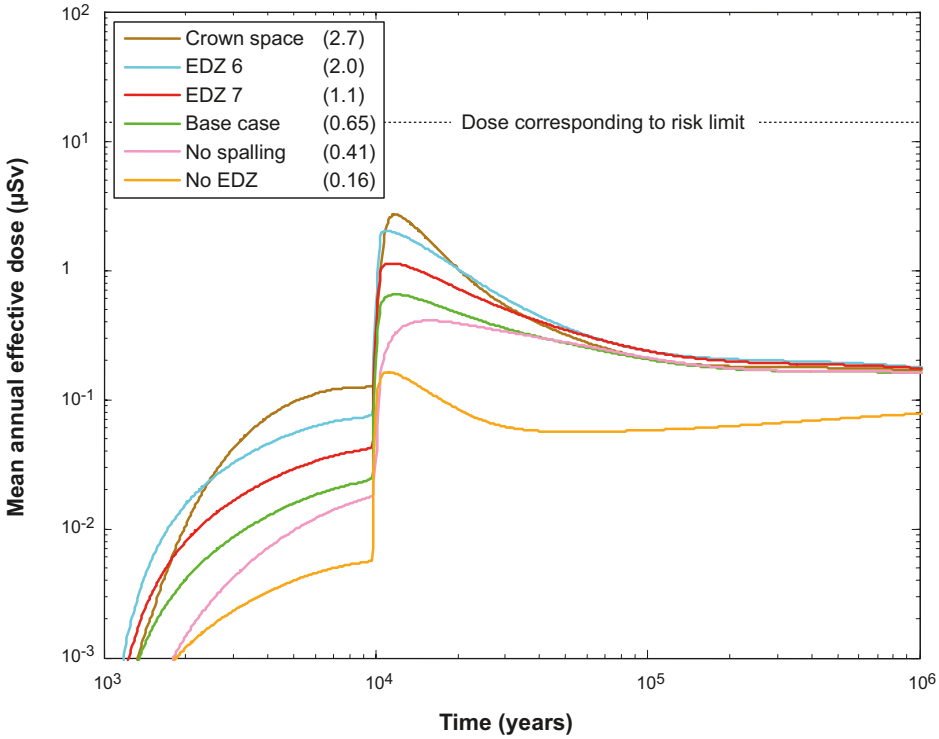


***Figure 13-58.*** *Far-field mean annual effective dose for the probabilistic calculations of the pinhole base case and cases with no spalling, with different assumptions regarding EDZ properties (EDZ6 and EDZ7 correspond to transmissivities of $10^{-6}$ $m^2/s$ and $10^{-7}$ $m^2/s$, respectively) and with a crown space in the deposition tunnel. The legends are sorted according to descending peak mean annual effective dose over one million years.*

The base case has an excavation damage zone (EDZ) transmissivity of $10^{-8}$ m$^2$/s. The effects of different EDZ transmissivities are examined by considering probabilistic variant cases with no EDZ and EDZ transmissivities of $10^{-6}$ m$^2$/s and $10^{-7}$ m$^2$/s. The latter two cases are included to clarify what the effects would be of using a potentially more damaging technique than that of the reference method for tunnel excavation. Eliminating the EDZ has virtually no impact on the Q1 release, whereas the Q2 release by definition vanishes. The Q3 release is somewhat reduced and this is due to the fact that many escape routes from the deposition tunnel are minor fractures connecting the tunnel to the EDZ in the base case. Increasing EDZ transmissivity above the base case value of $10^{-8}$ m$^2$/s does not increase the Q1 release. For Q2, each order of magnitude increase in transmissivity results in approximately a factor of 3 increases in near-field and far-field peak releases. Releases through Q3 are weakly affected. The increase in total far-field mean annual effective dose in going from the base case value of $10^{-8}$ m$^2$/s to $10^{-6}$ m$^2$/s is somewhat less than an order of magnitude, and the effect of assuming no EDZ is a reduction by somewhat less than an order of magnitude.

A flow model variant in which tunnel backfill has compacted with a resulting gap at the tunnel crown is also analysed, see Section 10.3.6. Early releases from the near field of C-14 are about 3 times higher compared to the pinhole case with an intact tunnel backfill, and Q3 is the dominating release path. In the longer term Ra-226 contributes considerably to the total dose. For the far field, early releases of C-14 are about 8 times higher compared to the pinhole case with an intact tunnel backfill, and also here Q3 is the dominating release mode. In the longer term, the total dose from the far field is comparable to that of the pinhole base case.

### *Calculations with MARFA*

Several variant cases of the growing pinhole failure mode have been investigated with MARFA to understand the sensitivity to various modelling assumptions, the potential for retention in engineered structures and soils, and the potential role of bentonite colloids in facilitating transport. MARFA was used for this assessment because it has capabilities to fully represent variability along pathways, including variability in the type of retention model. For example, MARFA can use an equilibrium sorption model for soils and tunnels in combination with matrix diffusion models for the fractured bedrock portions of the transport pathways.

Because the focus here is in understanding modelling sensitivities, a simplified treatment of uncertainty is adopted. Preliminary deterministic values are used for initial radionuclide inventories, near-field transport parameters, and matrix parameters. Details can be found in the **Radionuclide transport report**. However, full pathway-to-pathway variability is included for flow-related transport parameters (the equivalent flow rate, advective travel time, and flow-related transport resistance). MARFA uses a segmented pathway representation in which advective travel time and flow-related transport resistance vary from segment to segment. Within the DFN regions, a segment is that part of a pathline contained within a single fracture. This detailed representation of spatial variability is in contrast to that of FARF31, which uses global values for advective travel time and flow-related transport resistance for each flow path. The results discussed below are for annual dose as expected values taking into account all deposition holes.

#### Reference case

The reference pinhole case analysed with MARFA differs from the above base case analysed with the COMP23 and FARF31 models in two significant ways: The parts of the pathway in tunnels and soil layers are included in the travel time (but no sorption is assumed), and deterministic values are used as described above. In particular the first of these factors yields a reduction in the calculated mean doses of about an order of magnitude compared to those obtained with the COMP23/FARF31 models. The far-field geosphere reduces peak total dose by a factor of approximately 20 for the Q1 path, approximately 5 for Q2, and approximately 2 for Q3. I-129, C-14 and Ra-226 account for almost all the far-field and near-field doses for all three release paths.

**Sensitivity to flow and transport assumptions**

The reference case includes soils and tunnel segments in the transport pathway, but assigns these segments zero equilibrium partitioning coefficients for all elements. Thus, the delay introduced by a non-zero groundwater travel time through soils and tunnels is accounted for, but retardation of sorbing elements is ignored. Effects of the soils and tunnels are summarized in Figure 13-59 for the Q1 release path. The blue curve is near-field release and the green curve is the reference case. The pink curve neglects the effect of transport in tunnels and soils. The black curve incorporates transport with sorption in tunnels and soil layers. There are two main conclusions to be drawn. First, the travel time in the tunnels and soil layers decreases the peak dose by a factor of approximately 5 (compare pink to green curves). This decrease is mostly due to the effect on the non-sorbing I-129 and C-14. Second, sorption in tunnels and soils has no significant effect on total dose. This lack of sensitivity is a consequence of the dominant role that the non-sorbing I-129 and C-14 play in determining the total dose. Indeed, examination of the far-field releases for individual nuclides (Figure 13-60) reveals that releases of sorbing radionuclides such as Ra-226 are significantly reduced by sorption in tunnels and soils.

Cases with different assumptions regarding the EDZ transmissivity and with the assumption of a crown space in the deposition tunnel have also been analysed, with similar results to those reported above for the COMP23/FARF31 models, see the **Radionuclide transport report** for details.

The effect of releasing multiple tracer particles per deposition hole (see Section 10.3.6 for details of the flow case) is analysed in the **Radionuclide transport report**. Different tracer particles traverse different flow paths, which makes it possible to explore the dispersive effects of different flow paths diverging from a single source location. It is shown that the effect of multiple particles (ten) per release point relative to the case with a single particle implies very small differences in resulting doses. Thus, dispersion caused by having multiple flow paths connect a single source location to the biosphere is subordinate to other processes that spread radionuclide mass in time.

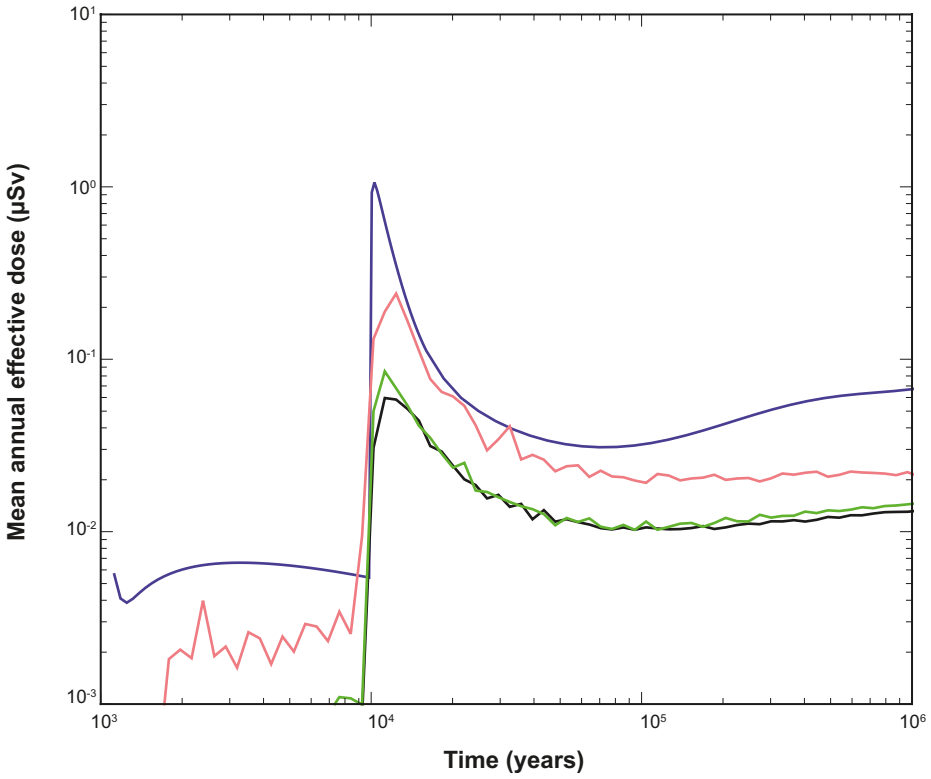


***Figure 13-59.*** *Expected values for all-nuclide releases for the Q1 pinhole release, expressed as equivalent doses. The blue curve is near-field release and the other curves are far-field releases as follows: pink neglects transport in tunnel and soil, green is the reference case (tunnels and soil layers included but with no sorption), black has sorption in tunnels and soils.*

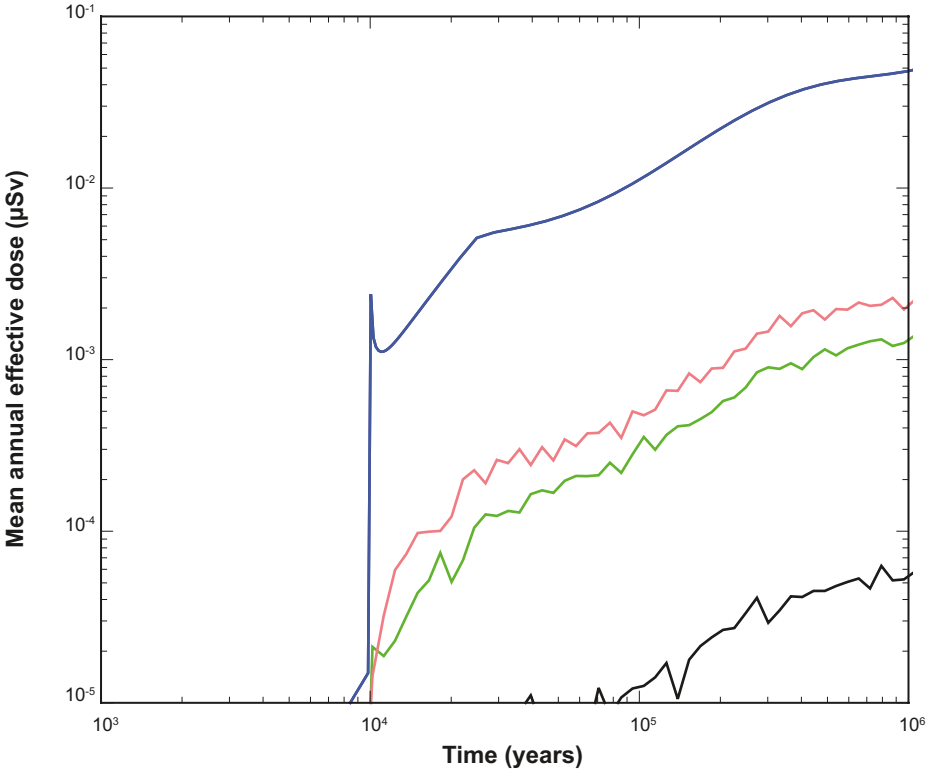


***Figure 13-60.*** *Expected Ra-226 release for pinhole Q1 release path and different assumptions about the role of tunnels and soils. The blue curve is near-field release and the other curves are far-field releases as follows: pink has no tunnel or soil segments in the pathway, green curve is the reference case (tunnels and soil layers included but with no sorption), black has sorption in tunnels and soils.*

#### Colloid facilitated transport

Colloid facilitated transport may be represented in MARFA by replacing two transport parameter groups by apparent values, see Section 13.5.6, sub-section 'Colloid facilitated transport'. The ratio of the colloid-free parameters and the apparent values in the presence of colloids depends only on the colloid mass density and the partitioning coefficient for sorption onto colloids, see the **Radionuclide transport report** for details. Assuming a colloid mass density of 10 mg/L /Wold 2010/, sorption onto colloids is found to have a negligible effect, see the **Radionuclide transport report**. The main reason that colloids do not enhance transport significantly is that the radionuclides I-129, C-14 and Ra-226 dominate the near-field and far-field releases, and I, C and Ra do not have a strong affinity for bentonite, see the **Data report**. Elements that have a strong affinity for bentonite and could potentially be transported significantly by bentonite colloids are not released from the bentonite buffer in sufficient quantities to affect the total dose.

### 13.7.3 Additional cases to illustrate barrier functions

Some conclusions regarding loss of barrier functions can be drawn from the analyses already presented. In order to provide a fuller treatment, the following cases of barrier deficiencies are postulated:

A. An initial absence of enough buffer causing advective conditions in the deposition hole for all deposition holes.

B. An initial pinhole in the copper shell for all canisters.

C. An initial, large opening in the copper shell and in the cast iron insert for all canisters.

D. A combination of cases A and C, i.e. an initial large opening in all canisters and advective conditions due to loss of buffer for all deposition holes.

E. A combination of case C with an assumption of fast fuel dissolution and fast corrosion of metal parts. An initial, large opening in every canister is combined with the assumption of a complete fuel dissolution and metal corrosion in only 100 years.

A loss of the radionuclide retention capability of the rock is combined with each of the five cases, yielding a total of ten release situations. The cases without geosphere retention are denoted A* through E*.

In all cases it is assumed that the backfill and closure are installed and perform as expected. Also, all aspects of the rock other than those related to retention, e.g. the near-field groundwater flow, which is generally low and with only about one sixth of the deposition holes connected to water conducting fractures, as well as the stable and favourable groundwater composition in the near field, are assumed to be present. Elemental solubilities are imposed on concentrations of radionuclides in the canister void volume only if the buffer is in place. This is the same approach as used in the analyses of the corrosion and shear load scenarios, Sections 13.5 and 13.6.

Table 13-10 gives an overview of the status of the retardation related safety functions, see Figure 8-3, for the cases.

The transport and dose calculations are probabilistic, since it is desirable to take into account both uncertainties due to lack-of-knowledge in general and the spatial variability of the properties of the deposition holes and their associated transport paths in the geosphere. The semi-correlated hydrogeological DFN model was used for these stylised calculations. Except for the case specific assumptions regarding failed barrier functions, all transport data are taken from the **Data report**. This applies to e.g. corrosion rates, fuel dissolution rate, sorption and diffusion data and LDF values.

**Table 13-10. Status of safety functions for the ten release situations. In cases denoted with an asterisk also geosphere retention is absent.**
**Green: Safety function intact**
**Yellow: Safety function deteriorates over time**
**Red: Safety function absent initially**

| | A. Buffer missing | A* | B. Pinhole damage | B* | C. Large canister defect | C* | D. Large canister defect and buffer missing | D* | E. Large canister defect, rapid fuel and metal conversion | E* |
|---|---|---|---|---|---|---|---|---|---|---|
| Limited fuel dissolution rate | | | | | | | | | | |
| Limited corrosion rate of metal parts | | | | | | | | | | |
| Limited solubilities | | | | | | | | | | |
| High transport resistance in canister/buffer interface | | | | | | | | | | |
| Retardation in buffer | | | | | | | | | | |
| High transport resistance in buffer/rock interface[1)] | | | | | | | | | | |
| Geosphere retention | | | | | | | | | | |

1) When this safety function is present, spalling is still pessimistically assumed in all deposition holes. When this safety function is not present, i.e. when the buffer is missing, the groundwater turnover in the deposition hole is still limited by the hydraulic properties of the rock.

The biosphere is here represented by the constant LDF values obtained when the release is distributed in the landscape according to the time dependent distribution of release locations from the repository during an interglacial. Furthermore, since the LDF values are suited primarily to handle releases that are constant over periods of time that are comparable to the duration of an interglacial, i.e. typically 10,000 years, the releases for these cases are, as a variant, also evaluated with fully time dependent modelling of the biosphere. Here, the releases are distributed in the landscape and the time dependent doses are presented, rather than a time dependent release converted to dose by a constant LDF value.

In the following, each case is discussed briefly using distributed, constant LDFs. The section is concluded with summarising accounts of all cases both with LDFs and with time dependent modelling of the biosphere.

### *Cases A and A*, initial absence of buffer*

A 0.5 m high section of the bentonite buffer is assumed to be missing, leaving a void in the form of a hollow cylinder between the canister and the wall of the deposition hole. The Q1 fracture, if it exists, intersects the deposition hole at the location of the void (see Figure 13-13). The deposition hole is otherwise filled with buffer and the deposition tunnel backfill is assumed to be intact. This case is analysed in Section 13.5.6, as a variant of the central corrosion case. For most of the deposition holes, the groundwater flow and sulphide concentrations are not sufficient to cause canister failure during the one million year assessment period. The corrosion calculation takes both the natural variability of flow rates for the ensemble of 6,000 deposition holes and the distribution of sulphide concentrations in the groundwater into account. This yields a calculated mean number of failed canisters of 0.17 at one million years, used also here. Only the deposition holes with the highest flow rates in the Q1 fracture contribute. This also means that releases to Q2 and Q3 release paths (Figure 13-13) are negligible for these positions. Canisters in positions without a Q1 fracture do not fail in this calculation case.

For a failed canister, radionuclide transport in the near field and the far field is modelled as follows.

- The instantaneous release fraction of the inventory dissolves in the water in the void volume of the canister and the void from the eroded buffer.
- Nuclides embedded in the metal parts of the fuel assemblies are released to the void water in congruence with the corrosion of the metals. This is pessimistically estimated to take on average 1,000 years.
- Nuclides embedded in the fuel matrix are released to the void water in congruence with the dissolution of the fuel matrix. This is estimated to take on average $10^7$ years.
- No solubility limits are imposed since the buffer is not in place to act as a filter for fuel colloids required in order to uphold solubilities.
- Releases occur from the water filled volume to the Q1 fracture, assumed to intersect the deposition hole where the buffer is missing. Only the highest flow rates cause failures. This also means that the release to the geosphere for these positions is essentially controlled by the release of nuclides from the metal parts and the fuel matrix, since the groundwater flow is sufficiently high to carry all the released nuclides away.
- The far-field development is modelled as in all other cases (see case B below), but the retention in the far field is generally poor since high flow rates at a deposition position are positively correlated with a low $F$ values in the geosphere.

The consequences are similar to those presented in Section 13.5.6, see Figures 13-28 and 13-29. The only differences is that the distributed LDF values are applied and the results are shown in Figure 13-67 later in this section. Many of the radionuclides have decayed to insignificance when the first failures occur after close to 50,000 years. Near-field release equivalent doses are dominated by Nb-94 from metal parts of the fuel and Ra-226, Pb-210 and Np-237 from the fuel matrix. Far-field doses are dominated by Nb-94, Se-79, Ra-226 and I-129.

### *Cases B and B*, initial, penetrating pinhole defect in all canisters*

The canister defects are assumed to be the same as those modelled in the growing pinhole failure, Section 13.7.2, i.e. an initial, penetrating pinhole that grows into a large failure after 10,000 years, but now in all canisters. The deposition hole buffer and the deposition tunnel backfill are assumed to be intact. The dose consequences in the biosphere are calculated with the distributed LDF values since this is a more realistic approach when releases occur from all over the repository.

The near-field development for this case is modelled as follows.

- Every canister is postulated to have an initial, penetrating defect. Water penetrates through the defect into the canister and the delay time to establish a continuous water pathway between the fuel and the canister exterior is pessimistically assumed to be 1,000 years.
- The instantaneous release fraction of the inventory dissolves in the water in the void volume of the canister.
- Nuclides embedded in the metal parts of the fuel assemblies are released to the void water in congruence with the corrosion of the metals. This is pessimistically estimated to take on average 1,000 years.
- Nuclides embedded in the fuel matrix are released to the void water in congruence with the dissolution of the fuel matrix. This is estimated to take on average $10^7$ years.
- Solubility limits are imposed since the buffer is in place and acts as filter for fuel colloids.
- Releases from the canister to the buffer commence after the 1,000 years' delay time, but the small size of the pinhole defect suppresses the release rate considerably compared to the case with a large degree of damage. After an additional pessimistically estimated 9,000 years, the pinhole suddenly grows so large that all transport resistance from the canister is lost.
- The nuclides are sorbed with varying efficiency in the buffer and the diffusion and sorption properties determine the time for diffusion through the buffer. If this time is shorter than a few half-lives of the nuclide, it passes to the Q1 fracture in the rock. Thermally induced spalling is assumed to have occurred in all deposition holes, reducing the transport resistance in the buffer/rock interface considerably. The release rate is determined by the nuclide concentration in the outer part of the buffer and the flow rate in the deposition hole. The flow is obtained from the base case of the semi-correlated hydrogeological DFN model.
- The release rate is multiplied by the LDF value for a release distributed in the landscape to obtain a dose equivalent release rate from the near field.

The far-field development for this case is modelled as for all cases:

- In the rock, the nuclide's sorption properties, together with the rock's transport properties, determine the time for transport through the rock to the biosphere. The half-life of the nuclide determines whether it passes through the geosphere before decaying to a substantial degree.
- This release rate is multiplied by the LDF value for a release distributed in the landscape to obtain a dose from the far field.

The consequences are similar to those in the pinhole scenario, see Figures 13-54 and 13-56 for the near field and the far field, respectively. The only difference is that all canisters are now assumed to have defects, meaning that the probabilistic single-canister results should be multiplied by 6,000 and that the distributed LDF values are applied, leading to a reduction of the consequences by typically one order of magnitude. The far-field results with all 6,000 canisters are shown in the summarising Figure 13-67 later in this section.

### *Cases C and C*, initial, large opening in all canisters*

The canister defects are assumed to be in the form of a large opening in the copper shell and the cast iron insert. The deposition hole buffer and the deposition tunnel backfill are assumed to be intact.

In the reference evolution, some of the deposition holes are affected by buffer erosion to the extent that advective conditions occur in the hole. For the stylised case considered here, no such erosion is, however, assumed, in order to more clearly demonstrate the role of the canister if all other barriers are intact. Combinations of canister and buffer defects are analysed in one of the cases described below.

The calculation case is similar to the isostatic collapse probabilistic case for the semi-correlated DFN model, applied to all canisters in the repository, with the difference that the failure is assumed to exist at deposition. The near-field and far-field releases are calculated with the radionuclide transport models used for the isostatic load scenario.

The near-field and far-field developments for this case are identical to those for the above case with initial pinhole defects in all canisters, with the following exceptions.

- After 100 years, all canisters are assumed to be filled with water and a continuous water pathway is established between the fuel and the canister exterior. 100 years is a rough estimate, corresponding to an inflow rate of 0.1 L/yr through the buffer to the canister similar to that assumed for canister failures due to shear load in Section 13.6. The saturation time of the near field is generally longer than 100 years at Forsmark.
- Releases from the canister to the buffer commence after the 100 years, and they are not suppressed by the canister due to the assumed, large degree of damage.

The dose equivalent release from the near field is shown in Figure 13-61. The dose is dominated over the initial 10,000 years by C-14, Cs-137, Sr-90, Ag-108m, I-129 and Se-79. After about 10,000 years Se-79, C-14, Ra-226 and I-129 contribute most to the total dose. Releases of nuclides that sorb strongly in the buffer, e.g. Pu-238 and Pu-239, are strongly reduced compared to case D* below where the buffer is also assumed to be missing. There is a considerable reduction also of releases of Cs-137, Sr-90 and Ag-108m compared to the case in which the buffer is missing.

The dose from the far-field release is shown in Figure 13-62. The peak total dose is reduced by less than an order of magnitude compared to the near-field release, whereas doses from many of the short-lived or sorbing nuclides are considerably reduced.

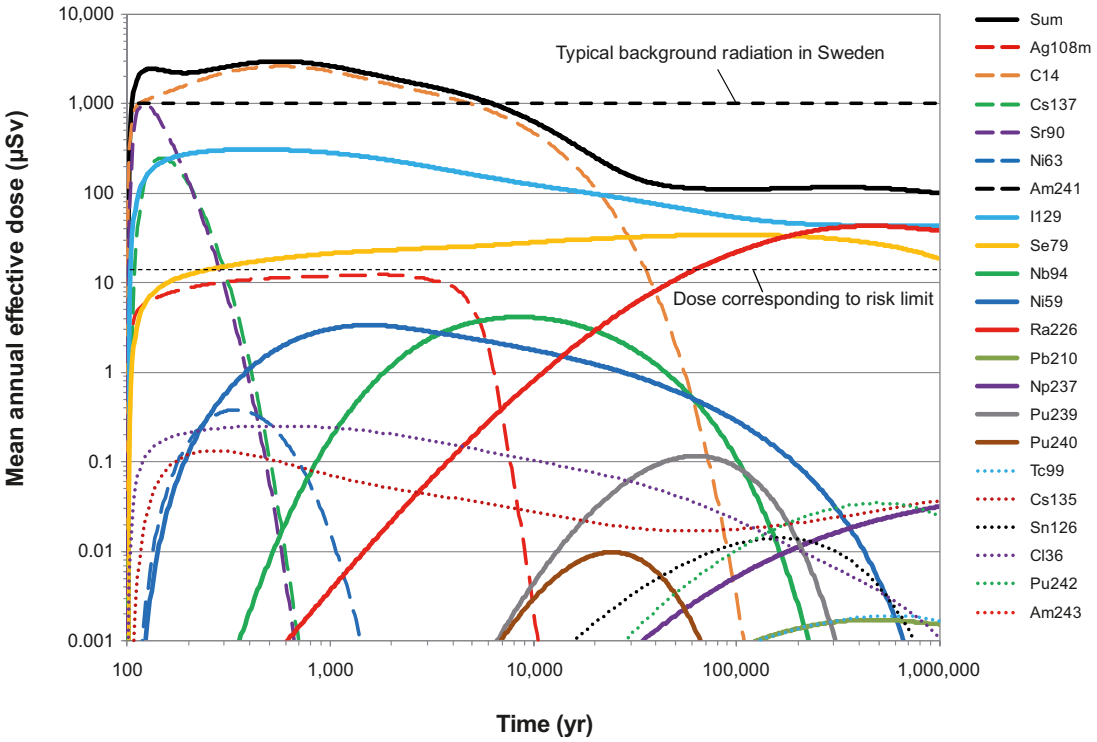


***Figure 13-61.*** *Near-field dose equivalent release for case C*, i.e. all canisters have an initial large defect and the buffer is intact.*

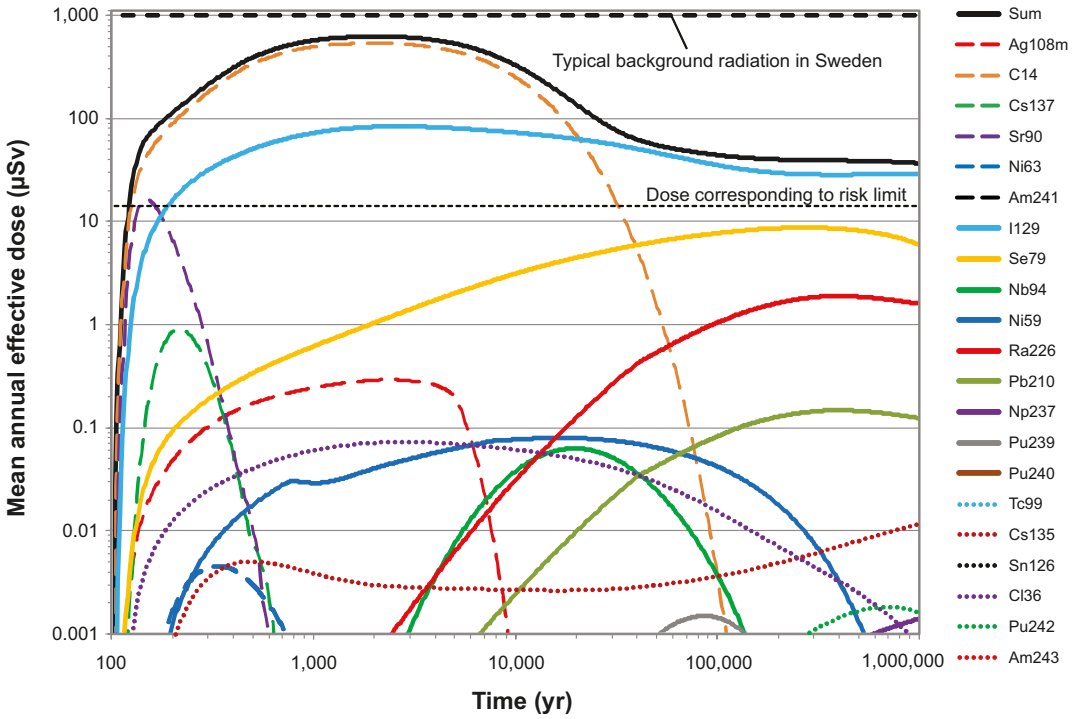


***Figure 13-62.*** *Far-field dose for case C, i.e. all canisters have an initial large defect and the buffer is intact.*

It is noteworthy that this completely unrealistic case of initial loss of containment function for all canisters in the repository yields far-field releases, converted to doses, which never exceed the background radiation. However, the containment function is required for a majority of the canisters in order to fulfil the regulatory requirement on risk at Forsmark.

The long-term release rate of I-129 equals, to a good approximation, the release rate of this nuclide from the fuel matrix. This is caused by the assumed absence of sorption and long half-life of I-129. Regarding the calculated dose from I-129 for this and other hypothetical cases in this section, it is noted that the mitigating effect of mixing of I-129 with naturally occurring stable iodine is disregarded in the biosphere models.

### *Cases D and D*, initial large opening in all canisters and advective conditions due to loss of buffer for all deposition holes*

The defects are assumed to be the same as those modelled in the corrosion scenario, i.e. a large opening in the copper shell and the cast iron insert and a section of the bentonite buffer is missing where the canister is damaged, leaving a void between the canister and the wall of the deposition hole in the form of a hollow cylinder. The deposition hole is otherwise filled with buffer and the deposition tunnel backfill is assumed to be intact. This means that releases occur predominantly to the Q1 fracture, if it exists. The near-field and far-field releases are calculated with the radionuclide transport models used for the corrosion scenario and applied to all deposition holes.

The near-field and far-field developments for this case are identical to those for the above case with initial pinhole defects in all canisters, with the following exceptions.

- After 100 years, all canisters are assumed to be filled with water and a continuous water pathway is established between the fuel and the canister exterior. 100 years is a rough estimate, corresponding to an inflow rate of 0.1 L/yr to the canister. The saturation time of the near field is generally longer than 100 years at Forsmark.
- No solubility limits are imposed since the buffer is not in place to act as a filter for fuel colloids.
- For deposition holes that have a Q1 fracture, releases occur from the water filled volume to this fracture, assumed to intersect the deposition hole where the buffer is missing. The release rate is determined by the flow rate in the fracture and the size of its intersection with the deposition hole, taken to be equal to the deposition hole diameter. The flow is obtained from the semi-correlated hydrogeological DFN model, and multiplied by a factor of two to account for the locally increased flow due to the void from the missing buffer.

The dose equivalent release from the near field is shown in Figure 13-63. The dose is dominated the initial 10,000 years by the IRF and/or CRF of Ag-108m, Cs-137, Sr-90, C-14 and Nb-94. Note that only the generally low flow rates at Forsmark limit the releases for the IRF/CRF. After about 10,000 years Nb-94, Pu-239, Pu-240, Np-237, Ra-226, Pb-210 and I-129 contribute most to the total dose.

The dose from the far-field release is shown in Figure 13-64. The total dose is reduced by about a factor of 10 compared to the near-field release. For the earliest releases this is an effect of the travel time in the geosphere. In the long term, strongly sorbing nuclides like Pu-239 and Pu-240 are retained in the geosphere. It is noteworthy that this completely unrealistic case of initial absence of all transport limitations in the engineered parts of the repository yields far-field releases, converted to doses, that exceed the background radiation by a factor of about five initially and that in the long term are less than a factor of ten above the risk limit.

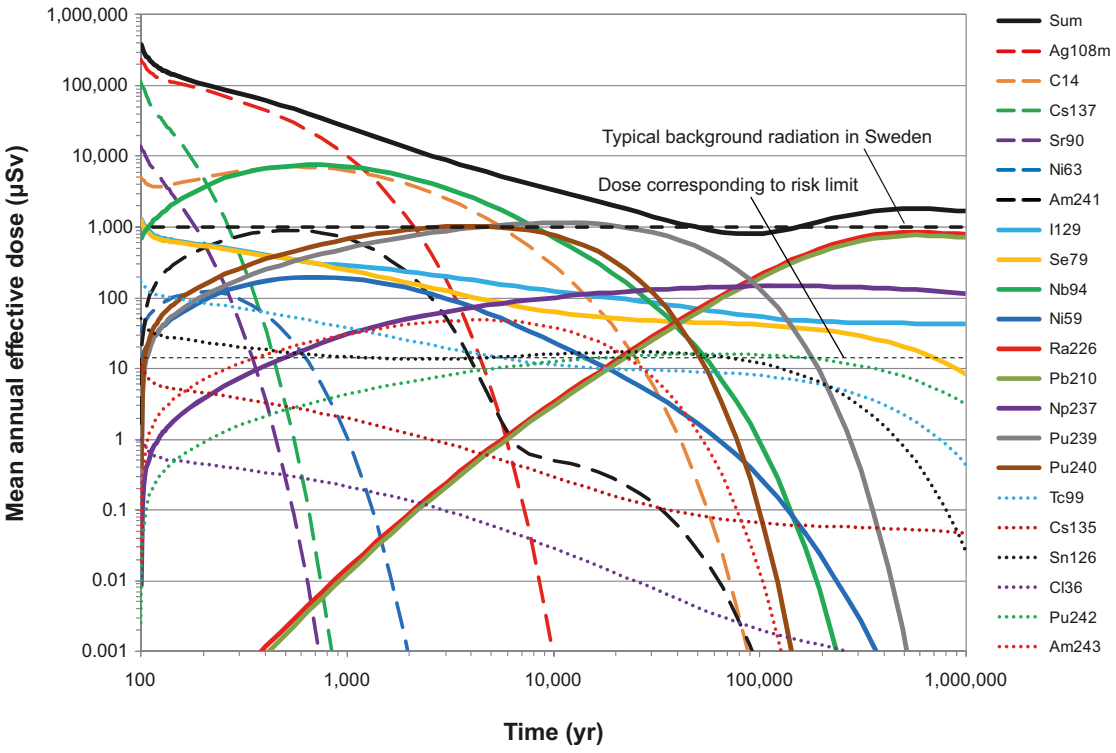


***Figure 13-63.*** *Near-field dose equivalent release for case D*, i.e. all canisters have an initial large defect and the buffer is missing between the defect in the canister and the wall of the deposition hole.*

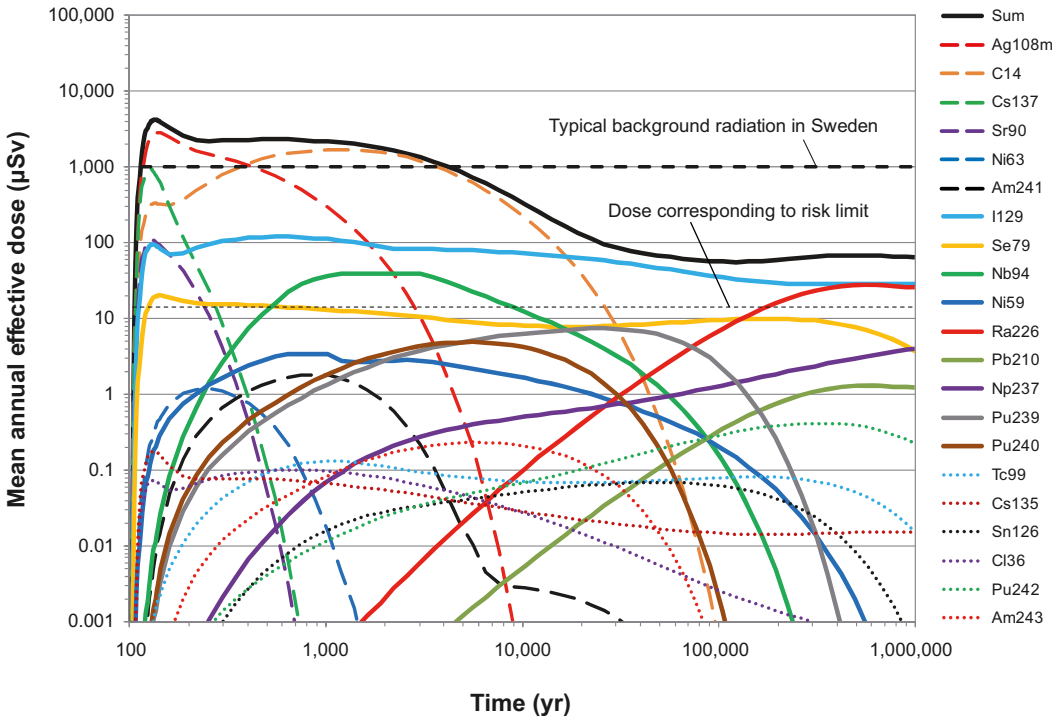


***Figure 13-64.*** *Far-field dose for case D, i.e. all canisters have an initial large defect and the buffer is missing between the defect in the canister and the wall of the deposition hole.*

### *Cases E and E*, initial, large opening in all canisters and rapid fuel dissolution and metal corrosion*

These cases are identical to cases C and C*, (all canisters have a large opening in the copper shell and the cast iron insert), except that for cases E and E* complete fuel dissolution and metal corrosion is assumed to occur in 100 years after water contacts the fuel. The containment function of not only the canister but also of the fuel matrix and the structural parts of the fuel is thus assumed to be absent. The deposition hole buffer and the deposition tunnel backfill are assumed to be intact.

The near-field and far-field developments for these cases are identical to those for cases C and C* with the exception of the fast fuel dissolution and metal corrosion.

The dose equivalent release from the near field is shown in Figure 13-65. The dose is dominated by C-14, Cs-137, Sr-90 and I-129 for more than 10,000 years. In the longer term, Ra-226 and Se-79 together with I-129 contribute most to the total dose. Note that the release of Ag-108m is identical to that in case C* since this release is controlled by the solubility of Ag and not by corrosion in the model. The early releases of Sr-90, Cs-137 and I-129 have increased in inversed relation to the IRF values for these nuclides; cases E and E* are similar to assuming 100% IRF for all nuclides. The decrease of I-129 at very long times is caused by depletion of I-129 from the repository and the host rock through outward transport and not through decay.

The dose from the far-field release is shown in Figure 13-66. The peak total dose is reduced by more than an order of magnitude compared to the near-field release, and doses from many of the short-lived or sorbing nuclides are considerably more reduced.

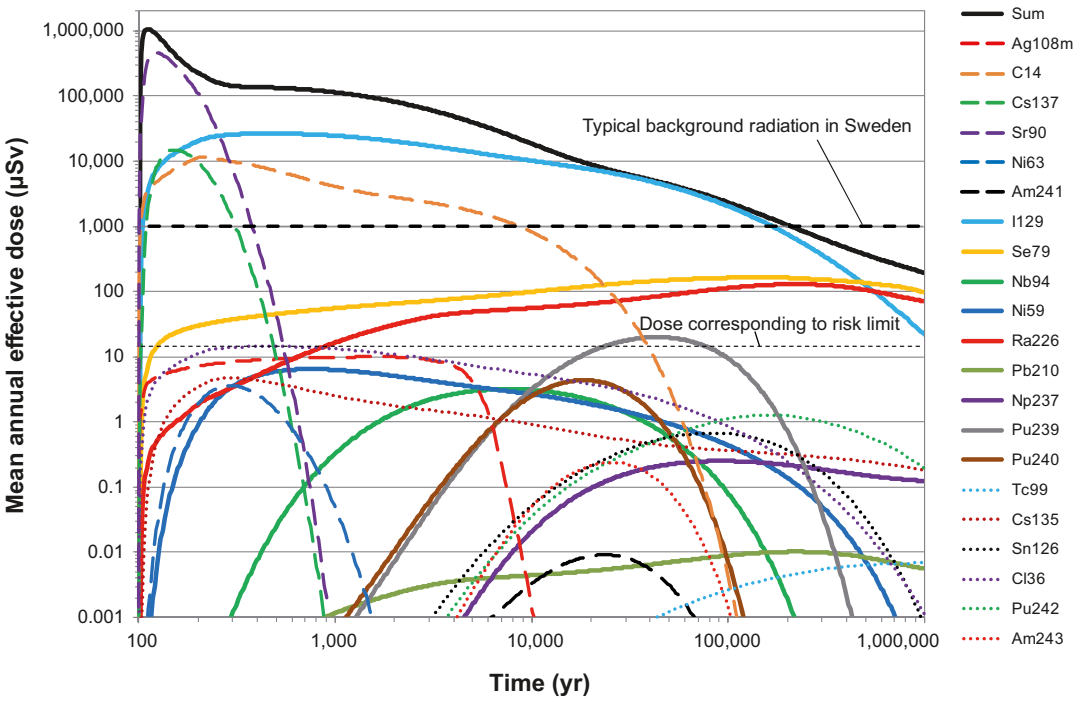


***Figure 13-65.*** *Near-field dose equivalent release for case E*, i.e. all canisters have an initial large defect in combination with a rapid fuel and metal conversion and the buffer is intact.*

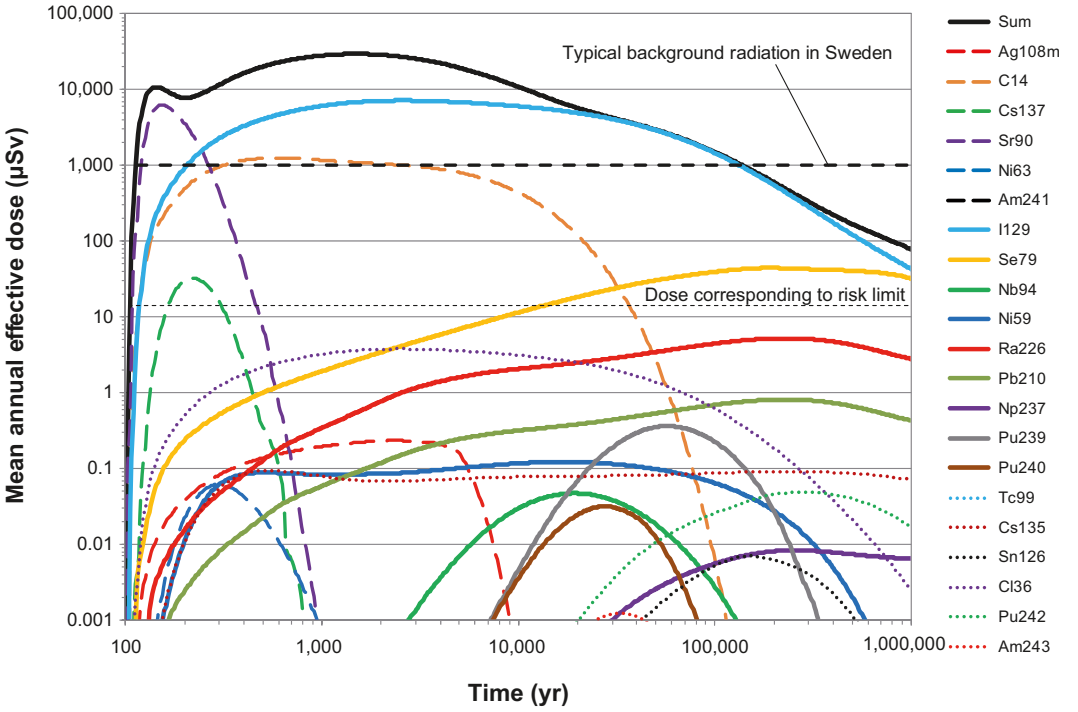


***Figure 13-66.*** *Far-field dose for case E, i.e. all canisters have an initial large defect in combination with a rapid fuel and metal conversion and the buffer is intact.*

### *Summary of results with distributed LDF values*

The summed dose for each case discussed above is given in Figure 13-67.

The following are noted.

After about 10,000 years, the doses for all cases are below the dose caused by typical background radiation in Sweden, except the case where retention properties of canisters, buffer and rock are all disregarded (case D*) and that with rapid fuel dissolution in combination with failed canisters (cases E and E*). The low flow and favourable groundwater chemistry of the rock and the presence of backfill and closure of the repository tunnel thus provide substantial protection from a fuel with unaltered dissolution rate.

If all canisters have large defects initially, but the barrier system is otherwise intact, case C, the peak annual dose to the most exposed individuals in the landscape does not exceed that caused by typical background radiation in Sweden, i.e. 1 mSv. Beyond 10,000 years this annual dose is less than an order of magnitude above the risk limit of 0.014 mSv.

If all canisters have large defects initially, and if also the buffer is assumed to be missing between the canister damage and the wall of the deposition hole, case D, the dose is around ten times the background radiation the first few hundred years, but is after 1,000 years quite similar to the case where the buffer is in place, case C. This suggests that the buffer is, from the point of view of total dose, not important as a retention barrier in this time perspective. However, a comparison between Figures 13-63 and 13-61 shows that the buffer has a considerable impact on near-field releases of many sorbing nuclides that do not dominate the dose.

With a large degree of damage to the canisters, the buffer missing and retention in the rock disregarded, case D*, the calculation results suggest annual doses in the Sievert range in the initial 1,000 years. This is a demonstration of the necessity of properly protecting man and the environment from

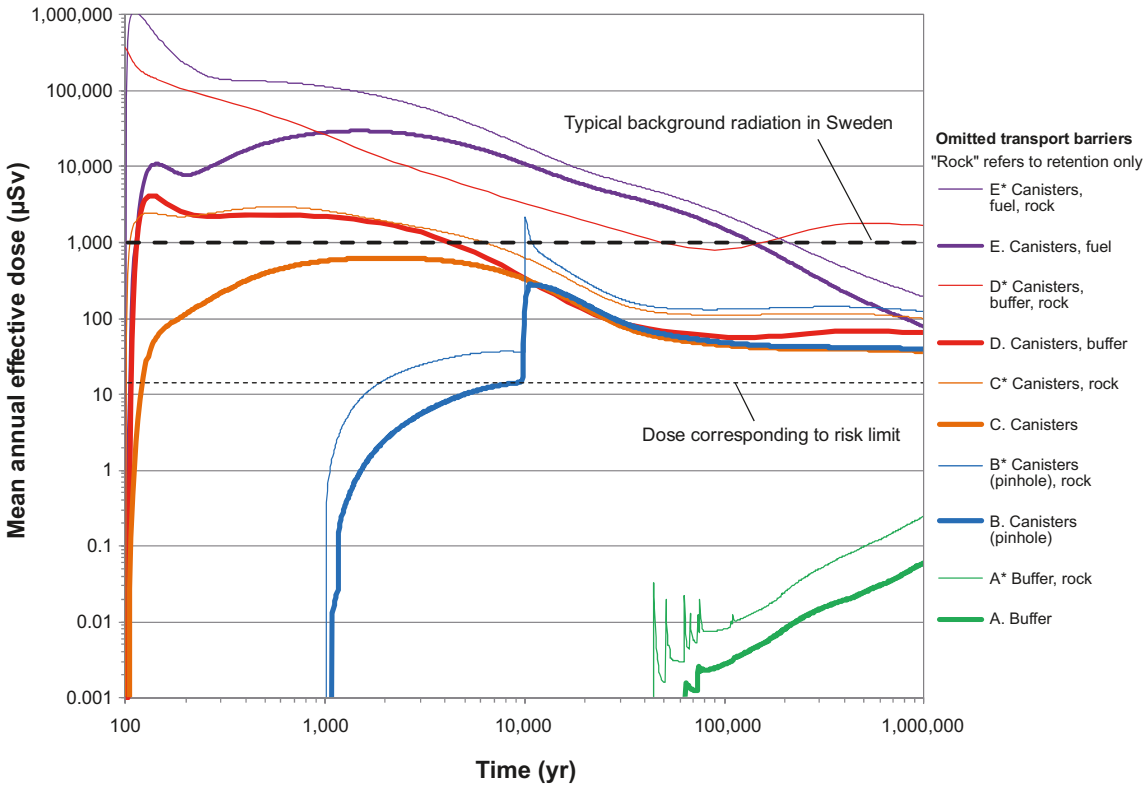


***Figure 13-67.*** *Results of stylised cases to illustrate loss of barrier functions. Note that an omission of the "rock" barrier in these cases refers to omission of retention of radionuclides in the rock fractures only, whereas the favourable, low flow rate at repository depth and the favourable geochemical conditions are still taken into account.*

the spent nuclear fuel, in particular in the 1,000 year time frame. It is noted that a more realistic treatment of corrosion of the AgInCd alloy of the PWR control rods would likely reduce the total dose, dominated by Ag-108m, by at least a factor of 10 the first 100 years and more between 100 and 1,000 years. Corrosion data for the control rods are discussed in the **Data report**, Section 3.2.7.

Beyond 10,000 years, the total dose is comparable to that caused by the background radiation even when neglecting the retention properties of all three barriers, case D*.

As expected, the cases with initial pinhole defects, case B, and that with large initial defects, case C, are quite similar beyond 10,000 years, when the pinhole defects are assumed to have grown into large defects. It is also noted that neglect of rock retention does not affect the total dose much for these cases after about 1,000 years. However, a comparison between Figures 13-62 and 13-61 shows that the rock has a considerable impact on far-field releases of many sorbing nuclides that do not dominate the dose.

A comparison of cases C and E shows the considerable containment function of the waste form for more than 100,000 years.

### *Summary of results with time dependent modelling of the biosphere*

As mentioned in the introduction, the LDF values are suited primarily to handle releases that are constant over periods of time that are comparable to the duration of an interglacial, i.e. typically 10,000 years. Therefore, the releases for most of the above cases were also evaluated with a fully time dependent modelling of the biosphere. Here, the releases are distributed in the landscape according to the time dependent spatial distribution of release points from the repository and the time dependent doses are presented, rather than a time dependent release converted to dose by a constant LDF value. This modelling was for assumed temperate conditions over a period of 60,000 years. The results are given in Figure 13-68. The solid curves are doses obtained with distributed LDF values (i.e. the same curves as in Figure 13-67) and the dashed curves are the corresponding doses obtained with time dependent modelling of the biosphere.

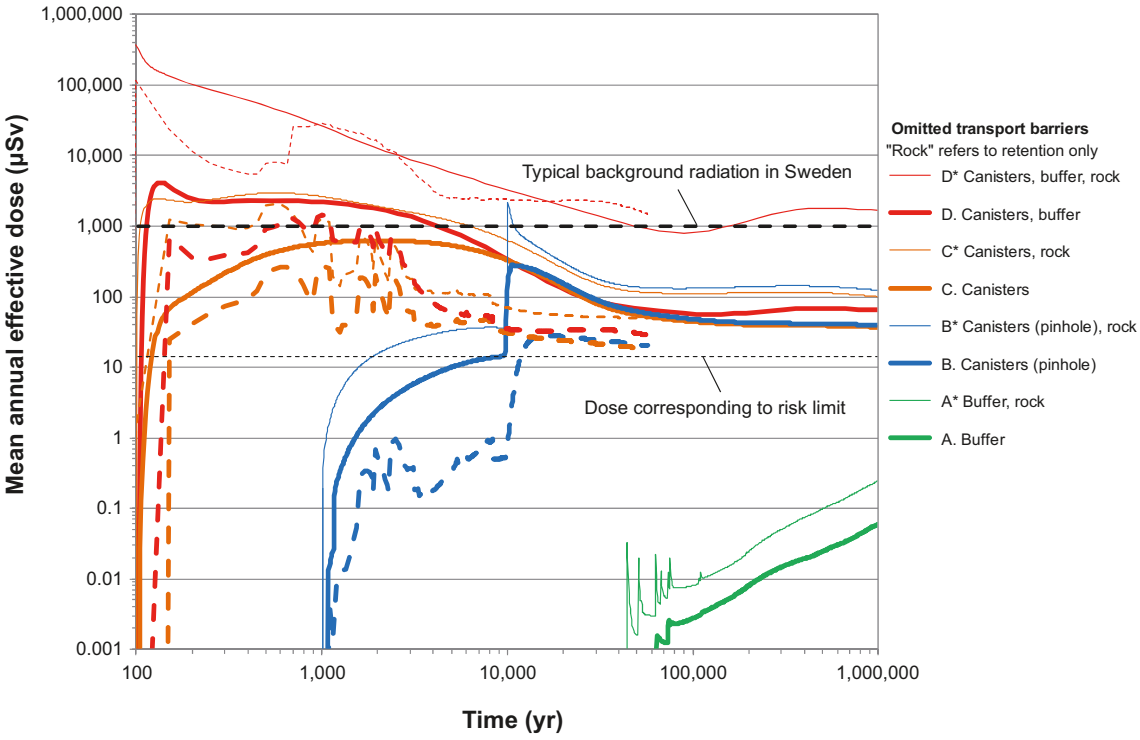


***Figure 13-68.*** *Results of stylised cases to illustrate loss of barrier functions.*
*Solid lines: Same as in Figure 13-67 (dose conversion through distributed LDF)*
*Dashed lines: Corresponding cases with time dependent dose modelling.*

The time dependent, dashed curves are generally within an order of magnitude of, but below, the curves obtained with LDF values. The one exception is the case where the retention properties of the canister, the buffer and the rock are all disregarded, case D*. Here, the time dependent doses from Ag-108m around 1,000 years and from C-14 around 20,000 years exceed those obtained using the LDF. This is caused by accumulation and delay effects in the biosphere: The release of Ag-108m from the near field decreases rapidly over the initial hundreds of years and hence also the release multiplied by the LDF value. In the time dependent case, some Ag-108m is accumulated in the landscape and this, in combination with the development of landscape objects, leads to a delayed release that exceeds the release obtained with the LDF values.

## 13.8 Radionuclide transport in the gas phase

Radionuclide transport in the gas phase, described by the processes Bu26, BfT22 and Ge25 for the buffer, the deposition tunnel backfill and the geosphere, is addressed in this section.

The formation of a gas phase is not possible for the corrosion scenario, since there is no buffer that can contain the gas in that case and the hydrogen is sufficiently soluble in water to be carried away by the advective flow i.e. gas can only accumulate if the buffer is intact. Hydrogen dissolution is a function of both the gas generation rate and water availability. The following description is valid for the shear load scenario, and the what-if cases treating the initial pinhole defect and the canister failure due to isostatic load.

The sealing properties of the buffer make it possible for a gas pressure to build up and a pulse of hydrogen gas to be released from a defective canister due to corrosion of the iron insert. Some radionuclides could potentially enter the gas phase and thereby be transported to the surface much more rapidly than would be the case for the aqueous pathway. In practice, only C-14 and Rn-222 are likely to enter the gas phase to any significant extent. (H-3 is expected to have decayed to insignificant levels before gas release could occur.)

It is assumed that if gas production exceeds the ability of the surrounding groundwater to take it into solution and transport it away from the canister that a pressure will build up within and adjacent to the canister. Based on experimental evidence /Harrington and Horseman 2003/, the bentonite is assumed to ultimately open by fracturing and release gas when the internal pressure exceeds 20 MPa. A rapid outflow would be expected until the pressure fell to values below ~10 MPa when the buffer would seal and further gas transport would be by diffusion (however, see also below). This means that half of the gas generated from corrosion inside the canister would be released instantaneously together with the radionuclides contained in that amount of gas. Neither the buffer nor the geosphere is expected to significantly delay the transport to the biosphere.

After the initial breakthrough pulse, the pathway is expected to stay open as long a there is substantial gas production in the canister. After the breakthrough pulse, the gas is expected to be released at the same rate as it is produced by corrosion. The buffer will only close if the gas production falls to levels where the gas can dissolve and diffuse away. This means that either the pathway will stay open as long as there is a gas source or the pathway will open and close, causing repeated gas cycles.

Due to the uncertainties of the chemical form of carbon in the spent fuel, it is pessimistically assumed that the entire inventory of C-14 can enter the gaseous phase. The full inventory of Rn-222 is also assumed to be in the gaseous phase.

The time for gas breakthrough is determined by the failure time of the copper shell and the corrosion rate of the canister insert (see Section 13.5.2). At the time of breakthrough, half of the inventory of C-14 and Rn-222 is taken to be released immediately to the biosphere. The remaining gaseous inventory (and the Rn-222 that is produced) is then taken to be released together with the gas that is produced continuously. However, this release is neglected, since it will be insignificant in comparison with the pulse release. If the release occurs in the first 10,000 years (unlikely) the release of C-14 would be about 25 GBq. A release of Rn-222 would be about 45 GBq if the release occurred after 100,000 years.

In /SKB 2006g, a/ the calculated exposures from pulse releases of C-14 and Rn-222 are presented. C-14 may be released as methane ($CH_4$) or carbon dioxide ($CO_2$). It is assumed that if C-14 is released as methane from the repository, it will be oxidised to carbon dioxide by soil organisms. There are several alternatives regarding the fate of methane in its travel towards the surface:

1. Nothing happens and it will be released as gas to the atmosphere.
2. Microorganisms incorporate methane in the biosynthesis of other organic substances (i.e. not an oxidation). Eventually this organic carbon will be released by respiration to $CO_2$. This may occur in the rock as well as in the regolith.
3. Other microorganisms utilise the carbon source and produce $CO_2$ (i.e. an oxidation). This may occur in the rock as well as in the regolith.
4. The produced $CO_2$ will either degass to the atmosphere or be used in the photosynthesis by aquatic or terrestrial algae/plants. This may occur in surface ecosystems.

Thus, if a pessimistic approach is taken, the release as $CO_2$ will at least be handled in the biosphere model before it is released to the atmosphere. Methane released to the atmosphere is unlikely to be utilised. However, the potentially increased mobility of a gas in the geosphere is not considered.

Radon is a noble gas and will not undergo chemical transformations. Two exposure cases are considered, one outdoors where radionuclides can be inhaled or consumed via uptake in plants in an area of 10,000 $m^2$, subject to a wind speed of 2 m/s and a mixing height of 20 m, the other inhalation of radionuclides indoors in a house with a volume of 1,000 $m^3$ and a ventilation rate of 2 $h^{-1}$. For C-14, exposure may occur via inhalation or ingestion, for Rn-222 only inhalation of Rn-222 and its radioactive daughter products needs to be taken into account. A summary of the results is given in Table 13-11. It is noted that no account for decay in transit from the repository to the surface is taken, making the results for Rn-222, with a half-life of only 3.8 days, further pessimistic.

If the gas pressure is built up during a period of glaciation, the hydrostatic pressure from the ice has to be added to the gas breakthrough pressure. This may lead to internal pressures of about 50 MPa inside the canister. If the retreat of the ice is rapid, this could lead to pressure drops of around 40 MPa and consequently 80% of the gaseous inventory would be instantaneously released.

The highest dose from a gas pulse of Rn-222 occurs in buildings. It is below the regulatory limits for an annual average life time risk for a repository, and it is considerably lower than the consequences of today's limit of 200 Bq/$m^3$ for radon in buildings in Sweden, which gives about 2 mSv/y.

**Table 13-11. Calculated annual mean life time risk from pulse releases of C-14 and Rn-222 for a single canister /SKB 2006g/, updated with inventory data used in SR-Site.**

| Pathway | C-14 (μSv) (25 GBq release) | Rn-222 (μSv) (45 GBq release) |
|---|---|---|
| Ingestion | 0.033 | – |
| Inhalation outdoors | $5.5 \cdot 10^{-5}$ | 0.20 |
| Inhalation indoors | 0.0035 | 8.3 |

## 13.9 Risk summation

### 13.9.1 Introduction

The calculated risk as a function of time is an essential component of the compliance demonstration for the final repository. This section gives a summation of the risk contributions from the analysed scenarios.

According to the previous sections of this chapter, radiological consequences may arise for the scenarios in which canister failures due to copper corrosion and due to shear load occur. In the following, each of these is considered in isolation and then the total risk associated with the repository is discussed.

It is noted that also the main scenario gives rise to consequences, but that these are assessed as equal to the central corrosion case and subsumed under the corrosion scenario.

As a basis for the discussion, a number of dose curves calculated in the analyses of the corrosion and shear load scenarios are converted to risk and shown in Figure 13-69. The effective dose to risk conversion factor of 0.073 $Sv^{-1}$ has been used in accordance with SSM's regulations (Appendix A).

### 13.9.2 Risk associated with the corrosion scenario

Consequences have been calculated for the six corrosion variants identified in the corrosion scenario, each with base case transport data and conditions. For the central corrosion variant, five additional cases have been calculated exploring alternative transport conditions and data.

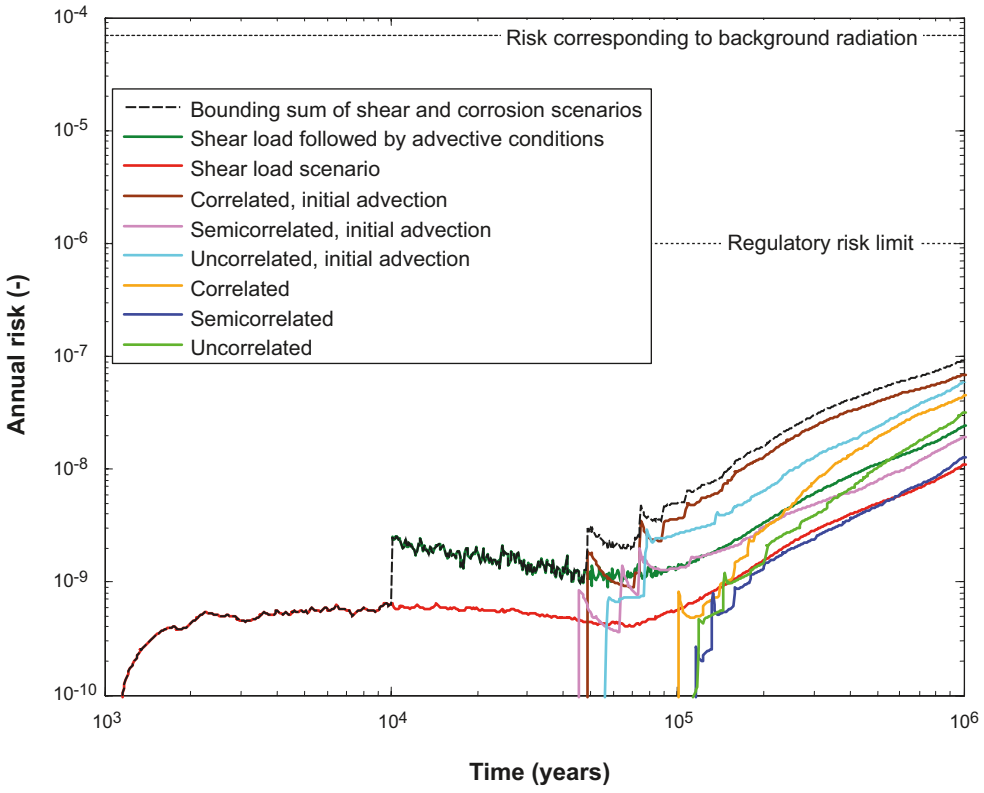


***Figure 13-69.*** *Risk curves, expressed as annual individual risk. Several alternatives for the corrosion scenario are shown, and two for the shear load scenario. The bounding, dashed curve is the sum of the curve for the shear load failure followed by advective conditions (dark green) and the curve for the variant of the corrosion scenario yielding the highest risk (brown). The risk associated with the main scenario is subsumed under the corrosion scenario as it is equal to the semi-correlated case (blue).*

### *Consideration of the six corrosion variants*

The uncertainties associated with the erosion process are illustrated by the differences between the case with the SR-Site erosion model and the case with the highly pessimistic assumption of initial advection, for a given hydrogeological DFN model. The initial advection cases put an upper bound on the possible consequences in terms of corrosion of the buffer erosion process. It bounds the impact on risk of uncertainties regarding the buffer erosion process, and covers impacts of gradually deteriorating functions of the buffer. It is, however, a highly pessimistic upper bound on the consequences. It is, therefore, argued that the central corrosion cases are reasonable and cautious representations of the risk associated with the corrosion scenario. However, since it is not possible to quantify several of the uncertainties associated with the erosion process, the pessimistically bounding cases of initial advection are also included as alternatives in the risk summation, noting that this case is clearly unrealistic as concerns the erosion process.

It is also noted that there are three corrosion variants where no advective conditions occur in deposition holes and where no canister failures due to corrosion occur. The risks associated with these variants are thus zero.

The uncertainties associated with the hydrogeological DFN model are illustrated by the differences between the cases with three different hydrogeological DFN models for a given assumption regarding buffer erosion. The semi-correlated DFN model is more compatible with the understanding of the water transmissive properties of fractures in crystalline rock. The uncorrelated and the fully correlated models are extreme variants of the correlation between fracture size and transmissivity, and are both seen as unrealistic. However, since the semi-correlated model gives the lowest consequences, and since it is not possible to quantify the degree of correlation in a strict sense, the uncorrelated and the fully correlated models are included as alternatives in the risk summation.

### *Consideration of the five alternative transport cases*

Regarding alternative transport conditions, five alternatives to the central corrosion case have been calculated for the semi-correlated hydrogeological DFN model (not included in Figure 13-69). The two cases with mobile thorium in the near field and inclusion of solubility limits yield somewhat lower dose consequences than the central corrosion case. The three calculations of time dependent flow and colloid facilitated transport in the geosphere suggest that the dose consequences are lowered if groundwater flow, rock $K_d$-values and LDF values are allowed to vary in accordance with a simplified climate development for the reference evolution. Furthermore, the dose consequences may temporarily be increased by a factor of less than three with colloid facilitated transport and for the highly pessimistic assumption that the colloid concentration is 10 g/L all along the geosphere transport path for 30 percent of both the temperate and the glacial climate domains, see Figure 13-34.

Based on these results, the central corrosion case, with base case transport conditions, is seen as a reasonable, cautious representation of the risk associated with the corrosion scenario for the semi-correlated hydrogeological DFN model, taking uncertainties in transport conditions into account. This also suggests that the other five corrosion variants, which have only been calculated for base case transport conditions, are appropriate representations with respect to assumptions regarding radionuclide transport.

### *Contribution from the IRF pulse*

The annual risk associated with the IRF pulse contribution is obtained by multiplying the contribution of the IRF to the mean annual dose (calculated as for the central corrosion case, see Table 13-6 in Section 13.5.4) by 0.073 $Sv^{-1}$. The result of this procedure is shown for the case yielding the highest risk, i.e. that with the fully correlated hydrogeological DFN model and assuming initial advection in Table 13-12. As seen in the table, the highest annual risk is $4.7 \cdot 10^{-10}$, i.e. more than three orders of magnitude below the risk limit. By comparing the pulse risk in each time interval to the risk curve, it is concluded that the pulse releases give negligible contributions to the calculated risk. They do, however, need to be considered in the account of risk dilution, see below. It is also noted that this treatment assumes that temperate conditions are prevailing. Including probabilities of periglacial and glacial climate conditions would reduce the calculated risk further.

**Table 13-12. Risk associated with the pulse release for the case with the correlated hydrogeological model and initial advection. See Section 13.5.4 for further explanation.**

| Time interval [yr] | $p_{Fail}$ | $p_{Expo}$ | $D_{TotPulse}$ [μSv] | Annual risk |
|---|---|---|---|---|
| 0–100,000 | $4.3 \cdot 10^{-2}$ | $4.3 \cdot 10^{-4}$ | 6.3[a] | $2.0 \cdot 10^{-10}$ |
| 100,000–200,000 | $1.1 \cdot 10^{-1}$ | $1.1 \cdot 10^{-3}$ | 5.9 | $4.7 \cdot 10^{-10}$ |
| 200,000–300,000 | $1.2 \cdot 10^{-1}$ | $1.2 \cdot 10^{-3}$ | 5.5 | $4.7 \cdot 10^{-10}$ |
| 300,000–400,000 | $9.0 \cdot 10^{-2}$ | $9.0 \cdot 10^{-4}$ | 5.3 | $3.5 \cdot 10^{-10}$ |
| 400,000–500,000 | $8.2 \cdot 10^{-2}$ | $8.2 \cdot 10^{-4}$ | 5.0 | $3.0 \cdot 10^{-10}$ |
| 500,000–600,000 | $7.3 \cdot 10^{-2}$ | $7.3 \cdot 10^{-4}$ | 4.8 | $2.6 \cdot 10^{-10}$ |
| 600,000–700,000 | $6.0 \cdot 10^{-2}$ | $6.0 \cdot 10^{-4}$ | 4.6 | $2.0 \cdot 10^{-10}$ |
| 700,000–800,000 | $9.0 \cdot 10^{-2}$ | $9.0 \cdot 10^{-4}$ | 4.5 | $3.0 \cdot 10^{-10}$ |
| 800,000–900,000 | $1.2 \cdot 10^{-1}$ | $1.2 \cdot 10^{-3}$ | 4.4 | $3.7 \cdot 10^{-10}$ |
| 900,000–1,000,000 | $8.2 \cdot 10^{-2}$ | $8.2 \cdot 10^{-4}$ | 4.3 | $2.5 \cdot 10^{-10}$ |

[a]This value determined for the time of the first canister failure, 48,000 years.

### 13.9.3 Risk associated with the shear load scenario

The two risk curves associated with the shear load scenario shown in Figure 13-69 are obtained from the calculated mean annual dose for the case with an intact buffer according to Figure 13-48 and the case with advective conditions in the deposition hole Figure 13-52, applied after a pessimistically chosen 10,000 years for reaching advective conditions through buffer erosion. These cases are both bounding with respect to the pessimistic treatment of the probability of earthquakes, of the transport conditions in the near field and to the neglect of geosphere retention. Between the two, the case with advective conditions is bounding.

In addition, since the occurrence of earthquakes is a stochastic process, it cannot be entirely ruled out that a detrimental earthquake would occur during the initial 1,000 years. The probability that one out of the 6,000 canisters has failed at the end of the initial 1,000 year period is estimated at $2.4 \cdot 10^{-5}$, see Section 10.4.5, i.e. 40,000 repositories, each with 6,000 canisters would have to be constructed in order for there to be an expectation of one failure during the initial 1,000 years. Despite this extremely low probability, a risk contribution was calculated for the first 1,000 years, with the result that the expected dose rate is around 0.001 μSv/yr, see Figure 13-49 in Section 13.6. This corresponds to an annual risk of $10^{-10}$/yr, i.e. below the risk scale of Figure 13-69.

Regarding the risk contribution from the IRF pulse, a similar treatment to that above can be made, where only the $p_{Fail}$ values would differ. Since these values are lower for the shear load scenario (the total failure probability over the entire one million year assessment period is 0.079) and since the risk for the corrosion scenario is very small, no such account is given.

### 13.9.4 Risk dilution

The issue of risk dilution is discussed in the methodology Section 2.6.2 and needs to be addressed both for the corrosion scenario and for the shear load scenario. Doses in both these scenarios are accounted for as a continuous contribution and as relatively short pulse contributions.

The total doses from the continuous contributions have, for a fixed failure time, an initial peak of limited duration followed by an increasing curve that generally grows beyond the value of the initial peak. Since this means that the maximum dose occurs at the end of the one million year assessment time, risk dilution is not an issue for the continuous contributions; the maximum risk is experienced by the same hypothetical generation living at the end of the assessment period irrespective of failure time. This is verified by comparing the peak-of-the-mean value (0.177 μSv/yr) to the mean-of-the-peaks value (0.179 μSv/yr) for the central corrosion case (see Section 2.6.2 for an explanation of these concepts). For the shear load scenario, the peak-of-the-mean is 0.15 μSv/yr and the mean-of-the-peaks is 0.28 μSv/yr.

Regarding the pulse contributions, the situation is different. Doses occur immediately after the canister failure and last short time intervals compared to the assessment time. The probabilistic treatment of the mean annual dose according to Table 13-12 leads to risk dilution as a consequence of the distribution of failure times. The peak doses given in Table 13-5 for the central corrosion case are an illustration of such doses. To address risk dilution for such short term releases, Appendix 1 to SSMFS 2008:37, reproduced in Appendix A of this report, suggests that risk dilution can be addressed by calculating an "accumulated short-term risk" (SKB's terminology) as

$$D_{TotPulse}(T) \cdot \int_{T_0}^{T} f(\tau)d\tau \cdot 0.073\ \mathrm{Sv}^{-1}$$

and comparing this entity to the risk limit. In this expression, $T_0$ is the time of closure of the repository, and $f$ is the time dependent frequency of canister failures. The results of such a calculation for the corrosion (correlated case with initial advection) and shear load scenarios are shown in Figure 13-70. The result shows the peak risk future individuals could be exposed to once during the one million year assessment period. The calculated entities in the figure are not comparable to the risk curves for the continuous releases and cannot be said to represent a true risk in the same sense as the continuous release. Rather, they represent a formal way of addressing the issue of risk dilution for short-term releases. The sum curves in Figure 13-70, and their total if they were to be added, are below the risk limit and hence the risk criterion is fulfilled also for this bounding way of addressing risk dilution.

It is also noted that both the LDF values used for the continuous releases and the pulse LDF values are derived by assuming that all of the release occurs to each biosphere object and the values obtained for the object giving the highest doses is then used for LDFs and pulse LDFs. There is hence no risk dilution due to uncertainty as to the biosphere object to which the release will occur.

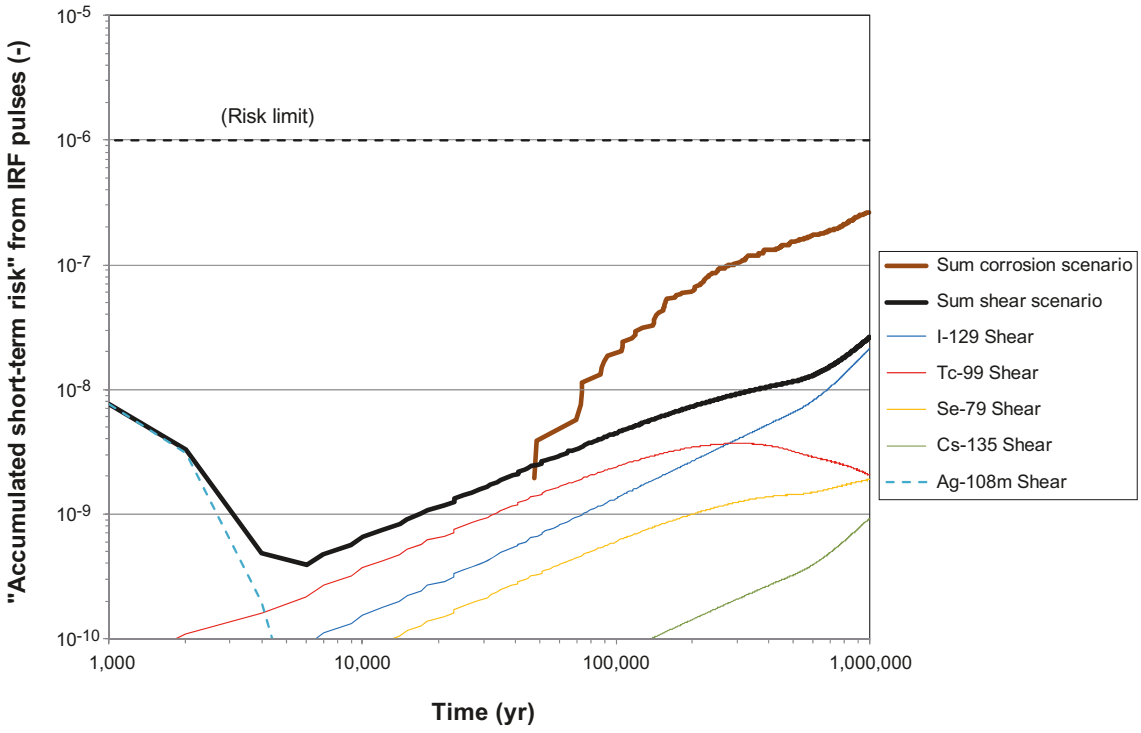


***Figure 13-70.*** *Accumulated short-term risk from IRF pulses in the corrosion (thick, brown curve) and shear (thick, black curve) scenarios. Also contributions from individual nuclides are shown for the shear scenario. The distribution of canister failure times for the corrosion scenario is taken from the fully correlated case assuming initial advection.*

### 13.9.5 Extended discussion of risk for the initial 1,000 years

#### *Introduction*

According to SSMFS 2008:37, a more detailed account of the protective capability of the repository is required for the initial 1,000 years after closure. Since the radiological hazard of the waste is highest for this time period it is particularly important to account for repository evolution, safety functions and risk in this time frame. Such an account is provided in the following, largely based on material from previous parts of this main report.

#### *Initial state*

All canisters are assessed to be tight at deposition. The initial copper coverage is discussed in the account of the initial state of the canister in Section 5.4.3. The initial minimum copper thickness is given as 47.5 mm in Table 5-9. Taking also the occurrence of local internal defects in the copper shell into consideration, no canisters are assessed to have local reductions exceeding 20 mm. This is the manufactured and inspected thickness of the corrosion barrier after the final machining of the canister components.

Also, according to Section 5.5.3, the buffer is expected to be emplaced according to the reference design leading to an initial state where the buffer will acquire its long-term safety related properties after water saturation.

#### *Modelling of the general evolution of the repository*

As required by SSM's regulations, many aspects of the repository evolution have been modelled in detail for the initial 1,000 years. This concerns the thermal, mechanical, hydraulic and chemical evolutions, as well as effects on the buffer and the canister. Detailed accounts are given in Sections 10.2 (the excavation and operational phases) and 10.3 (the initial period of temperate climate after closure). Also the biosphere development is modelled in detail during this time period.

According to Sections 10.2.5 and 10.3.13, no canister failures due to corrosion during the excavation/operational phase and during the initial 1,000 years of the reference evolution are expected. As concluded in Section 10.3.13 the total amount of copper corrosion during the excavation and operational phases and the first 1,000 year period can be estimated to be less than 1 mm, when taking into account the contributions from residual oxygen in the repository and possible microbial sulphate reduction as well as the contribution from sulphides in the bentonite and backfill. Given the initial state of the copper coverage above, the margin to failure due to corrosion is hence very large. No challenge to this conclusion was found in the analysis of the corrosion scenario in Section 12.6.

The same applies to failures due to isostatic loads on the canisters, briefly treated in the reference evolution Section 10.3.13 and further in the scenario addressing this failure mode in Section 12.7. The isostatic pressures during the initial 1,000 years are considerably lower than those that may occur during later, glacial conditions, that the canister is designed to withstand. Pressures from uneven swelling of the bentonite buffer have been addressed in the design analysis of the canister (Section 5.4), with the conclusion that the probability that the canister will not withstand the loads is negligible.

Shear loads on the canister may occur as a consequence of large earthquake induced secondary shear movements in fractures intersecting deposition holes. Although the likelihood for large earthquakes is higher during glacial rebound, it cannot be entirely ruled out that a detrimental earthquake would occur during the initial 1,000 years.

The probability that one out of the 6,000 canisters has failed at the end of the initial 1,000 year period is estimated at $2.4 \cdot 10^{-5}$, see further Section 10.4.5, i.e. hypothetically 40,000 repositories, each with 6,000 canisters would have to be constructed in order for there to be an expectation of one failure during the initial 1,000 years.

### *Calculated risk for the initial 1,000 years*

Of the three identified failure modes of the canister, i.e. failure due to corrosion, due to shear load and due to isostatic loads, corrosion and isostatic load induced failures can thus be ruled out with large margins for the first 1,000 years.

Failures due to shear load are extremely unlikely according to the above, and since no probability limit for excluding a risk is adopted in SR-Site, a risk contribution was calculated for the first 1,000 years, as reported in Section 13.6.2, with the result that the mean annual dose is at most around 0.001 μSv/yr corresponding to a risk of $10^{-10}$/yr, see Figure 13-49. This analysis builds on detailed modelling of the biosphere development and radionuclide transport in the developing landscape during the initial 1,000 years, as required by SSM's regulations.

It is noted that this calculation case is based on several pessimistic assumptions regarding the probability of shear failure, the modelling of the near field and in the neglect of geosphere retention (Table 13-13). Additional pessimistic assumptions of relevance for the initial 1,000 years concern the time to establish water contact with the fuel, assumed pessimistically to be 100 years neglecting the build-up of a counter pressure in the canister interior as water enters the canister and neglect of the containment function of the Zircaloy cladding.

Based on the above, it is concluded that the analysed repository at Forsmark complies with the regulatory risk criterion during the initial 1,000 years after closure with a considerable margin.

### *Discussion of the barrier system for the initial 1,000 years*

According to extensive analyses in the corrosion scenario, even a hypothetical initial absence of the buffer in all deposition holes does not lead to failure of canisters for tens of thousands of years. It is thus not relevant to discuss hypothetical buffer malfunction further in the 1,000 year perspective. For the same reason, the retention properties of the host rock are not further discussed here.

Regarding the canister, as mentioned above, all canisters are assessed to be tight at deposition. To discuss the barrier system in a 1,000 year perspective, a hypothetical case where a canister is not initially tight, may be considered. In such a case, there are several factors that contribute to safety according to the following.

- For the fuel:
  - The containment function of the fuel matrix.
  - The containment function of the structural parts of the fuel elements.
- For the canister:
  - The time required to fill the canister with water.
  - The containment function of the Zircaloy cladding.
- For the buffer:
  - Its contribution to delaying water saturation and limiting the rate at which the canister fills with water.
  - radionuclide retention.
- For the host rock:
  - Its favourable hydrogeological properties, contributing to slow water saturation and limited release rates.
  - Radionuclide retention.

In the following, each of these factors is briefly discussed.

#### The containment functions of the fuel matrix and of the structural parts of the fuel elements

These factors were discussed in the analyses of cases with assumed, complete losses of barrier functions in Section 13.7.3. There, it was concluded that the waste form has a considerable containment function for more than 100,000 years.

**The time required to fill the canister with water**

In the **Data report** it is shown that for a hypothetical, circular penetrating defect with a radius of 2 mm it will take more than 20,000 years to fill the canister with water. To cover any shape of the defect, the delay time is pessimistically estimated to be at least 1,000 years, used as the pessimistic delay time in the hypothetical pinhole case analysed in Section 13.7.2.

The derivations of all these delay times neglects the effect of gas generated by corrosion of the insert by the penetrating water, which could lead to substantially longer delay times /Bond et al. 1997/.

**The buffer's contribution to delaying water saturation and limiting the rate at which the canister is filled with water**

A prerequisite for water to enter into the canister is a fully water saturated buffer. The saturation times for both backfill and buffer are likely to range from a few tens of years to several thousand years, as a consequence of the rock properties (matrix hydraulic conductivity and presence and characteristics of fractures) at Forsmark. Consequently, in many deposition hole positions, no water would be expected to come into contact with the waste during the first 1,000 years even if there were an initial defect in the canister.

**The containment function of the Zircaloy cladding**

According to the **Fuel and Canister process report**, available data suggest a life of the cladding tubes of at least 100,000 years. Although Zircaloy is highly resistant to uniform corrosion, due to its potential susceptibility to local corrosion in groundwaters and to hydrogen induced cracking, cladding is not assumed to constitute a barrier to radionuclide release from the fuel in SR-Site. However, even a cladding with small cracks or corrosion defects would offer a large mass-transport resistance for water to get into contact with the fuel and for dissolved radionuclides to exit into the canister void.

**Radionuclide retention in the buffer**

The retention properties of the buffer are exemplified in the calculation cases with assumed complete losses of barrier functions in Section 13.7.3. A comparison between Figures 13-63 and 13-61 shows that the buffer has a considerable impact on near-field releases of many sorbing nuclides.

**The host rock's favourable hydrogeological properties**

In addition to contributing to long saturation times mentioned above, the limited flow rates at the deposition positions limits the release rate of radionuclides from the near field if releases occur from the canister.

**Radionuclide retention in the rock**

The retention properties of the rock are exemplified in the calculation cases with assumed complete losses of barrier functions in Section 13.7.3. A comparison between Figures 13-62 and 13-61 shows that the rock has a considerable impact on far-field releases of many sorbing nuclides.

### 13.9.6 Conclusions

The bounding, dashed curve in Figure 13-69 is the sum of the risk associated with the shear load scenario and that associated with the corrosion scenario. The former is represented by the case with advective conditions and the latter by the correlated case with initial advection, both of which give the highest risks within their scenarios. (Within the scenarios the cases are mutually exclusive, meaning that only one from each scenario should be used in the summation. Since the main scenario is represented by the central corrosion variant, also the main scenario is included as subsumed under the bounding corrosion case.)

Other scenarios did not yield any contributions to the calculated risk. In the account of combinations of scenarios and phenomena in Section 12.9.3 it was concluded that the consequences of a shear load failure followed by buffer erosion needs to be assessed and this is done in the bounding case of the shear load scenario. All relevant risk contributions are, therefore, assessed to be included in Figure 13-69.

Since the bounding curve in Figure 13-69 is below the risk limit for the duration of the one million year assessment period, the analysed KBS-3 repository at the Forsmark site is assessed to fulfil the regulatory risk criterion. Risk dilution was shown not to challenge this conclusion.

It is furthermore concluded that a more realistic risk may be anywhere in the area below the bounding curve, down to zero risk based on the zero results of the three cases with no erosion and a situation where no canisters would fail due to shear movements induced by large earthquakes, which could be reached if somewhat less pessimistic assumptions could be defended for the shear load scenario.

It is also noted that through the use of LDF factors to transform releases to doses, it is in the risk assessment implicitly assumed that the landscape to which the releases occur is always fully populated, including the object where the highest dose is calculated to occur and at the time when this occurs. Furthermore, long periods of glacial and submerged conditions are expected where no doses to humans occur since the site is not habitable. This has not been taken into account in the risk summation. Rather, temperate conditions yielding the highest doses are assumed throughout.

Factors that have the greatest impact on overall risk are identified in the sensitivity analyses e.g. in Section 12.2.2 (buffer erosion), 12.6.2 (canister corrosion) and 13.5.11 (consequences for the corrosion scenario). These are summarised in the next section where also references to sections discussing steps that could be taken to reduce or mitigate these impacts are given.

It is also noted that the calculated risk is one of several indicators of repository safety for distant time frames. Four additional indicators have been applied in Section 13.5.8 with the result that the calculated consequences are well below the reference values to which they are compared. This is further discussed in the conclusions of the assessment, see Section 15.3.

A KBS-3 repository at Forsmark is assessed to fulfil the regulatory risk criterion for the initial 1,000 years with a considerable margin. The barrier system has a number of functions that contribute to safety in a hypothetical case where the canister is assumed to be initially defective. Several of the factors would, with cautious assumptions, alone prevent any releases during the initial 1,000 years for an initially defective canister. This relates particularly to the time required for water to get into contact with the fuel elements and the integrity of the Zircaloy cladding.

Finally, it is noted that the risks due to both the corrosion scenario and to the shear load scenario are increasing at one million years. This is primarily caused by the increasing probabilities for barrier failures for the later parts of the assessment period, whereas radioactive decay plays a minor role for the development since the dose dominating nuclides, in particular the parent nuclides of Ra-226, are very long-lived. It is not seen as meaningful to continue the calculations beyond one million years (see further Section 14.5), but an account of the consequences for a number of hypothetical cases where all canisters fail early in the assessment period is given in Section 13.7.3. For the hypothetical case where all canisters are failed, where the buffer is absent and where retention in the rock is disregarded, the calculated risk at one million years is comparable with that caused by the background radiation. This indicates a bound on the development of the risk curve beyond one million years, when the extent of barrier failures may be expected to increase.

## 13.10 Summary of uncertainties affecting the calculated risk

### 13.10.1 Summary of main uncertainties affecting the calculated risk

A number of issues relevant for long-term safety are associated with considerable uncertainties. This is inevitable in an assessment of situations far into the future and where the parts of the system are not fully known. The following is an account of how main uncertainties affecting the calculated risk are handled in SR-Site with indications, through reference to the feedback Sections 15.4 to 15.7, of the potential of reducing them in later stages of the repository programme. The account deals with factors affecting the two scenarios contributing to the calculated risk, i.e. the corrosion scenario and the shear load scenario. A discussion of whether formal expert elicitations could be a means of reducing these uncertainties is provided in Section 13.10.2.

In the corrosion scenario, canister failures, and hence risk contributions, occur only in cases where the buffer has been eroded to the extent that advective conditions prevail in part of the deposition hole, leading to enhanced corrosion rates. In the sensitivity analyses of the extent of buffer erosion in Section 12.2.2, of canister corrosion for advective conditions in Section 12.6.2 and of dose consequences from canisters failed due to corrosion in Section 13.5.11, the main uncertain factors listed in Table 13-13 were identified. Means of reducing these uncertainties and the potential impact on risk this may have is also accounted for in the table. Regarding the shear load scenario, many of the uncertain factors are related to the assessment of the likelihood of earthquake induced shear failures in Section 10.4.5 and to the evaluation of consequences of such failures in Section 13.6. These are also listed in Table 13-13.

It is noted that, in addition to the factors mentioned in the table, more developed deposition position rejection criteria have a large potential of reducing risk. This is, however, a design issue rather than an uncertain factor in the risk calculations in SR-Site, see further Sections 14.3 and 15.3.5.

**Table 13-13 Main uncertain factors affecting the calculated risk and future plans for their reduction.**

| Factor | Type of uncertainty | Handling in SR-Site risk calculations | Means of reducing uncertainty | Potential impact on calculated risk | Plans in section |
|---|---|---|---|---|---|
| Mechanistic understanding of buffer erosion. | Conceptual. | Pessimistic.<br>Use of state-of-the-art model as central case. Demonstration of low negative impact on corrosion for a bounding case of initial advection.<br>Bounding case of initial advection included in risk summation and used to demonstrate risk compliance. | Further research. | Can only reduce risk, since bounding case is included in risk summation.<br>Potential to lead to exclusion of buffer erosion in the corrosion scenario would result in exclusion of canister failures in the corrosion scenario according to analyses in SR-Site. | 15.7.3 |
| Groundwater salinity; low salinity required for buffer erosion to occur. | Site data, conceptual understanding. | Pessimistic.<br>Cautious approach in modelling of salinity at high-flow deposition positions.<br>Demonstration of limited negative impact on erosion and corrosion for a bounding case of dilute conditions 100% of time.<br>Cases with initial advective conditions bound impact of uncertainties regarding dilute conditions in risk calculation. | Additional groundwater sampling.<br>See also groundwater flow as salinity evolution is strongly related to groundwater flow. | Can only reduce risk, since bounding case is included in risk summation.<br>Potential to lead to exclusion of buffer erosion from the corrosion scenario would result in exclusion of canister failures in the corrosion scenario according to analyses in SR-Site. | 15.6.9 |
| Groundwater flow.<br>Flow at deposition positions affects erosion and corrosion.<br>Flow in host rock affects radionuclide transport. | Conceptual as well as spatial and temporal variability. | Probabilistic modelling.<br>Input data from comprehensive hydrogeological modelling of several concepts (correlation structures), in turn based on evaluation of conceptual uncertainty in site modelling. Each model generates an input data distribution covering spatial variability. Each distribution propagated to risk calculations. Distribution yielding highest risk used to demonstrate risk compliance.<br>Temporal variability addressed by stylised glaciation case. Simplified results used in variant case of risk calculation and shown to have limited impact on overall risk when considered together with biosphere alterations. | Further development of models based on data from future underground characterisation. (Sensitivity to spatial variability difficult to reduce, other than by deposition hole rejection criteria.) | Limited, if developed model is within bounds of conceptual models used in SR-Site. | 15.6.4<br>15.6.5 |
| Sulphide concentrations over time; affect corrosion. | Incomplete understanding of causes for range in site data; both spatial variability and conceptual uncertainty. Incomplete understanding of temporal development. | Probabilistic.<br>Use of measured range of values at the Forsmark site combined with distribution of groundwater flow at deposition positions to obtain mean number of failed canisters.<br>Incomplete understanding of temporal development; pessimistically handled. | Additional site data.<br>Further research. | Potentially considerable reduction in risk if spatial variability could be reduced and/or demonstrated to reflect temporal variability at deposition positions (see Section 12.6.2, subheading ‘Groundwater concentrations of sulphide’). | 15.6.9<br>15.7.4 |
| Probability of earthquake; affects probability of shear failure. | Conceptual; incomplete understanding. | Pessimistic.<br>Frequency range, (several estimates) determined and upper bound of range chosen for risk calculations | Further research. | May further reduce risk. | 15.7.4 |

| Factor | Type of uncertainty | Handling in SR-Site risk calculations | Means of reducing uncertainty | Potential impact on calculated risk | Plans in section |
|---|---|---|---|---|---|
| Probability that a zone hosts an earthquake; affects probability of shear failure. | Conceptual uncertainty. | Pessimistic.<br>i) All zones affecting the repository assumed to host the largest earthquake compatible with their size.<br>ii) Zone with largest impact chosen for risk calculation. | Further research. | May further reduce risk. | 15.6.1<br>15.6.7<br>15.7.4 |
| Probability of a deposition position being intersected by a large fracture. | Conceptual uncertainty, spatial variability, insufficient information. | Pessimistic.<br>All DFN models identified in site modelling evaluated. Variant yielding highest probability of intersection used in risk calculation. | Further research, methodology development, data from underground investigations. | May further reduce risk. | 15.6.2<br>15.6.3<br>15.7.4 |
| Efficiency in deposition hole acceptance criteria. | Measurement techniques not sufficiently tested for this context. | All EFPC fractures assumed to be found.<br>No credit taken for additional signatures of large fractures; these may potentially be more efficient than EFPC in identifying deposition holes to reject. | Further development of methods to identify critical structures. | May further reduce risk. | 15.6.2 |
| Potential for damage if shear is larger than 5 cm; affects probability of shear damage. | Conceptual as well as spatial and temporal variability. | Pessimistic.<br>i) Case with angle of intersection and point of impact yielding maximum impact on canister used as basis for risk calculation.<br>ii) Upper bound on buffer density in design premise used; no credit for demonstrated lower maximum density in reference design, nor of distribution of densities. | Additional mechanical analyses to cover cases where the angle and the buffer density are more beneficial.<br>Probabilistic handling of impact location, angle of intersection and buffer density.<br>Revised design premises for buffer density. | Would further reduce risk. | 15.7.2<br>15.5.3, 15.5.7 |
| Failure criteria in assessment of canister response to shear loads; affects probability of shear damage. | Conceptual. | Pessimistic.<br>i) Pessimistically chosen, local, failure criterion for cast iron insert in design analysis of canister used as criterion for global failure.<br>ii) No allocation of containment potential to copper shell when insert fails locally. | Further development of criteria for global failure of canister.<br>Further development of models for copper creep behaviour.<br>Implementation in shear response modelling. | Would further reduce risk. | 15.7.2 |
| Hydraulic properties of shearing fracture and retention in migration pathway; affects retention. | Incomplete understanding of hydraulic properties resulting from shearing of a fracture. | Pessimistic.<br>Near field: i) Canister failure location assumed to fully coincide with location of shearing fracture; ii) Shear assumed to increase transmissivity of intersecting fracture such that its *Qeq* value is too high to contribute to transport resistance in the near field; iii) Geometric transport resistance of fracture/buffer intersection neglected.<br>Far field: No credit taken for radionuclide retention in the geosphere. | Analyses of the impact on the flow system if only the shearing fractures were affected. | Potentially reduction in risk since only the shearing fracture, and not the fractures it connects to, would be affected. A local increase of transmissivity in a fracture network would not necessarily increase flow or reduce retention. | |

| Factor | Type of uncertainty | Handling in SR-Site risk calculations | Means of reducing uncertainty | Potential impact on calculated risk | Plans in section |
|---|---|---|---|---|---|
| Fuel dissolution rate. | Incomplete knowledge. | Probabilistic.<br>Pessimistically derived distribution of rates from experiments. | Further research. | Reduction in risk if more favourable distribution can be defended. | 15.7.1 |
| Corrosion release rate. | Incomplete knowledge. | Probabilistic.<br>Pessimistically derived distribution of rates from experiments and dimensions.<br>Instantaneous corrosion of Ag-alloy in PWR control rods. | Further research, in particular for corrosion rate of Ag-alloy in PWR control rods. | Considerable reduction in corrosion related peaks for individual nuclides if more favourable distribution can be defended. Limited impact on overall risk. | 15.7.1 |
| Flow related transport parameters. | See groundwater flow. (Uncertainties in transport parameters are mainly due to uncertainties in flow. Conceptual understanding of channelling is an additional uncertain factor.) | See groundwater flow. | See groundwater flow. (Further data has impact on flow that influences transport parameters.) | Limited, if developed model is within bounds of conceptual models used in SR-Site. | 15.7.4 |
| Landscape specific dose conversion factors. | Conceptual. | Deterministic values, with pessimistic handling of several uncertainties, see further Section 13.2.6. | Further research and model development. | Potential to reduce risk by several orders of magnitude for specific nuclides. | 15.7.5 |

### 13.10.2 Candidate issues for formal expert elicitations

In planning SR-Site, an evaluation of candidate issues for expert elicitations was made and the following criteria were used to determine whether an issue could be considered for an elicitation.

- The issue should be associated with large uncertainties that have a considerable impact on the assessed level of safety.
- A formal expert elicitation can be deemed to contribute to the reduction of these uncertainties in addition to what is achievable through other means established in the methodology for the assessment (evaluation of conceptual uncertainties in the **Process reports**, of data uncertainty in the **Data report**, through quality assured modelling, etc. all of these leading to a well motivated and often pessimistic handling of the issue in the assessment).

As pointed out in Section 2.8.5 the conclusion of the evaluation was that, although a number of uncertainties could in principle be amenable to a formal expert elicitation, no issue was identified for which both the above criteria apply. Based on the sensitivity analyses of the calculated risk in SR-Site, presented in this chapter, the evaluation of candidate issues for expert elicitation can be updated. As was the case for SR-Can, it is the corrosion and the shear load scenarios that contribute to risk and consequently it would only be uncertainties related to these scenarios that would be of interest for formal expert elicitations. In particular, the issues listed in Table 13-13 are of interest to evaluate. In general, there is no issue in Table 13-13 that was not recognised already at the completion of SR-Can.

#### *Candidate issues for the corrosion scenario*

According to Table 13-13 issues related to the corrosion scenario mainly concern mechanistic understanding of the buffer erosion process, groundwater flow, evolution of groundwater salinity and sulphide levels, releases rates from the spent fuel and the flow related transport parameters. These are assessed in the following.

Mechanistic understanding of the buffer erosion process: This issue has been the target for intense research since it was identified as crucial for the safety evaluation in the SR-Can project. A group of experts recruited internationally has studied the process experimentally and theoretically. Several expert reports and a summary report have been produced in the project and regular seminars where the entire expert group has discussed intermediate results and possible ways forward have been held. The project reports have also been reviewed internationally. It is difficult to conceive of an additional group of experts that could, in a limited time, evaluate these findings in such a way that the years of efforts by this expert group could be further refined or qualified for the safety assessment. Although this is an important issue for safety, it is, on the above grounds, not deemed as suitable for an expert elicitation.

Neither uncertainties related to the fraction of a glacial cycle during which erosion is active nor the buffer mass loss required to reach advective conditions in a deposition hole, nor the strongly related corrosion geometry are sufficiently important for the overall safety evaluation to qualify these issues as candidates for a formal expert elicitation. Furthermore, they are both evaluated by cautious interpretation of results of direct modelling and are thus addressable through the standard methodology for the assessment. Similar arguments can be put forward regarding the concentration of canister corroding agents over a glacial cycle.

The distributions of the equivalent flow rate, of the Darcy flux and of the flow related transport parameters for the ensemble of deposition holes are affected by both conceptual uncertainties and spatial variability. In particular the Darcy flux has a considerable impact on the safety evaluation through its importance for the erosion and corrosion processes. These factors have been evaluated in several steps including the collection of site data, comprehensive modelling of the hydraulic properties of the site including the consideration of several conceptual models and data uncertainties, modelling of the hydraulic evolution within the safety assessment, and a thorough evaluation of the resulting distributions in the **Data report**. All these steps have been carried out by several expert groups with overlapping membership. The results have been externally reviewed. It is not deemed fruitful to attempt to further substantiate these findings, achieved through years of reviewed efforts, by a formal expert elicitation.

All data relating to the calculation of radionuclide transport and dose for the failed canisters are thoroughly evaluated in the **Data report**. A dominating factor, the fuel alteration rate, is evaluated in a dedicated report by a group of international experts forming the most important input to the evaluation in the **Data report**. The expert report has also been subject to peer review. It is difficult to conceive of an additional group of experts that would, in a limited time, reach better founded conclusions.

#### *Candidate issues for the shear load scenario*

According to Table 13-13 issues related to the shear load scenario mainly concern the probability of earthquakes; the probability that a zone hosts an earthquake; the probability of a deposition position being intersected by a large fracture, the efficiency of deposition hole acceptance criteria, the potential for canister failure if the shear is larger than 5 cm, the failure criteria in assessment of canister response to shear loads and the hydraulic properties of shearing fracture and retention in the migration pathway. As is clear from the table, these issues are generally handled by making pessimistic assumptions, combined with or evaluated by cautious interpretation of results of direct modelling and are thus accessible through the standard methodology for the assessment. For example:

- The probability of earthquake is handled by adopting a pessimistic frequency range based on estimates by a wide range of experts and input where an upper bound of range is chosen for the risk calculations.
- The probability that a zone hosts an earthquake and the resulting secondary movements in large fractures has been assessed by extensive modelling and final estimates and the zone with largest impact is chosen for risk calculations.
- The probability of a deposition position being intersected by a large fracture is handled by using the variant yielding highest probability of intersection in the risk calculation and a pessimistic assessment on the possibility of finding large fractures during detailed investigations.
- The potential for damage if the shear is larger than 5 cm has been assessed by extensive modelling and further modelling efforts appears a viable approach in case current pessimistic assumptions on failure need to be replaced by a more differentiated approach.

In short, the impact of remaining uncertainties on risk is bounded, and if there is a requirement to reduce the estimated risk by more knowledge, other means than formal expert elicitation appear more promising.

#### *Conclusions*

In conclusion, although a number of uncertainties could in principle be amenable to a formal expert elicitation, no issue has, in this evaluation, been identified for which both i) the calculated risk is highly sensitive to the uncertainty and ii) the uncertainty can be expected to be significantly reduced through a formal expert elicitation.

The procedures established for the qualification of processes and data in SR-Site, the considerable and concerted research activities on critical issues, the comprehensive site modelling by expert groups including thorough evaluation of uncertainties and the formulation of a confidence statement, the reviewing by external experts, and the pessimistic handling of many factors in the assessment all contribute to this conclusion. Also, the fact that the pessimistically calculated total risk in SR-Site is well below the regulatory limit for the entire one million year assessment period has influenced the view on the absence of a need for further reduction of uncertainties through expert elicitations.

## 13.11 Conclusions

The analyses of the retardation potential of the repository reported in this chapter have led to the following conclusions.

For the corrosion scenario, the calculated mean doses are at least one order of magnitude below the dose corresponding to the regulatory risk limit. In the most pessimistic variants of this scenario, the first canister failures and hence the first releases occur after around 50,000 years. In these variants,

the mean dose is about two orders of magnitude below the regulatory limit at 100,000 years and about one order of magnitude below the limit at one million years.

Different numbers of canister failures in the corrosion scenario propagated from the analysis of containment potential led to variations in calculated mean doses within one order of magnitude. Also uncertainties in the conceptualisation of the near-field transport conditions have a similarly limited impact on the calculation results.

For the shear load scenario, the calculated mean dose for the initial 1,000 years is negligible in comparison to the dose corresponding to the regulatory risk limit. Between 1,000 and 100,000 years, the calculated mean dose is about three orders of magnitude below the limit and then increases to become about two orders of magnitude below the limit at one million years.

The overall risk summation shows that a KBS-3 repository at Forsmark is assessed to comply with the regulatory risk criterion over the entire one million year assessment period. The margin to compliance is about one order of magnitude when pessimistically bounding a number of uncertainties in the risk calculation. Risk dilution has been analysed and found to not challenge the conclusion regarding compliance.

In the corrosion scenario, the geosphere provides only a modest attenuation of the dose-equivalent release from the near field. The safety relevant role of the geosphere is here rather i) its contribution to the containment function of the repository through favourable geochemical and hydrological conditions limiting the number of failed canisters and ii) through its contribution to limiting the releases from the near field by providing reducing conditions and hence limiting the fuel dissolution rate. In the shear load scenario the geosphere contributes to containment through favourable mechanical conditions and, as in the corrosion scenario, to limiting the fuel dissolution rate by providing reducing conditions.

Sensitivity analyses of the probabilistic calculation results show that input uncertainties for the fuel dissolution rate, the failure time of the canister and the flow related transport resistance in the geosphere account for most of the uncertainty in the calculated dose. Additional uncertainties are addressed through the formulation of variant calculation cases regarding e.g. different conceptual hydrogeological models or through pessimistic assumptions regarding, e.g. the likelihood of canister failure due to shear load. The influences of all important uncertainties on the calculated risk are evaluated based on the outcome of the risk summation, and possibilities of reducing the uncertainties are discussed as feedback from the assessment.

Application of four alternative indicators to risk show, for the central corrosion case, that release rates are about three orders of magnitude below the activity constraints issued by the Finnish regulator STUK, that the calculated concentrations in ecosystems at Forsmark from repository releases of Ra-226 are about three orders of magnitude below measured concentrations of naturally occurring Ra-226 at Forsmark and that geosphere fluxes caused by Ra-226 releases from the repository are about two orders of magnitude below naturally occurring fluxes of Ra-226 at the site, as estimated from site data. Similar conclusions are drawn for other relevant calculation cases.

Dose rates to non-human biota are well below the screening dose rate recommended in the ERICA Integrated Approach, meaning that the calculated radionuclide releases are not expected to lead to any detrimental biological effects on individuals of species found, or likely to be found, at the site. Hence, populations, communities and ecosystems are assured an adequate degree of protection.

Simplified analytical models applied to key variants of the corrosion and shear load scenarios are in good agreement with the numerical results. This enhances confidence in the calculation results i) by providing a quality assurance check on the numerical modelling of dose equivalent releases and ii) by demonstrating that releases for the cases in question are controlled by relatively simple processes that are straightforward to understand and model.

# 14 Additional analyses and supporting arguments

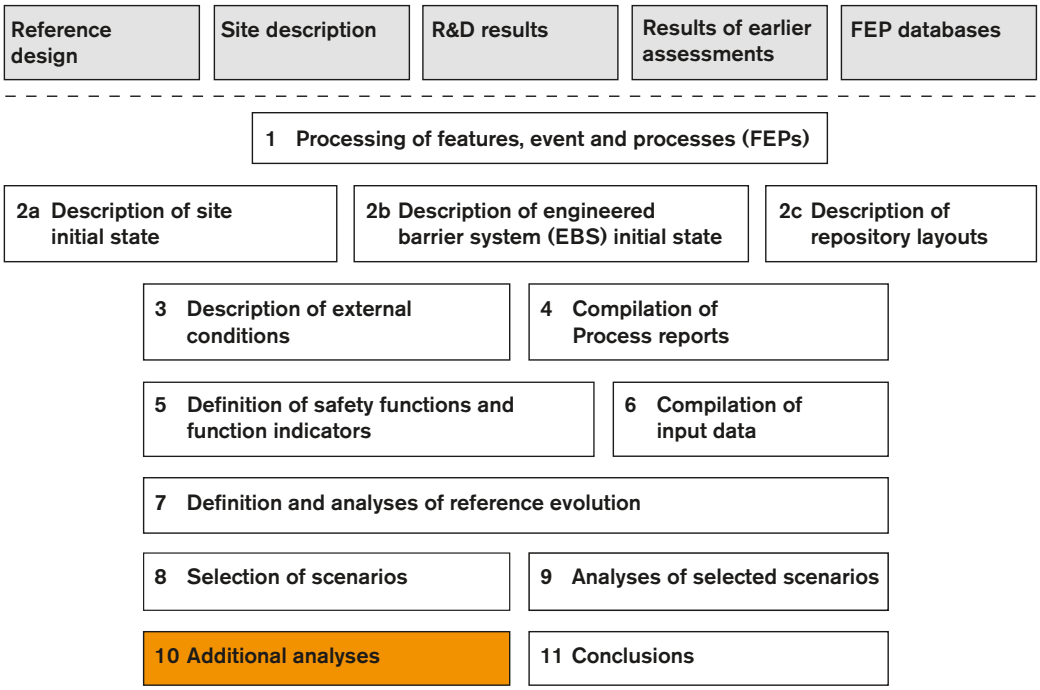


***Figure 14-1.*** *The SR-Site methodology in eleven steps (Section 2.5), with the present step highlighted.*

## 14.1 Introduction

In this chapter, additional analyses required to complete the safety assessment according to the methodology described in Chapter 2 are documented. The contents of the chapter are as follows.

Section 14.2 gives an account of the methodology used for the analysis of scenarios related to future human actions, followed by a summary of the analyses and their results.

An account of the additional analyses required in order to demonstrate optimisation and the use of best available technique is given in Section 14.3.

In Section 14.4, verification that FEP's omitted in earlier parts of the assessment are negligible in light of the completed scenario and risk analysis is undertaken.

Section 14.5 gives a brief account of the time period beyond one million years.

Finally, Section 14.6 gives an account of how natural analogues support the analyses and conclusions in the safety assessment.

## 14.2 Scenarios related to future human actions

### 14.2.1 Introduction

According to the scenario selection described in Section 2.5.8 and Table 11-1, two main categories of scenarios related to future human actions, FHA, were distinguished, scenarios related to a sealed repository and scenarios related to an unsealed or incompletely sealed repository. These categories of FHA scenarios were previously identified in SR-Can /SKB 2006a/, but only the former category was further analysed. In SR-Site, both categories are addressed and the analyses are provided in the **FHA report** and summarised in the following subsections.

The potential exposure to large quantities of radiotoxic material is an inescapable consequence of the deposition of spent nuclear fuel in a final repository, and consequently intrusion into the repository needs to be considered in repository design and safety assessment. To reduce the probability of inadvertent intrusion and resulting exposure to the spent fuel, in line with ICRP recommendations /ICRP 2000/, the following countermeasures have been applied in the repository siting and design.

- The repository is to be located at a site not containing exploitable natural resources.
- The repository depth is selected to be substantially greater than the depth of interest for water supply and more generally occurring sub-surface facilities.
- The repository will be sealed so as to make subsequent entry difficult.
- Measures will be taken to preserve institutional control and information on the repository for as long as possible.

Intrusion in the post-closure phase of institutional control and beyond is primarily prevented through the design of the repository. In addition to that there will presumably continue to be safeguards measures, preservation of information (record keeping) and possibly some sort of markers placed at the site. During the institutional control period, activities at the site have to be restricted or directed if they have the potential to interfere with or hinder surveillance of the site, but this does not necessarily rule out all forms of access to the area. Measures and land use restrictions during the period of institutional control are exemplified and further discussed in the **FHA report**.

The fact that the repository contains fissile materials is an important aspect. Regarding today's situation, control of safeguards measures will most likely be upheld by national as well as international agencies (SSM, IAEA and Euroatom) /Fritzell 2006, pp 11–14/. Furthermore, the authorities in their review of SR-Can /Dverstorp and Strömberg 2008/ maintain that the state, rather than SKB, is expected to be responsible for the supervision and monitoring of the repository after sealing /SKI 2007/.

### 14.2.2 Principles and method for handling FHA scenarios

Man is dependent on, and influences, the environment in which he lives. After closure of the repository, future generations should be able to utilise the repository site according to their needs without jeopardising their health. In the case of a final repository of the KBS-3 type, there are, however, inevitably examples of activities that, if carried out carelessly or without knowledge of the repository, could result in exposure to radiotoxic elements. Examples of such activities are drilling of deep boreholes and construction of tunnels, shafts or rock caverns to great depth within the repository area. Globally occurring human activities, such as the emission of greenhouse gases or pollution, may also affect the repository. There is, therefore, an international consensus that future human activities shall be considered in safety assessments of deep geological repositories /NEA 1995, ICRP 2000/.

Human actions of concern are those with a potential impact on the repository's safety functions. Human actions can be divided into different categories e.g. "recent and ongoing" or "future"; "global" or "local" /Wilmot et al. 1999/ and "inadvertent" or "intentional" /NEA 1995, ICRP 2000/. Recent and ongoing, local, intentional activities are considered in the description of the local ecosystems (see Sections 4.10 and 10.3.3). Mishaps can be regarded as local, inadvertent activities and the ones occurring during the excavation and operational phases are considered in the general handling of uncertainties in the main and additional scenarios. The global, recent and ongoing emissions of greenhouse gases have no direct impact on the repository, but may affect the climate and is considered in the global warming variant of the reference evolution, Section 10.6. That leaves global pollution other than the emission of greenhouse gases and local, future activities for further analysis.

If people in the future for some reason deliberately enter the repository they are responsible for the consequences of their actions. Society today cannot protect future societies from their own actions if the latter are aware of the consequences /NEA 1995, ICRP 2000/. However, in developing a system for final disposal of spent fuel, as much consideration as possible should be given to future generations. Based on these generally accepted principles and the Swedish Radiation Safety Authority's, SSM's, regulations concerning safety in connection with the disposal of nuclear material and nuclear waste

/SSM 2008a/ and on the protection of human health and the environment in connection with the final management of spent nuclear fuel and nuclear waste /SSM 2008b/, the future human actions considered in this part of the safety assessment are restricted to global pollution and actions that:

- Are carried out after the sealing of the repository.
- Take place at or close to the repository site.
- Are unintentional, i.e. are carried out when the location of the repository is unknown, its purpose forgotten or the consequences of the action are unknown.
- Impair the safety functions of the repository's barriers.

A problem when discussing future human actions is that the future of man and society cannot be predicted. On time spans of tens of years or more, the best we can do is to identify some important parameters or factors and combine them to explore possible outcomes. On time spans of hundreds of years and longer the future of man and society is, however, unpredictable and the uncertainties are indeterminate or unspecified, i.e. the outcome space is not known and cannot be described. It is for instance impossible to determine what scientific discoveries will be made the next 1,000 years. One commonly applied approach to handle this and to avoid speculation as to the future is to assume that the future conditions of society and technical practice are essentially the same as today /NEA 1995/. This provides a practical and comprehensible procedure to illustrate the potential hazards related to future human actions at the repository site which is applied in this assessment.

In the General Guidance to their Regulations, SSM recommends the inclusion of direct intrusion by means of drilling as well as examples of activities that indirectly may affect the safety functions in the safety assessment /SSM 2008b/. They also recommend basing the future human activity scenarios on current habits and technical practise. Regarding the consequences, SSM in its regulations SSMFS 2008:37 /SSM 2008b/ states that only doses due to the impaired repository need to be calculated, whereas the consequences for the individuals performing the intrusion need not to be assessed. This is not in agreement with the direction of SSMFS 2008:21 /SSM 2008a/ which states that cases to illustrate damage to humans intruding into the repository should be included. The need of a stylised calculation of injuries to humans who intrude into the repository was also pointed out by the authorities in their review of SR-Can /Dverstorp and Strömberg 2008/ and this direction has been followed in the analyses of FHA scenarios in SR-Site.

Finally, in line with SSM's General Guidance /SSM 2008a/, future human actions and their impact on the repository are evaluated separately, and are not included in the reference evolution or the risk summation.

#### *Method*

Human actions can affect the repository in different ways. The impact of the action on the repository as well as its consequences is the result of a combination of technical and societal factors. Examples of such factors are the level of technology and knowledge, existence of institutional control, infrastructure and settlement pattern and food supply system. For the purpose of providing as comprehensive a picture as possible of different human actions that may impact the deep repository as well as their background and purpose, the following approach has been used, see the **FHA report**.

- Technical analysis:
  Identifies human actions that may impact the safety functions of the repository, describes such actions and, in technical terms, justifies that they may occur.
- Analysis of societal factors:
  Identifies framework scenarios (framework conditions) that describe feasible societal contexts for future human actions that can affect the radiological safety of a deep repository.
- Choice of representative cases:
  The results of the technical and societal analyses are put together and one or several illustrative cases of future human activities are chosen.
- Scenario description and consequence analysis of the chosen cases.

The three first steps are mainly based on work carried out in conjunction with the safety assessment SR 97 /SKB 1999a/. Results from the development of the SKB FEP database, Chapter 3, and a review of some relevant literature published after SR 97 are also considered, as well as the authorities review

of SR-Can /Dverstorp and Strömberg 2008/. The last step is an update and extension of the work conducted for SR-Can, also here considering the authorities review of SR-Can /Dverstorp and Strömberg 2008/. A summary of the work is provided in the following subsections.

### 14.2.3 Technical and societal background

#### *Technical analysis*

The technical analysis was based on the results from a workshop carried out within the framework of SR 97 /Morén et al. 1998/. For SR-Can, the relevance of the results from the workshop regarding recent technical developments was reviewed based on consultation with technical experts within SKB. Furthermore, an audit against the NEA FEP database and linked national projects resulted in some minor amendments and the addition of the action "subsurface bomb or blast" /SKB 2006e/. The complementary FEP work conducted for SR-Site (see Chapter 3) did not result in any modifications to the list of human actions developed for SR-Can.

The human actions identified for SR-Can and also applicable for SR-Site are listed in Table 14-1. Based on their principal impacts, the actions are divided into the categories human actions with thermal (T), hydraulic (H), mechanical (M) or chemical (C) impact. From the technical analysis it was concluded that actions that include drilling and/or construction in rock are those with the greatest potential influence on the repository. Furthermore, the repository site was regarded as more favourable than other places for building a heat store or heat pump plant, due to the heat generated by the spent fuel. For the other actions, the repository site was considered to be equivalent to, or less favourable than, other places with similar bedrock.

**Table 14-1. Human actions that may impact repository safety.**

| Category | Action |
|---|---|
| Thermal impact | T1: Build heat store* |
| | T2: Build heat pump system* |
| | T3: Extract geothermal energy (geothermics)* |
| | T4: Build plant that generates heating/cooling on the surface above the repository |
| Hydrological impact | H1: Construct well* |
| | H2: Build dam |
| | H3: Change the course or extent of surface water bodies (streams, lakes, sea) and their connections with other surface water bodies |
| | H4: Build hydropower plant* |
| | H5: Build drainage system |
| | H6: Build infiltration system |
| | H7: Build irrigation system* |
| | H8: Change conditions for groundwater recharge by changes in land use |
| Mechanical impact | M1: Drill in the rock* |
| | M2: Build rock cavern, tunnel, shaft, etc* |
| | M3: Excavate open-cast mine or quarry* |
| | M4: Construct dump or landfill |
| | M5: Bomb or blast on the surface above the repository |
| | M6: Subsurface bomb or blast* |
| Chemical impact | C1: Store/dispose hazardous waste in the rock* |
| | C2: Construct sanitary landfill (refuse tip) |
| | C3: Acidify air, soil and bedrock |
| | C4: Sterilise soil |
| | C5: Cause accident resulting in chemical contamination |

* Includes or may include drilling and/or construction of rock cavern.

#### *Analysis of societal factors*

Prevailing societal conditions are of importance both for the possible occurrence of inadvertent human actions impairing repository safety and for evaluation of their consequences. Important issues are why the disruptive action is being carried out and contemporary societal conditions such as general knowledge and regulations. These primarily humanistic and socio-economic questions were analysed at a workshop for SR 97 (see the **FHA report** and /SKB 2006e, Morén et al. 1998, SKB 1999a/). Experts in the fields of cultural geography, history of science and technology and systems analysis participated in this workshop. So called framework scenarios that describe plausible societal contexts for future human actions with an influence on the radiological safety of the deep repository were formulated. The framework scenarios were developed by means of morphological field analysis /Morén et al. 1998, Ritchey 1997/, a group- and process-oriented interactive method for structuring and analysing complex problem fields that are non-quantifiable, contain non-determinable uncertainties and require a judgmental approach.

From the study of societal aspects, it was concluded that it is difficult to imagine inadvertent intrusion, given a continuous development of society and knowledge. Owing to the long time horizon, however, it is not possible to rule out the possibility that the repository and its purpose will be forgotten, even if both society and knowledge make gradual progress. Nor is it possible to guarantee that institutional control over the repository site will be retained in a long time perspective. With a discontinuous development of society, where the development of society and technology contains a sudden, large change, it seems likely that knowledge will be lost and institutions will break down. It is also reasonable to assume that knowledge is lost if society degenerates.

### 14.2.4 Choice of representative cases

#### *Sealed repository*

It is probable that the repository site will be used by people in the future. Human actions that influence radiological safety and are carried out without knowledge of the repository and/or its purpose cannot be ruled out. Actions that influence the containment or the function indicators for containment are the most severe, followed by actions that influence retardation or the function indicators for retardation. Changes in the biosphere may result in an increase in the doses to which human beings may be exposed if the containment has been violated and there are leaking canisters in the repository.

A KBS-3 repository will be situated at a minimum depth of 400 metres in the rock, and the suggested repository depth is below 450 m at Forsmark. One reason for this is the wish to locate the repository in an environment where the containment of the fuel will be retained even in the event of extensive changes on the surface. Changes considered in the determination of the depth for a KBS-3 repository are natural changes and changes caused by man. Examples of natural changes are change of the repository's location in relation to the sea, and the presence of permafrost and ice sheets, see further Sections 5.2.2 and 14.3.4. These natural changes will also influence factors of importance for future human actions at the site e.g. settlement, society and man's opportunities to use the repository site.

Large uncertainties are associated with the development of technology and society. To reduce speculation, the NEA working group on assessment of future human actions /NEA 1995/ as well as SSM in the general guidelines to their regulations /SSM 2008b/ suggested an approach based on present-day knowledge and experience. However, applying this approach literally or with consistency there would be no inadvertent human actions yielding radiological consequences. The current activities at the repository site will not impact the safety. Drilling to great depth is solely performed to investigate the site for repository construction. If this were to result in hazardous conditions or circumstances, measures to avoid or minimise consequences for man and environment would be taken. There is another dilemma in the assessment of future human actions. In order to quantify the consequences, detailed descriptions of the human actions are required. Such descriptions will inevitably include speculations as to the course of actions which always can be questioned. However, both the technical and societal analyses can, even if they do not depict conditions that exist today, be said to be based on current practise and their results can be used for the selection of representative cases. When describing scenarios based on the selected cases, speculation is avoided by assuming the most severe among simplified and plausible alternatives.

All actions in Table 14-1 influence the migration of radionuclides in the biosphere. However, actions that are performed on or near the surface, down to a depth of a few tens of metres, are judged not to be able to directly affect the technical barriers and the containment of the fuel. This applies to the actions

T4, H2, H3, H4, H5, H6, H7, H8, M3, M4, C2, C3, C4 and C5 (though some of them could include drilling of relatively deep wells). Activities near the surface that belong to categories M and H are deemed to have less influence on the repository than natural changes in conjunction with future climate change. Of the actions that entail a chemical influence (C2–C5), acidification of air and land (C3) has been studied in most detail. In realistic cases of acidification by atmospheric sulphur and carbon dioxide, the environment at repository depth is not affected /Nebot and Bruno 1991, Wersin et al. 1994b/. Soil layers and bedrock are judged to work efficiently as both a filter and buffer against other chemical compounds as well.

Bombing or blasting on the ground surface above the repository (M5) cannot affect the containment of the spent fuel, except if blasting is done with a powerful nuclear weapon. Such an event implies a nuclear war and the consequences of the war and the blast itself would be much greater than the consequence of the hypothetical leakage from the repository. However, sub-surface testing of nuclear bombs (M6) close to the repository may violate the containment in a similar way to an earthquake. The test would need to be carried out close to the deposited canisters. Testing of bombs could be combined with identified societal contexts to form a plausible scenario. However, tests of nuclear bombs require knowledge of nuclear fission and its associated risks and are carried out below the surface to avoid environmental impact. Since measurements are carried out in connection with the tests it is plausible that if a detectable leakage from the repository exists, it would be distinguished from the releases from the bomb and handled by a society performing sub-surface weapon tests.

Some of the actions in Table 14-1 can, besides influencing radionuclide transport, indirectly influence the containment of the spent fuel if they affect the capability of the geosphere to provide favourable hydrological or chemical conditions. Such actions would have to be performed directly above or very close to the repository and include drilling and/or construction in the rock (M1, M2). These categories include actions that have to do with heat extraction (T1, T2, T3), well drilling (H1) and disposal of hazardous waste in the rock (C1). Hydropower plants (H5) and open-cast mines and quarries (M3) may also involve drilling or rock works at great depth. Before a rock facility is built, drilling is carried out to investigate the rock. Therefore, if present day technology is applied, all these cases involve drilling in the rock.

Large rock facilities adjacent to the repository are deemed to be out of the question in a short time perspective, i.e. within a few hundred years, for several reasons. For example, the repository is itself a large rock facility, the only one of its kind in Sweden that is very unlikely to be forgotten over such a short time span. Institutional control can be expected to endure on this timescale. The enumerated actions that encompass major rock works are less likely at the repository site, based on current technology and economics. In a slightly longer time perspective, i.e. a few or several hundred years or more, it is difficult to predict how knowledge, technology and society will develop, and thereby how, where and why rock facilities will be built. Based on current practice, rock facilities at depth down to around 50 metres may very well occur and actually exist at Forsmark (the SFR facility, a repository for low- and intermediate level radioactive waste). In the far future, the potential ore resources to the south-west of the investigated area in Forsmark may be exploited.

Of the actions in Table 14-1, “Drill in the rock” is judged to be the only one that can directly lead to penetration of the copper canister and breach of waste containment, while at the same time being inadvertent, technically possible, practically feasible and plausible. “Drill in the rock” is furthermore a conceivable action in the light of the results of the societal analysis. Even if it is possible to build a rock cavern, tunnel or shaft or to excavate an open-cast mine which leads to penetration of the copper canister, doing so without having investigated the rock in such a way that the repository is discovered, i.e. without knowledge of the repository, is not considered to be technically plausible. However, the construction of a rock facility at shallow depth or a mine in the vicinity of the Forsmark site may occur in the future. Therefore, the cases “Canister penetration by drilling” and “Rock facility in the vicinity of the repository” and “Mine in the vicinity of the Forsmark site” were selected as representative cases for scenarios related to a sealed repository, and which should be further described and analysed.

#### *Unsealed or incompletely sealed repository*

According to regulations, it is also necessary to define and analyse a case that illustrates the consequences of an unsealed repository /SSM 2008a/. Since the repository is gradually excavated and operated, the

case selected for analysis represents an incompletely sealed repository rather than an unsealed repository. The strategy for deposition of canisters implies that deposition tunnels are successively filled with canisters and then backfilled and sealed as soon they are filled. Abandoning the repository in the middle of this process is judged as rather unlikely because this would mean that canisters are left at the surface where they would constitute a larger risk than if emplaced in the repository. It is judged more plausible that the repository is abandoned when all canisters are deposited and all deposition tunnels backfilled and sealed, but all other repository volumes are still open due to, for example, political decisions not to seal the repository completely. Therefore, this is the basic assumption in the case selected as representative for scenarios related to an unsealed or incompletely sealed repository.

### 14.2.5 Assessment of the drilling case

#### *Introduction and specification of the case analysed*

Only drilling done without knowledge of the location and purpose of the repository is considered. Various countermeasures to reduce the likelihood of inadvertent intrusion into the repository have been discussed /NEA 1995, Eng et al. 1996/. When the repository is sealed the countermeasures then deemed to be most efficient will be implemented. Examples of such countermeasures are conservation of information in archives, marking the site and various types of institutional control, for example physical surveillance, ownership restrictions and restrictions on land use. All these countermeasures are assumed to have lost their preventive and warning effect at the time for the drilling.

As discussed in Section 14.2.3, it is hard to imagine a societal evolution resulting in the loss of knowledge of the repository, its purpose and content in combination with preservation or development of knowledge, technology and society. It is likely that a society having the technical capability to drill to great depth also has the knowledge to analyse the findings and possibly will act to prevent harmful effects on man and the environment. In the drilling scenario, it is assumed that technology to drill to great depth is available, that the knowledge of the location and purpose of the repository is lost, that the intruders are incapable of analysing and understanding what they have found and that no societal regulations on drilling exist. It is assumed that an evolution rendering this situation will require some time. Countermeasures to prevent inadvertent intrusion are generally assumed to be preserved for between 100 and 500 years, whereas physical markers may be effective on a longer time perspective of up to a couple of thousand years /NEA 1995, Wilmot et al. 1999/. A KBS-3 repository is a large industrial establishment that will be under operation for several decades and this type of facility has been debated, investigated and analysed since the first nuclear power plants commenced operation in Sweden. It is plausible that it will take some time before the knowledge about the repository is lost and also for society and land owners to give up the control of activities such as drilling at the repository site. Based on this, it is assumed that the drilling will take place 300 years or longer after repository closure.

The technical practise is assumed to be similar to that at present. Today, drilling is done to sink wells, for the extraction of heat from the ground, and for exploratory purposes. Rock wells are normally drilled to a depth of between 50 and 100 metres, but occasionally wells are drilled down to 130–150 metres. Deeper wells are more uncommon. The reason is that it is expensive to drill and the probability of finding potable water in sufficient quantity declines with depth. For extracting heat, deeper drilling may occur. Even though drilling to depths down to 500 m or more for the extraction of heat is performed today and may become more common in the near future, drilling to great depth is generally done for exploratory purposes, most often prospecting.

Prospecting generally involves surface-based investigations prior to drilling. Results from modelling of the geophysical response of a spent fuel repository at Forsmark indicate that the repository will comprise an anomaly that could be detected by reflection seismics, but not with the other geophysical methods studied (magnetics, gravity, induced polarisation, resistivity, transient electromagnetics) /Isaksson et al. 2010/. The seismic response is due to the contrasts in velocity between the bentonite and the surrounding rock. Most likely, this type of anomaly would not be interpreted as a mineralisation, but it cannot be ruled out that the anomaly would be further investigated. Therefore, it is assumed that drilling through the repository is done for exploratory purposes.

Diamond (core) drilling is normally employed for exploratory drilling. The drill core is retrieved, placed in boxes and inspected by a geologist. Selected samples may be analysed more thoroughly. The cuttings (the pulverised rock mixed with the drill's cooling water) are normally removed with

water, which also cools the drill. The water with cuttings is usually spread on the ground around the borehole. When the drilling is finished, the cores are sent to core mapping and the borehole is abandoned. If the hole has passed a zone with high water flow, so that a great deal of water is brought up to the surface, the borehole may be backfilled. This is generally only done if the flow entails a problem for local residents.

The direction of the borehole varies depending on the purpose and what is known about the rock volume to be investigated. In general the drill is inclined; the angle with the ground plane is usually 60–85 degrees. If there are no known obstacles or underground facilities, the drillers always try to continue the drilling even if they run into problems. If the drill reaches the buffer and the canister these may very well be penetrated and the drilling continued and not stopped until the drill core is inspected, or the agreed depth is reached. If penetration of the backfilled deposition tunnel occurs, the water cooling the drill and bringing the cuttings to the surface will be glutted with fine-grained material. The usual procedure is then to try to flush the fine grained material away. If this does not succeed, which is plausible if trying to drill through the backfill, the borehole is frequently grouted and the drilling continued though the concrete.

It is assumed that the purpose of the drilling is to reach great depth and that the drill rig therefore is placed at a low point in the terrain. The drilling angle is assumed to be 85° and the cuttings are assumed to be spread on the ground. When the backfilled tunnel is reached the borehole is assumed to be grouted and the drilling continued. The buffer is assumed to be grouted as well, the drilling continued and the canister penetrated. When the drill core containing canister material and spent fuel is brought to the surface the anomalous situation is taken to be recognised and the drilling is stopped.

Since the assessment should not only consider the impact to the intruder, but also assess how the safety functions of the repository may be impaired, the following additional assumptions are made: The site and the borehole are abandoned without further measures. About a month later, a family moves to the site and operates a domestic production farm there. The abandoned borehole is used as a well by the family. The consequences for the repository and the annual effective doses to the family as well as the dose to the drilling personnel are assessed.

### *Function indicator(s) considered*

Because this drilling case presumes that one canister as well as the buffer and backfill above the canister are penetrated by a borehole, function indicators related both to containment and retardation properties of the canister, buffer and deposition tunnel backfill are affected. In addition, the function indicators related to the capacity of the geosphere to provide favourable hydraulic and chemical conditions may be affected. Therefore, the following function indicators are considered in this drilling case:

- Can1, Provide corrosion barrier; ensure containment.
- Buff1, Limit advective transport in buffer; ensure tightness and self-sealing.
- BF1, Counteract buffer expansion; high density and self-sealing of backfill.
- R1, Provide favourable chemical conditions; ensure reducing conditions.
- R2, Provide favourable hydrologic and transport conditions; ensure high transport resistance in fractures and low equivalent flow rate at buffer/rock interface.

Further, the safety function Buff 5, Prevent canister sinking may be affected if sufficiently much buffer material is lost. However, if this occurs, the other buffer safety functions will have already been violated.

### *Qualitative description of the consequences of unintentionally penetrating a canister when drilling*

It is assumed that one canister has been penetrated by core drilling. The borehole above the penetrated canister is assumed to be grouted and the buffer's capability to prevent advective transport, self seal and prevent colloid transport are lost in the grouted area. Some buffer and backfill material is lost, but excluding the grouted parts both backfill and buffer are assumed to retain their safety functions. The water containing the cuttings from the drilling is brought the surface and spread on the ground on a circular area.

The grouted borehole has left an open pipe from the penetrated canister to the surface. As long as the grout remains intact, the tunnel backfill in the deposition tunnel and the buffer in the remainder of the deposition holes in the deposition tunnels are not directly affected by the presence of the borehole. However, the open borehole may, at least locally, affect the groundwater flow pattern. This, in turn, may affect the chemical conditions in and around the repository. Therefore, the impact on the groundwater flow field of an open borehole from the surface through the backfill into a deposition hole has been analysed.

With time, it is likely that the grout is degraded and that the buffer and backfill above the penetrated canister expands to fill the empty volume of the borehole in these barriers. Considering the self-sealing capacity of the buffer and backfill (Section 10.2.4) and the quite large amounts of buffer and backfill materials that can be lost before advective conditions occur (see Sections 10.3.9 and 10.3.11) it seems likely that this expansion will re-establish favourable hydraulic and mechanical conditions in the buffer in the deposition hole with the penetrated canister and the backfill above this deposition hole. However, even if this is not the case, the borehole will most likely not affect the backfill in other parts of the deposition tunnel. This implies that the buffer in other deposition holes in the tunnel also should be unaffected by the borehole.

#### *Quantitative assessment of the radionuclide release and dose consequences of a penetrated canister when drilling*

In the analysis of the dose consequences of this drilling case, the dose to the drilling personnel as well as to a family settled on the site are analysed. The analysis is provided in the **FHA report** (Section 6.3), and summarised below. The data used in the analysis are compiled in Table 14-2.

It is assumed that one canister is penetrated by drilling and that this takes place at the earliest 300 years after repository closure. The water containing the cuttings from the drilling is brought to the surface together with the drill core comprising damaged or undamaged fuel. The fuel is contained as fuel rods in fuel assemblies in the cast iron insert in the copper canisters. Based on the geometry and arrangement of the fuel rods in the canister and assuming a diameter of the borehole of 0.056 m, the portion of the fuel in the canister that is brought to the surface is set to 3%. It is further pessimistically assumed that all fuel brought to the surface remains at the site, and that radionuclides in this fuel, as well as the instantaneous release fraction of the inventory in the penetrated canister are spread on the ground. This is assumed to occur over a circular area with a radius of the contaminated area of 3 m and a thickness of the contaminated soil layer of 0.1 m. The drilling personnel receives dose from these radionuclides spread on the ground.

In this drilling case it is further assumed that a family settles on the site one month after the site is abandoned by the drillers. The grouted borehole has left an open pipe from the penetrated canister to the surface and the family uses the borehole as a well. In addition, the contaminated soil is used for cultivation purposes. The family receives dose from radionuclides in the borehole water as well as from radionuclides in agricultural products and air, the latter originating from radionuclides in the contaminated soil. The assumptions in the calculations of the dose obtained from using the abandoned borehole as a well are the same as those in the dose calculations for other scenarios analysed in SR-Site /Avila et al. 2010/. It is assumed that the water from the borehole is used for irrigation and as drinking water for the family and for cattle. In the calculation of dose from radionuclides spread on the ground, it is assumed that the family uses the contaminated soil to establish a domestic garden for cultivation of vegetables. This garden is assumed to be large enough to produce vegetables for five persons, which implies that the radionuclides brought to the surface are spread over a larger area. The members of the family are also exposed to external radiation and through inhalation of dust when spending time in the garden.

The release of radionuclides from the fuel to the water in the penetrated canister is determined by the fuel alteration rate and the corrosion rate of the metal components. However, elemental solubility limits may govern the release of some radionuclides, depending on the magnitude of the water flow in the deposition hole containing the penetrated canister. Based on results of the hydrogeological modelling /Joyce et al. 2010/, the water flow in the deposition hole is set to 0.1 $m^3$/year. With this water flow and elemental solubility limits representative of groundwater chemical conditions between 2000 and 3000 AD, the release of $^{237}Np$, $^{99}Tc$, $^{93}Zr$ and the uranium isotopes from the spent fuel becomes solubility limited.

**Table 14-2. Compilation of data used in the analysis of dose consequences of unintentionally penetrating a canister when drilling.**

| Parameter | Value/assumption | Comment/reference |
|---|---|---|
| Time of drilling | 300 years after closure of the repository or later | |
| Time the exposed individual in the family spends in the middle of the contaminated area | 365 hours | One hour per day every day of the year |
| Radionuclide inventory | Average canister | **Data report**, Section 3.1 |
| IRF | Included in the inventory left on the ground | Median values according to **Data report**, Section 3.2 |
| Portion of fuel in the canister brought to surface | 0.03 | **FHA report**, Appendix B |
| Fuel alteration rate | $10^{-7}$ per year | **Data report**, Section 3.3 |
| Corrosion rate of metal parts in fuel | $10^{-3}$ per year | **Data report**, Section 3.2 |
| Water flow through deposition hole | 0.1 $m^3$ per year | **FHA report**, Appendix B |
| Elemental solubility limits | Representative for site conditions in the period 2000 to 3000 AD | **FHA report**, Section 6.3. |
| Volume of initially contaminated soil | 2.8 $m^3$ (radius 3 m, thickness 0.1 m) | – |
| Dose conversion factors for contaminated ground | Dose factors for external irradiation, inhalation and ingestion of food cultivated at the site | /Nordén et al. 2010/ |
| Sorption coeffecients | Element specific sorption coefficients for soil in the irrigated area | /Nordén et al. 2010/ |
| Density of agricultural soil | 323 kg dry weight/$m^3$ | /Löfgren 2010/ |
| Area of land used to grow vegetables | 102 $m^2$ | Large enough to produce vegetables for 5 persons, assuming a fraction of 2.5% vegetables in the diet. |
| Productivity of vegetables on irrigated land | 0.135 kgC per $m^2$ and year | /Löfgren 2010/ |
| Productivity of root crops on irrigated land | 0.127 kgC per $m^2$ and year | /Löfgren 2010/ |
| Productivity of cereals on irrigated land | 0.114 kgC per $m^2$ and year | /Löfgren 2010/ |
| Dust concentration in the air | $5 \cdot 10^{-8}$ kg dry weight/$m^3$ | /Nordén et al. 2010/ |
| Inhalation rate | 1 $m^3$ per hour | /Nordén et al. 2010/ |
| Yearly intake of carbon | 110 kg carbon per year | /Nordén et al. 2010/ |
| Yearly intake of water | 0.6 $m^3$/year | /Nordén et al. 2010/ |
| Volume of irrigation water used each year | 0.15 $m^3/(m^2\ y)$ | /Nordén et al. 2010/ |
| Number of irrigation events per year | 5 | /Nordén et al. 2010/ |
| Runoff | 0.186 m/y | /Löfgren 2010/ |
| Well capacity | 82,502 $m^3$/year | /Löfgren 2010/ |

### Dose to drilling personnel

The dose to the drilling personnel originates from the radionuclides in cuttings, drilling water and fuel pieces spread on the ground around the borehole. The dose rate that a member of the drilling personnel would be exposed to while working in the highly contaminated area 300 years after repository closure is calculated to be 130 mSv/hour and the dose rate is totally dominated by exposure to Ag-108m, see the **FHA report**. If drilling occurs at c. 5,000 years after repository closure, the dose rate has decreased to values below 1 mSv/hour and is dominated by exposure to Nb-94 and Sn-126.

These calculated dose rates are very high. This is primarily a result of the cautious assumption regarding the amount of Ag-108m brought to the surface when drilling. In the spent fuel, Ag-108m is contained in the Ag-In-Cd alloy of the control rods, but in the calculations assumed to be part of the radionuclides that are instantly released when a canister is penetrated and therefore the entire amount is taken to be brought to the surface. In the case of drilling intrusion Ag-108m would not be instantaneously released, so 3% instead of 100% of the inventory of Ag-108m would be brought to the surface when drilling. Due to the total dominance of Ag-108m in determining the dose rate, this would reduce the dose rate to workers to 3% of the value, i.e. the dose rate 300 years after repository closure would be about 4 mSv/hour.

**Dose to family settled on the site**

The doses to the family that settles on the site originates from two sources. The abandoned borehole used as a well by the family and the cuttings containing the instant release fraction and the fuel particles spread on the ground. The calculated annual effective doses from using the abandoned borehole as a well and from the radionuclides spread on the ground are shown in Figures 14-2 and 14-3, respectively. The calculated annual effective dose is that which an adult member of the family would be exposed to during the first year at the site.

The total dose from using the borehole as a well 300 years after repository closure is 0.31 mSv/year (Figure 14-2) and is dominated by the contribution from Am-241. This dose is above the regulatory risk limit of 0.014 mSv/year, but below the dose of 1 mSv/year from background radiation. At 2,000 years after repository closure, the dose is dominated by Pu-240 and if drilling takes place at still later times, Pu-239 and Nb-94 becomes more significant.

The maximum total annual effective dose from the use of the contaminated soil for agricultural purposes is about 10 Sv/year and this dose is obtained 300 years after repository closure. The dose is dominated by ingestion of vegetables contaminated with Tc-99 and there is also a significant dose contribution due to external radiation from Ag-108m. The calculated annual dose is very high, but it should be noted that there are a number of simplified, cautious assumptions made in the calculations (see further section on uncertainties below).

### *Quantitative assessment of the effects on the repository of unintentionally penetrating a canister when drilling*

The impact of an open borehole on the groundwater flow in the repository and the surrounding rock has been studied by introducing boreholes at various locations in the hydrogeological base case model applied for analyses of the temperate period in SR-Site /Joyce et al. 2010, Section 5.6/. The results show that a borehole through the backfill and buffer above a canister will act as a sink for many flow paths and that the water flow in the borehole is directed upwards. Although the flow paths are affected

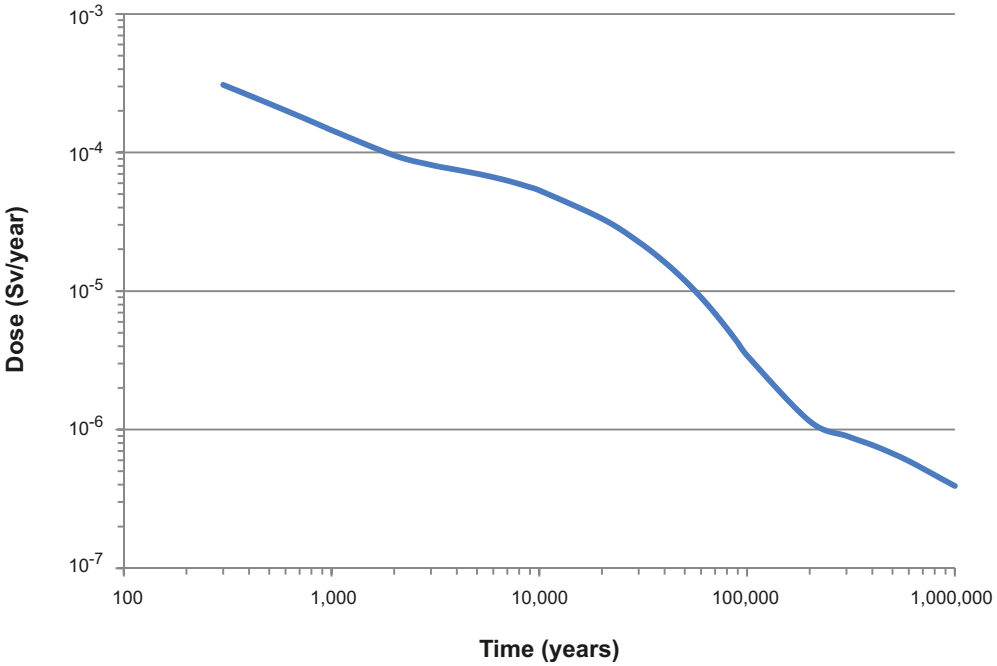


***Figure 14-2.*** *Calculated annual effective doses from using the borehole as a well for drinking water and irrigation at Forsmark. The dose is that which an adult member of the family would be exposed to during the first year at the site and the time is the year after repository closure when drilling takes place and the family settles on the site. This means that the only loss of radionuclides accounted for is that through radioactive decay (Figure 6-2 in the* ***FHA report****).*

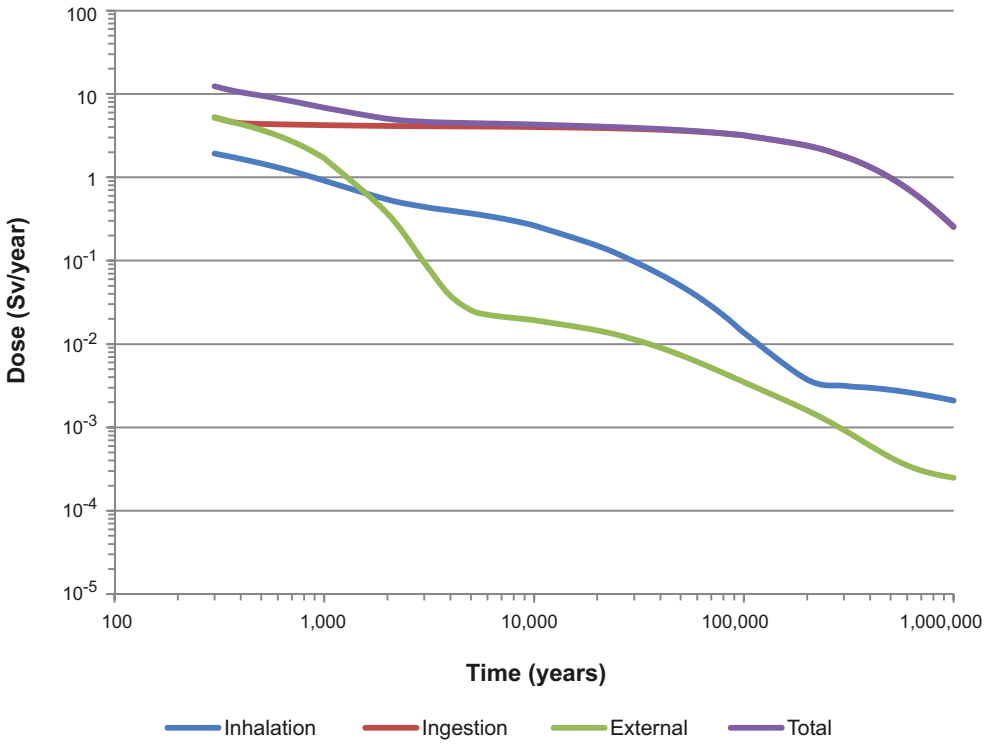


***Figure 14-3.*** *Calculated annual effective doses from exposure to the radionuclides brought to the surface as drill cuttings and fuel pieces (3% of the inventory in a canister) via the use of the contaminated soil for domestic farming and through spending time in the contaminated area. The dose is that which an adult member of the family would be exposed to the first year at the site and the time is the year after repository closure when drilling takes place and the family settles on the site. This means that the only loss of radionuclides accounted for is that through radioactive decay (Figure 6-3 in the* ***FHA report****).*

by the borehole, the results indicate only small effects of the borehole on the performance measures as compared with the hydrogeological base case model (see Section 10.3.6). This indicates that the flow paths established by the presence of the borehole have similar transport characteristics to the flow paths without a borehole. Furthermore, the upward directed flow in the borehole implies that reducing conditions prevail inside the penetrated canister. The modelling results do not show explicitly where the flow paths continue from the borehole, but the interpretation is that the water in the borehole exits into the highly transmissive fractures in the upper part of the bedrock and continues towards low points in the terrain.

### *Uncertainties*

As stated in the **FHA report**, there are a number of uncertainties in the assumed drilling case regarding the impact on the deposition hole hit by the drilling and in the calculations of the doses that this action gives rise to. One major uncertainty concerns the amount of the inventory brought to surface by the drilling, and especially the amount of the dose-dominating radionuclide Ag-108m. In the calculations it is assumed that the whole inventory of Ag-108m is instantaneously released from the spent fuel and brought to the surface by the drilling. This is a pessimistic assumption, since Ag-108m is contained in metal parts of the fuel and would thus be brought to the surface in a quantity proportional to the amount of fuel brought to the surface. Furthermore, Ag-108m comes from control rods. These only exist in canisters with PWR fuel, i.e. in about 25% of all canisters. The assumed radius of the borehole will also affect the amount of radionuclides brought to the surface, and the handling of the fuel and cuttings will affect their spreading and dilution in the biosphere. For example, unbroken fuel rods may be removed from the site for further inspection instead of left on the ground as it is assumed in the calculations. All these factors will affect the calculated doses from the fuel and cuttings left on the ground.

Another major uncertainty relates to the availability in, and loss of, radionuclides from the contaminated soil. The whole radionuclide inventory in the contaminated area is assumed to be instantaneously available for transfer to the agricultural production and air with contaminated dust. This assumption leads to a pessimistic value of the annual effective dose, since most likely only a fraction of the inventory will be available from the beginning. Further, it is assumed that there are no losses of radionuclides from the contaminated area other than by radioactive decay. However, in reality, other loss processes, such as leaching in percolating waters, are likely to be of importance. Note that the calculated annual effective dose from the radionuclides brought to the surface is valid only for the first year after the intrusion given these assumptions and that the land is assumed to be cultivated during that year.

It is not certain that the family finds the borehole and uses it as a well. Current practice is to place the pump just above the borehole for the well. Non-manual pumps are most often covered and some space is left around them to allow maintenance. Manual pumps require some space for pumping. The combination of using the borehole as a well and the contaminated soil from the area around it for cultivation therefore seems unlikely. Based on current practice the most likely situation seems to be that the contaminated area will either be used for cultivation or the borehole will be used as a well. Consequently, the person can be assumed to either receive the dose from the use of the contaminated area for agricultural purposes or from using the borehole as a well.

Uncertainties in the analyses of the impact of the borehole on parts of the repository other than the deposition hole directly affected by the borehole are judged as small compared to those associated with the calculations of dose from the canister penetrated by the drilling. The conclusion that a borehole through the backfill above, and buffer in, the deposition hole hit by drilling does not affect the backfill and the buffer in a neighbouring deposition hole, is based on results of analyses reported by /Åkesson et al. 2010a, Appendix F/. These analyses addressed loss of backfill above a deposition hole or in the middle between two deposition holes. Although the results reported by /Åkesson et al. 2010a/ are associated with uncertainties, their results in combination with the situation in this case, where a potential loss of backfill occurs still further away from a deposition hole, seem firm enough for the conclusion drawn. There are also uncertainties in the analyses of the impact of open boreholes on the groundwater flow in and around the repository, but these uncertainties are judged to not significantly affect the results, see the **FHA report**.

### *Conclusions*

If a canister is penetrated and the borehole is used as a well for drinking and irrigation, the annual effective doses to representative members of critical groups will exceed the individual limit on annual effective dose for members of the public but not the annual effective dose due to background radiation. Assuming the site-specific median water yield of percussion holes drilled in the repository rock at Forsmark, the dose corresponding to the regulatory risk limit is exceeded if the intrusion occurs during the first c. 35,000 years after repository closure.

If the instant release fraction and crushed material, pieces, and even unbroken fuel rods, from the fuel elements are brought to the surface by drilling, the persons executing the drilling will receive very high doses. After about eight hours of exposure, the threshold of 1 Sv for suffering from radiation sickness is exceeded. Further, if the contaminated soil surrounding the borehole is used for agricultural purposes, the exposed persons in the case illustrated may be severely injured. However, as discussed above, the case analysed involves a number of simplified and cautious assumptions. Therefore, the calculated annual effective doses should be seen as illustrations of possible consequences rather than estimations of what the consequences would be.

An open borehole might affect the long-term properties of the backfill in the deposition tunnel in the vicinity of the borehole but the effect on the backfill above neighbouring deposition holes is assessed as negligible. This implies that the buffer surrounding canisters in neighbouring deposition holes in the deposition tunnel is also unaffected by the borehole. An open borehole through the backfill will also change the pattern of flow paths in the rock beneath the highly transmissive fractures in the upper part of the bedrock. However, the new paths established have similar transport characteristics as those prevailing without an open borehole through the backfill. Therefore, it is judged that even though drilling a borehole that penetrates a canister will severely affect the deposition hole hit by

drilling, the impact of the borehole on the containment potential of other parts of the repository as well as on the retardation potential of the geosphere is negligible. No significant additional doses would be incurred by people other than those directly using the contaminated borehole water or the land affected by contaminated drillcore.

### 14.2.6 Assessment of the rock excavation or tunnel case

#### *Introduction and specification of the case analysed*

As discussed in Section 14.2.3 and in the **FHA report**, there are several plausible reasons for constructing tunnels or other types of underground excavations in the bedrock. Today, existing and planned underground excavations constructed to repository depth of 400 metres or deeper include mines, hard rock laboratories and deep geological repositories for radioactive material. These kinds of facilities are considered unrealistic at or close to the repository site. Mines are excluded, since sites including exploitable natural resources are excluded in the site selection. Hard rock laboratories and deep geological repositories are excluded, since it is probable that societies planning the construction of these kinds of facilities will discover and understand that the site is already used for a similar purpose and either construct their facility so that is does not intrude on the existing one or chose another site. For the other kinds of facilities mentioned in Table 14-1 the depth is generally as shallow as possible with regard to the geology and purpose of the facility. Generally, tunnels are constructed down to a depth of 50 metres, which is considered to be plausible also at Forsmark. This is, for instance, the depth of the final repository for low- and intermediate level waste (SFR), located close to the planned final repository for spent fuel.

For most purposes, tunnels or rock excavations are sealed to prevent water inflow and reinforced to mechanically stabilise the tunnel and to avoid the fallout of rock blocks when they are in operation. In many cases, the tunnel walls are lined with concrete. If the tunnel is used for final storage, it is assumed that measures are taken to prevent hazardous quantities of the unknown stored material from escaping from the tunnel.

The size of a tunnel or rock excavation depends on its purpose. Tunnels can have cross sections from about four up to 100–200 $m^2$ and excavations can have volumes from 10,000 to 100,000 $m^3$ or more.

Based on these considerations, the following case is analysed.

- A tunnel constructed at 50 metres depth with a cross section of 100 $m^2$ and with a length corresponding to the whole repository footprint along the centre line of the deposition areas is considered. The justification for this assumption is that it is plausible in relation to current practice and does not underestimate the possible impact on the repository.
- The purpose of the tunnel or rock excavation is not specified.
- The operational phase of the tunnel and the designed working life of sealing and reinforcement is assumed to be a couple of hundred years. After operation, it is assumed that the tunnel is abandoned and becomes saturated with groundwater.
- As in the drilling case, it is assumed that the existence of the repository is forgotten and that the technical standards for making underground constructions are similar to those used at the present. Further, it is assumed that the construction of the rock excavation (tunnel) is not initiated before 300 years after repository closure.

#### *Function indicator(s) considered*

The function indicator relevant for this case is:

- R2, Provide favourable hydrologic and transport conditions.

During operation of the tunnel, the hydraulic gradients in its vicinity may be affected. Indirectly, if the impact on the hydrologic conditions is substantial, the function indicator R1, Provide favourable chemical conditions, could be affected.

### *Assessment of the consequences of the construction of a tunnel above the repository*

At Forsmark, the bedrock selected for hosting the final repository for spent fuel (the target volume) comprises the north-westernmost part of a tectonic lens (Section 4.3). The upper part of the bedrock (down to about 150 metres depth) in the target volume is recognised for its large horizontal fractures/sheet joints /SKB 2008a/. Due to these structures and the high fracture frequency close to the rock surface, the upper part of the bedrock is much more water conductive than the lower part, especially below 400 metres depth. A measure of the hydraulic importance of these sheet joints in the upper part of the bedrock is provided by the exceptionally high water yields in the percussion boreholes drilled during the site investigation. The median yield of the first 22 percussion-drilled boreholes is c. 12,000 L/h /SKB 2008a, Section 8.4.4/. This is c. 20 times higher than the median yield of the domestic water wells drilled outside the tectonic lens, which is no different from the median yield of all bedrock wells registered at the Geological Survey of Sweden /SKB 2008a, Section 8.4.4/. The high water yield at shallow depth in the target volume of the bedrock inside the tectonic lens is not only due to these large horizontal structures in the upper part of the bedrock and the high fracture frequency close to the rock surface, but also due to the closeness to the sea, which acts as an endless source of water (positive hydraulic boundary).

If a tunnel is constructed at 50 metres depth, despite the high conductivity in the upper part of the bedrock in the target volume, this would place limitations on constructability and require extensive grouting. Grouting would, in turn, considerably limit the impact of the tunnel on the hydrogeology in the surrounding superficial rock. There is no reason to expect that an open tunnel at 50 metres depth located above the repository should result in up-coning of groundwater that significantly affects the hydrogeology in the repository bedrock at 450 metres depth. This conclusion is supported by the significant decrease in the frequency of water-conducting fractures with depth observed in the site investigations. It is noted that not even the spent fuel repository is expected to give noticeable up-coning during the construction and operational phase, as shown by modelling results for an open repository reported in /Svensson and Follin 2010, Section 5.2/.

The future uplift at Forsmark during the next 1,000 years is on the order of 7 m, see the **Climate report**. This decrease in shoreline elevation is not expected to change the importance of the horizontal fractures/sheet joints in the upper part of the bedrock for the hydrogeological system in the target volume of the rock as the horizontal fractures/sheet joints in the upper part of the bedrock occur also at greater depths than 7 m. The potential construction and operation of a tunnel above the repository during the next 1,000 years would then not negatively impact the performance of the repository. Abandoning the tunnel during this period would imply that the tunnel becomes filled with water as the grout in the tunnel degrades. The abandoned tunnel might act as a conductor for near-surface flows, but no significant impacts on the magnitude of the water flow in the rock surrounding the deposition holes in the repository is expected. This is based on the results from hydrogeological analyses of an abandoned, partially open repository /Bockgård 2010/, which show very small changes in the magnitude of Darcy flux at deposition hole positions if it is assumed that all excavations in the repository except deposition tunnels and deposition holes are open, as compared with the expected case that the repository is completely backfilled and sealed, see also Section 14.2.8. Consequently, there is little reason to expect that an abandoned open tunnel restricted to 50 m depth should impact the magnitude of the water flow at repository depth. Furthermore, similar arguments could be made for tunnels located down to at least the 150 m level.

### *Conclusions*

The above assessment indicates that the upper 150 m of the bedrock above the repository is an unfavourable location for a tunnel from an engineering point of view, due to the exceptionally high water yield in this part of the bedrock. These conditions also imply that a tunnel constructed in this part of the bedrock would not affect the groundwater flow at repository depth such that the presence of the tunnel violates the safety functions of the deep repository. The design consideration to locate the repository to a depth that allows utilisation of the site for generally occurring future human activities should, therefore, be fulfilled at Forsmark.

### 14.2.7 Assessment of a mine in the vicinity of the Forsmark site

#### *Introduction and specification of the case analysed*

The ore potential at Forsmark has been analysed within the site investigations. In an area south-west of the Forsmark site a felsitic to metavolcanic rock, judged to have a potential for iron oxide mineralisation, has been identified /Lindroos et al. 2004/ (see Section 4.3.2 and Figure 14-4). The mineral deposits have been assessed to be of no economic value. Nevertheless, as this judgement may be revised in the future due to economic reasons, the potential exploitation of this mineralisation is addressed.

Since the mineralisation at the present is judged to be of no value, it is impossible to describe the design of a mine exploiting the mineralisation based on current mining standards. It could be a quarry or a mine and the depth could be from tens to hundreds of metres or for mines a thousand metres or even deeper.

#### *Function indicator(s) considered*

The function indicator relevant for this case is:

- R2, Provide favourable hydrologic and transport conditions.

During operation of the mine, the hydraulic gradients in its vicinity may be affected. Indirectly, if the impact on the hydrologic conditions is substantial, the function indicator R1, Provide favourable chemical conditions, could be affected.

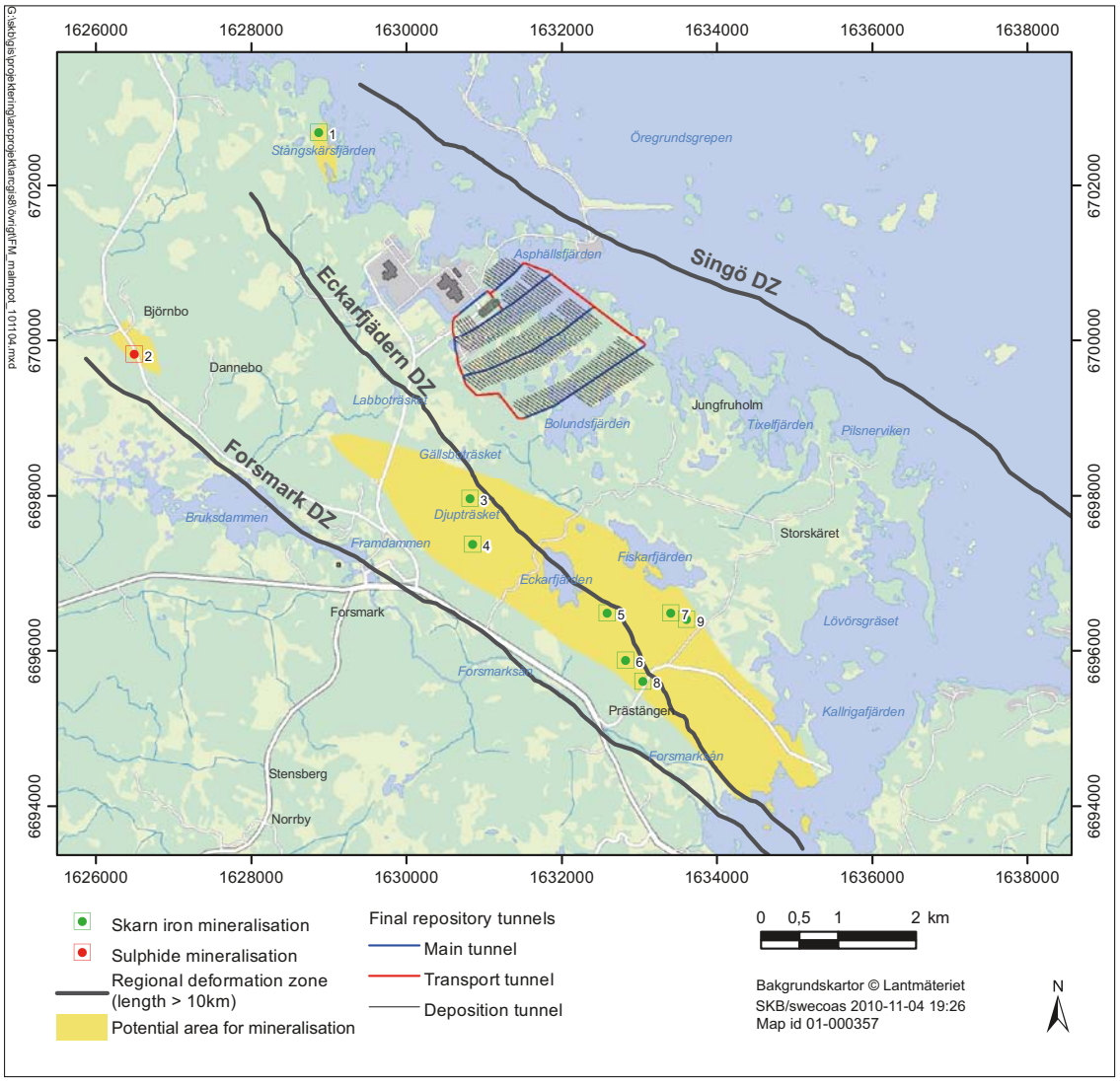


***Figure 14-4.*** *Map showing the areas on the surface that are judged to have some exploration potential for mineral deposits (Figure 6-5 in the* ***FHA report****).*

#### *Assessment of the consequences of a mine in vicinity of the Forsmark candidate area*

If a mine, or other sub-surface rock excavation, were to be constructed in the vicinity of the Forsmark site, it may be assumed that the greatest influence on the repository for spent nuclear fuel would occur if the construction took place at the same depth and in close proximity to the repository for spent nuclear fuel. Since the south-westernmost part of the repository is located west of Lake Bolundsfjärden (Figure 14-4), the closest distance between the repository and a hypothetical mine in the potential area for mineralisation (Figure 14-4) would be on the order of 1 to 1.5 km.

In order to assess the potential influence on the repository, results from analyses of the hydraulic impact of an open repository are used. Calculations of the effects of water inflow to an open repository show that the drawdown of the hydraulic head is large in the rock close to the repository at a depth of 450 m /Mårtensson and Gustafsson 2010, Figure 7-20 lower insert/. However, the drawdown decreases rapidly with distance from the open repository in a westerly direction to about 50 m within tens of metres from the repository and at distance of c. 1 km from the repository, the drawdown at 450 m depth is negligibly small. The reason for the small radius of influence is the low hydraulic conductivity of the rock mass volumes at depth in proximity to the repository. This constraining hydraulic condition is valid also for a potential future mine outside the tectonic lens. Therefore, it is reasonable to expect a very limited hydraulic impact from the mine on the repository because of the low-conductive bedrock in the target volume.

#### *Conclusions*

The assessment indicates that exploitation of the potential mineral resources in the vicinity of the Forsmark site would not impact the safety functions of the repository. The design consideration to locate the repository at a site without natural resources is, therefore, considered to be fulfilled.

### 14.2.8 Incompletely sealed repository

#### *Introduction and specification of the case analysed*

According to regulations, it is also necessary to define and analyse a case that illustrates the consequences of an unsealed repository /SSM 2008a/. The basic assumption in the case selected as representative for scenarios related to an unsealed or incompletely sealed repository is that the repository is abandoned when all canisters are deposited and all deposition tunnels backfilled and sealed, but the main and transport tunnels as well as the central area, repository access (ramp and shafts) and the ventilation shafts in the deposition area (see Figures 5-21 and 10-7) are still open due to, for example, political decisions not to seal completely. This assumption is based on the strategy for deposition of canisters, which implies that deposition tunnels are successively filled with canisters and then backfilled and sealed as soon they are filled. Abandoning the repository in the middle of this process is judged as rather unlikely because this would mean that canisters are left at the surface where they would constitute a larger risk than if emplaced in the repository.

#### *Function indicator(s) considered*

This case relates to the following function indicators:

- Can1, Provide corrosion barrier; ensure containment.
- Buff1, Limit advective transport in buffer; ensure tightness and self-sealing.
- Buff2, Reduce microbial activity.
- BF1, Counteract buffer expansion; high density and self-sealing of backfill.
- R1, Provide favourable chemical conditions; ensure reducing conditions.
- R2, Provide favourable hydrologic and transport conditions.

#### *Qualitative description of the consequences of an incompletely sealed repository*

If the repository is abandoned when the main and transport tunnels, central area, repository access and ventilation shafts in the deposition area are still open, these open volumes will successively be water filled. Water will flow through the open volumes with a magnitude and direction dependent on the magnitude and direction of the hydraulic gradient. In addition, the open volumes may affect the groundwater flow pattern in the repository bedrock.

All deposition tunnels will be plugged towards the main tunnels when the repository is abandoned. When the main tunnels have become filled with water, the cement and other components in the concrete plugs may be dissolved in the water and transported away. At some point in time the plugs will lose their function and the backfill in the deposition tunnel will swell out into the main tunnels. This swelling out into the main tunnels will decrease the density of the backfill in the deposition tunnels. How far into the deposition tunnel the decrease in density reach depends on the amount of backfill material that is lost from the deposition tunnel. If the density in the backfill above a deposition hole is significantly reduced, the buffer in the deposition hole may expand into the backfill above with the consequence that the density of the buffer also decreases.

Abandoning the repository without sealing the access from the surface may facilitate recharge of oxygenated water from the surface down to the central area and the main tunnels. In addition, the unsealed parts of the repository will contain air which will dissolve in the water that successively intrudes into the empty, unfilled parts of the repository. If dissolved oxygen reaches the canisters via the backfill in the deposition tunnels and the bentonite buffer or via fractures in the rock that intersect the deposition tunnel and further through the bentonite buffer, the oxygen will corrode the copper canisters. This may lead to corrosion breakthrough in the canisters and release of radionuclides from the spent fuel.

If and when corrosion breakthrough occurs depends on the supply of oxygen to the canister surface. Groundwater recharging from fractures and fracture zones intersecting the unfilled volumes deeper down in the rock will most likely not contain dissolved oxygen due to the large reduction capacity of both the rock and the overburden through which this water has infiltrated, see Section 10.2.5. The major supply of oxygen from the surface down into the open volumes of the repository will likely occur during glacial periods when glacial meltwater can be forced down due to the high hydraulic gradients established by the ice sheet. However, oxygen dissolved in the water in the empty volumes of the repository may also be consumed by both biotic and abiotic processes. For example, biological degradation of organic materials, already present in the empty volumes as well as supplied with incoming water, will continue until either the oxygen or the biodegradable organic material is depleted, and oxygen may react chemically with reducing minerals in the rock such as chlorite, biotite and pyrite /Sidborn et al. 2010/, as well as be consumed by aerobic corrosion of iron construction materials left in the unfilled volumes of the repository.

Further transport of dissolved oxygen from the unfilled main tunnels in the repository to the canisters in the deposition holes will take place by advection or diffusion in the backfill in the deposition tunnels and in the bentonite surrounding the canisters, depending on the properties of these barriers. Alternatively, transport of dissolved oxygen may take place with groundwater flowing in fractures that intersect the deposition holes and are connected to either the unfilled main tunnel or to the deposition tunnel at a location close to the intersection with the main tunnel (see e.g. Figure 5-21). Both in the backfill and the buffer, oxygen consumption may take place by chemical reactions with accessory minerals in the bentonite. In addition, microbial activity in the backfill is expected to consume oxygen (Section 10.2.5).

As described in Section 10.2.5, the bentonite contains organic materials that under anoxic conditions potentially could be utilised for microbial reduction of sulphate to sulphide. As long as the backfill above a deposition hole does not loose density to the extent that the buffer in the deposition hole can expand upwards into the backfill, microbial sulphate reduction in the bentonite buffer is not expected to take place to any extent (Section 10.2.5). If the backfill density is reduced to such extent that the buffer expands into the backfill, the buffer density may become too low to rule out microbial activity in the buffer. However, as noted in Section 10.2.5, although the amount of organic material in the bentonite accessible for microbial degradation is highly uncertain, it consists mainly of humic and fulvic acids that have molecules that are too large to be used by bacteria as a carbon source.

#### *Quantitative assessment of the containment potential of an incompletely sealed repository*

The assessment of the containment potential is based on analysis of expansion of deposition tunnel backfill into open main tunnels, on results from groundwater flow modelling of the effects of open tunnels and on simple estimates of oxygen supply and canister corrosion, see the **FHA report**, Section 6.6.3.

**Expansion of deposition tunnel backfill**

The expansion of deposition tunnel backfill into the main tunnels after degradation of the plug has been analysed by /Åkesson et al. 2010a, Section 22/. With the assumption that the entire plug is lost and that the backfill may freely swell out into the main tunnel, the results indicate that deposition holes located closer than 25 to 35 m from the degraded plug/backfill interface will experience a backfill with a dry density that is below the acceptance criterion of 1,240 kg/m$^3$. Since no deposition hole will be located closer than 20.6 m from the deposition tunnel entrance /SKB 2009b/, this implies that the loss of backfill from deposition tunnels could lead to density reduction of the buffer in at most four to five deposition holes located closest to the tunnel entrance.

The case analysed presumes that the plug is lost from neighbouring deposition tunnels and that the swelling is similar from all these tunnels, which implies that the backfill at most can expand 20 metres along the main tunnel since the distance between two deposition tunnels is 40 metres. The consequences of free swelling of the backfill in a deposition tunnel for a case where the plug in a neighbouring deposition tunnel is intact and the backfill in this tunnel remains in place have not been analysed quantitatively. Clearly, more backfill will expand out into the main tunnel and it is envisaged that a few additional deposition holes will experience a backfill with a density below the acceptance criteria, as compared with the case with expansion of tunnel backfill in two neighbouring deposition tunnels. However, the exact number of such deposition holes is not important for the approach selected for analysis of the dose consequences of this case.

**Hydrogeological impact**

In order to investigate the hydraulic influence of an abandoned, partially open repository, as compared to the reference closure of the repository, the effects of open tunnels have been studied for two situations with different boundary conditions; a temperate situation with present-day boundary conditions and a generic future glacial situation with an ice sheet covering the repository /Bockgård 2010/. The boundary conditions in the glacial simulation represent a case with an advancing ice margin, but without permafrost, where the ice front is located above the repository at ice front location IFL II, as defined in Figure 10-127.

The results from the calculations imply that the open tunnels will cause a drawdown in the surrounding rock during temperate conditions, meaning that the tunnels will capture many flow paths from canister positions and thereby act as a conductor for flow to the surface. The general flow direction in the tunnels is recharge through the ventilation shafts in the deposition area and discharge through the ramp and shafts above the central area (see Figure 10-7 for locations of the repository features). The water flow in the open system amounts to 0.42 L/s (13,230 m$^3$/year) of which c. 60% (0.26 L/s) recharge from the transmissive surface layer and sheet joints above elevation – 40 m. The impact of open tunnels on the Darcy flux at deposition hole positions is, however, small, with an increase of about 10% in the median value compared with the reference closure case. The open tunnels decrease the median transport resistance to about 30% of the reference value.

The consequences of open tunnels for the glacial conditions assumed in the calculations are, on the other hand, considerable. The high hydraulic head established by the ice sheet may cause a significant flow, about 250 m$^3$/s, through the tunnel system, with recharge through the ramp and shafts above the central area and discharge through the ventilation shafts in the deposition area. The high hydraulic gradient will be transmitted by the tunnels to repository depth and water will be injected into the rock. The Darcy flux at deposition hole positions will in general increase and at certain deposition hole positions, a considerable increase in Darcy flux is indicated, but the open tunnels decrease the median transport resistance in the rock by only about 50%.

**Oxygen supply and canister corrosion**

To illustrate the potential consequences for canister corrosion by oxygen dissolved in the water in the open tunnels in the repository, some simple calculations have been carried out, see the **FHA report**, Section 6.6.3 and Appendix B. In the calculations it is assumed that the water in the backfilled deposition tunnels above a deposition hole is saturated with dissolved oxygen and that oxygen is further transported to the canister lid by diffusion through the 1.5 m thick bentonite buffer above

the lid (see Figure 5-11). For temperate conditions, the concentration of oxygen at the upper boundary of the buffer is set to 0.3 mol/$m^3$, i.e. in equilibrium with atmospheric oxygen, and a concentration of 1.5 mol/$m^3$ is assumed for glacial conditions, i.e. corresponding to the concentration in glacial meltwater /Sidborn et al. 2010/.

With an effective diffusivity of $1 \cdot 10^{-10}$ $m^2$/s for dissolved oxygen, an approximate value representative for uncharged species (see the **Data report**) and assuming 1D-diffusion through the entire cross-sectional area of the buffer (diameter 1.75 m, Figure 5-12), the flux of oxygen after diffusion through 1.5 m buffer is calculated to $1.5 \cdot 10^{-3}$ mol/year. If it is further assumed that this oxygen instantly reacts with the copper according to the stoichiometry 4 mol Cu/mol $O_2$, it would take 1 million years before corrosion breakthrough occurs in the 50 mm thick copper lid. If diffusion through the bentonite occurs through a cross-sectional area corresponding to the area of the canister lid, the time for corrosion breakthrough will be approximately three times longer. With a ten times higher diffusivity, representative of diffusion in unconfined water, it would still take on the order of 100,000 to 300,000 years before breakthrough occurs. With the higher concentration of dissolved oxygen, corresponding to glacial conditions, it would take on the order of 200,000 to 600,000 years for corrosion breakthrough provided that the buffer has retained its properties and about 20,000 to 60,000 years if the buffer above the canister is lost and diffusion of oxygen occurs through water only.

Sulphide as a corrosion agent is neglected in this scenario, since the corrosion breakthrough times are expected to be significantly longer than those estimated for oxygen. The main reasons for this are that the natural concentrations expected are at most in the order of $10^{-5}$ M /Tullborg et al. 2010/, which is orders of magnitudes lower than the concentration of oxygen assumed in the simplified calculations, and that the stoichiometry of the corrosion reaction imply that less copper is consumed per mol sulphide (2 mol) compared with the consumption by oxygen (4 mol). The organic material contained in the bentonite material in buffer and backfill (see Section 10.2.5) is not expected to be utilised for microbial reduction of sulphate in the groundwater to sulphide as long as oxygen is present, if indeed they are at all susceptible to biodegradation.

**Conclusion regarding containment potential**

According to the reference glacial cycle evolution described in Section 10.4.1 and displayed in Figure 10-107, extensive glacial conditions are not expected to be established within the next c. 58,000 years. Even if the density of the buffer in deposition holes close to the intersection between the deposition tunnel and the main tunnel significantly decreases, the calculations carried out indicate that no corrosion breakthrough is to be expected within the next c. 58,000 years. Furthermore, the results of the hydrogeological analysis indicate that the hydraulic gradients during temperate conditions are directed towards the open tunnels and, hence, would act against oxygen transport from the open tunnels to the deposition holes. The hydrogeological results for temperate conditions also indicate only small effects of the open tunnels on the Darcy flux at deposition hole positions. Although the open tunnels change the flow paths with somewhat reduced flow related transport resistances in the rock as a result, these resistances are still high. The fact that flow paths are captured by the open tunnels and discharge through the shafts and ramp above the central area is also considered as insignificant, since discharge points occur close to the repository also in the reference evolution and also because periglacial conditions with permafrost in the upper parts of the ramp and shafts will prevail for large parts of the 58,000 year time period. This implies that the impact of the open tunnels for deposition holes other than those directly affected by the expanding tunnel backfill is small. Therefore, no analyses of radionuclide release and dose consequences are carried out for the period prior to the next glaciation.

At the onset of the glacial period at Forsmark (c. 58,000 years after present), the hydrogeology at the site is expected to change and high groundwater flows in the open tunnels cannot be excluded. According to the reference evolution, Figure 10-107, this glacial period will last for c. 8,000 years. No corrosion breakthrough in canisters is expected during an 8,000 year long period with glacial conditions as long as diffusion is the dominating transport process in the buffer for corrosive agents in the groundwater. However, backfill that has expanded out into the main tunnels may be carried away during periods of high groundwater flow in the open tunnels. This may, in turn, result in further expansion of deposition tunnel backfill out into the main tunnels, exposing the buffer in deposition

holes close to the intersection with the main tunnel to less and less counter pressure from the remaining backfill in the deposition tunnels. This may lead to expansion of the buffer upwards into the deposition tunnel, leading to a decrease in buffer density. Furthermore, if the deposition hole is intersected by a fracture large enough to carry substantial flow, buffer and backfill material could be carried away by groundwater flowing through the deposition hole and the deposition tunnel. Whether this situation is likely to occur during the 8,000 year long glacial period has not been quantitatively assessed. However, here it is assumed that it does and that this also implies that the groundwater flow through the deposition hole is large enough to supply the amount of corrosive species needed for corrosion breakthrough in the canister to occur before the end of this glacial period. This should be a cautious assumption, since permafrost prevails in the upper part of the bedrock, at least down to c. 70 m depth, during the whole period (Figure 10-107), which should limit the water turnover in the open tunnels in the repository.

#### *Quantitative assessment of the radionuclide release and dose consequences of an incompletely sealed repository.*

According to the reference glacial cycle evolution (Figure 10-107), deglaciation at the site will occur at 66,200 AP after which the site will be submerged during the following c. 8,000 years before periods with alternating periglacial and temperate conditions occur. In the analysis of the radionuclide release and dose consequences of this case, see the **FHA report**, the sequence of submerged and alternating periglacial and temperate conditions is not considered. Instead it is for simplicity assumed that temperate conditions prevail when calculating the radionuclide release from the repository and the subsequent dose impact. Further assumptions made in the calculations are listed below and data used in the calculations are the same as those provided in Table 14-2, except for the water flow through the deposition hole, which is set to the value of high water flow in the analyses of the scenario "canister failure due to corrosion (0.73 $m^3$/year).

- No corrosion breakthrough in canisters occurs during the first period of temperate conditions lasting until c. 58,000 years after present.
- During the subsequent glacial period lasting until 66,200 years after present, corrosion breakthrough occurs in a canister in a deposition hole that is intersected by a fracture with high groundwater flow and which is located close to the intersection between a deposition tunnel and an open main tunnel.
- At year 66,200 after present, radionuclides are released from the spent fuel in the failed canister at a rate determined by the advective flow in the fracture intersecting the deposition hole. The released radionuclides are transported with the flowing water from the deposition hole to the central area and the access ramp and shafts above the central area via the deposition tunnel and open main and transport tunnels. The concentration of radionuclides in the water in the open system is determined by the groundwater turnover in the open tunnels as estimated for temperate conditions.
- The water in the access ramp and shafts is utilised by humans for agricultural purposes and as drinking water.

The calculated total effective dose (Figure 14-5) during the first 1,000 years after canister failure is 56 μSv/year and the dose is dominated by the intake of food and water contaminated by Pu-239 and by external radiation from Nb-94. Thereafter, the effective dose remains at a fairly constant level of about 25 μSv/year for the remaining period until the start of glacial conditions about 90 thousand years after present. During this period, the dose is dominated by the intake of food and water contaminated with Pu-239 and Ra-226.

The calculated effective dose is above the regulatory risk limit of 14 μSv/year during the whole time period analysed, but below the dose of 1 mSv/year from background radiation. The calculated effective dose is obtained for a postulated failure of one canister in the repository during the glacial period prior to 66,200 years after present. In order to receive an effective dose that is comparable to that received from background radiation, approximately 20 canisters can fail during this period.

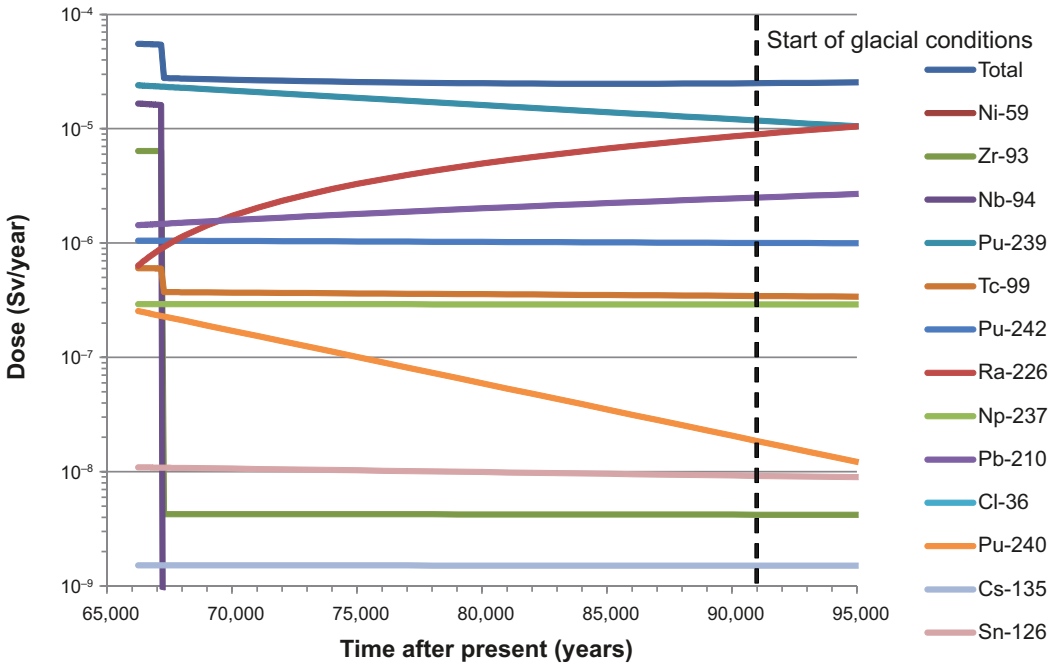


***Figure 14-5.*** *Calculated effective dose from using water in the open shafts and ramp as drinking water and for irrigation (Figure 6-19 in the* ***FHA report****).*

### *Uncertainties*

The uncertainties in the analyses of expansion of deposition tunnel backfill are rather large. The friction angle is a function of the swelling pressure and increases with decreasing swelling pressure. The values at low swelling pressure are not well known, but laboratory measurements indicate that the friction angle is higher than 20 degrees at low density and that the lateral stresses (corresponding to the normal stresses towards the rock surface) are higher than the stress in the swelling direction. This means that the resisting force from friction is probably larger than that modelled, which implies that the results are probably pessimistic in the sense that the swelling and thus density loss would be smaller than modelled /Åkesson et al. 2010a/.

There are a number of uncertainties in the analyses of the impact on groundwater flow of open tunnels in the repository, especially for the simulations with glacial conditions. One important uncertainty relates to the accessibility of water. In reality the flow in an open tunnel below the ice front will probably be limited by the supply of subglacial melt water in the transmissive subglacial layer at the ice-subsurface interface. If the supply of water is insufficient, there will be a drawdown of the pressure and the flow will decrease. In order to give such a high flow as adopted above, the tunnel entrances have to coincide with a major melt water tunnel under the ice. It should also be noted that the calculations assume a worst case location of the ice front in terms of hydraulic gradient. The hydraulic gradient below the ice sheet when the repository is completely covered by ice may be even lower than during the temperate conditions /Vidstrand et al. 2010/.

Several simplified assumptions are made in the calculations of oxygen supply to the canister surface. The only transport resistance accounted for is that in the buffer surrounding the canister, whereas transport resistances in the backfill on top of the buffer in the deposition hole and in the deposition tunnel as well as in fractures in the rock are neglected. This is judged as very pessimistic, at least for temperate conditions. Even if the tunnel backfill expands out into the main tunnel and the density of the backfill above a deposition hole is significantly reduced, the transport resistance in the deposition tunnel should still be significant. This is supported by the results of the hydrogeological modelling that indicate that the hydraulic gradients are directed towards the open tunnels in the repository. Any oxygen transport from the open tunnels to the deposition holes then has to take place in a direction opposite to the hydraulic gradient. Other pessimistic assumptions concern the oxygen concentration and that it remains constant over a long time period. There are both biotic and abiotic processes that may consume oxygen in the repository environment.

The assumption that the tunnels will remain open after the advance and retreat of an ice sheet is also uncertain. Although the surface denudation is quite small at Forsmark, see Section 4.5.7 in the **Climate report**, it seems very likely that eroded materials will fall down and fill in at least parts of the open tunnels.

The assumption that one canister fails due to corrosion during the next glacial period is not backed-up by any quantitative assessments, but is postulated based on cautious assumptions and therefore associated with large uncertainties. For example, it is assumed that the water flow in a fracture intersecting a deposition hole is large enough to carry away buffer in the deposition hole and backfill material above the deposition hole and to supply enough corrosive species for corrosion breakthrough to occur within an 8,000 year long period. Considering that in the design premises for the final repository there are limits on the water inflow to a deposition hole that will be accepted for hosting a canister /SKB 2009a/, the potential for deposition holes that have intersecting fractures with high flow rates should be low.

#### *Conclusions*

From the simplified analyses carried out it can be concluded that abandoning the repository without backfilling and sealing all parts of the repository may imply that backfill in the deposition tunnels is lost and that the safety functions for containment are violated for deposition holes located close to the entrance of the deposition tunnels. Therefore, the general conclusion is that the repository should not be abandoned prior to complete backfilling and sealing.

The analyses of a not completely sealed repository further demonstrate that the repository system adapted to the Forsmark site is robust over a long period of time. Even without backfill in parts of the system, no canister failures are expected as long as diffusion dominates the transport of corrosive species in the backfill in deposition tunnels and buffer in deposition holes. The hydrogeological results for temperate conditions also indicate only small effects of the open tunnels on the Darcy flux at deposition hole positions. Although the open tunnels change the flow paths with somewhat reduced flow related transport resistances in the rock as a result, these resistances are still high. The fact that flow paths are captured by the open tunnels and discharge through the shafts and ramp above the central area is also considered as insignificant, since discharge points occur close to the repository also in the reference evolution and also because periglacial conditions with permafrost in the upper parts of the ramp and shafts will prevail for large parts of the 58,000 year time period. This implies that the impact of the open tunnels for deposition holes other than those directly affected by the expanding tunnel backfill is small.

If corrosion breakthrough in canisters occurs during the next period with glacial conditions, i.e. from 58,000 years to 66,200 years after present according to the reference evolution, the annual effective dose from radionuclides in the failed canisters will exceed the regulatory risk limit. However, as long as the number of failed canisters is limited to less than c. 20, the effective dose from radionuclides in these canisters will be lower than the dose obtained from background radiation. Considering the large uncertainties and cautious assumptions made in the analysis, the calculated annual effective dose should be seen as an illustration of possible consequences rather than an estimation of what the consequence would be if the repository is not completely backfilled and sealed.

## 14.3 Analyses required to demonstrate optimisation and use of best available technique

### 14.3.1 Introduction

As stated in Section 2.7 some aspects of the demonstration of best available technique (BAT) need to be addressed in the assessment of long-term safety supporting the licence application, i.e. in the SR-Site reporting. While a general account of the use of BAT is a broad issue spanning from the selection of method for the management of nuclear waste to fine details of the selected method, a limited part of this issue can and should be addressed in the safety assessment of the preferred method. Here, the account of BAT is, therefore, confined to the KBS-3 method with vertical deposition, using copper/cast iron canisters, buffer and backfill at the selected site.

Within the SR-Site assessment final judgements on BAT cannot be made, but a basis for such judgements can be provided. As stated in the introduction, Section 1.2, SR-Site is based on a reference design of the engineered parts of the repository, including reference methods to achieve the specified design, taking into account methods of controlling that the specifications of the reference design have been achieved. Feedback can be given as to whether alterations in relation to this reference design could lead to reductions in risk or in reduction in uncertainties that potentially could affect risk. For aspects of the design where no such reduction in risk or uncertainty in fulfilment of safety functions can be seen to be realistically obtainable, the solution will be claimed to be optimal and BAT. However, SR-Site is not an assessment of all conceivable technical solutions. SKB will continue technical development of several aspects of the design in order to further simplify construction and implementation, but will only adopt these developments if they lead to the same or lower risk than found in SR-Site.

The BAT related assessment focuses on the scenarios, with their related safety functions, contributing to risk, i.e. the scenarios treating canister corrosion failure and canister shear failure. For these scenarios aspects of the design influencing the occurrence of the scenario and its calculated risk are assessed considering whether realistic alterations of the design would significantly reduce risk. In addition, also the main features of the design, such as backfill, sealing or repository depth, that do not directly contribute to risk are assessed, in order to clarify whether there are aspects of these features that could be detrimental to any safety functions and whether changes to these features could enhance safety.

The analysis of the containment potential for the relevant scenarios presented in Chapter 12 and the analyses of retardation potential and risk, presented in Chapter 13, with associated sensitivity analyses, are the bases of the BAT related assessment presented in the following subsections, since they point to the most important issues to consider in the BAT discussion. Furthermore, in order to evaluate the calculated risk results in the assessment of long-term safety from the point of view of BAT and optimisation, some additional analyses of the sensitivity of the risk with respect to important barrier dimensions and layout rules have been carried out and are presented below. The overall assessment of whether the current reference design is in compliance with this aspect of BAT is left to Section 15.3.5.

### 14.3.2 Potential for corrosion failure

Canister failure due to corrosion, i.e. violation of safety function criterion Can 1, copper shell thickness, according to Figure 8-3, is the main contributor to calculated risk. According to the corrosion scenario assessed in Section 12.6, corrosion failure could only occur if advective conditions develop in the buffer. Factors of the design influencing the potential for advective conditions in the buffer are (Section 12.2):

- Buffer density – amount of dry mass deposited.
- Backfill density – amount of dry mass deposited above the deposition hole.
- Type of buffer material used.
- Geosphere conditions yielding very high or very low ionic strengths of groundwater.
- Geosphere conditions leading to increased flow.

Factors of the design affecting the potential for corrosion failure in case of an eroded buffer are (see Section 12.6):

- Copper shell thickness.
- Deposition hole acceptance criteria – since these may affect the Darcy flux of the groundwater around the deposition hole.

In the following it is assessed, based on results already presented in this report complemented by some additional sensitivity analyses, whether realistic changes of the current reference design would lead to reduced risk.

### *Copper shell thickness*

The mean number of failed canisters at one million years in the corrosion scenario has been calculated for cases where the reference design copper thickness of 5 cm is changed to 10 cm and to 2.5 cm. All other input data are as for the central corrosion variant, see Section 12.6.3, meaning e.g. that the result is based on a weighted mean of all semi-correlated hydrogeological DFN realisations. The results show that increasing the copper thickness to 10 cm reduces the mean number of failed canisters at one million years by a factor of about 3 while halving the thickness to 2.5 cm increases the number by about a factor of 2, see Figure 14-6.

The maximum dose and hence the risk depends on the canister thickness in a similar way to the mean number of failed canisters at one million years, see the **Radionuclide transport report**.

Since the calculated risk with the reference design is below the regulatory limit, the selected copper thickness is deemed adequate from the point of view of BAT. Potential problems of manufacturing and sealing a thicker canister have not been considered in this analysis.

### *Buffer material – potential for avoiding buffer erosion*

The assessment of buffer erosion/colloid release, summarised in Section 10.3.11, demonstrates that the phenomenon cannot be ruled out in the assessment of long-term safety. There is still uncertainty with regard to modelling of colloid formation and subsequent erosion of the buffer material and the modelling approach thus tends to be pessimistic. It also seems clear that it cannot with current understanding be defensibly mitigated by e.g. selection of another buffer material. A continued R&D program is needed.

Furthermore, it is possible that the erosion process will be hindered, from an early stage, by accessory material in the eroded buffer filling up the fractures in which the erosion process occurs /Neretnieks et al. 2009/. Continued R&D is required before such a phenomenon could be taken credit for in the safety assessment.

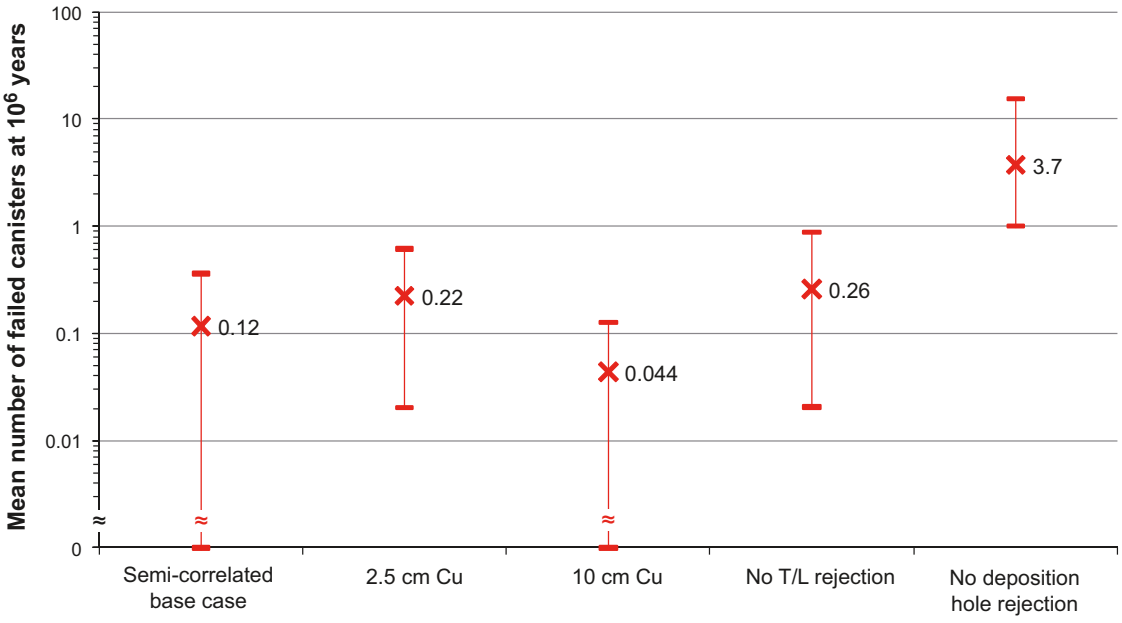


***Figure 14-6.*** *Sensitivity cases relating to BAT for the corrosion scenario. Cases with 2.5 and 10 cm copper thickness are shown as are two cases where the rejection criteria for deposition holes are eased and omitted, respectively. The crosses denote mean values and the bars denote the variability over the several realisations of the hydrogeological DFN models.*

### *Buffer mass and thickness*

A thicker buffer and hence a larger deposition hole diameter, would to a limited extent mitigate the effects of buffer erosion, since an increased buffer mass would allow more buffer to be lost without advective conditions arising. This is however counteracted by the increased deposition hole diameter, which to some extent would increase the erosion rate /Moreno et al. 2010/ and also increase the probability of having a water-conducting fracture intersecting the deposition hole.

In conclusion, a larger buffer mass is not seen as a practical means of mitigating the effects of buffer erosion. A larger buffer mass may offer a slightly longer time before advective conditions are encountered in the deposition hole, but this is not seen as a solution to the issue. It is also concluded that continued R&D on the erosion process is required. It may also be noted that changing the buffer thickness would also imply a need for revising the thermal design of the repository.

### *Backfill density – Amount of dry mass deposited above the deposition hole*

According to Section 10.3.9 a maximum backfill material loss of 220 tonnes in a deposition tunnel section can be allowed before advective conditions have to be considered in the deposition hole below. As concluded in Section 10.3.11 none of the tunnel intersecting single fractures will cause erosion of the backfill to this extent. For a few positions where the tunnel is intersected by a transmissive deformation zone, potentially more than 220 tonnes could be lost, but this is not relevant from the point of view of canister integrity. Such local loss of backfill by erosion does not mean that the hydraulic conductivity of the entire tunnel will be affected and these occurrences are not judged to impair safety. In conclusion, the amount of dry mass deposited above the deposition hole according to current design is deemed appropriate.

### *Deposition hole acceptance criteria*

The groundwater flow around and through deposition holes has a large impact on both the loss of bentonite which may potentially lead to advective conditions and on the rate of corrosion by sulphide in the groundwater as illustrated by Figures 10-72 and 10-158. These figures also show the large impact of applying EFPC as a means to avoid deposition holes with high groundwater flow. As described in Section 5.2.3, in addition to the 'pure' EFPC criterion, also an additional deposition hole rejection criterion related to the combination of a high transmissivity and length of the intersecting fracture (T/L filtering) is assumed in the reference design of the repository and in the analyses carried out in SR-Site.

In order to further investigate the importance of the deposition hole acceptance criteria some additional cases have been studied.

The mean number of failed canisters at one million years in the corrosion scenario has been calculated for cases where i) the transmissivity-fracture length (T/L) filter is omitted and ii) no rejection is applied, i.e. neither the T/L-filter nor the 'pure' EFPC criterion are applied. All other input data are as for the central corrosion variant, see Section 12.6.3. The results show that omitting the T/L-filter increases the mean number of failed canisters at one million years by a factor of about 2 while the omission of all rejection criteria increases the number by about a factor of 30, see Figure 14-6. In particular the latter of these two results demonstrate the necessity of applying appropriate rejection criteria.

The maximum dose and hence the risk depends on the rejection criteria in a similar way to the mean number of failed canisters at one million years, see the **Radionuclide transport report**.

Furthermore, with the assumptions used in the corrosion calculations for advective conditions in SR-Site, in a deposition hole with a Darcy flux of 0.001 m/yr it takes more than 900,000 years to corrode through a canister after the buffer has been eroded away, even with the highest sulphide concentration considered in the corrosion calculations (0.00012 M). Also, the time to erode the buffer is of the order of 100,000 years for such a hole if the aperture of the fracture to which buffer is lost is $10^{-3}$ m and assuming dilute conditions 25% of the time. This means that if deposition positions with long term Darcy fluxes of 0.001 m/yr or more could be identified and rejected, then the risk over the one million year assessment time associated with the corrosion scenario should vanish. It is also noteworthy that a Darcy flux limit of 0.01 m/yr would not reduce the risk much compared to what is obtained with the EPFC criterion, since almost all of the few positions with such Darcy fluxes

are already avoided. Typically less than one percent of the deposition positions have Darcy fluxes above 0.001 m/yr and around one in a thousand have fluxes above 0.01 m/yr without any rejection, meaning that if an efficient criterion more directly related to the Darcy flux could be formulated, the potential losses of deposition positions would be small.

It should be noted that since SR-Site considers the application of the EFPC (including the T/L criterion), in practise also a hydraulic consideration is applied. Since there is a correlation, although uncertain, between fracture size and transmissivity, application of the EFPC in fact reduces the number of high Darcy flux deposition holes significantly. This observation highlights the fact that it is not the EFPC as such that is important, but the finding of an observable property that would identify potentially flowing fractures.

A more direct criterion that could further reduce the calculated risk, explored within SR-Site, is to adopt an inflow criterion since there has to be a correlation between high inflows during open repository conditions and high future Darcy fluxes. As is discussed in Section 10.2.3 and further elaborated in /Selroos and Follin 2010, Section 7.1/, such a correlation indeed exists, at least for the higher inflows and Darcy fluxes. For example, this analysis suggests that avoiding inflows above 0.1 L/min implies that Darcy fluxes above $10^{-2}$ m/yr during saturated temperate conditions would not occur. To further study the potential effects of such a criterion, the identified deposition positions with high inflow rates under open repository conditions were omitted in an analysis of the central corrosion variant of the corrosion scenario, for the base case realisation of the semi-correlated hydro-DFN model. This led to the result that no canister failures occurred in the scenario, i.e. all the unsuitable deposition positions were identified by this procedure.

In conclusion, there appears to be a potential for further enhancing safety by avoiding deposition holes with high inflows, even if the correlation is not one-to-one given the differences in boundary condition. Furthermore, the inflows will be disturbed by skin effects and grouting and there will also be a practical lower detection limit. Partly, these disturbances may be overcome by requiring that deposition holes intersected by fractures capable of providing inflows above a certain value are to be avoided. This suggests that the hydraulic properties of the fractures intersecting the borehole should be tested in the pilot hole prior to drilling the full size hole, thereby avoiding skin effects, and that deposition holes intersected by fractures showing visible grout also should be rejected, since the presence of grout suggests that the fracture was quite transmissive before grouting.

#### *Deposition tunnel acceptance criteria – including the EDZ*

According to current design premises, excavation induced damage in deposition tunnels should be limited and not result in a connected effective transmissivity, along a significant part (i.e. at least 20–30 m) of the disposal tunnel and averaged across the tunnel floor, higher than $10^{-8}$ m$^2$/s. Evidence presented in the **Underground openings construction report** and further elaborated in the **Data report** and in Section 10.2.2 suggests there is ample evidence that a potential EDZ formed during excavation will be kept below the maximum allowed transmissivity as set out by the design premises and data suggests that a continuous EDZ would not develop at all. However, as also stated in the **Underground openings construction report**, further development of the method to control the EDZ as well as demonstration of the reliability of this method is needed.

As shown in Table 14-3 the number of corroded canisters is identical between cases without an EDZ and with the basic assumption of an EDZ transmissivity of $10^{-8}$ m$^2$/s.

The table also shows that a more transmissive EDZ could affect risk since the number of failed canisters starts to increase, although moderately when the transmissivity is increased. It is thus concluded that the transmissivity limit of $10^{-8}$ m$^2$/s is adequate.

The EDZ appears even less important for radionuclide transport. For the pin-hole scenario, see Section 13.7.2, the presence of an EDZ with a transmissivity of $10^{-8}$ m$^2$/s increases the dose only marginally compared with the case without an EDZ, and making the EDZ transmissivity larger does not further increase the dose.

**Table 14-3. Calculated mean number of failed canisters at one million years for various assumptions regarding the properties of the EDZ and the existence of a crown space.**

| | Mean number of failed canisters at one million years |
|---|---|
| Semi-correlated base case realisation without EDZ | 0.083 |
| Semi-correlated base case realisation (includes EDZ with $T = 10^{-8}$ m²/s) | 0.083 |
| Semi-correlated base case realisation with $T = 10^{-7}$ m²/s EDZ | 0.19 |
| Semi-correlated base case realisation with $T = 10^{-6}$ m²/s EDZ | 0.33 |
| Semi-correlated base case realisation with crown space (includes EDZ with $T = 10^{-8}$ m²/s) | 0.25 |

### 14.3.3 Potential for shear failure

Canister failure due to shear, i.e. violating safety function criterion Can 3 "Withstand shear load", according to Figure 8-2, is a contributor to calculated risk, even if the contribution is small. As concluded in Section 10.4.5, pessimistic estimates of canister failure due to rock shear indicate that the probability that one out of the 6,000 canisters has failed at Forsmark at the end of the one million year assessment period is 0.079. This leads to a peak mean dose of 0.15 μSv, occurring at one million years, Section 13.6. It could well be argued that further reductions of this very low risk contribution are not very meaningful, but it is nevertheless worthwhile to consider what factors of the design influence the potential for shear failure. According to the assessment of the canister shear scenario (Section 12.8) these factors are:

- Insert strength and the occurrence of defects.
- Copper shell mechanical properties.
- Buffer density and buffer material properties.
- Efficiency in the implementation of deposition hole rejection.

These factors are assessed in the following, mainly using the findings of the studies by /Raiko et al. 2010/ of the canister-buffer system response to shear loads within the canister design analysis, forming an important basis for the **Canister production report**. As stated in Section 10.4.5 the current design premises are the result of a balance between achievable requirements on the canister and on the layout of the repository, given the understanding of earthquakes and secondary shear movements on the one hand and of the response of the buffer-canister system on the other. A lower design premise shear displacement would give a higher probability for shear with given layout rules, but lower requirements on the canister design and material (especially the non-destructive testing of the insert) and vice versa. Furthermore, the cited analyses of the response of the buffer-canister system to a shear load also suggest that if the real variability in buffer density, fracture orientation and impact location on the canister were to be taken into account, then in many cases not even a 10 cm shear movement would jeopardise the integrity of the canister. This conclusion is further corroborated by the fact that the criteria used to evaluate the modelling results relate to local properties, and the violating of these criteria would not, in many cases, lead to loss of the integrity of the copper shell.

#### *Insert strength and the occurrence of defects*

The capability of the insert to withstand shear load depends mainly on the occurrence of surface defects in the cast iron. According to the damage tolerance analyses /Raiko et al. 2010/, discussed in Sections 10.4.5 and 5.4.3, the maximum acceptable depth of crack-like surface defects with a semi-elliptical shape is quite small (4.5 mm). Larger shear displacement will lessen the acceptable depth, while decreasing the buffer density will increase it.

While the **Canister production report** concludes that the current canister reference design conforms to the stated design premises, it is also noted that rigorous requirements on manufacturing and NDT capability are needed for the insert. Revising the design of the canister/buffer system such that the loads in the insert decrease, e.g. by reducing buffer density, would thus allow relaxation of the manufacturing and NDT capability requirements relating to the insert.

It should also be noted that the initial state for the shear load case does not take into account PWR inserts as representative materials data for strength and damage tolerance analysis are not yet available. Formally, SR-Site cannot assess the adequacy of PWR inserts. However, the PWR design is more robust due to the higher material thickness in the cast iron insert.

### *Copper shell mechanical properties*

The results from inspections of manufactured canister components, presented in the **Canister production report**, show that the specified values for elongation and creep ductility in the copper shells conform to the reference design. These design values are used in the subsequent damage tolerance analysis /Raiko et al. 2010/ and are found appropriate. While formal sensitivity analyses of the importance of the copper shell mechanical properties are not made, it is judged that there is little prospect that changing these properties would enable the canister to withstand even larger loads.

### *Buffer density and buffer material properties*

Alteration of the buffer material due to cementation yields small effects in the shear analyses. In the shear calculation made for SR-Can /Börgesson and Hernelind 2006b/ an 8.75 cm thick zone of the buffer material around the canister was assumed to be converted to cement like material, with no swelling pressure, with an E-modulus increased by a factor of 100 and a shear strength increased by a factor of 5 compared to the unaltered buffer. No new calculations of this case have been done for SR-Site since such strong changes of bentonite properties are unrealistic, the properties of converted material are unknown and the effect rather small. Conversely it is not judged feasible to change the buffer composition such that the E-modulus and shear strength are reduced considerably, while keeping the needed swelling pressure.

Lowering the bentonite density lessens both the strain and the stress on the insert, as demonstrated in Section 10.4.5, Table 10-22. Given the experience in producing and controlling the buffer density, as assessed in the **Buffer production report**, a feasible approach for relaxing the requirements on the canister would be to tighten the requirements on the maximum allowed buffer density. As discussed in Section 5.5.3 the derived initial state of the buffer implies a maximum bentonite density of 2,022 kg/m$^3$ around the canister, which would increase the margins for the effects of rock shear on the canister. Further reductions of the maximum allowed buffer density, still practically compatible with the requirements on minimum buffer density may also be feasible, at least in the form of a statistical distribution. Consequently, SR-Site provides this feedback for updating the design premises and for revising the buffer design, see Section 15.5.7.

### *Efficiency in the implementation of deposition hole rejection*

As stated in Section 12.8.2, the number of canisters that may fail due to shear load during the assessment period depends on the success of detecting and avoiding large fractures in deposition holes. The FPI deposition hole rejection criteria have been shown to be effective in finding critical structures and enable the detection of > 97% of the critical canister positions irrespective of DFN model /Munier 2010/. The remaining positions are propagated to the assessment of seismic impact (Section 10.4.5). However, the FPI simulations are based on idealisations of fractures as being perfectly planar, infinitesimally thin discs for computational convenience. Most real fractures are not anonymous and, rather, display many properties that can be used as proxies for size /Cosgrove et al. 2006/. It is therefore, as argued in /Munier 2010/, likely that critical fractures that escaped detection in the simulations used as input for this assessment will indeed be detected by a carefully designed investigation programme /SKB 2010b/. Hence, it is likely that the number of potentially damaged canisters will be lower than predicted in this assessment. From the viewpoint of BAT it may thus be argued that while the current EFPC provides adequate protection against shear failure, there is reason to continue the efforts envisaged in the detailed investigation programme to be able to find critically large fractures by other means. Such efforts are also likely to be economically attractive, since application of EFPC implies that many deposition holes are rejected, even if they are not intersected by sufficiently large fractures to be of any concern.

### 14.3.4 Design related factors that do not contribute to risk

#### *Failure due to isostatic overpressure*

The assessment of the scenario "Canister failure due to isostatic load", presented in Section 12.7.5, concludes that a maximum swelling pressure of 15 MPa could occur in the buffer, the groundwater pressure is around 4.5 MPa at Forsmark for ice-free conditions and an additional ground water pressure of at most 30 MPa could occur as a result of a maximum glacial load supported by geological evidence. The sum of these loads is 49.5 MPa. However, considering that the combined impact of swelling pressure and hydrostatic load is somewhat smaller than this sum, this, as suggested in Section 12.7.5, results in a total pressure of around 46.5 MPa.

The assessment of canister strength concludes that local collapse is avoided with substantial margin for 45 MPa and the margin to total collapse (90 MPa), i.e. the criterion for canister failure, is considerable. For the given reference design there is ample margin to prevent canister failure due to isostatic load, even for the most extreme load situations and there seems to be no need to change the design in order to increase this margin.

#### *Dimensions and material properties of the deposition tunnel backfill*

The backfill safety functions BF1, according to Figure 8-3, are to keep the buffer in place and to have sufficiently low hydraulic conductivity. These safety functions are achieved and maintained with the current backfill design.

It is concluded in Section 10.3.9 that the swelling pressure of the buffer and the associated safety functions will be maintained during the expansion of the buffer into the backfill for all possible combinations of buffer and backfill conditions. Furthermore, several likely pessimistic assumptions are made in this analysis including assuming the buffer to be completely water saturated and homogenised from the start, assuming weak mechanical contacts between the backfill blocks, not including the local crushing of the blocks that may occur close to the floor and assumed that the backfill blocks are not overlapping.

It is also important that the backfill maintains its swelling pressure, thereby avoiding e.g. the formation of a water conductive crown space immediately beneath the tunnel ceiling. As demonstrated by the last row of Table 14-3, such a crown space could alter the flow situation e.g. such that it affects canister failures due to corrosion negatively. The swelling pressure is indeed assessed to be maintained with the current design.

- According to Section 10.3.9, there will be a remaining density gradient in the backfill after saturation. The calculated lowest density is 1,370 kg/m$^3$, which according to Figure 5-19 would give a swelling pressure of ~1 MPa. This is an order of magnitude higher than the swelling pressure needed to fulfil backfill safety function Bf2 (Figure 8-3). Thus, the backfill self-sealing ability should be sufficient.
- As seen in Section 10.3.9, erosion of backfill in a tunnel intersected by a highly conductive fracture is important for the properties of the buffer in the deposition hole, but is not expected to have any significant importance for the transport properties itself. There will be a local volume with low swelling pressure and high hydraulic conductivity. However, the main part of the tunnel volume will be unaffected.
- Since the temperature is low under all conditions, montmorillonite alteration, in the form of illitization can be neglected in the backfill. It is also assumed that the cement in the repository will be of the "low-pH" type and will have insignificant impact on the properties of the backfill (see the **Buffer, backfill and closure process report**, Section 4.4.7).
- In Sections 10.4.8 it is shown that future changes in temperature and groundwater chemistry will have limited or no effect on the hydromechanical properties of the backfill material.

For the case when backfill material is lost, a maximum loss of 220 tonnes in a deposition tunnel section can be allowed before advective conditions have to be considered in a deposition hole. As found in Section 10.3.11 none of the tunnel intersecting single fractures will cause erosion of the backfill to the extent that it loses so much swelling pressure that advective conditions must be assumed in underlying deposition holes. For a few positions where the tunnel is intersected by a very transmissive deformation zone, potentially more than 220 tonnes could be lost, but this is not relevant from the point of view of canister integrity. Such local loss of backfill by erosion does not mean that the hydraulic conductivity of the entire tunnel will be affected and these occurrences are not judged to impair safety.

In conclusion, while there possibly could be improvements in the backfill design from an installation point of view, there does not seem to be a need to change the design to further improve its safety functions.

### *Dimensions and material properties of the closure*

There are no direct safety functions connected to the closure of the repository, but its impact has been assessed in SR-Site. The reference design presented in the **Underground openings construction report** and in the **Closure production report** conforms to these design premises and the analyses in SR-Site show that a design following these rules would be appropriate. Furthermore, based on the findings from varying the transmissivity of the EDZ, discussed in Section 14.3.2 it is not obvious that these rules can be relaxed. However, it is likely that the direct impact on risk would only apply to the EDZ in the deposition tunnels, whereas a higher transmissivity probably could be accepted in the other tunnels. Such a situation has, however, not been analysed in SR-Site.

### *Repository depth*

As explained in the **Underground openings construction report** and further discussed in Section 5.2.2, the repository depth has mainly been decided by considering the hydraulic conditions of the Forsmark site, i.e. frequency and occurrence of transmissive fractures and their dependence on depth, while the constructability is mainly related to rock mechanical issues, e.g. the likelihood and extent of spalling in deposition holes prior to emplacement. It is judged that remaining uncertainties in the geological description can be sufficiently resolved using methods and techniques that were implemented during the site investigations and would only require minor re-adjustments of the available areas. Uncertainties in the orientation of maximum horizontal stress can only be significantly reduced by in situ tests at depth during access construction. The finding may necessitate a re-orientation of the deposition tunnels, but would not affect the overall suitability of the designated depth and repository areas.

### Chemical stability – Salinity, redox and sulphide

Factors relating to the chemical stability safety function R1 “Provide chemically favourable conditions” are generally favourable at the selected depth. The only remaining chemical stability issues of concern for repository safety relate to the potential for a few deposition holes to experience groundwater with too low ionic strength and presence of sulphide. The other R1 safety function indicator criteria regarding favourable chemically favourable conditions are upheld for the entire assessment period.

As already concluded in Section 14.3.2, the ionic strength of the groundwater; $\Sigma q[M^{q+}]$, will fall below 4 mM charge equivalent i.e. violating safety indictor criterion R1c, for some deposition holes during some time of the glacial cycle. This may, in turn, lead to loss of buffer in a few deposition holes and that a few (between 0 and 2) canisters would fail due to corrosion by the end of the $10^6$ year assessment period. As already discussed this latter problem could probably be further mitigated by applying more strict inflow rejection criteria when selecting deposition holes. Generally, the risk of penetration of dilute waters would also decrease with increased repository depth. However, the few occurrences of such potential penetration are related to the scarce occurrence of highly transmissive migration paths in the generally very tight rock. There is no evidence that a practically realistic increase of the depth (i.e. in the order of a 100 m) would dramatically reduce the occurrence of such isolated paths – and it seems a better strategy to try to avoid them locally.

The sulphide contents of groundwaters at Forsmark have been examined in /Tullborg et al. 2010/. The data show that there is no indication that sulphide concentrations should be correlated with depth. No dependence has been found between the sulphide concentrations and the transmissivity of the fractures where the groundwaters were sampled. Other parameters that could be involved in the process of bacterial sulphate reduction are concentrations of dissolved organic carbon (DOC), methane and hydrogen. Organic carbon concentrations are higher in the upper 100 m of the rock, but at depth the values are low, less than $2 \cdot 10^{-4}$ mol/L, and no depth trend can be discerned. The data on methane and hydrogen are scarce and show no depth dependency either. The conclusion is therefore that a change in the repository depth would not affect the number of failed canisters due to corrosion by sulphide.

**Lengths and transport resistances of hydraulic travel paths to and from the repository**

Safety function R2a "Transport resistance in fractures, F" is affected by repository depth. The length of the travel paths of solutes in the groundwater will increase with increasing depth, but the resulting impact on the transport resistance would only be marginal, i.e. increasing depth by 100 m would only imply an increase in path length by about 25%. More importantly, the transport resistances offered by these paths would increase with depth if the hydraulic conductivity decreases with depth at the site, see further below.

**Fracture frequency and fracture transmissivity**

Both safety functions R2a "Transport resistance in fractures, F" and R2b "Equivalent flow rate in buffer/rock interface, $Q_{eq}$" are affected by repository depth, since fracture frequency and fracture transmissivity show depth dependence. However, the selected repository depth is well below the depth at about 400 m where the already low frequency of water conducting fractures drops dramatically. Nothing in the data suggests that this extremely low frequency would drop further at realistically reachable greater depths. In summary, the chosen repository depth below 450 m is sufficient to reach the low fracture frequency and low permeability volumes of Forsmark, and there does not seem to be any advantage in going deeper.

**Groundwater pressure**

Groundwater pressure, safety function R3a, contributing to the isostatic load on the canister, increases with depth. However, compared with the buffer swelling pressure and hydrostatic pressures from a glacial overburden, the increased pressures are of marginal importance. An increased pressure will also increase the inflow to the repository during construction, unless this is counteracted by grouting – this is however mainly an issue for repository engineering. Furthermore, there will only be limited needs for grouting at depth in Forsmark, since the frequency of water conducting fractures and deformations zones is very low.

**Rock stress**

Rock stress indirectly affects safety function R2b "Equivalent flow rate in buffer/rock interface, $Q_{eq}$", since the in situ stress determines the potential for spalling. Stress in general increases with depth, but as concluded in the **Underground openings construction report** (and its underlying references), below 300 m depth, there appears to be little evidence that the horizontal stress magnitudes in fracture domain FFM01 increase significantly with depth. Hence placing the repository at 400 m or 500 m depth does not significantly increase the risk for spalling in the deposition holes.

**Initial temperature**

The *in situ* temperature, relates to safety function R4 "Provide favourable thermal conditions". Temperature increases with depth, although the thermal gradient is relatively low in the considered depth range. This needs to be considered in the repository layout, when determining the necessary canister spacing that would ensure that the peak buffer temperature lies below stipulated limits, and this means that the canister spacing needs to increase with depth, leading to a larger footprint for a deeper location. However, given that this is considered in the repository design, there are no other detrimental effects of the elevated *in situ* temperature with depth.

**Freezing**

A colder future climate may in principle ultimately lead to freezing and relates to safety function R4 "Provide favourable thermal conditions, of the buffer and the deposition tunnel backfill". Such freezing could in turn have detrimental effects on the canister and the near-field rock. The likelihood of freezing decreases with increasing depth. The analyses in SR-Site have, however, demonstrated that freezing of the buffer can be considered as a residual scenario, i.e. no reasonable way that this could occur has been identified for a depth of 450 m at Forsmark. For an eroded buffer, the freezing point is higher than for an intact buffer. At the current depth it is unlikely but cannot be fully ruled out. The effects are, however, not assessed to threaten the integrity of the canister. As demonstrated in Section 12.3 freezing of the deposition tunnel backfill at these depths can also be ruled out.

**Surface erosion**

Surface erosion of the host rock will occur, in particular by glacial erosion. This means that the repository depth will decrease somewhat for each glacial phase. The extent has been estimated to 1–2 m per glacial cycle, see the **Climate report**, Sections 3.5.4 and 4.5.7, when considering the repository site located in bedrock without major valleys and deformation zones. Therefore, erosion does not have to be considered when determining repository depth within the reference interval 400–700 metres.

**Inadvertent human intrusion**

The probability of inadvertent human intrusion into the repository decreases with increasing depth. Intrusion may have consequences both for the intruders and for the long-term performance of the repository after the intrusion. Intrusion scenarios are evaluated separately from other scenarios in the safety assessment, in accordance with Swedish regulations. Therefore, it is not straight-forward to assign this factor an importance measure in a sense comparable to the other factors discussed here. In general, intrusion to several hundred metres is considered unlikely in resource poor rock.

#### *Other layout issues*

SR-Site has assessed a specific repository layout adapted to the Forsmark site and fulfilling the design premises stated for layout adaptation. The analyses show that for the scenarios contributing to risk (corrosion and shear failure) it is essentially the details of the layout, like the exact position of deposition holes and what deposition holes would be accepted that is important. These details can only be finalised during repository construction and operation and by application of the observational method using findings from the underground based detailed investigations and applying the design premises for accepting deposition holes discussed in previous sections. Thus, the question whether the repository layout is BAT can at this stage only be assessed based on these design premises. More specific feedback on these premises is given in Section 15.5.

## 14.4 Verification that FEP's omitted in earlier parts of the assessment are negligible in light of the completed scenario and risk analysis

### 14.4.1 Introduction

FEP's are omitted at various stages in the assessment. In establishing the SR-Can FEP catalogue, and the update of this to the SR-Site FEP catalogue, audits of FEP's in the NEA FEP databases were carried out (see Chapter 3). The first step in this process was to screen out Project FEP's in the NEA FEP database assessed as not relevant for SR-Can and SR-Site using some pre-defined screening criteria, see the **FEP report**. A FEP could be screened out if one or more of the criteria listed below are fulfilled.

- The FEP is not appropriate to the actual waste, canister design, repository design, geological or geographical setting.
- The FEP is defined by a heading without any description of what is meant by the heading, but from the interpretation of the heading it is judged that the FEP is covered by other NEA Project FEP's.
- The FEP is very general and covered by other more specific NEA Project FEP's.

The outcome of this first screening of FEP's is documented in the SKB FEP database and is not further addressed here. It should be noted that the general strategy in the screening of FEP relevance was to judge FEP's as relevant rather than to screen them out at this stage, unless it is clearly obvious that they are irrelevant.

As described in Section 3.3 and in the **FEP report**, all NEA Project FEP's remaining after the initial relevance screening were mapped to FEP's in the SR-Can and SR-Site FEP catalogues. The result was used to create check lists for updating process descriptions and for the descriptions of the initial states of the repository system components. In addition, FEP lists from the audit were used as checklists for the selected handling of external factors as described in the SR-Can Climate report /SKB 2006c/ and

the SR-Site **Climate report**, the SR-Can FHA report /SKB 2006e/ and the SR-Site **FHA report**, as well as for the establishment of SKB FEP's for further consideration in the selection of scenarios. In this process, additional NEA Project FEP's were omitted by the various experts involved and the reason for omitting each FEP was documented together with the handling of NEA Project FEP's assessed as relevant. A common justification provided for not considering a NEA Project FEP, or an aspect of it, is that it is not relevant for a KBS-3 repository in Swedish crystalline rock, i.e. corresponding to the first screening criterion listed above. This documentation is included in the SKB FEP database, linked to the SR-Can and SR-Site FEP catalogues, and also as appendices in the **FEP report**, and is not further addressed here.

Since the SR-Site FEP catalogue, which is an update of the SR-Can version, is the compilation of FEP's assessed as relevant for a KBS-3 repository located at Forsmark, the remainder of this section is devoted to verification of the legitimacy of omission of FEP's included in the SR-Site FEP catalogue. FEP's considered are processes relevant for the reference evolution, whereas methodology-FEP's are excluded (see Section 3.3).

In the following subsections, the process tables in Section 7.4 are revisited and the legitimacy of omission of all processes assigned as "not relevant" or "neglected" is verified in the light of the completed scenario and risk analysis. The verification of the omission of process FEP's is restricted to the system components of primary concern for repository safety, i.e. the fuel, the canister, the buffer, the backfill and the geosphere. Process FEP's for the remainder of the engineered barrier system are generally judged as of secondary importance for safety and are, therefore, not considered. In particular, the following considerations are identified as being of secondary importance.

- The bottom plate in the deposition holes may degrade (Section 10.3.12), but the impact is less than the impact from assuming spalling in the deposition hole and this effect is thus covered by the assessment assumption that spalling occurs in all deposition holes.
- Disintegration of tunnel plugs will only have a local impact around the plug. As assessed in Section 10.3.12, there will be no effect on the backfill above the nearest deposition hole.
- The only function of the closure of the cavities in the central area is to occupy the space with no other design premise than to prevent substantial convergence and subsidence of the surrounding rock. The only purposes of the backfill in the upper part of the ramp and shaft are to hinder unintentional intrusion into the repository and to keep the lower backfill in place. Both these areas are filled with crushed rock with an assumed high hydraulic conductivity.
- To ensure that they do not act as preferential transport paths, a number of investigation boreholes, holes drilled both from the surface and from underground openings have to be sealed, at the closure of the deep repository. As concluded in Section 10.3.6, the impact of improper sealing of the boreholes is very moderate. Furthermore, according to the assessment presented in Section 10.3.14, the reference design of the borehole seals will perform as intended.

Climate FEP's of importance to the safety of a geological repository are those affecting biosphere and geosphere conditions. Climate issues, corresponding to the climate FEP's in the SR-Site FEP catalogue, and their impact on geosphere conditions as well as their handling in the assessment are documented in Chapter 3 in the **Climate report**. All these issues are considered in the assessment as well as couplings between them. One exception is the impact of surface denudation on the estimated depth of permafrost. However, as discussed in Section 6.1, surface denudation (erosion and weathering) of the host rock has been estimated to generally be limited to a few metres or less per glacial cycle for the Forsmark repository site and some tens of metres for 1 million years. This is of minor importance for repository safety considering that the assessment of permafrost depth (see Sections 10.4.1 and 10.4.3) shows that freezing can be excluded at the repository level. No further treatment of climate issues of relevance to geosphere conditions is made here.

Climate issues of relevance to biosphere conditions as well as biosphere processes are described and handled in the Biosphere process report /SKB 2010c/ and Ecosystem reports /Andersson 2010, Aquilonius 2010, Löfgren 2010/. These are not further addressed here, since the LDF's used in the assessment are bounding values over the full range of climatic conditions of relevance and high utilisation of discharge areas has been assumed. Therefore, most biosphere FEP's will tend to mitigate rather than augment assessed doses.

### 14.4.2 Fuel

According to Table 7-2, the following fuel processes are omitted from the assessment for parts or a whole glacial cycle:

- F3 Induced fission (criticality).
- F7 Structural evolution of the fuel matrix (failed canister).
- F9 Residual gas radiolysis/acid formation (intact canister).
- F10 Water radiolysis (except for fuel dissolution).
- F15 Helium production (intact canister).
- F16 Chemical alteration of fuel matrix (failed canister).

#### *F3 Induced fission (criticality)*

Acceptance criteria for encapsulation of fuel assemblies in canisters are defined to ensure that intact canisters are sub-critical (see Section 5.3.4). Furthermore, analyses of the potential for criticality in failed canisters as well as outside failed canisters indicate that this is highly unlikely (see Section 13.3). Therefore, omission of this process is considered justified as long as the acceptance criteria for fuel encapsulation are met.

#### *F7 Structural evolution of the fuel matrix*

Structural evolution of the fuel matrix due to radioactive decay, mainly alpha decay, could possibly affect the distribution of radionuclides in the fuel matrix. The main impact of this process would be on the segregation of fission products to the grain boundaries of the fuel matrix. However, reported results indicate that radiation-enhanced diffusion in the fuel matrix is too limited to have any effects in the timescale of interest in the safety assessment. Therefore, the judgement in the **Fuel and canister process report** is that this process is negligible for the fuel types and burnup relevant for SR-Site. There are no results of the complete scenario and risk analyses that challenge this neglect, although there are some uncertainties in the gap inventory for future BWR and PWR fuel with higher burnup than the fuel produced so far. However, the cautious handling of the instantly released fractions of the radionuclide inventory (Section 13.5.2) in the assessment calculations is judged to cover remaining uncertainties in this respect. No other coupling than to the instantly released fraction is identified as relevant for this process.

#### *F9 Residual gas radiolysis/acid formation*

There are restrictions on the maximum amount of water and air that the canister shall contain at sealing (Section 5.3.1). With these amounts of oxidants available, the depth of insert penetration by general corrosion is of the order of ten micrometres, see the **Fuel and canister process report**. In addition, the restrictions on water and air (nitrogen) content (more than 90% argon in the canister is required) should constrain the formation of corrosive gases, such as nitric and nitrous acids, implying that stress corrosion cracking of the insert is not likely, see the **Fuel and canister process report** and further Section 14.4.3. Since the restrictions on water and air content are considered to be fulfilled in the reference design, the legitimacy of omission of this process is considered verified.

#### *F10 Water radiolysis*

Any water initially present in the canister, at most 600 g according to the design premises, is expected to be consumed by nitric acid formation or cast iron corrosion (see above). Radiolysis of water intruding into a failed canister will lead to the formation of oxidants and hydrogen. The contribution to hydrogen formation is negligibly small compared with hydrogen formation due to corrosion of the cast iron insert and therefore neglected, see the **Fuel and canister process report**. The formation of oxidants by radiolysis of water is considered in determining the range of fuel dissolution rates explored in the assessment.

In the assessment calculations, it is assumed that the spent fuel is accessible to intruding groundwater once the copper shell has failed and no credit is taken for any transport resistances in the canister interior. These cautious assumptions thus implicitly cover effects of build-up of hydrogen gas that would mechanically impact the cast iron insert and the fuel assemblies and disregard any beneficial effects of build up of hydrogen that could counteract ingress of groundwater. These assumptions also justify the omission of the small contribution from radiolysis of water to hydrogen formation.

#### *F15 Helium production*

Helium is produced in the spent fuel due to alpha decay of actinides. This could lead to a pressure build-up inside the fuel rods, which, in turn, could lead to mechanical rupture of the rods. Based on estimates of the amount of helium that can be generated and the assumption that all generated helium is released to the canister interior, the pressure increase in the canister interior has been calculated and found to be considerably lower than the pressure external to the canister. Based on these results, reported in the **Fuel and canister process report**, the consequence of helium production for the mechanical stability of the canister is neglected. There is nothing in the completed scenario- and risk assessment that questions this neglect, since the reference design conforms to the design premises for the fuel and canister. Concerning the fuel rods, the assumption in the assessment calculations is that they all are ruptured and therefore provide no resistance to release or transport of radionuclides from the fuel once the canister has failed. Concerning the impact of helium build-up on the mechanical stability of the fuel matrix and thus the gap inventory, it is concluded in the **Fuel and canister process report** that there are no detrimental effects, but that there are remaining uncertainties on this point relating to future fuel with a potential higher burn-up level than produced so far. However, as stated above for FEP *F7 Structural evolution of the fuel*, the cautious handling of the instantly released fractions of the radionuclide inventory (Section 13.5.2) in the assessment calculations is judged to cover remaining uncertainties in this respect.

#### *F16 Chemical alteration of the fuel matrix*

Chemical alteration of the fuel matrix refers to the alteration of the uranium dioxide matrix through the formation of coffinite in contact with silica-rich groundwater in a failed canister. According to the **Fuel and canister process report**, this will most likely occur through a dissolution and re-precipitation process where radionuclides in the fuel matrix are released during dissolution of the uranium dioxide. Therefore, assuming that the dissolution rate of uranium dioxide is determining the release of matrix-bound radionuclides in the assessment calculations should be appropriate even if this process is disregarded.

### 14.4.3 Canister

According to Table 7-3, the following canister processes are omitted from the assessment for parts or a whole glacial cycle:

- C4 Deformation of copper canister from external pressure (failed canister).
- C5 Thermal expansion (both cast iron insert and copper canister).
- C7 Radiation effects.
- C9 Galvanic corrosion (failed canister).
- C10 Stress corrosion cracking of cast iron insert.
- C12 Stress corrosion cracking, copper canister.
- C13 Earth currents – stray current corrosion.
- C14 Deposition of salts on canister surface.

#### *C4 Deformation of copper canister from external pressure (failed canister)*

Deformation of a failed copper canister from external pressure, such as the groundwater pressure and the buffer swelling pressure, as well as the load from rock shear, is neglected in the assessment. The assessment results show that failure of a canister by corrosion requires that advective conditions prevail

in the buffer, i.e. the buffer is eroded. Therefore, pessimistic assumptions are made in the calculations of dose impact from a corrosion failure, implying that no transport resistance in the failed canister is accounted for (Section 13.5). In the consequence analyses of canister failure due to shear load (Section 13.6), the same pessimistic assumption concerning the state of the failed canister is made, i.e. that the failure is massive and, therefore, no transport resistance in the canister is accounted for. The assumptions made in the consequence calculations thus cover the effects of any subsequent deformation of a failed canister by external impact.

### *C5 Thermal expansion (both cast iron insert and copper canister)*

This process concern the effects of differences in thermal expansion of the copper canister and cast iron insert. During temperature decrease in the repository, the shrinking of the copper canister is larger than that of the iron insert, which causes tensile stresses in the copper. These effects are neglected based on calculations provided in the **Fuel and canister process report** showing that the change in tensile strain in the copper is negligible compared to the creep ductility of copper. This is valid for temperatures up to the maximum temperature expected in the canister materials given by the design criteria for maximum temperature in the buffer and the canister. Since these design premises are conformed to in the reference design, and also verified in the thermal analyses, see Section 10.3.4, the neglect of these effects is considered justified.

### *C7 Radiation effects*

This process refers to changes in material properties of the cast iron insert and copper canister due to neutron and gamma radiation from the fuel. In order to avoid irradiation-induced hardening and embrittlement of the cast iron insert, a design premise is set on the upper limit on Cu content in the cast iron insert. Since this design premise is considered to be conformed to in the reference design of the canister with its content of fuel, the omission of these effects is justified.

### *C9 Galvanic corrosion (failed canister)*

This process refers to the galvanic corrosion of the cast iron insert when the copper canister has failed. In the **Fuel and canister process report**, it is concluded that this process does not need any specific treatment since the influence of galvanic corrosion under oxygen-free, reducing conditions lies within the margins of error for the corrosion rate of the iron insert. Furthermore, no credit is taken for the cast iron insert either as a corrosion barrier or as providing any resistance to the release of radionuclides from a failed canister in the scenario- and risk assessment. Consequently, the omission of a specific treatment of galvanic corrosion of the cast iron insert is considered justified.

### *C10 Stress corrosion cracking of the cast iron insert*

Stress corrosion cracking of the cast iron insert requires a combination of static tensile stresses, a corrosive environment and a susceptibility of the material. In the **Fuel and canister process report**, stress corrosion cracking is considered as unlikely and even if it occurred it would have no consequences for stability of the insert. A corrosive environment can be established by the radiolysis of water and air in the canister. In order to prevent this, a design premise is set on the maximum allowable water (600 g) and air (nitrogen) content in the canister (see Sections 14.4.2, process F9, and 5.3.1). Since this design premise is considered to be conformed to in the reference design, the neglect of this process is considered justified.

### *C12 Stress corrosion cracking, copper canister*

In the **Fuel and canister process report**, stress corrosion cracking of the copper canister is assessed as negligible due to the combined effect of very low expected (if any) concentrations of SCC promoting agents and the insufficient availability of oxidants. The chemical species that support SCC of copper are nitrite, ammonia and acetate ions. No further analyses of this have been made in SR-Site.

### *C13 Earth currents – stray current corrosion*

According to Section 3.5.6 of the **Fuel and canister process report** the effect of natural earth currents on canister corrosion can be neglected as it is unlikely that sufficiently large potential gradients can be maintained over the deposition hole to affect the copper corrosion as the electrical resistance of a fully saturated bentonite buffer and the rock surrounding the deposition hole is low.

For the existing high voltage direct current (HVDC) cable at Forsmark, operated in monopolar mode, measured self potential gradients can be used to estimate the influence on copper canister corrosion of the installations. The self potential measurements in open boreholes may serve as a proxy for the case where the entire buffer is fully saturated, whereas packed-off boreholes correspondingly may serve as a proxy for the case with less saturated bentonite around the canister than above and below. The maximum potential difference over the 5 m long canister is in a pessimistic case suggested to be about 0.5 V, but a more realistic assumption is a typical potential difference over the canister of about 0.05 V, which occasionally may increase up to 0.25 V. The present and possible future cable installations will, however, exist for only short times, compared to the total assessment time for SR-Site.

The corrosion of the canister in the presence of an external field would still be limited by the availability of groundwater constituents for either the cathodic reaction (oxygen), the anodic reaction (sulphide), or ions causing stress corrosion cracking (nitrite, ammonium, acetate). Cathodic reactions would also be counteracted by any present dissolved hydrogen gas. The external field would thus not increase the extent of corrosion in the assessment.

The effect of earth currents on canister corrosion can thus be neglected in the long-term perspective, based on the discussion presented above. No analyses, in addition to the ones presented in the **Fuel and canister process report** were considered necessary in relation to this issue.

### *C14 Deposition of salts on canister surface*

According to the **Fuel and canister process report**, Section 3.5.7, it is possible that salts in the bentonite will be redistributed, enriched and deposited on the canister surface. The salts that may be of concern are chlorides and sulphates from the groundwater and sulphates and carbonates from the impurities in the bentonite. Of these, the chlorides are most important since the presence of high chloride concentrations may have an effect on the corrosion properties of copper. Sulphate and carbonate deposits are not electrically conductive, so they are not expected to increase the risk of pitting corrosion. An increase in the chloride concentration would, however, lower the susceptibility of copper to pitting corrosion, since it would favour general corrosion /King et al. 2010/.

Section 12.6 demonstrates that the groundwater pH is always expected to be slightly alkaline. The water reaching the canister will be influenced by the reactions with the bentonite, but the pH would not be below 6, even for a groundwater pH of 6 (see Section 10.3.10), and the chloride concentration would not be changed to any large extent. A high chloride concentration will, consequently, not lead to increased general corrosion, and the extent of the corrosion will be determined by the amount of available oxygen (and sulphide). The process can thus be neglected.

## 14.4.4 Buffer

According to Table 7-4, the following buffer processes are omitted from the assessment for parts or a whole glacial cycle:

- Bu1 Radiation attenuation/heat generation (intact canister).
- Bu3 Freezing (resaturation/thermal phase and intact canister).
- Bu6 Gas transport/ dissolution (gas phase transport) (intact canister).
- Bu9 Liquefaction (intact canister).
- Bu17 Iron-bentonite interactions (resaturation/thermal phase and intact canister).
- Bu19 Radiation-induced transformations (intact canister).
- Bu20 Radiolysis of porewater (intact canister).
- Bu21 Microbial processes (unsaturated conditions and intact canister).

In addition, processes related to radionuclide transport, e.g. diffusion, sorption, speciation and colloid transport are neglected for the excavation/operational period based on the assumption that no canister failure occurs over this period. This is confirmed by the analyses of the reference evolution for the excavation/operational phase as summarised in Section 10.2.7.

#### *Bu1 Radiation attenuation/heat generation (intact canister)*

Radiation attenuation and the resulting heat generation in the buffer is neglected in the **Buffer, backfill and closure process report** since quantifications have shown that the dose rate from an intact canister is too low to be of importance for the properties of the buffer (see processes Bu19 and Bu20 below). This is at least true if the dose rate is below 1 Gy/h, which is the limit stated as a design premise, see Section 5.4.1. Furthermore, the highest obtained radiation dose rate stated in the **Spent fuel report** is 0.18 Gy/h. Therefore, the neglect of this process is considered justified.

#### *Bu3 Freezing (resaturation/thermal phase and intact canister)*

Freezing of the buffer is ruled out during the resaturation and thermal phase since this requires a temperature of – 4°C at repository depth, which will not occur during this phase of repository evolution (or any later phase).

#### *Bu6 Gas transport/dissolution (intact canister)*

As described in the **Buffer, backfill and closure process report**, any gas present in the buffer surrounding an intact canister is expected to be dissolved in the buffer porewater. Air that is trapped in the buffer during resaturation of the buffer is considered in THM-modelling of the resaturation phase. As long as the copper canister is intact, there are no processes occurring in the canister or buffer that are expected to produce gases in such amounts that the solubility of the gas in the buffer porewater is exceeded. Radiolysis of porewater in the buffer can produce hydrogen and oxygen, but the radiation level outside the canister is too low for this process to produce significant amounts (see Bu20 below). Furthermore, oxidants are expected to be consumed by copper corrosion. Microbial processes may also lead to formation of gaseous species, but as long as the high swelling pressure in the buffer is maintained, microbial activity in the buffer is expected to be low.

#### *Bu9 Liquefaction*

A process that could affect the canister significantly is liquefaction of the buffer. According to the **Buffer, backfill and closure process report**, liquefaction is a process implying that a stiff material (e.g. soil) turns into liquid due to an effect with short duration, see e.g. /Lambe and Whitman 1969/. It may take place in a loose sand when the porewater pressure is increased either due to a vibration that makes the sand particles float in the porewater (since they tend to go into a higher degree of compaction, but the water temporarily prevents this) or due to a strong upward water flow that releases the effective stresses between the particles (quicksand). It may also take place in clay that has been settled in salty water (forming an open structure with a high water ratio). If the salt is partly washed out by fresh water, the clay structure cannot hold the high amount of water at moulding or when subject to vibrations, meaning that the structure collapses when exposed to vibrations.

These two types of liquefaction cannot take place in a bentonite with high density, since the effective stress that holds the clay together is high due to the swelling pressure. This conclusion was also made by /Pusch 2000b/. However, a similar phenomenon has been observed during compaction of bentonite blocks at very high water ratios. If the bentonite is compacted at a very high stress to a state where the bentonite is completely water saturated, all further increases in stress will be taken up by the water and the bentonite will behave like a liquid. This phenomenon has been observed during uniaxial compaction when liquid bentonite has squirted from the mould.

The process requires a very strong impact of pressure and is rather unlikely to occur in a deposition hole. It can probably only result from an earthquake and requires a reduction in the volume of the deposition hole due to an increase in rock stress. A combination of factors may lead to an increase in rock stress of about 15 MPa /Bäckblom et al. 2004/. Estimation according to Kirsch /Brady and Brown 1994/ of the convergence of a deposition hole at such an increase in rock stress yields a convergence of the hole of about 1 mm. This is not sufficient for liquefaction to occur.

Neither earthquakes nor high hydrostatic pressure during a glacial event are expected to lead to a loss in effective stress in the buffer sufficient for liquefaction (see also Section 10.4.8).

### *Bu17 Iron-bentonite interaction*

Reactions between metallic iron and montmorillonite in the buffer may lead to breakdown of the montmorillonite structure. As long as the copper canister is not breached, the iron insert will not be in contact with the bentonite buffer. Furthermore, the installation procedure of the buffer requires that the deposition hole is cleaned prior to the emplacement of bentonite blocks and pellets, see the **Buffer production report**, Section 5.4.3. Therefore, omitting this process for intact copper canisters is considered justified.

The scenario- and risk analysis shows that corrosion failure of the copper canister requires that advective conditions in the buffer have been established. In this case, the subsequent contact between the iron insert and the buffer is no longer significant, since the diffusion barrier is already lost. If canister failure occurs due to shear movements in a fracture intersecting the deposition hole, the buffer surrounding the canister will still be a diffusion barrier at the time of the shear failure. However, the analysis of a combination of the shear load and corrosion scenarios (Section 13.6) shows that both the retardation in the buffer and the limited solubility of the dose determining Ra-226, which requires an intact buffer, are of limited importance for the result. A loss of the buffer as a diffusion barrier subsequent to a shear failure of the canister is therefore not of significance for the dose impact, and the omission of a specific analysis of the consequences of iron-bentonite interaction is considered justified.

### *Bu19 Radiation-induced transformations*

This process refers to the direct breakdown of montmorillonite in the buffer by radiation from the spent fuel in the canister. The process is neglected in the **Buffer, backfill and closure process report** for intact canisters based on experimental results that show no effect for absorbed dose rates from γ-radiation well above 1 Gy/hour. Consequently, as long as the copper canister is intact, the design requirement of 1 Gy/h on the canister surface will ensure that the dose rate outside the canister is too low to have any effect on the buffer properties.

If a canister fails, radionuclides that are released from the canister and sorbed in the buffer may expose the montmorillonite in the buffer to α-radiation. Based on results from radionuclide calculations for the safety assessment SR 97 /SKB 1999a/ on the concentration of α-emitters in the buffer and the total dose they would give during one million years in case of an early canister failure, it is concluded in the **Buffer, backfill and closure report** that the consequences can be neglected. Considering that these results are for an early failure of the canister, which is not expected to occur, and that there is a large margin to absorbed dose rates where impact on buffer occurs, these results justify the omission of this process. Furthermore, corrosion failure in SR-Site implies that advective conditions are established in the buffer prior to failure and that no credit is taken for retardation in the buffer in the assessment calculations. Therefore any consequences of radiation-induced changes of buffer properties after corrosion failure of the canister are of no concern. This is also the case for canister failure due to shear movements in a fracture intersecting the deposition hole for the same reasons as given above for the potential consequences of iron-bentonite interactions (see Bu17).

### *Bu20 Radiolysis of porewater*

Radiolysis of porewater in the buffer by γ-radiation penetrating the canister leads to the formation of oxidants and hydrogen. This process is of primary concern for the corrosion of the copper canister and is neglected in the **Buffer, backfill and closure process report** as well as in the **Fuel and canister process report** based on an estimate of the maximum possible amounts of oxidised copper that can be produced before the γ dose rate has substantially declined and on available experimental information that shows no evidence for enhanced corrosion rates caused by γ-radiation (see Section 10.3.13).

### *Bu21 Microbial processes (unsaturated conditions)*

Microbial processes are neglected during the initial period of unsaturated conditions in the buffer. The reason for this is that the extent of aqueous reactions during this period is limited, see the **Buffer, backfill and closure process report**. This is further substantiated in Section 10.3.13, subtitle

"Corrosion during not fully saturated conditions". While it is concluded that during saturation it cannot be excluded that conditions will be more favourable to microbial activity, even saturation times in the order of thousands of years are short in the assessment time perspective. Furthermore, only limited amounts of sulphide possibly formed in the backfill can reach the canister due to the limited transport capacity, and that this transport capacity would be lower in the unsaturated buffer than in the saturated. The phase of partly unsaturated conditions will thus not increase the maximum amount of sulphide reaching the canister. For corrosion processes bounded by mass balances of corrosive agents, there will be no addition from changed saturation conditions.

### 14.4.5 Backfill

According to Table 7-5, the following backfill processes are omitted from the assessment for parts or a whole glacial cycle:

- BfT2 Freezing (resaturation/thermal period, intact canister).
- BfT5 Gas transport/ dissolution (long term for intact canister, failed canister).
- BfT8 Liquefaction.
- BfT10 Diffusive transport of species (early stage, intact canister).
- BfT11 Sorption (including ion-exchange) (early stage, intact canister).
- BfT13 Aqueous speciation and reactions (early stage, intact canister).
- BfT17 Radiation-induced transformations.

In addition, processes related to radionuclide transport, e.g. diffusion, sorption, speciation and colloid transport are neglected for the excavation/operational period based on the assumption that no canister failure occurs at this period. This is confirmed by the analyses of the reference evolution for the excavation/operational phase as summarised in Section 10.3.7.

#### *BfT2 Freezing (resaturation/thermal period, intact canister)*

Freezing of the backfill in deposition tunnels is ruled out during the resaturation and thermal phase since this requires a temperature of lower than – 2°C at repository depth, which will not occur during this phase of repository evolution.

#### *BfT5 Gas transport/dissolution (long term for intact canister, failed canister)*

Corrosion of the cast iron insert in a failed canister would lead to the formation of hydrogen gas. This gas could potentially escape through the backfill in the deposition tunnel above the failed canister as could radionuclides in the gaseous phase released from the canister. This transport route for gas is neglected in the assessment because the impact on the saturation conditions in the backfill is assessed as small, see the **Buffer, backfill and closure process report**, Section 4.2.3. Furthermore, an instant transfer of the radionuclides in the gas phase to the biosphere after gas breakthrough through the bentonite is assumed. Neither the buffer nor the geosphere is expected to significantly delay the transport to the biosphere. Also, it is not certain that gas generated by corrosion of the iron insert will reach the tunnel. An alternative escape route is through fractures in the rock intersecting the deposition hole. This is related to FEP Ge4 and is further discussed in Section 14.4.6.

#### *BfT8 Liquefaction*

Liquefaction in the backfill is discarded using the same arguments as for the buffer, see Section 14.4.4, subheading "Bu9 Liquefaction".

#### *BfT10 Diffusive transport of species (early stage, intact canister)*

Diffusion is suggested to be neglected in the **Buffer, backfill and closure process report** for the period before saturation of the backfill since advection is the dominating process during resaturation. However, the process is considered in the coupled hydrogeochemical analyses reported by /Sena et al. 2010/.

#### *BfT11 Sorption (including ion-exchange) (early stage, intact canister)*

The argument in the **Buffer, backfill and closure process report** for neglecting sorption before saturation is that there are no continuous water paths available prior to water saturation of the backfill. However, the process is considered in the coupled hydrogeochemical analyses reported by /Sena et al. 2010/.

#### *BfT13 Aqueous speciation and reactions (early stage, intact canister)*

Aquous speciation and reactions are suggested to be neglected for the period prior to saturation since the geochemical processes are expected to be the same before and after saturation, see the **Buffer, backfill and closure process report**. However, consumption of oxygen by reactions with minerals in the backfill is addressed by /Sena et al. 2010/ as discussed in Section 10.2.5 also for the resaturation phase.

#### *BfT17 Radiation-induced transformations*

Radiation-induced transformations of the backfill are neglected in the **Buffer, backfill and closure process report** since the dose rate in the backfill is too low to have any effect. Since the dose rate in the buffer is too low to have any effect because the design premise on the maximum dose rate on the canister surface is conformed to (Section 14.4.4, FEP Bu19), it is considered verified also that the dose rate in the backfill, which is more shielded than the buffer, is too low to have any effect.

### 14.4.6 Geosphere

According to Table 7-6, the following geosphere processes are omitted from the assessment for parts or a whole glacial cycle:

- Ge1 Heat transport (excavation/operational period).
- Ge4 Gas flow/dissolution.
- Ge6 Reactivation – displacement along existing discontinuities (excavation/operational period).
- Ge8 Creep.
- Ge10 Erosion/sedimentation in fractures.
- Ge14 Reactions groundwater/rock matrix (excavation/operational period, temperate- and periglacial climate domains).
- Ge18 Colloid processes.
- Ge20 Methane hydrate formation.
- Ge22 Radiation effects (rock and grout).
- Ge23 Earth currents.

In addition, processes related to radionuclide transport, e.g. diffusion, sorption and speciation, are neglected for the excavation/operational period based on the assumption that no canister failure occurs during this period. This is confirmed by the analyses of the reference evolution for the excavation/operational phase as summarised in Section 10.2.7.

#### *Ge1 Heat transport (excavation/operational period)*

According to the **Geosphere process report**, Section 2.17, it is concluded that the thermal dimensioning of the repository neglects heat transport in the rock for the excavation/operational period in the sense that all canisters are assumed to be deposited simultaneously. This is based on calculations that show that the peak temperature in the buffer, which is the safety relevant issue (safety function indicator Buff4), is underestimated by less than 0.2°C if simultaneous canister deposition is assumed, compared to a case where canisters are deposited in an orderly fashion (i.e. panel by panel) at a rate of 2 or 4 days per canister (Section 10.2.1 and /Hökmark et al. 2009/). However, as discussed in Section 10.2.1 there are deposition sequences for which this simplification does not apply, but these could be avoided by proper management of the disposal sequence. Therefore, it is judged that the legitimacy of omission of the disposal sequence in the evaluation of heat transport and the buffer peak temperature is verified.

Since the treatment of heat transport for the excavation/operational period is a simplification of the deposition sequence rather than an omission of the process, all relevant couplings to other processes are considered.

### *Ge4 Gas flow/dissolution*

According to the **Geosphere process report**, an unsaturated region may be induced in the vicinity of the tunnels and an unsaturated zone above the repository during repository pre-closure operations, but that these unsaturated zones only have a marginal effect on inflows to the tunnels. Therefore, details of gas flow and dissolution during the excavation and operational period are neglected and the effect of gas flow is taken into account in a simplified manner in the calculations of the resaturation of the tunnels after repository closure.

Concerning repository generated gas, the main source is hydrogen produced by anaerobic corrosion of the cast iron insert in a failed canister. Calculations conducted for SR-Can /Hartley et al. 2006/ showed that gas generated in the repository and released through the buffer can rapidly escape through the geosphere without causing a pressure build-up. Based on this result and the small change in bedrock properties between the hydrogeological models in SR-Can and SR-Site, the impact on geosphere performance is neglected in the **Geosphere process report**. Substantial localised gas generation in the repository implies that a canister has failed so that corrosion of the iron insert can occur. The assessment shows that failure by corrosion requires advective conditions in the buffer which in turn implies that the deposition hole is intersected by a highly transmissive fracture. Since there is no buffer to contain the gas, hydrogen formed will dissolve and be carried away by water flowing in the intersecting fracture. This supports the neglect of impact of gas flow in case of corrosion failure of a canister.

In the case of canister failure by shear movement, the buffer is still acting as a barrier and gas pressure build-up inside the buffer will have to occur before gas is released to the geosphere. In the assessment, this scenario with build-up of gas pressure inside the buffer is addressed to analyse the dose consequences of the release of radionuclides in the gas phase (see Section 13.8). Since it cannot be excluded that the fracture causing the shear failure of the canister is transmissive or becomes transmissive after the shear movement, no credit is taken for any radionuclide retention in the geosphere in the analysis of the dose consequences in the shear failure scenario (Section 13.6) or in the scenario for release of radionuclides in the gas phase (13.8). Any potential impact of build-up of gas pressure or gas flow in the geosphere on the dose impact is then implicitly covered in the analyses and there is no need for a specific treatment of this process.

### *Ge6 Reactivation – displacement along existing discontinuities (excavation period)*

Construction-induced seismicity is neglected based on an assessment in the **Geosphere process report**. It is concluded that in order for a fault slip larger than 0.05 m to be triggered by the excavation activities, an induced earthquake of approximately magnitude 5 is required. To host such an earthquake, the structure must have a rupture area exceeding a square kilometre. It is unlikely that such a structure would remain undetected after tunnel mapping, which makes it possible to avoid the structure during deposition. In addition, there is no evidence that present-day deviatoric stresses in Swedish bedrock at repository depth are sufficient to power seismic events of magnitude 5. Furthermore, the largest seismic events recorded in very deep mines in South Africa, for instance, where stresses are high and where the rate of excavation is much higher than it will be in the deep repository, are less than magnitude 5. In the light of the completed scenario- and risk assessment, there is no reason for modification of this conclusion.

### *Ge8 Creep*

Creep along fractures and in intact rock is neglected in the **Geosphere process report** and is also discussed in Section 10.3.5. For the Forsmark fractures, creep displacements are likely to be insignificant compared to displacements caused by the direct changes in load and pore pressure projected for the different phases of the assessment period. Concerning creep in intact rock, it is concluded in the **Geosphere process report** that this requires stresses that will be found only in small volumes of the rock around the walls of the openings. These effects are accounted for in the assessment of thermally-induced spalling. Therefore, the neglect of this process is considered justified.

These conclusions are further justified by the assessment presented in Section 10.3.5. A recent study by /Damjanac and Fairhurst 2010/ assessing whether there is a lower bound to the long-term strength of rocks demonstrates that there is always a stress threshold for confined conditions, because confinement acts to suppress the tension stresses associated with crack growth. If spalling is encountered and a notch forms, the stress adjustments that can occur at the notch tip may cause additional time-dependent/creep deformations. The monitoring of the unconfined open notch in the APSE Experiment showed that the majority of the new displacements occurred in the existing notch /Andersson 2007/. When the spalled notch is confined, any time-dependent deformations are expected to be insignificant, compared to the deformations that formed the notch. It can also be noted that the effects of fracture creep, in terms of fracture displacement under constant shear load because of time-dependent material strength properties, can be estimated using the modelling approach for fracture reactivation described in /Hökmark et al. 2010/. Even if the strength is reduced to zero over the entire fracture plane, only very minor fracture displacements would occur. Creep deformation and related issues like "sub-critical crack growth" are, therefore, not further considered in SR-Site.

#### *Ge10 Erosion/sedimentation in fractures*

Erosion and sedimentation in fractures is neglected for the excavation/operational phase because high-transmissive fractures in the repository rock will be grouted and the flow rates in non-grouted fractures are expected to be too low to cause significant erosion. After closure of the repository, the hydraulic gradients during the temperate period will be so low that the potential for erosion is negligible. During glacial advance and retreat, the hydraulic gradient will dramatically increase, but the shear stresses will still be low.

As noted in Section 10.4.8, /Birgersson et al. 2009/ found that the shear strength of MX-80 at a water ratio of 100 ($\varphi$=0.0037) for sodium concentration of 10 and 100 mM is larger than 5 Pa. The hydro-geological modelling of the "expanding ice front" case in SR-Site shows that the calculated shear stresses are always below 5 Pa and much lower most of the time. It can thus be concluded that the loss of bentonite from shearing of particles can be neglected for all reasonable conditions.

#### *Ge14 Reactions groundwater/rock matrix*

Chemical reactions between groundwater and rock matrix minerals are neglected in the **Geosphere process report** since they are judged not to cause appreciable changes in groundwater composition or matrix porosity for the whole time period during which the function of the repository must be considered. The primary effects are expected to be caused by reactions between groundwater and fracture-filling minerals. This standpoint is based on observations of drillcores from the repository volume at Forsmark which show very little alteration of the rock matrix surrounding fractures (see also Section 4.4.4). These observations justify the neglect of reactions between groundwater and the rock matrix in comparison with reactions between groundwater and fracture filling minerals.

#### *Ge18 Colloid processes*

In the **Geosphere process report**, the impact of colloids on the geochemical conditions of the geosphere is judged as negligible. However, colloids may act as carriers for radionuclides. It is further noticed that the current salinities of the groundwater at Forsmark are higher than that required to keep the concentration of colloids suspended in groundwaters to a low level. During the excavation and operational phases, substantial amounts of colloids may be formed, but the colloid concentrations will quickly resume the natural values under the saline water conditions that will be re-established (see also Section 10.2.5). Since the assessment shows that no canister failures occur during this period, the neglect of colloid processes for the excavation and operational period is considered justified.

#### *Ge20 Methane hydrate formation*

The potential for formation of methane hydrate during periglacial conditions at Forsmark is neglected in the **Geosphere process report**, Section 5.11, based on a modelling simulation. The conclusion from that study is that methane hydrate formation is unlikely at the methane concentrations and water salinities reported for Forsmark. This conclusion is also brought forward in Section 10.4.7, where estimates of maximum fluxes and production of methane are used to support this conclusion. Hence, the neglect of this process is considered justified.

### *Ge22 Radiation effects (rock and grout)*

Radiation effects on ground supporting material are ruled out in the **Geosphere process report** based on findings from the Yucca Mountain project. According to the **Geosphere process report**, Section 5.13.4 no degradation of the mechanical properties of cement have been observed for a fast neutron fluence as high as $8.2 \cdot 10^{19}$ n/cm$^2$, i.e. no change in dimension, weight, compressive strength, bending strength, or Young's Modulus of cement paste due to irradiation alone. This neutron fluence can be compared with the highest obtained initial radiation dose rate stated in the **Spent fuel report**, and summarised in Section 5.3.4. The maximum flux is for a PWR element with a burn-up of 42.2 MWd/kgU after 34.1 years, and according to the specifications for the type canisters, the initial source strength of neutrons is $1.2 \cdot 10^8$ /s. Assuming all this flux to be concentrated on one cm$^2$, without considering radioactive decay and the moderation due to the water in the bentonite and the rock it would take in the order of $10^{11}$ seconds, i.e. some thousands of years to reach these high fluence levels. In reality the neutron flux will be dispersed, decrease due to radioactive decay and it will also be absorbed, which implies that the omission of the process is clearly justified.

### *Ge23 Earth currents*

The impact of earth currents, both natural and anthropogenically induced, are neglected in the **Geosphere process report** since expected electrical potential fields are too small to affect groundwater flow or solute transport. There are a number of reasons behind this conclusion. The main ones are that the fields usually are weak or become weak at repository level for geometrical reasons and that most of the fields are alternating and the effects, therefore, are reversible. There is nothing in the light of the completed scenario- and risk analysis that questions the neglect of this impact of earth currents, see also Section 14.4.3, sub heading "C13 Earth currents – stray current corrosion".

## 14.5 A brief account of the time period beyond one million years

For the time beyond one million years, no risk calculation is required. SSM's General Recommendations related to SSMFS 2008:21 suggest that an account of the evolution of radiotoxicity may be the only meaningful way of illustrating the further development of the repository. Such an account is given in Figure 2-1 in Section 2.4. It is obvious from the figure that the radiotoxicity of the spent nuclear fuel decreases somewhat between $10^6$ and $10^7$ years. The radiotoxicity then stays constant for very long times beyond $10^7$ years. The following is a brief, qualitative discussion of the development of the site for the time period beyond one million years, based essentially on general tectonic considerations and indications from natural analogues.

### *Tectonics*

Although geological processes are generally slow, the evolution of the site over a period larger than the one million year time frame is difficult to predict. The analysis in, for example, Section 10.4.5 regarding earthquakes cannot readily be extended to larger timeframes without taking into account additional effects that are beyond the scope of SR-Site. For instance, although it can be assumed that the Fennoscandian shield will remain a tectonically stable craton with most of its deformation localised at its margins, it cannot be assumed that pattern and properties of the deformation zones and fractures within the site will remain sufficiently constant over this time frame for enabling an earthquake hazard assessment. The site is expected to experience substantial surface denudation but also, occasionally, be loaded by an unknown amount of sediments originating from the denudation of mountainous areas, imposing mechanical, thermal and chemical effects that could surpass the effects of repeated glaciations.

On the other hand, the rocks, the ductile deformation and the brittle deformation zones at Forsmark all formed at least one billion years ago, and have experienced numerous episodes of burial, both by sediments and glaciations. The effects of such events have been extensively studied during site investigations and it appears as if the pattern of localised strains, manifested as deformation zones of various orientations, has remained fairly constant for much longer than 10 million years. It is reasonable, therefore, to assume that essentially the same deformation zones will act as planes of weakness, thereby enabling release of accumulated stress in a manner similar to the past 10 million years or so.

It is also reasonable to assume that the fracture intensity will increase, but reach an unknown level of intensity saturation beyond which jostling (reactivation) of the blocks within the brittle upper crust will largely dominate over fragmentation (creation of new fractures). Due to the power law nature of fractures sizes, fractures able to host slip exceeding 5 cm will still be rare even if both the intensity and the mean fracture size are increased.

### *Qualitative discussion of canister failures and releases*

The above means that the probability of intersection of a fracture able to host slip exceeding 5 cm with an individual deposition hole will remain low even in the time beyond one million years from now, indicating that the extent of canister failures due to shear load would be limited also in a ten million year perspective.

Likewise, if geochemical and flow conditions were, when averaged over very long time periods, similar to those today, the extent of canister failures due to corrosion would be limited to a few failed canisters, compared to, e.g. on average 0.12 at one million years for the central corrosion variant (Section 12.6.2).

It is also noted that radioactive decay plays a minor role for the development of release curves beyond one million years since the dose dominating nuclides, in particular the mother nuclides of Ra-226, are very long-lived. Related to this, the scientific understanding of the fuel dissolution process suggests that the longevity of the spent fuel matrix is several million years in the repository environment (see Section 13.5.5).

Finally, the hypothetical case in Section 13.7.3, where all canisters are failed, where the buffer is absent and where retention in the rock is disregarded, yields releases that correspond to dose consequences that are comparable to the natural background radiation after one million years. The releases are in that case controlled by the flow at repository depth and the inventory of radionuclides, the latter of which decreases with time.

### *Indications from natural analogues*

In the time beyond one million years from now, the radiotoxicity of the spent nuclear fuel in the repository will be comparable to a concentrated uranium deposit, as indicated in Figure 2-1, Section 2.4. The performance of the engineered barriers after one million years becomes increasingly uncertain. The further discussion regarding the evolution of the repository during the time beyond the one million years may, however, draw on existing knowledge of natural uranium ores and the behaviour of uranium in a geological environment.

One undisputable fact that emerges from geological observation is the existence of uranium ores that are many millions and even billions of years old. Studies of, for example, Cigar Lake in Canada, reveal a uranium ore body found today at a depth of 450 m, which has persisted for 1,300 million years e.g. /Ruiz López et al. 2004, Miller et al. 2000/. There are today no geochemical indications of the Cigar Lake uranium ore body on the surface, indicating the possibility for a reducing, uranium rich environment with low hydraulic permeability to retain a majority of the elements associated with the ore for a time period well in excess of one million years.

Pockets of rich uranium ore at Oklo (Gabon) reached critical mass nearly two billion years ago. The natural spent fuel which was formed during this criticality has, to a large extent, been retained in the deposit for the almost two billion years that followed /Gauthier-Lafaye et al. 1996/. This can be explained partly by the low mobility of uranium in a reducing environment, and partly by the relatively stable geology of the area. This does not mean that there has been a complete lack of tectonic events; one example is an episode of regional extension, c. 860 million years ago, which caused the intrusion of mafic magma in the sedimentary basin which hosts the uranium. The magma cooled and solidified and is now found as a network of dolerite dykes in the area. One of these dykes, c. 20 m wide, is found cutting across the Oklo deposit. The intrusion and regional extension caused elevated heat and circulation of hydrothermal fluids that have affected the Oklo deposit. In spite of this event, and the solid-fluid interactions that were associated with it, the uraninite in the natural fossil fission reactors is remarkably well preserved and has even retained fission-related impurities within the uraninite grains /Evins et al. 2005/.

From the above, it seems clear that, in the case of stable tectonics and maintained reducing conditions in the repository, the uranium oxide which constitutes the fuel matrix can be stable for many millions of years. Another observation is that dissolution experiments in the laboratory yield faster dissolution rates than are estimated from observations of minerals in natural settings. This has been observed and discussed in the literature and may, in part, be explained by evolution of the surface of the dissolving mineral which occurs on a time scale that cannot be studied in a normal laboratory experiment /White and Brantley 2003/.

Further discussion regarding knowledge gained from natural analogue studies is found in the next Section 14.6.

## 14.6 Natural analogues

Natural systems provide two things that cannot be achieved in the laboratory: The full complexity of the natural environment, and very long time scales. By making comparisons with natural systems in which some feature, event or process is deemed similar to what is expected in the repository system, the response of the repository to the natural environment in which it will evolve for such a long time can be assessed with better confidence.

There are different parts of the repository system – spent fuel, copper canister, bentonite buffer – for which comparisons with natural analogues have proven useful. Knowledge about many processes occurring in the geosphere, for example transport of uranium and other elements, has been enhanced by studies at natural analogue sites.

### 14.6.1 The role of natural analogue studies in safety assessments

Since the concept of natural analogues first started to take form in the 1980's /Chapman et al. 1984/, the relationship between natural analogue studies and safety assessments of high-level waste repositories has changed. The quantification necessary in a safety assessment is difficult to extract from the natural analogue studies; however, these studies have a significant qualitative value in that it can be shown that a feature or process does exist in nature and that it has persisted in a natural environment for a very long time. This is an important aspect, especially for raising public awareness and understanding. Much of what is needed in order to understand safety assessment falls outside the realm of common knowledge. Here, analogues and demonstration experiments can, to some extent, provide also the general public with insights into conditions and processes of importance for long-term safety. Material analogues, especially, have been useful for that purpose.

It is now clear that the two main reasons natural analogue studies are interesting, namely the exposure to natural complexity and long time scales, introduce uncertainties which render them difficult to use in a systematic safety analysis. For natural analogues, one limitation is often a lack of information about boundary conditions. The need for well known initial conditions for quantitative evaluations of effects of processes is one example of where difficulties arise. In addition, analogues are never perfect: The difference between an analogue and the actual component under investigation will always be a source of doubt. Therefore, most natural analogue studies do not lead to quantitative data that can be used in safety assessment models. However, in spite of these limitations, these studies have significantly enhanced the understanding of natural processes relevant to those considered in safety assessments. The role natural analogue studies play in identifying relevant processes, and also in verifying that all relevant processes have been incorporated in the models, is significant. Examples to illustrate this role are given by /Miller et al. 2000/.

A different aspect of the natural analogue studies has been the opportunities these studies have provided to drive development of equipment and methods intended for investigation of repository sites. For the comprehensive studies of ore bodies, mainly uranium, site investigation methods had to be applied. In this case, the differences between individual analogues and typical repository sites present an opportunity rather than a difficulty. The differences make it possible to better test the methods used to interpret measurements of, for example, redox conditions in groundwater, pH, colloids, and microbial activity.

Many studies of natural analogues have been performed as international projects. These projects have gathered scientists from different fields and contributed to discussions generating valuable critiques of the hypotheses being tested. Long-term safety, like science in general, ultimately rests on the combination of openness and critique.

The following is a short review of main outcomes from some of the analogue studies performed in the last three decades. These have been more extensively reviewed by /Miller et al. 2000/ and /Ruiz López et al. 2004/. Preference has been given to the ones recognised as relevant to the KBS-3 concept. Other groups of experts have also found these analogues to be of interest in this context /Apted et al. 2009, pp 23–24, Bath and Hermansson 2009, pp 58–68, Neall et al. 2008, pp 35–42/.

### 14.6.2 Analogues of repository materials and processes affecting them

Natural materials and archaeological objects found in nature have been studied as analogues of repository materials. These materials have been subjected to the complex variety of natural processes for different amounts of time, and what we see today is the result of this "natural experiment".

#### *Spent nuclear fuel*

The natural mineral uraninite (uranium dioxide) has many similarities with $UO_2$-based spent nuclear fuel. These materials are uranium oxides with the same crystallographic structure (fluorite structure), they form solid solutions with oxides of Th, Ca and REE, they are resistant to radiation damage (self-annealing), and they are similarly affected by oxidation /Janeczek et al. 1996/. However, this does not mean that these materials are identical – there are many important differences. Examples of major differences are the amount of oxidized uranium, which is higher in uraninite, and the amount of radiogenic Pb, which can be almost 20 wt% PbO in 2 billion year old uraninite, but is very low in spent nuclear fuel even after 10,000 years (0.00014 wt% Pb /Janeczek et al. 1996/).

Many natural analogue sites, for example Oklo (Gabon), Cigar Lake (Canada), Poços de Caldas (Brazil) and Palmottu (Finland), are centred on uranium deposits which formed many millions of years ago. The sites have been chosen partly due to the opportunity they provide to study how uraninite, as an analogue to spent nuclear fuel, behaves in different geological environments.

At *Cigar Lake*, the ore body is found at c. 450 m depth in a reducing environment, and dissolution of uranium oxide in the ore has been extensively discussed /Bruno et al. 1997/. However, in spite of the reducing environment, the oxidation state of uraninite is somewhat higher in Cigar Lake uraninite than in uranium dioxide in spent fuel, which makes it difficult to draw parallels to dissolution of spent nuclear fuel in the KBS-3 repository. However, it is noteworthy that all natural processes that have affected this ore body since its formation, c. 1,300 million years ago, have not resulted in any geochemical indications of its existence at the ground surface.

Another feature of importance for spent fuel dissolution that has been studied in Cigar Lake is radiolysis. Ionising radiation causes chemical reactions and the total energy deposited by radioactive decay is considerable. Therefore, early pessimistic evaluations of this effect on spent fuel dissolution tended to be grossly exaggerated. Observations of ferric iron precipitations in the clay nearest to the ore in Cigar Lake were, to begin with, interpreted as a result of oxidation by radiolysis. However, it could be demonstrated that the likely origin was hydrothermal alterations during ore formation. This and other observations stimulated the development of more realistic models /Smellie and Karlsson 1996/.

As stated before, natural uraninite contains elements other than uranium and oxygen, for example Th and REE. Many of these elements also form in the nuclear fuel during reactor operation, or they can function as so-called "chemical analogues" for the elements in spent fuel. These chemical analogues are abundant in the *Poços de Caldas* ore deposits, and played an important role in the natural analogue studies performed at this site /Chapman et al. 1993/.

The most striking natural analogue of spent nuclear fuel is the uraninite in the 2 billion year old *Oklo* natural fossil fission reactors, which is, in fact, a natural spent nuclear fuel /Neuilly et al. 1972, Naudet 1991, Gauthier-Lafaye et al. 1996/. These fossil reactors are found in a uranium ore bearing formation in Gabon, western Africa, where they form reactor zones shaped by nuclear criticality.

Some sixteen of these reactor zones were discovered in the mines at Oklo, at nearby Okélobondo and during prospecting in Bangombé, which is situated about 20 kilometres to the south. The nuclear reactions occurred some 2,000 million years ago when the U-235 content was still high enough for a sustained nuclear fission reaction. Geological studies involving Precambrian rocks elsewhere have failed to locate any sign of a similar fossil reactor. This is likely due to the many coincidences that allowed nuclear chain reactions to start naturally: High uranium concentration, the right isotopic composition of uranium, the presence of a neutron moderator (water) due to high porosity, and the unusually low abundance of neutron poisons (e.g. vanadium and manganese), which capture neutrons /Naudet 1991/. In addition, the sedimentary formation that hosts these natural reactors is essentially unaffected by tectonic processes, despite 2 billion years of existence.

The Oklo uraninite and spent nuclear fuel have many striking similarities, but also important differences. These differences stem partly from the very different operating histories of the natural reactors and man-made power producing reactors. The nuclear reactions in Oklo uraninite proceeded at a very low rate and at low power, intermittently for some hundreds of thousands of years /Naudet 1991/. Spent fuel from power producing reactors has a much more intense thermal history, a higher burn-up and contains higher concentrations of fission products. Another notable difference is the presence of hydrocarbons in Oklo which might have helped to keep the conditions reducing.

Knowledge regarding the requirements for criticality at Oklo was used in the evaluation of the possibility of achieving criticality in a spent fuel repository. There is still fissile material left in the spent fuel. A model based on Oklo conditions was therefore applied to the KBS-3 repository case /Oversby 1998/. The result was negative in so far that no criticality was to be expected in the repository.

One aspect which makes Oklo uraninite unique among analogues for spent nuclear fuel is that reactor zone uraninite contains elements formed during the fission reactions (fission products). The reactor zones are also remarkably well preserved considering their age, so that few of the components have been lost to mass transport which would otherwise have complicated the evaluation of the nuclear reactions. For example, rare earth elements generated by fission are well preserved and contained in the uraninite, but volatile elements such as Cs have been lost. Analogues of the metallic aggregates, in spent nuclear fuel called ε-particles, are also found in the Oklo reactor zones. In spent nuclear fuel these ~1 μm sized ε-particles consist of alloys of Mo, Tc, Ru, Rh, and Pd. There are also observations of the fission product Te associated with these particles /Cui et al. 2004/. In the Oklo reactors, similar segregations of metallic fission products also occur, as evidenced by records of Ru-, Pd- and Pb-containing particles /Gauthier-Lafaye et al. 1996/. These particles are up to ~100 μm diameter and are not metallic alloys but are aggregates of different sulphide phases. Interestingly these aggregates are also associated with Te and Se, illustrating the chemical affinity between the noble metals and these chalcogenic metalloids.

### *Cast iron*

A waterlogged archeological site at Nydam Mose in Denmark contains buried iron objects of military equipment, sacrificed in the period 200–500 AD. Here, siderite was identified as a main corrosion product, which indicates an oxygen-free, carbonate-rich ($10^{-2}$ M) corrosion environment /Matthiesen et al. 2003, 2004/. The estimated corrosion rates range from an upper limit of 5 μm/year down to 0.03 μm/year or less. The average corrosion rate for 151 analysed lances is about 0.2 μm/year.

Corrosion of archeological cast iron artefacts has been studied by /Neff et al. 2003, 2005/, who analysed the corrosion products on artefacts from the 2nd century AD to the 16th century AD. Also low carbon steel objects, buried for long periods /Neff et al. 2006/, were analysed to determine the average corrosion rate. The presence of oxygen in the corrosion process was indicated by the corrosion products. It was found that the measured or estimated corrosion rates varied over a relatively large range, but that the estimated average corrosion rates do not exceed 4 μm/year.

### *Copper*

Finds of native copper in geochemical environments relevant to repository conditions are illustrative examples of the long-term stability of copper canisters. Ore bodies containing native copper have therefore been investigated and particularly the processes corroding or potentially corroding copper. Archaeological copper objects have been used for the same purpose /Johnson and Francis 1980, Miller et al. 2000/.

The world's largest deposit of native copper occurred on the *Keweenaw Peninsula* in Northern Michigan, USA. The native copper lodes, which are associated with conglomerate sediments interbedded in the host basalt, formed about 1.1 billion years ago /Brown 2006/. About five million tonnes of native copper has reportedly been mined /Johnson and Francis 1980/. Some native copper has been transported by glaciers from primary copper deposits in upper Michigan, like Keweenaw Peninsula. Sizes ranges from small pebbles to blocks of more than one tonne, such as the famous Ontonagon copper boulder. This is referred to as "float copper". Well preserved pieces of float copper have been found in banks of sand and gravel left by the glaciers. Two such pieces with evidence of glacial abrasion were investigated /Johnson and Francis 1980/. The last glacier receded 8,000 to 11,000 years ago. Still, the pieces are well preserved with relatively thin layers of corrosion products identified as cuprite ($Cu_2O$) and malachite ($Cu_2CO_3(OH)_2$). The abraded areas had a maximum oxide thickness of only 0.6 mm. One of the pieces was reportedly found at less than a metre depth (about two feet).

The *Hyrkkölä* copper-uranium mineralisation in Finland is situated in a geologic setting similar to the sites considered for disposal of spent nuclear fuel in Finland and Sweden. Native copper and uraninite in Hyrkkölä are hosted in granite pegmatite veins. The age of the mineralisations is estimated to about 1,700 million years. Native copper together with copper sulphide and secondary uranium minerals occurs in open fractures at several depth intervals in these pegmatites. One interval with altered granite pegmatite contains native copper together with cupric oxide and the fracture surfaces were coated with smectite with adsorbed uranium and copper /Marcos et al. 1999/. Investigations have been made by core drilling down to depths of about one hundred metres. Groundwater compositions related to the mineralised fractures were analysed using the SKB mobile field laboratory. Native copper in Hyrkkölä has evidently persisted despite exposure to sulphide-containing water as well as current oxidising conditions. Uranium series studies corroborate the exposure to groundwater and indicate together with other observations that sulphidisation ceased a few hundred thousand years ago to be later replaced by oxidation. Native copper grains as large as one millimetre were found with thin rims of cuprite. Some of the smallest grains were totally oxidised. Some well preserved grains of native copper were found embedded in smectite /Marcos et al. 1999/.

Native copper in Hyrkkölä is one of many examples where copper found in nature has survived geochemical conditions similar to those expected in a repository for geologic time periods /Marcos 1989/. However, native copper deposits in general are mainly associated with basalts, such as the Keweenaw Peninsula case, or supergene weathering of copper sulphide deposits /Amcoff 1998/. Hyrkkölä is valuable in comparison because the geochemical setting is so close to that of a potential repository in Finland or Sweden.

Sheets of native copper, about 1–2 millimetres thick and up to more than ten centimetres across, have been found in outcrops of Permian mudstone at *Littleham Cove* in the UK /Milodowski et al. 2002/. Apart from some signs of corrosion the copper is remarkably well preserved despite the indicated age of more than 176 million years. The copper sheets are associated with uranium containing nodules, formed within a halo caused by contemporaneous reduction of ferric iron in the mudstone. These uraniferous concretions and the native copper were formed early, before compaction of the mudstone, by mineral deposition from fluids. Then, for most of their history, the mudstone host rocks have been well below the present water table and remained saturated with water. Both the native copper and the uranium nodules have been evaluated as analogues to spent fuel disposal in copper canisters buried in compacted clay /Milodowski et al. 2002/.

At Littleham Cove, copper precipitated along bedding lamina and thin fractures in the mudstone. A narrow, less than a millimetre, diffusive halo of copper has been measured in the mudstone next to the copper. This could be the result of either enhancement during formation or loss of copper later. Either way it indicates that diffusion occurred over distances of only a few hundreds of micrometres. Some early partial alteration to cuprite has been identified but, apart from that, the native copper remained relatively inert until the sequence was uplifted and exposed to surface erosion and oxidative weathering in the present-day environment. The radioactivity of the uranium-containing nodules has been used for evaluation of the effects of radiolysis. Methods used to calculate the production of hydrogen peroxide due to radiolysis of water by alpha particles from spent nuclear fuel were applied to a typical nodule. The calculated maximum production of peroxide was enough to oxidise over a gram of pyrite. However, there were no observations or measurements to indicate that radiolysis had been a significant process for inducing oxidation of ferrous iron or other reduced species in the water-saturated clay matrix of the mudstone /Milodowski et al. 2002/.

The man-of-war *Kronan* exploded and sank south east of Öland in 1676, and its cannons scattered on the sea floor. One cannon made of bronze was chosen for investigations of corrosion. It was almost entirely buried, near vertically with its muzzle down in shallow marine clay. The copper content of the bronze was as high as 96.3% and the surrounding relatively compact marine clay consisted partly of montmorillonite /Hallberg et al. 1988/. Known boundary conditions such as age of the burial and the composition of the environment made it valuable as an analogue for a copper canister in a saturated clay buffer, despite the comparatively short time of burial. The surface of the cannon was analysed together with the surrounding clay. Cuprite ($Cu_2O$) and some malachite ($Cu_2CO_3(OH)_2$) were found on the surface, and slag inclusions of tenorite (CuO) in the bronze matrix below the surface. Diffusion of copper was traced four centimetres into the clay. The slag inclusions, and the fact that the cannon must have been covered with a layer of corrosion products before the ship sank, complicated the investigation. The facts at hand were carefully evaluated and a maximum corrosion of less than ten micrometres per hundred years was reported /Hallberg et al. 1988/.

This study was later revisited and reassessed with reference to a corrosion mechanism developed for copper nuclear waste containers in a Canadian concept /King 1995/. This mechanism included the formation of soluble copper species and the so called disproportionation reaction. The latter implies that divalent copper, for example from the tenorite slag inclusions, together with copper metal produces monovalent copper. The developed mechanism was able to satisfactorily explain the earlier reported observations and refine the conclusions /King 1995/.

Three *lightning conductor plates*, located at separate places in middle and southern Sweden, were excavated after having spent more than fifty years in the ground /Hallberg et al. 1984/. The three plates had been buried at depths ranging from 1.2 to 3.3 metres in soil of clay and/or silt. The corrosion of the plates was studied in relation to the chemical properties of the soil. Two of the plates were affected by pitting corrosion with a pitting factor of five, while the third and deepest plate showed no such signs. Copper oxides were found on the two former plates and copper sulphides on the latter. *Copper water pipes* also provided useful information about pitting.

Later evaluations of copper canister corrosion regarding pitting have had more benefit of experiments and theoretical considerations which were previously not available /King et al. 2010, Section 5.3/.

### *Bentonite*

Bentonite clay used in the buffer and backfill are usually taken from natural deposits with very little further processing, apart from drying, crushing and sieving. The deposits themselves and other occurrences of bentonite in different geological settings have been studied as analogues for buffer and backfill in a repository. Processes of interest are, for example, thermal and chemical influences, resistance to hydraulic flow and diffusion of dissolved substances.

Alteration of smectite to illite (illitization) is the most common transformation of smectite observed in natural sediments, and it has been reproduced under laboratory conditions. One of the requirements for illite to form is availability of potassium. Potassium is found both dissolved in groundwater and in rock-forming minerals. For kinetic considerations relating to smectite-illite alteration, the initial potassium concentration in groundwater and the dissolution rate of surrounding potassium-bearing minerals are of importance. Any other mineral formation that may compete with illite for the potassium may also be important.

The conditions for transformation of smectite to illite have been investigated in *deep wells in sedimentary basins* /Velde and Vasseur 1992/. These studies of illitization in natural systems are not connected to any specific natural analogue site but have instead been performed in a variety of sedimentary basins in order to better describe the time and temperature relations of smectite-illite mineral changes. Samples from wells from the Texas Gulf Coast (USA), the Niigata basin (Japan), Los Angeles basin (USA), and the Paris Basin (France) were studied by /Velde and Vasseur 1992/. These wells, drilled in sedimentary basins of varying age (4.5 to 210 Ma), provide data on an almost complete burial sequence. The resulting model shows that the reaction rate at repository relevant temperatures is very slow in relation to the timescale considered for a repository (~1 Ma).

Thermal effects on bentonite have been studied at *Kinnekulle* in Sweden, where a two m thick bed of bentonite clay formed from volcanic ash deposits c. 450 million years ago. Samples from the bentonite clay, situated about 95 metres below a cap of a c. 300 million year old diabase, were investigated

/Pusch et al. 1998/. The diabase formed when molten lava penetrated laterally into the sediment series. This magmatic event exposed the sediments to heat that reached down to the bentonite layers. The bentonite layers at Kinnekulle have been known for some time and they were studied early as analogues to compacted bentonite clay buffers to test current understanding of heat effects /Pusch 1983/. These early studies were later supplemented by investigations of samples from *Gotland* and *Sardinia* where episodes of lava flows have likewise heated smectite clay minerals but with different time-temperature profiles /Pusch and Karnland 1988/.

Due to the magmatic intrusion, the centre of the bentonite layer reached a peak temperature of 140ºC after about 200 years, stayed above 100ºC for another 600 years and slowly decreased towards ambient for more than one thousand years /Pusch et al. 1998/. Cementation of the clay by silica ($SiO_2$) and occurrence of the clay mineral illite have been interpreted as caused by the heating. Both of these processes, cementation by precipitation of silica and production of illite from smectite, can lower the swelling capacity of bentonite which is essential for its function as a buffer. Early observations /Pusch 1983, Pusch and Karnland 1988/ confirmed the view that compacted bentonite will retain its swelling capacity providing the heat pulse is limited in temperature and time, and provided that the geochemical environment is not aggressive to smectite in any other aspect. Later investigations of Kinnekulle used a simplified one-dimensional diffusion-reaction model to simulate the observed development of the clay /Pusch et al. 1998/. Sea water composition was assumed and two different options for the reaction were tested: Solid state conversion of smectite to illite versus dissolution of smectite followed by precipitation of illite. The second option was the better one and an even better agreement was reached by assuming that illite formation is non-reversible. Potassium, as expected, proved to be an essential component for the production of illite. Silica produced by the reaction was, according to the calculations, consumed by diffusion into the surrounding sediments and precipitation of quartz.

A number of bentonite deposits in the Cabo de Gata region in *Almería*, Spain, were selected for sampling and studies of different long-term buffer aspects (Barra project) /Villar et al. 2006/. After a first phase, the studies were narrowed to three deposits and two processes: Morrón de Mateo for thermal effects; Cala del Tomate and Cortijo de Archidona for the effect of salinity. The thermal effect in Morrón de Mateo had been caused by a volcanic dome. Bentonite near the volcano was shown to be iron- and magnesium-rich smectite compared to normal aluminium smectite in more distant samples, but properties such as cation exchange capacity and specific surface were found to be the same. The presence of iron and magnesium in the smectite mineral structure was explained as due to a reaction of smectites with contaminants present near the volcanic dome at moderate temperatures (below 100ºC). Conditions may not have been extreme enough to transform the smectite to other minerals. The bentonite clays at Cala del Tomate and Cortijo de Archidona have evidently experienced changes in water composition. Sodium and magnesium are the dominating exchangeable cations in smectites at depth in Cala del Tomate as compared to magnesium and calcium near the surface. Observations from Cortijo de Archidona indicate a sea water intrusion later followed by infiltration of meteoric water, rich in calcium and magnesium. The ionic strength of porewater had varied between 0.02 and 0.23 moles per litre but the clay minerals had seemingly remained stable.

In *Wyoming*, USA, bentonite was formed by alteration of volcano ashes that fell over the shallow, now relict, Mowry Sea. The ashes formed thin but widespread layers on the sea floor and were subsequently altered to bentonite /Smellie 2001/. These bentonite layers were formed about 100 million years ago and their remains are mined in some locations for their content of high grade sodium bentonite. The brand MX-80 has long been used by SKB as reference buffer material. Scientific studies support the view that the bentonite formed under shallow, brackish and partially reducing conditions, and that no further alteration occurred. However, isolation by subsequent depositions of mud and silt may have served to protect the bentonite clay. Consequently, it was not possible to address the question of what would happen under conditions more open to saline groundwater.

The protective and preserving potential of a clay buffer is demonstrated by clay deposits in *Dunarobba*, Italy, which contain a fossil forest /Valentini et al. 1997/. Tree trunks were identified as *Taxodioxylon gypsaceum* which became extinct during the Plioscene indicating that they have been preserved by the clay deposits for more than one million years. The deposit hosting the trees was regarded as dense, consolidated clay with some cementation by calcium carbonate (hydraulic conductivity less than $2 \cdot 10^{-10}$ m/s and yield pressure 1.5–9 MPa). The original cover was supposedly 80 metres before erosion took place. The tree wood is remarkably well preserved. Very little alteration has taken place and the material is still in all aspects wood, with a cellulose content not far from modern

wood. Evaluation of the site suggested that the clay formation had acted on a local scale to protect the fossil trees from unsuitable conditions. The low hydraulic conductivity of the clay has prevented the ingress of oxygenated water which could otherwise have caused aerobic decomposition of the wood. More surprisingly the clay seems to have protected from anaerobic decomposition as well. Anaerobic bacteria are known to decompose organic and in particular cellulosic material. It is also known from archaeological excavations that clay can help to preserve such materials where conditions are generally anaerobic, for example in lake sediments. The Dunarobba fossil forest is in line with these examples but more striking due to its great age. The usual assumption in safety assessments of radioactive waste disposal, that organic material will always become degraded by anaerobic bacteria, which thereby generate gas, is probably pessimistic in many cases where clay is used as buffer and backfill. One possible explanation as to why the clay so efficiently has hindered anaerobic degradation is that essential nutrients were kept out by the clay /Valentini et al. 1997, p 216/.

At the *Cigar Lake* uranium deposit, in Canada, clay (mainly illite and kaolinite) surrounds the uranium ore body. The ore is situated at c. 450 m depth and the ore cannot be geochemically detected on the surface. This isolation of the ore, and the elements related to it, for many millions of years, is partly due to the low hydraulic permeability of the surrounding clay /Cramer and Smellie 1994/. Results from the Cigar Lake studies also illustrate the colloid filtering capacity of clay /Vilks, pp 219–241 in Cramer and Smellie 1994/. Sorption of radionuclides on sheet silicates, mainly chlorite and illite, in the natural fission reactor zones at *Oklo*, have also been shown to have played an important role in limiting the dispersion of these elements around the reactor zones /Bros et al. 2003/.

### 14.6.3 Transport and retardation processes in the geosphere

Scientific investigations aimed at enhancing our knowledge about transport and retardation of radionuclides in the geosphere is based on studies of the geochemical behaviour of these elements (or their chemical analogues).

#### *Subsurface conditions*

The uranium ore zone at *Lake Palmottu* in Finland forms a steeply dipping zone that extends down to a depth of about 300 metres. Geology, hydrogeology, groundwater chemistry, climate, and landscape are similar to those of investigated potential repository sites in Finland and Sweden. It was therefore investigated as an analogue for disposal of spent fuel in crystalline rock /Blomqvist et al. 2000/. At Palmottu, the conditions at depth are generally oxygen-free and reducing, whereas oxidising groundwater conditions were typically encountered in the topmost 100 metres. Reducing conditions at depth are also found at Forsmark. The 1,700 million year old uranium deposit at Palmottu has experienced several periods of glaciations, which may have temporarily subjected the ore to oxidising conditions; however, if so, reducing conditions were efficiently restored. Despite the low grade of ore (0.1%), uranium was found to be abundant enough to be an additional sink for reduction of infiltrating oxygen. The observations in Palmottu illustrate the capacity of the rock to remain stable and maintain reducing conditions despite a long geologic history including periods of permafrost and glaciations.

Freezing conditions, causing salt exclusion, may have caused the unusual groundwater chemistry observed at Palmutto, with elevated sodium and sulfate. Freezing and subsequent dissolution of $NaSO_4$ minerals may lie behind this; however, this is still an open question/Blomqvist et al. 2000/. Another aspect of subsurface conditions during permafrost and glaciations is the possible formation of methane gas hydrates. This has been studied mainly in Canada, where gas-hydrate bearing core samples were collected from the sediments in the present natural permafrost environment of the Mallik sea, Canada, e.g. /Clark et al. 1999/. Gas hydrates were also one aspect of the studies at the Lupin Mine, Canada; no methane hydrates were found during the studies, but there are indications of their presence in the past /Stotler et al. 2009a/. The studies of natural permafrost environments support the conclusion that hydrate formation is unlikely at expected repository conditions.

Reducing conditions are prevailing at *Cigar Lake* in Canada, where a 1,300 million year old uranium deposit is situated at c. 450 m depth. The uraninite at Cigar Lake has interacted with groundwater at different times in the geological history of the ore, as is evidenced by oxygen isotopic composition as well as the presence of secondary uranium minerals; however, the conditions were still such that this has caused only minor disturbances to the uraninite chemical composition and texture, and limited actinide migration /Fayek et al. 2002/.

Surface weathering processes and groundwater conditions at shallow depth are affecting the *Bangombé* natural fission reactor zone in Gabon. The Bangombé reactor is located at 12 m depth in a subtropical, variably oxidizing environment. Thus, the effects of such groundwater conditions on the reactor zone have been studied. The groundwater redox potential at Bangombé was found to be more sensitive to lithological variations than to depth and confinement. The interaction between reactor zone and oxygen-rich groundwater has been in progress for at least c. 70,000 years (and probably much longer), as evidenced by the age of the secondary uranyl-mineral torbernite encountered at Bangombé /Gauthier Lafaye et al. 2000/. The concentration of colloids in the Bangombé groundwater was found to be low (less than 0.3 ppm), in spite of the dynamic subtropical conditions /Gauthier Lafaye et al. 2000, pp 55–56/.

### *Radionuclide transport and retardation*

One important aspect of natural analogue projects is investigation of geochemical behaviour and geochemical reactions of elements of interest for nuclear waste disposal. This was a significant part of the studies at the *Poços de Caldas* natural analogue site in Brazil /Chapman et al. 1993/. In this project, it was shown that the redox front played a significant role in retarding many trace elements, even those considered non-redox sensitive. In this study, colloids were not found to contribute to the transport; rather it was shown that particulate material and colloids in deep groundwater were immobile. Microbes in the system at Poços de Caldas were found to catalyse specific redox reactions, thereby affecting the redox front. Results of the Poços de Caldas project indicate that large-scale, rapid transport of radionuclides and trace elements has not occurred at this site /Chapman et al. 1993/.

The *Cigar Lake* studies indicate a similar absence of large-scale transport since there are no geochemical indications of the 1,300 million year old uranium ore body on the surface. This apparent immobility of relevant elements may be due to the clay that surrounds the ore; the low hydraulic permeability of the clay may have been a contributing factor. This property has been simulated by mass-transport models of the kind that are used for performance assessment of repositories /Cramer and Smellie 1994/. Observations at Cigar Lake also supported conclusions on the role of colloids in the transport of radionuclides. Filtering of colloids by the clay was indicated. There were also examples of irreversible sorption of radionuclides on colloids which is a mechanism that may enhance radionuclide transport /Vilks, pp 219–241 in Cramer and Smellie 1994/. However, as was noted in the *Poços de Caldas* project, particles and colloids may be more or less immobile, in which case irreversible sorption on these particles and colloids will act as a sink, and work in favour of retardation /Chapman et al. 1993/.

The natural fission reactors in Gabon, *Oklo, Okélobondo* and *Bangombé*, provide unique opportunities to study the dispersion of fission products and actinides in the geosphere as a result of 2 billion years of exposure to a natural geological environment. Despite the great age few of the components have been transported out of the zones. However, volatile elements, such as Cs, have been lost /Gauthier-Lafaye et al. 1996/. Retention of plutonium is traced in some locations by anomalous concentrations of the U-235 that has been generated by the decay of Pu-239 /Bros et al. 1996/.

The first and possibly most important episode of mobilization of radionuclides in and around the reactor zones relates to the thermal influence of nuclear reactions. The nuclear reactions themselves heated the groundwater which caused geochemical reactions and rearrangements of matter close to the zones. The clay halo surrounding the core of the reactors formed as a result of this episode of hydrothermal alteration. Transport of rare earth elements in the near field of an Oklo reactor by circulation of heated water has been calculated. The near-field models were reasonably successful in simulating the pattern of rare earth elements distributed in the few metres above the reactor. No fissiogenic rare earth elements were detected further away from the reactor zones /Gauthier-Lafaye et al. 2000, pp 77–79/. The hydrothermal clay in and around the reactor zones has been shown to effectively retain U, REE, Zr and, to some degree, Mo through sorption on the sheet silicates (illite and chlorite) /Bros et al. 2003/.

After the reactor zones cooled down followed c. 1,000 million years during which no major geological event affected the reactor zones. Around 860 million years ago, the Franceville sedimentary basin, which hosts the reactor zones, was subjected to regional extension associated with mafic magmatic dike intrusions. This event caused uraninite recrystallisation and lead loss. During this time radiogenic lead, expelled from the uraninite, precipitated as galena (PbS) crystals in and around the reactor

zones /Evins et al. 2005/. The association between galena, fissiogenic platinum metals (Ru, Rh, Pd), and chalcogens (Se, Te) found in aggregates in or near the uraninite grain boundaries, suggest the mobilisation and redistribution within the reactor zones of these elements during the main episode of galena crystallisation /Gauthier-Lafaye et al. 2000, p 16/.

Transport and redistribution of actinides and radionuclides occur today in the reactor zones. This is most clearly demonstrated by studies performed at Bangombé, where oxidative alteration and dissolution of uraninite is observed as different varieties of secondary uranyl-minerals that have precipitated in and around the reactor zone, and by the uranium isotopic composition measured 50 m downflow from the reactor zone /Gauthier-Lafaye et al. 2000, p 53/. Studies of the migration behaviour of REE have showed that only very small amounts of REE's have left the reactor zone, and the groundwater samples from the reactor zone are depleted in REE's. It was indicated that the uraninite and secondary uranium phases (including coffinite, $U[SiO_4]_nH_2O$) played an important role in retaining the REE /Gauthier-Lafaye et al. 2000, p 51/.

Uranium transport has been studied also at *Palmottu*, in Finland, where the groundwater conditions are similar to those at the Forsmark site. At Palmottu, groundwater facilitated uranium transport was only found to be significant in the oxidizing uppermost hundred metres. Colloids were also carefully analysed at Palmottu but found to be unimportant as carriers of uranium in this case /Blomqvist et al. 2000/. The importance of redox conditions was also observed at the *Koongarra* uranium deposit in the Alligator Rivers Region (Australia), where transport and retention mechanisms are to a large extent connected to oxidising weathering of minerals or the presence of unique constituents such as phosphates /Duerden et al. 1992/.

Transport of radionuclides has also been studied at the *Nevada Test Site* (USA), where groundwater samples from packed off sections in deep drilled wells contained detectable amounts of radionuclides from the nuclear tests /Kersting et al. 1999/. Underground nuclear tests melt the wall of the rock cavity that forms as a result of the explosion. Most of the actinides and rare earth elements produced in the explosion are incorporated in the molten glass that coalesces into a "puddle" at the bottom of the collapsing cavity. Plutonium found in the well had the same isotopic signature as samples from the melt glass of the "Benham" test, which had been performed under the groundwater table, 1.3 kilometres away, 29 years prior to sampling. Moreover, the plutonium and some other radionuclides were found to be associated with colloidal particles. This is probably the best indication so far that radionuclides can in fact be transported in the form of colloids, over substantial distances in a relatively short time.

### 14.6.4 Model testing and method development

A major part of many natural analogue projects concerns validation and testing of geochemical models used in performance assessment and safety analysis of radioactive waste repositories. In addition, the methods and equipment developed for use in natural analogue studies are important for detailed site investigations.

In the *Koongara* (Alligator Rivers, Australia) project, a total of 13 different mass transport models were tested to see how well they were able to reproduce the observed dispersion fan of uranium-238 and some of its daughter nuclides using the large amount of information and data gathered through extensive investigations at the site /Golian and Lever 1992/. The age of the dispersion fan, according to these calculations, was in the range 0.5–3 million years which compared reasonably well with the 1–6 million years obtained from geomorphologic observations. However, none of the models were ruled out which implies that the test was not a very severe one for the models, probably due to the complexity of the analogue and a lack of well defined boundary conditions. Also, loss of a small fraction travelling further than the measured dispersion fan could not be ruled out. Such an observation could have been important and possibly discriminated the models.

A unique approach for the Koongarra project was to test the scenario analysis method, originally developed as a safety analysis tool. It proved itself valuable in stimulating the evaluations, and also served to illustrate the complexity of the analogue /Skagius and Wingefors 1992/.

At *Poços de Caldas* (Brazil), mass-transport models and reaction models were tested, for example by simulating redox front development and hydrothermal transport /Chapman et al. 1993/. The models used in the predictive modelling were generally able to mimic the observed features, which involved

transport of oxidized iron and uranium by rainwater followed by precipitation of pitchblende by reduction when the uranium-bearing water encountered reducing conditions. The pattern confirmed the assumptions of mass-transport in fractured crystalline rock where features such as channelling and matrix diffusion play an important role and where continuum models are no longer adequate /Romero et al. pp 471–502 in Chapman et al. 1993/.

In the Poços de Caldas project different geochemical codes and databases for speciation and solubilities were tested and compared. It was observed that, for example, calculated solubilities tended to be on the pessimistic (over-estimated) side but not always. These exercises led to recommendations for amendments and improvements to the models and databases /Bruno et al. pp 451–470 in Chapman et al. 1993/.

In studies of the *Bangombé* natural fossil fission reactor (Gabon), comparisons were made between two codes used for geochemical evaluation: A statistical approach of principal component analysis and a deterministic approach simulating coupled transport and chemical reactions along groundwater flow lines. Both were able to distinguish chemical reactions from mixing and both independently identified an increase in alkalinity around the Bangombé reactor zone /Gurban et al. 1998/. This observation was explained by microbial analysis of iron reducing bacteria, capable of decomposing organic matter and generating carbon dioxide causing the alkalinity to increase. The code (M3) for principal component analysis has been used since for geochemical evaluations of results from investigations of potential repository sites in Sweden. The fact that availability of reliable and relevant thermodynamic data is a requirement for adequate modelling is illustrated by the improvements made in calculated predictions of mineral assemblages at Bangombé, which after an update of the thermodynamic database reached a much better agreement with observed mineralogy /Jensen et al. 2002/.

Blind predictive modelling was used in studies of the *Palmottu* natural analogue site in Finland, where a flow path in the "Eastern Flow System" was covered by boreholes with packed-off sections for groundwater sampling. Mass transport models were applied to explain the measured concentrations and isotope ratios of uranium along the flow path /Blomqvist et al. 2000/. The first attempts were made "blind", based on a limited amount of data. These first simplified approaches were not adequate to explain the observations. In the second phase, additional data on groundwater chemistry were distributed and two advanced models were applied, one fully coupled reaction-transport model and another model incorporating matrix diffusion. Both of them were successfully used to explain the development of uranium concentrations. The coupled model closely explained the measurements of groundwater composition in the boreholes. The assumption of matrix diffusion in the second model, to explain uranium dissolution by gradual oxidation of the rock matrix, was supported by independent measurements of uranium series disequilibrium.

In addition to model testing, the Palmottu project also provided an opportunity to test equipments developed for investigation of repository sites, such as flow-logging devices, borehole video camera, borehole radar, mobile groundwater chemistry laboratory, down-hole chemistry probes etc. Measuring and sampling in boreholes were thoroughly exercised and the results used to describe the site, for example, the distribution of fractures and composition of the rock, as well as flow and chemistry of the groundwater. Much of this approach was later repeated during investigations of potential repository sites.

### 14.6.5 Concluding remarks

An important contribution from natural analogue studies to long-term safety assessments is to provide qualitative information on which processes and features to include in the assessments. The relevant processes are not limited to the well-known natural analogue sites, but can be studied in many natural systems. However, by focussing research efforts in these international projects, much site specific information has been made available, and researchers from different disciplines have been brought together to discuss the results.

Natural analogues can be considered experiments that have run for vast time periods in a complex, natural environment. Thus, observations of the results of these "experiments" can be made, from which hypotheses regarding processes that have affected the investigated feature can be formulated. These hypotheses can be tested with various methods. In this way, information from natural analogue studies can be used in development of conceptual models.

A central issue for many natural analogue projects has been to test the adequacy of the geochemical tools, and the mathematical models incorporated in them, that are used in analyses of long-term safety. In practice this has resulted in an assessment of the applicability of associated databases used in geochemical models under natural conditions, and has helped to establish some of the uncertainties associated with these models.

There are, however, aspects of natural analogue studies that limit the use of the results acquired. The difficulty in extracting the quantitative data necessary for the safety analyses is the main limitation. Information regarding the initial state of the feature as well as details regarding events and processes affecting the feature through all of its history is normally not fully available. This is often a result of the long timescales involved and the complexity of the systems, which is inherent in the concept of a natural analogue.

In conclusion, the outcome of the natural analogue studies has been of a more qualitative than quantitative nature. The gathering of scientists and modellers in these international projects has focussed the research efforts and method development, so that enough information is available for identifying processes and scenarios relevant to safety assessments. Also, many natural analogues provide support to long-term safety analyses by improving general perception and understanding of the concept of a deep repository.

**Table 14-4. Selected references for some natural analogue studies with relevance for the KBS-3V safety assessment. This list is not exhaustive. Large and interesting overviews of analogue studies are given in /Miller et al. 2000/ and /Ruiz López et al. 2004/.**

| **Spent nuclear fuel, transport and retardation in the geosphere, method development and model testing** | |
|---|---|
| Oklo, Gabon | Gauthier-Lafaye et al. 2000 |
| Cigar Lake, Canada | Cramer and Smellie 1994 |
| Poços de Caldas, Brazil | Chapman et al. 1993 |
| Palmottu, Finland | Blomqvist et al. 2000 |
| Koongarra (Alligator Rivers), Australia | Duerden et al. 1992 |
| Nevada Test Site, USA | Kersting et al. 1999 |
| **Copper canister** | |
| Keweenaw Peninsula, USA | Johnson and Francis 1980 |
| Hyrkkölä, Finland | Marcos et al. 1999 |
| Littleham Cove, UK | Milodowski et al. 2002 |
| Kronan cannon, Sweden | Hallberg et al. 1988 |
| Lightning plates, Sweden | Hallberg et al. 1984 |
| **Buffer and backfill** | |
| Deep wells in sedimentary basins | Velde and Vasseur 1992 |
| Kinnekulle, Sweden | Pusch et al. 1998 |
| Wyoming, USA | Smellie 2001 |
| Almería, Spain | Villar et al. 2006 |
| Dunarobba, Italy | Valentini et al. 1997 |

# 15 Conclusions

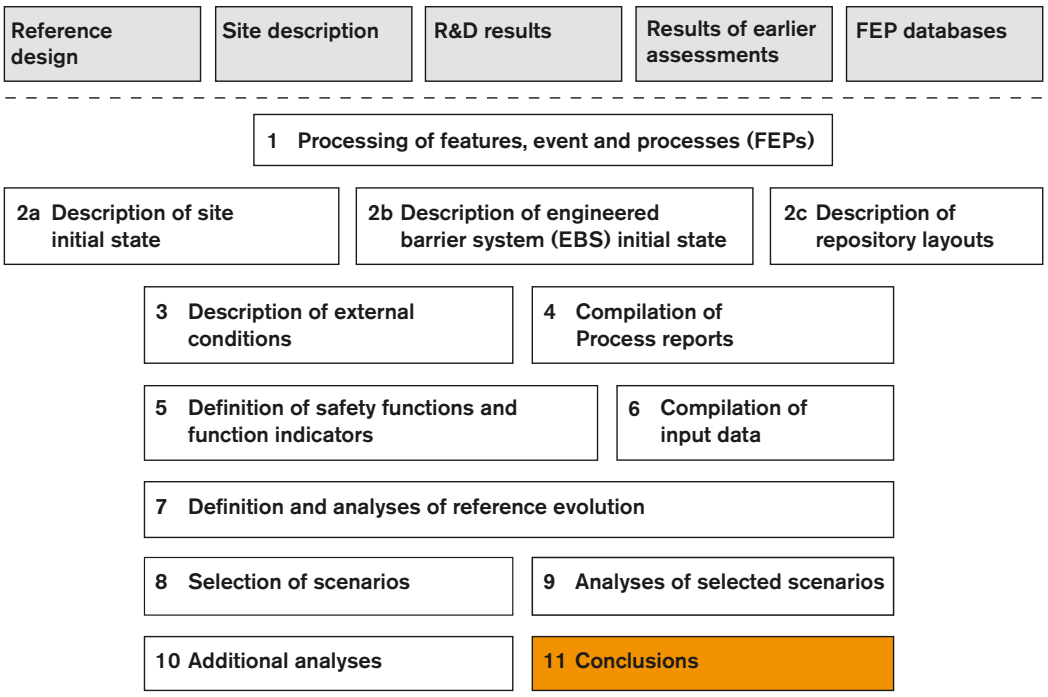


***Figure 15-1.*** *The SR-Site methodology in eleven steps (Section 2.5), with the present step highlighted.*

## 15.1 Introduction

The central conclusion of the safety assessment SR-Site is that a KBS-3 repository that fulfils long-term safety requirements can be built at the Forsmark site.

This conclusion is reached because the favourable properties of the Forsmark site ensure the required long-term durability of the barriers of the KBS-3 repository. In particular, the copper canisters with their cast iron insert have been demonstrated to provide a sufficient resistance to the mechanical and chemical loads to which they may be subjected in the repository environment.

The conclusion is underpinned by the following considerations.

- The reliance of the KBS-3 repository on i) a geological environment that has long-term stability with respect to properties of importance for long-term safety, i.e. mechanical stability, low groundwater flow rates and the absence of high concentrations of detrimental components in the groundwater, and ii) the choice of naturally occurring materials (copper and bentonite clay) for the engineered barriers that are sufficiently durable in the repository environment to provide the barrier longevity required for safety.
- The understanding, through decades of research at SKB and in international collaboration, of the phenomena that affect long-term safety, resulting in a mature knowledge base for the safety assessment.
- The understanding of the characteristics of the site through several years of surface-based investigations of the conditions at depth and of scientific interpretation of the data emerging from the investigations, resulting in a mature model of the site, adequate for use in the safety assessment.
- The detailed specifications of the engineered parts of the repository and the demonstration of how components fulfilling the specifications are to be produced in a quality assured manner, thereby providing a quality assured initial state for the safety assessment.

The detailed analyses, performed systematically according to a well-defined methodology, demonstrate that canister failures in a one million year perspective are rare. Even with a number of pessimistic assumptions regarding detrimental phenomena affecting the buffer and the canister, they are sufficiently rare that their cautiously modelled radiological consequences are well below one percent of the natural background radiation.

As a background to the discussion of conclusions in this chapter, the main features of the KBS-3 safety concept are repeated.

- The waste is isolated from the human and near-surface environment by placing the repository at depth in a long-term stable geological environment. This means that the repository is not strongly affected by either societal changes or by the direct effects of long-term climate change at the ground surface.
- The risk of human intrusion is reduced by locating the repository at a site where the host rock can be assumed to be of no economic interest to future generations.
- The spent fuel is surrounded by several engineered and natural safety barriers.
- The primary safety function of the barriers is to contain the fuel within a canister.
- Should containment be breached, the secondary safety function of the barriers is to retard a potential release from the repository.
- The engineered barriers are made of naturally occurring materials that are stable in the long term in the repository environment.
- The repository is designed and constructed so that temperatures that could have significant detrimental effects on the long-term properties of the barriers are avoided.
- The repository is designed and constructed so that radiation-induced processes that could have significant detrimental effects on the long term behaviour of the engineered barriers or of the rock are avoided.
- The barriers function passively, i.e. without human intervention and without artificial supply of matter or energy.

This chapter presents the detailed conclusions from the SR-Site project.

Two major roles for the presentation of the conclusions from the SR-Site project can be distinguished:

1. To demonstrate compliance with applicable Swedish regulations for a KBS-3V repository at the Forsmark site.
2. To provide feedback to design development, to SKB's RD&D Programme, to detailed site investigations and to future safety assessment projects.

The first purpose is addressed in Section 15.3 and the second in Sections 15.4 through 15.8. Before the formal discussion of compliance-related issues and the detailed feedback, an overview of the results of the analyses is given in Section 15.2 immediately below.

## 15.2 Overview of results

This section gives a summary of the most important findings in the SR-Site project. The conclusions are further discussed and substantiated in the following sections of this chapter.

### 15.2.1 Compliance with regulatory risk criterion

**A repository at Forsmark is assessed to comply with the regulatory risk criterion**

The analyses carried out in SR-Site show that a KBS-3V repository at Forsmark constructed in accordance with the current reference design will comply with the regulatory risk criterion issued by SSM.

**The likelihood of canister failures during the initial one thousand years, is assessed as negligible**

The pessimistically calculated mean number of canisters failing due to earthquakes during the initial one thousand years is of the order of one in a hundred thousand. All other failure types are assessed as ruled out for this period. Furthermore, the evaluations of the canister sealing procedure, have led to the conclusion that all canisters will be tight at deposition.

**In a one million year time perspective, there is a small risk contribution from canister failures due to enhanced corrosion following buffer erosion**

Loss of buffer may occur from exposure to low ionic strength waters but the extent is uncertain. The Forsmark site has a large potential to maintain a sufficient ionic strength at repository depth over a glacial cycle. Loss of buffer mass, to the extent that advective conditions arise in the deposition hole, may, however, occur in a 100,000 year perspective for typically less than ten deposition positions with high flow rates.

Advective conditions in a deposition hole will enhance the canister corrosion rate. In a one million year time perspective, this may lead to failures of a few canisters when applying the most pessimistic of the hydraulic interpretations made of the Forsmark site, with cautious assumptions regarding concentrations of corrosive agents and deposition hole acceptance rules.

With pessimistic assumptions regarding buffer erosion, copper corrosion and radionuclide transport conditions, the radiological risk from such canister failures is pessimistically calculated to be around 1/100 of the regulatory limit in a 100,000 year perspective and around 1/10 of the regulatory limit in a one million year time perspective.

**In a one million year time perspective, there is a small risk contribution from canister failures due to earthquakes**

Canister failures due to large earthquakes cannot be categorically ruled out. However, the probabilistic analyses imply that, on average, it would take considerably more than one million years for even one such canister failure to occur.

The contribution to radiological risk from earthquakes is pessimistically calculated to be less than 1/100 of the regulatory limit in a 100,000 year perspective and less than 1/10 of the regulatory limit in a one million year time perspective.

### 15.2.2 Issues related to altered climate conditions

Several issues of importance for long-term safety are related to future glacial, periglacial or warmer climate conditions. A number of conclusions regarding effects of such conditions can be drawn.

**Freezing of the buffer is ruled out – even for very pessimistically chosen climate conditions**

According to the analyses, freezing of the buffer clay is ruled out, even for the most pessimistic periglacial climate conditions considered, which includes the large uncertainties related to future climate development. Also freezing of a deposition tunnel backfill material or of a water-filled cavity in an eroded buffer is ruled out for the most pessimistic climate development at Forsmark.

**Canister failure due to isostatic load is ruled out – even for very pessimistically chosen climate conditions**

According to the analyses, canister failure due to isostatic load is ruled out for the most severe future glacial conditions considered based on the glacial development of the past two million years.

**Oxygen penetration is very unlikely – even for very pessimistically chosen climate conditions – and the consequences are small**

Oxygen penetration to canister positions is ruled out, except for enhanced flow situations occurring during the unlikely event when an ice sheet margin is temporarily stationary above the repository in combination with several other pessimistic assumptions. Even in such a case, the consequences in terms of canister corrosion are small.

**Repository safety for a prolonged period of warm climate before the next glacial period is assessed as comparable to safety for a climate unperturbed by enhanced global warming**

A prolonged period of warm climate (global warming due to an enhanced greenhouse effect) may lead to increased exposure to dilute groundwater of a repository at Forsmark and hence to increased buffer erosion. The sensitivity of the calculated risk to such a perturbation is, however, low.

The occurrence of large earthquakes is likely to increase during deglaciation, and this effect is thus delayed by a prolonged initial period of warm climate.

### 15.2.3 Other issues related to barrier performance and design

**The reference design, forming the basis for the assessed initial state in SR-Site, yields a safe repository when implemented at the Forsmark site**

Since the analyses in SR-Site show that the regulatory risk criterion is fulfilled, it is concluded that the assessed reference design implemented through the selected production and control procedures will yield a safe repository. Conclusions regarding design issues important for long-term safety yielding feedback to future refinement of the design have been drawn.

**It is crucial to avoid deposition positions intersected by large or highly water conductive fractures and the low frequency of water conducting fractures allows efficient application of such rejection criteria**

The risk contributors in SR-Site are related to the occurrence of large and/or highly conductive fractures intersecting deposition holes. This applies to the buffer colloid release process and the impact of major earthquakes in the vicinity of the repository. These two phenomena are related to canister failures due to canister corrosion and to secondary rock shear movements, respectively. As also the retention in large, highly transmissive fractures is small, such failures are in general associated with high consequences. Accordingly, such fractures need to be avoided once identified.

Cautious assumptions regarding the likelihood of occurrence of such fractures and regarding deposition hole rejection criteria are adopted in SR-Site. The results of the analysis are sensitive to these assumptions. It is important to continue the development of acceptance criteria for deposition holes as a basis for future assessments. This needs to be studied both by simulation of the effects of applying potential criteria and by exploring the practicability of applying the criteria.

**The heat from the canister will likely fracture the rock in the deposition hole wall, which would enhance the in- and outward transport of dissolved substances, but this has little impact on risk**

Thermally induced spalling around deposition holes at Forsmark cannot be ruled out and may have a considerable impact on mass exchange between the flowing groundwater and the buffer as long as diffusion is the dominant transport mechanism in the buffer. For diffusive conditions, there is, however, a considerable margin to canister failures even when spalling is pessimistically assumed in all deposition positions at Forsmark. If advective conditions prevail in the buffer, the effects of spalling are much less pronounced because it adds little to the already increased flow rate. In consequence, the overall effect on the calculated risk is small.

**The importance of the excavation damaged zone in the rock around the deposition tunnels as a transport path for radionuclides is limited**

The importance of the excavation damaged zone (EDZ) around deposition tunnels is limited in comparison to other transport routes for radionuclides. Very pessimistic assumptions about the EDZ in relation to the reference excavation method could affect the extent of canister corrosion for advective conditions.

This confirms the suitability of the cautious reference excavation methods adopted in the reference design of the repository.

**In most deposition holes groundwater will not reach the canister for thousands of years due to the favourable rock properties at Forsmark**

The saturation times for both backfill and buffer are likely to range from a few tens of years to several thousand years, as a consequence of the rock properties (matrix hydraulic conductivity and presence and characteristics of fractures) at Forsmark. The majority of deposition holes are not intersected by water conducing fractures, yielding slow saturation (with water from the deposition tunnel and the buffer) and slow inflow of e.g. corrosive agents in the groundwater both during unsaturated and saturated conditions. Transport of corrosive agents within the bentonite will be very limited and diffusion-dominated also during the unsaturated phase. During saturation the microbial activity may be enhanced before the swelling pressure is established. However, this is of little consequence, since the corrosion is limited by mass balance and transport. Since the groundwater flow during saturation is towards the deposition holes, no erosion of the bentonite can occur during the unsaturated period. The effects of the unsaturated period on the geochemical, mineralogical and thermal property changes in the buffer have been investigated in SR-Site. They are found to be small and without any significant impact on long-term performance.

### 15.2.4 Confidence

**The confidence in the results obtained is sufficient to form a basis for a decision regarding application for a licence to construct a repository.**

In summary, the elements contributing to the overall confidence in the assessment results are as follows.

- The knowledge of the Forsmark site from the completed, surface based investigations is sufficient for the assessment of long-term safety. The site has favourable conditions for safety and no site-related issues requiring resolution in order to demonstrate safety have been identified.
- There is a well established reference design with specified and achievable production and control procedures yielding an initial state of the repository system with properties favourable for long-term safety at the Forsmark site. There is potential for additional optimisation when this reference design is developed and implemented, as is further discussed in Sections 15.3.5 and 15.5.
- The scientific understanding of issues relevant for long-term safety is mature as a result of decades of research both within the Swedish and other national programmes and in international collaboration projects.
- A complete analysis of issues identified as relevant to long-term safety has been carried out in SR-Site according to an established assessment methodology comprising e.g. cautious approaches when addressing uncertainties.
- Documented quality assurance routines, including peer reviewing, have been applied in the assessment of the initial state, in the development of the site description and in the analysis of long-term safety.

The discussion of confidence is further developed in Section 15.3.6.

## 15.3 Demonstration of compliance

### 15.3.1 Introduction

From applicable regulations from SSM and general recommendations and guidance associated with these regulations, a number of requirements on presentation of a compliance evaluation can be derived. The requirements are here categorised and addressed as follows:

1. Account of calculated risk to individuals, Section 15.3.3.
2. Account of effects on the environment from release of radionuclides, Section 15.3.4.
3. Demonstration of use of best available technique, BAT, Section 15.3.5.
4. A discussion of confidence, Section 15.3.6.
5. Other, general requirements on the system, e.g. demonstration of a multi-barrier system, Section 15.3.7.
6. General requirements on the safety assessment (adequate handling of uncertainties, quality assurance, etc), Section 15.3.8.

The above structure does not, however, address all aspects of the regulations. For a complete account of how the SR-Site report meets these requirements, the reader is referred to Appendix A, where the regulations are reproduced and where references are given to sections in this report where each issue is addressed.

The analyses and conclusions in SR-Site are based on an established reference design with specified and achievable production and control procedures yielding an initial state of the repository system with properties favourable for long-term safety at the Forsmark site. The engineered parts of the repository system are based on demonstrated technology and established quality assurance procedures to achieve the initial state of the system, including the construction of the repository facility. This is systematically documented in the **Production reports** and their underlying references as summarised in Chapter 5.

As an introduction to the discussion of compliance, a brief account of the safety concept, evaluated by results from the SR-Site assessment is given in Section 15.3.2 immediately below.

### 15.3.2 The safety concept and allocation of safety

The main safety function of the KBS-3 concept is containment and the secondary safety function, mobilised if the containment function is not upheld, is retardation.

#### *Containment*

The containment function is provided by an intact copper shell of the canister. The extent to which this function is upheld is dependent on the buffer's function of limiting advective transport between the host rock and the canister and on favourable mechanical, hydrogeological and geochemical properties of the host rock: i) limited flow rates and a minimum charge concentration of the groundwater to avoid erosion of the buffer ii) limited flow rates and low groundwater concentrations of sulphide to limit corrosion, in particular if the buffer has been eroded, and iii) a low probability of large fractures intersecting deposition holes in order to limit the potential impact on the canister of large earthquakes in the vicinity of the repository.

The analyses in SR-Site indicate that containment is maintained even in the one million year perspective for a vast majority of canisters. Deterioration of the barrier system to the extent that containment is lost is assessed to only occur, as a statistical average, for less than one canister due to buffer erosion leading to advective conditions and enhanced corrosion. The other failure mode that could not be ruled out, that due to earthquake-induced secondary shear movements in fractures intersecting deposition holes, is even less likely and affects on average considerably less than one canister when this failure mode is evaluated statistically with a number of pessimistic assumptions. This means that containment is assessed to be maintained for the vast majority of the 6,000 canisters throughout the assessment period.

All safety functions related to containment are shown in Figure 8-2. Many of these, like the canister's ability to withstand isostatic loads or the "ability" of the host rock to provide a favourable rock temperature, are assessed as upheld thought the assessment period.

It is also noted that the consequences of a postulated, complete loss of containment for all canisters decrease with time, and are about a factor of 3 higher than the regulatory risk limit at the end of the assessment period (hypothetical case C in Figure 13-67).

#### *Retardation*

Both the failure mechanisms that could not be ruled out are of the common mode type, i.e. the canister, the buffer and the rock are all affected, either through a detrimental shear movement or through a high flow rate in the geosphere, affecting both erosion and corrosion. The causes of the failures affect also the retention properties through high flow rates and, in the case of erosion, through the absence of the buffer after failure. Hence the retarding potential of the repository is limited in these particular cases, for the canisters that have failed. Instead, safety is to a considerable extent achieved through the slow dissolution of the fuel and, to a lesser extent, through the limited corrosion rate of radionuclide-containing metallic structural parts of the fuel elements.

For the canisters that maintain their containment potential, retardation is a latent safety function throughout the assessment period. A more general view of the retarding potential of the buffer and the host rock is obtained from the analyses of hypothetical, complete losses of barrier functions in Section 13.7.3.

Retention in the buffer is important for the initial 1,000 years and limited in longer time frames (compare cases C and D in Figure 13-67). The latter is due to the fact that the total dose in the long term is dominated by non-sorbing or very long lived nuclides. However, a nuclide specific comparison (Figures 13-63 and 13-61) reveals that the buffer has a considerable retention function for sorbing nuclides also in the long term, masked in the total dose by the dominance of the non-sorbing species.

The role of retention in the rock is similar; it is important for the initial 1,000 years and limited in longer time frames (compare cases C and C* in Figure 13-67) as concerns total dose, again since total dose is then dominated by nuclides that do not sorb in the rock. A nuclide specific comparison (Figures 13-62 and 13-61) reveals that the rock has a considerable retention function for sorbing nuclides also in the long term, masked in the total dose by the dominance of the non-sorbing species. The low flow rates at repository depth also play an important role in limiting the release rate of radionuclides to the rock.

#### *Summary*

In summary, containment is the primary safety function of the KBS-3 repository and it is demonstrated to be efficiently upheld at the Forsmark site throughout the assessment period, directly through the properties of the canister and indirectly by the favourable hydrogeological and geochemical properties of the host rock. For the rare failures of containment, retardation is of limited importance due to the common mode nature of the failure mechanisms in question and since only very long-lived nuclides remain when these failures occur. As a latent function, retardation is significant for hypothetical releases of, in particular, sorbing species throughout the assessment period. For hypothetical failure modes affecting the canister only, retardation of sorbing nuclides is significant in the buffer and in the host rock.

### 15.3.3 Compliance with SSM's risk criterion

This section contains a discussion of the compliance with SSM's risk criterion in different time frames. A discussion of confidence in the results, e.g. that the assumed initial state or site properties in the assessment are justified, is given in Section 15.3.6.

#### *Regulatory requirements*

The primary compliance criterion in Swedish regulations is SSM's risk criterion. An account of the calculated risk is, therefore, an essential component of a compliance demonstration for the first 1,000 years. This is also explicitly stated in SSM's General Guidance, where a reporting of contributions to risk from each analysed scenario is also requested.

Also for the initial glacial cycle, a risk calculation is required. SSM states the following regarding this period in its General Guidance:

"Reporting should be based on a quantitative risk analysis in accordance with the guidelines to Sections 5-7. Supplementary indicators of the repository's protective capability, such as barrier functions, flow of radionuclides and concentrations in the environment should be used to strengthen the confidence in the calculated risks. The given period of time of one hundred thousand years is approximate and should be selected in such a way that the effect of expected large climate changes, for instance, a glaciation cycle, on the protective capability of the repository and consequences to the surroundings can be illustrated."

Regarding the time beyond the initial glacial cycle, SSM states the following in its General Guidance: "The risk analysis should illustrate the long-term development of the repository's barrier functions and the importance of major external disturbances on the repository such as earthquakes and glaciations. Taking into consideration the increasing uncertainties over time, the calculation of doses to people and the environment should be made in a simplified way with respect to climate development, biosphere conditions and exposure pathways. Climate development can simplified be described as a repetition of identical glaciation cycles."

A strict quantitative comparison of calculated risk in relation to the criterion for individual risk in the regulations is not meaningful. The assessment of the protective capability of the repository should instead be based on reasoning on the calculated risk together with several supplementary indicators of the protective capability of the repository such as barrier functions, flows of radionuclides and concentrations in the environment. If the calculated risk exceeds the criterion of the regulations for individual risk or if there are other indications of substantial disruptions of the protective capability of the repository, the underlying causes of this should be reported on as well as possible measures to improve the protective capability of the repository."

### *Calculated individual risk in SR-Site*

A detailed summary account of the calculated individual risk for a repository at Forsmark is given in Section 13.9. The details are not repeated here, but the numerical result of the risk summation of the two contributing scenarios, the corrosion scenario and the shear load scenario is reproduced in Figure 15-2, as a background to the discussion below.

### *Compliance for the first 1,000 years*

All canisters are assessed to be tight at deposition. The initial copper coverage is discussed in the account of the initial state of the canister in Section 5.4.3. The initial minimum copper thickness is given as 47.5 mm in Table 5-9. Taking also the occurrence of local internal defects in the copper shell into consideration, no canisters are assessed to have local reductions exceeding 20 mm. This is the manufactured and inspected thickness of the corrosion barrier after the final machining of the canister components.

As required by SSM's Regulations, many aspects of the repository evolution have been modelled in detail for the initial 1,000 years. This concerns the thermal, mechanical, hydraulic and chemical evolution, as well as effects on the buffer and the canister. Detailed accounts are given in Sections 10.2 (the excavation and operational phases) and 10.3 (the initial period of temperate climate after closure). Also the biosphere development is modelled in detail during this time period.

Of the three identified failure modes of the canister, i.e. failure due to corrosion, due to shear load and due to isostatic loads, corrosion and isostatic load induced failures can be ruled out with large margins for the first 1,000 years, as demonstrated in the reference evolution (Chapter 10) and the analyses of the corrosion and isostatic load scenarios (Sections 12.6 and 12.7, respectively).

Shear loads on the canister may occur as a consequence of large earthquake induced secondary shear movements in fractures intersecting deposition holes. Although the likelihood for large earthquakes is higher during periods of tectonic stress, for example during glacial rebound, it cannot be entirely ruled out that a detrimental earthquake would occur during the initial 1,000 years.

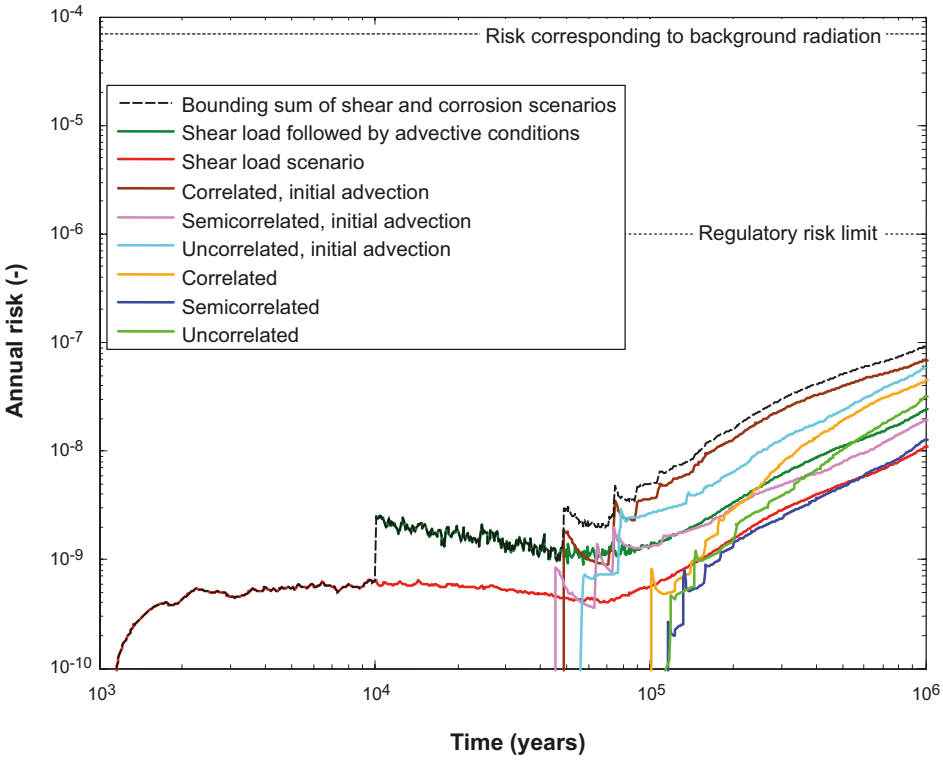


***Figure 15-2.*** *Risk curves, expressed as annual individual risk. Several alternatives for the corrosion scenario are shown, and two for the shear load scenario. The bounding, dashed curve is the sum of the curve for the shear load failure followed by advective conditions (dark green) and the curve for the variant of the corrosion scenario yielding the highest risk (brown). The risk associated with the main scenario is subsumed under the corrosion scenario as it is equal to the semi-correlated case (blue).*

The probability that one out of the 6,000 canisters has failed at the end of the initial 1,000 year period is estimated at $2.4 \cdot 10^{-5}$, see further Section 10.4.5, i.e. hypothetically 40,000 repositories, each with 6,000 canisters would have to be constructed in order for there to be an expectation of one failure during the initial 1,000 years. Despite this extremely low probability, a risk contribution was calculated for the first 1,000 years, with the result that the mean annual dose is at most around 0.001 μSv/yr corresponding to a risk of $10^{-10}$/yr, see Figure 13-49 in Section 13.6. This analysis builds on a detailed modelling of the biosphere development and radionuclide transport in the developing landscape during the initial 1,000 years, as required by SSM's Regulations.

It is, therefore, concluded that the analysed repository at Forsmark complies with the regulatory risk criterion during the initial 1,000 years after closure.

In hypothetical cases of initially defective canisters, there are several properties of the barrier system that provide protection, some of which are not important, or more difficult to claim, in longer time frames. As discussed in Section 13.9.5, some of these would, with cautious assumptions, alone prevent any releases during the initial 1,000 years for an initially defective canister. This relates particularly to the time required for water to get into contact with the fuel elements and the integrity of the Zircaloy cladding.

### *Compliance for the initial glacial cycle*

As reported in Section 13.9 and reproduced in Figure 15-2, the calculated, pessimistically bounded risk during the initial 120,000 year glacial cycle is at most about $10^{-8}$/yr, i.e. about two orders of magnitude below the regulatory limit.

Only the shear load scenario contributes to risk for the first tens of thousands of years. Consequences in the corrosion scenario occur after about 50,000 years for the highly pessimistic and bounding case where initial advection in all deposition holes is assumed. With cautious estimates of the extent of buffer erosion, the first consequences of the corrosion scenario occur at the earliest after around 100,000 years.

### *Repository performance for the time beyond the initial glacial cycle up to one million years*

As reported in Section 13.9 and reproduced in Figure 15-2, the calculated, pessimistically bounded risk beyond the first 120,000 year glacial cycle up to one million years is at most about $10^{-7}$/yr, i.e. about one order of magnitude below the regulatory limit.

In this time frame, both the shear load scenario and the corrosion scenario contribute to the calculated risk. The contributions are comparable in magnitude. However, since both are represented by pessimistic bounding cases, and because the pessimistic assumptions differ between the scenarios, the two risk contributions cannot be directly compared.

Alternative safety indicators for this time period are discussed below.

### *Risk dilution*

Risk dilution was analysed in connection with the risk summation in Section 13.9 and found not to challenge the conclusion regarding compliance with the risk criterion in any of the time frames.

### *Alternative safety indicators*

In particular for times far into the future, the calculated risk becomes less useful as an indicator of repository safety, and SSM's Regulations suggest that alternative indicators should, therefore, also be evaluated. Four alternative indicators to risk are used in SR-Site, as described in Section 13.5.8. The following results emerged for the central corrosion case.

- Peak releases of activity from the geosphere are about three orders magnitude below the activity constraints issued by the Finnish regulator STUK.
- The peak radiotoxicity flux from the geosphere is more than three orders of magnitude lower than the reference value for radiotoxicity flux from the geosphere suggested by the EU SPIN project.
- Calculated radionuclide peak concentrations in ecosystems at Forsmark from repository releases of Ra-226 are about three orders of magnitude below measured concentrations of naturally occurring Ra-226 at Forsmark.
- Peak geosphere fluxes caused by Ra-226 releases from the repository are about two orders of magnitude below naturally occurring fluxes of Ra-226 at the site, as estimated from site data; the difference is larger for U-234 and U-238. The total release of all repository derived nuclides converted to dose is also around two orders of magnitude lower than the summed dose from fluxes of the three mentioned naturally occurring nuclides.

The results are readily applicable to other corrosion cases, for most indicators by simply scaling by the release of Ra-226, which is, at most, one order of magnitude higher than that for the central corrosion case.

Similar conclusions are reached for the shear load scenario, as accounted for in the **Radionuclide transport report**.

In summary, the application of alternative indicators shows that releases from the repository are orders of magnitude below the adopted reference values for the indicators. This suggests that the future radiological consequences on man and on the environment of releases from the repository are negligible, independent of assumptions in the biosphere model.

### *The time beyond one million years*

The evolution of the repository after 1 million years is discussed in Section 14.5.

An account of the development of the radiotoxicity of the spent nuclear fuel up to ten million years is given in Figure 2-1 in Section 2.4.

Although the rocks, the ductile deformation and the brittle deformation zones at Forsmark all formed at least one billion years ago, the increasing uncertainties regarding the external conditions makes it not meaningful to predict the development of the site and of the repository for time periods beyond one million years.

It is noted that the hypothetical case in Section 13.7.3, where all canisters are failed, where the buffer is absent and where retention in the rock is disregarded, yields releases that correspond to dose consequences that are comparable to the natural background radiation after one million years. The releases are in that case controlled by the flow at repository depth and the inventory of radionuclides, the latter of which decreases with time and is dominated by radionuclides that also occur in natural ore bodies.

Finally, the scientific understanding of the fuel dissolution process suggests that the longevity of the spent fuel matrix is several million years in the repository environment (see Section 13.5.5). Furthermore, uranium ores that are many millions and even billions of years old are known through geological observations. This indicates that, in the case of stable tectonics and maintained reducing conditions in the repository, the uranium oxide which constitutes the fuel matrix can be stable for many millions of years.

#### *Uncertainties linked to the risk calculation for different time periods*

Uncertainties that have a significant influence on the calculated risk are discussed in Section 13.10, Table 13-13, where the handling of the uncertain factors in SR-Site is summarised together with references to plans for the reduction of these uncertainties. As seen in the table, most of the uncertain factors have been treated pessimistically, whereas some have been included as probability distributions in the risk calculations, where their full uncertainty range is used in the determination of mean annual doses, the relevant metric for determining the calculated risk.

The combination of pessimistic handling of uncertainties for which probability distributions could not be determined with the probabilistic handling of quantified uncertainties means that the total risk as determined in the risk summation in Section 13.9 is claimed to represent an upper bound on risk. Since this upper bound is below the risk limit throughout the one million year assessment period, there are no uncertainties of critical importance to resolve with respect to risk.

### 15.3.4 Effects on the environment from release of radionuclides

Doses to non-human biota for the central corrosion case have been calculated according to the methodology described in Section 13.2.5. The results are presented in Section 13.5.7. The highest dose rates to organisms in marine, freshwater and terrestrial ecosystems in Forsmark, both in total and for the dose-dominating radionuclides are well below the screening dose rate (10 $\mu$Gy $h^{-1}$) recommended in the ERICA Integrated Approach. It is therefore concluded that radionuclide releases predicted for this case will not lead to significant detrimental biological effects on individuals of species found, or projected to occur in future, at the site. In consequence, there will be no detrimental impact on populations, communities or ecosystems.

The results are readily applicable to other corrosion cases, by scaling the releases of the nuclides in question, which are at most about one order of magnitude higher than that for the central corrosion case. This means that the conclusion for the central corrosion case holds also for all other corrosion cases considered in SR-Site.

Releases for the shear load scenario have not been analysed with respect to doses to biota in SR-Site. However, since the releases are generally lower for this scenario than for the corrosion scenario, and since the margin to the reference value is several orders of magnitude in the latter, it is concluded that the effects on the environment for the shear load scenario are of no concern.

### 15.3.5 Optimisation and best available technique, BAT

The basis for the SR-Site contribution to the demonstration of optimisation and best available technique (BAT), as well as existing regulatory requirements and general guidance is provided in Section 2.7. While, a general account of the use of BAT is a broad issue spanning from the selection of method for the management of nuclear waste to fine details of the selected method, a limited part of this broad issue can and should be addressed in the safety assessment of the preferred method.

Based on the findings from SR-Site, and especially the specific assessment presented in Section 14.3, feedback can be given whether alterations in relation to the analysed reference design could lead to

reductions in risk or in reduction in uncertainties that potentially could affect risk. For aspects of the design where no such reduction in risk or uncertainty in fulfilment of safety functions can be seen to be realistically obtainable, SR-Site claims the solution to be optimal and BAT. However, SR-Site is not an assessment of all conceivable technical solutions. SKB will continue technical development of several aspects of the design in order to further simplify construction and implementation, but will only adopt these developments if they lead to a risk comparable to or lower than that found in SR-Site.

### *The canister*

The assessment presented in Section 14.3 shows the following.

- Increasing the copper thickness to 10 cm reduces the mean number of failed canisters at one million years by a factor of about 3 while halving the thickness to 2.5 cm increases the number by about a factor of 2. However, since the calculated risk with the reference design is below the regulatory limit, the risk reduction obtained by increasing the thickness is moderate. Furthermore, considering the added problems of manufacturing and sealing a thicker canister, the selected copper thickness is deemed adequate from the point of view of BAT.
- The specified values for elongation and creep ductility in the copper shells are found appropriate and it is judged that there is little prospect that changing these properties would enable the canister to withstand even larger shear loads.
- The ability of the cast iron insert to withstand shear load depends mainly on the occurrence of surface defects in the insert. While it is concluded in the **Canister production report** that the current canister reference design conforms to the stated design premises, it is also noted that rigorous requirements are placed on manufacturing and NDT (non-destructive testing) capability. Revising the design of the canister/buffer system such that the loads on the insert decrease, e.g. by reducing the buffer density, would thus allow relaxation of the requirements on manufacturing and NDT capability for the insert. Furthermore, the adequacy of inserts for PWR fuel have not formally been assessed, but the PWR design is more robust due to its larger material thickness in the cast iron insert.
- For the given reference design, there is ample margin to prevent canister failure due to isostatic load, even for the most extreme load situations and there seems to be no need to change the design in order to increase this margin.

In conclusion, there seems to be little need to alter the canister design from a safety perspective, but the formal analyses of the adequacy of the PWR inserts need, of course, to be made eventually.

### *The buffer*

The assessment presented in Section 14.3 shows the following.

- A larger buffer mass, e.g. by increasing buffer thickness or buffer density, is not seen as a practical means of mitigating the effects of buffer erosion. A larger buffer mass may offer a slightly longer time before advective conditions are created in the deposition hole, but this is not seen as a solution to the buffer erosion issue.
- The assessment of buffer erosion/colloid release, summarised in Section 10.3.11, demonstrates that the phenomenon cannot be ruled out in the assessment of long-term safety. Furthermore, there is still uncertainty with regard to modelling of colloid formation and subsequent erosion of the buffer material and the modelling approach thus tends to be pessimistic. It also seems clear that it cannot, with the current understanding, be defensibly mitigated by e.g. selection of another buffer material. A continued R&D programme on buffer erosion mechanisms is needed and is being implemented.
- Lowering the bentonite density lessens the stress on the cast iron insert. Further reductions of the maximum allowed buffer density, still practically compatible with the requirements on minimum buffer density, may be feasible, at least in the form of a statistical distribution. Consequently, SR-Site will provide this feedback for updating the design premises and for revising the buffer design, see Section 15.5.7.

In conclusion, there is potential to further reduce risk by developing the buffer design and adapting the production of the buffer and deposition holes to conform to this design.

### *The deposition tunnel backfill*

The assessment presented in Section 14.3 shows that the buffer and the associated safety functions will be maintained during the expansion of the buffer into the backfill for all possible combinations of buffer and backfill conditions. For the case when backfill material is lost, a maximum loss of 220 tonnes in a deposition tunnel section can be allowed before advective conditions have to be considered in the deposition hole. However, none of the single fractures intersecting the tunnel close to deposition holes will cause erosion of the backfill to the extent that it loses so much swelling pressure that advective conditions must be assumed in underlying deposition holes. For a few positions, where the tunnel is intersected by a very transmissive deformation zone, potentially more than 220 tonnes could be lost, but since these positions are far away from deposition holes, this is judged not to impair safety. In conclusion, while there possibly could be improvements in the backfill design from an installation point of view, there does not seem to be a need to change the design to further improve its safety functions.

### *Repository layout and acceptance criteria for deposition tunnels and deposition holes*

As demonstrated in Section 14.3, the application of deposition acceptance criteria in the form of EFPC is important for limiting risk, both directly for mitigating the potential for canister shear failure due to earthquakes and indirectly for limiting the future high flows affecting the potential for advective conditions in the buffer and the potential for subsequent canister failure by corrosion.

With regard to shear failure, it is, as argued in /Munier 2010/ likely that critical fractures that escaped detection by strict application of EFPC will indeed be detected by a carefully designed investigation programme and that it is likely that the number of potentially damaged canisters will be lower than predicted in this assessment.

Regarding corrosion failure, application of EFPC significantly reduces the number of deposition holes with high Darcy flux, since there is a correlation, of uncertain magnitude, between fracture size and transmissivity. However, it can also be concluded that if it were possible to even better identify the few deposition hole positions having the largest Darcy flux during saturated conditions before canister emplacement, this would further reduce the already low risk, without any significant loss of useful canister positions.

From the viewpoint of BAT, the current EFPC provides adequate protection against shear failure, but there is reason to continue the efforts envisaged in the detailed investigation programme to be able to find critically large fractures by other means, since such efforts are also likely to result in criteria where fewer deposition holes would need to be rejected. Thereby, both a safer and a more efficient repository may be designed.

Application of EFPC is also important for protection against corrosion failures, but criteria directly connected to the flow properties would be preferable to such indirect criteria. In addition, there appears to be a potential for further enhancing safety by avoiding deposition holes with high inflows, even if the correlation between inflows during the operational phase and long-term flow characteristics is not one-to-one given the differences in boundary condition. Furthermore, the inflows will be disturbed by the open hole ("skin effects") and grouting and there will also be a practical lower detection limit. Partly, these disturbances may be overcome by requiring that deposition holes intersected by fractures capable of providing inflows above a certain value are to be avoided. This suggests that the hydraulic properties of the fractures intersecting the borehole should be tested in the pilot hole prior to drilling the full size hole, thereby minimising skin effects, and that deposition holes intersected by fractures showing visible grout also should be rejected, since the presence of grout suggests that the fracture was quite transmissive before grouting.

The assessment in Section 14.3 also shows that the number of failed canisters due to corrosion would increase if there is an EDZ that is much more transmissive than the currently stipulated limit of $10^{-8}$ $m^2/s$, but the assessment also shows that there is no need to apply a more restrictive limit, i.e. the number of failed canisters would not decrease even if there was no EDZ at all.

In conclusion, the analyses show that for the scenarios contributing to risk (corrosion and shear failure) it is essentially the details of the layout, like the exact position of deposition holes and what deposition holes would be accepted that is important. These details can only be finalised during

repository construction and operation and by application of the observational method using findings from the underground based detailed investigations and by applying the design premises for accepting deposition holes, as discussed above. Thus, the question as to whether the repository layout is BAT can at this stage only be assessed based on these design premises. More specific feedback on these is given in Section 15.5.

### *Repository depth*

As concluded from the assessment of the adequacy of the selected repository depth, presented in Section 14.3.4, the depth has mainly been decided by considering the hydraulic conditions at the Forsmark site, i.e. frequency and occurrence of transmissive fractures and their dependence on depth, whereas the constructability is mainly related to rock mechanical issues, e.g. the likelihood and extent of spalling in deposition holes prior to emplacement. More detailed conclusions are given below.

- Factors relating to the chemical stability safety function R1, "Provide chemically favourable conditions", are generally favourable at the selected depth. The only remaining chemical stability issues of concern for repository safety relate to the potential for a few deposition holes to experience groundwater with too low an ionic strength and to the presence of sulphide. Generally, the risk of penetration of dilute waters would decrease with increased repository depth. However, the few occurrences of such potential penetration are related to the scarce occurrence of highly transmissive migration paths in the generally very tight rock. There is no evidence that a practically realistic increase of the depth (i.e. in the order of a 100 m) would dramatically reduce the occurrence of such isolated paths – and it seems a better strategy to try to avoid them locally. Furthermore, there is no indication that the occurrence of sulphide is correlated to depth.
- Safety function R2a "Transport resistance in fractures, F" is affected by repository depth. The length of the travel paths of solutes in the groundwater will increase with increasing depth, but the resulting impact on the transport resistance would only be marginal.
- Both safety functions R2a "Transport resistance in fractures, F" and R2b "Equivalent flow rate in buffer/rock interface, $Q_{eq}$" are affected by repository depth, since fracture frequency and fracture transmissivity show depth dependence. However, the chosen repository depth below 450 m is sufficient to reach the low fracture frequency and low permeability rock volumes at Forsmark, and there does not seem to be any advantage in going deeper.
- Groundwater pressure, safety function R3a, increases with depth. However, compared with the buffer swelling pressure and hydrostatic pressures from a glacial overburden, the increased pressures are of marginal importance.
- Rock stress indirectly affects safety function R2b "Equivalent flow rate in buffer/rock interface, $Q_{eq}$", since the in situ stress determines the potential for spalling. Stress in general increases with depth, but placing the repository at 400 m or 500 m depth does not significantly increase the risk for spalling in the deposition holes.
- The in situ temperature relates to safety function R4 "Provide favourable thermal conditions". The temperature increases with depth and this needs to be considered in the repository layout. However, given that this is considered in the repository design, there are no other detrimental effects of the elevated in situ temperature with depth.
- The likelihood of freezing, safety function R4, decreases with increasing depth. The analyses in SR-Site have, however, demonstrated that freezing of the buffer can be considered as a residual scenario and also freezing of the deposition tunnel backfill at these depths can be ruled out.
- Surface denudation (erosion and weathering) of the host rock is has been estimated to generally be limited to a few metres or less per glacial cycle for the Forsmark repository site and some tens of metres for 1 million years. Therefore, surface denudation does not have to be considered when determining repository depth within the reference interval 400–700 metres.
- The probability of inadvertent human intrusion into the repository decreases with increasing depth. In general, intrusion to several hundred metres is considered unlikely in rock poor in resources.

In conclusion, the selected repository depth is adequate and changing the depth is not deemed to significantly reduce the calculated risk. Furthermore, a shallower location, e.g. above the 400 m level, might increase the risk, since the frequency of water conducting fractures is higher there.

Placing the repository some 100 m deeper would probably result in a risk contribution similar to the one obtained from the selected depth, whereas much deeper locations would imply that additional factors, such as very high stress levels, might need to be considered.

### 15.3.6 Confidence

The SR-Site assessment supports SKB's application for a final repository, i.e. a major decision point in SKB's programme for the management of spent nuclear fuel. A statement on the confidence in the results obtained in SR-Site is, therefore, appropriate. The confidence in the results obtained is assessed as sufficient for the decision at hand based on the following.

- The knowledge of the Forsmark site from the completed, surface based investigations is sufficient for the assessment of long-term safety. The site has favourable conditions for safety and no site-related issues requiring resolution in order to demonstrate safety have been identified. Confidence in the site-descriptive model and in the understanding of the site is obtained by a systematic and quality assured programme for site investigations and site modelling. The confidence in the site model is assessed in detail and documented in the **Site description Forsmark**. Key properties of the site are documented in Chapter 4 of this main report.
- There is a well established reference design with specified and achievable production and control procedures yielding an initial state of the repository system with properties favourable for long-term safety at the Forsmark site. The engineered parts of the repository system are based on demonstrated technology and established quality assurance procedures to achieve the initial state of the system. This is systematically documented in the **Production reports** and their underlying references as summarised in Chapter 5. Examples of important aspects of the initial state of the engineered barriers include:
  a. The copper canister sealing quality.
  b. The cast iron insert casting quality.
  c. Buffer properties such as density and content of montmorillonite and impurities.
  d. Backfill properties ensuring its ability to keep the buffer in place and to swell.
  e. The quality of the approach to adapt the repository to the detailed conditions found underground and the quality of the excavation technique.
  f. The quality of the deposition technique.

  There is potential for additional optimisation when this reference design is developed and implemented, as is further discussed in Sections 15.3.5 and 15.5.
- The scientific understanding of issues relevant for long-term safety is mature as a result of decades of research both within the Swedish and other national programmes and in international collaboration projects. The R&D efforts to understand repository evolution and safety have led to the understanding of key processes like copper corrosion, shearing of canisters and other potential canister failure causes, and of key phenomena controlling retardation. This knowledge is, in SR-Site, systematically documented in several reports in a format suitable for use in the safety assessment, see further Chapters 6 and 7.
- The SR-Site main report and its supporting documents have undergone comprehensive peer reviewing. In particular the scientific basis of the safety assessment has undergone review by recognised experts in the relevant fields of science.
- A complete analysis of issues identified as relevant to long-term safety has been carried out in SR-Site according to an established assessment methodology, described in Chapter 2 and comprising e.g. cautious approaches when addressing uncertainties.
  – The understanding of safety is built on a systematic identification of safety functions and criteria for the safety functions, see Chapter 8.
  – Repository evolution is analysed with a structured approach in several time frames, addressing in each of these the processes that have been identified as relevant and with the safety of the system, as expressed by the safety functions, as a focus, see Chapter 10. Data uncertainties and data quality are assessed and documented according to a pre-established template, described in Chapter 9. Quality assurance of models and modelling is achieved by following procedures documented in the **Model summary report**. The assessment is then broken down into a set of scenarios to exhaustively scrutinise all possible ways in which the identified safety functions could be impaired and the consequences of such situations, see further Chapters 11, 12 and 13.

  - Confidence in the key results of radionuclide transport and risk calculations is enhanced by the fact that they can often be closely reproduced with simple, analytical models, using the same input data as the fully qualified numerical models.
  - The key results of radionuclide transport and risk calculations are overestimates since a number of pessimistic assumptions were made in the analyses, both regarding the extent of canister failures and regarding their consequences.
- Documented quality assurance routines have been applied in the assessment of the initial state, in the development of the site description and in the analysis of long-term safety. A QA-plan, encompassing most of the routines followed in undertaking the steps described in the above points, has been established and implemented in SR-Site. This is part of the overall methodology followed in the assessment, as documented in Chapter 2.

#### *Completeness, comprehensiveness*

Also relevant for the confidence discussion is the issue of completeness or comprehensiveness of the assessment. This issue may be formulated through the following questions.

1. Have all factors relevant for long-term safety been identified?
2. Have all identified factors been adequately treated in the assessment?

The following two points summarise the efforts made to ensure that all relevant factors have been identified, see also Section 2.8.3, in particular the subheading ‘System uncertainty’.

- Decades of systematic and documented R&D, in international collaboration has been performed to achieve a sufficient knowledge of the repository system and its evolution. New phenomena have only rarely been identified in recent years, indicating that the scientific and technical foundation is mature. Several safety assessments have been performed throughout the years to obtain an integrated evaluation of the knowledge base and to provide feedback to the research programme.
- Systematic and documented studies of factors identified by other organisations have been made, e.g. by comparisons to internationally available FEP databases

The question of whether all identified issues have been adequately handled in the assessment is partly addressed in the confidence discussion above. A more complete answer is provided by the description of the methodology for the assessment described in Chapter 2. Of particular relevance is the systematic handling of uncertainties described in Section 2.8.3. The scenario selection and analysis is claimed to be comprehensive based on the systematic focussing of the scenario selection on safety functions and a systematic handling of factors that could impair safety functions, followed by a handling of combinations of scenarios. A formal check whether FEP’s omitted in earlier parts of the assessment are of negligible importance to safety in light of the completed scenario and risk analysis has also been made and is reported in Section 14.4.

The above points support the claim that the SR-Site assessment is comprehensive, whereas completeness in a strict sense can never be proved. In this context it is, therefore, relevant to discuss possible consequences if completeness has not been achieved, for example if an important detrimental process remains unidentified despite all efforts to ensure the opposite. In its most extreme form, such a discussion may take the form of the consequences of complete, early loss of safety functions. As evidenced by the section below, even very extreme and completely unrealistic assumptions regarding early barrier losses yield calculated doses that are comparable with those caused by natural background radiation.

Based on the above reasoning, it is concluded that the SR-Site assessment is sufficiently comprehensive for its purposes.

### 15.3.7 Bounding cases, robustness

In Section 13.7.3, a number of stylised, bounding cases illustrating complete, initial loss of important safety functions are analysed. The analyses led to the following conclusions.

- A highly hypothetical calculation case with an initial, large defect in all 6,000 canisters would yield peak dose consequences to the most exposed individuals in a fully populated landscape of about 700 μSv/yr, corresponding to a risk of about $5 \cdot 10^{-5}$/yr, occurring in the 10,000 year time frame. After about 100,000 years, the calculated risk is about a factor of two above the risk limit of $10^{-6}$/yr.
- An even more hypothetical case with a large defect in all 6,000 canisters and with no buffer barrier present would yield peak dose consequences to the most exposed individuals in a fully populated landscape of about 4,000 μSv/yr, corresponding to a risk of about $10^{-4}$/yr, occurring in the 10,000 year time frame. After about 100,000 years, the calculated risk is about a factor of two above the risk limit of $10^{-6}$/yr.

Several pessimistic assumptions, in addition to the completely fictitious losses of barrier functions, were made in the calculations of these cases.

The results reported in Section 13.7.3 indicate that the calculated doses are comparable to or below the natural background radiation also for very severe losses of safety functions. For example, an initial total loss of the canister and buffer in all deposition holes yields, for the Forsmark site, doses that are comparable to those arising from background radiation.

The bounding analyses also demonstrate the multi-barrier character of the KBS-3 system, which may be less evident from results of other analyses. For example, with intact canister and buffer properties the rock appears relatively unimportant, since most nuclides are retained already in these barriers. However, for the unrealistic case of complete initial failure of the canister and buffer barrier, the results in Figures 13-67 and 13-68 indicate that retention in the rock reduces the doses by about two orders of magnitude, clearly illustrating the importance of the rock. Furthermore, the rock is always important in providing a low groundwater flow, suitable chemical conditions and stable mechanical conditions.

### 15.3.8 Additional, general requirements on the safety assessment

#### *Use of natural analogues*

An account of natural analogues as a support for a safety assessment of a KBS-3 repository is given in Section 14.6. Both the role of natural analogues in safety assessments and the actual supporting arguments for specific repository materials and processes affecting them are discussed.

In Section 14.6.5 it is concluded that the outcome of the natural analogue studies has been of a more qualitative than quantitative nature. The gathering of scientists and modellers in the international projects studying natural analogues has focussed the research efforts and method development, so that enough information is available for identifying processes and scenarios relevant to safety assessments. Also, many natural analogues provide support to long-term safety analyses by improving general perception and understanding of the concept of a deep repository.

Furthermore, in cases where natural analogues provide useful information for the understanding of specific processes, this information is given in the **Process reports**, under a dedicated heading.

#### *Quality assurance*

A quality assurance plan has been developed and implemented, as described in Section 2.9. The plan encompasses e.g. the reviewing of central documents, quality assured FEP management and the following of pre-established templates when documenting essential information regarding e.g. process understanding and input data in the safety assessment. A description of quality assurance relating to models and modelling is given in the SR-Site **Model summary report**.

More generally, SKB applies a management system that fulfils the requirements of ISO 9001:2000 and that has been certified by DNV Certification AB, Sweden. In accordance with SKB's procedures for project management, described in the management system, quality assurance plans for the Spent fuel project (Kärnbränsleprojektet), of which SR-Site is a sub-project, and for the SR-Site project have been developed and implemented. The QA plan for the SR-Site project (SDK-003) builds on the QA-plan developed for the SR-Can project /SKB 2006a/, which has been extended and adapted to fulfil the general requirements on a project supporting the application to build a final repository, as specified in the QA plan for the Spent Fuel project (SDK-001). Other sub-projects of the Spent Fuel project have their own specific quality assurance plans, developed so as to conform to the general requirements in the QA plan for the Spent fuel project. In addition, all sub-projects that provide input to the SR-Site project are required to fulfil the general requirements on quality assurance as specified in the SR-Site QA plan.

#### *Handling of uncertainties*

A systematic handling of uncertainties, addressing system uncertainty, conceptual/model uncertainty and data uncertainty has been applied. The systematic handling of FEP's, as documented in the **FEP report** is a key component in assuring that all relevant factors are considered in the assessment. Uncertainties regarding the understanding and modelling of processes of importance for long-term safety are addressed in the **Process reports**, according to the template for process documentation. Data and data uncertainties for modelling are qualified in the **Data report**, according to the template for data qualification.

The analyses in the reference evolution aim at reducing the number of uncertainties requiring further consideration and at identifying and quantifying uncertainties that need to be propagated to subsequent parts of the assessment. These latter uncertainties are addressed in later parts of the reference evolution and/or in the subsequent analyses of additional scenarios.

Further details regarding the integrated handling of uncertainties in SR-Site are provided in Section 2.8.4.

## 15.4 Design basis cases

Feedback from assessments of long-term safety is a key input to the refinement of the design of the KBS-3 repository and is also recommended by regulations. The recommendations to the regulation SSMFS 2008:21 state the following: "Based on scenarios that can be shown to be especially important from the standpoint of risk, a number of design basis cases should be identified. Together with other information, such as on manufacturing method and controllability, these cases should be used to substantiate the design basis[22] such as requirements on barrier properties."

A first set of design basis cases was formulated in the SR-Can main report /SKB 2006a, Section 13.4/ and feedback to canister and repository design was given in Sections 13.5–13.6 of the SR-Can main report /SKB 2006a/. This was further developed into requirements termed *design premises* in a report entitled "Design premises for a KBS-3V repository based on results from the safety assessment SR-Can and some subsequent analyses", /SKB 2009a/. Design premises typically concern specification on what mechanical loads the barriers must withstand, restrictions on the composition of barrier materials or acceptance criteria for the various underground excavations.

As further described in Chapter 5, and in the **Production reports**, these design premises formed the basis for establishing and justifying the reference design being assessed in SR-Site, although most of the design was developed before these design premises were formally established.

As already envisaged when the design basis cases and the design premises were first presented in /SKB 2009a/, the design premises may be modified in future stages of SKB's programme, e.g. after major updates of the safety assessment or as a result of reviews of the safety assessment. Reasons for

[22] The cited text is from the current SSM, unofficial, translation of the regulation. In the official Swedish version, the word "design basis" is "konstruktionsförutsättningar", which in most other cases, including the SKB usage, is translated into "design premises".

such modifications include results of analyses based on more detailed site data and a more developed understanding of processes of importance for long-term safety. Based on the findings of SR-Site, feedback to a potential update of the design basis cases is provided in this section, whereas detailed feedback to the design premises is provided in Section 15.5.

### 15.4.1 General

The approach for arriving at design basis cases was outlined in the SR-Can main report /SKB 2006a/, Section 13.4, and was further elaborated in /SKB 2009a/. This approach is judged adequate, but is for completeness repeated here, with obvious modifications with regard to references.

As stated in SSM's recommendations, the purpose of identifying design basis cases is to provide input to the formulation of requirements on barrier properties. This process is *iterative* and contains several elements.

1. Establishment of a repository reference design, i.e. a barrier system *with a chosen set of properties*, see the **Production reports** and Chapter 5 of this report.
2. Identification of the safety functions the system should fulfil over time, see Chapter 8.
3. Identification of the stresses the system will be subject to over time, potentially jeopardising safety. This is done in Chapter 10 (the reference evolution) and further in the scenario analyses in Chapter 12.
4. A quantitative analysis of how the identified stresses affect safety for the established design. This analysis is provided in Chapters 10, 12 and 13. The load situations occurring in the scenarios that are particularly important from the standpoint of risk, i.e. a set of design basis cases, are briefly summarised below in this section. These provide important input to the formulation of the design premises.
5. Conclusions regarding the sufficiency of the chosen set of properties or recommendations regarding possible improvements. This is important feedback to the design process.
6. The derivation of modified requirements on barrier properties based on step 5, leading to a modified design for which the above steps can be repeated.

For a particular safety assessment, a certain repository design, step 1, is hence provided. Steps 2, 3, 4 and 5 essentially constitute the safety assessment. Step 6 is, however, not formally within the scope of the safety assessment, see further below.

#### *Scenarios*

It is clear from the analyses in the SR-Site assessment, as it was in SR-Can, that scenarios related to canister corrosion for an eroded buffer and to shear movements are most important from the standpoint of risk. In addition to these most important scenarios from the standpoint of risk, canister failure scenarios that did not contribute to risk, since the assumed design was sufficient to prevent failures, have also been considered among the design basis cases, although this is not a strict requirement in the nuclear safety regulations. The only such scenario identified in SR-Site is canister failures due to isostatic loads. Although such failures do not contribute to the calculated risk, the canister's resistance to isostatic loads is an important component of the design basis. Other scenarios than those leading to canister failures are not considered, since such scenarios do not, by definition, cause any risk. However, the canister failure scenarios encompass a number of other scenarios relating to the buffer and to the host rock and these are thus included in the design basis cases.

#### *Time scale*

The design basis cases also depend on the time scale considered. For times longer than 100,000 years the recommendations to the regulation SSMFS 2008:37 state that: "A strict quantitative comparison of calculated risk in relation to the criterion for individual risk in the regulations is not meaningful. The assessment of the protective capability of the repository should instead be based on reasoning on the calculated risk together with several supplementary indicators of the protective capability of the repository such as barrier functions, radionuclide fluxes and concentrations in the environment."

The likelihood that detrimental events, like large earthquakes and major ice sheets, would occur increases with time. The detrimental effects of some continuous processes, like canister corrosion, also increase with time. Following the recommendation, a strict application of the risk criterion is relevant in a 100,000 year time scale and since the design basis cases are to be derived from scenarios that are important from the standpoint of risk, this could be taken as an indication that the design basis should also be developed for this time frame. However, the principle of best available technique (BAT) applies over the one million year assessment time. It does not seem reasonable to develop the design premises for the timescale of 100,000 years and then use the one million year time scale when the principle of BAT is applied. Therefore, the one million year time scale is considered also when the design premises are developed.

This does not, however, mean that the repository must be designed to withstand all loads identified in the safety assessment in a one million year perspective. The design must be such that the requirements on risk and BAT are met and this may well be compatible with the occurrence of some detrimental effects on the barriers during the assessment period.

#### *Integrated approach*

There is a considerable amount of information in SR-Site that can be used to evaluate the current design premises for a KBS-3 repository, but as concluded already in SR-Can, there are few, if any, load cases *on individual barriers* that can be directly derived from the external conditions alone. For example, the isostatic load on the canister will depend not only on the external conditions like the size of a future glacial load and associated groundwater pressure, but also on the depth of the repository and the design of the buffer, that determines its maximum swelling pressure. The situation regarding shear movements on the canister is even more complex: This depends on external factors like probabilities of future large earthquakes, but also on the fracture distribution in the rock in the deposition area, how the layout of the deposition area and deposition holes is adapted to the site conditions, and the material properties of the buffer.

The load on one barrier will thus depend on the design of other barriers and on the site properties, meaning that the design premises must be determined for the entire barrier system in an integrated manner, and in some respects also site specifically. It also means that there is a range of different combinations of barrier and site properties that could provide a similar performance of the repository. The role of the safety assessment in this context is to provide input to the derivation of design premises, in the form of external loads the barrier system should sustain, informed by the calculated risk and, later, to audit the specific design and construction outcomes. It is, however, beyond the scope of the safety assessment report to develop the specific design. However, safety assessment competence is required for the appropriate formulation of the design premises.

The following is a summary of the most important results, *concerning the external loads the barrier system will be exposed to*, that need to be considered when the design premises are developed. It furthermore serves as an introduction to the more detailed discussion on feedback to canister and repository design in Section 15.5.

### 15.4.2 Canister: Isostatic load

The isostatic load on the canister depends on groundwater pressure and on the swelling pressure of the buffer. It is pessimistically assumed that the sum of these two pressures determines the isostatic load. The detailed assessment of the isostatic collapse load scenario in Section 12.7 concludes that a maximum swelling pressure of 15 MPa could occur in the buffer, the groundwater pressure is around 4.5 MPa at Forsmark for ice-free conditions and an additional ground water pressure of at most 30 MPa could occur as a result of a maximum glacial load supported by geological palaeo-ice-sheet evidence. The sum of these loads is 49.5 MPa. However, considering that the combined impact of swelling pressure and hydrostatic load is somewhat smaller than this sum, this, as suggested in Section 12.7.5, results in a total pressure of around 46.5 MPa. The assessment of canister strength concludes that the margin to total collapse (90 MPa), i.e. the criterion for canister failure, is considerable.

In SR-Can it was concluded that "If the canister is emplaced in a buffer with a density in the range 1,950–2,050 kg/m$^3$, corresponding to swelling pressures up to 15 MPa, the canister should withstand an isostatic load of 45 MPa. Thereby the global collapse due to isostatic load will remain a residual scenario, with no risk contribution."

While the essential message is still true, there is a need to revise this statement such that it takes into account the uncertainty in future ice thickness. An upper bound is the largest ice thickness inferred for Pleistocene ice sheets, including today's largest ice thickness that is found in East Antarctica (~4,500 m). This corresponds to an isostatic load from the ice of 40 MPa. This would correspond to a total load of 60 MPa, but this upper bound is judged extreme.

From the standpoint of risk, it is important to realise that the isostatic loads mentioned above, at least the (dominating) contribution from the groundwater pressure at repository depth, is likely to affect *all canisters simultaneously*. If the canisters are not designed to sustain these loads, a substantial number of canisters could potentially fail simultaneously. This is different from cases where the natural variability of the host rock affects the load situation, e.g. as concerns the likelihood of a large fracture intersecting a deposition hole.

The canister may be subjected to asymmetric loads during different phases in the repository evolution. This could temporarily occur due to uneven water saturation in the buffer and lack of straightness of the deposition hole. Permanent asymmetric loads may occur due to an uneven buffer density distribution after water saturation in combination with lack of straightness of the deposition hole. However, as seen in Section 10.3.9, the swelling pressure around the canister is expected to be homogenised and significant asymmetric loads are expected to be rare and thus to affect only a small fraction, if any, of the deposition positions. Such cases are useful to consider when assessing the isostatic load case but have too low a probability to be considered to coincide with the low probability shear load case discussed in the next section.

### 15.4.3 Canister: Shear movements

In rare cases, detrimental shear movements may occur as a consequence of earthquakes that could induce secondary movements in fractures intersecting deposition holes. As was concluded in /SKB 2009a/, the response of the canister to shear loads depends on a number of factors. The most important ones are:

- The magnitude and location of the earthquake.
- The length over which the intersecting fracture is sheared.
- The velocity of the fracture shear movement.
- The angle of intersection of the fracture and its position in relation to the main axis of the canister.
- The buffer mechanical properties, many of which depend strongly on the buffer density.
- The canister geometry and properties of the canister materials like Young's modulus and fracture toughness.
- The temperature of the canister and buffer at the time of the event.

The combined effect of all these factors determines if the canister will withstand a shear load.

The following design basis case was formulated in /SKB 2009a/ with respect to shear movements: "The copper corrosion barrier should remain intact after a 5 cm shear movement at 1 m/s for buffer material properties of a 2,050 kg/m$^3$ Ca-bentonite, for all locations and angles of the shearing fracture in the deposition hole and for temperatures down to 0°C. The insert should maintain its pressure-bearing properties to isostatic loads."

The **Canister production report**, see also Section 5.4, demonstrates that the current canister reference design fulfils these requirements. However, in order to meet these requirements rigorous requirements on manufacturing and NDT capability (especially of the insert) need to be imposed.

The potential for shearing is further assessed in SR-Site, Section 10.4.5 and in Section 12.8, and it is found that on average less than one deposition hole will experience shear movements larger than 0.05 m over $10^6$ years, resulting in canister failure if it is assumed that the canister will actually fail if the load exceeds that of the design basis value. In reality, there will be even less failures, since i) the buffer in most deposition holes will have lower density than the maximally allowed value, ii) since there are only a few fracture angles and locations that would lead to failure at 5 cm shear, and iii) the copper shell elongation and creep ductility achieved in the pilot production implies there is a margin between the now assumed direct failure of the copper shell when the acceptable defect size in the insert is exceeded and the actual performance of the copper shell during a shear movement.

Furthermore, only few canisters would potentially be subject to shear movements of a detrimental magnitude. The majority of the canisters would be expected to experience only negligible shear movements, since their deposition holes would be intersected by only small fractures, if any. It is thus only a small fraction of the deposition holes that are expected to have properties that require the canisters to withstand a 5 cm shear movement. To the extent that a distribution of shear movement resilience can be determined for the ensemble of canisters, taking into account e.g. manufacturing flaws, the potential part of the distribution not fulfilling the design requirements should be evaluated against the distribution of deposition hole properties in order to estimate the likelihood that a canister will experience shear failure.

Generally, the canister's resilience to a shear movement decreases with decreasing temperature. The thermal analyses in Sections 10.4.3 and 12.3 show that extreme and unrealistic climate conditions are required to obtain temperatures below 0°C at repository depth. Therefore, temperatures below 0°C need not be considered for the shear case.

As described in Section 10.3.10 there is no reason to believe that there would be mineralogical changes in the buffer that would lead to substantial changes of the mechanical or hydraulic properties over the assessment timescale. However, there are experimental results showing that the mechanical properties of bentonite can be altered if the material is exposed to an elevated temperature in a saturated state /Dueck 2010/. On the other hand, assuming that buffer material around the canister is converted to a cement-like material with no swelling pressure, an increased E-modulus and shear strength, yields small effects in the shear analyses. It is thus considered that cementation of buffer material does not need to be included in the design basis case for shear movement.

The following are concluded.

- The risk contribution from canister failures due to shear movement is considerably lower than the regulatory risk limit, meaning that the current design basis case is sufficiently restrictive.
- The design basis case constitutes a balance between requirements on the canister, on the buffer and on the repository layout, the latter through the requirement on a maximum shear magnitude of 5 cm. In a revision of this design basis case, for example the following may be considered, provided that the resulting calculated risk from shear movements is comparable to or smaller than that in SR-Site:
  - Given the technical challenges in meeting the rigorous requirements on manufacturing and NDT capability, it might be appropriate to relax the requirement on the canister, e.g. by requiring resilience to a smaller allowed shear movement or to a less stiff bentonite.
  - There is a potential to redefine the requirements on buffer density, i.e. to lower the upper bound in the density interval in light of the achieved limits in the current pilot production. This would lessen the requirements on manufacturing and NDT for the canister.
  - The maximum shear movement may be reconsidered. However, increasing the limit beyond 5 cm would mean increased demands on the canister design given the current capability of analysing the response of the canister/buffer system to shear movements. Decreasing the limit would mean an increased calculated risk with the current repository design, since more canisters would experience such movements, alternatively a decreased limit would impose unrealistic demands on the repository layout in order to avoid the movements.

### 15.4.4 Canister: Corrosion load

One of the three long-term safety functions of the canister is to provide a corrosion barrier and a discussion of design basis cases as regards corrosion is, thus, required. The role of the safety assessment regarding corrosion loads is not merely to specify the loads, but also to calculate the resulting corrosion depths. A more direct feedback can therefore be given in terms of the sufficiency of the canister thickness assumed in the safety assessment and sensitivities to variations in that thickness.

In /SKB 2009a/ the following was concluded with regard to the design basis case related to the corrosion load: "…the copper thickness should be chosen so that the number of failed canisters due to corrosion does not exceed what is acceptable with respect to the risk criterion for 100,000 years. In SR-Can it was shown that 5 cm is sufficient for meeting the risk criterion. Thus a nominal thickness of 5 cm will be the required design premise for SR-Site."

While SR-Site generally shows that the requirement on nominal thickness provides an adequate corrosion barrier, it is nevertheless justified to assess the findings from the updated corrosion assessments made in SR-Site.

In Sections 10.2.5 and 10.3.13, the resulting corrosion depths for various corrosion processes are shown to be in the order of a few mm for an intact buffer, with its intended swelling pressure and transport properties.

In Section 10.4.9, the corrosion for a case with a partially eroded buffer is assessed, and the sensitivity is further analysed in the corrosion scenario (Section 12.6.2). The results show that the calculated mean number of failed canisters in one million years is between 0 and 2. This span of number of failed canisters covers uncertainties regarding the buffer erosion process, the variability in the hydrogeological DFN models and uncertainties in the sulphide concentration distribution, as well as uncertainties in the conceptual model of corrosion geometry (part of the copper surface that is corroded by the sulphide transported to the canister).

When assessing BAT, see Section 14.3.2, copper thicknesses of 2.5 and 10 cm have been evaluated. The results show that increasing the copper thickness to 10 cm reduces the mean number of failed canisters at one million years by a factor of about 3 while halving the thickness to 2.5 cm increases the number by about a factor of 2, see Figure 14-6. Potential problems of manufacturing and sealing a thicker canister have not been considered in this analysis.

In the evaluation of the corrosion, the copper thickness achieved for the reference design with current production and QA procedures is used. For the shell and the bottom and lid, the manufactured thickness is considered not to be less than 45 mm, which can be taken as a lower limit for the manufactured thickness. To evaluate the significance of the occurrence of small areas with lesser copper thickness (weld area, or surface defects from transportation and handling) probability aspects (small areas for a few canisters to coincide with a few deposition holes with high flow) are considered in the assessment.

In conclusion, corrosion in the case of a partially eroded buffer is the only risk contribution from canister failures due to corrosion. The design basis case relevant for the assessed repository at Forsmark should be the one assessed in SR-Site, considering uncertainties regarding the buffer erosion process, the variability in the hydrogeological DFN models and uncertainties in the sulphide concentration distribution, as well as uncertainties in the conceptual model of corrosion geometry. Furthermore, given the relative insensitivity of the number of failed canisters to the copper thickness it is clear that design premises derived from this design basis case cannot be given in the same detail as the production specification and thus specifying the thickness in the centimetre scale is seen as a more appropriate output.

### 15.4.5 Buffer

The design basis cases for the buffer formulated in /SKB 2009a/ consisted of a list of external chemical, mechanical and thermal loads the buffer will be subjected to during the $10^6$ years assessment period. Generally, this list of loads has not changed much, but since the understanding of factors influencing buffer stability has evolved since SR-Can this design basis is reformulated here.

The listed external loads that may affect the buffer are based on a thorough understanding of the safety-related functions of the buffer in the repository, i.e. on the role of the buffer in the safety concept and the expected variations in the chemical environment of the buffer, see Chapter 10. Based on this, the following chemical and thermal environment for the buffer should be considered.

- Generally, most deposition holes will experience a salinity with ionic strength $\Sigma q[M^{q+}] > 4$ mM charge equivalent. However, up to 2 percent of all deposition holes may experience salinities below this value at some time in the overall glacial cycle.
- Groundwaters with a TDS up to 20g/L may occur in the scenarios analysed in SR-Site. This should not pose a threat to the buffer functions.
- The pH may, at least for short periods be up to pH 11. Specifically, an initial, short term high pH load cannot be excluded and should also be acceptable, based on mass balance arguments. Consequently, the buffer should sustain such conditions, as indeed is shown to be the case for the reference buffer design assessed in SR-Site (see Section 10.3).
- The buffer may also be exposed to isostatic pressures up to 34.5 MPa. As was concluded in SR-Can, the buffer materials analysed are not negatively affected by such pressures, see Section 10.4.8, sub-heading Liquefaction.
- Regarding shear movements, see the discussion of this issue for the canister above.
- The function indicator criterion for buffer freezing is pessimistically assessed to be −4°C, see Section 8.3.2. As shown in Section 12.4, the groundwater at repository depth will never freeze, which means that the −4°C criterion for the buffer material is an achievable design premise for the buffer.

## 15.5 Feedback to assessed reference design and related design premises

### 15.5.1 Introduction

SR-Site has assessed a specific reference design based on specific design premises. In this feedback section, the safety aspects of the reference design are addressed and feedback given as to whether there is reason to consider revisions of the reference design and/or of the design premises as they were formulated in /SKB 2009a/.

The reassessment of the design basis cases, as well as other conclusions reached within SR-Site, can also be used as input for revising the specific design premises listed in /SKB 2009a/.

Since SR-Site demonstrates a sufficient level of safety for a repository at Forsmark constructed in accordance with the reference design, conforming to the design premises presented in /SKB 2009a/, the remaining reasons to revise these design premises are:

- Considering whether a refined formulation or requirement could significantly enhance the resulting safety, while considering if such a change is realistically achievable.
- Feedback from the design and production (**Production reports**) including possibilities to verify the design premises both in design and production.
- Adjustment of premises proven to be unnecessary or providing no or little enhancement of safety.
- Clarification of wording, corrections and other minor modifications in order to enhance clarity.

Reasons to revise the reference design include:

- Challenges, e.g. complex or less well founded demonstrations verifying that the reference design will conform to given design premises.
- Proposed changes in design premises.
- Further refinement and development of methods for production, installation and inspection promoting improvements within the framework of the reference design.
- Research and development resulting in alternative designs that are e.g. easier to implement and with potential to maintain the barrier functions and safety.

Based on these general principles most of the already stated design premises and associated reference designs are judged adequate as they are, whereas some can usefully be modified or elaborated. A more detailed assessment is presented in the following subsections.

### 15.5.2 Canister mechanical stability – withstand isostatic load

In /SKB 2009a/ it is stated that:

"The canister shall withstand an isostatic load of 45 MPa, being the sum of maximum swelling pressure and maximum groundwater pressure."

As stated in Chapter 5, and shown in the **Canister production report**, canisters can be designed and manufactured in conformity to the stated design premise with respect to isostatic load. The detailed assessment of the isostatic collapse load scenario in Section 12.7 confirms the conclusion reached already in SR-Can that such canisters will not fail due to any foreseeable isostatic load during the assessment period. However, the analysis also suggests that future loads may be somewhat higher than 45 MPa, and a value of 46.5 MPa is considered. Considering the uncertainty in future ice thickness, a margin to the largest ice thickness analysed in SR-Site might be considered. It should also be noted that the potential changes of buffer density would in principle affect this design premise, but the changes suggested are too small to be of significance for this aspect.

#### *Feedback to design premises*

Current design premises on isostatic load should be revised to consider the uncertainty in future ice thickness. One upper bound for such a margin would be the largest ice thicknesses inferred for Pleistocene ice sheets, including today's largest ice thickness found in East Antarctica, which is ~4,500 m. This corresponds to an isostatic load from the ice of 40 MPa. This would correspond to a total load of 60 MPa, but this upper bound is judged extreme.

#### *Feedback to reference design*

The current reference design is appropriate with regard to its insensitivity to the isostatic load.

### 15.5.3 Canister mechanical stability – withstand shear movement

In /SKB 2009a/ it is stated that: "The copper corrosion barrier should remain intact after a 5 cm shear movement at a velocity of 1 m/s for buffer material properties of a 2,050 kg/m$^3$ Ca-bentonite, for all locations and angles of the shearing fracture in the deposition hole, and for temperatures down to 0°C. The insert should maintain its pressure-bearing properties to isostatic loads."

As already concluded in Section 15.4.3, a canister in conformity to the stated design premises would on average result in less than one failed canister over $10^6$ years, even if it is assumed that the canister will fail directly if the load exceeds the design value. In reality, there will be even less failures, since i) the buffer in most deposition holes will have lower density than the maximally allowed value, ii) since there are only a few fracture angles and locations that would lead to failure at 5 cm shear, and iii) the copper shell elongation and creep ductility achieved in the pilot production implies that there is a margin between the currently assumed immediate and complete failure of the copper shell when the acceptable defect size in the insert is exceeded and the actual performance of the copper shell during a shear movement.

As stated in Section 5.4, and shown in the **Canister production report**, the current canister reference design conforms to the stated design premises, but it is also noted that this implies that rigorous requirements on manufacturing and NDT capability need to be imposed. On the other hand, the sensitivity to shear load is an integrated canister/buffer problem and larger loads could be managed if the buffer density was lower. Given the experience in producing and controlling the buffer density, as assessed in the **Buffer production report**, a feasible approach for relaxing the requirements on the canister would be to modify the requirements on the maximum allowed buffer density.

#### *Feedback to design premises*

Given the technical challenges in meeting the rigorous requirements on manufacturing and NDT capability, it might be considered appropriate to relax the requirement on the canister, provided that the requirement on the buffer density is modified such that the risk contribution from shear load is less or equal to that than in SR-Site.

The probability of shearing more than 5 cm is very low, and there seems to be little to gain from changing this shear magnitude criterion in either direction (see further Section 15.4.3).

#### *Feedback to reference design*

The current reference design is judged adequate. However, there is the potential for an adjustment of the design premises that may allow some relaxation of the requirements on manufacturing and NDT capability.

### 15.5.4 Provide corrosion barrier – Copper thickness

In /SKB 2009a/ it is stated that there should be a: "A nominal copper thickness of 5 cm, also considering the welds."

As already concluded in Sections 14.3.2 and 15.4.4, the requirement of a 5 cm nominal thickness provides an adequate corrosion barrier and the derivation of more detailed criteria on copper thickness is not warranted.

#### *Feedback on design premises*

Even though the design premise is expressed as a nominal copper thickness of 5 cm, a more detailed criterion can be derived, allowing for tolerances in the manufacturing. For the shell, and the bottom and lid, the manufactured copper thickness achieved for the reference design with current production and QA procedures is considered to be not less than 45 mm, which can be taken as a lower limit for the manufactured thickness.

#### *Feedback on reference design*

Current reference design is considered adequate, but is should be clarified that the lower limit for the manufactured thickness for the shell, the bottom and lid, including tolerances, is 45 mm.

### 15.5.5 Canister material etc

/SKB 2009a/ provides some detailed design premises regarding the copper content in the cast iron, limits on other elements in the copper, the maximum amount of water left in the insert, the hydrogen content in copper material, maximum temperatures and allowed radiation levels. The risk analysis in SR-Site does not provide any direct feedback on these design premises, but the further analyses made and presented in e.g. the **Fuel and canister process report** may allow some further elaboration of these design premises, by enhancing the foundations for the limits given and for adjustment of some limits also to address allowable tolerances.

### 15.5.6 Durability of the hydromechanical properties of the buffer material

In /SKB 2009a/, regarding "durability of the buffer material with respect to chemical and thermal loads", it is stated that:

"After swelling, the buffer should uphold the minimum swelling pressure 2 MPa and the hydraulic conductivity should not exceed $10^{-12}$ m/s independently of dominating cation and for chloride concentrations up to 1 M. After swelling, the shear strength of the buffer must not exceed the strength used in the verifying analysis of the canisters resistance against shear loads. These conditions apply for temperatures down to 0°C and temperatures up to 100°C."

As concluded in Section 15.4.5, the design basis concerning the external chemical, mechanical and thermal loads that the buffer will be subjected to during the $10^6$ years should be revised relative to the one formulated in /SKB 2009a/. Consequently, the related design premises should be revised to reflect this change.

The assessment in Chapter 10 shows that the buffer function indicator criteria are upheld for all conceivable chemical and thermal conditions during the assessment period, as long as not too much buffer mass is lost, initially or due to erosion. The initial state is to be ensured by the procedures described in the **Buffer production report**. Mitigating loss of buffer due to piping erosion can be handled by selecting deposition holes where the potential for excessive piping erosion is avoided (see further Section 15.5.13).

It is concluded in Section 10.3.9 that when large amounts of bentonite are lost or missing from start, the bentonite swells and fills the empty space but the density and resulting swelling pressure is locally rather low due to the friction in the buffer and the friction against the rock surface. In such cases, the swelling pressure may at least locally fall below 1 MPa, depending on internal friction in the material and the smoothness (friction) of the rock wall. Advective conditions in the buffer can occur if the hydraulic conductivity is sufficiently high. The buffer function indicators prescribe a hydraulic conductivity of $10^{-12}$ m/s and a swelling pressure of 1 MPa to rule out advection in the buffer. These values do, however, have some safety margins included in them.

In the discussion about margins for the safety function indicator criteria, in Section 8.3.5, it is stated that, for the hydraulic conductivity, the margin is related to the hydraulic gradient and the diffusivity of the species in question, and that the margin is considerable. In practice, the hydraulic conductivity of the buffer will rarely determine whether diffusion will prevail as the dominating mechanism for transport. As the swelling pressure drops, the possibility for pathway formation in the buffer increases. There is an effect of the hydraulic gradient and possibly of salinity. Laboratory samples show piping at ~60 kPa. In a situation with piping, the bulk hydraulic conductivity becomes irrelevant. According to the analysis a minimum dry density of 1,000 kg/m$^3$ is required, corresponding to a void ratio of 1.75. This requirement is still met across almost the entire buffer diameter when two whole bentonite rings are omitted, corresponding to a dry mass loss of 2,400 kg. It should be noted that even though the margin for the safety function indicator criterion for the swelling pressure is more than an order of magnitude, the margin for mass (density) loss is only about a factor of two.

For the case when the buffer erodes by colloid formation, the mass loss may be quite local and it is appropriate to consider the limit for losses over typically half the circumference, i.e. a loss of 1,200 kg, which also would cover the situation when the loss occurs closer to the centre of the canister. This value still includes some pessimism, since homogenisation in the horizontal direction is neglected.

As concluded in Section 10.4.7, the ionic strength of the groundwater; $\Sigma q[M^{q+}]$, will fall below 4 mM charge equivalent i.e. violating safety indictor criterion R1c, for some deposition holes during some part of the glacial cycle. This means that colloid release may occur from these holes and from sections of the backfill. More specifically, it is concluded in Section 10.4.7 that less than two percent of the deposition hole positions may be assumed to experience dilute conditions during a glacial cycle, and they will only experience these conditions during a fraction of the time. While there still is uncertainty with respect to modelling of colloid formation and subsequent erosion of the buffer material and the modelling approach thus tends to be pessimistic, as discussed in Section 10.3.11, it seems clear that the process as such is real and that it cannot with current understanding be defensibly mitigated by e.g. selection of another buffer material.

It is concluded in Section 10.3.10 that an increased temperature may have an effect on the mechanical properties of the bentonite, but the effect is not very pronounced even at 150°C and does not seem to progress with time. However, this effect is discussed in the evaluation of shear load on the canister, see Section 10.4.5. In Sections 10.3.10 and 12.4 it is concluded that the increased temperature will have no significant effect on the mineralogical properties of the buffer.

As demonstrated in Sections 10.4.3 and 12.3, buffer freezing can be excluded also for the case of a partially eroded buffer.

#### *Feedback to design premises*

The requirements on minimum swelling pressure and hydraulic conductivity should be revised such that they reflect the current safety function indicator criteria, i.e. the minimum swelling pressure should be 1 MPa rather than 2 MPa. The design premises should also be revised such that the conditions under which minimum swelling pressure, hydraulic conductivity and shear strength should be maintained reflect the conditions listed in the design basis. However, as SR-Site shows that safety is maintained, even if a very small fraction of deposition holes loses the buffer due to a groundwater composition with the ionic strength $\Sigma q[M^{q+}]$ below 4 mM charge equivalent and since the impact of such conditions cannot be dramatically mitigated by e.g. selection of another buffer material, the design premise would not need to consider groundwaters with ionic strength $\Sigma q[M^{q+}]$ below 4 mM charge equivalent.

#### *Feedback to reference design*

Currently analysed examples of buffer materials are judged adequate. There are differences between the two considered bentonites. The differences mainly concern their geochemical evolution. However, as shown in Section 10.3.10, both materials are affected by the geochemical conditions at the site and their differences will decrease with time. There are no identified significant differences in the long- term performance of the two materials.

### 15.5.7 Installed buffer mass

In /SKB 2009a/ it is stated, regarding "buffer density", that: "The initially deposited buffer mass should be such that it corresponds to a saturated buffer density in the volume initially filled with buffer that is: less than 2,050 kg/m$^3$ to prevent too high shear impact on canister (see 3.1.2), and higher than 1,950 kg/m$^3$, i.e. sufficiently high to ensure a swelling pressure of 2 MPa with margin for possible loss of material."

As shown in Sections 5.5.2 and 5.5.3, the installed average buffer density in a deposition hole will be well within the desired range. The final distribution of buffer density is dependent on:

- Homogenisation of blocks and pellets.
- Material loss from piping/erosion during the early period after emplacement.
- Expansion of buffer into the backfill.

In the long term, loss due to colloid release may also affect the density in a deposition hole.

The initial state of the buffer after emplacement is unsaturated bentonite blocks and rings with a much higher density than the average density for the entire hole and one empty slot at the canister surface and a pellet filled slot with very low density at the rock surface. A shown in Section 10.3.9, the homogenisation process leads to residual density gradients in the material, mainly due to internal friction. This means that the density in the original pellet volume may be slightly below 1,950 kg/m$^3$, but the safety function indicators will still be upheld.

Piping followed by erosion during the water saturation may lead to a local loss of buffer mass in some deposition holes (Section 10.2.4). For the allowed water flows in deposition holes, according to Section 5.2.1, the density may drop locally below 1,950 kg/m$^3$, but the safety function criteria will still remain upheld.

Expansion of buffer into the backfill and the interaction between the buffer blocks and pellets are discussed in Section 10.3.8. The expansion into the backfill will lead to a drop in the installed density, but the effect is limited even for unfavourable calculation cases.

The colloid release from buffer and backfill case, presented in Section 10.3.8, may lead to a substantial drop in buffer density.

As a result of a loss of buffer mass/density, sulphide may be formed as a result of microbial activity in the highly compacted bentonite, see Section 10.3.13. Though the factors limiting the activity are not fully understood, experimental results indicate that a minimum saturated density of 1,800 kg/m$^3$ is required to keep the copper corrosion caused by microbial activity to a negligible level.

#### *Feedback to design premises*

A buffer with a density of 1,950 kg/m$^3$ will have good margins to the safety functions. However, this design premise refers to the average installed density in a cross-section of the deposition hole and may not be upheld at all locations within the volume. While it is shown that there is a margin to ensure a safe function of the buffer, it is nevertheless suggested to keep this lower limit as a design premise in order to ensure a sufficient margin to buffer loss by piping/erosion etc. The design premise needs therefore to be clarified such that when assessing its fulfilment, buffer losses, e.g. due to piping erosion and homogenisation, need not be considered, since the potential for and significance of such losses are addressed in the safety assessment.

Furthermore, additional assessments should be performed to increase the understanding of the significance of limited local volumes of the buffer with a lower density than the main volume. This relates both to the mechanical properties and the possibility for significant microbial activity.

The findings from SR-Site suggest that the risk contribution from shear loads on the canister would be further reduced if the buffer density was lower than the maximum value of 2,050 kg/m$^3$. Experience from the buffer design work suggests that it would be possible to replace the upper limit with a distribution of allowed densities such that only a small fraction of deposition holes would have densities close to 2,050 kg/m$^3$. Such a distribution could also consider the montmorillonite content of the dry buffer material, see Section 15.5.9. The exact formulation of such a distribution can, however, only be set in cooperation with the buffer and rock excavation designers, such that it can also be ensured that conformity with the revised design premise can be achieved.

#### *Feedback to reference design*

The manufacturing method presented in Section 5.5.2 produces a buffer with a much narrower density interval than allowed in the design premises. From the point of view of long- term performance, this strengthens the confidence in the assessment. The main reason for this is the strong dependence of swelling pressure on density. A narrowed range of initial density means that a smaller range of swelling pressures needs to be considered.

If the design premise regarding initial buffer density are revised, the buffer reference design and quality control procedures for deposition hole geometry and buffer installation will need to be revised accordingly.

### 15.5.8 Buffer thickness

In /SKB 2009a/ it is stated that: “The buffer dimensions used as reference dimensions in SR-Can shall be used, in addition to other requirements affecting the buffer and deposition hole geometry.”

As concluded in Section 14.3 a larger buffer mass is not seen as a practical means of mitigating the effects of buffer erosion. A larger buffer mass may offer a slightly longer time before advective conditions occur in the deposition hole, but it is not seen as a solution to the issue. It is also concluded that continued R&D on the erosion process is required.

#### *Feedback to design premises*

While the current design premise, referring to dimensions assessed in SR-Can, essentially is adequate, it is suggested that it be reformulated in a way that provides better guidance to designers, e.g. by formulating some minimum dimensions, considering also the maximum allowed gaps between buffer and canister and buffer and rock wall.

#### *Feedback to reference design*

The current reference design is judged adequate.

### 15.5.9 Buffer mineralogical composition

In /SKB 2009a/ it is stated that: "The montmorillonite content of the dry buffer material shall be 75–90% by weight. The content of organic carbon should be less than 1 wt-%. The sulphide content should not exceed 0.5 weight percent of the total mass, corresponding to approximately 1% of pyrite. The total sulphur content (including the sulphide) should not exceed 1 wt-%."

The requirement on montmorillonite content relates to the buffer swelling properties. Assessment in SR-Site shows that extreme combinations of densities and montmorillonite contents result in a wider range of swelling pressures than previously assumed. However, it is still the density that is the key factor for the swelling pressure.

The requirements on carbon, sulphide and sulphur concern the impact of these materials on the copper. As shown in Chapter 10, as long as the buffer is intact copper corrosion by contaminants in the buffer, backfill or groundwater does not pose a threat to canister integrity for the initial temperate period and even during the one million year overall assessment period the expected corrosion of the canister for an assumed temperate climate would cause corrosion depths of the order of a few millimetres, even for the most unfavourable deposition positions at Forsmark.

The shear properties of the buffer may be affected by the charge compensating cation. However, it is stated that the requirements should be fulfilled for any composition of cations.

#### *Feedback to design premises*

The current design premises are judged adequate.

#### *Feedback to reference design*

The current reference design is judged adequate. The range for montmorillonite content is judged adequate. It could still be worthwhile to investigate the possibility of adjusting the block density in the manufacturing for bentonite shipments that are outside of the 80-85% range.

### 15.5.10 Deposition hole bottom plate

In /SKB 2009a/ there are no specific design premises related to the bottom plate. However, since this plate is part of the current reference design, feedback on its adequacy is required.

In Section 10.2.4 it is concluded that additional assessments and possibly development work is needed for the bottom plate. There are uncertainties regarding the current design that are unresolved. These are connected to the thickness and the compressibility of the bottom plate and to the possibility for a lifting of the buffer/canister package before the backfill is in place. A thick, compressible bottom plate may lead to loss of density to a level below the design target of 1,950 kg/m$^3$ in the bottom of the buffer. Furthermore, Section 10.3.12 concludes that while the effect of a degraded bottom plate on the mass transfer resistance in the near field is less than the impact from assuming spalling in the deposition hole, the degraded bottom plate will be the main transport path if spalling can be avoided and if the bottom plate is intersected by a fracture. Another issue is the chemical interaction between the bottom plate and the buffer. This was found to be acceptable in SR-Site, but must be considered as an unnecessary disturbance.

#### *Feedback to design premises*

There is no reason to add design premises directly addressing the bottom plate. Its presence does not affect risk.

#### *Feedback to reference design*

Given the question marks around the current design of the bottom plate, alternative solutions should be strived for. Ideally, only the canister and bentonite should be allowed in a deposition hole.

### 15.5.11 Deposition tunnel backfill

In /SKB 2009a/ it is stated that: "Packing and density of the backfill, both at initial dry state and after complete water saturation, must be sufficient to ensure a compressibility that results in a minimum buffer saturated density according to the conditions set out (i.e. 1,950 kg/m$^3$) with sufficient margin to loss of backfill and to uncertainties."

Furthermore, *the following function indicator criteria should be upheld in the backfill to limit migration:*

- *Hydraulic conductivity < $10^{-10}$ m/s.*
- *Swelling pressure > 0.1 MPa.*

It is concluded in Section 10.3.9 that the swelling pressure of the buffer and the associated safety functions will be maintained during the expansion of the buffer into the backfill for many possible combinations of buffer and backfill conditions. Furthermore, several likely pessimistic assumptions are made in this analysis, including assuming the buffer to be completely water saturated and homogenised from the start, assuming weak mechanical contacts between the backfill blocks, not including the local crushing of the blocks that may occur close to the floor and assuming that the backfill blocks are not stacked overlapping each other.

For the case when backfill material is lost, a maximum loss of 220 tonnes in a deposition tunnel section can be allowed before advective conditions have to be considered in the deposition hole. As concluded in Section 10.3.11, advective conditions may not be excluded in some very few deposition hole closest to the tunnel intersecting fracture but the contribution of loss of deposition tunnel backfill to the possible generation of advective conditions in deposition holes is considered negligible. For a few positions where the tunnel is intersected by a very transmissive deformation zone, potentially more than 220 tonnes could be lost, but this is not relevant from the point of view of canister integrity. Such local loss of backfill by erosion does not mean that the hydraulic conductivity of the entire tunnel will be affected and these occurrences are not judged to impair safety.

Generally, a requirement on the bulk hydraulic conductivity of the backfill has very little practical meaning and could probably be removed, whereas the requirement on swelling pressure is important to ensure a sufficiently tight contact between the backfill and the rock wall.

#### *Feedback to design premises*

Current design premises on the deposition tunnel backfill are judged adequate. However, they should be refined to reflect that backfill properties need not be retained where the deposition tunnel intersects very transmissive fractures (that would certainly not be allowed to intersect deposition holes).

#### *Feedback to reference design*

The current reference design appears adequate. There are very few identified uncertainties regarding the long- term performance of the current backfill design. However, the ongoing detailed design and testing of the tunnel plug needs to verify that it will be sufficiently tight to ensure that the inflow to deposition holes will be below the values that would lead to unacceptable piping and erosion of the buffer.

### 15.5.12 Selecting deposition holes – mechanical stability

In /SKB 2009a/ it is stated that:

- *Deposition holes are not allowed to be placed closer than 100 m to deformation zones with trace length longer than 3 km.*
- *Deposition holes should, as far as reasonably possible, be selected such that they do not have potential for shear larger than the canister can withstand. To achieve this, the EFPC criterion should be applied in selecting deposition hole positions.*

As shown in Section 10.4.5, application of these design premises leads to a very small probability of shear movements larger than 5 cm in a deposition hole. The resulting risk contribution from failed canisters due to this is very small, even considering the current pessimistic assumption of failure for all cases in which the shear exceeds 5 cm. There is thus no reason to strengthen the design premise. However, the analyses in Section 10.4.5 also demonstrate that only some of the 3 km long deformation zones may host earthquakes and that the EFPC rule is a proxy for avoiding excessively large fractures. Furthermore, previously /SKB 2009a/ noted that it may be possible to reduce the respect distance of 100 m to some deformation zones based on an a site-specific detailed and individual assessment of the actual extent of the damage zone including splays combined with revised criteria for what fractures should be avoided in deposition holes.

#### *Feedback to design premises*

The potential to revise current design premises is directly linked to the potential progress within the detailed investigation programme in characterising the actual extents of damage zones and splays for the few deformation zones longer than 3 km that exist at the Forsmark site and to find alternative means for determining the size of fractures intersecting deposition holes. Before specific progress is made on this, the current design premises should apply, but a reformulation might be considered such that it would allow for these potential breakthroughs, without the need of further altering the design premise. It is thus suggested to change the last sentence to: "The EFPC criterion is a tool to identify such fractures, but can be replaced or complemented by other tools in cases where the application of such tools is shown not to increase the risk contribution."

#### *Feedback to reference design*

The current reference design is judged adequate. Further efforts in characterising the actual extent of damage zone and splays for the few deformation zones longer than 3 km that exist at the Forsmark site and to find alternative means for determining the sizes of fractures intersecting deposition holes are warranted. If these efforts are successful, the design rules may be changed accordingly.

### 15.5.13 Selecting deposition holes – hydrological and transport conditions

Large fractures and fractures with high flow rates intersecting deposition holes are common factors for many identified safety related issues. Flow in fractures intersecting deposition holes affects:

- Piping.
- Colloid release.
- Oxygen penetration.
- Inflow of corrodants, potentially leading to canister failure.
- Outflow of radionuclides (in both the corrosion and shear displacement cases, in particular for eroded buffer).

High flow rates in deposition holes are also generally associated with low *F*-values in the geosphere for both recharge and discharge flow paths.

In /SKB 2009a/ it is stated that:

- *The total volume of water flowing into a deposition hole, for the time between when the buffer is exposed to inflowing water and saturation, should be limited to ensure that no more than 100 kg of the initially deposited buffer material is lost due to piping/erosion. This implies, according to the present knowledge, that this total volume of water flowing into an accepted deposition hole must be less than 150 m$^3$.*
- *Fractures intersecting the deposition holes should have sufficiently low connected transmissivity (specific value cannot be given at this point).*

The findings from SR-Site suggest that these premises should be revised, both with regard to piping erosion and with regard to implications for correlation to Darcy flux during the assessment period.

### *Piping erosion*

It is concluded in Section 10.2.4 that piping followed by erosion cannot be ruled out. Up to about 100 kg of dry bentonite may be lost due to erosion without jeopardising the function of the buffer. The uncertainty in the assessment of the corresponding eroded volume needs to be considered when revising the design premises for acceptable inflow conditions to the deposition holes.

Furthermore, the stated rule on a maximum allowed total volume of inflow to a deposition hole is judged of limited practicality by designers and also is related to how much water would pass the deposition tunnel plug before saturation.

### *Correlation to Darcy flux and far-field transport resistance*

The analyses in SR-Site suggest that risk would be much further reduced if it was possible to identify the deposition holes having the largest Darcy flux during saturated conditions. As shown in Chapter 10, due to the very low frequency of water conducting fractures at the Forsmark site, only a few percent of all deposition holes might have dilute conditions and of these only a handful, having the largest Darcy fluxes would lose the buffer over the $10^6$ year time period and then even less canisters would fail due to these conditions. It can thus be concluded that if it was possible to identify these few deposition hole position before emplacement, this would significantly reduce the already low risk, without any significant loss of useful canister positions. The design and detailed investigation challenge is instead to find these positions.

It should be noted that since SR-Site considers the application of the EFPC, in practise also a hydraulic consideration is applied. Since there is a correlation, although uncertain, between fracture size and transmissivity, application of EFPC in fact reduces the number of high Darcy flux deposition holes significantly. This observation highlights the fact that, for avoiding high flows, it is not the EFPC as such that is important, but to find an observable property that would identify potentially flowing fractures.

As is concluded in Section 14.3.2, there appears to be a potential for further enhancing safety by avoiding deposition holes with high inflows, even if the correlation with long-term Darcy flux is not one-to-one given the differences in boundary condition. Furthermore, the inflows will also be disturbed by skin effects and grouting and there will also be a practical lower detection limit. Partly, these disturbances may be overcome by requiring that deposition holes intersected by fractures capable of providing inflows below a certain value are to be avoided. This means that the hydraulic properties of the fractures intersecting the borehole should be tested in the pilot hole prior to drilling the full size hole, thereby avoiding skin effects, and that deposition holes intersected by fractures showing visible grout should also be rejected, since the presence of grout suggests that the fracture was quite transmissive before grouting.

### *Feedback to design premises*

Regarding piping erosion, the stated limit of 150 $m^3$ volume of water entering the deposition hole before saturation appears appropriate. However, a more practical design rule than limiting the total amount of water entering the deposition hole must be strived for, but input for such an updated rule requires further R&D.

It is suggested that the current design premises be revised such that deposition holes with potential for high Darcy flux during the assessment period are avoided. The practical formulation of the rule needs further elaboration, but a tentative rule may be to avoid deposition holes intersected by connected transmissive fractures capable of producing higher inflows than 0.1 L/min. Deposition holes intersected by fractures showing visible grout should also be rejected. Making this rule more restrictive, i.e. by reducing the allowable inflow to 0.01 L/min, would potentially further reduce risk, but application of this rule may be hard in practice. Instead, it is suggested that this criterion should be combined with the application of the EFPC, for the entire deposition hole as explained in Section 5.2.2, but only for fractures showing potential for groundwater flow. Completely healed fractures would not be considered for this reason.

#### *Feedback to reference design*

Further development is needed in order to derive a more practical design rule than limiting the total amount of water that could enter a deposition hole for the time between when the buffer is exposed to inflowing water and saturation. One factor of importance in this respect concerns the practical possibilities of limiting the flow through the deposition tunnel plug before backfill saturation.

The revised design premise with regard to the allowed transmissivity of fractures intersecting the deposition holes, indications of grouting and application of EFPC needs to be considered when updating the repository design and when further developing the detailed investigation programme.

### 15.5.14 Hydraulic properties in deposition hole wall

In /SKB 2009a/ it is stated that: "Before canister emplacement, the connected effective transmissivity integrated along the full length of the deposition hole wall and as averaged around the hole, must be less than $10^{-10}$ $m^2/s$."

There are essentially two reasons why this condition may not be upheld. These are damage from excavation and new fracturing due to spalling. The conformity with the design premise is demonstrated in the **Underground openings construction report** and there is no reason to revise the design premise based on SR-Site findings. However, since spalling may also result from the thermal load it is worthwhile to consider its importance.

The rock mechanics assessment, see Section 10.3.5, concludes that thermally induced spalling, is likely to occur but the counter pressure exerted by bentonite pellets in the slot between buffer and rock wall, may suppress the spalling, or at least keep the spalled slabs in place and minimise the hydraulic transmissivity of the spalled damage zone.

The assessment of the impact of spalling, Section 10.3.6, demonstrates that spalling may increase the mass transfer (the equivalent flow rate $Q_{eq}$) for the Q1 path by more than an order of magnitude, but the other paths are not affected. However, this increase has essentially no impact on risk, since spalling will not affect the local Darcy flux in the case of advective conditions in the deposition hole or if the canister is damaged by a shearing fracture.

#### *Feedback to design premises*

Since thermally induced spalling has a minor impact on risk, it is suggested to keep the current design premises and not specify any design rule connected to its occurrence.

#### *Feedback to reference design*

While occurrence of thermally induced spalling has a minor impact on risk, efforts to handle and mitigate thermally induced spalling should continue.

### 15.5.15 Canister positions – adapted to the thermal conditions

According to current design premises "Buffer geometry (e.g. void spaces), buffer water content and distances between deposition holes should be selected such that the temperature in the buffer is < 100°C".

As discussed in Section 10.3.10, the temperature requirement is adequate to protect the buffer, but possibly too strict at least if the temperature evolution is considered. It is found that an increased temperature will have an effect on the mechanical properties of the bentonite, but the effect is not very pronounced even at 150°C and does not seem to progress with time.

The thermal analysis, see Section 10.3.4 demonstrate that with the current repository design, with its deposition hole spacing, buffer geometry and maximum residual power, there is an adequate margin to the peak temperature criterion for the buffer, even when the spatial variability of the rock thermal properties is taken into account and with other data essential for computing the result chosen pessimistically. However, it is possible to envisage deposition sequences, e.g. when a canister is

deposited centrally in a deposition area where nearby positions were deposited several years before, where the resulting temperature in the buffer would exceed the maximum allowed. Such situations could always be avoided, but this possibility highlights the need for careful thermal management of the disposal sequence.

#### *Feedback to design premises*

There does not seem to be an immediate need to revise the design premise relating to the buffer temperature. However, it is noted that in the practical design of the canister encapsulation facility there is a need to have a more refined rule concerning the maximum allowed residual power in the canister, e.g. if it can be acceptable that some canister have slightly higher power. In order to provide such refined rules the strictness of the current requirement on maximum temperature in the buffer could be reconsidered.

#### *Feedback to reference design*

The current reference design, stating maximum residual power, buffer geometry and minimum deposition hole spacing, appears appropriate, but may of course be revised if the design premises are revised. However, restrictions regarding the canister emplacement sequence should be added to ensure that temperature requirement would not be violated during the operational period.

### 15.5.16 Controlling the Excavation Damage Zone (EDZ)

In /SKB 2009a/ it is stated that: "Excavation induced damage should be limited and not result in a connected effective transmissivity, along a significant part (i.e. at least 20–30 m) of the disposal tunnel and averaged across the tunnel floor, higher than $10^{-8}$ m$^2$/s. Due to the preliminary nature of this criterion, its adequacy needs to be verified in SR-Site."

The sufficiency of the upper transmissivity limit of $10^{-8}$ m$^2$/s is indeed demonstrated in SR-Site. As further assessed in Section 14.3.2, the number of corroded canisters is virtually unaffected comparing a case without an EDZ with the basic assumption of an EDZ transmissivity of $10^{-8}$ m$^2$/s. However, the analysis also shows that a more transmissive EDZ could affect risk since the number of failed canisters starts to increase, although moderately, when the transmissivity is increased. The EDZ seem to be even less important for radionuclide transport. For the pin-hole scenario, see Section 13.7.2 the presence of an EDZ at $10^{-8}$ m$^2$/s increases the dose compared to a case without an EDZ, but only marginally, and making the EDZ transmissivity larger does not further increase the dose.

Evidence presented in the **Underground openings construction report** and further elaborated in the **Data report**, see also Section 10.2.2, suggests that there is ample evidence that a potential EDZ formed during excavation will be kept below the maximum allowed transmissivity as set out by the design premises and the data further suggests that a continuous EDZ would not develop at all. However, as also stated in the **Underground openings construction report** further development of the method to control and inspect the EDZ as well as demonstration of the reliability of this method is needed.

#### *Feedback to design premises*

The variation cases analysed in SR-Site confirm that the suggested upper limit of the connected EDZ transmissivity of $10^{-8}$ m$^2$/s is adequate and need not be decreased. However, connected EDZ transmissivity above this value will start to affect risk and needs to be avoided.

#### *Feedback to reference design*

The importance of clearly establishing that there is no connected EDZ or that its connected transmissivity is less than $10^{-8}$ m$^2$/s demonstrates that further development of the method to control the development of the EDZ as well as development of techniques to verify the excavation results are needed.

### 15.5.17 Materials for grouting and shotcreting

According to /SKB 2009a/ the following restrictions apply in deposition tunnels

- *Only "low pH" materials (pH < 11).*
- *No continuous shotcrete.*
- *Continuous grouting boreholes outside tunnel perimeter should be avoided.*

According to the **Underground openings construction report**, the reference design contains low pH cement that is used in shotcrete support, for embedding various rock support elements and in grout mixes used for sealing purposes. Various recipes that would generate porewater with pH< 11 have been developed for the purpose of grouting in rock types with potential for unacceptable inflows as well as for rock support elements that need to be embedded in cement. Furthermore, the assessment of repository evolution presented in Chapter 10 confirms that the currently estimated amounts of engineered and residual materials left at deposition, backfill or closure of the underground openings would have negligible impact on the safety functions. The modelling presented in Section 10.3.12 shows that the given cement composition will yield a pH > 11 in the bottom plate for a short duration, but that this has negligible impact on the buffer.

#### *Feedback to design premises*

Current design premises are judged adequate, but should be more correctly formulated to state that only materials with sufficiently low alkalinity, not resulting in a pH over 11 in the groundwater exposed to that material, will be allowed. Furthermore, it should be clarified that a short duration pulse above pH 11 when the concrete is setting may be acceptable.

#### *Feedback to reference design*

The current reference design is judged appropriate, although it is recognised that the practical applicability of the suggested materials needs to be further tested and that final recipes may be modified. While the amounts of grout and reinforcement material presented in the **Underground openings construction report** would not jeopardise safety and that probably even larger amounts and more alkaline materials would be acceptable, it is also noted that it will be important to keep a careful record of all materials that are brought into (and taken out of) the repository, allowing for updated assessments of whether the amounts would come close to detrimental levels.

### 15.5.18 Repository depth

In /SKB 2009a/ it is stated that:

- *The repository volumes and depth need to be selected where it is possible to find large volumes of rock fulfilling the specific requirements on deposition holes.*
- *With respect to potential freezing of buffer and backfill, the requirement of temperatures favouring the mechanical properties of the canister, surface erosion and inadvertent human intrusion the depth should be considerable. Analyses in the SR-Can assessments corroborate that this is achieved by prescribing the minimum depth to be as specified for a KBS-3 repository i.e. at least 400 m.*

The analyses in SR-Site corroborate the adequacy of the selected repository depth. A more detailed assessment is given in Section 14.3.4.

#### *Feedback to design premises*

Current design premises are adequate.

#### *Feedback to reference design*

There is no reason to revise the selected repository depth based on the findings from SR-Site.

### 15.5.19 Main tunnels, transport tunnels, access tunnels, shafts and central area, and closure

In /SKB 2009a/ it is stated that:

- *Below the location of the top sealing, the integrated effective connected hydraulic conductivity of the backfill in tunnels, ramp and shafts and the EDZ surrounding them must be less than $10^{-8}$ m/s. This value need not be upheld in sections where e.g. the tunnel or ramp passes highly transmissive zones. There is no restriction on the hydraulic conductivity in the central area.*
- *The top sealing has no demands on hydraulic conductivity.*
- *The depth of the top sealing can be adapted to the expected depth of permafrost during the assessment period, but must not be deeper than 100 m above repository depth.*

The reference design presented in the **Closure production report** and in the **Underground openings construction report** conforms to these design premises and the analyses in SR-Site show that a design following these rules would be appropriate. Furthermore, based on the findings from varying the transmissivity of the EDZ, discussed in Section 15.5.16, it is not obvious that these rules can be further relaxed. However, it is likely that the direct impact on risk would only apply for the EDZ in the deposition tunnels, whereas a higher transmissivity probably could be accepted in the other tunnels. Such a situation has, however, not been analysed in SR-Site.

#### *Feedback to design premises*

Current design premises appear adequate. To further relax the demands would require additional sensitivity analyses focusing on the hydraulic properties of the access, main and transport tunnels.

#### *Feedback to reference design*

The current reference design, based on the deposition tunnel concept, could likely be simplified without violating current design premises. Furthermore, additional simplifications could probably be made if the design premises could be revised as discussed above.

### 15.5.20 Sealing of boreholes

In /SKB 2009a/ it is stated that: "Boreholes must be sealed such that they do not unduly impair containment or retention properties of the repository. This is preliminarily achieved if the hydraulic conductivity of the borehole seal < $10^{-8}$ m/s, which is ensured if the swelling pressure of the seal is > 0.1 MPa. This value needs not be upheld in sections where e.g. hole passes highly transmissive zones."

The impact of an open borehole on the groundwater flow in the repository and the surrounding rock has been studied by introducing boreholes at various locations in the hydrogeological model applied for analyses of the temperate period in SR-Site /Joyce et al. 2010/. As concluded there and in Section 10.3.6, the impact of improper seals of the boreholes is very moderate. Furthermore, according to the assessment presented in Section 10.3.14, the reference design of the borehole seals will perform as intended. Clearly, the bentonite may be lost in sections intersecting highly flowing fractures, but in the reference design there is no bentonite in such sections. The only problem with the seals is to demonstrate their performance. The keys issue is that it is difficult to inspect the quality of the seals after installation. A loss of bentonite in the range of a few metres in the seals will lead to a total loss of performance in that section, but the rest of the seal will be virtually unaffected. The function of the seal is not to hinder flow in the intersecting fractures, but to hinder flow along the borehole, so loss of function over a few metres is not a significant consideration.

#### *Feedback to design premises*

Current design premises appear adequate. However, it may be argued that current design premises for the borehole seals are too strict, since even open boreholes seem to have a limited impact on the flow. Since it might be difficult to inspect the outcome of the current design of the sealing, it could be of interest to assess whether a solution that may result in higher effective permeability of the borehole seals, but that would be more robust to control, would provide sufficiently good protection. However, relaxing the design premises in this way would require additional sensitivity analyses.

***Feedback to reference design***

The assessment in SR-Site indicates that the reference design is appropriate for the purpose. However, if design premises are relaxed, more robust designs might be worth investigating.

## 15.6 Feedback to detailed investigations and site modelling

Previous chapters have demonstrated that several site-specific conditions have a large impact on repository evolution and also, in some cases, on individual risk. While, the confidence in the site understanding is judged adequate and remaining uncertainties are sufficiently well constrained to allow upper bound risk estimates to be made, the repository might still be further optimised with respect to efficiency and risk reduction. Furthermore, as should be clear from the assessment of the design premises in the previous section, most of such potential improvements concern possibilities for local adaptation of the deposition tunnels and deposition holes to the conditions found in the rock. In addition, some issues remain concerning the properties of the rock mass outside the immediate vicinity of the deposition areas. Feedback to the detailed site investigations and site modelling can thus be given, considering the confidence and uncertainty in the **Site description Forsmark** as outlined in Chapter 4.

A framework programme for the detailed investigations and associated site descriptive modelling has been developed and is documented in /SKB 2010b/ It is generally found that this framework programme and the presented plans for developing this into the actual detailed and investigation programme are adequate. However, the findings from SR-Site are still important for prioritising and further specifying the development needs.

### 15.6.1 Further characterisation of the deformation zones with potential to generate large earthquakes

In order to ensure mechanical stability of deposition holes, it is a necessary condition that deposition holes are located with appropriate respect distances to deformation zones with the potential to host larger earthquakes, see Section 15.5.12. According to the **Site description Forsmark**, there is a very high confidence that only the few such zones already identified exist at the site and that even less of them intersect the repository volume in such a way that respect distances need to be considered.

It will also be important to locally establish the adequacy of applied respect distances in relation to observed occurrences (e.g. as mapped in transport tunnels) of the few zones able to host larger earthquakes that exist in the immediate vicinity of the repository. The detailed investigation programme needs thus spend further efforts in:

- Determining the extent of the damage zone for the few deformation zones able to host larger earthquakes at the Forsmark site.
- Identifying and characterising splays from these deformation zones.

According to the detailed investigation framework programme /SKB 2010b/ currently available tools are sufficient for such a characterisation allowing for more specific characterisation plans to be developed.

### 15.6.2 Further develop the means to bound the size of fractures intersecting deposition holes

The mechanical stability of canisters also requires that the canisters are not intersected by fractures sufficiently large to cause shear failures of the canister in case of an earthquake. As noted in Section 15.5.12, the currently applied criterion, the EFPC, is only a proxy for avoiding such large fractures. Application of EFPC implies that several deposition positions might be rejected, even if the fracture intersecting them is not large enough to represent a problem. Furthermore, the efficiency of EFPC, i.e. the risk of not identifying the problematic fracture, to some extent depends on the statistical distribution of fracture sizes. Consequently, it is of high interest to further develop the means for bounding the size of fractures intersecting deposition holes. Plans for such development work are outlined in the detailed investigation framework programme /SKB 2010b/.

### 15.6.3 Reduce the uncertainty of DFN models

The risk contribution from large earthquakes partly depends on the applied statistical description of the fractures, although the uncertainty in this description to a large extent is mitigated by applying the design rule that large fractures are not allowed to intersect the canister. Uncertainty in the geological DFN models is still an issue. Furthermore, reducing the uncertainty in the geological DFN model would also be of importance for reducing uncertainty in the hydrogeological DFN model, see Section 15.6.5.

The DFN model of the site is still quite uncertain and several alternatives are presented and assessed in SR-Site, see Section 10.4.5. The assessment of earthquake risk thus considers this wide range of uncertainty and even considering this, the risk contribution is very small. However, further efforts in reducing uncertainties are warranted.

In the **Site description Forsmark** it was concluded that the uncertainties in the geological DFN model can only be significantly reduced by data from underground. Such data include tunnel mapping and evaluations from boreholes (such as pilot holes drilled during the underground excavation work) and such data are, according to the detailed investigation framework programme /SKB 2010b/ planned to be obtained and assessed.

### 15.6.4 Identifying connected transmissive fractures

The analyses in SR-Site suggest that if it was possible to identify the few deposition hole positions having the largest Darcy flux during saturated conditions, this would dramatically reduce risk, without any significant loss of useful canister positions, see Section 15.5.13. Means of finding (and then avoiding) connected transmissive fractures capable of producing higher inflows and high Darcy fluxes into and around deposition holes should thus be a priority task of the detailed investigations. This challenge is also acknowledged in the detailed investigations framework programme /SKB 2010b/, where it is stated that there are hydraulic testing methods available for meeting this challenge, but that further development is needed for interpreting such tests, together with other information from the tunnel.

### 15.6.5 Hydraulic properties of the repository volume

The hydraulic properties of the repository volume, expressed as the hydrogeological DFN model, together with the hydraulic description of the deformation zones, has a large impact on repository performance, even if some of the importance may be reduced by introducing more efficient deposition hole acceptance criteria, as discussed previously.

While confidence is high with regard to the very low frequency of connected transmissive fractures, there are still large uncertainties in the actual distribution of hydraulic properties within these fractures. This is expressed by formulating and propagating different variants concerning the correlation between fracture size and transmissivity. As shown in Chapters 10, 12 and 13, the selection of this correlation has an impact both on the number of failed canisters, due to corrosion for advective conditions in the buffer, and on the resulting migration of released radionuclides. It is thus concluded that better bounds, especially on the size versus transmissivity correlation, on the hydrogeological DFN model would be beneficial. Uncertainties in the flow-related transport resistance, due to the fact that individual fractures are treated as having homogeneous properties, are considered to be small based on the arguments provided in Section 10.3.6.

As for the geological DFN model, it is concluded in the **Site description Forsmark** that the uncertainties in the hydrogeological DFN model can only be significantly reduced by data from the underground characterisation. Combining hydraulic data obtained from underground, e.g. by hydraulic tests in boreholes (such as pilot holes drilled during the underground excavation work) with the geological characterisation of the fractures responsible for the measured flow will allow further integration between the geological and hydrogeological modelling. Such integrated modelling is also foreseen in the detailed investigation framework programme /SKB 2010b/.

### 15.6.6 Verifying the conformity to the EDZ design premise

According to Section 15.5.16, the current design premise requiring that excavation induced damage should be limited and not result in a connected effective transmissivity higher than $10^{-8}$ $m^2/s$ along a significant part (i.e. at least 20–30 m) of the disposal tunnel and averaged across the tunnel floor, is adequate. It was also concluded that a more transmissive EDZ starts to affect risk, even though the impact is moderate.

As already discussed, there is ample evidence that a potential EDZ formed during excavation will be kept below the maximum allowed transmissivity as set out by the design premises, and data suggest that a continuous EDZ would not develop at all. It is also clear that further development of the methods to control the EDZ as well as demonstration of the reliability of these methods is needed.

The methods to control the development of an EDZ are to a large extent connected to the quality of the drill and blast operation, but some aspects of confirming that these measures actually result in an EDZ in conformity with the design premises belong to the detailed investigation programme and need thus to be developed therein. This is acknowledged in the detailed investigation framework programme /SKB 2010b/, where some relevant plans are presented. However, the detailed investigation framework programme also concludes that it is neither possible nor necessary to continuously verify these hydraulic design premises. The conformity would instead be built on verifying that the reference method for rock excavation can be managed such that it conforms to the design premises.

### 15.6.7 Rock mechanics

As discussed in Section 15.5.14, the *in situ* rock stress and the properties of the intact rock are such that thermally induced spalling is likely to occur. The hydraulic assessment of the impact of spalling, Section 10.3.6, demonstrates that spalling may increase the equivalent flow rate for the Q1 path by more than an order of magnitude, whereas the other paths are not affected. However, this increase has essentially no impact on risk, since spalling will not affect the local Darcy flux in the case of advective conditions in the deposition hole or if the canister is damaged by a shearing fracture.

According to the **Site description Forsmark**, there are remaining uncertainties with regard to the stress magnitude at Forsmark. There is also uncertainty in the spalling strength. While resolving these uncertainties is important for the design and layout of the repository, especially since the occurrence and amount of spalling affects the number of usable deposition positions, these uncertainties are of somewhat less importance for safety. Nevertheless, the potential for thermally induced spalling is evident considering the current uncertainty range and, since spalling affects one of the safety functions, although not risk itself, further efforts in finding methods to mitigate the spalling are warranted. This also includes a need for further characterisation of both the rock stress and the spalling strength of the rock.

In conclusion, the plans for rock mechanics assessment presented in the detailed investigation framework programme /SKB 2010b/ are judged adequate.

### 15.6.8 Thermal properties

For a specific residual power in the canister the thermal conductivity and in situ temperature determine, together with the repository layout and the thermal properties and geometry of the buffer, the buffer peak temperature. The thermal analyses, see Section 10.3.4, demonstrate that the suggested layouts would conform to the thermal design premises by a substantial margin, even considering remaining uncertainties in the thermal data. In fact, most deposition holes will have a temperature much below the allowed maximum. From a strictly safety point of view, further detailed investigations and modelling of thermal properties is only needed if SKB decides to aim for a more compact design, with adaptation of deposition hole distances and/or residual power in the canisters to the local thermal conditions in the tunnel. In conclusion, the plans for thermal property assessment presented in the detailed investigation framework programme /SKB 2010b/ are judged adequate.

### 15.6.9 Hydrogeochemistry

The chemical environment directly controls the evolution of the repository. The most important parameters are redox properties, salinity and ionic strength, which directly affect the canister and buffer safety functions, but also other factors are important, including the groundwater content of

potassium, sulphide and iron(II), as they might affect the chemical stability of the buffer and the canister. In particular, as shown in Chapter 10 and Chapter 12, the levels of sulphide affect risk, since these levels control the canister corrosion rate and thus the number of canister failures due to corrosion in the case of advective conditions in the buffer.

Available hydrogeochemical data are clearly sufficient to prove that suitable conditions prevail at the Forsmark site today and also during the temperate period that should persist for at least the next few thousand years. Estimating possible changes in the groundwater composition for longer times and during a glacial cycle are more challenging and this has been done pessimistically in SR-Site. As shown in Section 10.4.7, upconing during glaciation will not result in excessively high salinity values, whereas intrusion of dilute glacial melt water, which may result in buffer erosion, cannot be excluded. Furthermore, for the case of an eroded buffer, the sulphide content becomes important, since excessively high values may lead to corrosion failure of the copper canister (see Section 10.4.9).

In order to enhance the confidence in these important evaluations and potentially also to be able to exclude the possibility of intruding dilute glacial melt water, more information would be valuable. Groundwater sampling data on sulphide, as well as dissolved organic carbon, microbial populations, hydrogen and methane, giving their concentrations and isotopic ratios would improve the possibility of estimating the future sulphide content. Isotope data on noble gases would also improve the understanding of diffusion of gaseous species. Also more uranium and radium analyses are needed in order to understand the heterogeneous distribution of these elements in Forsmark. The methods outlined in the detailed investigations framework programme /SKB 2010b/ are judged adequate to fulfil these needs.

### 15.6.10 Surface ecosystems

The assessment of long term effects on humans and the environment is based on two main foundations: i) a conceptual understanding of ecosystem function today, in the near and in the far future, and during different climate regimes, and ii) input data to assessment models, synthesised from the site description, from the literature and from models describing the landscape development.

Some important input data to the biosphere radionuclide model, like partitioning coefficients ($K_d$ values) and parameters describing biological uptake (CR) of some important radionuclides, rely today partly or completely on the use of literature data and data on analogue elements. It would probably be possible to increase model precision if estimates of these parameters could, to a higher extent, reflect site conditions and rely less on generic data from other sites. The upcoming detailed site investigations should therefore aim at providing a better coverage of concentration measurements of a few elements (including Ra and I) in all environmental media. There is also a need to measure concentrations of all elements in locally produced agricultural products and in the soils where these products are cultivated. Moreover, additional chemistry data from precipitation samples will enhance knowledge regarding elemental distribution and transport in the landscape.

## 15.7 Feedback to RD&D Programme

In accordance with a proper safety culture, general research on processes of importance for safety should continue even if the current view is that existing knowledge is sufficient to demonstrate long-term safety. More specifically, there are some issues which SR-Site shows to contribute to risk and where the basis for the assessment can be improved through more R&D.

### 15.7.1 Spent fuel

#### *Gap and grain boundary inventory*

SR-Site has revised the gap inventory (see the **Spent fuel report**) considering the plans for increased burn-up of future BWR and PWR fuel and the planned increased thermal power of the nuclear power plants. Since the gap release is important in relation to risk, see Section 13.5.11, it is essential that this work continues. The SR-Site estimates of fission gas release from high-burnup fuel should be complemented with actual measurements of fission gas release and releases in solution of mobile elements such as Cs and I.

#### *Corrosion release rate*

In SR-Site, the rate of corrosion of structural metallic parts of the fuel elements was based on published data for their corrosion under anoxic conditions. The corrosion of the Cd-In-Ag alloy of the control rods was, on the other hand, treated very pessimistically by assuming instant dissolution, given the paucity of data. Available unpublished in-reactor data indicate a potential de-alloying and release of In and Cd. Silver is a noble metal that under anoxic conditions is expected to corrode only in the presence of e.g. sulphide ions /McNeil and Little 1992/. Some research effort will be devoted to the study of the corrosion of the Cd-In-Ag alloy, with emphasis on silver corrosion and release. This is expected to make possible a less pessimistic treatment of silver releases in the future.

#### *Spent fuel dissolution*

Given the importance of the spent fuel dissolution for the amount of radionuclides released, see Section 13.5.11, research on fuel dissolution should continue. This research should focus both on data under repository like conditions and on understanding of basic processes contributing to fuel dissolution. Findings from this research could reduce the calculated risk further.

### 15.7.2 Canister

#### *Corrosion of copper canister*

Understanding copper corrosion is fundamental for the safety concept. While confidence is judged high it is still essential to continue ongoing research. Such research includes studying the reactions that could occur on copper surfaces in an oxygen-gas free environment both in laboratory experiments and by theoretical quantum mechanical modelling, studies of copper sulphide films as well as further assessing the role of bentonite in determining corrosion rates.

#### *Stress corrosion cracking of copper canister*

Conditions for stress corrosion cracking are not judged to occur in the repository but the basic research focusing on identifying the necessary conditions needed for stress corrosion cracking to occur on copper should continue.

#### *Deformation of cast iron*

Understanding the deformation of cast iron is essential for the confidence in the assessment of the impact of mechanical load on the canister. While confidence is judged high for the design analyses presented in the **Canister production report**, further work is warranted since this is a key issue and since pessimisms regarding e.g. failure criteria applied in the design analysis could be reduced. The ongoing development work on manufacturing and testing of cast iron inserts, including the PWR inserts should thus continue. The impact of hydrogen on mechanical properties, in relation to the hydrogen levels that could be expected to be created by corrosion by potentially remaining water in the sealed canister, also would benefit from further understanding.

#### *Deformation of copper canister from external pressure*

Also the understanding of copper deformation under external pressure is essential for the confidence in the assessment of the impact of mechanical load on the canister. While confidence is judged high for the design analyses presented in the **Canister production report**, further work is warranted since this is a key issue and since pessimisms regarding e.g. failure criteria applied in the design analysis could be reduced. The ongoing work on assessing creep properties of copper should continue and include welded material as well as the effects of different disturbances such as cold working and the impact from hydrogen on mechanical properties.

### 15.7.3 Buffer and backfill

#### *Water transport*

As shown in Chapter 10, there is sufficient understanding of water transport in the buffer and backfill material to make adequate predictions with respect to long-term safety. However, uncertainties

remain, which when resolved might enhance current designs. Laboratory and field tests of different materials and calibration of models in order to optimise parameter values in the models to enhance knowledge of water transport in both dry and wet conditions are thus warranted.

#### *Gas transport*

Further assessment of parameters critical to gas transport in clay materials is warranted. Findings from Lasgit, being part of the EU project Forge which will end 2012, should be assessed and laboratory experiments to study critical parameters that are difficult to evaluate in a full-scale test should be carried out.

#### *Piping/erosion*

The understanding of piping/erosion is much advanced since SR-Can and has allowed formulation of design premises with regard to inflow into deposition holes. For fine tuning these design premises and for developing the designs, further understanding of the importance of geometry, enhanced knowledge of when piping does not occur, the applicability of the erosion model, self-sealing of cracks and enhanced ability to quantify the process would be valuable. Such studies should consider the processes occurring during water saturation with a focus on homogenisation.

#### *Mechanical processes*

Homogenisation and self-sealing are important processes for the evolution of the buffer and the backfill. Ongoing research should continue.

#### *Integrated THM development*

Also the ongoing development of the integrated coupled buffer THM model should continue. This should be facilitated by assessing different projects at Äspö, further development of the codes used and by new experiments on a smaller scale for studying hydromechanical processes. Effort should be focused on processes occurring during water saturation: Piping, erosion, water saturation, self-sealing, and homogenisation of both buffer and backfill.

#### *Montmorillonite alteration*

Buffer and backfill performance depends on understanding montmorillonite alteration. The impact from potential construction and grouting materials, such as low alkalinity cements and silica sol should continue to be studied, especially to further specify restrictions on their use in the repository.

#### *Cementation*

The studies on rheological effects of cementation should be continued.

#### *Buffer erosion/Colloid release*

From the studies of buffer erosion/colloid release conducted since SR-Can it has been concluded that the process cannot be ruled out in the assessment of long-term safety and that a continued R&D programme is needed. The transport model basically considers a pure sodium system and the loss of bentonite is most likely overestimated. Further studies could reduce the pessimism. Some areas of interest are:

- The effect of calcium and mixed Ca/Na systems on swelling/colloid formation behaviour.
- Erosion in fractures or slots (instead of open pipes or filters as has been the case in most of the earlier experimental work).
- The effect of flow and water velocity on the erosion.
- Sealing of erosion damage.

These studies are already progressing.

### 15.7.4 Geosphere

Much of the R&D related to the geosphere is covered by the detailed investigation programme, but research on some processes should also continue.

#### *Spalling*

Since SR-Can, several efforts have been made to enhance the understanding of the conditions under which thermal spalling will occur, as well as the extent of the spalled zone. As already concluded, thermally induced spalling, is likely to occur, but the counter pressure exerted by bentonite pellets in the slot between buffer and rock wall, may suppress the spalling, or at least keep the spalled slabs in place and minimise the hydraulic transmissivity of the spalled damage zone. Furthermore, the assessment of the impact of spalling demonstrates that spalling may increase the equivalent flow rate for the Q1 path by more than an order of magnitude and that this increase has essentially no impact on risk, since spalling will not affect the local Darcy flux in the case of advective conditions in the deposition hole or if the canister is damaged by a shearing fracture. Other exit paths than Q1 are not affected by spalling. Consequently, further progress in the actions to assess spalling is not critical to safety, but efforts to handle and mitigate thermally induced spalling should continue as this affects one of the safety functions.

#### *THM assessment of the geosphere*

The assessment of coupled thermo-hydro-mechanical processes presented in Chapter 10 clearly demonstrates that such processes have limited impact on safety. Continued research on the underlying processes is still warranted, although possibly primarily for input to the rock engineering design of the repository. With respect to long term safety issues, those worth further assessment include revisiting the current assumptions on stress-transmissivity couplings for fractures and deformation zones and revisiting current assumptions on excess porewater pressure during the glacial cycle. Current assumptions are judged to overstate the importance of these effects.

#### *Glacially induced stresses and earthquake simulations*

There have been major advances regarding the potential for earthquakes and their implications for safety since SR-Can. Potentially, there is some risk contribution from this mechanism, but it is low. Furthermore, the adaptation of the repository to deformation zones and fractures is handled within the detailed investigation programme, see Section 15.6. Considering that mechanical stability is fundamental, research on the prerequisites (e.g. state of stress) for glacially induced fault triggering should still continue. Further development of the earthquake simulation tools and approaches is also considered worthwhile.

#### *DFN methodology*

A better understanding of the fracture network in crystalline bedrock is essential for gaining a more realistic understanding, decreasing the uncertainty of models representing geological, mechanical, and hydrological aspects of the rock. Thus, efforts will be made to: Investigate how estimated fracture intensity depends on measuring methods, identify what extra data are needed for limiting values for input parameters that would limit the possible range of model outputs, develop an efficient method in order to evaluate differences between different models, further investigate the distribution of fracture apertures over the fracture surface, study effects of connectivity of fractures, for example through channelling, truncation, or alternative methods for generating fracture networks, and evaluate alternative concepts for generation of fractures.

#### *Groundwater chemistry – sulphide*

As shown in Section 13.6, the future sulphide levels in the groundwater have a strong influence on risk. The sulphide distribution applied in SR-Site is judged to pessimistically overestimate the consequences of future sulphide concentrations, especially since it is assumed that locations with high sulphide levels will remain at high levels throughout the assessment period. Further research

to better bound the expected evolution of sulphide and the processes affecting this evolution at the Forsmark site is thus warranted. Such research would include further assessments of errors introduced by the sampling and monitoring equipment.

#### *Microbial processes*

Redox conditions and sulphide levels directly affect risk. Since these conditions are strongly affected by microbial activity, the ability of microbes to maintain a low and stable redox potential in the near field and the far field and their role for sulphide formation and oxygen consumption still warrants further research.

#### *Radionuclide migration*

In Section 10.3.6 it is argued that the calculated flow-related transport resistance values do not need to be reduced due to channelling effects. This argument is based on motivations provided in the **Radionuclide transport report** and also summarised in the **Data report**. In short, the argument is based on calculations showing that channelling leads to stagnant water in the fracture planes (between the channels) enhancing the potential for matrix diffusion due to the fast diffusion from the flowing channels into the stagnant parts of the fracture. Furthermore, supporting calculations using the alternative conceptual model CHAN3D /Liu et al. 2010/ indicate that broadly consistent flow-related transport resistance values to those presented in /Joyce et al. 2010/ are obtained, see Section 10.3.6 for details. This further supports the assumption made on channelling.

However, in order to shed additional light on the assumptions made in SR-Site, continuing research in the field of channelling should be pursued. Specifically, high resolution numerical simulations of fractures with spatially variable apertures are planned. The objective is to study the effects of channelling within fractures, and between fractures in a network, with variable apertures. With a more detailed understanding of channelling phenomena, more conclusive statements concerning the assumptions made in SR-Site can be drawn.

### 15.7.5 Biosphere

A number of potential improvements have been identified that may contribute to gaining further confidence, reducing uncertainties or reducing the level of pessimism in the assessment. The detailed site investigations include mainly additional data collection, whereas the RD&D Programme spans from improving assessment models with existing information, to compilation of new knowledge by reviews and by basic research. Collection of additional site data, compilation of new knowledge and implementation of the knowledge in assessment models is an iterative process, often involving the same individuals and research groups.

Collection of additional site data on concentrations of elements in different media is one way to reduce uncertainties in parameters describing radionuclide retention and biological uptake (see Section 15.6.10). In order to predict retention and biological uptake of radionuclides in the future landscape, when environmental conditions may be different from today, it is also important to increase the understanding of important processes. A better process understanding may be achieved by complementary and deepened analyses of data on element and isotope concentrations.

For some nuclides it may also be possible to describe sorption and/or biological uptake by alternative modelling approaches that are less sensitive to parameter uncertainties. The coming RD&D Programme will therefore aim at developing assessment tools that explicitly describe biological uptake as determined by physiological processes /Kumblad and Kautsky 2004/. For primary producers this means that both active and passive uptake will be modelled, and that the bioavailability of radionuclides and the competition between radioactive and stable isotopes will be considered e.g. /Avila 2006/. Beside additional collection of site data, further studies on radionuclide transport in the regolith by chemical modelling, see /Piqué et al. 2010/, are needed to reduce uncertainty in $K_d$ values. Together with mass balance calculations of different elements, studies of element fluxes in the landscape should be continued with new data to explore element transport and limits for element retention in the landscape /Tröjbom et al. 2007/.

The biosphere assessment is in the current calculation chain implemented by the concept of maximum LDF for a unit release (1 Bq/y), i.e. the maximum LDF is taken across all biosphere objects and all times, separately for each radionuclide. This decoupling between the LDF's on the one hand and the space and time dimensions on the other, will most likely result in overestimated doses. The degree of overestimation may be evaluated in studies where hydrogeological models are connected to the biosphere models. Such studies are necessary to evaluate the pessimism that follows from the simplifications of a presumed pulsed release, and should contribute to a more thorough understanding of important processes for radionuclide transport from the repository to the biosphere. The conceptual understanding and description of future landscapes will gain considerably from data collected from environmental regimes other than today's Forsmark, e.g. Greenland, as well as from a further review of how other cultures explore and utilise the landscape they inhabit.

The methodology used to evaluate dose to non-human biota needs further development to fully utilise site data.

### 15.7.6 Climate

In order to further assess the degree of pessimism in various assumptions made in SR-Site modelling of groundwater flow and chemistry under glacial and periglacial climate conditions, further research is needed. In order to increase the conceptual knowledge necessary for the set up of such model simulations, the use of present-day analogues, such as observations of glacial hydrological processes from the Greenland ice sheet and hydrological interpretations of paleodrainage systems from the last glacial cycle in Fennoscandia, should be used.

Apart from the work of identifying and describing extremes within which climate and climate related processes may vary, the work within SR-Site also focussed on describing climate and climate related processes within each of the climate domains, and during some of the transitions between domains. Future research should include further description and analysis of transitions between climate domains, and the potential changes in processes that may relate specifically to such transition phases. This work should also include the coupling to the representation of processes and features in the biosphere and other programmes under such transition phases.

## 15.8 Conclusions regarding the safety assessment methodology

The assessment methodology outlined in Chapter 2 has been found adequate for analysing long-term safety of a KBS-3 repository according to requirements in applicable Swedish regulations. It is also in line with international practice for safety assessments. Much of the technical feedback given in the above sections is expected to lead to updated input to future assessments and will influence the approach used when addressing the issues in such future assessments.

# 16 References

SKB's (Svensk Kärnbränslehantering AB) publications can be found at www.skb.se/publications. References to SKB's unpublished documents are listed separately at the end of the reference list. Unpublished documents will be submitted upon request to document@skb.se.


### *References with abbreviated names*

**Backfill production report, 2010.** Design, production and initial state of the backfill and plug in deposition tunnels. SKB TR-10-16, Svensk Kärnbränslehantering AB.

**Biosphere synthesis report, 2010.** Biosphere analyses for the safety assessment SR-Site – synthesis and summary of results. SKB TR-10-09, Svensk Kärnbränslehantering AB.

**Buffer, backfill and closure process report, 2010.** Buffer, backfill and closure process report for the safety assessment SR-Site. SKB TR-10-47, Svensk Kärnbränslehantering AB.

**Buffer production report, 2010.** Design, production and initial state of the buffer. SKB TR-10-15, Svensk Kärnbränslehantering AB.

**Canister production report, 2010.** Design, production and initial state of the canister. SKB TR-10-14, Svensk Kärnbränslehantering AB.

**Climate report, 2010.** Climate and climate-related issues for the safety assessment SR-Site. SKB TR-10-49, Svensk Kärnbränslehantering AB.

**Closure production report, 2010.** Design, production and initial state of the closure. SKB TR-10-17, Svensk Kärnbränslehantering AB.

**Data report, 2010.** Data report for the safety assessment SR-Site. SKB TR-10-52, Svensk Kärnbränslehantering AB.

**FEP report, 2010.** FEP report for the safety assessment SR-Site. SKB TR-10-45, Svensk Kärnbränslehantering AB.

**FHA report, 2010.** Handling of future human actions in the safety assessment SR-Site. SKB TR-10-53, Svensk Kärnbränslehantering AB.

**Fuel and canister process report, 2010.** Fuel and canister process report for the safety assessment SR-Site. SKB TR-10-46, Svensk Kärnbränslehantering AB.

**Geosphere process report, 2010.** Geosphere process report for the safety assessment SR-Site. SKB TR-10-48, Svensk Kärnbränslehantering AB.

**Model summary report, 2010.** Model summary report for the safety assessment SR-Site. SKB TR-10-51, Svensk Kärnbränslehantering AB.

**Radionuclide transport report, 2010.** Radionuclide transport report for the safety assessment SR-Site. SKB TR-10-50, Svensk Kärnbränslehantering AB.

**Site description Forsmark, 2008.** Site description of Forsmark at completion of the site investigation phase – SDM-Site Forsmark. SKB TR-08-05, Svensk Kärnbränslehantering AB.

**Spent fuel report, 2010.** Spent nuclear fuel for disposal in the KBS-3 repository. SKB TR-10-13, Svensk Kärnbränslehantering AB.

**Underground openings construction report, 2010.** Design, construction and initial state of the underground openings. SKB TR-10-18, Svensk Kärnbränslehantering AB.

### *Other public references*

**Aastrup M, 1981.** Naturligt förekommande uran-, radium- och radonaktiviteter i grundvatten (in Swedish). SKBF/KBS TR 81-08, Svensk Kärnbränsleförsörjning AB.

**Ahokas H, Hellä P, Ahokas T, Hansen J, Koskinen K, Lehtinen A, Koskinen L, Löfman J, Mészáros F, Partamies S, Pitkänen P, Sievänen U, Marcos N, Snellman M, Vieno T, 2006.** Control of water inflow and use of cement in ONKALO after penetration of fracture zone R19. Posiva Working Report 2006-45, Posiva Oy, Finland.

**Ahonen L, Vieno T, 1994.** Effects of glacial meltwater on corrosion of copper canisters. Report YJT-94-13, Nuclear Waste Commission of Finnish Power Companies.

**Allard B, Banwart S, Bruno J, Ephraim J, Grauer R, Grenthe I, Hadermann J, Hummel W, Jakob A, Karapiperis T, Plyasunov A, Puigdomenech I, Rard J, Saxena S, Spahiu K, 1997.** Modelling in aquatic chemistry. Paris: Nuclear Energy Agency, Organisation for Economic Co-operation and Development.

**Amcoff Ö, 1998.** Mineral formation on metallic copper in a "future repository site environment": textural considerations based on natural analogs. SKI Report 98:7, Statens kärnkraftinspektion (Swedish Nuclear Power Inspectorate).

**Anderson J G, 1986.** Seismic strain rates in the central and eastern United States. Bulletin of the Seismological Society of America, 76, pp 273–290.

**Andersson E (ed), 2010.** The limnic ecosystems at Forsmark and Laxemar-Simpevarp. SR-Site Biosphere. SKB TR-10-02, Svensk Kärnbränslehantering AB.

**Andersson J, 1999.** Data and data uncertainties. Compilation of data and data uncertainties for radionuclide transport calculations. SKB TR-99-09, Svensk Kärnbränslehantering AB.

**Andersson J C, 2007.** Rock mass response to coupled mechanical thermal loading: Äspö pillar stability experiment. Ph. D. thesis. Royal Institute of Technology, Stockholm, Sweden.

**Andersson J, Ström A, Svemar C, Almén K-E, Ericsson L O, 2000.** What requirements does the KBS-3 repository make on the host rock? Geoscientific suitability indicators and criteria for siting and site evaluation. SKB TR-00-12, Svensk Kärnbränslehantering AB.

**Andersson P, Garnier-Laplace J, Beresford N A, Copplestone D, Howard B J, Howe P, Oughton D, Whitehouse P, 2009.** Protection of the environment from ionising radiation in a regulatory context (protect): proposed numerical benchmark values. Journal of Environmental Radioactivity, 100, pp 1100–1108.

**Andra, 2005.** Dossier 2005 Argile. Safety evaluation of a geological repository. Châtenay-Malabry: Agence nationale pour la gestion des déchets radioactifs (Andra).

**Apted M J, Bennett D G, Saario T, 2009.** A review of evidence for corrosion of copper by water. Report 2009:30, Strålsäkerhetsmyndigheten (Swedish Radiation Safety Authority).

**Aquilonius K (ed), 2010.** The marine ecosystems at Forsmark and Laxemar-Simpevarp. SR-Site Biosphere. SKB TR-10-03, Svensk Kärnbränslehantering AB.

**Arcos D, Grandia H, Domènech C, 2006.** Geochemical evolution of the near field of a KBS-3 repository. SKB TR-06-16, Svensk Kärnbränslehantering AB.

**Arenius M, Hansen J, Juhola P, Karttunen P, Koskinen K, Lehtinen A, Lyytinen T, Mattila J, Partamies S, Pitkänen P, Raivio P, Sievänen U, Vuorinen U, Vuorio M, 2008.** R20 summary report: The groundwater inflow management in ONKALO – the future strategy. Posiva Working Report 2008-44, Posiva Oy, Finland.

**Arvidsson R, 1996.** Fennoscandian earthquakes: whole crustal rupturing related to postglacial rebound. Science, 274, pp 744–746.

**Auqué L F, Gimeno M J, Gómez J B, Puigdomenech I, Smellie J, Tullborg E-L, 2006.** Groundwater chemistry around a repository for spent nuclear fuel over a glacial cycle. Evaluation for SR-Can. SKB TR-06-31, Svensk Kärnbränslehantering AB.

**Avila R, Bergström U, 2006.** Methodology for calculation of doses to man and implementation in Pandora. SKB R-06-68, Svensk Kärnbränslehantering AB.

**Avila R, Pröhl G, 2008.** Models used in the SFR 1 SAR-08 and KBS-3H safety assessments for calculation of $^{14}C$ doses. SKB R-08-16, Svensk Kärnbränslehantering AB.

**Avila R, Ekström P-A, Åstrand P-G, 2010.** Landscape dose conversion factors used in the safety assessment SR-Site. SKB TR-10-06, Svensk Kärnbränslehantering AB.

**Bamber J L, Layberry R L, Gogineni S P, 2001.** A new ice thickness and bed data set for the Greenland ice sheet 1: Measurement, data reduction, and errors. Journal of Geophysical Research, 106, pp 33773– 33780.

**Bamber J L, Riva R E M, Vermeersen B L A, LeBrocq A M, 2009.** Reassessment of the potential sea-level rise from a collapse of the West Antarctic ice sheet. Science, 324, pp 901–903.

**Banwart S A, 1999.** Reduction of iron(III) minerals by natural organic matter in groundwater. Geochimica Cosmochimica Acta, 63, pp 2919–2928.

**Banwart S A, Gustafsson E, Laaksharju M, 1999.** Hydrological and reactive processes during rapid recharge to fracture zones: the Äspö large scale redox experiment. Applied Geochemistry, 14, pp 873–892.

**Bath A, Hermansson H-P, 2009.** Biogeochemistry of redox at repository depth and implications for the canister. Report 2009:28, Strålsäkerhetsmyndigheten (Swedish Radiation Safety Authority).

**Bath A, Lalieux P, 1999.** Technical summary of the SEDE Workshop on the use of hydrogeochemical information in testing groundwater flow models. In: Use of hydrogeochemical information in testing groundwater flow models: proceedings of an NEA Workshop, Borgholm, Sweden, 1–3 September 1997. Paris: Nuclear Energy Agency, Organisation for Economic Co-operation and Development, pp 13–30.

**Becker D-A, Buhmann D, Storck R, Alonso J, Cormenzana J-L, Hugi M, van Gemert F, O'Sullivan P, Laciok A, Marivoet J, Sillen X, Nordman H, Vieno T, Niemeyer M, 2002.** Testing of safety and performance indicators (SPIN). EUR 19965 EN, European Commission.

**Behrenz P, Hannerz K, 1978.** Criticality in a spent fuel repository in wet crystalline rock. KBS TR 108, Svensk Kärnbränslehantering AB.

**Beresford N, Brown J, Copplestone D, Garnier-Laplace J, Howard B J, Larsson C-M, Oughton O, Pröhl G, Zinger I (eds), 2007.** D-ERICA: An integrated approach to the assessment and management of environmental risks from ionising radiation. Description of purpose, methodology and application. ERICA Project, contract number FI6R-CT-2004-508847, European Commission.

**Berger A, 1978.** Long-term variations of daily insolation and Quaternary climatic changes. Journal of the Atmospheric Sciences, 35, pp 2362–2367.

**Berger A, Loutre M F, 2002.** An exceptionally long interglacial ahead? Science, 297, pp 1287–1288.

**BIOCLIM, 2003.** Deliverable D7. Continuous climate evolution scenarios over western Europe (1,000 km scale). Work package 2: Simulation of the future evolution of the biosphere system using the hierarchical strategy. Châtenay-Malabry: Agence nationale pour la gestion des déchets radioactifs (Andra).

**BIOCLIM, 2004.** Deliverable D10-D12. Development and application of a methodology for taking climate-driven environmental change into account in performance assessments. Work package 4: Biosphere system description. Châtenay-Malabry: Agence nationale pour la gestion des déchets radioactifs (Andra).

**Birgersson M, Börgesson L, Hedström M, Karnland O, Nilsson U, 2009.** Bentonite erosion. Final report. SKB TR-09-34, Svensk Kärnbränslehantering AB.

**Birgersson M, Karnland O, Nilsson U, 2010.** Freezing of bentonite. Experimental studies and theoretical considerations. SKB TR-10-40, Svensk Kärnbränslehantering AB.

**Blomqvist R, Ruskeeniemi T, Kaija J, Ahonen L, Paananen M, Smellie J, Grundfelt B, Pedersen K, Bruno J, Pérez del Villar L, Cera E, Rasilainen K, Pitkänen P, Suksi J, Casanova J, Read D S, Frape S, 2000.** The Palmottu natural analogue project Phase II: Transport of radionuclides in a natural flow system at Palmottu. Project Report EUR 1961, European Commission.

**Bockgård N, 2010.** Groundwater flow modelling of an abandoned partially open repository. SR-Site Forsmark. SKB R-10-41, Svensk Kärnbränslehantering AB.

**Bond A E, Hoch A R, Jones G D, Tomczyk A J, Wiggin R W, Worraker W J, 1997.** Assessment of a spent fuel disposal canister. Assessment studies for a copper canister with cast steel inner component. SKB TR 97-19, Svensk Kärnbränslehantering AB.

**Bosson E, Sassner M, Sabel U, Gustafsson L-G, 2010.** Modelling of present and future hydrology and solute transport at Forsmark. SR-Site Biosphere. SKB R-10-02, Svensk Kärnbränslehantering AB.

**Boulton G S, Kautsky U, Morén L, Wallroth T, 2001.** Impact of long-term climate change on a geological repository for spent nuclear waste. SKB TR-99-05, Svensk Kärnbränslehantering AB.

**Bowman C D, Venneri F, 1994.** Underground supercriticality from plutonium and other fissile material. LA-UR-94-4022A, Los Alamos National Laboratory. (Also published in Science and Global Security 1996, 5, pp 279–302.)

**Bradbury M H, Baeyens B, 2005.** Modelling the sorption of Mn(II), Co(II), Ni(II), Zn(II), Cd(II), Eu(III), Am(III), Sn(IV), Th(IV), Np(V), and U(VI) on montmorillonite: Linear free energy relationships and estimates of surface binding constants for some selected heavy metals and actinides. Goechimica et Cosmochimica Acta, Vol. 69, No. 4, pp. 875-892. doi:10.1016/j.gca.2004.07.020.

**Brady B H G, Brown E T, 1994.** Rock mechanics for underground mining. 2nd ed. London: Chapman & Hall.

**Brandefelt J, Otto-Bliesner B L, 2009.** Equilibration and variability in a Last Glacial Maximum climate simulation with CCSM3. Geophysical Research Letters 36, L19712, doi:10.1029/2009GL040364.

**Broed R, 2008.** Landscape model configuration for biosphere analysis of selected cases in TILA-99 and in KBS-3H safety evaluation, 2007. Posiva Working Report 2007-108, Posiva Oy, Finland.

**Bros R, Carpéne J, Sere V, Beltritti A, 1996.** Occurrence of Pu and fissiogenic REE in hydrothermal apatites from the fossil nuclear reactor 16 at Oklo (Gabon). Radiochimica Acta, 74, pp 277–282.

**Bros R, Hidaka H, Kamei G, Ohnuki T, 2003.** Mobilization and mechanisms of retardation in the Oklo natural reactor zone 2 (Gabon) – inferences from U, REE, Zr, Mo and Se isotopes. Applied Geochemistry, 18, pp 1807–1824.

**Brown A C, 2006.** Genesis of native copper lodes in the Keweenaw District, northern Michigan: a hybrid evolved meteoric and metamophogenic model. Economic Geology, 101, pp 1437–1444.

**Brown G H, 2002.** Glacier meltwater hydrochemistry. Applied Geochemistry, 17, pp 855–883.

**Brown J E, Alfonso B, Avila R, Beresford N A, Copplestone D, Pröhl G, Ulanovsky A, 2008.** The ERICA Tool. Journal of Environmental Radioactivity, 99, pp 1371–1383.

**Bruno J, Casas I, Cera E, Duro L, 1997.** Development and application of a model for the long-term alteration of $UO_2$ spent nuclear fuel: test of equilibrium and kinetic mass transfer models in the Cigar Lake ore deposit. Journal of Contaminant Hydrology, 26, pp 19–26.

**Brydsten L, 2004.** A mathematical model for lake ontogeny in terms of filling with sediments and macrophyte vegetation. SKB TR-04-09, Svensk Kärnbränslehantering AB.

**Brydsten L, 2009.** Sediment dynamics in the coastal areas of Forsmark and Laxemar during an interglacial. SKB TR-09-07, Svensk Kärnbränslehantering AB.

**Brydsten L, Strömgren M, 2010.** A coupled regolith-lake development model applied to the Forsmark site. SKB TR-10-56, Svensk Kärnbränslehantering AB.

**Brydsten L, Engqvist A, Näslund J-O, Lindborg T, 2009.** Expected extreme sea levels at Forsmark and Laxemar-Simpevarp up until year 2100. SKB TR-09-21, Svensk Kärnbränslehantering AB.

**BSC, 2003.** Total system performance assessment – license application methods and approach. TDR-WIS-PA-000006 REV 00, Bechtel SAIC Company, Las Vegas, Nevada.

**Bungum H, Olesen O, Pascal C, Gibbons S, Lindholm C, Vestøl O, 2010.** To what extent is the present seismicity of Norway driven by post-glacial rebound? Journal of the Geological Society, 167, pp 373–384.

**Bäckblom G, 2009.** Excavation damage and disturbance in crystalline rock – results from experiments and analyses. SKB TR-08-08, Svensk Kärnbränslehantering AB.

**Bäckblom G, Almén K-E, 2004.** Monitoring during the stepwise implementation of the Swedish deep repository for spent fuel. SKB R-04-13, Svensk Kärnbränslehantering AB.

**Bäckblom G, Munier R, 2002.** Effects of earthquakes on the deep repository for spent fuel in Sweden based on case studies and preliminary model results. SKB TR-02-24, Svensk Kärnbränslehantering AB.

**Bäckblom G, Munier R, Hökmark H, 2004.** Earthquake data and modelling to study the effects of future earthquakes on a final repository of spent nuclear fuel in Sweden. Paper 3238. 13th World Conference on Earthquake Engineering, Vancouver, Canada, 1–6 August 2004.

**Böðvarsson R, 2002.** Swedish National Seismic Network (SNSN). A short report on recorded earthquakes during the third quarter of the year 2002. SKB P-02-04, Svensk Kärnbränslehantering AB.

**Böðvarsson R, 2002–2009.** Swedish National Seismic Network (SNSN). Series of short reports on recorded earthquakes during the period 2002–2009. Svensk Kärnbränslehantering AB.

**Böðvarsson R, 2009.** Swedish National Seismic Network (SNSN). A short report on recorded earthquakes during the fourth quarter of the year 2008. SKB P-09-03, Svensk Kärnbränslehantering AB.

**Böðvarsson R, Lund B, Roberts R, Slunga R, 2006.** Earthquake activity in Sweden. Study in connection with a proposed nuclear waste repository in Forsmark or Oskarshamn. SKB R-06-67, Svensk Kärnbränslehantering AB.

**Bøggild C E, Mayer C, Podlech S, Taurisano A, Nielsen S, 2004.** Towards an assessment of the balance state of the Greenland Ice Sheet. Geological Survey of Denmark and Greenland Bulletin, 4, pp 81–84.

**Börgesson L, Hernelind J, 2006a.** Consequences of loss or missing bentonite in a deposition hole. A theoretical study. SKB TR-06-13, Svensk Kärnbränslehantering AB.

**Börgesson L, Hernelind J, 2006b.** Earthquake induced rock shear through a deposition hole. Influence of shear plane inclination and location as well as buffer properties on the damage caused to the canister. SKB TR-06-43, Svensk Kärnbränslehantering AB.

**Börgesson L, Hernelind J, 2009.** Mechanical interaction buffer/backfill. Finite element calculations of the upward swelling of the buffer against both dry and saturated backfill. SKB R-09-42, Svensk Kärnbränslehantering AB.

**Börgesson L, Johannesson L-E, 2006.** Consequences of upwards swelling from a wet deposition hole into a dry tunnel with backfill made of blocks. A preliminary study. SKB TR-06-12, Svensk Kärnbränslehantering AB.

**Börgesson L, Sandén T, 2006.** Piping and erosion in buffer and backfill materials. Current knowledge. SKB R-06-80, Svensk Kärnbränslehantering AB.

**Börgesson L, Johannesson L-E, Sandén T, Hernelind J, 1995.** Modelling of the physical behaviour of water saturated clay barriers. Laboratory tests, material models and finite element application. SKB TR 95-20, Svensk Kärnbränslehantering AB.

**Börgesson L, Fälth B, Hernelind J, 2006.** Water saturation phase of the buffer and backfill in the KBS-3V concept. Special emphasis given to the influence of the backfill on the wetting of the buffer. SKB TR-06-14, Svensk Kärnbränslehantering AB.

**Calais E, Mattioli G, DeMets C, Nocquet J-M, Stein S, Newman A, Rydelek P, 2005.** Seismology: tectonic strain in plate interiors? Nature, 438, E9-E10, doi:10.1038/nature04428.

**Calais E, Han J Y, DeMets C, Nocquet J M, 2006.** Deformation of the North American plate interior from a decade of continuous GPS measurements. Journal of Geophysical Research, 111, B06402, doi:10.1029/2005JB004253.

**Carlsten S, Stråhle A, 2000.** Borehole radar and BIPS investigations in boreholes at the Boda area. SKB TR-01-02, Svensk Kärnbränslehantering AB.

**Chapman N A, McKinley I G, Smellie J A T, 1984.** The potential of natural analogues in assessing systems for deep disposal of high-level radioactive waste. SKB TR 84-16, Svensk Kärnbränslehantering AB.

**Chapman N A, McKinley I G, Shea M E, Smellie J A T (eds), 1993.** The Poços de Caldas project: natural analogues of processes in a radioactive waste repository. Amsterdam: Elsevier. (Reprinted from the Journal of Geochemical Exploration, 45, 1992.)

**Christiansson R, Ericsson L O, Gustafson G, 2009.** Hydraulic characterisation and conceptual modelling of the Excavation Disturbed Zone (EDZ). Proceedings of the 2009 International Symposium on Rock Mechanics "Rock Characterisation, Modelling and Engineering Design Methods" (Sinorock 2009), Hong Kong, 19–22 May 2009.

**Claesson Liljedahl L, Munier R, Sandström B, Drake H, Tullborg E-L, 2010.** Assessment of fractures classified as non-mineralised in the SICADA database. SKB R-11-02, Svensk Kärnbränslehantering AB.

**Clark I D, Matsumoto R, Dallimore S R, Lowe B, Loop J, 1999.** Isotope constraints on the origin of pore waters and salinity in the permafrost and gas-hydrate core intervals of the JAPEX/JNOC/GSC Mallik 2L-38 gas-hydrate research well. Geological Survey of Canada Bulletin, 544, pp 177–188.

**Cliffe K A, Kelly M, 2006.** COMP23 version 1.2.2 user's manual. SKB R-04-64, Svensk Kärnbränslehantering AB.

**Colleoni F, Krinner G, Jakobsson M, Peyaud V, Ritz C, 2009.** Influence of regional parameters on the surface mass balance of the Eurasian ice sheet during the peak Saalian (140 kya). Global and Planetary Change, 68, pp 132–148.

**Collins G S, Melosh H J, Marcus R A, 2005.** Earth Impact Effects Program: a web-based computer program for calculating the regional environmental consequences of a meteoroid impact on Earth. Meteoritics & Planetary Science, 40, pp 817–840.

**Coope G R, Lemdahl G, Lowe J J, Walkling A, 1998.** Temperature gradients in northern Europe during the last glacial–Holocene transition (14–9 $^{14}$C kyr BP) interpreted from coleopteran assemblages. Journal of Quaternary Science, 13, pp 419–433.

**Cooper R J, Wadham J L, Tranter M, Hodgkins R, Peters N E, 2002.** Groundwater hydrochemistry in the active layer of the proglacial zone, Finsterwalderbreen, Svalbard. Journal of Hydrology, 269, pp 208–223.

**Cosgrove J, Stanfors R, Röshoff K, 2006.** Geological characteristics of deformation zones and a strategy for their detection in a repository. SKB R-06-39, Svensk Kärnbränslehantering AB.

**Couture R A, 1985.** Steam rapidly reduces the swelling capacity of bentonite. Nature, 318, pp 50–52.

**Cowie P A, Scholz C H, 1992a.** Growth of faults by accumulation of seismic slip. Journal of Geophysical Research, 97, pp 11085–11095.

**Cowie P A, Scholz C H, 1992b.** Displacement-length scaling relationship for faults: data synthesis and discussion. Journal of Structural Geology, 14, pp 1149–1156.

**Cox P M, Hungingford C, Jones C D, 2006.** Conditions for sink-to-source transitions and runaway feedbacks from the land carbon cycle. In: Schellnhuber H J, Cramer W, Nakicenovic N, Wigley T, Yohe G (eds). Avoiding dangerous climate change. Cambridge: Cambridge University Press, pp 155–161.

**Cramer J J, Smellie J A T (eds), 1994.** Final report of the AECL/SKB Cigar Lake Analogue Study. SKB TR 94-04, Svensk Kärnbränslehantering AB. (Also published as AECL-10851, COG-93-147.)

**Cuadros J, Linares J, 1996.** Experimental kinetic study of the smectite-to-illite transformation. Geochimica et Cosmochimica Acta, 60, pp 439–453.

**Cui D, Low J, Sjöstedt C J, Spahiu K, 2004.** On Mo-Ru-Tc-Pd-Rh-Te alloy particles extracted from spent fuel and their leaching behaviour under Ar and $H_2$ atmospheres. Radiochimica Acta, 92, pp 551–555.

**Damjanac B, Fairhurst C, 2010.** Evidence for a long-term strength threshold in crystalline rock. Rock Mechanics and Rock Engineering, 43, pp 513–531.

**Dansgaard W, Johnsen S J, Clausen H B, Dahl-Jensen D, Gundestrup N S, Hammer C U, Hvidberg C S, Steffensen J P, Sveinbjörnsdottir A E, Jouzel J, Bond G, 1993.** Evidence for general instability of past climate from a 250-kyr ice-core record. Nature, 364, pp 218–220.

**Dawers, N H, Anders M H, Scholz C H, 1993.** Growth of normal faults: displacement-length scaling. Geology, 21, pp 1107–1110.

**Degueldre C, Baeyens B, Goerlich W, Riga J, Verbist J, Stadelmann P, 1989.** Colloids in water from a subsurface fracture in granitic rock, Grimsel Test Site, Switzerland. Geochimica et Cosmochimica Acta, 53, pp 603–610.

**Degueldre C, Grauer R, Laube A, Oess A, Silby H, 1996.** Colloid properties in granitic groundwater systems. II: Stability and transport study. Applied Geochemistry, 11, pp 697–710.

**Delos A, Trinchero P, Richard L, Molinero J, Dentz M, Pitkänen P, 2010.** Quantitative assessment of deep gas migration in Fennoscandian sites. SKB R-10-61, Svensk Kärnbränslehantering AB.

**Dillström P, Bolinder T, 2010.** Damage tolerance analysis of canister inserts for spent nuclear fuel in the case of an earthquake induced rock shear load. SKB TR-10-29, Svensk Kärnbränslehantering AB.

**Domènech C, Arcos D, Duro L, Grandia F, 2006.** Effect of the mineral precipitation-dissolution at tunnel walls during the operational and post-operational phases. SKB R-06-108, Svensk Kärnbränslehantering AB.

**Drew M C, 1983.** Plant injury and adaptation to oxygen deficiency in the root environment: a review. Plant and Soil, 75, pp 179–199.

**Dueck A, 2010.** Thermo-mechanical cementation effects in bentonite investigated by unconfined compression tests. SKB TR-10-41, Svensk Kärnbränslehantering AB.

**Duerden P, Lever D A, Sverjensky D A, Townley L R, 1992.** Summary of findings. Alligator Rivers Analogue Project, final report. Vol. 1. An OECD/NEA International Project Managed by ANSTO. SKI Report 92:20-1, Statens kärnkraftinspekton (Swedish Nuclear Power Inspectorate).

**Duro L, Grivé M, Cera E, Gaona X, Domènech C, Bruno J, 2006.** Determination and assessment of the concentration limits to be used in SR-Can. SKB TR-06-32, Svensk Kärnbränslehantering AB.

**Dverstorp B, Strömberg B, 2008.** SKI's and SSI's review of SKB's safety report SR-Can. SKI Report 2008:23, Statens kärnkraftinspektion (Swedish Nuclear Power Inspectorate), SSI Report 2008:04 E, Statens strålskyddsinstitut (Swedish Radiation Protection Authority).

**Dvinskikh S V, Szutkowski K, Furó I, 2009.** MRI profiles over very wide concentration ranges: application to swelling of a bentonite clay. Journal of Magnetic Resonance, 198, pp 146–150.

**Ekman M, 1996.** A consistent map of the postglacial uplift of Fennoscandia. Terra Nova, 8, pp 158–165.

**Ekström P-A, 2011.** Pandora – a simulation tool for safety assessments. Technical description and user's guide. SR-Site Biosphere. SKB R-11-01, Svensk Kärnbränslehantering AB.

**Elert M, Gylling B, Lindgren M, 2004.** Assessment model validity document FARF31. SKB R-04-51, Svensk Kärnbränslehantering AB.

**Eng T, Norberg E, Torbacke J, Jensen M, 1996.** Information, conservation and retrieval. SKB TR 96-18, Svensk Kärnbränslehantering AB.

**Engqvist A, Andrejev O, 2000.** Sensitivity analysis with regard to variations of physical forcing including two possible future hydrographic regimes for the Öregrundsgrepen. A follow-up baroclinic 3D-model study. SKB TR-00-01, Svensk Kärnbränslehantering AB.

**Enssle C P, Poppei J, 2010.** Implementation and testing of an improved methodology to simulate resaturation processes with DarcyTools. SKB R-09-54, Svensk Kärnbränslehantering AB.

**Ericsson L O, Brinkhoff P, Gustafson G, Kvartsberg S, 2009.** Hydraulic features of the Excavation Disturbed Zone. Laboratory investigations of samples taken from the Q- and S-tunnels at Äspö HRL. SKB R-09-45, Svensk Kärnbränslehantering AB.

**Eriksson S, 2007.** Äspö Hard Rock Laboratory. Prototype repository. Analysis of microorganisms, gases and water chemistry in buffer and backfill, 2004–2007. SKB IPR-08-01, Svensk Kärnbränslehantering AB.

**Eshelby J D, 1957.** The determination of the elastic field of an ellipsoidal inclusion, and related problems. Proceedings of the Royal Society of London. Series A, Mathematical and Physical Sciences, 241, pp 376–396.

**Evans D F, Wennerström H, 1999.** The colloidal domain: where physics, chemistry, biology, and technology meet. 2nd ed. New York: Wiley-VCH.

**Evins L Z, Jensen K A, Ewing R C, 2005.** Uraninite recrystallization and Pb loss in the Oklo and Bangombé natural fission reactors, Gabon. Geochimica et Cosmochimica Acta, 69, pp 1589–1606.

**FASSET, 2004.** FASSET – Framework for Assessment of Environmental Impact. Final report. A project within the EC 5th Framework Programme, Contract No FIGE-CT-2000-00102, project co-ordinator: Swedish Radiation Protection Authority.

**Fastook J L, 1994.** Modelling the Ice Age: the finite-element method in glaciology. Computational Science and Engineering, 1, pp 55–67.

**Fastook J L, Chapman J E, 1989.** A map plane finite-element model: three modelling experiments. Journal of Glaciology, 35, pp 48–52.

**Fastook J L, Holmlund P, 1994.** A glaciological model of the Younger Dryas event in Scandinavia. Journal of Glaciology, 40, pp 125–131.

**Fayek M, Harrison M T, Ewing R C, Grove M, Coath C D, 2002.** O and Pb isotopic analyses of uranium minerals by ion microprobe and U–Pb ages from the Cigar Lake deposit. Chemical Geology, 185, pp 205–225.

**FENCAT, 2007.** Historical earthquakes in northern Europe. [Online]. Available at: http://www.seismo.helsinki.fi/english/bulletins/catalog_northeurope.html. Institute of Seismology, University of Helsinki, Finland.

**Fenton C, Adams J, Halchuk S, 2006.** Seismic hazards assessment for radioactive waste disposal sites in regions of low seismic activity. Geotechnical and Geological Engineering, 24, pp 579–592.

**Follin S, 2008.** Bedrock hydrogeology Forsmark. Site descriptive modeling, SDM-Site Forsmark. SKB R-08-95, Svensk Kärnbränslehantering AB.

**Follin S, Johansson P-O, Hartley L, Jackson P, Roberts D, Marsic N, 2007a.** Hydrogeological conceptual model development and numerical modelling using CONNECTFLOW, Forsmark modelling stage 2.2. SKB R-07-49, Svensk Kärnbränslehantering AB.

**Follin S, Levén J, Hartley L, Jackson P, Joyce S, Roberts D, Swift B, 2007b.** Hydrogeological characterisation and modelling of deformation zones and fracture domains, Forsmark modelling stage 2.2. SKB R-07-48, Svensk Kärnbränslehantering AB.

**Forsyth R, 1997.** The SKB Spent Fuel Corrosion Programme. An evaluation of results from the experimental programme performed in the Studsvik Hot Cell laboratory. SKB TR 97-25, Svensk Kärnbränslehantering AB.

**Forsyth R S, Werme L O, 1992.** Spent fuel corrosion and dissolution. Journal of Nuclear Materials, 190, pp 3–19.

**Fox A, La Pointe P, Hermanson J, Öhman J, 2007.** Statistical geological discrete fracture network model. Forsmark modelling stage 2.2. SKB R-07-46, Svensk Kärnbränslehantering AB.

**Frape S K, Stotler R L, Ruskeeniemi T, Ahonen L, Paananen M, Hobbs M Y, 2004.** Hydrogeochemistry of groundwaters at and below the base of the permafrost at Lupin: Report of phase II. Report 06819-REP-01300-10047-R00, Ontario Power Generation, Nuclear Waste Management Division, Canada.

**Fredén C (ed), 2002.** Sveriges nationalatlas. Berg och jord (in Swedish). Stockholm: SNA publishing.

**French H M, 2007.** The periglacial environment. 3rd ed. Chichester: John Wiley and Sons.

**Fritz B, Kam M, Tardy Y, 1984.** Geochemical simulation of the evolution of granitic rocks and clay minerals submitted to a temperature increase in the vicinity of a repository for spent nuclear fuel. SKB/KBS TR 84-10, Svensk Kärnbränslehantering AB.

**Fritzell A, 2006.** Concerns when designing a safeguards approach for the back-end of the Swedish nuclear fuel cycle. SKI Report 2008:18, Statens kärnkraftinspektion (Swedish Nuclear Power Inspectorate).

**Funehag J, 2008.** Injekteringen av TASS-tunneln. Delresultat t o m september 2008. SKB R-08-123, Svensk Kärnbränslehantering AB.

**Fälth B, Hökmark H, 2006.** Seismically induced slip on rock fractures. Results from dynamic discrete fracture modeling. SKB R-06-48, Svensk Kärnbränslehantering AB.

**Fälth B, Hökmark H, 2007.** Mechanical and thermo-mechanical discrete fracture near-field analyses based on preliminary data from the Forsmark, Simpevarp and Laxemar sites. SKB R-06-89, Svensk Kärnbränslehantering AB.

**Fälth B, Hökmark H, Munier R, 2007.** Seismically induced shear displacements in repository host rock fractures. In: Proceedings of the 9th Canadian Conference on Earthquake Engineering, Ottawa, 26–29 June 2007.

**Fälth B, Hökmark H, Munier R, 2008.** Seismically induced slip on rock fractures – expanded study with particular account of large earthquakes. In: Yale D, Holtz S, Breeds C, Ozbay U (eds). Proceedings of the 42nd U.S. Rock Mechanics Symposium, San Fransisco, 29 June – 2 July 2008.

**Fälth B, Hökmark H, Munier R, 2010.** Effects of large earthquakes on a KBS-3 repository. Evaluation of modelling results and their implications for layout and design. SKB TR-08-11, Svensk Kärnbränslehantering AB.

**Galíndez J M, Molinero J, 2010.** Assessment of the long-term stability of cementitious barriers of radioactive waste repositories by using digital-image-based microstructure generation and reactive transport modeling. Cement and Concrete Research, 40, pp 1278–1289.

**Gascoyne M, 1999.** Long-term maintenance of reducing conditions in a spent nuclear fuel repository. A re-examination of critical factors. SKB R-99-41, Svensk Kärnbränslehantering AB.

**Gaucher E, Blanc P, Matray J-M, Michau N, 2004.** Modeling diffusion of an alkaline plume in a clay barrier. Applied Geochemistry, 19, pp 1505–1515.

**Gauthier-Lafaye F, Holliger P, Blanc P-L, 1996.** Natural fission reactors in the Franceville basion, Gabon: a review of the conditions and results of a "critical event" in a geologic system. Geochimica et Cosmochimica Acta, 60, pp 4831–4852.

**Gauthier-Lafaye F, Ledoux E, Smellie J, Louvat D, Michaud V, Pérez del Villar, Oversby V, Bruno J, 2000.** OKLO – natural analogue Phase II. Behaviour of nuclear reaction products in a natural environment: final report. EUR 19139, European Commission.

**Gierszewski P, Avis J, Calder N, D'Andrea A, Garisto F, Kitson C, Melnyk T, Wei K, Wojciechowski L, 2004.** Third case study – postclosure safety assessment. Report 06819-REP-01200-10109-R00, Ontario Power Generation, Nuclear Waste Management Division, Canada.

**Glamheden R, Fredriksson A, Röshoff K, Karlsson J, Hakami H, Christiansson R, 2007.** Rock mechanics Forsmark. Site descrpitive modelling Forsmark stage 2.2. SKB R-07-31, Svensk Kärnbränslehantering AB.

**Glamheden R, Fälth B, Jacobsson L, Harrström J, Berglund J, Bergkvist L, 2010.** Counterforce applied to prevent spalling. SKB TR-10-37, Svensk Kärnbränslehantering AB.

**Golian C, Lever D A, 1992.** Radionuclide Transport. Alligator Rivers Analogue Project. Final report. Vol. 14. An OECD/NEA International Project Managed by ANSTO. SKI Report 92:20-14, Statens kärnkraftinspektion (Swedish Nuclear Power Inspectorate).

**Grandia F, Domènech C, Arcos D, Duro L, 2006.** Assessment of the oxygen consumption in the backfill. Geochemical modelling in a saturated backfill. SKB R-06-106, Svensk Kärnbränslehantering AB.

**Grandia F, Galíndez J-M, Arcos D, Molinero J, 2010a.** Quantitative modelling of the degradation processes of cement grout. Project CEMMOD. SKB TR-10-25, Svensk Kärnbränslehantering AB.

**Grandia F, Galíndez J-M, Molinero J, Arcos D, 2010b.** Evaluation of low-pH cement degradation in tunnel plugs and bottom plate systems in the frame of SR-Site. SKB TR-10-62, Svensk Kärnbränslehantering AB.

**Gregory J M, Huybrechts P, 2006.** Ice-sheet contributions to future sea-level change. Philosophical Transactions of the Royal Society A, 364, pp 1709–1731.

**Grivé M, Domènech C, Montoya V, Garcia D, Duro L, 2010.** Determination and assessment of the concentration limits to be used in SR-Can. Supplement to TR-06-32. SKB R-10-50, Svensk Kärnbränslehantering AB.

**Gubner R, Andersson U, 2007.** Corrosion resistance of copper canister weld material. SKB TR-07-07, Svensk Kärnbränslehantering AB.

**Guimerà J, Duro L, Jordana S, Bruno J, 1999.** Effects of ice melting and redox front migration in fractured rocks of low permeability. SKB TR-99-19, Svensk Kärnbränslehantering AB.

**Gurban I, Laaksoharju M, Ledoux E, Made B, Salignac A L, 1998.** Indications of uranium transport around the reactor zone at Bagombé (Oklo). SKB TR 98-06, Svensk Kärnbränslehantering AB.

**Gustafsson B G, 2004.** Millennial changes of the Baltic Sea salinity. Studies of the sensitivity of the salinity to climate change. SKB TR-04-12, Svensk Kärnbränslehantering AB.

**Hallbeck L, 2009.** Microbial processes in glaciers and permafrost. A literature study on microbiology affecting groundwater at ice sheet melting. SKB R-09-37, Svensk Kärnbränslehantering AB.

**Hallbeck L, 2010.** Principal organic materials in a repository for spent nuclear fuel. SKB TR-10-19, Svensk Kärnbränslehantering AB.

**Hallbeck L, Pedersen K, 2008.** Explorative analysis of microbes, colloids and gases. SDM-Site Forsmark. SKB R-08-85, Svensk Kärnbränslehantering AB.

**Hallberg R, Engvall A-G, Wadsten T, 1984.** Corrosion of copper lightning conductor plates. British Corrosion Journal, 19, pp 85–88.

**Hallberg R, Östlund P, Wadsten T, 1988.** Inferences from a corrosion study of a bronze cannon, applied to high level nuclear waste disposal. Applied Geochemistry, 3, pp 273–280.

**Hamby D M, 1994.** A review of techniques for parameter sensitivity analysis of environmental models. Environmental Monitoring and Assessment, 32, pp 135–154.

**Harrington J F, Birchall D J, 2007.** Sensitivity of total stress to changes in externally applied water pressure in KBS-3 buffer bentonite. SKB TR-06-38, Svensk Kärnbränslehantering AB.

**Harrington J F, Horseman S T, 2003.** Gas migration in KBS-3 buffer bentonite. Sensitivity of test parameters to experimental boundary conditions. SKB TR-03-02, Svensk Kärnbränslehantering AB.

**Hartikainen J, 2004.** Permafrost modeling in DECOVALEX III for BMT3. In: Eloranta E (ed). DECOVALEX III, 1999–2003. An international project for the modelling of coupled thermo-hydro-mechanical processes for spent fuel disposal. Finnish national contributions. STUK-YTO-TR 209, Finnish Centre for Radiation and Nuclear Safety (STUK), Helsinki.

**Hartikainen J, Kouhia R, Wallroth T, 2010.** Permafrost simulations at Forsmark using a numerical 2D thermo-hydro-chemical model. SKB TR-09-17, Svensk Kärnbränslehantering AB.

**Hartley L, Hoch A, Jackson P, Joyce S, McCarthy R, Rodwell W, Swift B, Marsic N, 2006.** Groundwater flow and transport modelling during the temperate period for the SR-Can assessment. Forsmark area – version 1.2. SKB R-06-98, Svensk Kärnbränslehantering AB.

**Hartmann W K, 1965.** Terrestrial and lunar flux of large meteorites in the last two billion years. Icarus, 4, pp 157–165.

**Hedenström A, Risberg J, 2003.** Shore displacement in northern Uppland during the last 6500 calendar years. SKB TR-03-17, Svensk Kärnbränslehantering AB.

**Hedin A, 1997.** Spent nuclear fuel – how dangerous is it? A report from the project "Description of risk". SKB TR 97-13, Svensk Kärnbränslehantering AB.

**Hedin A, 2002a.** Safety assessment of a spent nuclear fuel repository: sensitivity analyses for prioritisation of research. In: Bonano E J, Camp A L, Majors M J, Thomson R A (eds). Proceedings of the 6th International Conference on Probabilistic Safety Assessment and Management, PSAM6, San Juan, Puerto Rico, 23–28 June 2002. Oxford: Elsevier.

**Hedin A, 2002b.** Integrated analytic radionuclide transport model for a spent nuclear fuel repository in saturated fractured rock. Nuclear Technology, 138, pp 179–205.

**Hedin A, 2003.** Probabilistic dose calculations and sensitivity analyses using analytic models. Reliability Engineering & System Safety, 79, pp 195–204.

**Hedin A, 2004a.** Methodology for risk assessment of an SNF repository in Sweden. In: Spitzer C, Schmocker U, Dang V N (eds). Proceedings of the 7th International Conference on Probabilistic Safety Assessment and Management, PSAM7, Berlin, 14–18 June 2004. London: Springer-Verlag.

**Hedin A, 2004b.** Integrated near-field evolution model for a KBS-3 repository. SKB R-04-36, Svensk Kärnbränslehantering AB.

**Hedin A, 2008a.** Risk, Uncertainty and Sensitivity Analyses in a Recent Safety Assessment of a Spent Nuclear Fuel Repository in Sweden. In: Kao T M, Zio E, Ho V (eds). Proceedings of the 9th International Conference on Probabilistic Safety Assessment and Management, PSAM9, Hong Kong, 18–23 May 2008. Hong Kong: Edge Publication Group.

**Hedin A, 2008b.** Semi-analytic stereological analysis of waste package/fracture intersections in a granitic rock nuclear waste repository. Mathematical Geosciences, 40, pp 619–637.

**Helmens K F, 2009.** Climate, vegetation and lake development at Sokli (northern Finland) during early MIS 3 at ~50 kyr. Revising earlier concepts on climate, glacial and vegetation dynamics in Fennoscandia during the Weichselian. SKB TR-09-16, Svensk Kärnbränslehantering AB.

**Helton J C, 1993.** Uncertainty and sensitivity analysis techniques for use in performance assessment for radioactive waste disposal. Reliability Engineering & System Safety, 42, pp 327–367.

**Hernelind J, 2010.** Modelling and analysis of canister and buffer for earthquake induced rock shear and glacial load. SKB TR-10-34, Svensk Kärnbränslehantering AB.

**Hetzel F, Doner H E, 1993.** Some colloidal properties of beidellite: comparison with low and high charge montmorillonites. Clays and Clay Minerals, 41, pp 453–460.

**Hohl V, 2005.** Northern European long term climate archives. SKB TR-05-01, Svensk Kärnbränslehantering AB.

**Holden B, Stotler R L, Frape S K, Ruskeeniemi T, Talikka M, Freifeld B M, 2009.** High Lake permafrost comparison site: permafrost phase IV. NWMO TR-2009-11, Nuclear Waste Management Organization, Canada.

**Hora S, 2002.** Expert opinion in SR 97 and the SKI/SSI joint review of SR 97. SSI Report 2002:20, Statens strålskyddsinstitut (Swedish Radiation Protection Authority).

**Hora S, Jensen M, 2002.** Expert judgement elicitation. SSI report 2002:19, Statens strålskyddsinstitut (Swedish Radiation Protection Authority).

**Hora S, Jensen M, 2005.** Expert panel elicitation of seismicity following glaciation in Sweden. SSI Report 2005:20, Statens strålskyddsinstitut (Swedish Radiation Protection Authority).

**Howard B J, Beresford N A, Andersson P, Brown J E, Copplestone D, Beaugelin-Seiller K, Garnier-Laplace J, Howe P D, Oughton D, Whitehouse P, 2010.** Protection of the environment from ionizing radiation in a regulatory context – an overview of the PROTECT coordinated action project. Journal of Radiological Protection, 30, pp 191–194.

**Huang W-L, Longo J M, Pevear D R, 1993.** An experimentally derived kinetic model for smectite-to-illite conversion and its use as a geothermometer. Clays and Clay Minerals, 41, pp 162–177.

**Huertas F J, Rozalen M L, Garcia-Palma S, Iriarte, Linares J, 2005.** Dissolution kinetics of bentonite under alkaline conditions. In: Ecoclay II: effects of cement on clay barrier performance – Phase II. Final report. EUR 21921, European Commission, pp 132–142.

**Humlum O, Houmark-Nielsen M, 1994.** High deglaciation rates in Denmark during the late Weichselian – implications for the palaeoenvironment. Geografisk Tidsskrift, 94, pp 26–37.

**Huybrechts P, 1990.** A 3-D model for the Antarctic ice sheet: a sensitivity study on the glacial-interglacial contrast. Climate Dynamics, 5, pp 79–92.

**Huybrechts P, de Wolde J, 1999.** The dynamic response of the Greenland and Antarctic ice sheets to multiple-century climate warming. Journal of Climate, 12, pp 2169–2188.

**Hökmark H, Karnland O, Pusch R, 1997.** A technique for modeling transport/conversion processes applied to smectite-to-illite conversion in HLW buffers. Engineering Geology, 47, pp 367–378.

**Hökmark H, Fälth B, Wallroth T, 2006.** T-H-M couplings in rock. Overview of results of importance to the SR-Can safety assessment. SKB R-06-88, Svensk Kärnbränslehantering AB.

**Hökmark H, Lönnqvist M, Kristensson O, Sundberg J, Hellström G, 2009.** Strategy for thermal dimensioning of the final repository for spent nuclear fuel. SKB R-09-04, Svensk Kärnbränslehantering AB.

**Hökmark H, Lönnqvist M, Fälth B, 2010.** THM-issues in repository rock. Thermal, mechanical, thermo-mechanical and hydromechanical evolution of the rock at the Forsmark and Laxemar sites. SKB TR-10-23, Svensk Kärnbränslehantering AB.

**IAEA, 1994.** Safety indicators in different time frames for the safety assessment of underground radioactive waste repositories. First report of the INWAC Subgroup on Principles and Criteria for Radioactive Waste Disposal. IAEA-TECDOC-767, International Atomic Energy Agency.

**IAEA, 2010.** Handbook of parameter values for the prediction of radionuclide transfer to humans in terrestrial and freshwater environments. Vienna: International Atomic Energy Agency. (IAEA Technical Reports Series 472)

**ICRP, 2000.** Radiation protection recommendations as applied to the disposal of long-lived solid radioactive waste. Oxford: Pergamon. (ICRP Publication 81; Annals of the ICRP 28)

**ICRP, 2007.** The 2007 recommendations of the International Commission on Radiological Protection. Oxford: Pergamon. (ICRP Publication 103; Annals of the ICRP 37)

**Iman R L, Conover W J, 1979.** The use of the rank transform in regression. Technometrics, 21, pp 499–509.

**Imbrie J, Hays J D, Martinson D G, McIntyre A, Mix A C, Morley J J, Pisias N G, Prell W L, Shackleton N J, 1984.** The orbital theory of Pleistocene climate: support from a revised chronology of the marine $\delta^{18}O$ record. In: Berger A L, Imbrie J, Hays J D, Kukla G, Saltzman B (eds). Milankovitch and climate: understanding the response to astronomical forcing. Dordrecht: Reidel, pp 269–305.

**INSITE/OVERSITE, 2008.** International expert review of SR-Can: site investigation aspects. External review contribution in support of SKI's and SSI's review of SR-Can. SKI Report 2008:09, Statens kärnkraftinspektion (Swedish Nuclear Power Inspectorate), SSI Report 2008:11, Statens strålskyddsinstitut (Swedish Radiation Protection Authority).

**IPCC, 2007.** Climate Change 2007: the physical science basis. Contribution of Working Group I to the Fourth Assessment Report of the Intergovernmental Panel on Climate Change, 2007. Solomon S, Qin D, Manning M, Chen Z, Marquis M, Averyt K B, Tignor M, Miller H L (eds). Cambridge: Cambridge University Press.

**Isaksson H, Keisu M, Lindholm T, Martinson O, Mattsson H, Thunehed H, Triumf C-A, 2010.** The geophysical response from a KBS-3 repository for spent nuclear fuel. Theoretical modelling based on physical properties of underground constructions at Forsmark. SKB P-10-39, Svensk Kärnbränslehantering AB.

**Itasca, 2007.** 3DEC – 3-Dimensional Distinct Element Code. Version 4.1. User's guide. Minneapolis: Itasca Consulting Group.

**Janeczek J, Ewing R C, Oversby V M, Werme L O, 1996.** Uraninite and $UO_2$ in spent nuclear fuel: a comparison. Journal of Nuclear Materials, 238, pp 121–130.

**Jansson, P, 1997.** Longitudinal coupling effects in ice flow across a subglacial ridge. Annals of Glaciology, 24, pp 169–174.

**Jansson P, Näslund J-O, 2009.** Spatial and temporal variations in glacier hydrology on Storglaciären, Sweden. SKB TR-09-13, Svensk Kärnbränslehantering AB.

**Jansson P, Näslund J-O, Rodhe L, 2007.** Ice sheet hydrology – a review. SKB TR-06-34, Svensk Kärnbränslehantering AB.

**Jensen K A, Palenik C S, Ewing R C, 2002.** $U^{6+}$ phases in the weathering zone of the Bangombé U-deposit: observed and predicted mineralogy. Radiochimica Acta, 90, pp 761–769.

**JNC, 2000.** H12 – Project to establish the scientific and technical basis for HLW disposal in Japan main report and four supplementary reports. JNC Technical Report TN1410 2000-001, JNC TN1410 2000-002 – 005, Japan Nuclear Fuel Cycle Development Institute.

**Jockwer N, Wieczorek K, 2003.** Gas generation measurements in the FEBEX project (Abstract). In: Clays in natural and engineered barriers for radioactive waste confinement: proceeding from the international meeting held in Reims, 9–12 December 2002. Châtenay-Malabry: Agence nationale pour la gestion des déchets radioactifs (Andra), pp 108–117.

**Johannesson L-E, 2007.** Äspö Hard Rock Laboratory. Canister Retrieval Test. Dismantling and sampling of the buffer and determination of density and water ratio. SKB IPR-07-16, Svensk Kärnbränslehantering AB.

**Johannesson L-E, Nilsson U, 2006.** Deep repository – engineered barrier systems. Geotechnical behaviour of candidate backfill materials. Laboratory tests and calculations for determining performance of the backfill. SKB R-06-73, Svensk Kärnbränslehantering AB.

**Johannesson L-E, Sandén T, Dueck A, Ohlsson L, 2010.** Characterization of a backfill candidate material, IBECO-RWC-BF. Baclo Project – Phase 3. SKB R-10-44, Svensk Kärnbränslehantering AB.

**Johnson A B, Francis B, 1980.** Durability of metals from archeological objects, metal meteorites, and native metals. Report PNL-3198, UC-70, Pacific Northwest Laboratory, U.S. Department of Energy, Richland, Washington.

**Johnston A C, 1987.** Suppression of earthquakes by large continental ice sheets. Nature, 330, pp 467–469.

**Johnston A C, 1996.** A wave in the Earth. Science, 274, p 735.

**Jonsson M, Bäckström A, Quanhong F, Berglund J, Johansson M, Mas Ivars D, Olsson M, 2009a.** ÄSPÖ Hard Rock Laboratory. Studies of factors that affect and control the Excavation Damaged/Disturbed Zone. SKB R-09-17, Svensk Kärnbränslehantering AB.

**Jonsson M, Hakami H, Ekneligoda T, 2009b.** Analysis of the effect of vibrations on the bentonite buffer in the canister hole. SKB R-09-40, Svensk Kärnbränslehantering AB.

**Joyce S, Applegate D, Hartley L, Hoek J, Swan D, Marsic N, Follin S, 2010.** Groundwater flow modelling of periods with temperate climate conditions – Forsmark. SKB R-09-20, Svensk Kärnbränslehantering AB.

**Kahn A, 1958.** The flocculation of sodium montmorillonite by electrolytes. Journal of Colloid Science, 13, pp 51–60.

**Karlsson A, Eriksson C, Borell Lövstedt C, Liungman O, Engqvist A, 2010.** High-resolution hydrodynamic modelling of the marine environment at Forsmark between 6500 BC and 9000 AD. SKB R-10-09, Svensk Kärnbränslehantering AB.

**Karnland O, 2010.** Chemical and mineralogical characterization of the bentonite buffer for the acceptance control procedure in a KBS-3 repository. SKB TR-10-60, Svensk Kärnbränslehantering AB.

**Karnland O, Birgersson M, 2006.** Montmorillonite stability with special respect to KBS-3 conditions. SKB TR-06-11, Svensk Kärnbränslehantering AB.

**Karnland O, Olsson S, Nilsson U, 2006.** Mineralogy and sealing properties of various bentonites and smectite-rich clay materials. SKB TR-06-30, Svensk Kärnbränslehantering AB.

**Kautsky U (ed), 2001.** The biosphere today and tomorrow in the SFR area. SKB R-01-27, Svensk Kärnbränslehantering AB.

**Kellner E, 2003.** Wetlands – different types, their properties and functions. SKB TR-04-08, Svensk Kärnbränslehantering AB.

**Kelly M, Cliffe K A, 2006.** Validity document for COMP23. SKB R-06-76, Svensk Kärnbränslehantering AB.

**Kersting A B, Efurd D W, Finnegan D L, Rokop D J, Smith D K, Thompson J L, 1999.** Migration of plutonium in ground water at the Nevada Test Site. Nature, 397, pp 56–59.

**Kim Y-S, Sanderson D J, 2008.** Earthquake and fault propagation, displacement and damage zones. In: Landowe S J, Hammler G M (eds). Structural geology: new research. New York: Nova Science.

**Kim Y-S, Peacock D C P, Sanderson D J, 2004.** Fault damage zones. Journal of Structural Geology, 26, pp 503–517.

**King F, 1995.** A natural analogue for the long-term corrosion of copper nuclear waste containers – reanalysis of a study of a bronze cannon. Applied Geochemistry, 10, pp 477–487.

**King F, Lilja C, Pedersen K, Pitkänen P, Vähänen M, 2010.** An update of the state-of-the-art report on the corrosion of copper under expected conditions in a deep geologic repository. SKB TR-10-67, Svensk Kärnbränslehantering AB.

**King-Clayton L, Chapman N, Ericsson L O, Kautsky F (eds), 1997.** Glaciation and hydrogeology. Proceedings of the workshop on the impact of climate change & glaciations on rock stresses, groundwater flow and hydrochemistry: past, present and future. Hässelby, Sweden, 17–19 April 1996. SKI Report 97:13, Statens kärnkraftinspektion (Swedish Nuclear Power Inspectorate).

**Kjellander R, Marčelja S, Quirk J P, 1988.** Attractive double-layer interactions between calcium clay particles. Journal of Colloid and Interface Science, 126, pp 194–211.

**Kjellström E, Strandberg G, Brandefelt J, Näslund J-O, Smith B, Wohlfarth B, 2009.** Climate conditions in Sweden in a 100,000 year time perspective. SKB TR-09-04, Svensk Kärnbränslehantering AB.

**Koistinen T, Stephens M, Bogatchev V, Nordgulen Ø, Wennerstrom M, Korhonen J V, 2004.** Geological map of the Fennoscandian Shield 1:2,000,000. Espoo: Geological Survey of Finland, Trondheim: Geological Survey of Norway, Uppsala: Geological Survey of Sweden, Moscow: Ministry of Natural Resources of Russia.

**Krabill W, Abdalati W, Frederick E, Manizade S, Martin C, Sonntag J, Swift R, Thomas R, Wright W, Yungel J, 2000.** Greenland ice sheet: high elevation balance and peripheral thinning. Science, 289, pp 428–430.

**Kujansuu R, 1964.** Nuorista siirroksista Lapissa (Recent faulting in Lapland) (in Finnish). Geologi, 16, pp 30–36.

**Kumblad L, Kautsky U, 2004.** Models for transport and fate of carbon, nutrients and point source released radionuclides to an aquatic ecosystem. SKB TR-04-13, Svensk Kärnbränslehantering AB.

**Laaksoharju M, Smellie J, Tullborg E-L, Gimeno M, Hallbeck L, Molinero J, Waber N, 2008.** Bedrock hydrogeochemistry Forsmark. Site descriptive modelling, SDM-Site Forsmark. SKB R-08-47, Svensk Kärnbränslehantering AB.

**Lagaly G, Ziesmer S, 2003.** Colloid chemistry of clay minerals: the coagulation of montmorillonite dispersions. Advances in Colloid and Interface Science, 100-102, pp 105–128.

**Lagerbäck R, 1979.** Neotectonic structures in northern Sweden. Geologiska Föreningens i Stockholm Förhandlingar, 100, pp 263–269.

**Lagerbäck R, Sundh M, 2008.** Early Holocene faulting and paleoseismicity in northern Sweden. Research Paper C 836, Sveriges Geologiska Undersökning.

**Lagerbäck R, Sundh M, Svedlund J-O, Johansson H, 2005.** Forsmark site investigation. Searching for evidence of late- or postglacial faulting in the Forsmark region. Results from 2002–2004. SKB R-05-51, Svensk Kärnbränslehantering AB.

**Lagerbäck R, Sundh M, Svantesson S-I, 2006.** Oskarshamn site investigation. Searching for evidence of late- or postglacial faulting in the Oskarshamn region. Results from 2005. SKB P-06-160, Svensk Kärnbränslehantering AB.

**Lambe T W, Whitman R V, 1969.** Soil mechanics. New York: Wiley.

**Lambeck K, Purcell A, Funder S, Kjær K H, Larsen E, Möller P, 2006.** Constraints on the Late Saalian to early Middle Weichselian ice sheet of Eurasia from field data and rebound modelling. Boreas, 35, pp 539–575.

**Lambeck K, Purcell A, Zhao J, Svensson N-O, 2010.** The Scandinavian Ice Sheet: from MIS 4 to the end of the Last Glacial Maximum. Boreas, 39, pp 410–435.

**Lang C, Leuenberger M, Schwander J, Johnsen S, 1999.** 16°C rapid temperature variation in Central Greenland 70,000 years ago. Science, 286, pp 934–937.

**Lantenois S, Lanson B, Muller F, Bauer A, Jullien M, Plançon A, 2005.** Experimental study of smectite interaction with metal Fe at low temperature: 1. Smectite destabilization. Clays and Clay Minerals, 6, pp 597–612.

**La Pointe P R, Cladouhos T T, Outters N, Follin S, 2000.** Evaluation of the conservativeness of the methodology for estimating earthquake-induced movements of fractures intersecting canisters. SKB TR-00-08, Svensk Kärnbränslehantering AB.

**La Pointe P R, Cladouhos T, Follin S, 2002.** Development, application, and evaluation of a methodology to estimate distributed slip on fractures due to future earthquakes for nuclear waste repository performance assessment. Bulletin of the Seismological Society of America, 92, pp 923–944.

**Lemdahl G, 1988.** Palaeoclimatic and palaeoecological studies based on subfossil insects from Late Weichselian sediments in southern Sweden. Ph. D. thesis. Department of Quaternary Geology, Lund University, Sweden.

**Lidmar-Bergström K, Näslund J-O, 2002.** Landforms and uplift in Scandinavia. In: Doré A G, Cartwright J A, Stoker M S, Turner J P, White N (eds). Exhumation of the North Atlantic margin: timing, mechanisms, and implications for petroleum exploration. London: Geological Society. (Special publication 196), pp 103–116.

**Lindborg T (ed), 2008.** Surface system Forsmark. Site descriptive modelling, SDM-Site Forsmark. SKB R-08-11, Svensk Kärnbränslehantering AB.

**Lindborg T (ed), 2010.** Landscape Forsmark – data, methodology and results for SR-Site. SKB TR-10-05, Svensk Kärnbränslehantering AB.

**Lindroos H, Isaksson H, Thunehed H, 2004.** The potential for ore and industrial minerals in the Forsmark area. SKB R-04-18, Svensk Kärnbränslehantering AB.

**Liu J, Neretnieks I, 2006.** Physical and chemical stability of the bentonite buffer. SKB R-06-103, Svensk Kärnbränslehantering AB.

**Liu L, Moreno L, Neretnieks I, 2009.** A dynamic force balance model for colloidal expansion and its DLVO-based application. Langmuir, 25, pp 679–687.

**Liu L, Moreno L, Neretnieks I, Gylling B, 2010.** A safety assessment approach using coupled NEAR3D and CHAN3D – Forsmark. SKB R-10-69, Svensk Kärnbränslehantering AB.

**Lokrantz H, Sohlenius G, 2006.** Ice marginal fluctuations during the Weichselian glaciation in Fennoscandia, a literature review. SKB TR-06-36, Svensk Kärnbränslehantering AB.

**Loutre M F, Berger A, 2000.** Future climatic changes: are we entering an exceptionally long interglacial? Climatic Change, 46, pp 61–90.

**Ludvigson J-E, 2002.** Brunnsinventering i Forsmark (in Swedish). SKB R-02-17, Svensk Kärnbränslehantering AB.

**Luna M, Arcos D, Duro L, 2006.** Effects of grouting, shotcreting and concrete leachates on backfill geochemistry. SKB R-06-107, Svensk Kärnbränslehantering AB.

**Lund B, 2005.** Effects of deglaciation on the crustal stress field and implications for endglacial faulting: a parametric study of simple Earth and ice models. SKB TR-05-04, Svensk Kärnbränslehantering AB.

**Lund B, 2006.** Stress variations during a glacial cycle at 500 m depth in Forsmark and Oskarshamn: Earth model effects. SKB R-06-95, Svensk Kärnbränslehantering AB.

**Lund B, Näslund J-O, 2009.** Glacial isostatic adjustment: implications for glacially induced faulting and nuclear waste repositories. In: Connor C B, Chapman N A, Connor L J (eds). Volcanic and tectonic hazard assessment for nuclear facilities. Cambridge: Cambridge University Press, pp 142–155.

**Lund B, Schmidt P, Hieronymus C, 2009.** Stress evolution and fault stability during the Weichselian glacial cycle. SKB TR-09-15, Svensk Kärnbränslehantering AB.

**Lundquist J, Lagerbäck R, 1976.** The Pärve Fault: a late-glacial fault in the Precambrian of Swedish Lapland. Geologiska Föreningens i Stockholm Förhandlingar, 98, pp 45–51.

**Luukkonen A, 2008.** Äspö Hard Rock Laboratory. Prototype repository. Inverse modelling of a prototype repository using near-field groundwater samples from July 1998 – March 2004. SKB IPR-08-06, Svensk Kärnbränslehantering AB.

**Lythe M, Vaughan D G, the BEDMAP Consortium, 2001.** BEDMAP: a new ice thickness and subglacial topographic model of Antarctica. Journal of Geophysical Research, 106, pp 11335–11351.

**Löfgren A (ed), 2010.** The terrestrial ecosystems at Forsmark and Laxemar-Simpevarp. SR-Site Biosphere. SKB TR-10-01, Svensk Kärnbränslehantering AB.

**Lönnqvist M, Hökmark H, 2010.** Assessment of potential for glacially induced hydraulic jacking at different depths. SKB R-09-35, Svensk Kärnbränslehantering AB.

**Marcos N, 1989.** Native copper as a natural analogue for copper canisters. Report YJT-89-18, Nuclear Waste Commission of Finnish Power Companies.

**Marcos N, Ahonen L, Bros R, Roos P, Suksi J, Oversby V, 1999.** New data on the Hyrkkölä native copper mineralization: a natural analogue for the long-term corrosion of copper canisters. In: Wronkiewicz D J, Lee J H (eds). Scientific basis for nuclear waste management XXII: symposium held in Boston, Massachusetts, 30 November – 4 December 1998. Warrendale, PA: Materials Research Society. (Materials Research Society Symposium Proceedings 556), pp 825–832.

**Marrett R, Allmendinger R W, 1990.** Kinematic analysis of fault-slip data. Journal of Structural Geology, 12, pp 973–986.

**Martin C D, 2005.** Preliminary assessment of potential underground stability (wedge and spalling) at Forsmark, Simpevarp and Laxemar sites. SKB R-05-71, Svensk Kärnbränslehantering AB.

**Martin C D, Kaiser P K, 1996.** Mine-by Experiment Committee Report, Phase 1: excavation response, summary and implications. AECL Report AECL-11382, Atomic Energy of Canada Limited.

**Martinerie P, Raynaud D, Etheridge D M, Barnola J-M, Mazaudier D, 1992.** Physical and climatic parameters which influence the air content in polar ice. Earth and Planetary Science Letters, 112, pp 1–13.

**Masurat P, Eriksson S, Pedersen K, 2010a.** Evidence of indigenous sulphate-reducing bacteria in commercial Wyoming bentonite MX-80. Applied Clay Science, 47, pp 51–57.

**Masurat P, Eriksson S, Pedersen K, 2010b.** Microbial sulphide production in compacted Wyoming bentonite MX-80 under in situ conditions relevant to a repository for high-level radioactive waste. Applied Clay Science, 47, pp 58–64.

**Matthiesen H, Hilbert L R, Gregory D J, 2003.** Siderite as a corrosion product on archaeological iron from a waterlogged environment. Studies in Conservation, 48, pp 183–194.

**Matthiesen H, Hilbert L R, Gregory D, Sørensen B, 2004.** Corrosion of archaeological iron artefacts compared to modern iron at the waterlogged site Nydam, Denmark. Prediction of long term corrosion behaviour in nuclear waste system. In: Andra (ed). Long term prediction and modelling of corrosion: proceedings of the 2nd International Workshop organized by the Working Party on nuclear corrosion (WP4) of the European Federation of Corrosion (EFC), Nice, 12–16 September 2004 (Eurocorr 2004), pp 114–127.

**Mazotti S, James T S, Henton J, Adams J, 2005.** GPS crustal strain, postglacial rebound, and seismic hazard in eastern North America: the Saint Lawrence valley example. Journal of Geophysical Research, 110, B11301, doi:10.1029/2004JB003590.

**McNeil M B, Little B J, 1992.** Corrosion mechanisms for copper and silver objects in near-surface environments. Journal of the American Institute for Conservation, 31, pp 355–366.

**Melosh H J, 1989.** Impact cratering: a geologic process. New York: Oxford University Press.

**Miller W, Alexander R, Chapman N, McKinley I, Smellie J, 2000.** Geological disposal of radioactive wastes and natural analogues: lessons from nature and archaeology. Amsterdam: Pergamon. (Waste Management Series 2)

**Miller B, Lind A, Savage D, Maul P, Robinson P, 2002.** Natural elemental concentrations and fluxes: their use as indicators of repository safety. SKI Report 02:3, Statens kärnkraftinspektion (Swedish Nuclear Power Inspectorate), SSI report 2002:02, Statens strålskyddsinstitut (Swedish Radiation Protection Authority).

**Milne, G A, Gehrels W R, Hughes C W, Tamisiea M E, 2009.** Identifying the causes of sea-level change. Nature Geoscience, 2, pp 471–478.

**Milodowski A E, Styles M T, Horstwood M S A, Kemp S J, 2002.** Alteration of uraniferous and native copper concretions in the Permian mudrocks of south Devon, United Kingdom. A natural analogue study of the corrosion of copper canisters and radiolysis effects in a repository for spent nuclear fuel. SKB TR-02-09, Svensk Kärnbränslehantering AB.

**Mitrovica J X, Milne G A, 2003.** On post-glacial sea level: I. General theory. Geophysical Journal International, 154, pp 253–267.

**Mitrovica J X, Gomez N, Clark P U, 2009.** The sea-level fingerprint of West Antarctic collapse. Science, 323, p 753.

**Moberg A, Sonechkin D M, Holmgren K, Datsenko N M, Karlén W, 2005.** Highly variable Northern Hemisphere temperatures reconstructed from low- and high-resolution proxy data. Nature, 433, pp 613–617.

**Moberg A, Gouirand I, Wohlfarth B, Schoning K, Kjellström E, Rummukainen M, de Jong R, Linderholm H, Zorita E, 2006.** Climate in Sweden during the past millennium – Evidence from proxy data, instrumental data and model simulations. SKB TR-06-35, Svensk Kärnbränslehantering AB.

**Molinero-Huguet J, Samper-Calvete F J, Zhang G, Yang C, 2004.** Biogeochemical reactive transport model of the Redox Zone experiment of the Äspö Hard Rock Laboratory in Sweden. Nuclear Technology, 148, pp 151–165.

**Morbidelli A, Bottke W F, Froeschlé C, Michel P, 2002.** Origin and evolution of near-Earth objects. In: Bottke W F, Cellino P, Paolicchi P, Binzel R P (eds). Asteroids III. Tucson: University of Arizona Press, pp 409–422.

**Morén L, Ritchey T, Stenström M, 1998.** Scenarier baserade på mänskliga handlingar. Tre arbetsmöten om metod- och säkerhetsanalysfrågor (Scenarios based on human actions. Three workshops on issues related to method and safety assessment) (in Swedish). SKB R-98-54, Svensk Kärnbränslehantering AB.

**Moreno L, Neretnieks I, Liu L, 2010.** Modelling of erosion of bentonite by gel/sol flow. SKB TR-10-64, Svensk Kärnbränslehantering AB.

**Motamedi M, Karnland O, Pedersen K, 1996.** Survival of sulfate reducing bacteria at different water activities in compacted bentonite. FEMS Microbiology Letters, 141, pp 83–87.

**Muir Wood R, 1993.** A review of the seismotectonics of Sweden. SKB TR 93-13, Svensk Kärnbränslehantering AB.

**Muir Wood R, 1995.** Reconstructing the tectonic history of Fennoscandia from its margins: The past 100 million years. SKB TR 95-36, Svensk Kärnbränslehantering AB.

**Muir Wood R, 2000.** Deglaciation seismotectonics: a principal influence on intraplate seismogenesis at high latitudes. Quaternary Science Reviews, 19, pp 1399–1411.

**Muir Wood R, Gregersen S, Basham P W, 1989.** Extraordinary deglaciation reverse faulting in northern Fennoscandia. In: Gregersen S, Basham P W (eds). Earthquakes at North-Atlantic passive margins: neotectonics and postglacial rebound. Boston: Kluwer Academic Publishers. (NATO Advanced Study Institutes Series C, Mathematical and Physical Sciences 266), pp 141–173.

**Munier R, 2006.** Using observations in deposition tunnels to avoid intersections with critical fractures in deposition holes. SKB R-06-54, Svensk Kärnbränslehantering AB.

**Munier R, 2007.** Demonstrating the efficiency of the EFPC criterion by means of sensitivity analyses. SKB R-06-115, Svensk Kärnbränslehantering AB.

**Munier R, 2010.** Full perimeter intersection criteria. Definitions and implementations in SR-Site. SKB TR-10-21, Svensk Kärnbränslehantering AB.

**Munier R, Hökmark H, 2004.** Respect distances. Rationale and means of computation. SKB R-04-17, Svensk Kärnbränslehantering AB.

**Munier R, Stenberg L, Stanfors R, Milnes A G, Hermanson J, Triumf C-A, 2003.** Geological Site Descriptive Model. A strategy for the model development during site investigations. SKB R-03-07, Svensk Kärnbränslehantering AB.

**Munier R, Hökmark H, Fälth B, 2008.** Respect distances: rationale and means of computation. In: Ahlbom K, Stephens M (eds). Investigations of potential repository sites for spent nuclear fuel at Forsmark and Laxemar-Simpevarp, Sweden. Abstracts, 33rd International Geological Congress, Oslo. SKB R-08-97, Svensk Kärnbränslehantering AB, p 57.

**Muzeau B, Jégou C, Delaunay F, Broudic V, Brevet A, Catalette H, Simoni E, Corbel C, 2009.** Radiolytic oxidation of $UO_2$ pellets doped with alpha emitters ($^{238/239}Pu$). Journal of Alloys and Compounds, 467, pp 578–589.

**Mårtensson E, Gustafsson L-G, 2010.** Hydrological and hydrogeological effects of an open repository in Forsmark. Final MIKE SHE flow modelling results for the Environmental Impact Assessment. SKB R-10-18, Svensk Kärnbränslehantering AB.

**Mäder U, Frieg B, Puigdomenech I, Decombarieu M, Yui M, 2004.** Hyperalkaline cement leachate-rock interaction and radionuclide transport in a fractured host rock (HPF Project). In: Oversby V M, Werme L O (eds). Scientific basis for nuclear waste management XXVII: symposium held in Kalmar, Sweden, 15–19 June 2003. Warrendale, PA: Materials Research Society. (Materials Research Society Symposium Proceedings 807), pp 861–866.

**Mörner N-A, 1989.** Postglacial faults and fractures on Äspö. SKB HRL Progress Report 25-89-24, Svensk Kärnbränslehantering AB.

**Mörner N-A, 2003.** Paleoseismicity of Sweden: a novel paradigm. Stockholm: N.-A. Mörner.

**Mörner N-A, 2004.** Active faults and paleoseismicity in Fennoscandia, especially Sweden: primary structures and secondary effects. Tectonophysics, 380, pp 139–157.

**Nagra, 2002.** Project Opalinus Clay. Safety report. Demonstration of disposal feasibility of spent fuel, vitrified high-level waste and long-lived intermediate-level waste (Entsorgungsnachweis). Nagra Technical Report NTB 02-05, National Cooperative for the Disposal of Radioactive Waste, Switzerland.

**Naudet R, 1991.** Oklo: des réacteurs nucléaires fossiles, étude physique. Paris: Commisariat à l'Energie Atomique.

**NEA, 1991.** Disposal of radioactive waste: review of safety assessment methods: a report of the Performance Assessment Advisory Group of the Radioactive Waste Management Committee, OECD Nuclear Energy Agency. Paris: Nuclear Energy Agency, Organisation for Economic Co-operation and Development.

**NEA, 1993.** Palaeohydrogeological methods and their application: proceedings of a NEA workshop, Paris, 9–10 November 1992. Paris: Nuclear Energy Agency, Organisation for Economic Co-operation and Development.

**NEA, 1995.** Future human actions at disposal sites: a report from the NEA Working Group on Assessment of Future Human Actions at Radioactive Waste Disposal Sites. Paris: Nuclear Energy Agency, Organisation for Economic Co-operation and Development.

**NEA, 1997a.** Lessons learnt from ten performance assessment studies. Paris: Nuclear Energy Agency, Organisation for Economic Co-operation and Development.

**NEA, 1997b.** The Probabilistic System Assessment Group: history and achievements 1985–1994. Paris: Nuclear Energy Agency, Organisation for Economic Co-operation and Development. (Disposal of radioactive waste)

**NEA, 1999a.** Confidence in the long-term safety of deep geological repositories: its development and communication. Paris: Nuclear Energy Agency, Organisation for Economic Co-operation and Development.

**NEA, 1999b.** Safety assessment of radioactive waste repositories – An international database of Features, Events and Processes. A report of the NEA working group on development of a database of Features, events and Processes relevant to the assessment of post-closure safety of radioactive waste repositories. Nuclear Agency of the Organisation for Economic Cooperation and Development (OECD/NEA), Paris, France. Electronic version 1.2 of the NEA FEP database developed on behalf of the Nuclear Energy Agency by Safety Assessment Management Ltd with support of Quintessa Ltd.

**NEA, 2001.** Scenario development methods and practices: an evaluation based on the NEA Workshop on Scenario Development, Madrid, Spain, May 1999. Paris: Nuclear Energy Agency, Organisation for Economic Co-operation and Development.

**NEA, 2004a.** The handling of timescales in assessing post-closure safety: lessons learnt from the April 2002 Workshop in Paris, France. Paris: Nuclear Energy Agency, Organisation for Economic Co-operation and Development.

**NEA, 2004b.** Post-closure safety case for geological repositories: nature and purpose. Paris: Nuclear Energy Agency, Organisation for Economic Co-operation and Development.

**NEA, 2005.** Management of uncertainty in safety cases and the role of risk: workshop proceedings. Paris: Nuclear Energy Agency, Organisation for Economic Co-operation and Development.

**NEA, 2006.** Electronic version 2.1 of the NEA FEP database developed on behalf of the Nuclear Energy Agency by Safety Assessment Management Ltd.

**NEA, 2009.** International Experiences in Safety Cases for Geological Repositories (INTESC): Outcomes of the INTESC Project. Paris: Nuclear Energy Agency, Organisation for Economic Co-operation and Development.

**Neall F, Pastina B, Snellman M, Smith P, Gribi P, Johnson L, 2008.** Safety assessment of a KBS-3H spent nuclear fuel repository at Olkiluoto. Complementary evaluation of safety. SKB R-08-35, Svensk Kärnbränslehantering AB.

**Nebot J, Bruno J, 1991.** The implications of soil acidification on a future HLNW repository. Part I: The effects of increased weathering, erosion and deforestation. SKB TR 91-45, Svensk Kärnbränslehantering AB.

**Neff D, Dillmann P, Beranger G, 2003.** An analytical study of corrosion products formed on buried ferrous archaeological artefacts. In: Féron D, Macdonald D D (eds). Prediction of long term corrosion behaviour in nuclear waste systems (EFC 36). Leeds: Maney Publishing, pp 295–315.

**Neff D, Dillmann P, Bellot-Gurlet L, Beranger G, 2005.** Corrosion of iron archaeological artefacts in soil: characterisation of the corrosion system. Corrosion Science, 47, pp 515–535.

**Neff D, Dillmann P, Descostes M, Beranger G, 2006.** Corrosion of iron archaeological artefacts in soil: estimation of the average corrosion rates involving analytical techniques and thermodynamic calculations. Corrosion Science, 48, pp 2947–2970.

**Neretnieks I, 1986.** Some uses for natural analogues in assessing the function of a HLW repository. Chemical Geology, 55, pp 175–188.

**Neretnieks I, 2006a.** Flow and solute transport in a zone damaged due to spalling. SKB R-06-91, Svensk Kärnbränslehantering AB.

**Neretnieks I, 2006b.** Flow and transport through a damaged buffer – exploration of the impact of a cemented and an eroded buffer. SKB TR-06-33, Svensk Kärnbränslehantering AB.

**Neretnieks I, Liu L, Moreno L, 2009.** Mechanisms and models for bentonite erosion. SKB TR-09-35, Svensk Kärnbränslehantering AB.

**Neretnieks I, Liu L, Moreno L, 2010.** Mass transfer between waste canister and water seeping in rock fractures. Revisiting the Q-equivalent model. SKB TR-10-42, Svensk Kärnbränslehantering AB.

**Neuilly M, Bussac J, Frejacques C, Nief G, Vendreys G, Yvon J, 1972.** Sur l'éxistance dans un passé reculé d'une réaction en chaine naturelle de fission, dans le gisement d'uranium d'Oklo (Gabon). Comptes rendus Hebdomadaires des Séances de l'Académie des Sciences, Série D: Sciences Naturelles, 275, pp 1847–1849.

**Nicot J-P, 2008.** Methodology for bounding calculations of nuclear criticality of fissile material accumulations external to a waste container at Yucca Mountain, Nevada. Applied Geochemistry, 23, pp 2065–2081.

**Nordén S, Avila R, de la Cruz I, Stenberg K, Grolander S, 2010.** Element-specific and constant parameters used for dose calculations in SR-Site. SKB TR-10-07, Svensk Kärnbränslehantering AB.

**Nordstrom D K, Ball J W, Donahoe R J, Whittemore D, 1989.** Groundwater chemistry and water-rock interactions at Stripa. Geochimica et Cosmochimica Acta, 53, pp 1727–1740.

**Norman S, Kjellbert N, 1990.** FARF31 – A far field radionuclide migration code for use with the PROPER package. SKB TR 90-01, Svensk Kärnbränslehantering AB.

**Näslund J-O, Fastook J L, Holmlund P, 2000.** Numerical modelling of the ice sheet in western Dronning Maud Land, East Antarctica: impacts of present, past, and future climates. Journal of Glaciology, 46, pp 54–66.

**Näslund J-O, Jansson P, Fastook J L, Johnson J, Andersson L, 2005.** Detailed spatially distributed geothermal heat-flow data for modelling of basal temperatures and meltwater production beneath the Fennoscandian ice sheet. Annals of Glaciology, 40, pp 95–101.

**Näslund J-O (ed), Wohlfarth B, Alexanderson H, Helmens K, Hättestrand M, Jansson P, Kleman J, Lundqvist J, Brandefelt J, Houmark-Nielsen M, Kjellström E, Strandberg G, Knudsen K L, Krogh Larsen N, Ukkonen P, Mangerud J, 2008.** Fennoscandian paleo-environment and ice sheet dynamics during Marine Isotope Stage (MIS) 3. Report of a workshop held September 20–21, 2007 in Stockholm, Sweden. SKB R-08-79, Svensk Kärnbränslehantering AB.

**Ochs M, Talerico C, 2004.** SR-Can. Data and uncertainty assessment. Migration parameters for the bentonite buffer in the KBS-3 concept. SKB TR-04-18, Svensk Kärnbränslehantering AB.

**Olesen O, Dehls J, Bungum H, Riis F, Hicks E, Lindholm C, Blikra L H, Fjeldskaar W, Olsen L, Longva O, Faleide J I, Bockmann L, Rise L, Roberts D, Braathen A, Brekke H, 2000.** Neotectonics in Norway. Final report. NGU Report 2000.002, Geological Survey of Norway.

**Olsson M, Niklasson B, Wilson L, Andersson C, Christiansson R, 2004.** Äspö HRL. Experiences of blasting of the TASQ tunnel. SKB R-04-73, Svensk Kärnbränslehantering AB.

**Olsson M, Markström I, Pettersson A, Sträng M, 2009.** Examination of the Excavation Damaged Zone in the TASS tunnel, Äspö HRL. SKB R-09-39, Svensk Kärnbränslehantering AB.

**Olsson S, Karnland O, 2009.** Characterisation of bentonites from Kutch, India and Milos, Greece – some candidate tunnel backfill materials? SKB R-09-53, Svensk Kärnbränslehantering AB.

**Olvmo M, 2010.** Review of denudation processes and quantification of weathering and erosion rates at a 0.1 to 1 Ma time scale. SKB TR-09-18, Svensk Kärnbränslehantering AB.

**ONDRAF/NIRAS, 2001.** SAFIR:2 Safety Assessment and Feasibility Interim Report 2, NIROND 2001-06E, ONDRAF/NIRAS.

**Oversby V M, 1996.** Criticality in a high level waste repository. A review of some important factors and an assessment of the lessons that can be learned from the Oklo reactors. SKB TR 96-07, Svensk Kärnbränslehantering AB.

**Oversby V M, 1998.** Criticality in a repository for spent fuel: lessons from Oklo. In: McKinley I G, McCombie C (eds). Scientific basis for nuclear waste management XXI: symposium held in Davos, Switzerland, 23 September – 3 October, 1997. Warrendale, PA: Materials Research Society. (Materials Research Society Symposium Proceedings 506), p 781.

**Painter S, Mancillas J, 2009.** MARFA version 3.2.2 user's manual: migration analysis of radionuclides in the far field. SKB R-09-56, Svensk Kärnbränslehantering AB.

**Painter S, Cvetkovic V, Mancillas J, Pensado O, 2008.** Time domain particle tracking methods for simulating transport with retention and first-order transformation. Water Resources Research, 44, W01406, doi:10.1029/2007WR005944.

**Parkhurst D L, Appelo C A J, 1999.** User's guide to PHREEQC (version 2): a computer program for speciation, batch-reaction, one-dimensional transport, and inverse geochemical calculations. Denver, CO: U.S. Geological Survey. (Water-resources investigations report 99-4259)

**Parkhurst D L, Kipp K L, Engesgaard P, Charlton S R, 2004.** PHAST: a program for simulating ground-water flow, solute transport, and multicomponent geochemical reactions. U.S. Geological Survey Techniques and Methods 6-A8. Denver, CO: U.S. Geological Survey.

**Paterson W S B, 1994.** The physics of glaciers. 3rd ed. Oxford: Pergamon.

**Pattyn F, De Smedt B, Souchez R, 2004.** Influence of subglacial Vostok lake on the regional dynamics of the Antarctic ice sheet: a model study. Journal of Glaciology, 50, pp 583–589.

**Payne A J, Huybrechts P, Abe-Ouchi A, Calov R, Fastook J L, Greve R, Marshall S J, Marsiat I, Ritz C, Tarasov L, Thomassen M P A, 2000.** Results from the EISMINT model intercomparison: the effects of thermomechanical coupling. Journal of Glaciology, 46, pp 227–238.

**Pedersen K, 2006.** Microbiology of transitional groundwater of the porous overburden and underlying fractured bedrock aquifers in Olkiluoto, Finland. Posiva Working Report 2006-09, Posiva Oy, Finland.

**Pedersen K, 2010.** Analysis of copper corrosion in compacted bentonite clay as a function of clay density and growth conditions for sulfate-reducing bacteria. Journal of Applied Microbiology, 108, pp 1094–1104.

**Pedersen K, Kennedy C, Nederfeldt K-G, Bergelin A, 2004.** Äspö Hard Rock Laboratory. Prototype repository. Chemical measurements in buffer and backfill; sampling and analyses of gases. SKB IPR-04-26, Svensk Kärnbränslehantering AB.

**Pers K, Skagius K, Södergren S, Wiborgh M, Hedin A, Morén L, Sellin P, Ström A, Pusch R, Bruno J, 1999.** SR 97 – Identification and structuring of process. SKB TR-99-20, Svensk Kärnbränslehantering AB.

**Petsev D N, Starov V M, Ivanov I B, 1993.** Concentrated dispersions of charged colloidal particles: sedimentation, ultrafiltration and diffusion. Colloids and Surfaces A: Physicochemical and Engineering Aspects, 81, pp 65–81.

**Piqué, A, Grandia, F, Sena, C, Arcos, D, Molinero, J, Duro, L, Bruno, J, 2010.** Conceptual and numerical modelling of radionuclide transport in near-surface systems at Forsmark. SR-Site Biosphere. SKB R-10-30, Svensk Kärnbränslehantering AB.

**Porcelli D, Andersson P S, Baskaran M, Wasserburg G J, 2001.** Transport of U- and Th-series in a Baltic shield watershed and the Baltic Sea. Geochimica et Cosmochimica Acta, 65, pp 2439–2459.

**Puigdomenech I, Ambrosi J-P, Eisenlohr L, Lartigue J-E, Banwart S A, Bateman K, Milodowski A E, West J M, Griffault L, Gustafsson E, Hama K, Yoshida H, Kotelnikova S, Pedersen K, Michaud V, Trotignon L, Rivas Perez J, Tullborg E-L, 2001.** $O_2$ depletion in granitic media. The REX project. SKB TR-01-05, Svensk Kärnbränslehantering AB.

**Pusch R, 1983.** Stability of deep-sited smectite minerals in crystalline rock – chemical aspects. SKBF/KBS TR 83-16, Svensk Kärnbränsleförsörjning AB.

**Pusch R, 2000a.** On the effect of hot water vapor on MX-80 clay. SKB TR-00-16, Svensk Kärnbränslehantering AB.

**Pusch R, 2000b.** On the risk of liquefaction of buffer and backfill. SKB TR-00-18, Svensk Kärnbränslehantering AB.

**Pusch R, 2008.** Rock fill in a KBS-3 repository. Rock material for filling of shafts and ramps in a KBS-3V repository in the closure phase. SKB R-08-117, Svensk Kärnbränslehantering AB.

**Pusch R, Karnland O, 1988.** Geological evidence of smectite longevity. The Sardinian and Gotland cases. SKB TR 88-26, Svensk Kärnbränslehantering AB.

**Pusch R, Ramqvist G, 2004.** Borehole sealing, preparative steps, design and function of plugs – basic concept. SKB IPR-04-57, Svensk Kärnbränslehantering AB.

**Pusch R, Ramqvist G, 2007.** Borehole project – Final report of Phase 3. SKB R-07-58, Svensk Kärnbränslehantering AB.

**Pusch R, Hiroyasu T, Steven B, 1998.** Chemical processes causing cementation in heat-affected smectite – the Kinnekulle bentonite. SKB TR-98-25, Svensk Kärnbränslehantering AB.

**Påsse T, 2001.** An empirical model of glacio-isostatic movements and shore-level displacement in Fennoscandia. SKB R-01-41, Svensk Kärnbränslehantering AB.

**Raiko H, Sandström R, Rydén H, Johansson M, 2010.** Design analysis report for the canister. SKB TR-10-28, Svensk Kärnbränslehantering AB.

**RETROCK, 2005.** Treatment of radionuclide transport in geosphere within safety assessments. Final report of the RETROCK Concerted Action. EUR 21230, European Commission.

**Riis F, 1996.** Quantification of Cenozoic vertical movements of Scandinavia by correlation of morphological surfaces with offshore data. Global and Planetary Change, 12, pp 331–357.

**Ritchey T, 1997.** Scenario Development and Risk Management using Morphological Field Analysis. In: Proceedings of the 5th European Conference on Information Systems. Cork: Cork Publishing Company, vol 3, pp 1053–1059.

**Roberts M J, 2005.** Jökulhlaups: a reassessment of floodwater flow through glaciers. Reviews of Geophysics, 43, RG1002, doi:10.1029/2003RG000147.

**Roberts M J, Russell A J, Tweed F S, Knudsen O, 2000.** Ice fracturing during jökulhlaups: implications for englacial floodwater routing and outlet development. Earth Surface Processes and Landforms, 25, pp 1429–1446.

**Romero A L, 1995.** The near-field transport in a repository for high-level nuclear waste. Ph. D. thesis. Department of Chemical Engineering and Technology, Royal Institute of Technology, Stockholm, Sweden.

**Romero L, Thompson A, Moreno L, Neretnieks I, Widén H, Boghammar A, 1999.** Comp23/ Nuctran user's guide. Proper version 1.1.6. SKB R-99-64, Svensk Kärnbränslehantering AB.

**Ruiz López C, Rodríguez J, Hernán P, Recreo F, Ruiz C, Prado P, Gimeno M J, Auqué L F, Gómez J, Acero P, González Á, Samper J, Montenegro L, Molinero J, Delgado J, Criado A, Martínez J A, Ruiz S, 2004.** Analogue application to safety assessment and communication of radioactive geological disposal. Illustrative synthesis. Colección Documentos I+D 11.2004, Consejo de Seguridad Nuclear, Madrid.

**Rummukainen M, 2003.** The Swedish regional climate modeling program, SWECLIM, 1996–2003. Final report. Norrköping: Sveriges meteorologiska och hydrologiska institut (Swedish Meteorological and Hydrological Institute). (SMHI Meteorologi 104)

**Ruskeeniemi T, Ahonen L, Paananen M, Frape S, Stotler R, Hobbs M, Kaija J, Degnan P, Blomqvist R, Jensen M, Lehto K, Moren L, Puigdomenech I, Snellman M, 2004.** Permafrost at Lupin: report of Phase II. Report YST-119, Geological Survey of Finland, Nuclear Waste Disposal Research.

**Sagar B, Egan M, Röhlig K-J, Chapman N, Wilmot R (eds), 2008.** International expert review of SR-Can: Safety assessment methodology. External review contribution in support of SSI's and SKI's review of SR-Can. SSI Rapport 2008:5, Statens strålskyddsinstitut (Swedish Radiation Protection Authority), SKI Rapport 2008:15, Statens kärnkraftinspektion (Swedish Nuclear Power Inspectorate).

**Salas J, Gimeno M J, Auqué L F, Molinero J, Gómez J, Juárez I, 2010.** SR-Site – hydrogeochemical evolution of the Forsmark site. SKB TR-10-58, Svensk Kärnbränslehantering AB.

**Saltelli A, Andres T H, Homma T, 1993.** Sensitivity analysis of model output: an investigation of new techniques. Computational Statistics & Data Analysis, 15, pp 211–238.

**Saltelli A, Chan K, Scott E M (eds), 2000.** Sensitivity analysis. Chichester: Wiley.

**Sandén T, Börgesson L, 2010.** Early effect of water inflow into a deposition hole. Laboratory test results. SKB R-10-70, Svensk Kärnbränslehantering AB.

**Sandén T, Börgesson L, Dueck A, Goudarzi R, Lönnqvist M, 2008.** Deep repository-Engineered barrier system. Erosion and sealing processes in tunnel backfill materials investigated in laboratory. SKB R-08-135, Svensk Kärnbränslehantering AB.

**Sandiford M, Wallace M, Coblentz D, 2004.** Origin of the in situ stress field in south-eastern Australia. Basin Research, 16, pp 325–338.

**Sandström B, Stephens M B, 2009.** Mineralogy, geochemistry, porosity and redox properties of rocks from Forsmark. Compilation of data from the regional model volume for SR-Site. SKB R-09-51, Svensk Kärnbränslehantering AB.

**Sandström B, Tullborg E-L, Smellie J, MacKenzie A B, Suksi J, 2008.** Fracture mineralogy of the Forsmark site. SDM-Site Forsmark. SKB R-08-102, Svensk Kärnbränslehantering AB.

**Sandström B, Tullborg E-L, Larsson S Å, Page L, 2009.** Brittle tectonothermal evolution in the Forsmark area, central Fennoscandian Shield, recorded by paragenesis, orientation and $^{40}Ar/^{39}Ar$ geochronology of fracture minerals. Tectonophysics, 478, pp 158–174.

**Savage D, Bennett D, Apted M, Sällfors G, Saario T, Segle P, 2008.** International expert review of SR-Can: Engineered barrier issues. External review contribution in support of SKI's and SSI's review of SR-Can. SKI Report 2008:10, Statens kärnkraftinspektion (Swedish Nuclear Power Inspectorate).

**Scherneck H-G, Lidberg M, Haas R, Johansson J M, Milne G A, 2010.** Fennoscandian strain rates from BIFROST GPS: a gravitating, thick-plate approach. Journal of Geodynamics, 50, pp 19–26.

**Schlesinger M E, Yin J, Yohe G W, Andronova N G, Malyshev S, Li B, 2006.** Assessing the risk of a collapse of the Atlantic thermohaline circulation. In: Schellnhuber H J, Cramer W, Nakicenovic N, Wigley T, Yohe G (eds). Avoiding dangerous climate change. Cambridge: Cambridge University Press, ch 5.

**Scholz C H, 2002.** The mechanics of earthquakes and faulting. 2nd ed. Cambridge: Cambridge University Press.

**Selroos J-O, Follin S, 2010.** Groundwater flow modelling methodology, setup and results. SKB R-09-22, Svensk Kärnbränslehantering AB.

**Selroos J-O, Walker D D, Ström A, Gylling B, Follin S, 2002.** Comparison of alternative modelling approaches for groundwater flow in fractured rock. Journal of Hydrology, 257, pp 174–188.

**Sena C, Salas J, Arcos D, 2010.** Aspects of geochemical evolution of the SKB near field in the frame of SR-Site. SKB TR-10-59, Svensk Kärnbränslehantering AB.

**Sidborn M, Neretnieks I, 2003.** Modelling of biochemical processes in rocks: Oxygen depletion by pyrite oxidation: model development and exploratory simulations. In: Finch R J, Bullen D B (eds). Scientific basis for nuclear waste management XXVI. Warrendale, PA: Materials Research Society. (Materials Research Society Symposium Proceedings 757), pp 553–558.

**Sidborn M, Neretnieks I, 2004.** Modelling biochemical processes in rocks: Analysis and exploratory simulationsof competition of different processes important for ferrous mineral oxidation and oxygen depletion. In: Oversby V M, Werme L O (eds). Scientific basis for nuclear waste management XXVII: symposium held in Kalmar, Sweden, 15–19 June 2003. Warrendale, PA: Materials Research Society. (Materials Research Society Symposium Proceedings 807), pp 829–834.

**Sidborn M, Neretnieks I, 2008.** Long-term oxygen depletion from infiltrating groundwaters: model development and application to intra-glaciation and glaciation conditions. Journal of Contaminant Hydrology, 100, pp 72–89.

**Sidborn M, Sandström B, Tullborg E-L, Delos A, Molinero J, Hallbeck L, Pedersen K, 2010.** SR-Site: Oxygen ingress in the rock at Forsmark during a glacial cycle. SKB TR-10-57, Svensk Kärnbränslehantering AB.

**Silver W L, Lugo A E, Keller M, 1999.** Soil oxygen availability and biogeochemistry along rainfall and topographic gradients in upland wet tropical forest soils. Biogeochemistry, 44, pp 301–328.

**Skagius K, Wingefors S, 1992.** Scenarios. Application of scenario development methods in evaluation of the Koongarra analogue. Alligator Rivers Analogue Project, final report. Vol. 16. An OECD/NEA International Project Managed by ANSTO. SKI Report 92:20-16, Statens kärnkraftinspektion (Swedish Nuclear Power Inspectorate).

**Skagius K, Ström A, Wiborgh M, 1995.** The use of interaction matrices for identification, structuring and ranking of FEPs in a repository system. Application on the far-field of a deep geological repository for spent fuel. SKB TR 95-22, Svensk Kärnbränslehantering AB.

**SKB, 1990.** Granskning av Nils-Axel Mörners arbeten avseende postglaciala strukturer på Äspö (in Swedish). SKB AR 90-18, Svensk Kärnbränslehantering AB.

**SKB, 1995.** SR 95. Template for safety reports with descriptive example. SKB TR 96-05, Svensk Kärnbränslehantering AB.

**SKB, 1999a.** Deep repository for spent nuclear fuel. SR 97 – Post-closure safety. Main report – Vol I, Vol II and Summary. SKB TR-99-06, Svensk Kärnbränslehantering AB.

**SKB, 1999b.** SR 97 – Processes in the repository evolution. Background report to SR 97. SKB TR-99-07, Svensk Kärnbränslehantering AB.

**SKB, 2004a.** Interim data report for the safety assessment SR-Can. SKB R-04-34, Svensk Kärnbränslehantering AB.

**SKB, 2004b.** Interim main report of the safety assessment SR-Can. SKB TR-04-11, Svensk Kärnbränslehantering AB.

**SKB, 2006a.** Long-term safety for KBS-3 repositories at Forsmark and Laxemar – a first evaluation. Main report of the SR-Can project. SKB TR-06-09, Svensk Kärnbränslehantering AB.

**SKB, 2006b.** FEP report for the safety assessment SR-Can. SKB TR-06-20, Svensk Kärnbränslehantering AB.

**SKB, 2006c.** Climate and climate-related issues for the safety assessment SR-Can. SKB TR-06-23, Svensk Kärnbränslehantering AB.

**SKB, 2006d.** Geosphere process report for the safety assessment SR-Can. SKB TR-06-19, Svensk Kärnbränslehantering AB.

**SKB, 2006e.** Handling of future human actions in the safety assessment SR-Can. SKB TR-06-24, Svensk Kärnbränslehantering AB.

**SKB, 2006f.** Data report for the safety assessment SR-Can. SKB TR-06-25, Svensk Kärnbränslehantering AB.

**SKB, 2006g.** The biosphere at Forsmark. Data assumptions and models used in the SR-Can assessment. SKB R-06-82, Svensk Kärnbränslehantering AB.

**SKB, 2007a.** Forsmark site investigation. Programme for long-term observations of geosphere and biosphere after completed site investigations. SKB R-07-34, Svensk Kärnbränslehantering AB.

**SKB, 2007b.** Final repository facility. Underground design premises/D2. SKB R-07-33, Svensk Kärnbränslehantering AB.

**SKB, 2008a.** Site description of Forsmark at completion of the site investigation phase. SDM-Site Forsmark. SKB TR-08-05, Svensk Kärnbränslehantering AB.

**SKB, 2008b.** Confidence assessment. Site descriptive modeling, SDM-Site Forsmark. SKB R-08-82, Svensk Kärnbränslehantering AB.

**SKB, 2009a.** Design premises for a KBS-3V repository based on the results from the safety assessment SR-Can and some subsequent analyses. SKB TR-09-22, Svensk Kärnbränslehantering AB.

**SKB, 2009b.** Underground design Forsmark. Layout D2. SKB R-08-116, Svensk Kärnbränslehantering AB.

**SKB, 2009c.** Site engineering report Forsmark. Guidelines for underground design. Step D2. SKB R-08-83, Svensk Kärnbränslehantering AB.

**SKB, 2010a.** Miljökonsekvensbeskrivning (MKB). Mellanlagring, inkapsling och slutförvaring av använt kärnbränsle (in Swedish). Svensk Kärnbränslehantering AB.

**SKB, 2010b.** Ramprogram för detaljundersökningar vid uppförande och drift av slutförvar för använt kärnbränsle (in Swedish). SKB R-10-08, Svensk Kärnbränslehantering AB.

**SKB, 2010c.** Components, processes and interactions in the biosphere. SR-Site Biosphere. SKB R-10-37, Svensk Kärnbränslehantering AB.

**SKB, 2010d.** Corrosion calculations report for the safety assessment SR-Site. SKB TR-10-66, Svensk Kärnbränslehantering AB.

**SKB, 2010e.** Platsval – lokalisering av slutförvaret för använt kärnbränsle (in Swedish). SKB R-10-42, Svensk Kärnbränslehantering AB.

**SKBF/KBS, 1983.** Kärnbränslecykelns slutsteg. Använt kärnbränsle – KBS-3. Del I–IV. Svensk Kärnbränsleförsörjning AB.

**SKI, 2007.** Statens ansvar för förslutning av använt kärnbränsle (The responsibility of the state for sealing of spent fuel) (in Swedish). SKI Rapport 2007:01, Statens kärnkraftinspektion (Swedish Nuclear Power Inspectorate).

**SKI/SSI, 2001.** SKI's and SSI's joint review of SKB's safety assessment report, SR 97, summary. SKI Report 01:3, Statens kärnkraftinspektion (Swedish Nuclear Power Inspectorate), SSI Report 2001:02, Statens strålskyddsinstitut (Swedish Radiation Protection Authority).

**Slunga R S, 1991.** The Baltic Shield earthquakes. Tectonophysics, 189, pp 323–331.

**Smellie J, 2001.** Wyoming bentonites. Evidence from the geological record to evaluate the suitability of bentonite as a buffer material during the long-term underground containment of radioactive wastes. SKB TR-01-26, Svensk Kärnbränslehantering AB.

**Smellie J, Karlsson F (eds), 1996.** A reappraisal of some Cigar Lake issues of importance to performance assessment. SKB TR 96-08, Svensk Kärnbränslehantering AB.

**Smith P, Johnson L, Snellman M, Pastina B, Gribi P, 2008.** Safety assessment for a KBS-3H spent nuclear fuel repository at Olkiluoto. Evolution report. SKB R-08-37, Svensk Kärnbränslehantering AB.

**Spiessl S M, MacQuarrie K T B, Mayer K U, 2008.** Identification of key parameters controlling dissolved oxygen migration and attenuation in fractured crystalline rocks. Journal of Contaminant Hydrology, 95, pp 141–153.

**SSI, 2007.** Strålmiljön i Sverige (in Swedish). SSI Rapport 2007:02, Statens strålskyddsinstitut (Swedish Radiation Protection Authority).

**SSM, 2008a.** Strålsäkerhetsmyndighetens föreskrifter och allmänna råd om säkerhet vid slutförvaring av kärnämne och kärnavfall (The Swedish Radiation Safety Authority's Regulations concerning Safety in connection with the Disposal of Nuclear Material and Nuclear Waste) (in Swedish). Stockholm: Strålsäkerhetsmyndigheten (Swedish Radiation Safety Authority). (SSMFS 2008:21)

**SSM, 2008b.** Strålsäkerhetsmyndighetens föreskrifter och allmänna råd om skydd av människors hälsa och miljön vid slutligt omhändertagande av använt kärnbränsle och kärnavfall (The Swedish Radiation Safety Authority's Regulations on the Protection of Human Health and the Environment in connection with the Final Management of Spent Nuclear Fuel and Nuclear Waste) (in Swedish). Stockholm: Strålsäkerhetsmyndigheten (Swedish Radiation Safety Authority). (SSMFS 2008:37)

**Stephens M B, Fox A, La Pointe P, Simeonov A, Isaksson H, Hermanson J, Öhman J, 2007.** Geology Forsmark. Site descriptive modelling Forsmark stage 2.2. SKB R-07-45, Svensk Kärnbränslehantering AB.

**Stephens M B, Bergman T, Isaksson H, Petersson J, 2008a.** Bedrock geology Forsmark. Modelling stage 2.3. Description of the bedrock geological map at the ground surface. SKB R-08-128, Svensk Kärnbränslehantering AB.

**Stephens M B, Simeonov A, Isaksson H, 2008b.** Bedrock geology Forsmark. Modelling stage 2.3. Implications for and verification of the deterministic geological models based on complementary data. SKB R-08-64, Svensk Kärnbränslehantering AB.

**Stotler R L, Frape S K, Ruskeeniemi T, Ahonen L, Onstott T C, Hobbs M Y, 2009a.** Hydrogeochemistry of groundwaters in and below the base of thick permafrost at Lupin, Nunavut, Canada. Journal of Hydrology, 373, pp 80–95.

**Stotler R L, Frape S K, Ruskeeniemi T, Ahonen L, Paananen M, Hobbs M Y, Lambie K E, Zhang M, 2009b.** Hydrochemistry of groundwaters at and below the base of the permafrost at Lupin: report of Phase III. NWMO TR-2009-10, Nuclear Waste Management Organisation, Toronto Ontario, Canada.

**Strömgren M, Brydsten L, 2008.** Digital elevation models of Forsmark. Site descriptive modelling, SDM-Site Forsmark. SKB R-08-62, Svensk Kärnbränslehantering AB.

**STUK, 2001.** Long-term safety of disposal of spent nuclear fuel. Guide YVL 8.4. STUK (Radiation and Nuclear Safety Authority), Finland.

**Sundberg J, Back P-E, Ländell M, Sundberg A, 2009.** Modelling of temperature in deep boreholes and evaluation of geothermal heat flow at Forsmark and Laxemar. SKB TR-09-14, Svensk Kärnbränslehantering AB.

**Svendsen J I, Astakhov V I, Bolshiyanov D Y, Demidov I, Dowdeswell J A, Gataullin V, Hjort C, Hubberten H W, Larsen E, Mangerud J, Melles M, Möller P, Saarnisto M, Siegert M J, 1999.** Maximum extent of the Eurasian ice sheets in the Barents and Kara Sea region during the Weichselian. Boreas, 28, pp 234–242.

**Svendsen J I, Alexanderson H, Astakhov V I, Demidov I, Dowdeswell J A, Funder S, Gataullin V, Henriksen M, Hjort C, Houmark-Nielsen M, Hubberten H W, Ingólfsson O, Jakobsson M, Kjær K H, Larsen E, Lokrantz H, Lunkka J P, Lyså A, Mangerud J, Matiouchkov A, Murray A, Moller P, Niessen F, Nikolskaya O, Polyak L, Saarnisto M, Siegert C, Siegert M J, Spielhagen R F, Stein R, 2004.** Late Quaternary ice sheet history of northern Eurasia. Quaternary Science Reviews, 23, pp 1229–1271.

**Svensson U, Follin S, 2010.** Groundwater flow modelling of the excavation and operation phases – SR-Site Forsmark. SKB R-09-19, Svensk Kärnbränslehantering AB.

**Svensson U, Ferry M, Kuylenstierna H-O, 2010.** DarcyTools, Version 3.4. Concepts, methods and equations. SKB R-07-38, Svensk Kärnbränslehantering AB.

**Swartzen-Allen S L, Matijević E, 1976.** Colloid and surface properties of clay suspensions III. Stability of montmorillonite and kaolinite. Journal of Colloid and Interface Science, 56, pp 159–167.

**Szakálos P, Hultquist G, Wikmark G, 2007.** Corrosion of copper by water. Electrochemical and Solid-State Letters, 10, pp C63–C67.

**Söderbäck B (ed), 2008.** Geological evolution, palaeoclimate and historical development of the Forsmark and Laxemar-Simpevarp areas. Site descriptive modelling. SDM-Site. SKB R-08-19, Svensk Kärnbränslehantering AB.

**Talbot C J, 1999.** Ice ages and nuclear waste isolation. Engineering Geology, 52, pp 177–192.

**Tarasov L, Peltier W R, 2004.** A geophysically constrained large ensemble analysis of the deglacial history of the North American ice-sheet complex. Quaternary Science Reviews, 23, pp 359–388.

**Thorne M C, Kane P, 2006.** Development of a series of narratives for climatic and landscape change. MTA/P0011a/2005-1: Issue 2, Mike Thorne and Associates Limited Report to United Kingdom Nirex Limited.

**Tohidi B, Chapoy A, Smellie J, Puigdomenech I, 2010.** The potential for methane hydrate formation in deep repositories of spent nuclear fuel in granitic rocks. SKB R-10-58, Svensk Kärnbränslehantering AB.

**Torudd J, 2010.** Long term radiological effects on plants and animals of a deep geological repository. SR-Site Biosphere. SKB TR-10-08, Svensk Kärnbränslehantering AB.

**Tröjbom M, Grolander S, 2010.** Chemical conditions in present and future ecosystems in Forsmark. Implications for selected radionuclides in the safety assessment SR-Site. SKB R-10-27, Svensk Kärnbränslehantering AB.

**Tullborg E-L, Smellie J, Nilsson A-C, Gimeno M J, Auqué L F, Brüchert V, Molinero J, 2010.** SR-Site – sulphide content in the groundwater at Forsmark. SKB TR-10-39, Svensk Kärnbränslehantering AB.

**Tushingham A M, Peltier W R, 1991.** ICE-3G: a new global model of late Pleistocene deglaciation based on geophysical predictions of post-glacial relative sea level change. Journal of Geophysical Research, 96, pp 4497–4523.

**UNSCEAR, 2000.** Sources and effects of ionizing radiation: UNSCEAR 2000 report to the General Assembly with scientific annexes. Vol. I. Annex A: Dose assessment methodologies: New York: United Nations Scientific Committee on the Effects of Atomic Radiation.

**UNSCEAR, 2008.** Sources and effects of ionizing radiation: UNSCEAR 2008 report to the General Assembly with scientific annexes. Vol. I. Sources. New York: United Nations Scientific Committee on the Effects of Atomic Radiation.

**Vahlund F, Hermansson H, 2006.** Compulink. Implementing the COMP23 model in Simulink. SKB R-06-86, Svensk Kärnbränslehantering AB.

**Valentini G, Lombardi S, Bozzano F, Scarascia Mugnozza G (eds), 1997.** Analysis of the geo-environmental conditions as morphological evolution factors of the sand-clay series of the Tiber valley and Dunarobba forest preservation. EUR 17479, European Commission.

**Van Konynenburg R A, 1995.** Comments on the draft paper "Underground supercriticality from plutonium and other fissile material" written by C. D. Bowman and F. Venneri (LANL). Report UCRL-ID-120990 COM, University of California.

**Velde B, Vasseur G, 1992.** Estimation of the diagenetic smectite to illite transformation in time-temperature space. American Mineralogist, 77, pp 967–976.

**Vidstrand P, Svensson U, Follin S, 2006.** Simulation of hydrodynamic effects of salt rejection due to permafrost. Hydrogeological numerical model of density-driven mixing, at a regional scale, due to a high salinity pulse. SKB R-06-101, Svensk Kärnbränslehantering AB.

**Vidstrand P, Follin S, Zugec N, 2010.** Groundwater flow modelling of periods with periglacial and glacial climate conditions – Forsmark. SKB R-09-21, Svensk Kärnbränslehantering AB.

**Vieno T, Nordman H, 1999.** Safety assessment of spent fuel disposal in Hästholmen, Kivetty, Olkiluoto and Romuvaara TILA-99. Posiva 99-07, Posiva Oy, Finland.

**Villar M V, Pérez del Villar L, Martín P L, Pelayo M, Fernández A M, Garralón A, Cuevas J, Leguey S, Caballero E, Huertas F J, Jiménez de Cisneros C, Linares J, Reyes E, Delgado A, Fernández-Soler J M, Astudillo J, 2006.** The study of Spanish clays for their use as sealing materials in nuclear waste repositories: 20 years of progress. Journal of Iberian Geology, 32, pp 15–36.

**Waber H N, Gimmi T, Smellie J A T, 2009.** Porewater in the rock matrix. Site descriptive modelling, SDM-Site Forsmark. SKB R-08-105, Svensk Kärnbränslehantering AB.

**Waddington E D, 1987.** Geothermal heat flux beneath ice sheets. In: Waddington E D, Walder J S (eds). The physical basis of ice sheet modelling. Wallingford, Oxfordshire: International Association of Hydrological Sciences. (IAHS Publication 170), pp 217–226.

**Wadham J L, Tranter M, Skidmore M, Hodson A J, Priscu J, Lyons W B, Sharp M, Wynn P, Jackson M, 2010.** Biogeochemical weathering under ice: size matters. Global Biogeochemical Cycles, 24, GB3025, doi:10.1029/2009GB003688.

**Walsh J J, Watterson J, 1987.** Distributions of cumulative displacement and seismic slip on a single normal fault surface. Journal of Structural Geology, 9, pp 1039–1046.

**Walsh J J, Watterson J, 1989.** Displacement gradients on fault surfaces. Journal of Structural Geology, 11, pp 307–316.

**Washburn A L, 1979.** Geocryology: a survey of periglacial processes and environments. 2nd ed. London: Arnold.

**Wells D L, Coppersmith K J, 1994.** New empirical relationships among magnitude, rupture length, rupture width, rupture area, and surface displacement. Bulletin of the Seismological Society of America, 84, pp 974–1002.

**Werner K, Hamrén U, Collinder P, 2010.** Vattenverksamhet i Forsmark (del I). Bortledande av grundvatten från slutförvarsanläggningen för använt kärnbränsle (in Swedish). SKB R-10-14, Svensk Kärnbränslehantering AB.

**Wersin P, Spahiu K, Bruno J, 1994a.** Time evolution of dissolved oxygen and redox conditions in a HLW repository. SKB TR 94-02, Svensk Kärnbränslehantering AB.

**Wersin P, Bruno J, Laaksoharju M, 1994b.** The implications of soil acidification on a future HLW repository. Part II: Influence on deep granitic groundwater. The Klipperås study site as test case. SKB TR 94-31, Svensk Kärnbränslehantering AB.

**White A F, Brantley S L, 2003.** The effect of time on the weathering of silicate minerals: why do weathering rates differ in the laboratory and field? Chemical Geology, 202, pp 479–506.

**Whitehouse P, 2009.** Glacial isostatic adjustment and sea-level change. State of the art report. SKB TR-09-11, Svensk Kärnbränslehantering AB.

**Wilmot R D, Wickham S M, Galson D A, 1999.** Elements of a regulatory strategy for the consideration of future human actions in safety assessments. SKI Report 99:46, Statens kärnkraftinspektion (Swedish Nuclear Power Inspectorate).

**Wilmot R D, Galson D A, 2000.** Expert judgement in performance assessment. SKI Report 00:4, Statens kärnkraftinspektion (Swedish Nuclear Power Inspectorate).

**Wilmot R D, Galson D A, Hora S C, 2000.** Expert judgements in performance assessments. Report of an SKI/SSI seminar, SKI Report 00:35, Statens kärnkraftinspektion (Swedish Nuclear Power Inspectorate).

**Wimelius H, Pusch R, 2008.** Backfilling of KBS-3V deposition tunnels – possibilities and limitations. SKB R-08-59, Svensk Kärnbränslehantering AB.

**Witt A, Schumann A Y, 2005.** Holocene climate variability on millennial scales recorded in Greenland ice cores. Nonlinear Processes in Geophysics, 12, pp 345–352.

**Wohlfarth B, 2009.** Ice-free conditions in Fennoscandia during Marine Oxygen Isotope Stage 3? SKB TR-09-12, Svensk Kärnbränslehantering AB.

**Wold S, 2010.** Sorption of prioritized elements on montmorillonite colloids and their potential to transport radionuclides. SKB TR-10-20, Svensk Kärnbränslehantering AB.

**Wu P, Wood R, Stott P, 2004.** Does the recent freshening trend in the North Atlantic indicate a weakening thermohaline circulation? Geophysical Research Letters, 31, L02301, doi:10.1029/2003GL018584.

**Wänstedt S, 2000.** Geophysical and geological investigations of the Boda area. SKB R-00-23, Svensk Kärnbränslehantering AB.

**Yang C, Samper J, Molinero J, Bonilla M, 2007.** Modelling geochemical and microbial consumption of dissolved oxygen after backfilling a high level radioactive waste repository. Journal of Contaminant Hydrology, 93, pp 130–148.

**Yershov E D, 1998.** General geocryology. Cambridge: Cambridge University Press.

**Åkesson M, Kristensson O, Börgesson L, Dueck A, Hernelind J, 2010a.** THM modelling of buffer, backfill and other system components. Critical processes and scenarios. SKB TR-10-11, Svensk Kärnbränslehantering AB.

**Åkesson M, Börgesson L, Kristensson O, 2010b.** SR-Site Data report. THM modelling of buffer, backfill and other system components. SKB TR-10-44, Svensk Kärnbränslehantering AB.

**Åstrand P-G, Broed R, Jones J, 2005.** Pandora technical description and user guide. Posiva Working Report 2005-64, Posiva Oy, Finland.

**Öhman J, Follin S, 2010.** Site investigation SFR. Hydrogeological modelling of SFR. Model version 0.2. SKB R-10-03, Svensk Kärnbränslehantering AB.

### Unpublished documents


| SKBdoc id, version | Title | Issuer, year |
|---|---|---|
| 1077122 ver 2.0 | Strålskärmsberäkningar för kopparkapslar innehållande BWR, MOX och PWR bränsleelement. | SKB, 2010 |
| 1175162 ver 4.0 | Svetsning vid tillverkning och förslutning. | SKB, 2011 |
| 1193244 ver 4.0 | Criticality safety calculations of disposal canisters. | SKB, 2010 |
| 1221567 ver 2.0 | SKB – Simulering av inkapsling av använt kärnbränsle för slutförvaring i KBS-3-förvar. | SKB, 2010 |

# Appendix A

## Applicable regulations and SKB's implementation of these in the safety assessment SR-Site

This Appendix contains regulatory texts issued by SSM applicable to a safety assessment for a nuclear waste repository. References to SKB's plan for complying with the regulations have been inserted in italics at relevant places in Sections A1.1 (SSMFS 2008:21) and A2.1 (SSMFS 2008:37).

### A1 SSMFS 2008:21

SSM has issued Regulations concerning Safety in connection with the Disposal of Nuclear Material and Nuclear Waste and General Recommendations concerning the application of those Regulations, both in SSMFS 2008:21.

Whereas the Regulations have a clear legal status, General Recommendations are described in 1 § Ordinance on Regulatory Codes (1976:725) as: Such general recommendations on the application of regulations that stipulate how someone can or should act in a certain respect.

#### A1.1 Regulations in SSMFS 2008:21

The Swedish Radiation Safety Authority's Regulations concerning Safety in connection with the Disposal of Nuclear Material and Nuclear Waste decided on December 19, 2008.

On the basis of 20 a and 21 §§ of the Ordinance (1984:14) on Nuclear Activities, the Swedish Radiation Safety Authority has issued the following regulations and decided on the following general recommendations.

**Application**

1 § These regulations apply to facilities for the disposal of spent nuclear fuel and waste (repositories). The regulations do not apply to facilities for landfill disposal of low-level nuclear waste in accordance with 19 § of the Ordinance (1984:14) on Nuclear Activities.

The regulations contain supplementary provisions to the Swedish Radiation Safety Authority's regulations (SSMFS 2008:1) concerning Safety in Certain Nuclear Facilities.

**Barriers and their Functions**

2 § Safety after the closure of a repository shall be maintained through a system of passive barriers.

3 § The function of each barrier shall be to, in one or several ways, contribute to the containment, prevention or retardation of dispersion of radioactive substances, either directly, or indirectly by protecting other barriers in the barrier system.

***Handling in SR-Site:*** *The ways in which the barriers contribute to safety is discussed in detail in Chapter 8. The calculation cases in Section 13.7.3 address this issue directly. In general, most of the safety assessment is aimed at demonstrating barrier safety.*

4 § A deficiency in any of the repository's barrier functions that is detected during the construction or operational surveillance of the repository and that can lead to a deterioration in safety after closure in addition to that anticipated in the safety report[23], shall be reported to the Swedish Radiation Safety Authority without delay[24]. The same applies if such a deficiency is suspected to occur or if the possibility that such a deficiency can occur in the future is suspected.

[23] Cf. Chapter 4. 2 § of the Swedish Radiation Protection Authority's regulations (SSMFS 2008:1) concerning Safety in Certain Nuclear Facilities.

[24] Cf. Chapter 2. 2 § of the Swedish Radiation Protection Authority's regulations (SSMFS 2008:1) concerning Safety in Certain Nuclear Facilities.

**Design and Construction**

5 § The barrier system shall be able to withstand such features, events and processes that can affect the post-closure performance of the barriers.

***Handling in SR-Site:*** *The overall purpose of the safety assessment can be said to demonstrate this point.*

6 § The barrier system shall be designed and constructed taking into account the best available technique[25].

***Handling in SR-Site:*** *The issue of BAT is addressed in Sections 2.7, 14.3 and 15.3.5.*

7 § The barrier system shall comprise several barriers so that, as far as possible, the necessary safety is maintained in spite of a single deficiency in a barrier.

***Handling in SR-Site:*** *This issue is addressed in many of the analyses. In particular, a set of calculation cases to illustrate this issue is presented in Section 13.7.3.*

8 § The impact on safety of such measures that are adopted to facilitate the monitoring or retrieval of disposed nuclear material or nuclear waste from the repository, or to make access to the repository difficult, shall be analysed and reported to the Swedish Radiation Safety Authority.

**Safety Assessment**

9 § In addition to the provisions of Chapter 4. 1 § of the Swedish Radiation Safety Authority's Regulations (SSMFS 2008:1) concerning the Safety in Certain Nuclear Facilities, the safety assessments shall also comprise features, events and processes which can lead to the dispersion of radioactive substances after closure, and such analyses shall be made before repository construction, before repository operation and before repository closure.

***Handling in SR-Site:*** *The systematic management in a database of the mentioned features, events and processes in SR-Site is discussed in Chapter 3 and in the* ***FEP report****. The detailed management of many of these factors is discussed throughout the report. Verification that FEPs omitted in earlier parts of the assessment are of negligible significance in light of the completed scenario and risk analysis is provided in Section 14.4.*

10 § A safety assessment shall comprise as long time as barrier functions are required, but at least ten thousand years.

***Handling in SR-Site:*** *The timescales of relevance for SR-Site are discussed in Section 2.4.*

**Safety Report**

11 § The safety report for a repository shall, in addition what is required in Chapter 4 2 § of the Swedish Radiation Safety Authority's Regulations (SSMFS 2008:1) concerning Safety in Certain Nuclear Facilities, contain the information required in Appendix 1 of these regulations and which concerns the time after closure.

Prior to repository closure, the final safety assessment must be renewed and subjected to a safety review in accordance with Chapter 4. 3 § of the Swedish Radiation Safety Authority's regulations (SSMFS 2008:1) Concerning Safety in Certain Nuclear Facilities and must be reviewed and approved by the Swedish Radiation Safety Authority.

**Exceptions**

12 § The Swedish Radiation Safety Authority may grant exceptions, if particular grounds exist, from these regulations if this can be achieved without departing from the purpose of the regulations and on condition that safety can be maintained.

[25] Cf. Chapter 2. 3 § of the Swedish Environmental Code.

**Appendix 1**

**The following shall be reported with regard to analysis methods:**

– how one or several methods have been used to describe the passive system of barriers in the repository, its performance and evolution over time; the method or methods shall contribute to providing a clear view of the features, events and processes that can affect the performance of the barriers and the links between these features, events and processes,

***Handling in SR-Site:*** *The format for system description is discussed in Chapter 5 (initial state), Chapter 6 (external conditions) and Chapter 7 (processes). The description of system evolution is related to the entire assessment and is analysed in detail as a reference evolution in Chapter 10. Variants of this evolution are analysed for a number of scenarios in Chapter 12.*

– how one or several methods have been used to identify and describe relevant scenarios for sequences of events and conditions that can affect the future evolution of the repository; the scenarios shall include a main scenario that takes into account the most probable changes in the repository and its environment,

***Handling in SR-Site:*** *The scenario selection method for SR-Site is described in Section 2.5.8 and its implementation in Chapter 11.*

– the applicability of models, parameter values and other conditions used for the description and quantification of repository performance as far as reasonably achievable,

***Handling in SR-Site:*** *This is done in the* ***Model summary report****, see e.g. Section 7.5 and the* ***Data report****, see Chapter 9.*

– how uncertainties in the description of the functions, scenarios, calculation models and calculation parameters used in the description as well as variations in barrier properties have been handled in the safety assessment, including the reporting of a sensitivity analysis which shows how the uncertainties affect the description of barrier performance and the analysis of consequences to human health and the environment.

***Handling in SR-Site:*** *The management of uncertainties permeates the safety assessment. A plan for the management of uncertainties is given in Section 2.8.3. Sensitivity analyses occur in a number of places in the reference evolution and the analyses of different scenarios, see e.g. Sections 12.2.2, 12.6.2, 13.5.11 and 13.6.2. Sensitivity of the main risk contributors to various conceptual uncertainties is analysed in Section 13.10.*

**The following shall be reported with respect to the analysis of post-closure conditions:**

– the safety assessment in accordance with 9 § comprising descriptions of the evolution in the biosphere, geosphere and repository for selected scenarios; the environmental impact of the repository for selected scenarios, including the main scenario, with respect to defects in engineered barriers and other identified uncertainties.

***Handling in SR-Site:*** *This is essentially the reporting of the analyses of the reference evolution in Chapter 10 and of the selected scenarios in Chapter 12.*

## A1.2 Excerpts from the General Recommendations in SSMFS 2008:21

**The Swedish Radiation Safety Authority's General Recommendations concerning the Application of the Regulations concerning Safety in connection with the Disposal of Nuclear Material and Nuclear Waste (SSMFS 2008:21)**

*The following is the unabbreviated Recommendations relevant to 9 and 10 § and Appendix of SSMFS 2008:21, i.e. those sections that concern the safety assessment.*

**On 9 § and Appendix**

The safety of a repository after closure is analysed quantitatively, primarily by estimating the possible dispersion of radioactive substances and how it is distributed in time for a relevant selection

of future possible sequences of events (scenarios). The purpose of the safety assessment is to show, inter alia, that the risks from these scenarios are acceptable in relation to the requirements on the protection of human health and the environment issued by the Swedish Radiation Safety Authority (SSMFS 2008:37). The safety assessment should also aim at providing a basic understanding of the repository performance on different time-periods and at identifying requirements regarding the performance and design of different repository components.

A ***scenario*** in the safety assessment comprises a description of how a given combination of external and internal conditions affect repository performance. Two groups of such conditions are:

- external conditions in the form of features, events and processes which occur outside repository barriers; this includes climate changes and their consequential impact on the repository environment, such as permafrost, glaciation, land subsidence and elevation as well as the impact of human activities,
- internal conditions in the form of features, events and processes which occur inside the repository; this includes properties, including defects, of nuclear material, nuclear waste and engineered barriers and related processes as well as properties of the surrounding geological formation and related processes.

Based on an analysis of the probability of occurrence of different types of scenarios in different time-periods, scenarios with a significant impact on repository performance should be divided into different categories:

- main scenario,
- less probable scenarios,
- other scenarios or residual scenarios.

***The main scenario*** should be based on the probable evolution of external conditions and realistic, or where justified, pessimistic assumptions with respect to the internal conditions. It should comprise future external events which have a significant probability of occurrence or which cannot be shown to have a low probability of occurrence during the time covered in the safety assessment. Furthermore, it should be based, as far as possible, on credible assumptions with respect to internal conditions, including substantiated assumptions concerning the occurrence of manufacturing defects and other imperfections, and which allow for an analysis of the repository barrier functions (it is, for example, not sufficient to always base the analysis on leak-tight waste containers, even if this can be shown to be the most probable case). The main scenario should be used as the starting point for an analysis of the impact of uncertainties (see below), which means that the analysis of the main scenario also includes a number of calculation cases.

***Less probable scenarios*** should be prepared for the evaluation of scenario uncertainty (see also below). This includes variations on the main scenario with alternative sequences of events as well as scenarios that take into account the impact of future human activities such as damage inflicted on barriers. (Damage to humans intruding into the repository is illustrated by residual scenarios, see below). The analysis of less probable scenarios should include analyses of such uncertainties that are not evaluated within the framework of the main scenario.

***Residual scenarios*** should include sequences of events and conditions that are selected and studied independently of probabilities in order to, *inter alia*, illustrate the significance of individual barriers and barrier functions. The residual scenarios should also include cases to illustrate damage to humans intruding into the repository as well as cases to illustrate the consequences of an unclosed repository that is not monitored.

***Handling in SR-Site:*** *The methodology for selection of scenarios is described in Section 2.5.8 and its implementation is described in Chapter 11.*

The lack of knowledge and other uncertainties in the calculation conditions (assumptions, models, data) is denoted in this context as uncertainties[26]. These uncertainties can be classified as follows:

- scenario uncertainty: uncertainty with respect to external and internal conditions in terms of type, degree and time sequence,
- system uncertainty: uncertainty as to the comprehensiveness of the description of the system of features, events and processes used in the analysis of both individual barrier performance and the performance of repository as a whole,
- model uncertainty: uncertainty in the calculation models used in the analysis,
- parameter uncertainty: uncertainty in the parameter values (input data) used in the calculations,
- spatial variation in the parameters used to describe the barrier performance of the rock (primarily with respect to hydraulic, mechanical and chemical conditions).

There are often no clear boundaries between the different types of uncertainties. The most important requirement is that the uncertainties should be described and handled in a consistent and structured manner.

The evaluation of uncertainties is an important part of the safety assessment. This means that uncertainties should be discussed and examined in depth when selecting calculation cases, calculation models and parameter values as well as when evaluating calculation results.

***Handling in SR-Site:*** *The management of uncertainties permeates the safety assessment. A plan for the management of uncertainties is given in Section 2.8.3.*

The assumptions and calculation models used should be carefully selected with respect to the principle that the application and the selection should be justified through a discussion of alternatives and with reference to scientific data. In cases where there is doubt as to a suitable model, several models should be used to illustrate the impact of the uncertainty involved in the choice of model.

***Handling in SR-Site:*** *This matter is mainly addressed in the* ***Process reports*** *and, for external influences, in the* ***Climate report****, see further Chapters 7 and 6, respectively. A structured account of important selected models is given in the* ***Model summary report****.*

Both deterministic and probabilistic methods should be used so that they complement each other and, consequently, provide as comprehensive a picture of the risks as possible.

***Handling in SR-Site:*** *Most of the calculations in SR-Site are deterministic. Probabilistic calculations are used essentially as a means of handling data uncertainty and spatial variability in modelling radionuclide transport and dose, in particular in Chapter 13.*

***The probabilities*** that the scenarios and calculation cases will actually occur should be estimated as far as possible in order to calculate risk. Such estimates cannot be exact. Consequently, the estimates should be substantiated through the use of several methods, for example, assessments by several independent experts. This can be done, for example, through estimates of when different events can be expected to have occurred.

***Handling in SR-Site:*** *Probabilities of scenarios that are not excluded from the risk summation as being "residual" are derived pessimistically. This is a component of the general approach to risk estimates, see Section 2.6.2. Of relevance is also the method for scenario selection described in Section 2.5.8 and implemented as described in Chapter 11. The analyses leading to the categorisation of the selected scenarios is provided in Chapter 12.*

Based on scenarios that can be shown to be especially important from the standpoint of risk, a number of ***design basis cases*** should be identified. Together with other information, such as on manufacturing method and controllability, these cases should be used to substantiate the design basis such as requirements on barrier properties.

***Handling in SR-Site:*** *See Section 15.4.*

[26] This explanation of the term uncertainty only makes sense in Swedish where the same word (säkerhet) is used to denote both certainty and safety.

Particularly in the case of disposal of nuclear material, for example spent nuclear fuel, it should be shown that criticality cannot occur in the initial configuration of the nuclear material. With respect to the redistribution of the nuclear material through physical and chemical processes, which can lead to criticality, it should be shown that such a redistribution is very improbable.

***Handling in SR-Site:*** *See Section 13.3 and further the* ***Fuel and canister process report****, Section 2.1.3.*

The result of calculations in the safety assessment should contain such information and should be presented in such a way that an overall judgement of safety compliance with the requirements can be made.

***Handling in SR-Site:*** *This is an overall requirement on the quality of the safety reporting, which has governed the compilation of the SR-Site report. Compliance is discussed in Section 15.3.*

The validity of assumptions used, such as models and parameter values, should be supported, for example through the citing of references to scientific literature, special investigations and research results, laboratory experiments on different scales, field experiments and studies of natural phenomena (natural analogues).

***Handling in SR-Site:*** *Justification of models, on the bases mentioned, is done in the* ***Process reports****, and for external influences, in the* ***Climate report****. A structured account of all important models is given in the* ***Model summary report****. Parameter values are justified in the* ***Data report****.*

Scientific background material and expert assessments should be documented in a traceable manner by thoroughly referring to scientific literature and other material.

***Handling in SR-Site:*** *This is addressed in much of the documentation of SR-Site, in particular the three* ***Process reports****, the* ***Climate report*** *and the* ***Data report****.*

**On 10 §**

The time-period for which safety has to be maintained and demonstrated should be a starting point for the safety assessment. One way of discussing and justifying the establishment of such a time period is to start from a comparison of the hazard of the radioactive inventory of the repository with the hazard of radioactive substances occurring in nature. However, it should also be possible to take into consideration the difficulties of conducting meaningful analyses for extremely long time-periods, beyond one million years, in any other way than through showing how the hazard of the radioactive substances in the repository declines with time.

In the case of a repository for long-lived waste, the safety assessment may have to include scenarios which take into account greater expected climate changes, primarily in the form of future glaciations. For example, the next complete glacial cycle which is currently estimated to be on the order of 100,000 years, should be particularly taken into account.

***Handling in SR-Site:*** *The timescale for SR-Site is discussed in Section 2.4.*

In the case of periods up to 1,000 years after closure, in accordance with the regulations of SSI FS 1998:1, the dose and risk calculated for current conditions in the biosphere constitute the basis for the assessment of repository safety and its protective capabilities.

Furthermore, in the case of longer periods, the assessment can be made using dose as one of several safety indicators. This should be taken into account in connection with the calculations as well as the presentation of analysis results. Examples of such supplementary safety indicators are the concentrations of radioactive substances from the repository which can build up in soils and near-surface groundwater or the calculated flow of radioactive substances to the biosphere.

(Compare the regulations in SSMFS 2008:37 and SSM's comments on those regulations).

***Handling in SR-Site:*** *Alternative safety indicators are selected in Section 2.6.3 and applied in Section 13.5.8 and further in the* ***Radionuclide transport report****.*

## A2 SSMFS 2008:37

SSM has in SSMFS 2008:37 issued Regulations concerning the Protection of Human Health and the Environment in connection with the Final Management of Spent Nuclear Fuel or Nuclear Waste, and General Guidance concerning the application of these regulations.

Whereas the Regulations have a clear legal status, General Recommendations are described in 1 § Ordinance on Regulatory Codes (1976:725) as: Such general recommendations on the application of regulations that stipulate how someone can or should act in a certain respect.

### A2.1 Regulations in SSMFS 2008:37

**The Swedish Radiation Safety Authority's Regulations concerning the Protection of Human Health and the Environment in connection with the Final Management of Spent Nuclear Fuel or Nuclear Waste; decided on December 19, 2008.**

On the basis of 7 and 8 §§ of the Radiation Protection Ordinance (1988:293), the Swedish Radiation Protection Institute stipulates the following.

**1 §** These regulations are to be applied to the final management of spent nuclear fuel or nuclear waste. The regulations do not apply to landfills for low-level nuclear waste in accordance with 19 § of the Ordinance (1984:14) on Nuclear Activities.

**Definitions**

**2 §** In these regulations, concepts are defined as follows:

- *best available technique:* the most effective measure available to limit the release of radioactive substances and the harmful effects of the releases on human health and the environment which does not entail unreasonable costs,
- *intrusion:* human intrusion into a repository which can affect its protective capability,
- *optimisation:* keeping the radiation doses to mankind as low as reasonably achievable, economic and social factors taken into account,
- *harmful effects:* cancer (fatal and non-fatal) as well as hereditary defects in humans caused by ionising radiation in accordance with paragraphs 47–51 of the International Radiation Protection Commission's Publication 60, 1990,
- *protective capability:* the capability to protect human health and the environment from the harmful effects of ionising radiation,
- *final management:* handling, treatment, transportation, interim storage prior to, and in connection with final disposal as well as the final disposal,
- *risk:* the product of the probability of receiving a radiation dose and the harmful effects of the radiation dose.

Terms and concepts used in the Radiation Protection Act (1988:220) and the Act (1984:3) on Nuclear Activities have the same meanings in these regulations.

**Holistic Approach etc.**

**3 §** Human health and the environment shall be protected from the harmful effects of ionising radiation, during the time when the various stages of the final management of spent nuclear fuel or nuclear waste are being implemented as well as in the future. The final management may not cause impacts on human health and the environment outside Sweden's borders that are more severe than those accepted inside Sweden.

**4 §** Optimisation must be achieved and the best available technique shall be taken into consideration in the final management of spent nuclear fuel or nuclear waste.

The collective dose, as a result of the expected outflow of radioactive substances during a period of 1,000 years after closure of a repository for spent nuclear fuel or nuclear waste shall be estimated as the sum, over 10,000 years, of the annual collective dose. The estimate shall be reported in accordance with 10–12 §§.

***Handling in SR-Site:*** *The aspects of optimisation and best available technique that can be addressed in the safety assessment are addressed in Sections 2.7, 14.3 and 15.3.5. Collective dose is addressed in Section 13.6.5.*

**Protection of human health**

**5 §** A repository for spent nuclear fuel or nuclear waste shall be designed so that the annual risk of harmful effects after closure does not exceed $10^{-6}$ for a representative individual in the group exposed to the greatest risk[27].

The probability of harmful effects as a result of a radiation dose shall be calculated using the probability coefficients provided in the International Radiation Protection Commission's Publication 60, 1990.

***Handling in SR-Site:*** *Estimation of risk and assessing compliance with the above criterion is one of the main purposes of SR-Site. Much of the methodology outlined in Chapter 2 is aimed at achieving this end-point. Issues directly related to the calculation of risk are discussed in Section 2.6. A summation of the calculated risk contributions from relevant scenarios is given in Section 13.9 and a discussion of compliance is given in Section 15.2.1.*

**Environmental Protection**

**6 §** The final management of spent nuclear fuel or nuclear waste shall be implemented so that biodiversity and the sustainable use of biological resources are protected against the harmful effects of ionising radiation.

**7 §** Biological effects of ionising radiation in living environments and ecosystems concerned shall be described. The report shall be based on available knowledge concerning the ecosystems concerned and shall take particular account of the existence of genetically distinctive populations such as isolated populations, endemic species and species threatened with extinction) and in general any organisms worth protecting.

***Handling in SR-Site:*** *This issue is addressed in Chapter 13, Sections 13.2.5 and 13.5.7. Conclusions are provided in Section 15.3.4.*

**Intrusion and Access**

**8 §** A repository shall be primarily designed with respect to its protective capability. If measures are adopted to make access easier or to make intrusion difficult, the effects on the protective capability of the repository shall be reported.

**9 §** The consequences of intrusion into a repository shall be reported for the different time periods specified in 11–12 §§.

The protective capability of the repository after intrusion shall be described.

***Handling in SR-Site:*** *Intrusion issues are discussed in Section 6.2.1 and analysed in Section 14.2 as further documented in the* ***FHA report****.*

[27] With respect to facilities in operation, the limitations and instructions that apply are provided in the Swedish Radiation Protection Institute's regulations (SSI FS 1991:5, amended 1997:2) concerning the limitation of releases of radioactive substances from nuclear power plants and the Swedish Radiation Protection Institute's regulations (SSI FS 1994:2, amended 1997:3) concerning health physics for activities involving ionising radiation at nuclear facilities.

**Time Periods**

**10 §** An assessment of a repository's protective capability shall be reported for two time periods of orders of magnitude specified in 11–12 §§. The description shall include a case, which is based on the assumption that the biospheric conditions which exist at the time that an application for a licence to operate the repository is submitted will not change. Uncertainties in the assumptions made shall be described and taken into account in the assessment of the protective capability.

*The first thousand years following repository closure*

**11 §** For the first thousand years following repository closure, the assessment of the repository's protective capability shall be based on quantitative analyses of the impact on human health and the environment.

*Period after the first thousand years following repository closure*

**12 §** For the period after the first thousand years following repository closure, the assessment of the repository's protective capability shall be based on various possible sequences for the development of the repository's properties, its environment and the biosphere.

***Handling in SR-Site (11 § and 12 §):*** *This is mainly addressed in the reference evolution, Chapter 10, which is divided into several time frames. The first 1,000 years are treated as part of the initial temperate period. A number of scenarios are analysed (Chapters 12 and 13), covering various possibilities for the repository evolution.*

**Exceptions**

**13 §** If special grounds exist, the Swedish Radiation Protection Institute may announce exceptions from these regulations.

## A2.2 General Guidance on SSMFS 2008:37

**The Swedish Radiation Safety Authority's guidelines on the application of the regulations (SSMFS 2008:37) concerning protection of human health and the environment in connection with the final management of spent nuclear fuel and nuclear waste; decided upon on 19 December 2008.**

### *Unofficial translation*

**Guidelines concerning geological disposal of spent nuclear fuel and nuclear waste**

**On Section 1: Area of application**

These guidelines are applicable to final geological disposal of spent nuclear fuel and nuclear waste. The guidelines cover measures undertaken with a view to develop, site, construct, operate and close a repository, which can affect the protective capability of the repository and environmental consequences after closure.

The guidelines are also applicable to measures that are to be undertaken with spent nuclear fuel and nuclear waste before final disposal and which can affect the protective capability of the repository and environmental consequences after closure. This includes activities at other installations such as the conditioning of waste that takes place by casting waste in concrete and by encapsulation of spent nuclear fuel, as well as transportation between installations and steering of waste to different repositories, including shallow land burials for low-level nuclear waste that are licenced in accordance with Section 19 of the Ordinance (1984:14) on Nuclear Activities. However, the guidelines, like the regulations, are not applicable to the land burial itself.

**On Section 2: Definitions**

Terms used in the Radiation Protection Act (1988:220), the Act (1984:3) on Nuclear Activities and SSM's Regulations on protection of human health and the environment in connection with final

management of spent nuclear fuel and nuclear waste have the same meaning in these guidelines. In addition, the following definitions are used:

| | |
|---|---|
| *Scenario:* | A description of the development of the repository given an initial state and specified conditions in the environment and their development. |
| *Exposure pathway:* | The migration of the radioactive substances from a repository to a place where human beings or an organism covered by the environmental protection regulations are present. This includes dispersion in the geological barrier, transport with water and air flows, migration in ecosystems and uptake in human beings or organisms in the environment. |
| *Risk analysis:* | An analysis with the aim to clarify the protective capability of a repository and its consequences with regard to the environmental impact and the risk for human beings. |

**On Sections 4, 8 and 9: Holistic approach etc. intrusion and access**

***Optimisation and Best Available Technique***

The regulations require that optimisation must be performed and that best available technique should be taken into account. Optimisation and best available technique should be applied in parallel with a view to improving the protective capability of the repository.

Measures for optimisation of a repository should be evaluated on the basis of calculated risks.

Application of best available technique in connection with final disposal means that the siting, design, construction, operation and closure of the repository and appurtenant system components should be carried out so as to prevent, limit and delay releases from both engineered and geological barriers as far as is reasonably possible. When striking balances between different measures, an overall assessment should be made of their impact on the protective capability of the repository.

In cases where considerable uncertainty is attached to the calculated risks, for instance, in analyses of the repository a long time after closure, or analyses made at an early stage of the development work with the repository system, greater weight should be placed on best available technique.

In the event of any conflicts between application of optimisation and best available technique, priority should be given to best available technique.

Experience from recurrent risk analyses and the successive development work with the repository should be used in the application of optimisation and best available technique.

***Handling in SR-Site:*** *The aspects of optimisation and best available technique that can be addressed in the safety assessment are addressed in Sections 2.7, 14.3 and 15.3.5.*

*Collective dose*

The regulations require an account of the collective dose from releases that take place during the first thousand years after closure. For final disposal the collective dose should also be used in comparisons between alternative repository concepts and sites. The collective dose need not be reported if the repository concept entails a complete isolation of the spent nuclear fuel or the nuclear waste in engineered barriers during the first thousand years after closure.

***Handling in SR-Site:*** *An estimate of the collective dose is provided in Section 13.6.5*.

*Occupational radiation protection*

An account should be given of measures undertaken for radiation protection of workers that may have a negative impact on the protective capability of the repository or make it more difficult to assess.

***Handling in SR-Site:*** *No such measures have been identified in SR-Site.*

*Future human action and the preservation of information*

When applying best available technique, consideration should also be given to the possibility to reduce the probability and consequences of inadvertent future human impact on the repository, for instance, inadvertent intrusion. Increased repository depth and avoidance of sites with extractable mineral assets may, for instance, be considered to decrease the probability of unintentional human intrusion.

***Handling in SR-Site:*** *Ore potential is evaluated for the site, see Section 4.3.2. This information is propagated to the analyses of FHA-scenarios in Section 14.2. Inadvertent intrusion is discussed as one of many factors when feedback is given to the selection of repository depth in Section 14.3.4 and 15.5.18.*

Preservation of knowledge about the repository could reduce the risk of future human impact. A strategy for preservation of information should be produced so that measures can be undertaken before closure of the repository. Examples of information that should be taken into consideration are information about the location of the repository, its content of radioactive substances and design.

***Handling in SR-Site:*** *The production of such a strategy is not an issue for the safety assessment. As documented elsewhere in SKB's licence application, information about the repository will be collected and stored during construction, operation and closure of the repository according to applicable legal requirements. A strategy for preservation of information after closure will be developed by SKB, to some extent as part of international cooperation on this subject, in reasonable time before closure.*

**On Sections 5–7: Protection of human health and the environment**

***Risk for the individual from the general public***

*The relationship between dose and risk*

According to the regulations, the recommendations of the International Commission on Radiological Protection (ICRP) are to be used for calculation of the harmful effects of ionizing radiation. According to ICRP Publication No. 60, 1990, the factor for conversion of effective dose to risk is 7.3 percent per sievert.

*The regulation's criterion for individual risk*

According to the regulations, the risk for harmful effects for a representative individual in the group exposed to the greatest risk (the most exposed group) shall not exceed $10^{-6}$ per year. Since the most exposed group cannot be described in an unambiguous way, the group should be regarded as a way of quantifying the protective capability of the repository.

One way of defining the most exposed group is to include the individuals that receive a risk in the interval from the highest risk down to a tenth of this risk. If a larger number of individuals can be considered to be included in such a group, the arithmetic average of individual risks in the group can be used for demonstrating compliance with the criterion for individual risk in the regulations. One example of such exposure situation is a release of radioactive substances into a large lake that can be used as a source of drinking water and for fishing.

If the exposed group only consists of a few individuals, the criterion of the regulations for individual risk can be considered as being complied with if the highest calculated individual risk does not exceed $10^{-5}$ per year. An example of a situation of this kind might be if consumption of drinking water from a drilled well is the dominant exposure path. In such a calculation example, the choice of individuals with the highest risk load should be justified by information about the spread in calculated individual risks with respect to assumed living habits and places of stay.

***Handling in SR-Site:*** *The most exposed group is defined as the group of individuals that receives the highest exposure across all potential release areas (i.e. biosphere objects) in the landscape, see further Section 13.2.3 and the* ***Biosphere synthesis report****.*

*Averaging risk over a lifetime*

The individual risk should be calculated as an annual average on the basis of an estimate of the life-time risk for all relevant exposure pathways for every individual. The lifetime risk can be calculated as the accumulated lifetime dose multiplied by the conversion factor of 7.3 percent per sievert.

***Handling in SR-Site:*** *This approach is used in SR-Site, see Section 13.2.3 and the* ***Biosphere synthesis report****.*

*Averaging risk between generations*

Deterministic and probabilistic calculations can both be used to illustrate how risk from the repository develops over time. A probabilistic analysis can, however, in certain cases give an insufficient picture of how an individual detrimental event, for instance, a major earthquake, would affect the risk for a particular generation. The probabilistic calculations should in this case be supplemented as specified in Appendix 1.

***Handling in SR-Site:*** *This so called risk dilution phenomenon is addressed in general terms in Section 2.6.2, subheading "Risk dilution" and analysed in Section 13.9.4.*

***Selection of scenarios***

The assessment of the protective capability of the repository and the environmental consequences should be based on a set of scenarios that together illustrate the most important courses of development of the repository, its surroundings and the biosphere.

*Handling of climate evolution*

Taking into consideration the great uncertainties associated with the assumptions on climate evolution in a remote future and to facilitate the interpretation of the risk to be calculated, the risk analysis should be simplified to include a few possible climate evolutions.

A realistic set of biosphere conditions should be associated with each climate evolution. The different climate evolutions should be selected so that they together illustrate the most important and reasonably foreseeable sequences of future climate states and their impact on the protective capability of the repository and the environmental consequences. The choice of the climate evolutions that serve as the basis for the analysis should be based on a combination of sensitivity analyses and expert judgements. Additional guidance is provided in the section with guidelines on Sections 10–12.

The risk from the repository should be calculated for each assumed climate evolution by summing the risk contributions from a number of scenarios that together illustrate how the more or less probable courses of development in the repository and the surrounding rock affects the repository's protective capability and environmental consequences. The calculated risk should be reported and evaluated in relation to the criterion of the regulations for individual risk, separately for each climate evolution. The repository should thus be able to be shown to comply with the risk criterion for the alternative climate evolutions. If a lower probability than one (1) is stated for a particular climate evolution, this should be justified, for instance, by expert judgements.

***Handling in SR-Site:*** *The method for selection of scenarios is described in Section 2.5.8. A reference climate evolution is used in the definition of a base case of the main scenario. In a global warming variant of the main scenario, a climate perturbed by the effects of anthropogenic greenhouse gas emissions is assumed. In the analyses of each of the additional scenarios in Chapter 12, both these variants are considered. In addition, for each scenario, the impact of uncertainties regarding the climate related factors of concern in that particular scenario, are analysed. The results of all these scenarios are considered in the risk summation.*

*Future human action*

A number of scenarios for inadvertent human impact on the repository should be presented. The scenarios should include a case of direct intrusion in connection with drilling in the repository and some examples of other activities that indirectly lead to a deterioration in the protective capability of the repository, for example by changing groundwater chemistry or the hydrological conditions in the repository or its surroundings. The selection of intrusion scenarios should be based on present living habits and technical prerequisites and take into consideration the repository's properties.

The consequences of the disturbance of the repository's protective capability should be illustrated by calculations of the doses for individuals in the most exposed group, and reported separately apart from the risk analysis for the undisturbed repository. The results should be used to illustrate

conceivable countermeasures and to provide a basis for the application of best available technique (see guidelines on optimisation and best available technique).

An account need not be given of the direct consequences for the individuals intruding into the repository.

***Handling in SR-Site:*** *The above approach is used in SR-Site, see Section 14.2. Regarding countermeasures, the depth and location (away from ore potential) of the repository have been selected with the aim of minimising the risk of inadvertent human intrusion among several other considerations, see Section 14.3.4.*

*Special scenarios*

For repositories primarily based on isolation of the spent nuclear fuel or nuclear waste, an analysis of a conceivable loss, during the first thousand years after closure, of one or more barrier functions of key importance for the protective capability should be made separately from the risk analysis. The intention of this analysis should be to clarify how the different barriers contribute to the protective capability of the repository.

***Handling in SR-Site:*** *Such an analysis is provided in Section 13.7.3.*

***Biosphere conditions and exposure pathways***

The future biosphere conditions for calculations of consequences on human beings and the environment should be selected in agreement with the assumed climate state. Unless it is clearly unreasonable, however, today's biosphere conditions at the repository and its surroundings should be evaluated, i.e. agricultural land, forest, wetland (mire), lake, sea or other relevant ecosystems. Furthermore, consideration should be given to land uplift (or subsidence) and other predictable changes.

The risk analysis can include a limited selection of exposure paths, although the selection of these should be based on an analysis of the diversity of human use of environmental and natural resources which can occur in Sweden today. Consideration should also be given to the possibility of individuals being exposed to combinations of exposure pathways within and between different ecosystems.

***Handling in SR-Site:*** *The above approach is used in SR-Site, see Section 13.2.*

***Environmental protection***

The description of exposure pathways should also include exposure pathways to certain organisms in the ecosystems that should be included in the risk analysis. The concentration of radioactive substances in soil, sediment and water should be accounted for where this is relevant for the respective ecosystem.

When a biological effect for the identified organisms can be presumed, a valuation should be made of the consequence this may have for the affected ecosystems, with the view to facilitating an assessment of impact on biological diversity and a sustainable use of the environment.

The analysis of consequences for organisms in "today's biosphere", carried out as above, should be used for the assessment of environmental consequences in a long-term perspective. For assumed climates, where the present biosphere conditions are evidently unreasonable, for instance, a colder climate with permafrost, it is sufficient to make a survey based on knowledge currently available about applicable ecosystems. Additional guidelines are contained in Appendix 2.

***Handling in SR-Site:*** *The approach used in SR-Site is explained in Section 13.2.5.*

***Reporting of uncertainties***

Identification and assessment of uncertainties in for instance, site-specific and generic data and models should take place in accordance with the instructions given in general recommendations from the Swedish Nuclear Power Inspectorate. The different categories of uncertainties, which are specified there, should be evaluated and reported on in a systematic way and evaluated on the basis of their importance for the result of the risk analysis. The report should also include a motivation of the methods selected for handling different types of uncertainties, for instance, in connection with the selection of scenarios, models and data. All calculation steps with appurtenant uncertainties should be reported on.

Peer review and expert panel elicitation can, in the cases where the basic data is insufficient, be used to strengthen the credibility of assessments of uncertainties in matters of great importance for the assessment of the protective capability of the repository.

***Handling in SR-Site:*** *The approach to handling of uncertainties is described in Section 2.8.*

**On Sections 10–12: Time periods**

Two time periods are defined in the regulations: the period up to a thousand years after closure and the subsequent period.

For longer time periods, the result of the risk analysis should be successively regarded more as an illustration of the protective capability of the repository given certain assumptions.

***Limitation of the risk analysis in time***

The following principles should provide guidance for the limitation of the risk analysis in time:

- For a repository for spent nuclear fuel, or other long-lived nuclear waste, the risk analysis should at least include approximately one hundred thousand years or the period for a glaciation cycle to illustrate reasonably predictable external strains on the repository. The risk analysis should thereafter be extended in time as long as it provides important information about the possibility of improving the protective capability of the repository, although at the longest for a time period of up to one million years.
- For other repositories for nuclear waste, than those referred to in point 1, the risk analysis should at least cover the time until the expected maximum consequences in terms of risk and environmental impact have taken place, although at the longest for a period of time up to one hundred thousand years.

The arguments for the selected limitations of the risk analysis should be presented.

***Handling in SR-Site:*** *The assessment period in SR-Site is one million years, see Section 2.4.*

***Reporting on the first thousand years after closure***

The period of time of a thousand years should be regarded as the approximate time period for which a risk analysis can be carried out with high credibility with regard to factors such as climate and biosphere conditions. For this time period, available measurement data and other knowledge about the initial conditions should be used for a detailed analysis and reporting on the development of the protective capability of the repository and its surroundings.

The conditions and processes during the early development of the repository, which can affect its long-term protective capability, should be described in as much detail as possible. Examples of such conditions and processes are the resaturation of the repository, stabilisation of hydrogeological and geochemical conditions, thermal evolution and other transient events.

Biosphere conditions and known trends in the surroundings of the repository should also be described in detail, partly to be able to characterise "today's biosphere" (see guidelines to Section 5), and partly to be able to characterise the conditions applicable to a conceivable early release from the repository. Known trends here refer, for instance, to land uplift (or subsidence), any trends in climate evolution and appurtenant changes in use of land and water.

***Handling in SR-Site:*** *The above approaches are used in SR-Site, in particular in the analysis of the reference evolution, where the first thousand years after closure are included in the detailed evaluation of the excavation/operational phase, Section 10.2, and of the initial temperate period, Section 10.3.*

***Reporting on very long time periods***

*Up to one hundred thousand years*

Reporting should be based on a quantitative risk analysis in accordance with the guidelines to Sections 5–7. Supplementary indicators of the repository's protective capability, such as barrier functions, radionuclide fluxes and concentrations in the environment, should be used to strengthen the confidence in the calculated risks.

The given period of time of one hundred thousand years is approximate and should be selected in such a way that the effect of expected large climate changes, for instance, a glaciation cycle, on the protective capability of the repository and consequences to the surroundings can be illustrated.

***Handling in SR-Site:*** *The above approach is used in SR-Site, in particular in the analysis of the first glacial cycle after closure, as part of the reference evolution, see Section 10.4. See also the discussion of compliance for this time period in Section 15.3.3.*

*Beyond one hundred thousand years*

The risk analysis should illustrate the long-term development of the repository's barrier functions and the importance of major external disturbances on the repository such as earthquakes and glaciations. Taking into consideration the increasing uncertainties over time, the calculation of doses to people and the environment should be made in a simplified way with respect to climate development, biosphere conditions and exposure pathways. Climate development can be simplified by being described as a repetition of identical glaciation cycles.

A strict quantitative comparison of calculated risk in relation to the criterion for individual risk in the regulations is not meaningful. The assessment of the protective capability of the repository should instead be based on reasoning on the calculated risk together with several supplementary indicators of the protective capability of the repository such as barrier functions, radionuclide fluxes and concentrations in the environment. If the calculated risk exceeds the criterion of the regulations for individual risk or if there are other indications of substantial disruptions of the protective capability of the repository, the underlying causes of this should be reported on as well as possible measures to improve the protective capability of the repository.

***Handling in SR-Site:*** *The above approach is used in SR-Site, in particular in the analysis of the period after the first glacial cycle up to one million years, as part of the reference evolution, see Section 10.5. See also the discussion of compliance for this time period in Section 15.3.3.*

***Summary of arguments for demonstrating compliance with the requirements of the regulations***

The reporting should include an account of how the principles for optimisation and the best possible technique have been applied in the siting and design of the repository and appurtenant system components and how quality assurance has been used in the work with the repository and appurtenant risk analyses.

***Handling in SR-Site:*** *Regarding the account of optimisation and BAT in the safety assessment, see above and Section 15.3.5. Quality assurance for the safety assessment is described in Section 2.9.*

The arguments for the protective capability of a repository should be evaluated and reported on in a systematic way. The reporting should include a logically structured argument for the protective capability of the repository with information on calculated risks, uncertainties in the calculations made and the credibility of the assumptions made. To provide a good understanding of the results of the risk analysis, it should be evident how individual scenarios contribute to the risk from the repository.

***Handling in SR-Site:*** *The arguments for the protective capability of the repository are provided in the discussion of compliance in Section 15.3, and in the various parts of the analysis that support the conclusions in that section.*

**Appendix 1. Guidelines on the averaging of risk between generations**

For certain exposure situations an annual risk, calculated as an average of all conceivable outcomes of a probabilistic risk assessment, provides an insufficient picture of how risk is allocated between future generations. This applies in particular to events which:

- can be assessed as leading to doses during a limited period of time in relation to the time period covered by the risk analysis, and
- if they arise, can be assessed as giving rise to a conditional individual risk exceeding the criterion in the regulations for individual risk, and
- can be assessed as having such a high probability of occurring during the time period covered by the risk analysis that the product of this probability and the calculated conditional risk is of the same order of magnitude as, or larger than, the criterion for individual risk in the regulations.

For exposure situations of this kind, a probabilistic calculation of risk should be supplemented by calculating the risk for the individuals who are assumed to live after the event has taken place and who are affected by its calculated maximum consequence. The calculation can be made for instance by illustrating the importance of an event occurring at different times ($T_1$, $T_2$ …, $T_n$), taking into consideration the probability of the event occurring during the respective time interval ($T_0$ to $T_1$, $T_0$ to $T_2$,…, $T_0$ to $T_n$, where $T_0$ corresponds to the time of closure of the repository). The results from these, or similar calculations, can in this way be expected to provide an illustration of the effects of the spreading of risk between future generations and should, together with other risk calculations, be reported on and evaluated in relation to the regulation's criterion for individual risk.

***Handling in SR-Site:*** *This approach is used in the handling of risk dilution in Section 13.9.4.*

**Annex 2. Guidelines on the evaluation of environmental protection**

The organisms included in the analysis of the environmental impact should be selected on the basis of their importance in the ecosystems, but also according to their protection value according to other biological, economic or conservation criteria. Other biological criteria refers, among other things, to genetic distinctiveness and isolation (for example, presently known endemic species), economic criteria refers to the importance of the organisms for different kinds of obtaining a livelihood (for instance, hunting and fishing), and conservation criteria if they are protected by current legislation and local regulations. Other aspects, for instance, cultural history, should also be taken into consideration in the identification of such organisms.

The assessment of effects of ionising radiation in selected organisms, deriving from radioactive substances from a repository, can be made on the basis of the General Guidance provided in the International Committee for Radiation Protection's (ICRP) Publication 91[28]. The applicability of the knowledge and databases used for the analyses of dispersion and transfer of radioactive substances in ecosystems and for analysing the effects of radiation on different organisms should be assessed and reported on.

***Handling in SR-Site:*** *The approach used in SR-Site is explained in Section 13.2.5.*

[28] A Framework for Assessing the Impact of Ionising Radiation on Non-human Species, ICRP Publication 91, Annals of the ICRP 33:3, 2003

# Appendix B

## Glossary of abbreviations and specialised terms used in SR-Site

The glossary is intended to explain all acronyms, SKB-specific terms, and technical terms that occur often in this report. It is not intended to contain all technical terms found in the report. Chemical formulae and units are usually not included in the glossary. In the glossary, the letters *x*, found in for example KFMxxx, have replaced the numbers/letters in the name of for instance the specific deformation zone KFM01D.

It is noted that some of the explanations differ slightly from the corresponding explanations in other, less specialised reports. The more technical explanations given below are appropriate for the context of this report.

| | |
|---|---|
| 1-D/1D | One-dimensional. |
| 2-D/2D | Two-dimensional. |
| 3-D/3D | Three-dimensional. |
| 3DEC | A discrete element modelling code for analysis of rock and structural support in three dimensions, used to simulate the response of fractured rock that is subject to either static or dynamic loading. |
| ABAQUS | Finite element computer code used for the analysis of buffer homogenisation, canister sinking and earthquake induced shear loads on the canister-buffer system. |
| Albedo | The ratio of the intensity of light reflected from Earth to that of the light it receives from the sun. |
| AMF | Assessment Model Flow chart. |
| APSE | Äspö Pillar Stability Experiment. |
| Asha | An alternative to the reference backfill material also studied by SKB. |
| Backfill | The material used as filling in the deposition tunnels. |
| BAT | Best Available Technique. |
| BIOCLIM | EU research project on modelling sequential biosphere system under climatic change for radioactive waste disposal. |
| Biosphere object | An area in the landscape that potentially will receive radionuclides released from a future repository (instead of Landscape object). |
| Boundary condition | The set of conditions specified for behaviour of the solution to a set of differential equations at the boundary of its domain. |
| BP | Before Present. |
| Buffer | One of the barriers in the KBS-3 concept, consisting of bentonite clay that surrounds the canister. |
| Burnup | Energy extracted from fuel due to fission, normally given in MWd/kgU. |
| BWR | Boiling Water Reactor. |
| CBI | Cement och BetongInstitutet (Swedish Cement and Concrete Research Institute). |
| CCC | Critical Coagulation Concentration. |
| CDF | Cumulative Distribution Function. |
| CEC | Cation exchange capacity. A measure of sites available for ion-exchange. |
| CFT | Colloid-facilitated transport. |
| CHAN3D | Computer code for simulation of groundwater flow. |
| Clab | Central interim storage facility for spent nuclear fuel in Oskarshamn. |
| Climate domain | A climatically determined environment with a specific set of characteristic processes of importance for repository safety. |
| Clink | Central interim storage and encapsulation plant. Clab and the encapsulation plant as an integrated unit. |
| CMH | Canister Mid-Height. |
| Code-Bright | Computer code for thermal-hydraulic-mechanical calculations. |
| Colloids | Finely divided particles, approximately 10 to 10,000 angstroms in size, dispersed within a continuous medium in a manner that prevents them from being filtered easily or settled rapidly. |
| COMP23 | Near-field model calculating the release rate of radionuclides into the geosphere far field. |
| ConnectFlow | Computer code for simulation of groundwater flow. |
| Copper ingot | A piece of copper cast into a shape suitable for further processing. |
| CPM | Continuous Porous Medium. |

| | |
|---|---|
| Craton | A large portion of a continental plate that has been relatively undisturbed since the Precambrian era and includes both shield and platform layers. |
| CRF | Corrosion Release Fraction. The fraction of the radionuclide inventory released by corrosion of metal parts in the fuel assemblies. |
| Crown space | Space under the tunnel ceiling resulting from consolidation of the backfill material. |
| CRR | Corrosion Release Rate. |
| CRT | Canister Retrieval Test. Experiment at Äspö HRL. |
| CSH | Calcium silicate Hydrates. |
| D2 | The repository design and layout assessed in SR-Site. |
| Darcy flux | Specific discharge, or flux[L/T],is the groundwater flow rate [$L^3/T$] per unit area [$L^2$]. |
| DarcyTools | Computer code for simulation of groundwater flow. |
| $D_e$ | Effective diffusion coefficient. |
| Deformation zone | An essentially 2-dimensional structure (a sub planar structure with a small thickness relative to its lateral extent) in which deformation (strain) has been concentrated (or, in the case of active faults, is being concentrated). |
| Denudation | Surface weathering and erosion. |
| Deponit CA-N | A brand name of a bentonite clay, used as one of the reference materials for the buffer in SR-Can. |
| Design basis case | A calculation case formulated on the basis of a scenario that is shown to be especially important from the standpoint of risk. The result of the calculation of a design basis case is used as input to the formulation of requirements on barriers. |
| Design Premises | Requirements – usually stated as “specification on what mechanical loads the barriers must withstand, restrictions on the composition of barrier materials or acceptance criteria for the various underground excavations.” |
| DFN | Discrete Fracture Network. |
| DLVO | Derjaguin and Landau, Verwey and Overbeek. Theory used in modelling of processes in bentonite. |
| DOC | Dissolved Organic Carbon. |
| Drawdown | Change in groundwater level due to pumping in a well or underground excavation. |
| DZ | Deformation Zone. |
| EBS | Engineered Barrier System. |
| Ecolego | Calculation code for probabilistic radionuclide transport calculations. |
| ECPM | Equivalent Continuous Porous Medium. |
| EDPM | Equivalent Discontinuous Porous Medium. |
| EDZ | Excavation Damaged Zone. |
| Eemian | The penultimate interglacial (Marine Isotope Stage 5e) that preceded the Weichselian glaciation. |
| EFPC | Extended Full Perimeter intersection Criterion. |
| E-modulus | Elastic modulus. The mathematical description of an object or substance’s tendency to be deformed elastically (i.e. non-permanently) when a force is applied to it |
| ERICA tool | Computer software used to obtain activity concentrations and radiological effects on different types of non-human biota. |
| Eustatic change | Changes in the sea level due to water mass added to or removed from the oceans. |
| External conditions | Conditions occurring exterior to the final repository that are considered in the safety assessment and may impact the safety functions of the repository. |
| F | Flow-related transport resistance [T/L], an entity integrated along a flow path, that quantifies the flow-related aspects of the possible retention of a solute transported in a fractured medium. |
| FARF31 | Far-field model for calculation of radionuclide transport in geosphere. |
| FEM | Finite Element Method. |
| Fennoscandian Shield | The exposed Precambrian northwest segment of the East European Craton. |
| FEP | Features, Events and Processes. |
| FFMxx | Fracture domain in Forsmark. |
| FGR | Fission Gas Release. |
| FHA | Future Human Actions. |
| Flow channelling | Heterogeneously distributed flow along preferential flow paths within fractures and deformation zones. |
| Forebulge | Flexural bulge in front of e.g. an ice-sheet load on the lithosphere. |
| FPC | Full Perimeter intersection Criterion. |
| FPI | Full Perimeter Intersection. |

| | |
|---|---|
| FSW | Friction Stir Welding. |
| Fuel assembly | A group of fuel rods handled as a unit in the reactor. |
| Fuel rod | Zirconium alloy tubes filled with cylindrical fuel pellets. |
| GIA | Glacial Isostatic Adjustment. |
| Glacial | Cold period typically associated with ice sheet growth and decay. An alternative word is glaciation. |
| Glacial climate domain | Regions that are covered by ice sheets. |
| Glacial cycle | A period of c 100,000 years that includes both a glacial (e.g. the Weichselian) and an interglacial (e.g. the Holocene). |
| Glacial domain | See Glacial climate domain. |
| Global warming variant | A warm variant of the Main Scenario in which the future climate and hence external conditions are assumed to be substantially influenced by human-induced global warming, i.e. a situation with an increased greenhouse effect. |
| GRIP | European Greenland Ice Core Project. |
| HCD | Hydraulic Conductor Domain. |
| HM | Heavy Metal (but see also next). |
| HM | Hydro-Mechanical. |
| Holocene | Current interglacial period that began around 11,500 years ago. |
| HRD | Hydraulic Rock Domain. |
| HSD | Hydraulic Soil Domain. |
| Ibeco RWC | Possible material for backfill and pellet fill (called Deponit C-AN I SR-Can). |
| ICE3G | A global ice sheet reconstruction by W R Peltier. |
| ICRP | International Commission on Radiological Protection. |
| IFL | Ice Front Location. |
| Illitization | Alteration of smectite (swelling sheet silicate) to illite (non-swelling sheet silicate). |
| Initial state | The state at the beginning of an analysis, e.g. the time of deposition of the canister and buffer and backfilling and sealing of deposition tunnels. |
| Interglacial | A warm period between two glacials. In SR-Site an interglacial is defined as the time from when the ice sheet retreats from the site (time of deglaciation) to the time for the first occurrence of permafrost. |
| Internal processes | Processes occurring within the final repository that are considered in the safety assessment and may impact the safety functions of the repository. |
| Interstadial | A warm period during a glacial, sometimes with ice-free conditions. |
| IPCC | Intergovernmental Panel on Climate Change. |
| IRF | Instant Release Fraction. The instantaneously accessible fraction of radionuclides assumed to be rapidly dissolved in the water entering a failed canister. |
| Isostatic changes | Vertical movements of the Earth's crust due to changes in e.g. ice sheet loading. |
| ka | Kilo-annum or kiloyear, a unit of time. |
| $K_d$ | Partitioning coefficient for sorption [$L^3/M$]. |
| $K_{eff}$ | Effective neutron multiplication factor. The design-basis requirement with a view to criticality is that keff, including uncertainties, shall be less than 0.95 during handling and disposal of canisters. |
| KFMxxx | Core drilled borehole in Forsmark. |
| ky | Kilo year, a unit of time. |
| Landscape development model | A model at landscape level that describes the long-term development of a landscape. The model is used to describe time-dependent properties of the biosphere objects that are input parameters to the Radionuclide model. |
| Lasgit | Large Scale Gas Injection Test. Experiment at Äspö HRL. |
| LDF | Landscape Dose Conversion Factor. The Landscape Dose conversion Factor (LDF) is a radionuclide-specific dose conversion factor, expressed in Sv/y per Bq/y. The LDF relates a unit release rate to dose. |
| LGM | Last Glacial Maximum. |
| Liquefaction | A process by which a stiff material (soil) turns into liquid. |
| Lithosphere | The rigid outer layer of the earth, having an average thickness of about 75 km and comprising the earth's crust and the solid part of the mantle above the asthenosphere. |
| Loss on ignition | Measure of amount of volatile substances (mainly water) in a sample. |
| Low pH materials | Cementitious materials that when in contact with water do not elevate the pH of that water to values above 11. |
| Ma | Million years, a unit of time. |

| | |
|---|---|
| MARFA | Migration Analysis for Radionuclides in the Far Field. Computer code for calculation of radionuclide transport in the far field. |
| Matlab | Numerical computing environment and fourth-generation programming language. |
| MIKE SHE | Computer code for surface hydrogeological modelling. |
| Milos backfill | Bentonite corresponding to reference backfill material. |
| Montmorillonite | Swelling phyllosilicate; key component of bentonite. |
| MOX fuel | Mixed Oxide fuel, blend of plutonium and natural or depleted uranium. |
| MX-80 | A brand name of bentonite clay, used as one of the reference materials for the buffer in SR-Site. |
| Myr | Million years, a unit of time. |
| Natural analogues | A natural system studied in order to investigate processes that have proceeded for a much longer time than can normally be followed by experiments in the laboratory or in the field. |
| NDT | Non-Destructive Testing. |
| NWMO | Nuclear Waste Management Organization, Canada. |
| Observational Method | A risk-based approach to underground design and construction that employs adaptive management, including advanced monitoring and measurement techniques. |
| Pandora | SKB's and Posiva's modelling tool for dose calculations in the biosphere. |
| Peneplain | A low-relief bedrock plain representing the final stage of surface denudation during times of extended tectonic stability. |
| Periglacial climate domain | Regions with permafrost. |
| PhreeqC | Computer code for chemical speciation, batch-reaction, one-dimensional transport, and inverse geochemical calculations. |
| Piping | Formation of hydraulically conductive channels in the buffer clay by erosion. |
| Pleistocene | The penultimate geological epoch. The Pleistocene and ongoing Holocene epochs together constitute the Quaternary period. |
| Posiva | Short for Posiva Oy, the organisation responsible for the final disposal of spent nuclear fuel in Finland. |
| Precambrian | The span of time before the beginning of the Cambrian Period. |
| PWR | Pressurized Water Reactor. |
| Q1 path | Release path from the near-field radionuclide transport model. The Q1 path represents transport into a fracture intersecting the deposition hole. The Q2 path represents transport into the excavation damaged zone (EDZ) located below the floor of the deposition tunnel. The Q3 path represents transport in the backfilled tunnel and into a fracture intersecting the deposition tunnel. |
| Q2 path | See Q1 path. |
| Q3 path | See Q1 path. |
| QA | Quality Assurance. |
| $Q_{eq}$ | Equivalent flow rate used in e.g. COMP23. |
| Quaternary | The Quaternary Period (between 1.6 Ma and the present) is the most recent period of the Cenozoic Era in the geologic time scale. The Quaternary includes two geologic epochs: the Pleistocene and the Holocene. |
| R&D | Research and Development |
| Radionuclide model | Model used to calculate radionuclide inventories in different compartments of the biosphere, radionuclide fluxes between the compartments and radionuclide concentrations in environmental media (soil, water, air and biota). Exposure calculations for humans to estimate LDF's is included in the radionuclide model, whereas exposure of non-human biota is calculated separately. |
| RD&D | Research, Development and Demonstration. |
| Rebound | Uplift of the continental crust as a response to deglaciation. |
| Regolith | In this report the term is used to designate all deposits on bedrock, including Quaternary deposits, soils, sediments, peat, organic debris, surface of rock outcrops and man-made structures. |
| Repository layout | The layout in space of the repository components such as deposition tunnels, central area and access. |
| Respect distance | The perpendicular distance from a deformation zone that defines the volume within which deposition of canisters is prohibited, due to anticipated, future seismic effects on canister integrity. |
| RFMxxx | Rock domain in Forsmark. |
| RH | Relative Humidity. |
| Ridge push | Tectonic horizontal compression of continental plates due to seafloor spreading. |
| Risk criterion | A regulatory criterion to which a calculated risk is compared. |
| Risk dilution | The seemingly paradoxical situation where less knowledge about e.g. a detrimental phenomenon leads to lower calculated individual risks. |

| | |
|---|---|
| RN | Radionuclide. |
| Saalian | The penultimate glacial, preceding the Eemian interglacial. |
| SAFE | The renewed safety assessment of the low level waste repository (SFR) at Forsmark. |
| Safety function | A role through which a repository component contributes to safety. |
| Safety function indicator | A measurable or calculable property of a repository component that indicates the extent to which a safety function is fulfilled. |
| Safety function indicator criteria | A quantitative limit such that if the safety function indicator to which it relates fulfils the criterion, the corresponding safety function is achieved. |
| SCC | Stress Corrosion Cracking. |
| SDM | Site Descriptive Model. A synthesis of geology, rock mechanics, thermal properties, hydrogeology, hydrogeochemistry, bedrock transport properties and surface system properties of the site for the planned spent nuclear fuel repository. |
| SDM-Site | Short name for the Site Descriptive Model resulting from the completed surface based investigations. |
| SFR | Repository in Forsmark for low-and intermediate-level radioactive waste. |
| Sheet joints | Fractures that are oriented sub-parallel to the topographic surface at the time of unloading and lack alteration associated with hydrothermal alteration, i.e. sheet joints. |
| Silica sol | A suspension of nano-sized silica particles that may be converted into a gel by adding a concentrated salt solution. Silica sol may be used as an injection grout that has near-neutral pH. |
| Site description | A model of the site providing descriptions of the present geosphere and biosphere conditions. It is the same as site descriptive model (SDM). |
| SKI | Swedish Nuclear Power Inspectorate. SKI and SSI were merged into the Swedish Radiation Safety Authority (SSM) 1 July 2008. |
| Skin effect | Disturbance of the flow conditions of the interface between the formation (fractured rock) and the tunnel. It is described by the skin factor, which may be positive or negative depending on whether the permeability of the interface is reduced (positive skin factor) or increased (negative skin factor) in relation to the initial permeability of the formation. |
| SMOW | Standard Mean Ocean Water, a water standard defining the isotopic composition of water. |
| Sorption | In this report the term is used to designate all processes by which a dissolved species is retained at a solid surface. |
| Spalling | Rock surface failure in which rock chips are shed from the rock wall. |
| SR 97 | Safety Report 97. The previous safety assessment to SR-Can. |
| SRB | Sulphate-reducing bacteria. |
| SR-Can | The preliminary safety assessment for the planned spent nuclear fuel repository, published in 2006. |
| SSI | Swedish Radiation Protection Authority. SSI and SKI were merged into the Swedish Radiation Safety Authority (SSM) 1 July 2008. |
| SSM | Swedish Radiation Safety Authority. SSI and SKI were merged into the Swedish Radiation Safety Authority 1 July 2008. |
| SSMFS | Regulations of the Swedish Radiation Safety Authority. |
| STUK | Finnish Radiation and Nuclear Safety Authority. |
| Sub-catchment | The drainage area of a biosphere object minus the drainage area of the inlet(-s) to the object. |
| Talik | A layer or body of unfrozen ground occurring in a permafrost area due to a local anomaly in thermal, hydrological, hydrogeological, or hydrochemical conditions. |
| TASQ-tunnel | Tunnel at the Äspö Hard Rock Laboratory. |
| TASS-tunnel | Tunnel at the Äspö Hard Rock Laboratory. |
| TDS | Total Dissolved Solids. |
| Tectonic lens | A lenticular rigid body of rock that is surrounded by deformation zones. |
| Temperate domain | Regions without permafrost or ice sheet conditions. It is dominated by a temperate climate in a broad sense. Within the temperate domain, a site may also at times be submerged by the sea or by an ice dammed lake. |
| Tertiary | Geologic period 65 million to 2.6 million years ago. |
| Thermally induced spalling | Spalling induced by the stresses resulting from the added thermal load from the canister heat. |
| THM | Thermo-Hydro-Mechanical. |
| Till | Dominantly unsorted and unstratified material, generally unconsolidated, deposited directly by a glacier or an ice sheet. |
| $t_w$ | Advective travel time. |
| UCS | Uniaxial Compressive Strength. |

| | |
|---|---|
| Upconing | Raising of the interface between fresh water and saline water due to a drawdown of the groundwater level, e.g. due to pumping in a well or in and underground excavation. In SR-Site, upconing is also used to describe the significant changes in the position of this interface associated with the advance/retreat of an ice sheet margin. |
| Weichselian | Name of the last glacial in north-eastern Europe. |
| Weichselian glacial cycle | The last glacial cycle, defined as comprising the Weichselian glacial and the Holocene interglacial periods. |
| XRD | X-ray diffraction. |
| ZFMxx | Gently dipping zone in Forsmark. |
| ZFMXXXxxxxx | Steeply dipping zone in Forsmark (XXX replaces letters for geographical direction, i.e. ENE). |
| Zircaloy | Name for a group of high-zirconium alloys commonly used as cladding for nuclear fuel rods. |
| Äspö HRL | Äspö Hard Rock Laboratory. |
| $\delta^{18}O$ | Notation used for reporting oxygen isotope ratios, often used as a proxy for temperature in atmosphere or ocean. |

# Appendix C

Topography and place names in the Forsmark area